ISSN 2432-8308

Fourth Periodic Report on the State of Acid Deposition in East Asia

Part I : Regional Assessment

Cambodia
China
Indonesia
Japan
Lao PDR
Malaysia
Mongolia
Myanmar
Philippines
Republic of Korea
Russia
Thailand
Vietnam

Acid Deposition Monitoring Network in East Asia (EANET)

The Fourth Periodic Report
on the State of Acid Deposition in East Asia

Part I: Regional Assessment

Edited by:

Shiro Hatakeyama	Asia Center for Air Pollution Research, Japan
Erdenebat Eldev-Ochir	Asia Center for Air Pollution Research, Japan
Sergey Gromov	Institute of Global Climate and Ecology (IGCE), Roshydromet and RAS, Russia
Le Ngoc Cau	Ministry of Natural Resources and Environment, Vietnam
Kazuhide Matsuda	Tokyo University of Agriculture and Technology, Japan
Meng Fan	Chinese Research Academy of Environmental Sciences, China
Park Jin-soo	National Institute of Environmental Research, Republic of Korea
Atsushi Kume	Kyushu University, Japan
Toshimasa Ohara	National Institute for Environmental Studies, Japan
Tsuyoshi Ohizumi	Asia Center for Air Pollution Research, Japan

December 2021

Table of Contents

List of authors and contributors to the Fourth Periodic Report Part I

Chapter	Authors and Contributors	E-mail address
1	Erdenebat Eldev-Ochir *	erdenebat@acap.asia
	Thiv Sophearith	rith72@yahoo.com
	Dodo Gunawan	dodo.gunawan@bmkg.go.id
	Gantuya Ganbat	gantuyaG@gmail.com
	Jiro Sato	jsato@acap.asia
	Zhu Meihua	mhzhu@acap.asia
2	Sergey A. Gromov *	sergey.gromov@igce.ru
	Kyu Kyu Sein	sein.dmhmdy@gmail.com
	Tamara V. Khodzher	khodzher@lin.irk.ru
	Hiroshi Machida	machida@acap.asia
	Kumiko Nakamura	nakamura@acap.asia
3	Le Ngoc Cau *	caukttv@gmail.com
	Kazuhide Matsuda *	kmatsuda@cc.tuat.ac.jp
	Arcely C. Viernes	arcely_viernes@emb.gov.ph
	Ekaterina A. Zhadanovskaya	zhadanovskaya@gmail.com
	Alisa M. Trifonova-Yakovleva	trifonova@igras.ru
	Tsuyoshi Ohizumi	tohizumi@acap.asia
	Huo Mingqun	mqhuo@acap.asia
	Akie Yuba	yuba@acap.asia
4	Meng Fan *	mengfan@craes.org.cn
	Park Jin-soo *	airchemi@korea.kr
	Patcharawadee Suwanathada	patcharawadee.s@pcd.go.th
	Hu Min	minhu@pku.edu.cn
	Bae Min-Suk	minsbae@hotmail.com
	Ekaterina A. Zhadanovskaya	zhadanovskaya@gmail.com
	Alisa M. Trifonova-Yakovleva	trifonova@igras.ru
	Ken Yamashita	kyamashita@acap.asia
	Hiroaki Minoura	minoura@acap.asia
	Keiichi Sato	ksato@acap.asia
5	Atsushi Kume *	akume@agr.kyushu-u.ac.jp
	Yunting Fang	fangyt@iae.ac.cn

	Zhaozhong Feng	zhaozhong.feng@nuist.edu.cn
	Wilfredo M. Carandang	wmcarandang@up.edu.ph
	Roland Kueh Jui Heng	roland@upm.edu.my
	Ms. Ekaterina S. Zhigacheva	zhigacheva@igce.ru
	Hiroyuki Sase	sase@acap.asia
	Rieko Urakawa	urakawa@acap.asia
	Masayuki Morohashi	morohashi@acap.asia
	Hiroki Yotsuyanagi	yotsuyanagi@acap.asia
	Abubakari Said Mgelwa	abubakarimgelwa@iae.ac.cn
6	Toshimasa Ohara *	tohara@nies.go.jp
	Atsushi Kume	akume@agr.kyushu-u.ac.jp
	Kayo Ueda	uedak@health.env.kyoto-u.ac.jp
	Hiroyuki Sase	sase@acap.asia
	Ken Yamashita	kyamashita@acap.asia
	Keiichi Sato	ksato@acap.asia
	Junichi Kurokawa	kurokawa@acap.asia
	Zhu Meihua	mhzhu@acap.asia
	Yuusuke Kiriyama	kiriyama@acap.asia
	Xerxes T. Seposo	seposo.xerxestesoro@nagasaki-u.ac.jp
	Syuichi Itahashi	isyuichi@criepi.denken.or.jp
7	Shiro Hatakeyama *	hatakeyama@acap.asia
	Nongnout Phanphongsa	phanphongsa@gmail.com
	Mohan Kumar Sammathuria	mohan@met.gov.my
	Yang Xiaoyang	yangxy@craes.org.cn
	Ken Yamashita	kyamashita@acap.asia
	Hiroyuki Sase	sase@acap.asia
	Hiroaki Minoura	minoura@acap.asia
	Tsuyoshi Ohizumi	tohizumi@acap.asia

* : Lead Author

Drafting Committee members in Scientific Advisory Committee

Name	Country	E-mail address
Thiv Sophearith ❋	Cambodia	rith72@yahoo.com
Meng Fan※	China	mengfan@craes.org.cn
Dodo Gunawan	INndnesia	dodo.gunawan@bmkg.go.id
Toshimasa Ohara	Japan	tohara@nies.go.jp
Nongnout Phanphongsa ❋	Lao PDR	phanphongsa@gmail.com
Mohan Kumar Sammathuria	Malaysia	mohan@met.gov.my
Gantuya Ganbat	Mongolia	gantuyaG@gmail.com
Kyu Kyu Sein	Myanmar	sein.dmhmdy@gmail.com
Arcely C. Viernes ❋	Philippines	arcely_viernes@emb.gov.ph
Park Jin-soo ❋	R. of Korea	airchemi@korea.kr
Sergey A. Gromov	Russia	sergey.gromov@igce.ru
Patcharawadee Suwanathada	Thailand	patcharawadee.s@pcd.go.th
Le Ngoc Cau	Vietnam	caukttv@gmail.com

❋: Nominating through the Secretariat, ※: Chair

Foreword

This report is the Fourth Periodic Report on the State of Acid Deposition in East Asia (PRSAD4). The EANET data of 2015-2019 is utilized for evaluating the current status and impact of the acid deposition and air pollution in the EANET region. This report also includes the long-term analysis of the temporal trend and variation, spatial distribution, and possible impact on the eco-system of acid deposition and air pollution in East Asia based on the twenty-year monitoring data from 2000 to 2019. Other national and international monitoring results were also used as references for additional assessment for interpretation of EANET data.

To evaluate scientifically the monitoring data generated, this report also highlighted the data quality assurance and quality control (QA/QC) activities designed to ensure reliable data and coordinated research activities, which were implemented jointly by the EANET community. This report also includes recommendations for future EANET activities based on the results of EANET activities and relevant studies of atmospheric environment assessment in the region.

The commitment and contributions from the Lead Authors under the guidance of the Drafting Committee for PRSAD4 of the Scientific Advisory Committee (SAC) are gratefully acknowledged. I would also like to thank the other contributors for each chapter.

The sources, processes and effects of acid deposition and air pollution are complicated, especially when interactions and controls of climate change are also taken into account. Hence, monitoring data and analysis are essential for control policymaking and scientific research. It is hoped that this Fourth Periodic Report will promote better understanding of acid deposition and air pollution in our region and contribute to the further development of EANET.

Prof. Meng Fan

Chairperson, Scientific Advisory Committee of the EANET

1. Introduction

1.1 Background

Many countries in the world have been experiencing acid deposition and air pollution problems. Over the last couple of decades, there are various arising risks in the East Asian region due to fast-growing economies and fossil fuel consumption. One of the serious problems of the acid deposition and air pollution problems is that long-range transport of air pollutants affected the areas far from the emission sources of precursor substances. As a result, the pollutants cause harmful effects to the human body, plants, animals, materials, and cultural heritage.

Acid deposition is primarily the result of emissions of sulphur dioxide (SO_2) and nitrogen oxides (NO_x) that can be transformed into dry or moist secondary pollutants such as sulphuric acid (H_2SO_4), ammonium nitrate (NH_4NO_3) and nitric acid (HNO_3). Acid deposition is related to smog and visibility/regional haze through common emissions and precursors, production pathways, and meteorological processes. Acid deposition affects everything from plants, soil, trees, buildings, cultural heritages and even humans. Air pollution occurs when pollutants, such as particulate matter (PM), SO_2 and NO_x, are released into and build up in the atmosphere. Increased air pollutants in the air are associated with degradation of air quality and human health such as respiratory problems, heart disease, and premature death.

The Acid Deposition Monitoring Network in East Asia (EANET) is an intergovernmental regional network established for promoting cooperation among countries in East Asia to address acid deposition problem. EANET has gained international recognition for its success in promoting regional cooperation on acid deposition monitoring in East Asia and facilitating inter-regional exchange on data measurement and assessments of the state of acid deposition. Other than conducting technical acid deposition monitoring, the EANET also implements public awareness and research activities to promote a common understanding of the state of acid deposition and air pollution problems. Toward this end, the EANET periodically publishes five reports for scientists and a general audience. Specific publications include the Periodic Report on the State of Acid Deposition in East Asia (PRSAD), the Report for Policy Makers (RPM), EANET Country Fact sheets, the EANET Science Bulletin, the Data Report, and the Report of the Inter-laboratory Comparison Project. A special report titled Report for Policy Makers on Acid Deposition Monitoring Network in East Asia (EANET): Goals, Achievements and Way Forward was launched at a High-Level Meeting in 2005. EANET also publishes a Newsletter biannually which highlights its recent achievements and progress.

The PRSAD, as the most important publication of the EANET, is published every five years. The target audience of this publication is government officials, researchers, and the general public. The objective of issuing the PRSAD is to provide rigorous information to the international community on long-term trends and regional distribution of acid deposition and air pollution in East Asia. As of today, EANET published scientific assessment reports on the state of acid deposition in East Asia in 2006, 2011, and 2016 based on the EANET monitoring data for 2000-2004, 2005-2009 and 2010-2014, respectively.

1.1.1 Preparation of the fourth periodic report

The EANET published scientific assessment reports on the state of acid deposition in East Asia in 2006, 2011, and 2016 based on the EANET monitoring data accumulated from 2000 to 2004, 2005 to 2009, and 2010 to 2014, respectively. This report is the fourth periodic report on the state of acid deposition in East Asia based on the monitoring data from 2000 to 2019 (Twenty years), focusing on spatial distribution, trend analysis and, possibly, impact assessment of acid deposition and air

pollution in the region. The data 2015-2019 is also utilized for evaluating the current status of the environment in the EANET region, following the first, second, and third periodic reports to share the results of the past five years provided by the EANET in its regular phase, as well as to evaluate scientifically the monitoring data generated.

The Nineteenth Session of the Scientific Advisory Committee (SAC19) in October 2019 approved the establishment of the Drafting Committee (DC) for the Fourth Periodic Report on the State of Acid Deposition in East Asia (PRSAD4) to prepare the implementation plan and other related works. It was endorsed by the Twenty-First Session of the Intergovernmental Meeting (IG21) in November 2019, in Beijing, China. The first DC meeting for the PRSAD4 was held virtually on 12 May 2020 due to the COVID-19 pandemic. It was organized by the Network Center (NC) for the Acid Deposition Monitoring Network in East Asia (EANET) in Niigata, Japan. The DC members from 13 participating countries of the EANET participated in the meeting. Prof. Fan Meng, Institute of Chinese Research Academy of Environmental Sciences, China, was elected as the Chairperson of the DC.

The DC developed the format and contents of the PRSAD4. The PRSAD4 consists of three parts: Part I: Regional Assessment, Part II: National Assessment, and Part III: Executive Summary. The DC also nominated the Lead Authors and Contributors to draft the report. The contents of the PRSAD4 are as follows:

- Chapter 1: Introduction
- Chapter 2: Data Quality
- Chapter 3: Wet and Dry Deposition of Acidic Substances in East Asia
- Chapter 4: Gas and Aerosol Pollution in East Asia
- Chapter 5: Impacts on Ecosystems in East Asia
- Chapter 6: Relevant Studies on Atmospheric Environment Assessment in the EANET Region
- Chapter 7: Summary and Recommendations for Future Activities

The report was prepared as a scientific assessment of the state of acid deposition in East Asia based on the data accumulated from the network. A trend analysis was also implemented to investigate the long-term variation in acid deposition using data prior to 2015 in addition to the data from 2015-2019 for this report.

1.2 Brief introduction of EANET

Acid deposition and air pollution are the national and the regional or hemispherical problems affecting human health and the environment. Since 1993, expert meetings were held to discuss the state of acid deposition in the East Asian region, impacts on ecosystems, and future efforts toward regional cooperation on this issue. The experts recommended that acid deposition monitoring should be improved and strengthened. Thus, the expert meetings contributed the necessary knowledge for establishing a regional collaborative monitoring network. Therefore, multilevel bilateral and multilateral environmental cooperation is being actively conducted to discuss air pollution mitigation. In response to the growing concern on the adverse effects of acid deposition, countries in East Asia have established a coordinated monitoring network on acid deposition in the region using the knowledge and experiences from other similar regional and international networks.

The Acid Deposition Monitoring Network in East Asia (EANET) is a regional intergovernmental network established for promoting cooperation among countries in East Asia to address acid deposition and other related atmospheric pollutants. The EANET has made progress and important achievements in the understanding the state of air pollution and acid deposition in East Asian region

by monitoring acidic pollutants and compilation, evaluation, and storage of the relevant data. The EANET has been conducting monitoring, analysis, and evaluation of data and information from several dozen monitoring sites in the 13 participating countries, namely, Cambodia, China, Indonesia, Japan, Lao PDR, Malaysia, Mongolia, Myanmar, Philippines, Republic of Korea, Russia, Thailand, and Vietnam, as well as periodic assessment of the state of acid deposition for the whole region. The network also conducts capacity building and promotes scientific research and public awareness on acid deposition and related air pollution problems with relevant efforts to assist policymakers in decision making to mitigate atmospheric pollution and its impacts based on scientifically assessed information.

The participating countries have participated in monitoring acid deposition as part of EANET since its initial period. In addition, EANET has successfully promoted the cooperation with other regional initiatives, including with the Convention on Long- Range Transboundary Air Pollution (CLRTAP), and established strong links with international organizations such as the World Meteorological Organization (WMO) and World Health Organization (WHO). The experts from these initiatives have been regularly invited to attend EANET meetings, and contributed in enhancing the collective efforts.

The technical capabilities and skills of those involved in managing acid deposition in the participating countries were significantly enhanced through a number of EANET activities. Technical missions were dispatched annually to selected participating countries to monitor performance, laboratory operations, data management and other procedures. Other activities to enhance the skills and knowledge of personnel include national workshops, scientific workshops, individual training courses at the Network Center, and annual expert meetings.

Numerous EANET publications (technical manuals, monitoring guidelines, data publications, QA/QC programs, training materials, etc.) have been disseminated to EANET countries. They will continue to be produced by countries to enhance further capabilities of personnel in monitoring, assessment, and management of acid deposition.

Furthermore, EANET have organized various workshops to raise awareness of the public on acid deposition problems and the importance of community support to improve the environment. The target audience of the awareness activities include general public, including government officials, monitoring officers, academia, students, and teachers. In addition, several publications and video promotional have been developed in collaboration with the participating countries. The countries in collaboration with EANET organized national workshops on acid deposition problems.

Many scientific research projects on acid deposition and its effects were conducted by EANET in collaboration with scientists from the participating countries. The projects were conducted in countries with diverse natural environments and climatic conditions in the East Asian region to obtain a better understanding of the processes involved.

Since 2005, EANET has implemented a research fellowship program to encourage young scientists from the region to carry out air pollution research activities at the Network Center in Japan. Two researchers participate in this activity annually.

1.3 Objectives

The objectives of the EANET described in the "Instrument for Strengthening the Acid Deposition Monitoring Network in East Asia (EANET)" are:

- Create a common understanding of the state of acid deposition in East Asia;

- Provide useful inputs for decision making at local, national, and regional levels to prevent or reduce adverse impacts on the environment caused by acid deposition; and

- Contribute to cooperation on issues related to acid deposition among the participating countries.

To achieve the above objectives, EANET has conducted the following major activities:

- Monitoring acid deposition in the participating countries uses common methodologies in five areas: wet deposition, dry deposition, soil/vegetation, inland aquatic environment, and catchment-scale monitoring.
- Compilation, evaluation, storage, and provision of the data obtained through monitoring.
- Promotion of QA/QC activities to obtain high-quality monitoring data.
- Enhancement of data analysis and assessment.
- Capacity building of monitoring capabilities in participating countries including the implementation of training programs.
- Promotion of research, studies, and public awareness activities related to acid deposition.

1.4 Institutional arrangement

The Acid Deposition Monitoring Network in East Asia (EANET) was established in 2001 to support participating countries in achieving the objectives to tackle acid deposition problems.

As the institutional framework for EANET, the Intergovernmental Meeting is the decision-making body of EANET. The Scientific Advisory Committee was established under the Intergovernmental Meeting, and the Secretariat and the Network Center were designated to support the network. These organizations promote the network activities in close communication, coordination and collaboration with the national focal points, national centers and national QA/QC managers in the participating countries.

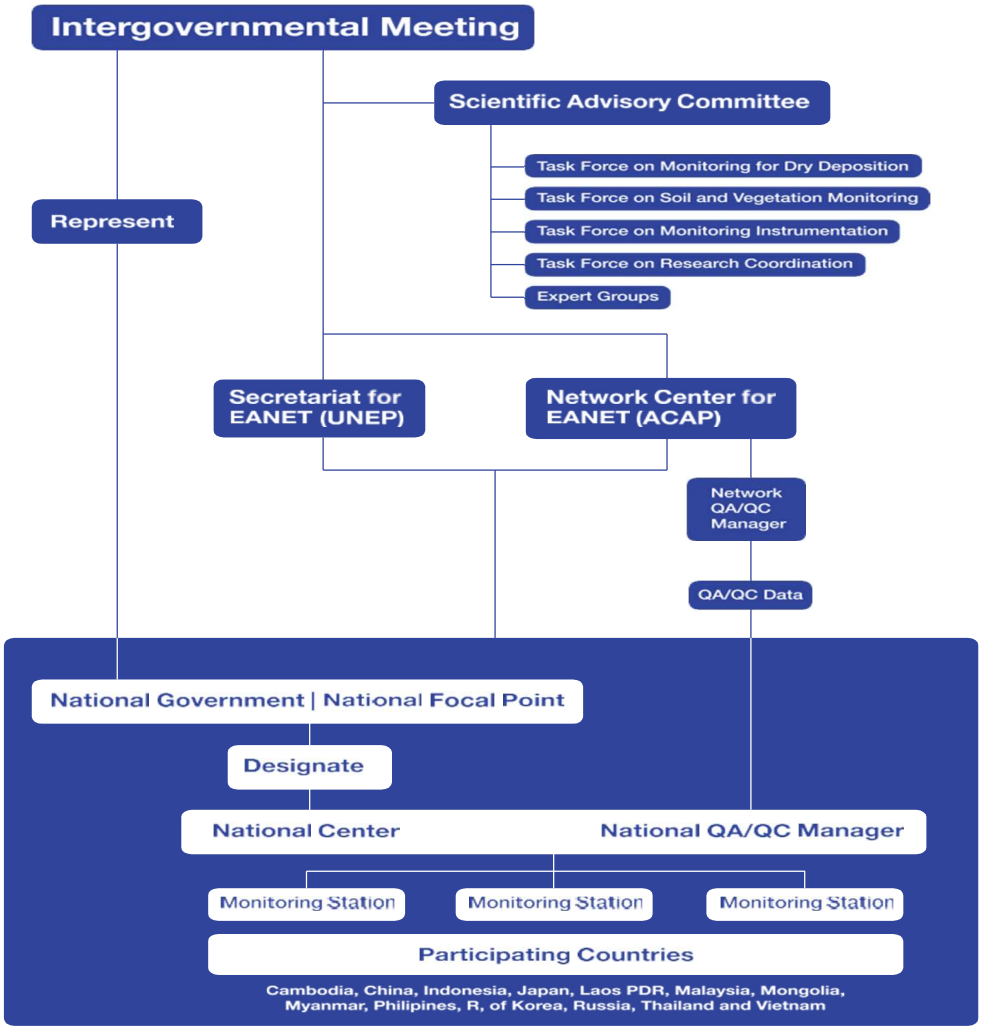

Figure 1.4.1. Institutional Framework for EANET.

Intergovernmental Meeting

The Intergovernmental Meeting (IG), Scientific Advisory Committee (SAC), Secretariat and Network Center (NC) are described in the "Tentative Design (TD) of the Acid Deposition Monitoring Network in East Asia (EANET)" (EANET/IG 2/5/3) as institutional bodies for implementing of the EANET activities on a regular basis.

The Intergovernmental Meeting, composed of the representatives of the participating countries, is the decision-making body of EANET and deals with the matters related to the management of the Network and implementation of the work program.

Scientific Advisory Committee

The Scientific Advisory Committee (SAC) incorporated scientific and technical experts from the participating countries, and have responsibilities to advise and assist the Intergovernmental Meeting with various scientific and technical matters related to the EANET activities.

Secretariat

The Secretariat ensures the effective management of the EANET and facilitates cooperation among Participating Countries in a transparent manner and carries out the following task under the guidance of the IG.

1) Communicate and coordinate with the participating countries concerning the network; Prepare for the EANET meetings such as the Intergovernmental Meeting, Scientific Advisory Committee Meeting, and Working Group Meeting;
2) Conduct necessary administrative and financial arrangement for the network;
3) Promote cooperation among participating countries and other initiatives; and Promotion of public awareness.

United Nations Environment Programme (UNEP) was designated as the Secretariat for EANET located in Bangkok, Thailand.

Network Center

ACAP was designated as the Network Center for EANET to handle scientific and technical matters of the EANET activities and to facilitate cooperation among the Participating Countries in a transparent manner. It carries out the following tasks under the guidance of the IG:

1) Central compilation, evaluation, and storage of monitoring data and related information;
2) Preparation of data reports on acid deposition in East Asia;
3) Dissemination of monitoring data and other relevant information;
4) Provision of technical assistance to the participating countries in implementing the network activities;
5) Implementation and coordination of QA/QC activities;
6) Development and implementation of education/training programs for those engaged in the network activities;
7) Implementation of research activities on acid deposition;
8) Provision of scientific and technical support for the Intergovernmental Meeting, Scientific Advisory Committee, and other subsidiary bodies; and
9) Other tasks as requested by the Intergovernmental Meeting.

The Asia Center for Air Pollution Research (ACAP) is designated as the Network Center for EANET located in Niigata, Japan.

Task Forces

Task Forces of Dry Deposition Monitoring, Soil and Vegetation Monitoring, Instrumentation Monitoring, and Research Coordination were established under the SAC supervising to assist in the development of a strategy for vital directions of monitoring as well as four Expert Groups of the Dry Deposition Flux Estimation, Technical Manual on Wet Deposition Monitoring, Technical Manual on Air Concentration Monitoring, and Technical Manual on Inland Aquatic Environment Monitoring.

Organizations in the participating countries

- National Focal Points

National Focal Point is a representative of the participating country responsible for communicating with the Secretariat and Network Center for EANET concerning the implementation of the network activities.

- National Centers

  National Center is responsible for developing and implementing the national monitoring plan; collecting the national monitoring data and submitting them to the Network Center; promoting national QA/QC activities; and dealing with technical matters on the network activities in the country.

- National QA/QC Managers

  National QA/QC Manager is responsible for developing the national monitoring plan and submitting it to the Network Center; promote national QA/QC activities in cooperation and coordination with the national centers.

1.5 EANET activities in 2000-2019

1.5.1 Main activities of the EANET

EANET was established as an important initiative for regional cooperation among the participating countries to create a common understanding of the state of acid deposition problems and provide useful inputs to policymakers at various levels.

Acid deposition monitoring

- Review and revision/establishment of the national monitoring plans where appropriate
- Implementation of monitoring using common methodologies wet deposition, dry deposition, soil/vegetation, inland aquatic environment, and catchment-scale monitoring

Compilation, evaluation, storage, and provision of data

- Submission of monitoring data to the Network Center
- Issuing of annual data report
- Preparation and publication of a periodic report on the state of acid deposition
- Dissemination of relevant information through the EANET website

Promotion of quality assurance and quality control (QA/QC) activities

- Development of QA/QC programs
- Development of Standard Operational Procedures (SOPs)
- Implementation of Inter-laboratory comparison projects

Implementation of technical support and capacity building activities

- Dispatch of technical missions
- Identification of training needs
- Individual training at the Network Center

Promotion of research and studies related to acid deposition problems

- Joint research programs
- Research fellowship program

Promotion of public awareness activities

- Development of brochures
- Workshop on public awareness

Other relevant activities

- Cooperation and exchange of information and experiences with other regional and global networks/initiatives

1.5.2 EANET meetings

The Fifth Session of the Intergovernmental Meeting (IG5) held in November 2003 in Pattaya, Thailand decided to establish a Working Group on Future Development of EANET (WGFD) to review the performance of the Secretariat and Network Center and develop guidelines on the administrative and financial management of the Secretariat and Network Center. In later years the functions of this Working Group were expanded to develop a five-year medium-term plan for EANET.

A High-Level Segment was held with the Seventh Session of the Intergovernmental Meeting (IG7) in November 2005 in Niigata, Japan at which the *Report for Policy Makers: Goals, Achievements and Way Forward* was launched. The IG7 also adopted Decision 1/IG7 (Niigata Decision) which decided that the participating countries of EANET should begin a process to discuss an appropriate instrument and legal status to provide a sound basis for a financial contribution to EANET.

The Strategy on EANET Development (2006-2010), which was approved by the Eighth Session of the Intergovernmental Meeting (IG8) in November 2006, focused on the whole activities of EANET with clearly stated targets, activities to be undertaken, and expected results. The implementation of the Strategy activities since 2006 and the regular activities of the Secretariat and the NC since the start of EANET, have brought EANET closer towards achieving its objectives.

The Twelfth Session of the Intergovernmental Meeting on EANET (IG12), held in November 2010 in Niigata, Japan adopted the Decision 1/IG12 on "Instrument for Strengthening the Acid Deposition Monitoring Network in East Asia (EANET)". Based on the performance review of the Strategy on EANET Development (2006-2010), the "Medium Term Plan for EANET (MTP) (2011-2015)" was adopted at the IG12 in 2010.

The MTP for the EANET (2016-2020) is the third medium-term plan for the EANET by considering the results of the review of the activities of the Medium Term Plan (2011-2015) and the outcomes of the Feasibility Study on the Expansion of the Scope of the EANET conducted by the Network Center (NC) for EANET. The MTP focuses on enhancing the monitoring network, supported by the participating countries, through the implementation of strategic activities to improve geographical coverage, ensure site representativeness, and strengthen monitoring procedures, particularly sampling and analysis, to achieve more comprehensive and precise data. It also includes capacity building activities, activities for the promotion of research on acid deposition and other priority chemical species, including activities relevant to the modeling and emission inventories.

The *Periodic Report on the State of Acid Deposition in East Asia* was produced in 2006, 2011, 2016 by the Scientific Advisory Committee of EANET. The Periodic Report consisted of 3 volumes: Executive Summary, Part I: Regional Assessment, Part II: National Assessments.

At the Ninth Session of the Intergovernmental Meeting (IG9) several new subsidiary bodies were established under the Scientific Advisory Committee of EANET:

- Task Force on Monitoring Instrumentation
- Task Force on Research Coordination
- Expert Group on Dry Deposition Flux Estimation under the Task Force on Dry Deposition Monitoring
- Expert Group on Revision of Technical Manual on Wet Deposition Monitoring
- Expert Group on Revision of Technical Manual on Inland Aquatic Environment Monitoring

1.5.3 Monitoring activities

EANET monitoring covers five environmental media, wet deposition, dry deposition, soil/vegetation, inland aquatic environment, and catchment-scale monitoring. The monitoring activities have been conducted following a set of monitoring guidelines and technical manuals. Monitoring for wet and dry deposition is implemented to measure concentrations and fluxes of acidic and other substances to the ground. In addition, monitoring soil/vegetation, inland aquatic environment, and catchment are being implemented to assess adverse impacts on terrestrial and aquatic ecosystems. Currently, wet and dry deposition monitoring is being carried out at dozens of sites in the EANET network (including remote, rural, and urban regions). Data and information for ecological impact studies are currently collected from more than dozens of inland aquatic monitoring sites and soil and forest vegetation monitoring sites. All the sites follow a standardized set of methodologies for site selection, sampling, and chemical analyses to ensure technical conformity within the network.

1. Wet Deposition
    - Monitoring Interval
        - every 24 hours or every precipitation event for an urban, rural or remote site
    - Major Parameters
        - Precipitation analysis: pH, electrical conductivity (EC), concentrations of sulfate (SO_4^{2-}), nitrate (NO_3^-), and other ions

2. Dry Deposition
    - Monitoring Interval
        - every day to two weeks, or every hour when measured by automatic instruments
    - Major Measurements
        - Gases: concentrations of sulfur dioxide (SO_2), nitrogen dioxide (NO_2), ozone (O_3) and others
        - Particulate components

3. Soil and Vegetation
    - Monitoring Interval
        - once three to five years
    - Major Parameters
        - Soil: pH, concentrations of exchangeable ions and effective cation exchange capacity (ECEC)
        - Vegetation (forest): survey of tree decline, and general description of a forest

4. Inland Aquatic Environment
    - Monitoring Interval
        - More than four times a year
    - Major Parameters
        - Inland water: pH, electrical conductivity (EC), alkalinity and ions

5. Catchment
    - Monitoring Interval
        - continuously (precipitation and discharge), every week to 2 weeks (chemical components)

- Major Parameters
  - Rainwater and stream water: Precipitation amount, discharge from the stream, major cations (Ca^{2+}, NH_4^+, etc.) and anions (SO_4^{2-}, NO_3^-, etc.), estimation of total deposition (wet + dry), etc.

EANET monitoring sites are classified into two basic categories: acid deposition monitoring sites and ecological survey sites. Acid deposition monitoring sites are sites for collecting fundamental data on the temporal and spatial distribution of acid deposition. They are further classified into three sub-categories: remote sites, rural sites, and urban sites for specific objectives of the monitoring. Ecological survey sites provide basic data for assessing the effects of acidification on terrestrial ecosystems. They are further classified into two sub-categories: basic survey sites and ecosystem analysis sites.

1.5.4 Monitoring activities in 2019

Thirteen EANET countries, namely Cambodia, China, Indonesia, Japan, Lao PDR, Malaysia, Mongolia, Myanmar, Philippines, Republic of Korea, Russia, Thailand, and Vietnam participated in acid deposition monitoring in 2019. A total of sixty-six sites were nominated for the monitoring, including 26 urban, 19 rural, and 21 remote sites. The map showing the locations of these sites with the classification information is provided in Figure 1.5.1. The details on the locations of the acid deposition monitoring sites are presented in Table 1.5.1

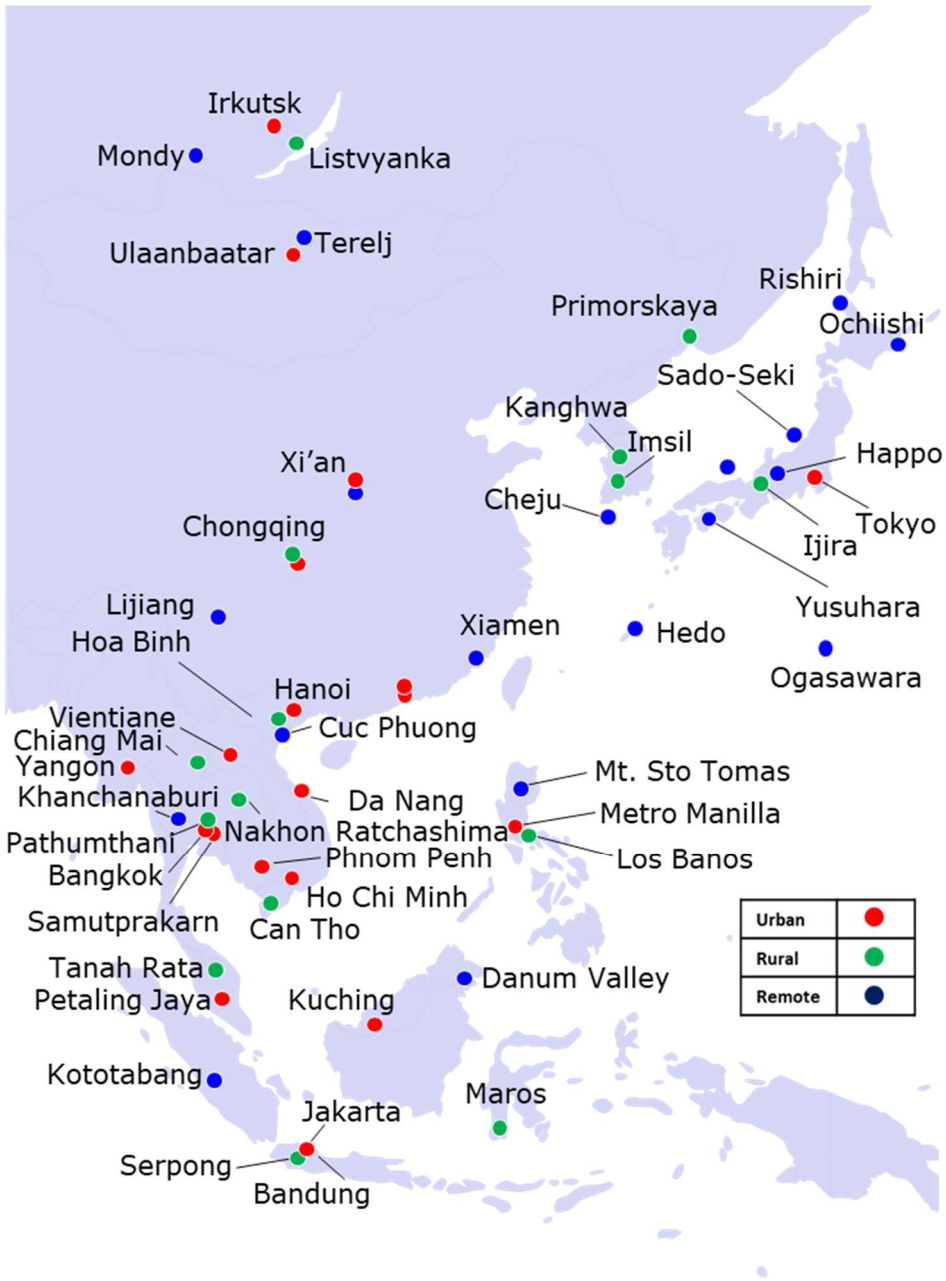

Figure 1.5.1. Locations of acid deposition monitoring sites in 2019.

Table 1.5.1 Locations of acid deposition monitoring sites

Country	Site	Code[*1]	Classification	Latitude[*2]	Longitude[*2]	Altitude /m
Cambodia	Phnom Penh	*KHA001*	Urban	11°33'18"N	104°56'20"E	12
China	Chongqing - Haifu	*CNA003*	Urban	29°37'30"N	106°30'34"E	317
	- Jinyunshan	*CNA004*	Rural	29°49'42"N	106°22'43"E	871
	Xi'an - Shizhan	*CNA005*	Urban	34°14'33"N	108°57'10"E	415
	- Jiwozi	*CNA007*	Remote	33°51'06"N	108°48'52"E	1,837
	Xiamen - Hongwen	*CNA008*	Urban	24°28'47"N	118°09'47"E	39
	- Xiaoping	*CNA009*	Remote	24°51'23"N	118°02'55"E	530
	Zhuhai - Xiang Zhou	*CNA010*	Urban	22°16'22"N	113°31'46"E	29
	- Zhuxiandong[*3]	*CNA011*	Urban	22°12'24"N	113°31'00"E	18
	- Haibin-Park	*CNA012*	Urban	22°15'40"N	113°34'25"E	10
	Wuzhishan - Wuzhishan [*4]	*CNA013*	Remote	18°50'11"N	109°29'26"E	958
	Lijiang - Lijiang [*4]	*CNA014*	Remote	27°13'38"N	100°14'48"E	3410
Indonesia	Jakarta	*IDA001*	Urban	06°09'22"S	106°50'32"E	7
	Serpong	*IDA002*	Rural	06°21'02"S	106°40'04"E	64
	Kototabang	*IDA003*	Remote	00°12'08"S	100°19'05"E	845
	Bandung	*IDA004*	Urban	06°53'41"S	107°35'11"E	753
	Maros	*IDA005*	Rural	04°59'50"S	119°34'17"E	1
	Jembrana[*4]	*IDA006*	Rural	08°20'27"S	114°37'02"E	24
	Lombok[*4]	*IDA007*	Rural	08°38'10"S	116°10'15"E	52
Japan	Rishiri	*JPA001*	Remote	45°07'30"N	141°14'30"E	40
	Ochiishi	*JPA002*	Remote	43°09'43"N	145°29'50"E	49
	Sado-seki	*JPA004*	Remote	38°15'02"N	138°24'01"E	129
	Happo	*JPA005*	Remote	36°41'48"N	137°47'53"E	1,850
	Ijira	*JPA006*	Rural	35°34'14"N	136°41'51"E	140
	Oki	*JPA007*	Remote	36°17'19"N	133°11'06"E	90
	Yusuhara	*JPA009*	Remote	33°22'46"N	132°56'06"E	790
	Hedo	*JPA010*	Remote	26°51'58"N	128°14'55"E	60
	Ogasawara	*JPA011*	Remote	27°05'32"N	142°13'02"E	212
	Tokyo	*JPA012*	Urban	35°41'30"N	139°45'10"E	26
	Niigata-maki[*4]	*JPA013*	Rural	37°48'33"N	138°51'09"E	47
	Tsushima[*4]	*JPA014*	Remote	34°14'48"N	129°17'17"E	390
Lao PDR	Vientiane[*3]	*LAA001*	Urban	17°59'53"N	102°34'56"E	175
Malaysia	Petaling Jaya	*MYA001*	Urban	03°06'07"N	101°38'42"E	51
	Tanah Rata	*MYA002*	Rural	04°29'03"N	101°22'17"E	1,545
	Danum Valley	*MYA003*	Remote	04°58'53"N	117°50'37"E	438
	Kuching	*MYA004*	Urban	01°29'25"N	110°21'09"E	20
Mongolia	Ulaanbaatar	*MNA001*	Urban	47°55'13"N	106°54'43"E	1,275
	Terelj	*MNA002*	Remote	47°59'00"N	107°27'04"E	1,550
Myanmar	Yangon	*MMA001*	Urban	16°51'53"N	96°09'13"E	21
	Mandalay	*MMA002*	Urban	21°54'46"N	96°03'51"E	70
Philippines	Metro Manila	*PHA001*	Urban	14°38'09"N	121°04'43"E	55
	Los Baños	*PHA002*	Rural	14°09'53"N	121°15'00"E	25
	Mt. Sto. Tomas	*PHA003*	Remote	16°25' N	120°36' E	1,500

Table 1.5.1 Locations of acid deposition monitoring sites (continued)

Country	Site	Code*1	Classification	Latitude*2	Longitude*2	Altitude /m
Republic of Korea	Kanghwa	*KRA001*	Rural	37°42'32"N	126°16'26"E	60
	Cheju (Kosan)	*KRA002*	Remote	33°17'32"N	126°09'43"E	37
	Imsil	*KRA003*	Rural	35°36'09"N	127°10'53"E	217
Russia	Mondy	*RUA001*	Remote	51°37'18"N	100°55'10"E	1,996
	Listvyanka	*RUA002*	Rural	51°50'47"N	104°53'34"E	646
	Irkutsk	*RUA003*	Urban	52°14'53"N	104°15'33"E	495
	Primorskaya	*RUA004*	Rural	43°37'45"N	132°14'13"E	85
Thailand	Bangkok	*THA001*	Urban	13°47'04"N	100°32'22"E	5
	Samutprakarn	*THA002*	Urban	13°39'58"N	100°36'21"E	4
	Pathumthani	*THA003*	Rural	14°02'46"N	100°42'43"E	6
	Khanchanaburi (Vajiralongkorn Dam)	*THA004*	Remote	14°47'05"N	98°36'05"E	130
	Chiang Mai					
	- Mae Hia	*THA005*	Rural	18°45'40"N	98°55'54"E	349
	- Chang Phueak	*THA006*	Urban	18°50'26"N	98°58'11"E	329
	- Si Phum	*THA007*	Urban	18°47'27"N	98°59'24"E	313
	Nakhon Ratchasima					
	- Sakaerat	*THA008*	Rural	14°28'04"N	101°54'05"E	409
	- Nai Mueang	*THA009*	Urban	14°58'46"N	102°05'53"E	184
Vietnam	Hanoi	*VNA001*	Urban	21°03'24"N	105°43'36"E	6
	Hoa Binh	*VNA002*	Rural	20°50'12"N	105°20'32"E	23
	Cuc Phuong	*VNA003*	Remote	20°18'01"N	105°41'38"E	155
	Da Nang	*VNA004*	Urban	16°02'35"N	108°12'24"E	5
	Can Tho	*VNA005*	Rural	10°05'18"N	105°41'45"E	2
	Ho Chi Minh	*VNA006*	Urban	10°47'04"N	106°42'00"E	5
	Yen Bai	*VNA007*	Rural	21°42'28"N	104°52'29"E	56

*1 Each code of acid deposition monitoring site is assigned in accordance with the following rules.
e.g.) *KH A 0 01*
(a) (b) (c) (d)

(a): country code (2 digits) (b): item code ("*A*" : acid deposition monitoring)
(c): sub-serial number for ecological monitoring
(d): serial number for each country (2 digits)

*2 The latitude and longitude are shown according to the World Geodetic System.

*3 The latitude of Vientiane and the longitude of Zhuxiandong and Vientiane were revised.

*4 Tappi and Banryu were closed in 2018, and Wuzhishan, Lijiang, Jembrana, Lombok, Niigata-maki, Tsushima started EANET monitoring in 2019.

The current situation on basic survey sites for ecological monitoring and their nearest acid deposition monitoring sites are shown in Table 1.5.2. The map showing the locations of these sites with the classification information is provided in Figure 1.5.2. Soil and vegetation monitoring and inland aquatic environment monitoring are conducted at 31 plots in 10 countries and 19 lakes/rivers in 11 countries. Most of the ecological monitoring sites correspond to the acid deposition monitoring sites. Moreover, both soil and vegetation monitoring and inland aquatic environment monitoring are conducted in the vicinity of four acid deposition monitoring sites in China, two sites in Japan, one site in Malaysia, one site in Mongolia, two sites in Philippines, two sites in Russia, one site in Thailand, and one site in Viet Nam. It is expected that the acid deposition monitoring data collected

in their nearest monitoring sites will be used for the interpretation of the data on ecological monitoring in these sites.

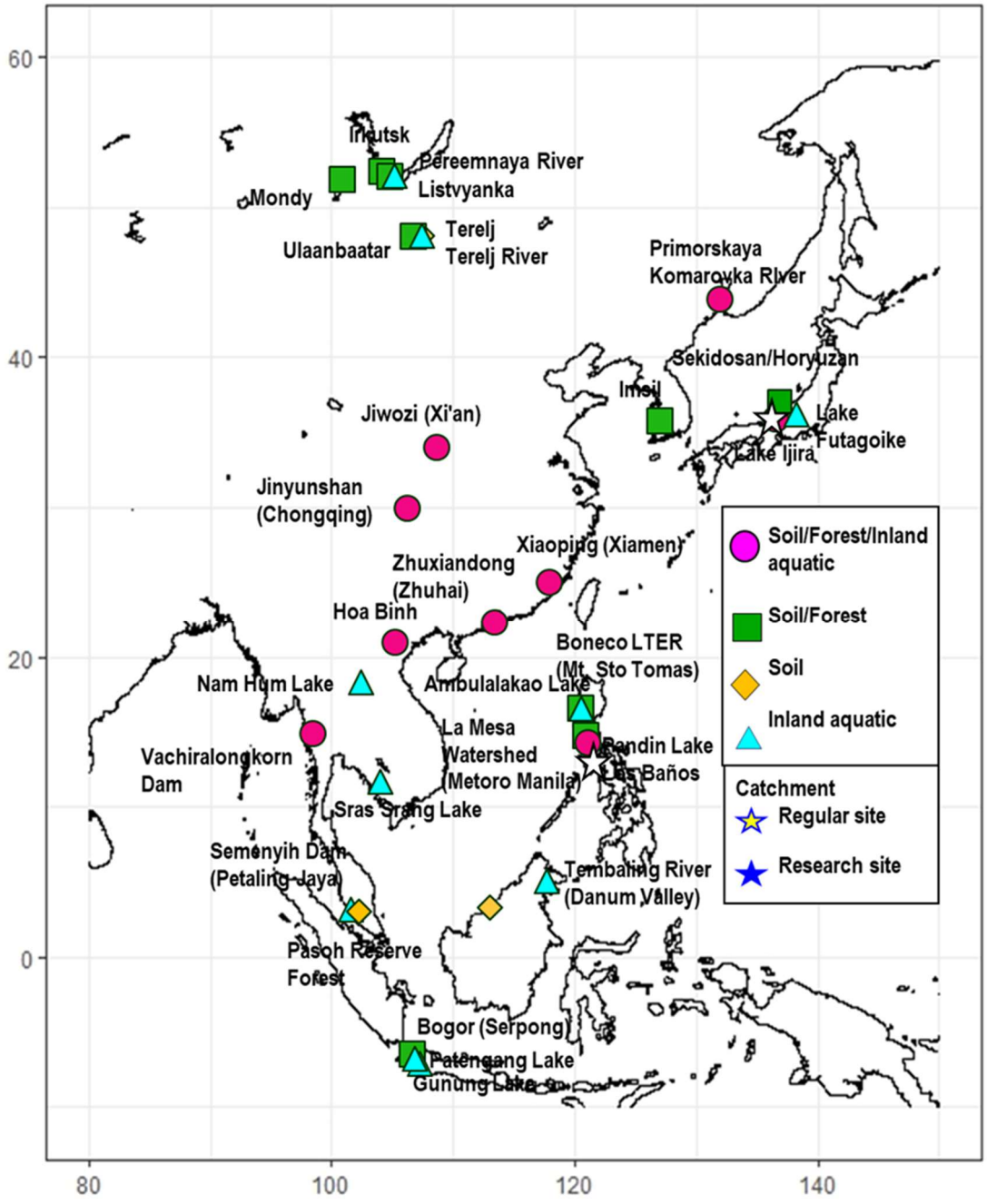

Figure 1.5.2. Locations of basic survey sites for ecological monitoring in 2019.

Table 1.5.2 Basic survey sites for ecological monitoring and their nearest acid deposition monitoring sites

Country	Site for acid deposition monitoring	Plot for soil and vegetation monitoring	Code for soil and vegetation monitoring[*1]	Site for inland aquatic environment monitoring	Code for inland aquatic environment monitoring[*1]
Cambodia	-	-	-	Sras Srang Lake	*KHI002*
China	Chongqing - Jinyunshan	Jinyunshan	*CNS004*	Jinyunshan Lake	*CNI004*
	Xi'an - Jiwozi	Dabagou	*CNS007*	Jiwozi River	*CNI007*
	Xiamen - Xiaoping	Xiaoping	*CNS009*	Xiaoping Dam	*CNI209*
	Zhuhai - Zhuxiandong	Zhuxiandong	*CNS011*	Zhuxiandong Stream	*CNI111*
Indonesia	Serpong	Bogor Research Forest (Dramaga Experimental Forest)	*IDS002*	-	-
	Bandung	-	-	Patengang Lake	*IDI004*
	-	-	-	Gunung Lake	*IDI006*
Japan	Happo	Sekido-san[*2]	*JPS005*	Futago-ike Lake[*2]	*JPI005*
		Horyu-zan[*2]	*JPS105*		
	Ijira	Ijira	*JPS006*	Ijira Lake	*JPI006*
		Yamato	*JPS106*		
Lao PDR	Vientiane	-		Nam Hum Lake	*LAI001*
Malaysia	Petaling Jaya	Pasoh Reserve Forest 1	*MYS001*	Semenyih Dam	*MYI001*
		Pasoh Reserve Forest 2	*MYS101*		
	-	UPMKB Rehabilitated Forest Planted in 1991	*MYS005*		
		UPMKB Rehabilitated Forest Planted in 2008	*MYS105*		
	Danum Valley	-	-	Tembaling River	*MYI003*
Mongolia	Ulaanbaatar	Bogdkhan Mountain	*MNS001*	-	-
	Terelj	Terelj Mountain	*MNS002*	Terelj River	*MNI002*

Table 1.5.2 Basic survey sites for ecological monitoring and their nearest acid deposition monitoring sites (continued)

Country	Site for acid deposition monitoring	Plot for soil and vegetation monitoring	Code for soil and vegetation monitoring*1	Site for inland aquatic environment monitoring	Code for inland aquatic environment monitoring*1
Philippines	Metro Manila	La Mesa Watershed	*PHS001*		
	Los Baños	Mt. Makiling	*PHS002*	Pandin Lake	*PHI102*
		UP Quezon, Land Grant	*PHS102*		
	Mt. Sto Tomas	Boneco Long Term Ecological Research Site	*PHS003*	Ambulalakaw Lake	*PHI003*
Republic of Korea	Imsil	Mt. Naejang	*KRS003*	-	-
Russia	Irkutsk	Irkutsk	*RUS003*	-	-
	Listvyanka	Bolshie Koty	*RUS002*		
		Pereemnaya river catchment	*RUS102*	Pereemnaya River	*RUI102*
	Mondy	Ilchir Lake	*RUS001*	-	-
		Okinskoe Lake	*RUS101*		
		Solar Observatory	*RUS201*		
	Primorskaya	Primorskaya	*RUS004*	Komarovka River	*RUI004*
Thailand	Khanchanaburi (Vajiralongkorn Dam)	Vajiralongkorn Dam	*THS004*	Vajiralongkorn Dam	*THI004*
		Vajiralongkorn Puye	*THS104*		
Vietnam	Hoa Binh	Cave of Heaven	*VNS002*	Hoa Binh Reservoir	*VNI002*
		Thang Ranh	*VNS102*		

*1 Each code of ecological monitoring sites is assigned in accordance with the following rules.
e.g.) *CN S 0 04*
(a) (b) (c) (d)

(a): country code (2 digits)
(b): item code ("*S*": soil and vegetation monitoring, "*I*": monitoring on the inland aquatic environment)
(c): sub-serial number when there are multiple ecological monitoring sites in the nearest acid deposition monitoring site
(d): 2-digit serial number corresponding to its nearest acid deposition monitoring site
(If there is no nearest acid deposition monitoring site within 50 km, another new serial number is assigned after the existing acid deposition monitoring site in its country.)

*2 Banryu site was closed in 2018, and Sekido-san/Horyu-zan and Futago-ike Lake sites started soil and vegetation monitoring and inland aquatic environment monitoring in 2019.

Table 1.5.3 shows the sites for catchment-scale monitoring.

Table 1.5.3 Site for catchment-scale monitoring

Country	Site for acid deposition monitoring	Site for catchment-scale monitoring	Code for catchment-scale monitoring[*1]
Japan	Ijira	Lake Ijira catchment	*JPC006*
Philippines	Mereo Manila	La Mesa Watershed	*PHC001*

*1 Each code of the catchment-scale monitoring sites is assigned in accordance with the following rules.
e.g.) *JP C 0 06*
(a) (b) (c) (d)

(a): country code (2 digits) (b): item code ("*C*": catchment-scale monitoring)
(c): Sub-serial number when there are multiple ecological monitoring sites in the nearest acid deposition monitoring site
(d): 2-digit number corresponding to its nearest acid deposition monitoring site
(If there is no nearest acid deposition monitoring site within 50 km, another new serial number is assigned after the existing acid deposition monitoring site in its country.)

1.5.5 Research activities

As one of the activities of the EANET, the promotion of research activity is specified in the Medium Term Plan for the Acid Deposition Monitoring Network in East Asia. Scientific findings from the research activities are shared with the scientists from participating countries and their scientific and technical research results are published in relevant international and national journals, including in the EANET Science Bulletin.

Research activities are implemented to improve acid deposition monitoring methodologies, deposition estimations, building capacity in the development of emission inventories and will also promote efforts to develop and use appropriate models to assess and analyze the trend of acid deposition and other relevant air pollutants at all scales.

Promotion of research activities related to acid deposition problems includes the following:

- Promotion of research studies, particularly on the applicability of various methodologies for measurement of air concentrations in East Asia;
- Promotion of studies on the effects of acid deposition and other priority chemical species on the ecosystem, human health, and other social aspects from the viewpoint of the socio-economics;
- Promotion of studies on proposed models to assess and analyze the trend of national and regional acid deposition and other air pollutants in East Asia by evaluation of existing models and providing a suitable one, and promotion of atmospheric simulation model through workshops, training courses, etc.; and

Promotion of emission inventories through workshops, training courses, pilot studies, preparation of reference materials, etc. Joint research projects are also implemented as well. A number of joint scientific research projects on acid deposition and its effects were conducted by the EANET participating countries.

The fellowship research program is also introduced annually. It has been promoted since 2005, which is an effective mechanism for encouraging young researchers from across the region to participate in air pollution research activities.

1.5.6 Capacity building activities

The EANET individual training course at the Network Center has been implemented once or twice a year from the beginning of the EANET activities. The training courses consist of wet deposition,

dry deposition, soil/vegetation and inland aquatic environment monitoring, and data management. The Network Center carry out the annual questionnaire survey on training activities conducted by the participating countries to gather information on training requirements and suggestions on new training areas.

The technical capabilities and skills of the participating countries for acid deposition monitoring and assessment were significantly enhanced through a number of EANET activities. The Network Center dispatch technical missions annually to the participating countries to assist them in monitoring performance, laboratory operations, data management, and other procedures. Other activities to enhance the skills and knowledge of personnel included national workshops, annual expert meetings and scientific workshops on ecological impacts and other topics related to acid deposition. Numerous EANET publications (Technical Manuals and Guidelines, Data Report, Reports on QA/QC projects, Training materials, etc.) have been produced for use by technical staff, specialists and researchers involved in the EANET monitoring, data quality, and data management. All of these materials are available on the EANET website (https://www.eanet.asia).

1.5.7 Public awareness activities

The promotion of public awareness on acid deposition and sharing a common understanding of atmospheric environmental issues is an important part of the EANET activities. Public awareness activities on acid deposition and other priority chemical species, including their effects, control and mitigation measures, are being regularly conducted by EANET.

Reports for policymakers were published titled **"**Goals, Achievements and Way Forward", "Clean Air for Sustainable Future", "EANET and Clean Air for Sustainable Development", and "Toward Clean Air for Sustainable Future in East Asia through Collaborative Activities". The EANET has undertaken joint public awareness projects with participating countries to develop brochures on acid deposition, conducted a "Workshop on Public Awareness on Acid Deposition Problems" in the participating countries. The capacity building workshops for the government officials, academicians, non-government organizations and private sectors were held in EANET to raise awareness of the adverse impacts on the environment caused by acid deposition. The Factsheets titled "Countries' efforts and achievements in combating acid deposition" was developed by all participating countries of the EANET through collaboration and coordination with the Network Center and the Secretariat. The published public awareness materials were also issued on the EANET website.

The Science Bulletin Vol.1-5 was published to share the research findings from the EANET Research Fellowship Program, Joint Research Project and other scientific papers using EANET monitoring data.

1.6 References

ACAP. 2011. ACAP Brochure. Asia Center for Air Pollution Research, Japan Environmental Sanitation Center (JESC). Niigata, Japan. 6 p.

ACAP. 2011. ACAP Brochure. Asia Center for Air Pollution Research, Japan Environmental Sanitation Center (JESC). Niigata, Japan. 6 p. EANET. 2011. EANET Brochure. Acid Deposition Monitoring Network in East Asia. Secretariat for the EANET, Pathumthani, Thailand and Network Center for the EANET, Niigata, Japan. 14 p.

EANET. 2011. Second Periodic Report on the State of Acid Deposition in East Asia. Executive Summary. Network Center for the EANET. Niigata, Japan. 41 p. EANET. 2011. EANET Brochure. Acid Deposition Monitoring Network in East Asia. Secretariat for EANET, Pathumthani, Thailand and Network Center for EANET, Niigata, Japan. 14 p.

EANET. 2014. Third Report for Policy Makers "EANET and Clean Air for Sustainable Development". Secretariat for the EANET, Pathumthani, Thailand and Network Center for the EANET, Niigata, Japan. 39 p.

EANET. 2016. Fourth Report for Policy Makers "Towards Clean Air for Sustainable Future in East Asia through Collaborative Activities". Secretariat for the EANET, UNEP Asia and Pacific Office, Thailand and Network Center for the EANET, Niigata, Japan.

EANET. 2014. Data Report 2014. Network Center for the EANET. Niigata, Japan. 311 p.

EANET. 2015. Medium Term Plan for the EANET (2016-2020). EANET/Ig 17/8 rev.1

EANET. 2020. Medium Term Plan for the EANET (2020-2025).

EANET IG19, 2017. Proceedings of the Nineteenth Session of the Intergovernmental Meeting on the Acid Deposition Monitoring Network in East Asia, Bangkok, Thailand.

EANET SAC17, 2017. Proceedings of the Seventeenth Session of the Scientific Advisory Committee, Acid Deposition Monitoring Network in East Asia, Bangkok, Thailand.

EANET PRSAD3, 2016. Third Periodic Report on the State of Acid Deposition in East Asia, Part III: Executive Summary. Acid Deposition Monitoring Network in East Asia, Bangkok, Thailand.

EANET PRSAD3, 2016. Third Periodic Report on the State of Acid Deposition in East Asia, Part II: National Assessments. Acid Deposition Monitoring Network in East Asia, Bangkok, Thailand.

EANET PRSAD3, 2016. Third Periodic Report on the State of Acid Deposition in East Asia, Part I: Regional Assessment. Acid Deposition Monitoring Network in East Asia, Bangkok, Thailand.

EANET RPM3, 2014. Third Report for Policy Makers: EANET and Clean Air for Sustainable Development. Acid Deposition Monitoring Network in East Asia, Pathumthani, Thailand.

EANET RPM2, 2009. Second Report for Policy Makers: Clean Air for a Sustainable Future. Acid Deposition Monitoring Network in East Asia, Pathumthani, Thailand.

EANET RPM, 2005. Report for Policy Makers on Acid Deposition Monitoring Network in East Asia (EANET): Goals, Achievements and Way Forward. Acid Deposition Monitoring Network in East Asia, Pathumthani, Thailand.

EANET RSAP, 2015. Review on the State of Acid Deposition in East Asia, Acid Deposition Monitoring Network in East Asia, Bangkok, Thailand.

2. Data Quality

2.1. Introduction

Quality Assurance of monitoring data is crucial condition to ensure reliable and proven results of measurements, which is a solid base to create a common understanding on the status of the acid deposition problems through EANET activities. At the regular phase of EANET the certain ultimate goals in this type of activity are:

- Increasing of the number of stations should be supported by appropriate data quality by which it can be realized into actual growth of real valid data;
- Involvement of EANET data into global and inter-regular evaluations of environmental issues as well as information exchange should be supported by the same level of data quality like in other networks;
- Prospective use of measurements for comprehensive trend analysis and model validation should provide them attribute as proven objective information.

EANET monitoring covers four environmental items – wet deposition of acidifying substances, dry deposition (air concentration) of related pollutants, soil chemistry, and inland aquatic environment. Monitoring of wet and dry deposition was implemented in order to evaluate fluxes of acidic substances to the land surface through measuring chemical composition of precipitation and atmospheric aerosols as well as gaseous pollutants, while monitoring for soil/vegetation and inland aquatic environment has been carried out to assess adverse impacts on terrestrial and aquatic ecosystems. All of these monitoring activities need to be accompanied with data quality procedures.

Quality Assurance and Quality Control (QA/QC) play an important role in acid deposition monitoring to ensure that the measurements are accurate, comparable and quantifiable quality. The EANET produced four QA/QC programs (Wet Deposition, Air Concentration, Soil and Vegetation, Inland Aquatic Environment) in 2000. Then, the Technical Manuals for Wet Deposition Monitoring, Air Concentration Monitoring, Soil and Vegetation Monitoring, and Inland Aquatic Environment Monitoring described the QA/QC matters. The QA/QC programs are composed of several procedure types: i) siting, ii) sampling procedures and sample handling, iii) chemical analysis, and iv) QA/QC for the measurement data at each site. Each National Center needs to execute various QA/QC activities, including development of national QA/QC programs, standard operating procedures (SOPs) and satisfaction of the data quality objectives (DQOs).

The Inter-Laboratory Comparison project is also used for all analytical laboratories for the EANET monitoring involved. The purposes of this project are to evaluate the analytical systems through the evaluation of analytical results, analytical instruments and their operating condition and other relevant and appropriate practices.

The QA/QC plays an indispensable role in acid deposition monitoring as well as other environmental measurements. QA/QC activities are also seen as an essential part of EANET monitoring to ensure that meaningful data are obtained. Through QA/QC activities, it is especially important that measured data satisfy specified levels of reliability and are accompanied by required information on the measurements themselves.

As mentioned above, several documents regarding QA/QC have been developed by EANET to guide receiving reliable data that can be comparable among the participating countries as well as with other monitoring networks outside of the East Asian region. The QA/QC programs cover activities for the components of the measurement/analysis system in a general way, i.e., in the field (sampling sites), laboratory, data management, and data reporting processes. According to EANET documents, QA/QC activities are documented by each relevant entity.

2.2. General procedures of QA/QC

The objectives of QA/QC programs are to obtain reliable and comparable monitoring data among the participating countries in East Asian region, as well as with other networks by ensuring data accuracy, precision, representativeness and completeness in the acid deposition monitoring.

2.2.1 Preparation of National Monitoring Plan (NMP)

Every participating country of EANET has been required to prepare its NMP in accordance with the "Data Reporting Procedures and Formats for Acid Deposition Monitoring in East Asia". The NMPs were prepared by participating countries after starting regular phase and have been reviewed every year with possible revision, if necessary.

The format of NMP consists of following items:
1) Information on established monitoring sites and their arrangement;
2) Measurement programs including sets of parameters and monitoring interval;
3) Metadata on participating laboratories for each field of monitoring activities, and;
4) Geoinformation on the respective monitoring sites with their scale maps.

The updating of information or making NMP actual to current national monitoring activities is under the responsibility of QA/QC Manager and NFP of country. All relevant information is prepared and discussed at the technical level with the NC at annual STM meeting. However, the certain kinds of information technology are necessary to integrate these data for summarizing or aggregating through network and to compare with advances of other monitoring initiatives or with recommendation of SAC or international bodies like WMO.

NMP is revised annually by participating countries to share information on the current status of EANET monitoring activities, both inside and outside EANET. NC has requested to prepare and revise NMP by using format in the "Quality assurance/Quality control (QA/QC) Guidebook for Acid Deposition Monitoring Network in East Asia -2016" (URL: https://www.eanet.asia/wp-content/uploads/2019/04/QAQC_Guidebook2016.pdf).

2.2.2 Siting

EANET monitoring sites are classified into two basic categories according to types of measurement programs, namely, acid deposition monitoring sites and ecological survey sites. Acid deposition monitoring sites are operating bodies collecting fundamental data on air concentrations and wet acidified deposition to investigate its temporal and spatial distribution,

They are classified into 3 sub-categories: remote sites, rural sites and urban sites with some differences in the objectives of the monitoring. Ecological survey sites are those that provide basic data for assessing the effects of acidification on terrestrial ecosystems, and they are principally classified into 2 sub-categories: survey sites and ecosystem analysis sites. The criteria used for classification of the sites are listed in Table 2.2.1.

Table 2.2.1 Classification of acid deposition monitoring sites

Site Category	Site Classification	Main Purpose and Siting Criteria
Acid Deposition Monitoring Site for wet deposition and dry deposition monitoring	Urban Site	- Assessment of the state of acid deposition in urban areas - Data can be used for evaluation of acid deposition effect on buildings and historical monuments or human health - Urban and industrial areas, and the areas immediately outside the urban area
	Rural Site	- Assessment of the state of acid deposition in rural areas and/or hinterlands - Data can be used for the evaluation of acid deposition on agricultural crops, forests, etc. - More than 20 km away from large pollution sources like cities, power plants and highways.
	Remote Site	- Assessment of the state of acid deposition in background areas - Data can be used for evaluation of long-range transport and deposition models - More than 50 km away from large pollution sources like cities, power plants and highways - More than 500 m away from main roads (less than 500 vehicles per day)
Ecological Survey Site for soil and vegetation monitoring and Inland aquatic monitoring	Basic survey site	- Accumulation of basic data on soil, forest, and inland aquatic environment and disclose trends in their properties - In the vicinity of the acid deposition monitoring site
	Ecosystem analysis site	- Assessment of acid deposition impacts on whole ecosystem through application of terrestrial ecosystem analysis and/or catchment analysis - Sensitive areas to changes in atmospheric acidity and ecologically conserved area

Generally the siting criteria of atmospheric deposition monitoring correspond to those been recommended by WMO-GAW (WMO, 2004) and EMEP (EMEP, 2001) for their design of the measurement networks on precipitation chemistry.

2.2.3 Sampling and sample handling

The sampling has been carried out according to the monitoring manuals for each monitoring category. Especially for the collected wet deposition samples, dry monitoring samples using the filter pack method, and inland water samples, samples are stored in the refrigerator or added a biocide such as thymol to prevent deterioration or at least minimize possible conversion of the chemical species in the collected sample before chemical analysis. The collected soil samples are air-dried, sieved and then stored in cool and dark place before the analysis.

2.2.4 Chemical analysis

The major ions, hydronium ion (H^+, as pH), ammonium ion (NH_4^+), calcium ion (Ca^{2+}), potassium ion (K^+), magnesium ion (Mg^{2+}), sodium ion (Na^+), sulfate ion (SO_4^{2-}), nitrate ion (NO_3^-), chloride ion (Cl^-) in the collected water samples are analyzed. Alkalinity as an indicator for acid neutralizing

capacity is also analyzed in the inland water samples, while exchangeable cations, including Ca^{2+}, Mg^{2+}, K^{+}, Na^{+}, H^{+}, and Al^{3+}, are analyzed in the soil samples. The operation manuals for each monitoring categories provide several acceptable analytical techniques to be applied in the laboratories of the participating countries.

2.2.5 QA/QC procedure prior to the data submission to the national and network center

The quality of the chemical analysis was evaluated in terms of ion balance and conductivity checks. The evaluation was quantified as R_1 and R_2 as defined below (WMO, 2004; EANET, 2010).

$$R_1 = \frac{(C - A)}{(C + A)} \times 100\ (\%) \qquad R_2 = \frac{(\Lambda_{obs} - \Lambda_{calc})}{(\Lambda_{obs} + \Lambda_{calc})} \times 100\ (\%)$$

where the symbols are defined as below and the symbols of the ion denote their concentration on an equivalent basis, and λ is the molar conductivity of the individual ion at infinite dilution at 25℃.

$$C = [H^+] + [NH_4^+] + [Ca^{2+}] + [K^+] + [Mg^{2+}] + [Na^+]$$
$$A = [SO_4^{2-}] + [NO_3^-] + [Cl^-]$$
$$\Lambda = \lambda_{H+}[H^+] + \lambda_{NH4+}[NH_4^+] + \lambda_{Ca2+}[Ca^{2+}] + \lambda_{K+}[K^+] + \lambda_{Mg2+}[Mg^{2+}] + \lambda_{Na+}[Na^+] + \lambda_{SO42-}[SO_4^{2-}] + \lambda_{NO3-}[NO_3^-] + \lambda_{Cl-}[Cl^-]$$

The acceptable ranges for R_1 and R_2 are defined as a function of the concentration sums of the analytical suites and presented in Table 2.2.2. Λmeas indicates the measured value of the electrical conductivity of the sample. When the value of either R_1 or R_2 does not meet the criteria, the samples are supposed to be a subject of reanalysis as well as more detailed examination of all analytical procedures is involved. Then, it is also recommended that some ionic species including hydrogen carbonate, HCO_3^-, or organic acids should be added to the analytical suites or the criteria should be modified as a function of pH. The acceptable ranges are encouraged to be revised in consideration of the ionic composition and concentration levels as well as the present state of arts of the analytical laboratories.

Table 2.2.2 Required criteria of analysis quality by R_1 and R_2

(C + A), μeq L^{-1}	R_1, %	Λmeas, mS m^{-1}	R_2, %
< 50	±30	< 0.5	±20
50–100	±15	0.5–3	±13
> 100	±8	> 3	±9

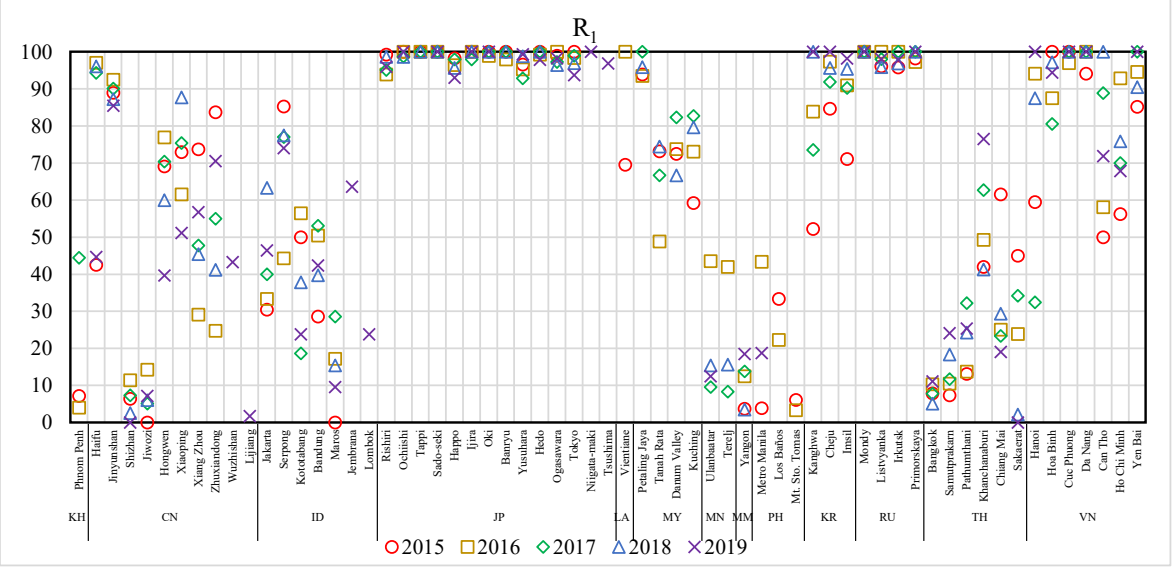

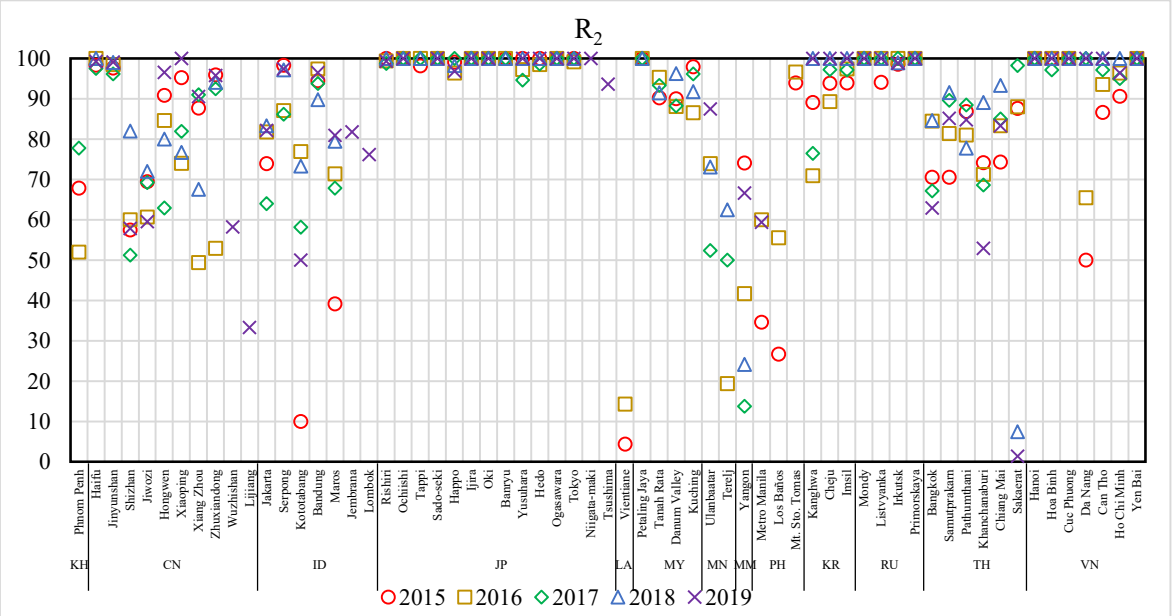

Figure 2.2.1. Annual percentage of the (precipitation chemistry) data that satisfied with the criteria for ion balance (R_1) and conductivity (R_2) from 2015 to 2019.

Figure 2.2.1 demonstrates the annual percentages of the data that satisfied with the criteria for ion balance (R_1) and conductivity (R_2) at each EANET monitoring site from 2015 to 2019. For R_1 values, some sites in China, Japan, Lao PDR, Malaysia, R. of Korea, Russia and Vietnam well satisfied the criteria. On the other hand, many sites in Southeast Asia countries could not meet these criteria because unanalyzed ionic species such as organic acids may be included in precipitation samples. For R_2 values, some sites in China, Indonesia, Japan, Malaysia, Philippines, R. of Korea, Russia, Thailand and Vietnam well satisfied the criteria. However, the data from other country did not satisfy completely the criteria with the same reason as of R_1.

2.3. Evaluation of Inter-Laboratory Comparison (ILC) Projects

Chemical analysis and evaluation of the analytical performance (as the part of QA/QC procedures) with help of Inter-Laboratory Comparison are very important for the data quality of EANET. It has been done annually since 1998 by starting on wet deposition (from the preparatory phase of EANET) in order to improve the quality assurance and quality control (QA/QC) of the network as a whole. There are different activities on analyzing media in the Inter-Laboratory Comparison projects, i.e., on wet deposition, dry deposition, soil, and inland aquatic environment.

The Inter-Laboratory Comparison project of EANET is a well-designed world-wide approach of the round-robin test performed with a common set of simulated water (artificial rainwater or surface water) or unified common samples in all analytical laboratories for the EANET monitoring. The purpose of this project is to evaluate the analytical systems through the evaluation of analytical accomplishments, analytical instruments and their operating condition and other relevant and appropriate practices. Particularly emphasis is placed on the issues: (i) to recognize the analytical precision and accuracy of the measurement of each laboratory, and provide an opportunity for the laboratories to improve the quality of the chemical analysis of wet deposition samples, and (ii) to improve reliability of analytical measurements through assessing the relevant techniques.

Throughout the Inter-Laboratory Comparison project, the outlier data and the actual procedure in each participating laboratory have been evaluated using artificial rainwater sample for wet deposition monitoring, artificial filter sample for the dry deposition monitoring with filter pack method, actual

soil sample for soil monitoring and artificial inland water sample for the inland aquatic environment monitoring.

2.3.1 Wet deposition

The Inter-Laboratory Comparison surveys were carried out 22 times from 1998 to 2019 with increasing participation of 24 to 37 laboratories in all thirteen countries of EANET. Figures 2.3.1 summarized the number of participating laboratories in each country.

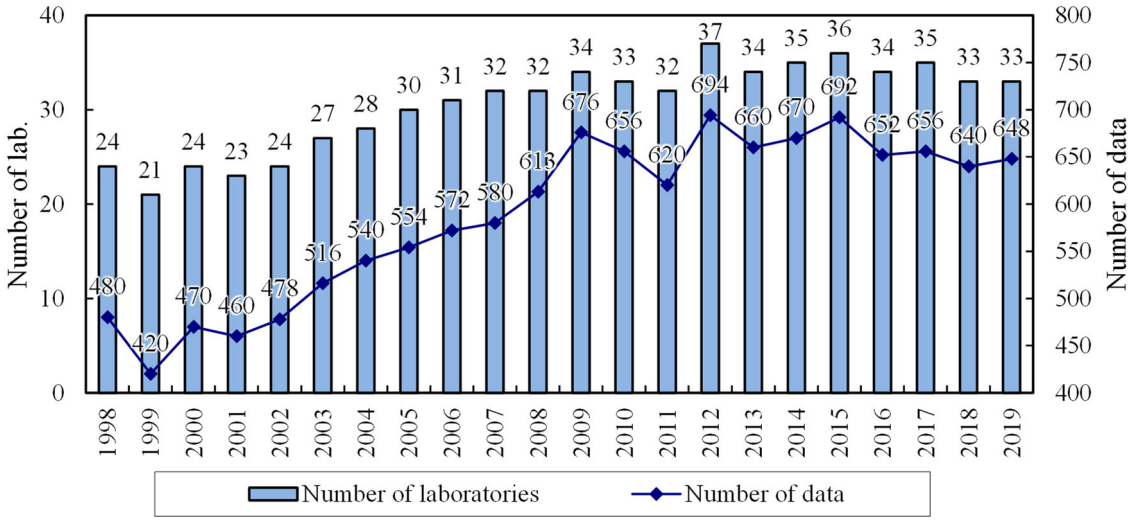

Figure 2.3.1. Number of participating laboratories and the number of data in the Inter-Laboratory Comparison Project on wet deposition for 1998-2019.

Two kinds of artificial rainwater samples of different levels of concentrations, higher and lower, were prepared by the NC to include all ions of analytical suites with the distribution of these samples to the participating laboratories at the end of every year.

The samples required to be diluted 100 times prior to analysis. Measurement of pH and electronic conductivity (EC), and determination of the concentrations of SO_4^{2-}, NO_3^-, Cl^-, Na^+, K^+, Ca^{2+}, Mg^{2+} and NH_4^+. Analytical results were submitted to the NC to summarize and review the results by comparing to the prepared values and further by carrying out some statistical analysis. The well-established design and format of the annual "Report of the Inter-Laboratory Comparison Project" includes all received analytical results, laboratory codes and statistical descriptions together with the lists of the participating laboratories in countries (EANET, 2019). The values of concentrations in the artificial rainwater samples from the 1st attempt (1998) to the 22th attempt (2019) were summarized in Table 2.3.1.

Table 2.3.1 The prepared values of each parameter in artificial rainwater for Inter-Laboratory Comparison project of EANET

year/sample #		pH	EC (mS m^{-1})	SO_4^{2-}	NO_3^-	Cl^-	Na^+	K^+	Ca^{2+}	Mg^{2+}	NH_4^+
				(μmol L^{-1})							
1998	No.1	4.05	7.94	83.5	93.3	129	95.8	11.1	41.1	13.1	84.8
	No.2	4.51	2.82	29.1	36.1	45.1	33.5	7.42	14.3	4.6	29.5
1999	No.1	4.14	6.38	67	75.0	104	77.0	8.9	33.0	11.0	68.0
	No.2	4.59	2.30	24.0	27.0	38.0	28.0	3.2	12.0	3.8	25.0
2000	No.1	4.10	6.23	59.7	63.3	101.3	51.3	9.9	29.4	11.7	60.5
	No.2	4.85	1.55	20.1	27.5	15.5	8.7	4.9	11.0	7.8	18.2
2001	No.1	4.10	7.45	85.0	93.3	108.4	68.4	15.8	41.1	18.7	87.8
	No.2	4.82	1.76	21.5	19.4	34.4	27.4	4.00	13.2	3.7	16.7

2002	No.1	4.30	3.75	40.3	51.0	33.7	13.7	6.92	19.1	7.02	42.4
	No.2	5.15	0.69	8.88	8.49	9.13	5.13	1.98	6.6	1.75	4.54
2003	No.031	4.52	3.44	44.7	30.9	66.0	46.1	6.9	20.5	7.0	48.3
	No.032	4.80	1.48	12.0	21.3	29.6	25.6	2.5	4.4	3.4	15.1
2004	No.041	4.60	3.93	58.5	41.4	76.6	66.6	7.0	38.9	9.7	39.3
	No.042	5.00	1.33	17.5	18.4	22.4	20.5	5.0	10.0	2.7	15.1
2005	No.051	4.66	3.32	43.7	40.3	68.5	56.5	6.9	23.2	11.7	40.9
	No.052	5.05	1.05	14.4	13.2	15.3	10.3	3.0	7.6	3.1	13.6
2006	No.061	4.72	3.10	45.8	36.3	57.5	44.5	6.9	23.8	11.7	43.9
	No.062	5.15	1.21	16.9	15.0	24.5	20.5	4.9	9.3	3.5	15.1
2007	No.071	4.64	3.72	54.9	43.6	69.0	53.4	8.3	28.6	14.0	52.7
	No.072	5.00	1.47	14.0	21.0	38.8	30.8	4.9	6.4	7.0	15.1
2008	No.081	4.49	3.97	49.5	47.4	75.8	56.8	9.1	25.7	12.6	47.5
	No.082	5.10	1.18	14.7	16.2	23.4	15.4	3.8	7.6	6.2	14.2
2009	No.091	4.52	4.23	57.8	46.7	81.9	59.9	9.1	29.0	14.8	57.5
	No.092	4.92	1.66	19.9	22.0	34.0	24.0	5.9	9.3	7.0	21.2
2010	No.101	4.54	3.97	52.0	47.0	77.0	60.0	8.9	26.0	13.0	52.1
	No.102	5.06	1.25	16.6	14.4	24.7	20.7	2.8	8.1	3.3	17.0
2011	No.111	5.52	3.52	76.4	37.8	56.7	53.7	10.4	47.6	13.7	57.5
	No.112	4.60	2.16	23.7	20.8	35.4	20.4	2.3	9.1	4.3	29.2
2012	No.121	4.60	3.25	37.1	32.9	78.7	58.7	6.3	18.6	10.8	37.1
	No.122	5.10	1.31	9.7	21.6	40.4	40.4	2.5	5.6	5.6	8.3
2013	No.131	4.60	3.19	46.2	36.4	49.4	34.4	7.1	22.0	9.7	48.4
	No.132	5.10	1.02	14.4	17.3	11.6	9.6	3.1	9.1	4.1	10.6
2014	No.141	4.70	3.20	49.0	37.1	54.8	44.8	6.9	24.7	10.1	48.6
	No.142	5.00	1.39	22.1	17.0	18.0	14.0	3.2	9.9	3.9	24.4
2015	No.151	4.74	3.05	44.1	38.9	56.8	48.8	7.8	22.2	10.5	43.9
	No.152	5.15	0.94	11.9	10.7	19.8	12.8	3.2	7.0	3.7	9.8
2016	No.161	4.85	2.39	44.5	21.0	32.3	18.3	6.9	28.8	7.0	31.5
	No.162	5.30	0.67	10.2	8.4	8.5	6.5	1.7	3.7	1.8	13.0
2017	No.171	4.85	2.98	60.0	30.9	33.2	26.2	4.8	33.9	9.5	52.1
	No.172	5.15	1.03	18.1	11.0	12.6	9.6	1.8	13.1	2.6	10.1
2018	No.181	4.92	2.44	50.7	33.6	14.3	11.3	4.4	27.1	10.1	47.1
	No.182	5.40	0.87	17.2	9.2	9.5	7.5	2.3	7.1	2.5	20.1
2019	No.191	4.89	2.80	42.9	25.9	65.2	55.2	5.3	23.4	8.8	38.9
	No.192	5.46	0.86	17.6	13.0	6.6	5.1	2.6	12.4	4.2	10.4

The results of the analysis in the project were evaluated in terms of the exceedance of the Data Quality Objectives (DQOs) values which had been prescribed in the EANET QA/QC program as a deviation of ±15% from prepared value for each analytical suite. The flag "E" was put to the data that exceed DQOs by a factor of 2 (±15%~±30%), and the flag "X" to the data exceeding DQOs by a factor of over 2 (<-30% or >30%). A set of the data for each sample was evaluated with the data checking procedures.

However, the room for improvement may be identified in the comparison with established DQO for other international measurement networks. The high quality targets are presented in Table 2.3.2 by the reference to requirement of regional WMO-GAW Precipitation Chemistry network and EMEP.

Table 2.3.2 Data Quality Objectives for Precipitation Chemistry analysis (accuracy in single analysis in laboratory)

Analyzed component in laboratory	DQO established for:	
	GAW-PC network (WMO, 2004)	EMEP network (EMEP, 2001)
pH	0.07 units	0.1 units
conductivity	7%	15 %
acidity	25%	15 %
sulfate	7%	10 %
nitrate	7%	10 %
ammonium	7%	15 %
chloride	10%	15 %

sodium	10%	15 %
potassium	20%	15 %
calcium	15%	15 %
magnesium	10%	15 %

It should be noted that DQO for the most of analyzed constituent in regional WMO-GAW PC laboratories are less in range of value accuracy, than in EANET, especially for the most interested compounds like oxidized sulfur and oxidized nitrogen. The similar limits (as in EANET) were established in EMEP, but the relevant documents on EMEP measurement strategy proposed the changes of those criteria (EMEP, 2009).

It is also useful to consider the comparison of approach being used by different international intercomparison projects for evaluation of analytical results and network laboratories performance as well as an application of some interesting tool like Yudgen plots (NIVA, 2011) and ring diagrams (WDCPC, 2011).

The Inter-Laboratory Comparison surveys were carried out 21 times, and the overall percentages of flagged data, "E" and "X" respectively, are shown in Figure 2.3.2. The percentage of data within the data quality objectives (DQOs) increased from 75.4-78.3% (1998) to 86.1-94.1% (2019). The percentage of the flagged data, which may be related to the concentration levels of the artificial rainwater, has been generally decreasing toward the 22nd attempt.

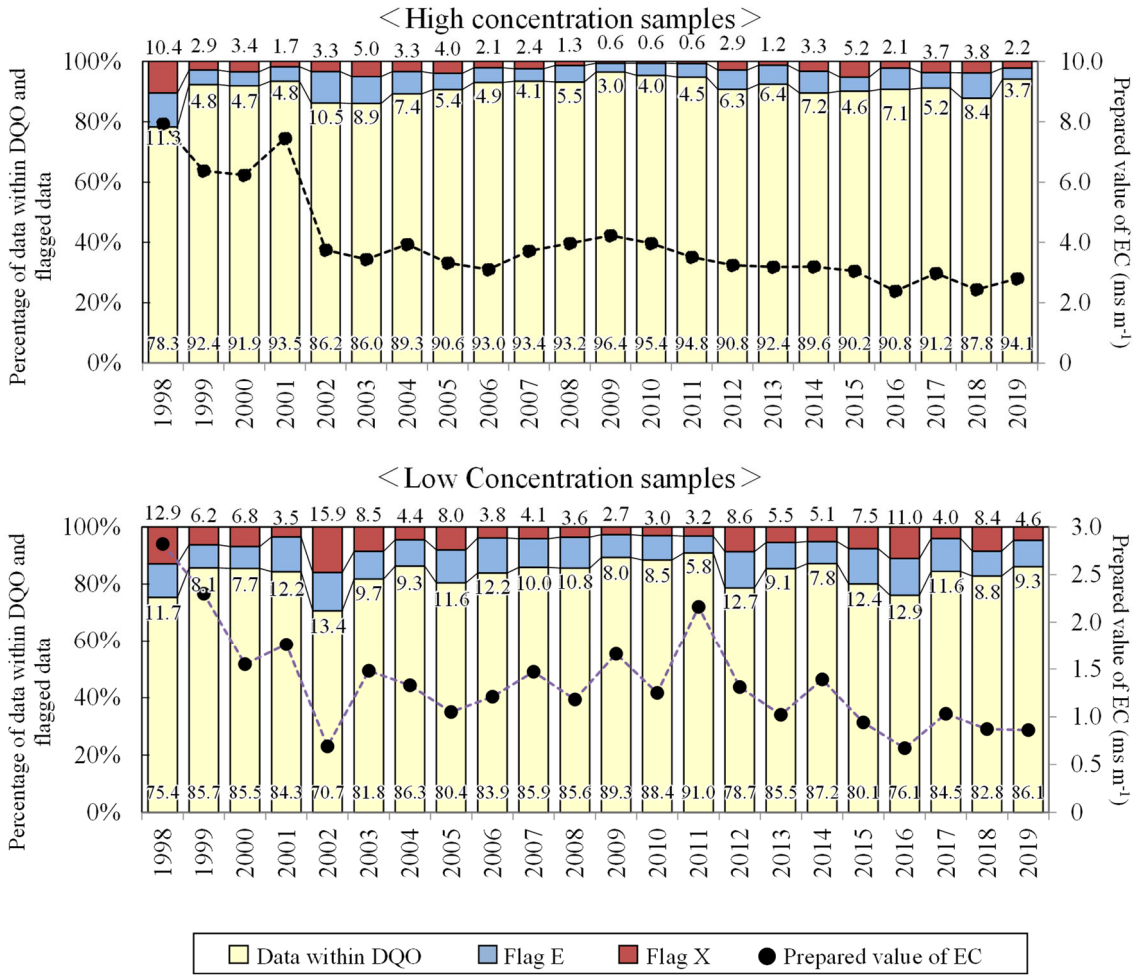

Figure 2.3.2. Overall comparisons of all Inter-Laboratory Comparison projects for 1998-2019.

2.3.2 Dry deposition

The Inter-Laboratory Comparison surveys on analysis of filters were carried out 15 times from 2005 to 2019 with participation of 19 to 27 laboratories in the thirteen countries: Cambodia, China, Indonesia, Japan, Lao PDR, Malaysia, Mongolia, Myanmar, Philippines, Republic of Korea, Russia, Thailand and Vietnam. Figure 2.3.3 shows the number of participating laboratories in each year.

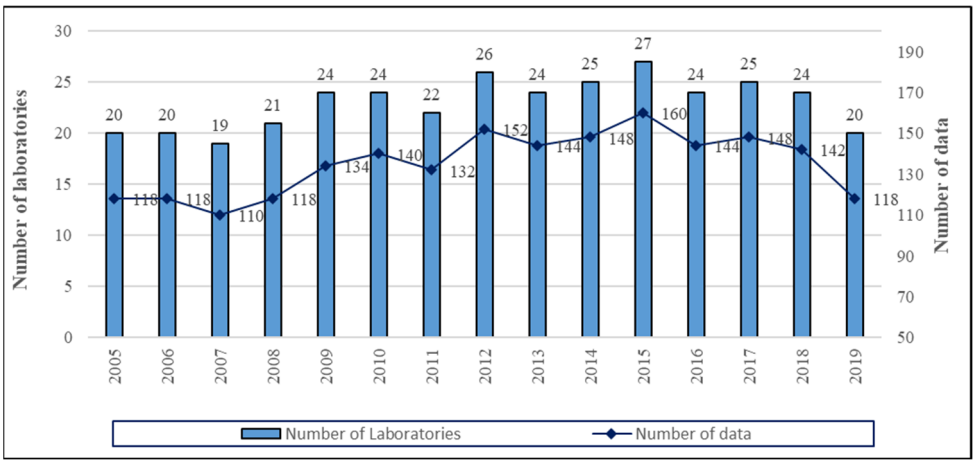

Figure 2.3.3. Number of participating laboratories the number of data in the Inter-Laboratory Comparison Project on dry deposition.

Two kinds of filter samples, one contained two ions ($SO_4^{2-}$and Cl^-), the other contained one ion (NH_4^+), were prepared and distributed to the laboratories. The blank filters, which were impregnated with K_2CO_3 or H_3PO_4 but did not contain any SO_4^{2-}, Cl^-, or NH_4^+, were also prepared and distributed these samples to the participating laboratories in October in each year. The preparation is correspondent to recommended procedure for the filter pack method described in "Technical Manual for Air Concentration Monitoring in East Asia" (EANET, 2013). Each filter sample was put in a centrifuge tube, a solvent was directly poured into the tube for extraction.

The prepared values of each parameter in the artificial filter samples from the 1st attempt (2005) to the 10th attempt (2014) are summarized in Table 2.3.3.

Table 2.3.3 The prepared values of each parameter in the artificial filter samples from the 1st attempt (2005) to the 15th attempt (2019) for Inter-Laboratory Comparison project of EANET

year/sample #		SO_4^{2-}	Cl^-	NH_4^+
		(μg)		
2005	No.051	25	2.8	5.3
	No.052	70	30	20
2006	No.061	40	3.5	6.5
	No.062	140	40	50
2007	No.071	20	1.6	4.6
	No.072	80	25	30
2008	No.081	30	2.5	5.6
	No.082	110	32	35
2009	No.091	35	3.0	5.3
	No.092	120	38	40
2010	No.101	30	6.0	5.8
	No.102	90	27	45
2011	No.111	73	3.0	8.0
	No.112	110	32	26
2012	No.121	22	2.5	20
	No.122	170	11	70
2013	No.131	10	2.6	6.0
	No.132	70	13	40
2014	No.141	25	9.0	16
	No.142	65	21	43
2015	No.151	18	3.5	9.5
	No.152	74	14	51
2016	No.161	15	4.0	8.8
	No.162	54	15	46
2017	No.171	11	4.4	9.6
	No.172	61	13	54
2018*	No.181	30.0	3.61	12.0
	No.182	62.0	9.63	62.1
2019	No.191	7.02	3.02	9.45
	No.192	70.1	17.1	58.3

Since Inter-laboratory Comparison Project 2018, the prepared values are officially disclosed 3 digits.

The Data Quality Objectives (DQOs) of EANET are specified that determined values are expected for fall within ±15% deviation from the prepared values in *Technical Manual for Air Concentration Monitoring in East Asia* (2013). Each laboratory analyzed each sample 3 times, and these average values are evaluated based on the deviation from the corresponding prepared values. A flag E indicates that its deviation exceeds ±15% but not ±30%, and a flag "X" indicates that its deviation exceeds ±30%.

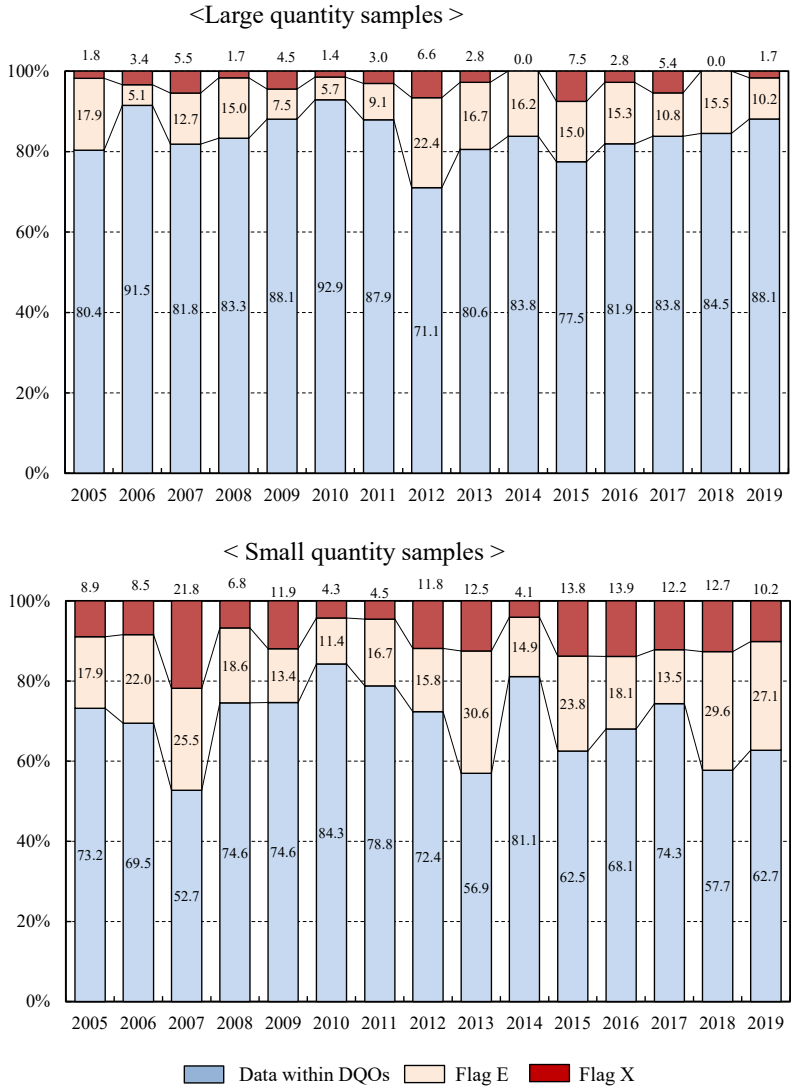

Figure 2.3.4. Overall comparisons of the Inter-Laboratory Comparison projects.

The Inter-Laboratory Comparison surveys were carried out 15 times, and the overall percentages of flagged data, "E" and "X" respectively, are shown in Figure 2.3.4. The percentage of data within the data quality objectives (DQOs) decreased from 73.2% (2005) to 62.7% (2019) for small quantity samples and increased from 80.4% (2005) to 88.1% (2019) for large quantity samples. The percentage of the flagged data for large quality samples has been generally decreasing in line with practice. Therefore, to improve completeness for sample analysis especially for the small quantity samples, analytical procedure including sample shipping, sample storage and extraction procedure, etc. should be confirmed hearing the situation in participating laboratories.

The relative standard deviations were varied. This variation was considered that the difference of the extraction procedure caused the variation of the results among the participating laboratories.

2.3.3 Soil

The project on soil sample analysis started in 1999 as one of the activities within the QA/QC programs. Twelve to sixteen laboratories participated from the following six to ten countries: China, Indonesia, Japan, Malaysia, Mongolia, Philippines, Republic of Korea, Russia, Thailand, and Vietnam. Air-dried soil samples, which were prepared by the NC, were distributed to the laboratories every year except 2001. The laboratories carried out the whole procedures of the soil analysis

including extraction, instrumental analysis or titration, and reporting. Performance at each step would be responsible for the inter-laboratory variations. In order to eliminate the differences in the sample preparation, therefore, samples of soil extract were also distributed in 2001 and 2002 to evaluate the procedures of respective steps. Distributed samples of the respective years and mandatory parameters to be measured for soil samples were listed in Tables 2.3.4 and 2.3.5, respectively.

Table 2.3.4 Distributed samples and their characteristics

Year	Sample 1	Sample 2
1999 (1st)	No. 991: Acrisols (red soil)	No. 992: Gleysols (gley soil)
2000 (2nd)	No. 001: Cambisols (brown forest soil)	No. 002: Andosols (black soil)
2001 (3rd)	No. 011: Soil extract by CH_3COONH_4 solution (for exchangeable base cations)	No. 012: Soil extract by KCl solution (for exchangeable acidity, Al, and H)
2002 (4th)	No. 021: Andosols (black soil: soil sample)	No. 022: Soil extract by CH_3COONH_4 solution (for exchangeable base cations)
2003 (5th)	No. 031: Cambisols (brown forest soil)	No. 032: Arenosols (red soil)
2004 (6th)	No. 041: Andosols (black soil)	No. 042: Cambisols (brown forest soil)
2005 (7th)	No. 051: *Quercus serrata* (secondary forest)	No. 052: *Pinus densiflora* (secondary forest)
2006 (8th)	No. 061: Eutric Cambisol (brown forest soil)	No. 062: Dystric Cambisol (brown forest soil)
2007 (9th)	No. 071: Acrisols (red soil)	No. 072: Cambisols (brown forest soil)
2008 (10th)	No. 081: Cambisols (brown forest soil)	No. 082: Acrisols (red soil)
2009 (11th)	No. 091: Cambisols (brown forest soil)	No. 092: Acrisols (red soil)
2010 (12th)	No. 101: Cambisols	No. 102: Andosols
2011 (13th)	No. 111: Cambisols	No. 112: Cambisols
2012 (14th)	No. 121: Cambisols	No. 122: Cambisols
2013 (15th)	No. 131: Dydstric Cambisol	No. 132: Eutric Fluvisol
2014 (16th)	No. 141: Andisols	No. 142: Cambisols
2015 (17th)	No. 151: Acrisols	No. 152: Cambisols
2016 (18th)	No. 161: Cambisols	No. 162: Cambisols
2017 (19th)	No. 171: Acrisols	No. 172: Cambisols
2018 (20th)	No. 181: Cambisols	No. 182: Cambisols
2019 (21st)	No. 191: Andosols	No. 192: Cambisols

Table 2.3.5 Mandatory parameters to be measured for the soil samples

Parameters	Unit
a) Moisture content	wt %
b) pH(H_2O), pH(KCl)	
c) Ex- base cations, such as Ca^{2+}, Mg^{2+}, K^+, and Na^+	cmol(+) kg^{-1}
d) Ex- acidity, Al^{3+}, and H^+	cmol(+) kg^{-1}

Note: Ex-, exchangeable

The laboratories analyzed each sample twice under the within-laboratory reproducibility condition (time, analysts, and/or instruments are different in a same laboratory). Moreover, triplicate analysis under the repeatability condition was carried out for each time. Therefore, six datasets could be obtained for each sample. Precisions on inter-laboratory reproducibility, within-laboratory reproducibility, and repeatability were estimated by analysis of variance (ANOVA) of the data, according to the method described in the Technical Manual for Soil and Vegetation Monitoring.

Each parameter is statistically evaluated according to the several procedures described in the "Technical Manual for Soil and Vegetation Monitoring in East Asia" (2nd ISAG, 2000). One of the procedures is detection of outliers by Cochran and Grubbs method. Evenness of within-laboratory precision (variation in each laboratory) and inter-laboratory precision (variation between participant laboratories) are verified by this method. Figure 2.3.5 shows the change of outlier ratio in all properties and laboratories from 2002 to 2019 [the ratio is calculated by {(N of entire dataset) – (N of verified dataset)} / (N of entire dataset)]. Although the ratio decreased from first experiment in 2002,

this is still high (10-25% from 2003 to 2019). The outlier ratio in 2019 was lower than the average outlier ratio from 2003 to 2018, which was around 14%. Outliers may disturb evaluation and understanding of actual monitoring data. For inter-laboratory comparison project on soil, a decrease in the outliers is most important task in near future. Appropriate standard solution, extraction solution, dilution rate and calculation should be checked to reduce extremely different values considered as outliers.

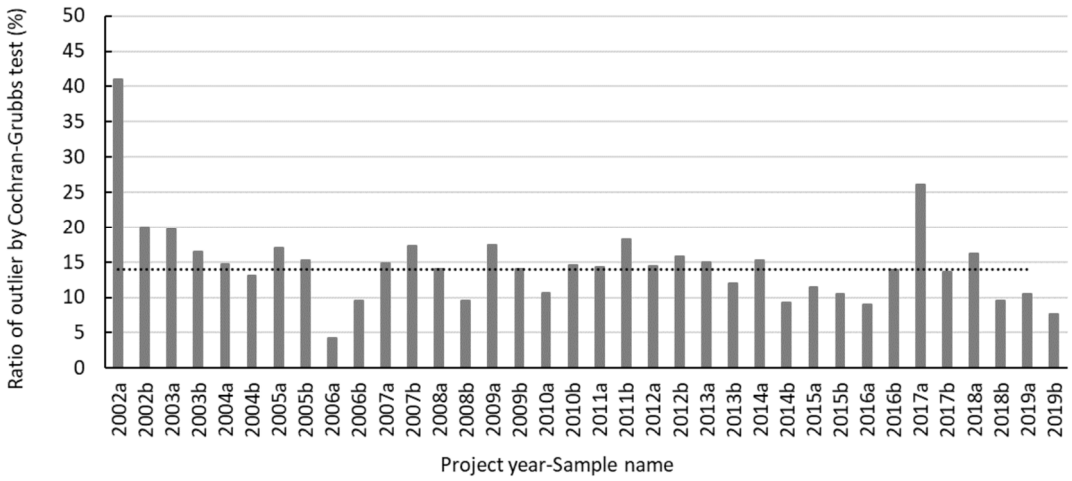

Figure 2.3.5. Change of the outlier ratio in all properties and laboratories from 2002 to 2019 calculated by {(*N* of entire dataset) – (*N* of verified dataset)} / (*N* of entire dataset). 'a' and ' b' show the two kind of sample in each year (e.g. 191s and 192s). Dotted line represents the average outlier ratio from 2003 to 2018.

Pretreatment procedures, such as extraction and dilution of the samples, and instrumental analysis may affect the inter-laboratory reproducibility. All the procedures should be checked step by step for improvement of the reproducibility. Moreover, all the distributed samples were collected in Japan, whose chemical and physical properties might be quite different from those monitored in the respective countries. This may also affect the inter-laboratory reproducibility. Thus, it was suggested that regional variation of exchangeable cations should carefully be evaluated taking uncertainties of the precision into consideration, while the pH values were enough comparable among the countries.

On the other hand, the high precisions of within-laboratory reproducibility and repeatability may allow to conclude that the analysis in the respective laboratories was conducted according to their standard procedures as appropriate. In the actual monitoring activities, soil samples collected from the permanent plots in the respective sites are analyzed periodically in the same laboratories. Temporal changes of soil chemical properties in the respective laboratories (respective sites) could be indicated and evaluated, although uncertainties of the actual values should still be taken into consideration.

2.3.4 Inland aquatic environment

The project on inland aquatic environment sample analysis started in 2000 as one of the activities within the QA/QC programs. Fourteen to sixteen laboratories participated from the following ten countries: China, Indonesia, Japan, Lao PDR, Malaysia, Mongolia, Philippines, Russia, Thailand, and Vietnam, participated in the projects. One artificial inland water sample, which contained all analyzed ions and was prepared by the NC, was distributed to the laboratories every year. The laboratories carried out the whole procedures of the inland water analysis including extraction, instrumental analysis or titration, and reporting. Performance at each step would be responsible for the inter-laboratory variations.

The Inter-Laboratory Comparison projects of EANET have been carried out 20 times, and the results showing the percentage of flagged data and the percentage of data that satisfied the DQOs are shown in Figure 2.3.6.

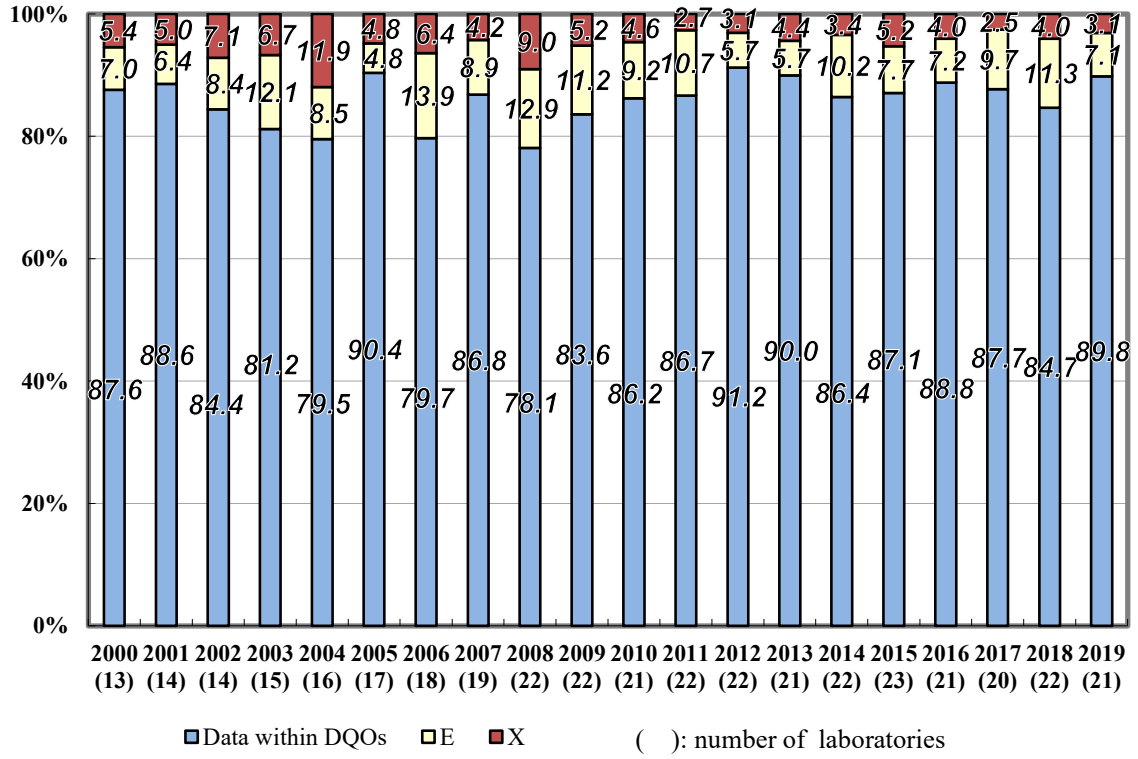

Figure 2.3.6. Comparison of the results from the Inter-Laboratory Comparison projects.

The graph includes the increased number of laboratories while the data within DQOs were temporary decreased. However, it was relatively good results in following attempts.

The comparison for each parameter from the 1st to 10th project with the percentage of flagged data is shown in Figure 2.3.7. There was no flagged data in pH, EC, and NO_3^- in this attempt. The analyses of SO_4^{2-}, Ca^{2+}, and NH_4^+ were improved, but flagged data were still appeared with significant percentage in Alkalinity, Ca^{2+} and NH_4^+. As for Na^+ and K^+, flagged data has decreased in spite of decreasing trends of prepared concentration.

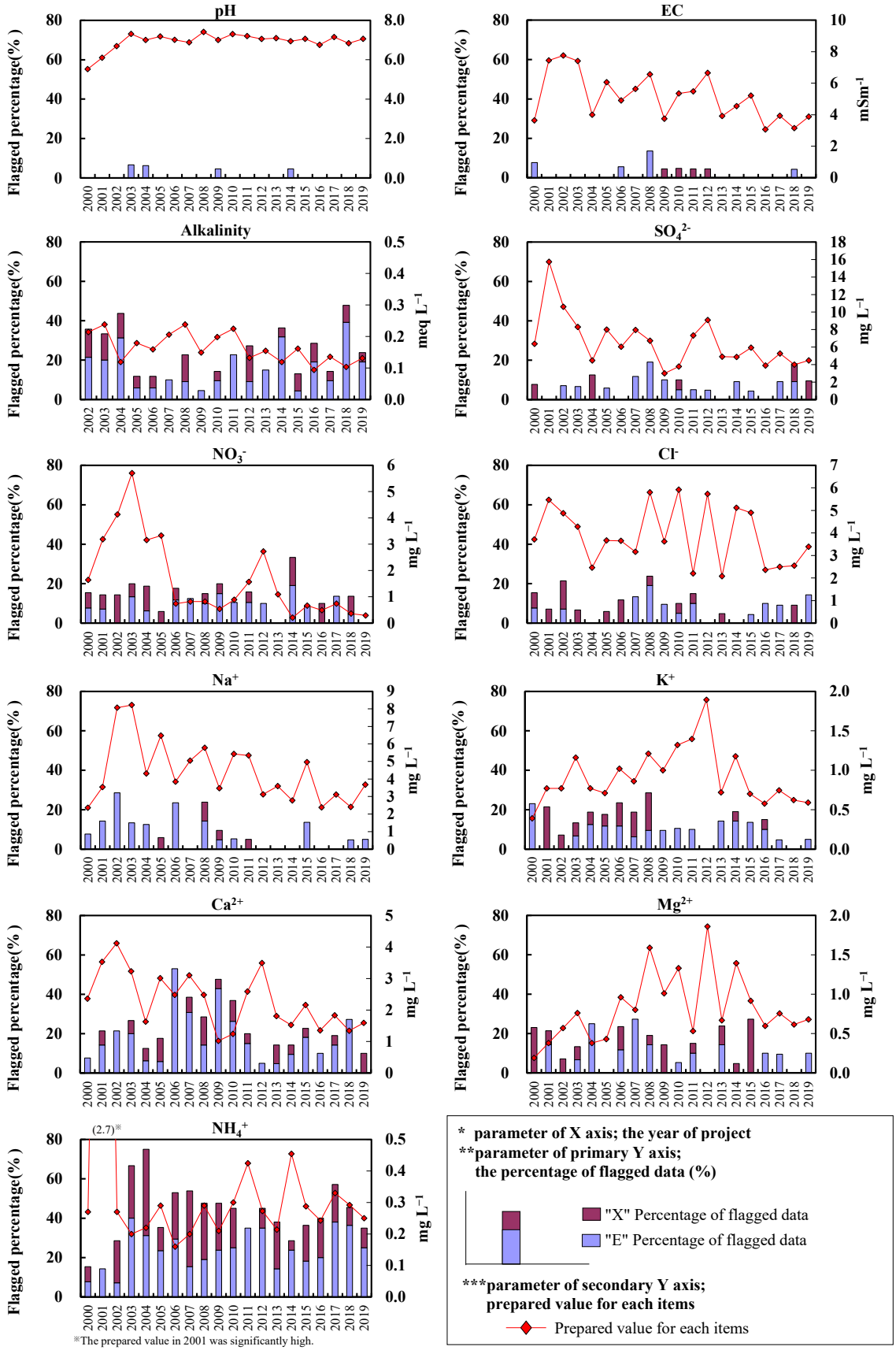

Figure 2.3.7. Comparison of the percentage of flagged data for each parameter in the Inter-Laboratory Comparison projects.

Furthermore, the percentage of flagged data was larger in NH_4^+ than for other parameters in every survey except for the 1st- 3rd project. The percentage of flagged Ca^{2+} in the 7th - 11th project was also comparatively high. In recent attempts, the number of flagged data in alkalinity increased to the similar level in NH_4^+ or Ca^{2+}. Therefore, in the inland water analysis, it is necessary to pay more attention not only to NH_4^+ and Ca^{2+} but also to alkalinity.

2.4 Evaluation of the measurements

The objectives of the QA/QC program are to obtain reliable data that can be comparable among the countries of the East Asian region, as well as with other networks by ensuring data accuracy, precision, representativeness and completeness in acid deposition monitoring. All activities of data management are directed to ensure acceptable quality assurance levels. This section describes data evaluation processes for QA/QC of the EANET monitoring.

2.4.1 Flow for the data reporting and verification

The annual measurements in a participating country are subjected to the data qualification by the National QA/QC manager and the national committee of data evaluation of each country. Some suspected datasets will be as feedback to the analytical laboratories or appropriate organizations. The principal flow chart of data reporting and verification is presented in Figure 2.4.1.

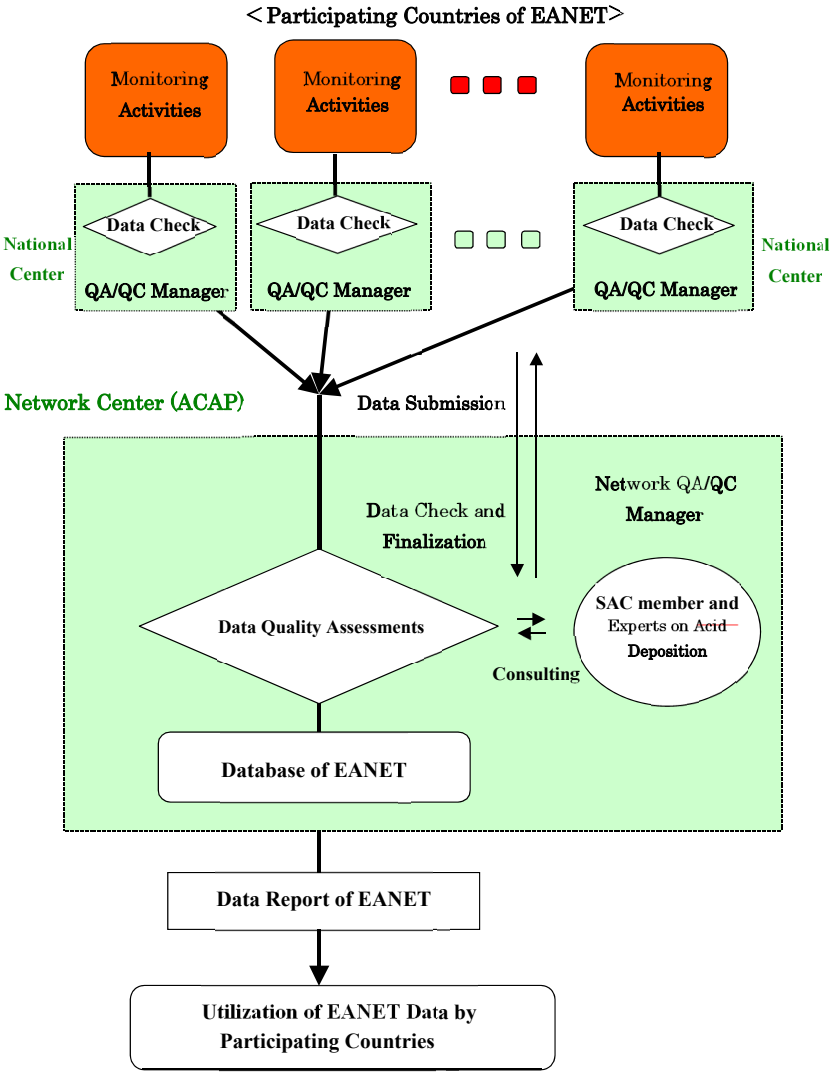

Figure 2.4.1. Flow Chart of reporting and verification for EANET Monitoring Data.

All datasets are eventually collected at the Network Center (NC) where the datasets are further examined and qualified through communications with national centers. The datasets qualified so far are submitted to the international data verification group for the final checking. The international experts of the monitoring activities qualify each of the datasets in a careful and detailed manner. After discussion between NC and national centers, the verified datasets are submitted to the Scientific Advisory Committee to be scientifically and technically approved. The annual data report is actually completed after SAC consideration, which will be officially and finally approved by the Intergovernmental Meeting.

2.4.2 Validation of the data for wet deposition

The tables with annual sets of wet deposition data include certain flags to reflect values out of criteria or questions to the individual samples or its analysis. The most frequent problems include an absence of value due to “insufficient sample volume” (for analysis) or “low precision”, therefore the correspondent flags are attached to those data, both for whole sample or individual datum. The list of flags is included into Technical Manual for Wet Deposition Monitoring in East Asia (2010). Most

of them are completely agreed with the similar flags recommended by EMEP or WMO in their manuals on precipitation chemistry monitoring (EMEP, 2001; WMO, 2004).

As the routine procedure for quality and completeness of sample chemical analysis, all the wet deposition data for individual sample are checked in terms of ion balance (R_1) and the conductivity agreement (R_2) as presented in 2.2.5. The three ranges of good values were established for the different levels of concentrations. This procedure is recommended by the most of monitoring networks, however, the values of R_1 and R_2 criteria could differentiate upon the network experience. Annual EANET Data Report presented information on the numbers of analyzed samples which meet mentioned criteria. The statistical analysis of long-term changes of data with good values of R_1 and R_2 criteria for each site demonstrated that more than 30% of sites has increased quality of their data analysis while for about 20% of sites the percentage of data out of ranges for R_1 and R_2 criteria is increasing. It has also to be mentioned that in some countries the number of data within allowable ranges of criteria are close to 100% for many years.

Table 2.4.1 Results of trend evaluation for wet deposition data with good R_1 and R_2criteria at EANET sites for 2000-2019

Country	Name of Sites	Years for R_1	R_1 %/year	R_1 conf	Years for R_2	R_2 %/year	R_2 conf	Years for R_1&R_2	R_1&R_2 %/year	R_1&R_2 conf
Cambodia	Phnom Penh	12	0.41	0.793	12	3.22	0.069	12	0.78	0.527
China	Haifu	12	-2.09	0.208	12	0.35	0.075	12	-1.74	0.284
China	Jinyunshan	19	0.51	0.069	19	0.74	0.015	19	0.85	0.036
China	Shizhan	19	-2.02	0.062	20	0.39	0.584	17	-1.78	0.090
China	Jiwozi	18	-1.66	0.055	18	1.40	0.095	15	-0.69	0.447
China	Hongwen	20	1.80	0.007	20	1.34	0.007	20	1.87	0.005
China	Xiaoping	20	2.17	0.000	20	2.01	0.001	20	2.39	0.000
China	Xiang Zhou	20	0.62	0.396	20	1.82	0.013	20	1.13	0.140
China	Zhuxiandong	16	1.10	0.197	16	2.26	0.016	16	1.66	0.081
China	Jakarta	18	0.88	0.232	19	1.52	0.055	17	1.26	0.131
Indonesia	Serpong	19	-0.91	0.268	19	0.03	0.917	19	-0.85	0.318
Indonesia	Kototabang	19	-0.38	0.636	18	0.52	0.566	18	-0.10	0.886
Indonesia	Bandung	19	-1.86	0.121	19	0.96	0.058	19	-1.59	0.195
Indonesia	Maros	11	-1.51	0.111	12	-0.23	0.833	11	-1.02	0.135
Japan	Rishiri	20	0.04	0.744	20	0.04	0.748	20	0.07	0.698
Japan	Ochiishi	17	0.02	0.862	17	0.05	0.647	17	0.07	0.713
Japan	Tappi	19	0.07	0.076	19	-0.01	0.520	19	0.06	0.225
Japan	Sado-seki	20	0.12	0.026	20	0.00	0.756	20	0.12	0.036
Japan	Happo	20	-0.02	0.813	20	-0.11	0.003	20	-0.09	0.402
Japan	Ijira	20	0.01	0.782	20	0.00	0.000	20	0.01	0.782
Japan	Oki	20	0.19	0.002	20	0.10	0.001	20	0.28	0.000
Japan	Banryu	19	0.19	0.066	19	0.02	0.481	19	0.21	0.044
Japan	Yusuhara	20	-0.06	0.631	20	-0.06	0.275	20	-0.09	0.505
Japan	Hedo	20	0.12	0.148	20	-0.02	0.594	20	0.09	0.280
Japan	Ogasawara	20	0.32	0.014	20	0.02	0.601	20	0.32	0.017
Japan	Tokyo	13	0.16	0.492	13	0.06	0.449	13	0.18	0.475
Lao P.D.R.	Vientiane	6	3.55	0.377	6	-5.86	0.149	5	-2.91	0.609
Malaysia	Petaling Jaya	19	2.26	0.015	19	2.17	0.005	19	2.61	0.004
Malaysia	Tanah Rata	19	1.93	0.039	19	1.68	0.037	19	1.77	0.050
Malaysia	Danum Valley	14	0.53	0.403	14	0.29	0.511	14	0.82	0.184
Malaysia	Kuching	11	-1.76	0.062	11	-0.84	0.149	11	-2.06	0.066
Mongolia	Ulanbaatar	15	0.52	0.606	17	-1.31	0.022	15	0.33	0.729
Mongolia	Terelj	15	0.16	0.844	16	-3.14	0.000	14	-0.27	0.744
Myanmar	Yangon	10	-3.71	0.066	11	-4.48	0.046	8	-3.84	0.096
Philippines	Metro Manila	17	-1.06	0.470	17	0.16	0.872	17	-0.90	0.516
Philippines	Los Baños	16	-0.39	0.821	16	0.56	0.674	14	-2.48	0.235
Philippines	Mt. Sto. Tomas	10	-9.98	0.000	11	1.42	0.087	10	-8.87	0.001
R of Korea	Kanghwa	19	0.56	0.390	19	-0.52	0.331	19	0.39	0.633
R of Korea	Cheju	19	1.69	0.004	19	0.08	0.853	19	1.63	0.018
R of Korea	Imsil	18	1.64	0.013	18	0.39	0.518	18	1.82	0.036
Russia	Mondy	20	0.08	0.546	20	0.00	0.000	20	0.08	0.546
Russia	Listvyanka	20	-0.05	0.469	20	-0.05	0.419	20	-0.07	0.382
Russia	Irkutsk	20	0.01	0.925	20	-0.04	0.128	20	0.01	0.935
Russia	Primorskaya	18	0.11	0.735	18	0.09	0.022	18	0.11	0.735

Increasing (improving) (significance level of5%)

Decreasing (worsening) (significance level of5%)

Table 2.4.1. Results of trend evaluation for wet deposition data with good R_1 and R_2 criteria at EANET sites for 2000-2019. (continued)

Country	Name of Sites	Years for R_1	R_1 %/year	R_1 conf	Years for R_2	R_2 %/year	R_2 conf	Years for R_1&R_2	R_1&R_2 %/year	R_1&R_2 conf
Thailand	Bangkok	19	-1.77	0.000	20	0.18	0.736	19	-1.41	0.003
Thailand	Samutprakarn	16	-2.58	0.002	17	0.45	0.390	16	-2.15	0.007
Thailand	Pathumthani	20	-0.94	0.023	20	-0.05	0.860	20	-0.70	0.069
Thailand	Khanchanaburi	19	0.13	0.832	20	-0.40	0.470	19	-0.90	0.112
Thailand	Mae Hia	19	0.12	0.831	19	1.58	0.010	18	0.02	0.972
Thailand	Sakaerat	13	-0.76	0.624	14	-4.47	0.022	12	0.69	0.607
Vietnam	Hanoi	20	-1.60	0.025	20	-0.01	0.558	20	-1.60	0.025
Vietnam	Hoa Binh	20	-0.65	0.227	20	-0.03	0.201	20	-0.65	0.227
Vietnam	Cuc Phuong	11	0.15	0.436	11	0.72	0.066	11	0.87	0.076
Vietnam	Da Nang	11	0.34	0.233	11	-0.39	0.862	11	-0.05	0.982
Vietnam	Can Tho	6	14.59	0.047	6	5.45	0.015	6	15.60	0.035
Vietnam	Ho Chi Minh	6	3.95	0.349	6	1.38	0.075	6	4.56	0.272
Vietnam	Yen Bai	5	2.55	0.252	5	0.00	0.000	5	2.55	0.252

Increasing (improving) (significance level of5%) Decreasing (worsening) (significance level of5%)

The examples of tendencies in submitted data within allowable criteria are presented in Figure 2.4.2. The statistical significance of the trends are marked in the Table 2.4.1 with the color. However, for some stations with higher percentage of data satisfied to R_1 and R_2 criteria the trends are not significant and could not characterized well the progress of performance.

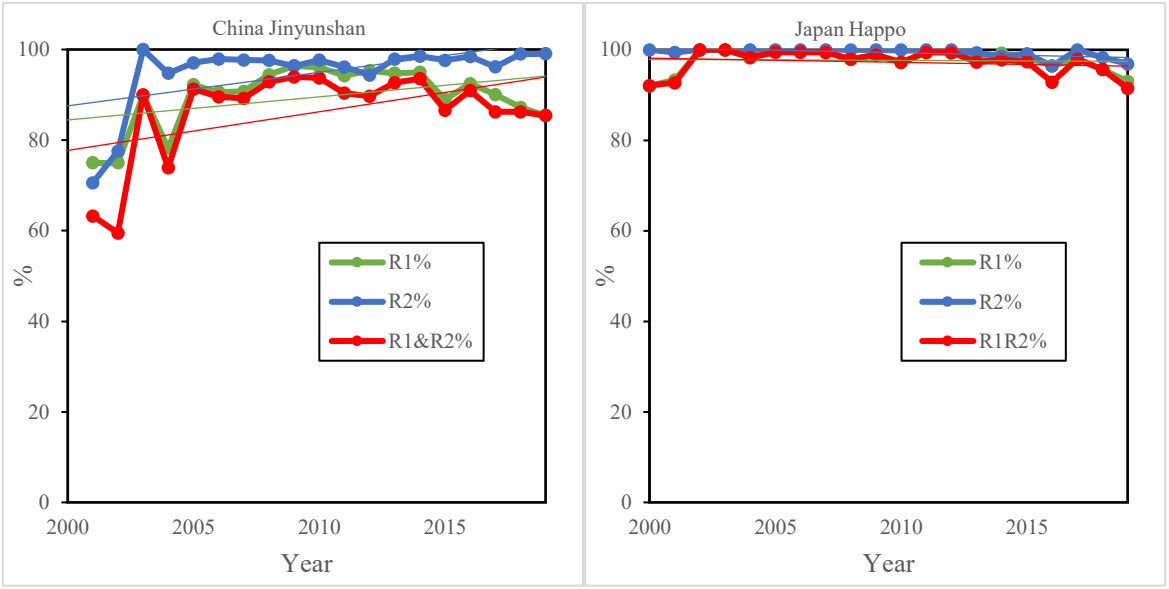

Figure 2.4.2. Percentage and trends of annually submitted data of some sites with R_1 and R_2 within allowable ranges for 2000-2019.

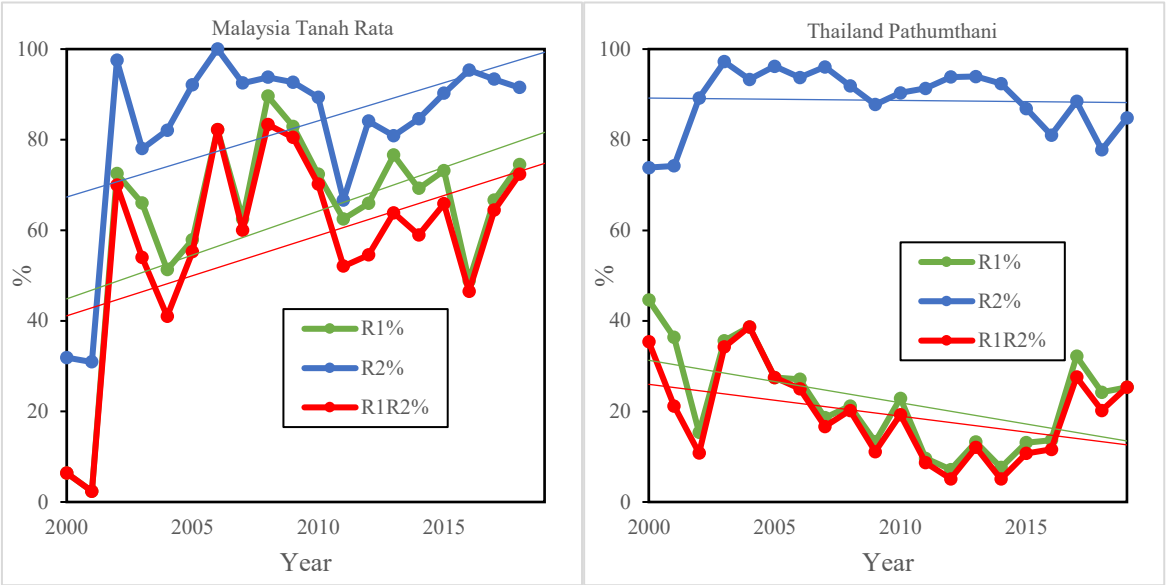

Figure 2.4.2. Percentage and trends of annually submitted data of some sites with R_1 and R_2 within allowable ranges for 2000-2019 (continued).

2.4.3 Data completeness

Data Completeness is one of the data quality indicators when measurement data are summarized statistically in monthly, seasonally or annual periods. If large amounts of data are missing or regarded as invalid during the summary period, the summarized statistics (e.g., the mean, median, maximum and minimum values) can be highly misleading. Therefore, periodic reporting of summarized data should be based on the full operation measurements without any missing data, which would be actually inevitable in the long-term regional monitoring network activities.

For the wet deposition monitoring, two Data Quality Objectives (DQOs) for data completeness are described in Technical Manual for Wet Deposition Monitoring in East Asia -2010, namely, Percent Precipitation Coverage Length (%PCL) and Percent Total Precipitation (%TP). %PCL is the percent of the summary period for which information on whether or not precipitation occurred is available. %TP is the percent of the total precipitation data measured during the summary period that is associated with valid samples. The requirement to be fulfilled in data is determined by the DQOs of %PCL and %TP are more than 80% (Technical Manual, 2010).

For the dry deposition (air concentration) monitoring, the data completeness should be evaluated in terms of the flagged or invalid data for automatic monitoring and the filter pack and other manual method. Data completeness describes the fraction of valid data coverage length in a certain monitoring period. The definition of data completeness is expressed as follows;

(Data completeness for automatic monitor)
= (Number of valid hourly data) / (Number of total measured hourly data)
(Data completeness for filter pack and other manual methods)
= (Number of valid measurement days) / (Number of total measurement days)

In order to evaluate monthly and annual air concentrations and monthly and annual dry deposition fluxes, the data completeness should be no less than 70%.

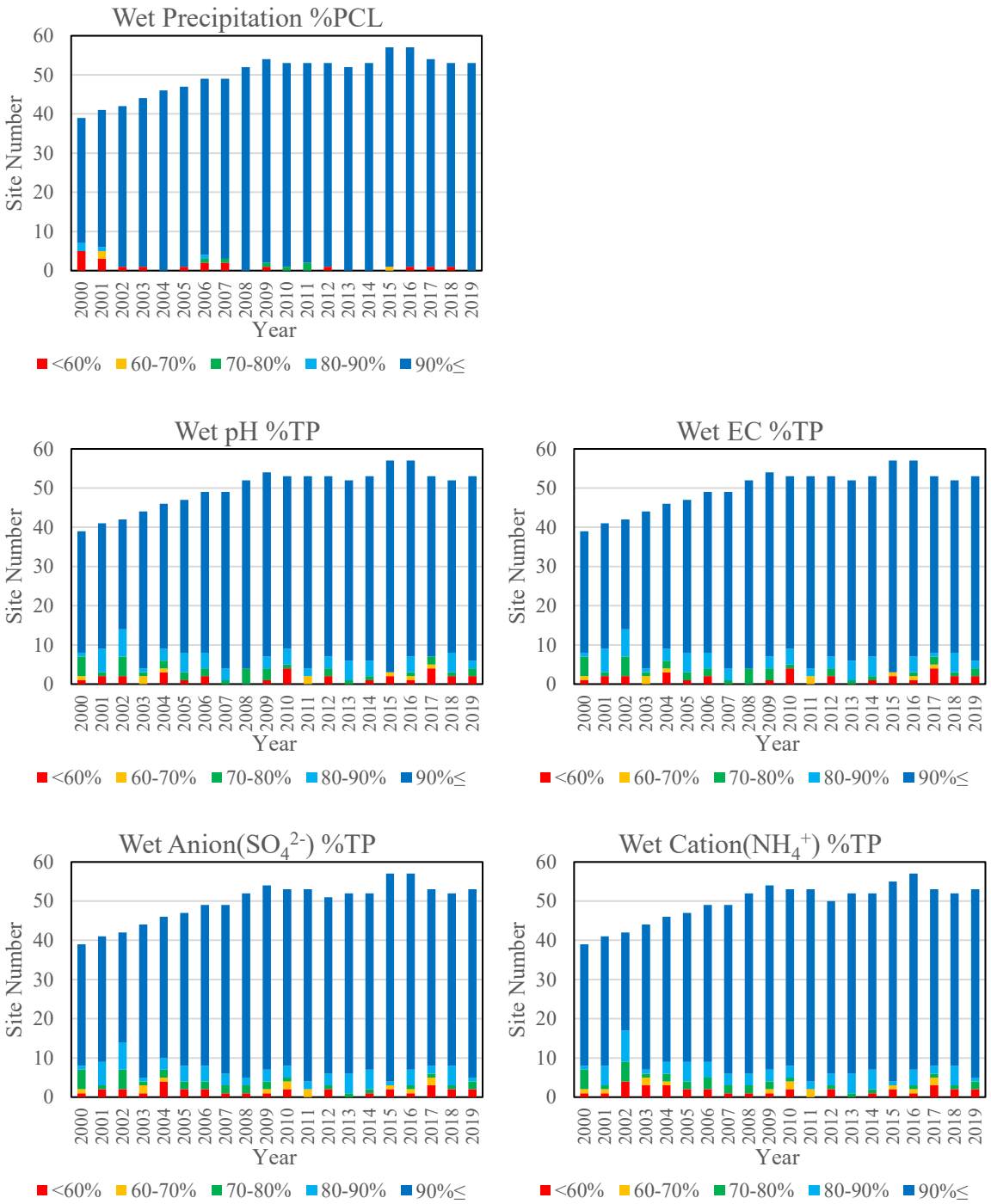

Figure 2.4.3. Annual variations of %PCL for precipitation and %TP for pH, EC, SO_4^{2-} and NH_4^+ in precipitation from 2000 to 2019.

Figure 2.4.3 shows annual variations of %PCL for precipitation and %TP for pH, EC and selected ions in precipitation from 2000 to 2019. The number of the sites in which %PCL for precipitation satisfies the DQO shows the increasing trend over 20 years.

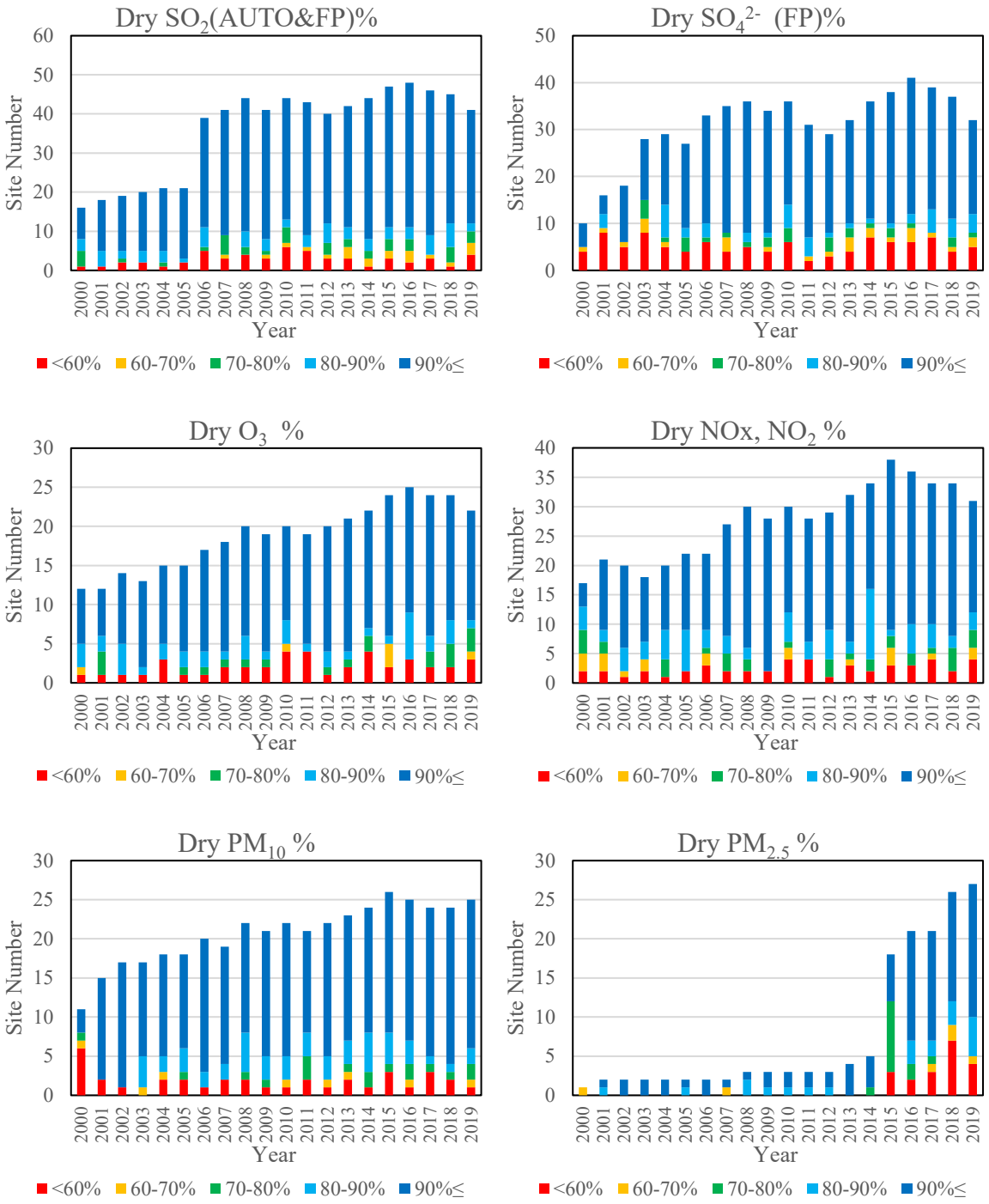

Figure 2.4.4. Annual variations of data completeness for SO_2 (measured by automatic monitor and filter-pack), particulate SO_4^{2-}, O_3, NOx/NO_2, PM_{10} and $PM_{2.5}$ from 2000 to 2019.

Figure 2.4.4 shows annual variations of data completeness for SO_2, particulate SO_4^{2-}, O_3, NOx/NO_2, PM_{10} and $PM_{2.5}$ from 2000 to 2019. In the beginning period, the number of monitoring stations was lower, and the data completeness was lower than the DQO at many stations. More than 80% of the sites satisfied the DQO of data completeness after 2005 except NOx/NO_2 in 2006, O_3 in 2010 and 2011, particulate SO_4^{2-} in 2013 and 2014, respectively.

The major reasons of long-term missing data and nonattainment of the DQOs are power failure at the site due to lightning damage or unstable power supply, failure of the sampling inlet, malfunction

of monitoring equipment due to deterioration over time or severe meteorological conditions, lack of financial and technical resources to repair the instruments, and so on. In order to improve data completeness, the alternative instruments for replacing the failed instruments should be kept in a laboratory, and lightning conductor, surge protector and/or uninterruptible power system (UPS) should be equipped in the station.

2.4.4 Site representativeness

The characteristics of the individual site were reported by the National Monitoring Plan of each EANET member country. It is important to consider the nature of the sites (e.g. urban, rural, remote, or ecological) for the evaluation of the monitoring data.

The specific features of EANET monitoring are to combine the measurements in different environmental media such as the atmosphere or surface water and more complicated soils or vegetation. The first ones are characterized by concentration levels of air or water pollutants while for latest we need also to take ecosystem peculiarities and their "annual life cycles" into account. The possible impact of anthropogenic sources (like emission, sludge discharge or land use) on level of pollution could be concerned during the site establishing. The environmental conditions have to be taken into account also in a view of possibility to trace ecosystem changes under influence of long range transport of air pollution.

EANET set up three categories for monitoring sites of atmospheric deposition presented in the Guidelines and Technical Manuals (ADORC, 2000b) with respect to the level of impact on surrounded area: urban, rural and remote stations. The site criteria define the distance of possible air pollution sources with different intensity, land use in the vicinity of different spatial scale, etc. The specific information are required and collected on site condition in accordance with formats of National Monitoring Plan for the surrounded areas in a distance to 150 m, 0.15-10 km and 10-50 km from place of measurements.

For the rural and remote sites the applied requirements were established based on the experience gained from activities of other networks in the world. These criteria specifications are closely correspondent to the similar requirements of well-operated monitoring networks such as EMEP or regional GAW-PC network (EMEP, 2001; WMO, 2004). However, mentioned networks are not concerned urban atmospheric pollution which became a serious problem in East Asian megacities and other big cities especially in tropics. Those kinds of measurements are particularly related to a number of national networks as well as to specific international initiatives directed to urban pollution.

Taking into account the differences in atmospheric processes and emission impact in urban and non-urban conditions and evaluation of regional pollution has to be done separately for mentioned areas. And the nature of the sites (e.g. urban, rural, remote, or ecological) was kept in mind for the analyses. The characteristics of the individual site were reported by answers on series of questions and photos from four or more directions. For the practical purposes, the brief overview of site conditions could be observed at EANET site (EANET, 2010a).

The site is evaluated from a perspective of available potential sources of sample contamination which could violate its representativeness of the area of interest on the three different spatial scales: on-site, local, and regional. Detailed examinations of the site by inspection and the related documents will evaluate the type of the site. Any changes of the site conditions on three different scales (on-site, local and regional) and relocation of the sampler may require a reevaluation of the type of the site (WMO, 2004).

The sites of fourth category have a focus on ecological monitoring of natural ecosystems which is also, might be referred to relevant conditions for the atmospheric deposition measurement. They are commonly stated as ecological sites being correspondent to one of these three mentioned above in

terms of the location conditions, but its focus of measurement programs is on the data acquisition of the input to the ecological elements of interest.

Guideline for Acid Deposition Monitoring in East Asia (ADORC, 2000b) recommended that ecological sites for soil and vegetation monitoring (basic survey program) and monitoring on inland aquatic environment have to be preferably established near the deposition monitoring sites or in their vicinity. In particular for soil and vegetation monitoring, more detailed criterion was proposed for the distance from the atmospheric deposition monitoring site as "within a radius of approximately 50 km". Moreover, it was suggested that two forest plots with different soil types be selected in each area within 50 km from the deposition site.

The current situation on co-location of basic survey sites for ecological monitoring and the nearest deposition monitoring sites was presented in Table 2.4.2. Soil and vegetation monitoring and monitoring on inland aquatic environment are conducted at 31 plots in 10 countries and 19 lakes/rivers in 11 countries, respectively. Most of ecological monitoring sites are corresponded to the deposition monitoring sites, however, their classification could be different.

Table 2.4.2 Basic survey sites for ecological monitoring and the nearest deposition sites

Country	Site for deposition monitoring	Plot for soil and vegetation monitoring	Site for monitoring on inland aquatic environment
Cambodia	-	-	Sras Srang Lake
China	Chongqing - Jinyunshan	Jinyunshan	Jinyunshan Lake
	Xi'an - Jiwozi	Dabagou	Jiwozi River
	Xiamen - Xiaoping	Xiaoping	Xiaoping Dam
	Zhuhai - Zhuxiandong	Zhuxiandong	Zhuxiandong Stream
Indonesia	Serpong	Bogor Research Forest (Dramaga Experimental Forest)	-
	Bandung	-	Patengang Lake
	-	-	Gunung Lake
Japan	Happo	Sekido-san*2	Futago-ike Lake*2
		Horyu-zan*2	
	Ijira	Ijira	Ijira Lake
		Yamato	
Lao PDR	Vientiane	-	Nam Hum Lake
Malaysia	Petaling Jaya	Pasoh Reserve Forest 1	Semenyih Dam
		Pasoh Reserve Forest 2	
	-	UPMKB Rehabilitated Forest Planted in 1991	
		UPMKB Rehabilitated Forest Planted in 2008	
	Danum Valley	-	Tembaling River
Mongolia	Ulaanbaatar	Bogdkhan Mountain	-
	Terelj	Terelj Mountain	Terelj River
Philippines	Metro Manila	La Mesa Watershed	
	Los Baños	Mt. Makiling	Pandin Lake
		UP Quezon, Land Grant	
	Mt. Sto Tomas	Boneco Long Term Ecological Research Site	Ambulalakaw Lake

Table 2.4.2 Basic survey sites for ecological monitoring and the nearest deposition sites (continued)

Country	Site for deposition monitoring	Plot for soil and vegetation monitoring	Site for monitoring on inland aquatic environment
Cambodia	-	-	Sras Srang Lake
Republic of Korea	Imsil	Mt. Naejang	-
Russia	Irkutsk	Irkutsk	-
	Listvyanka	Bolshie Koty	
		Pereemnaya river catchment	Pereemnaya River
	Mondy	Ilchir Lake	-
		Okinskoe Lake	
		Solar Observatory	
	Primorskaya	Primorskaya	Komarovka River
Thailand	Khanchanaburi (Vajiralongkorn Dam)	Vajiralongkorn Dam	Vajiralongkorn Dam
		Vajiralongkorn Puye	
Vietnam	Hoa Binh	Cave of Heaven	Hoa Binh Reservoir
		Thang Ranh	

However, the conventional monitoring system seems could not provide evident information on implication between the ecological and deposition data. Monitoring activities for ecosystems and atmospheric impact should be integrated more for discussion on both quantitative and qualitative relations. Catchment-scale monitoring may be one of approaches for this further investigation including some modeling. As shown in the Table 2.4.3, Catchment-scale monitoring has implemented currently in Japan and the Philippines. Japan submitted the data of the Lake Ijira Catchment, which was started in 2007. Moreover, the Philippines has just started the regular monitoring in 2019. Based on the catchment-scale dataset, the simulation model on biogeochemistry cycle is expected to be developed in near future.

Table 2.4.3 Site for catchment-scale monitoring

Country	Site for acid deposition monitoring	Site for catchment-scale monitoring
Japan	Ijira	Lake Ijira catchment
Philippines	Metro Manila	La Messa Watershed

2.4.5 Overall data quality

Evaluation of the datasets from the four viewpoints mentioned above would have ensured that a large fraction of the measurements in the early stage are acceptable, and recent datasets are improved in the data quality.

2.5 Conclusions and recommendations

Throughout the implementation of ILC project, the submitted data was evaluated by using the prepared values which was specified by the NC. Using this prepared value, the bias was observed on the statistic data. The possible likelihood value which should be used for the evaluation can be the

median of all of the compiled data.

The National Monitoring Plan (NMP) of each participating country was prepared after starting formal phase. The NMP should be reviewed every year and revised if necessary. The NC is now difficult to grasp current situation of the participating countries because of being kept the NMP unchanged. When there is a revision in the monitoring activity, the NMP shall be revised immediately and should be submitted to the NC.

The Technical Mission has been conducted as one of the additional activities of EANET. And it could be effective to build the acid deposition monitoring capacity in the participating countries. The potential problems in the laboratories in charge of the EANET monitoring in the participating countries may not be able to be stimulated to maintain and to improve their abilities and their data quality. Even in the laboratories which have been already regarded as high potential, there might be unrevealed problem. It may be significant to reconsider the modality of the Technical Mission.

Items for the improvement of the quality of monitoring data in EANET are considered as listed below:

1) Selection of the monitoring sites;
   The site selection should be done in accordance with the technical manuals. All of the site shall be prepared their regional scale, local scale and on-site scale descriptions. And the sites shall represent the circumstances around the site in each classified region, such as remote, rural or urban sites. The existing monitoring sites should be reviewed their suitability to the requirements.
2) Establishment of the common point of view to the methodology including sampling and measurement;
3) Implementation of the ILC project;
4) Implementation of the technical mission;
5) Establishment of quality management, and;
6) Reporting of the monitoring data.

2.6 References

ADORC. 2000b. Technical Documents for Acid Deposition Monitoring in East Asia 2000. The Second Interim Scientific Advisory Group Meeting of Acid Deposition Monitoring Network in East Asia adopted in March 2000, Guidelines for Acid Deposition Monitoring in East Asia, Technical Documents for Wet Deposition Monitoring in East Asia including, Technical Manual for Wet Deposition Monitoring in East Asia, Quality Assurance / Quality Control (QA/QC) Program for Wet Deposition Monitoring in East Asia, Technical Manuals for Soil and Vegetation Monitoring in East Asia, and Technical Documents for Monitoring on Inland Aquatic Environment in East Asia including Technical Manuals for Monitoring on Inland Aquatic Environment in East Asia and Quality Assurance / Quality Control (QA/QC) Program for Monitoring on Inland Aquatic Environment in East Asia. Niigata, Japan.

EANET. 2010a. EANET site information, http://www.eanet.cc/site/index.html.

EANET. 2010. Technical Manual for Wet Deposition Monitoring in East Asia. Niigata, Japan.

EANET. 2013. Technical Manual for Air Concentration Monitoring in East Asia. Niigata, Japan.

EANET. 2016. Quality Assurance / Quality Control (QA/QC) Guidebook for Acid Deposition Monitoring Network in East Asia - 2016, Niigata, Japan.

EANET. 2020. Report of the Inter-Laboratory Comparison Projects of 2019, Niigata, Japan.

EANET. 2020. Data Report 2019. Niigata, Japan.

EMEP. 2001. EMEP manual for sampling and chemical analysis. NILU EMEP/CCC-Report 1/95, Kjeller, Norway, rev. November 2001 (current update at http://www.nilu.no/projects/ccc/manual/index.html).

EMEP. 2009. EMEP monitoring strategy and measurement programme 2010-2019. Geneva, ECE/EB.AIR/GE.1/2009/15.

NIVA. 2011. Intercomparison 1125: pH, Conductivity, Alkalinity, NO_3-N, Cl, SO_4, Ca, Mg, Na, K, TOC, Al, Fe, Mn, Cd, Pb, Cu, Ni, and Zn. UN ECE International Cooperative Programme on Assessment and Monitoring of Acidification of Rivers and Lakes (ICP-Waters) Report 107/2011.

WDCPC. 2011. Quality Assurance/Science Activity Centre – Americas (QA/SAC-Americas): Ring Diagrams Overview, http://qasac-americas.org/ringdiagram.

WMO. 2004. Manual for the GAW Precipitation Chemistry Programme. Guidelines, Data Quality Objectives and Standard Operating Procedures. Ed. M. A. Allan. Geneva, WMO-GAW Report 160, WMO-TD No 1251.

3. Wet and Dry Deposition of Acidic Substances in East Asia

3.1 Introduction

When a chemical species is emitted into the atmosphere, it will undergo a series of processes, including transportation, transformation, and deposition into the earth's surface. In these processes, a complex chain of physical and chemical process and reactions take place, resulting in the deposition of the species to the earth's surface. Naturally, the deposition of chemical species to the earth's surface is an input to another complex processes that take place in land and aquatic environments. The deposited chemical species will impact both of the environment, and human health and crop productivity. This is particular truth for the deposition of acidic substances from the atmosphere to the earth's surface. The atmospheric deposition of acidic substances to the earth surface is categorized into two forms, namely wet deposition and dry deposition. Wet deposition happens when the sulfuric and nitric acids formed in the atmosphere fall to the ground mixed with rain, snow, fog, or hail. This is what we usually think of acid rain. Dry deposition is the deposition of acidic particles and gases from the atmosphere in the absence of moisture.

Under EANET framework, there are currently 61 wet deposition monitoring sites and 54 dry deposition monitoring sites located in 13 EANET member countries including Cambodia, China, Indonesia, Japan, Lao P.D.R, Malaysia, Mongolia, Myanmar, Philippines, Republic of Korea, Russia, Thailand, and Vietnam. In accordance with EANET criteria, the monitoring sites are categorized into three types: urban, rural, and remote. Sampling techniques, sample storage and analysis, and data processing and QA/QC procedures of all monitoring sites and laboratories participating in EANET are conducted according to EANET's guidelines.

This Chapter describes the status and trend of acid deposition (both wet deposition and dry deposition) in East Asia in the past 20 years (2000-2019) based on data analysis results obtained from 115 acid deposition monitoring stations installed in 13 EANET member countries. The Chapter is structured into 7 sections and References. Section 1 is Introduction. Section 2 presents details about methodologies for sampling, sample storage, sample analysis and QA/QC aggregation for both wet deposition and dry deposition. Section 3 discusses about air pollutants and their chemical reaction in the atmosphere and chemical composition of precipitation in East Asia in the past 20 years. Section 4 presents an analysis and discussion about spatial and temporal distribution of wet deposition in East Asia. A comparison of wet deposition among EANET, US and Europe was made. The section also discusses trends of wet deposition in some regions of EANET countries. Section 5 presents methodologies employed for assessing dry deposition in EANET. Section 6 presents an analysis and discussion about spatial and temporal variation of total deposition (wet and dry deposition) observed in EANET countries during the period from 2000 - 2019. Trends of annual amounts of total S deposition, total N deposition, total N deposition by oxidized N and reduced N, both wet and dry depositions, at remote, rural and urban sites were presented and analyzed. Final section, section 7 is the conclusion of this Chapter.

3.2 Methodology for sample collection and analysis

3.2.1 Wet deposition

Monitoring sites

The number of the wet deposition monitoring site is 61 in 2019 (Cambodia: 1, China: 10, Indonesia: 7, Japan: 12, Lao P.D.R: 1, Malaysia: 4, Mongolia: 2, Myanmar: 1, Philippines: 3, Republic of Korea: 3, Russia: 4, Thailand: 6, Vietnam: 7), which represent 52%-increase from 2000 (Figure 3.2.1). The monitoring site is classified into three categories (urban, rural, and remote) followed by the EANET

monitoring site criteria. Urban site is located at least 500 m far from the main road to estimate the comprehensive air pollution in the residential or industrial region. The rural site is at least 20 km far from the major emission source such as the highway and industrial area to estimate the effect on the agricultural and forestry products and ecosystem from the wet deposition. The remote site is located at least 50 km far from the major emission source to estimate the long-range transport of the air pollution. There are 21 urban sites, 19 rural sites, and 21 remote sites in EANET.

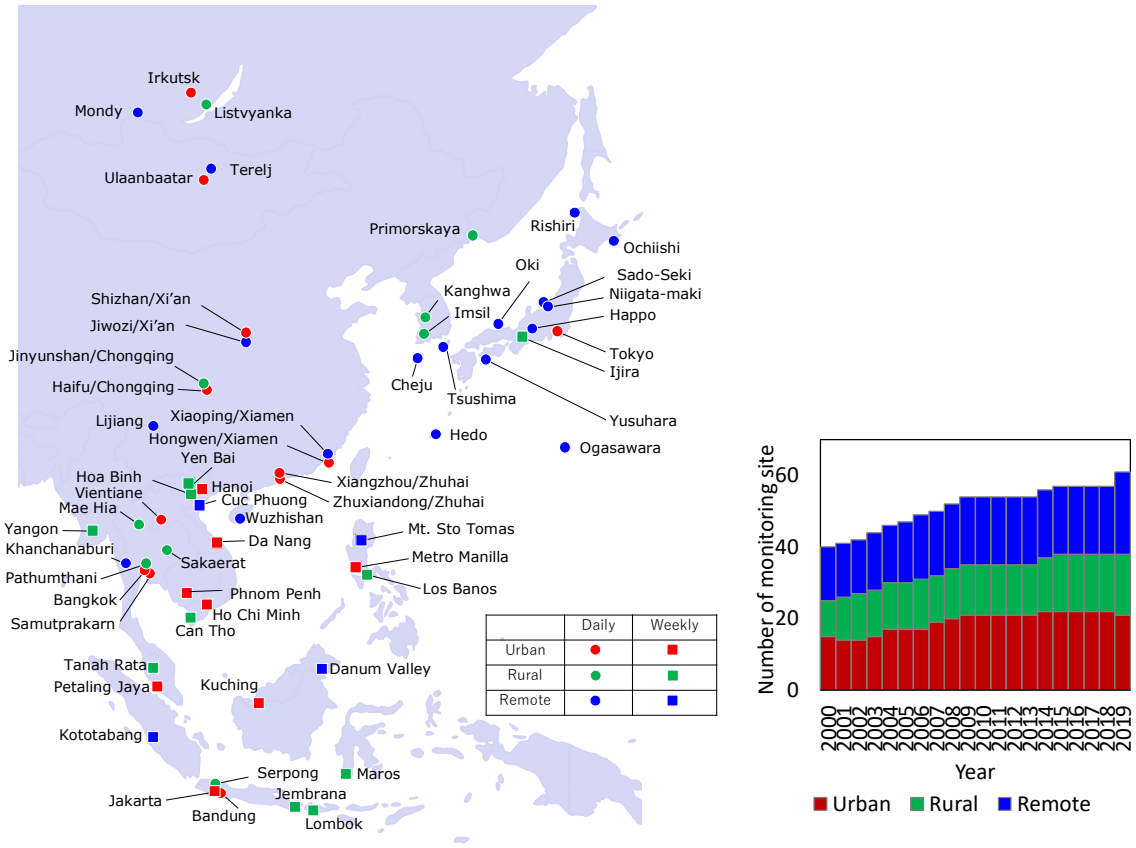

Figure 3.2.1. Location and number of wet deposition monitoring sites in EANET (2019).

Sample collection and analysis

Rain or snow samples should be collected by the wet only sampler which has the collecting funnel with the heater if necessary, lid, precipitation sensor, and sample container with the refrigerator. The lid of the wet only sampler should be opened automatically if the precipitation sensor detects the rainfall. It should be closed at the end of the precipitation event to avoid the contamination of the dry deposition. The sampling frequency is daily, weekly, or every precipitation event (in the past period) which is dependent on the climate in the participating countries.

The sample should be transported to the laboratory immediately and the following items should be measured; the precipitation amount, electric conductivity (EC), pH, ion concentrations (SO_4^{2-}, NO_3^-, Cl^-, NH_4^+, Na^+, K^+, Ca^{2+}, Mg^{2+} if possible, F^-, NO_2^-, PO_4^{3-}, HCO_3^-, etc.). The precipitation amount is obtained by the rain gauge or caliculated from the sample amount. EC is obtained by the conductivity cell. pH is obtained by the pH meter with the glass electrode. Ion concentrations are usually obtained by the ion chromatography, Atomic absorption/emission spectrometry and spectrophotometry.

QA/QC aggregation

The analytical results were confirmed by the personnel in charge of the laboratory as well as the QA/QC manager in the EANET participating countries. Data check or validation is conducted by the following procedure; the ion balance in precipitation samples, the conductivity balance between the measured EC and calculated EC using the ion concentration, the comparison with the data in the previous measurement, the relation between chemical components in air and precipitation.

The data completeness should be considered from the confirmation of Percent Precipitation Coverage Length (%PCL) and Percent Total Precipitation (%TP). %PCL is defined as the percent of the summary period for which information on whether or not precipitation occurred in available. If precipitation is known to have occurred during the particular sampling period but no measurement of the amount is available, then no knowledge of precipitation is assumed. %TP means the percent of the total precipitation data measured during the summary period that is associated with valid samples. Both %PCL and %TP should be no less than 80%. The detailed description of methodology is shown in the Technical Manual for Wet Deposition Monitoring in East Asia -2010 (https://www.eanet.asia/wp-content/uploads/2019/04/techwet.pdf).

3.2.2 Dry deposition

Air concentration (dry deposition) monitoring sites are expected to monitor the parameters of sulfur and nitrogen compounds associated with acid deposition problems, PM and O_3 associated with air quality issues, meteorological parameters associated with local meteorology and estimation of dry deposition flux. For evaluation of dry deposition, the sampling period of air concentrations could be longer than one day to one or two weeks. This monitoring might employ either of real-time monitors or integrating manual samplers (filter packs, denuders, or passive samplers, as may be determined appropriate). So far, there are 54 monitoring sites of dry deposition in EANET including 41 sites using filter pack method, 34 sites using automatic method and 6 sites using passive sampler method in 2019. The location of dry deposition monitoring sites is shown in the Fig 3.2.2. The number of wet/dry monitoring sites in ENAET is increasing in the past 20 years.

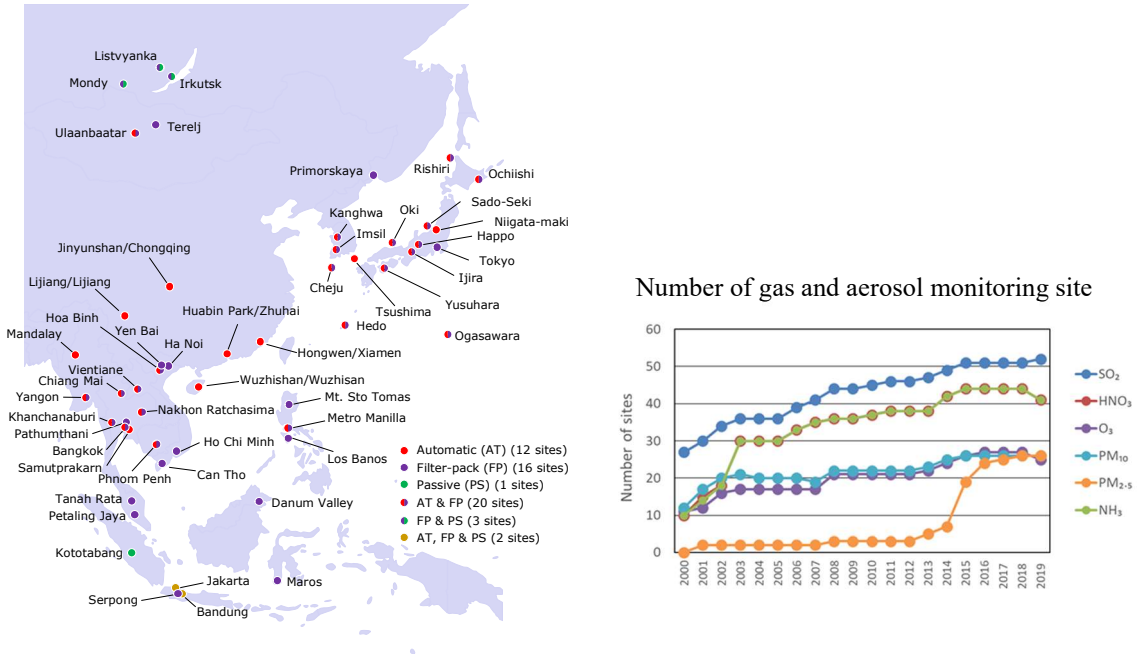

Figure 3.2.2. Location and number of dry deposition monitoring sites in EANET (2019).

Hourly data are required where diurnal cycles in deposition velocity are to be explicitly monitored. The pulsed fluorescence method is used for SO_2 measurements. Oxides of nitrogen, NOx, and nitric oxide, NO, are measured either by dual-channel or single-channel analyzers using the gas-phase

chemiluminescence method or differential optical absorption spectroscopy method. Ozone is measured by ultraviolet photometric method. PM_{10} and $PM_{2.5}$ are measured by β-ray absorption method or tapered element oscillating microbalance method. These one-hour averaged values can also be used for the purpose of the evaluation of dry deposition after averaging over longer periods.

The four-stage filter pack can measure both of the concentration of chemical species in particulate matter and gaseous compounds. Aerosols are collected on the first filter (F0: made of PTFE, Polytetrafluoroethylene), while the gaseous substances such as SO_2, HNO_3, HCl, NH_3 will pass though this filter. The second filter (F1: made of polyamide) collects all HNO_3 and partial SO_2, HCl and NH_3 from the sampling air. The remaining SO_2 and HCl react with alkali substance on the third filter (F2: made of cellulose). Oxidizing species in air such as ozone are believed to convert most of the sulfite to sulfate during the sampling. The remaining NH_3 reacts with acid substance on the fourth filter (F3: made of cellulose) after passing through the first, second and third filters. Ammonia is effectively retained on a filter impregnated with phosphoric, citric or oxalic acid.

A passive sampler is a very simple device consisting of an impregnated filter or molecular sieve which preferentially sorbs the gas to be analyzed, and a diffusion barrier (usually an entrapped air volume) that keeps the sampling rate constant. If the sampling efficiency is sufficiently high, then the sampling rate can be calculated using the Fick's first law of diffusion from the cross-sectional area perpendicular to the transport direction and the distance that the gas has to diffuse. Passive samplers provide a simple and cost-effective way of monitoring specific species at urban, regional and global scales, and offer broad capacity building opportunities. Passive samplers have been utilized in the network for the monitoring of ozone, SO_2, NO_2, and NH_3.

Typical data check procedures include routine data check, confirmation of measured data, and data screening. Records of the old data can be used to create simple statistics including percentiles, mean values and standard deviations. The statistical tests are comparisons between new measurement and calculated results and data already stored in the database. The tests are carried out to identify possible outliers. In some cases, respective air concentrations and calculated dry deposition fluxes may be compared with earlier data using the lognormal distribution. For manual monitoring method the precision test can be determined as relative standard deviation of duplicated measurement using blank filter or standard filter. Relations between various chemical components (including ion balance (R_1) of particulate matter components), relationship between sea salt components, and relationship between air concentrations from neighboring stations and time-series plots are also useful. In order to evaluate monthly and annual air concentrations and monthly and annual dry deposition fluxes, the data completeness should be no less than 70%. The detailed description of methodology is shown in the Technical Manual for Air Concentration Monitoring in East Asia (https://www.eanet.asia/wp-content/uploads/2019/04/techacm.pdf).

3.3. Precipitation chemistry in East Asia

3.3.1 Introduction

The process by which atmospheric substances are deposited on the earth’s surface together with moisture such as rain and fog is called wet deposition. Sulfur and nitrogen oxides released into the atmosphere due to the combustion of fossil fuels are converted into acids by gas or liquid phase reaction after being taken up by cloud water or precipitation. Some of the generated acid are neutralized by atmospheric ammonia gas and basic calcium aerosols. In addition, some of the acids produced in the gas phase reaction or particles produced by the reaction of them with basic compounds in the atmosphere are involved in cloud formation as condensation nuclei. In this process, acids and salts present in the atmosphere are deposited on the ground surface due to meteorological phenomena such as rain, snow, fog, dew, and frost. On the other hand, the deposition of air pollutants without precipitation is called dry deposition. The amount of wet deposition is calculated from the

precipitation amount and concentration of components collected by the open-type device during precipitation, while the amount of dry deposition is calculated as the product of the concentration of gas and particles in the atmosphere and the deposition velocity estimated from meteorological data.

3.3.2 Air pollutants and their reactions in the atmosphere

There are various substances in the atmosphere, but the main substances that are taken up by precipitation and involved in the acidification are (1) sulfur dioxide and nitrogen oxides derived from human activity, (2) sulfur compounds derived from volcanic activity and the reduction of marine sulfate, nitrogen compounds such as nitrogen oxides derived from forest fires, (3) acids generated in the atmosphere using them as precursors, (4) ammonia gas derived from agricultural activities, etc., (5) basic calcium particles contained in yellow sands, (6) hydrogen chloride derived from volcanic and human activities. Sea salt particles are also important substances for evaluating the balance of acids and bases in precipitation. The most important reactions of various compounds present in the atmosphere related to acid deposition are the following gas and liquid phase reactions of sulfur dioxide and nitrogen oxides (Hara et al., 1995).

(a) Gas phase reaction

OH radical plays an important role in gas phase reactions. The OH radical reacts 1:1 with SO_2 and NO_2.

$$SO_2 + OH + M \rightarrow HOSO_2 \quad (1)$$
$$HOSO_2 + O_2 \rightarrow SO_3 + HO_2 \quad (2)$$
$$SO_3 + H_2O \rightarrow H_2SO_4 \quad (3)$$
$$HO_2 + NO \rightarrow OH + NO_2 \quad (4)$$

OH radical is regenerated in (4) and SO_2 is oxidized by a chain reaction.

$$NO_2 + OH \rightarrow HNO_3 \quad (5)$$
$$NO_2 + O_3 \rightarrow NO_3 + O_2 \quad (6)$$
$$NO_2 + NO_3 \Leftrightarrow N_2O_5 \quad (7)$$
$$N_2O_5 + H_2O \rightarrow 2HNO_3 \quad (8)$$

For the oxidation of SO_2 and NO_2, the reactions of Eqs. (1) and (5) are rate-determining, respectively, and the rate constant of SO_2 is an order of magnitude smaller than that of NO_2. Therefore, NO_2 is oxidized 10 times faster than SO_2. In other words, the lifetime of NO_2 is much shorter than that of SO_2, and it is considered that the oxidation of NO_2 to nitric acid is completed closer to the source, comparing with the oxidation of SO_2 to sulfuric acid. Equation (7) is an equilibrium reaction.

(b) Liquid phase reaction

Only sulfuric acid is produced in the liquid phase reaction. SO_2 is efficiently oxidized by H_2O_2 and O_3 dissolved in the liquid phase from the atmosphere.

$$SO_2 + H_2O \rightarrow SO_2 \cdot H_2O \rightarrow HSO_3^- + H^+ \rightarrow SO_3^{2-} + 2H^+ \quad (9)$$
$$HSO_3^- + H_2O_2 \rightarrow SO_4^{2-} + H^+ + H_2O \quad (10)$$
$$SO_3^{2-} + O_3 \rightarrow SO_4^{2-} + O_2 \quad (11)$$

H_2O_2 is generated by the reaction of two HO_2 radicals ($2HO_2 \rightarrow H_2O_2 + O_2$). In addition, O_3 is a major oxidizing substance in the atmosphere together with H_2O_2, and is produced by a photochemical reaction of NO_2, and the reaction is promoted in the presence of VOC.

Some of the acids produced by the gas or liquid phase reaction are neutralized by basic compounds such as ammonia gas and basic calcium aerosols in the atmosphere.

The compounds produced by the above reactions or their precursors are deposited on the ground surface with precipitation. In general, the process by which precipitation away from clouds dissolves substances in the atmosphere and deposits on the ground is called below cloud scavenging (Washout). In cloud scavenging (Rainout) is a case in which reaction products in the atmosphere are involved in cloud formation as condensation nuclei or are directly taken up by cloud water and deposited on the ground. When the former is the main process, the component concentration changes greatly in a precipitation event, and the concentration of the initial precipitation is high. In the latter case, the fluctuation in concentration is small (Ohizumi, 2009).

3.3.3 Chemical composition and acidity of precipitation

The term “Acid Rain” was based on pH 5.6, which is the acidity when carbon dioxide with a concentration of about 380 ppm is in equilibrium with pure water in the atmosphere. However, volcanic sulfur dioxide and hydrogen sulfide are present in the atmosphere. And there is also DMS (Dimethyl sulfide) in which sulfate ions in seawater are reduced by sulfate-reducing bacteria and released into the atmosphere. These sulfur compounds are oxidized to sulfuric acid in the atmosphere. These acids are present in the atmosphere even in the absence of anthropogenic acids, and basic substances in the atmosphere neutralize those acids in precipitation. Since the acidity of precipitation is determined by their balance, pH 5.6 cannot be said to be an appropriate index value for anthropogenic pollution against precipitation, and pH alone cannot evaluate pollution due to anthropogenic activities. In addition, when considering the acute effects of initial precipitation on plant leaves using the precipitation pH as an index, different conclusions can be obtained depending on whether the target is initial 1 mm precipitation or 0.1 mm precipitation. This indicates that when dealing with concentrations in the study of wet deposition, it is very important to standardize by considering precipitation.

3.3.4 Twenty year’s observation of precipitation chemistry in East Asia

Figure 3.3.1 shows the average precipitation composition for 20 years at each EANET observation site. At about half of the sites, cations (upper side) and anions (lower side) are balanced, and it can be confirmed that the nine components shown in the figure are the main ions at those sites. On the other hand, at other sites, the cation sum tends to be higher than the anion sum. This suggests the existence of unmeasured anions, most of which are thought to be due to bicarbonate ions, fluorine ions, and organic acids, and actual measurements of those ions have been reported from many sites. Therefore, determination of dissolved components have been performed without defects in EANET and the uncertainty of the measured value is considered to be small.

In addition, when unmeasured anions are not dissolved in precipitation, sum of non-sea-salt anions (nss-SO_4^{2-}, NO_3^-) and sum of non-sea-salt cations (H^+, NH_4^+, nss-Ca^{2+}) are balanced as shown in Listvyanka in the upper left corner in the Figure 3.3.1. These relation between anions and cations can be understood as a result of the neutralization of sulfuric and nitric acids produced by the gas-phase and liquid-phase reactions by basic ammonia gas and calcium particles. In other words, it can be confirmed from actual observation data that the acidity (H^+ concentration) of precipitation is determined by the balance of acids and bases dissolved in precipitation.

From the figure 3.3.1, large averaged annual precipitation amounts are identified in Mt. Sto. Tomas (4570mm), Kuching (4319mm), and Petaling Jaya (3356mm), respectively. Small averaged annual precipitation amounts are observed in Ulaanbaatar (162mm), Terelj (166mm), and Mondy (239mm). Low pHs are reported in Petaling Jaya (4.34, urban), Jinyunshan (4.40, rural), and Haifu (4.55, urban) in average. On the other hands, high averaged pHs are observed in Yangon (6.51, urban), Jiwozi (6.10, remote), and Phnom Penh (6.09, urban), respectively.

Figure 3.3.2 shows the correlation between the pAi (Ai, input acidity, pAi = -log (nss-SO_4^{2-} + NO_3^-)/[μeq/L], Hara et. al., 1995) which in acidity calculated from the acid concentrations dissolved in precipitation and the precipitation pH observed by EANET. The figure placed in the center shows the correlation between the acid concentration sum (horizontal axis, nss-SO_4^{2-} + NO_3^-) and base concentration sum (vertical axis, NH_4^+ + nss-Ca^{2+}). At the site where the base concentration sum is lower than the acid concentration sum, it is highly possible that the pH is low. From the average composition of precipitation over 20 years, the sites in which the acid concentration sum is higher than the base concentration sum are Haifu, Jinyunshan, Hongwen, Guanyinqiao, and Xiaoping, Jakarta, Bandung, and Serpong, Kanghwa, Imsil, and Cheju, Listvyanka and Primorskaya, Petaling Jaya, Tanah Rata, Danum Valley, and Kuching, and all 12 sites in Japan. In other countries, in Vietnam and Malaysia, there were some sites in which the acid concentrations sum is almost equal to the base concentration sum.

Figure 3.3.2 also shows the annual correlation between pAi and precipitation pH at each site. pAi tended to be the lowest in Chinese EANET sites (<3.0), followed by Mongolian sites (≈3.0). On the other hand, pAi exceeds 5.0 in some sites of Thailand, Malaysia, Indonesia and Japan. In addition, the fluctuation range of precipitation pH is often wider than that of pAi, and it can be seen that the precipitation pH is influenced by the contribution of the basic components. On the other hand, Japan and Malaysia are characterized by the fact that the precipitation pH and pAi are distributed in a narrow range despite the large number of sites. This is considered to be because the amount of basic components taken into precipitation is small and their effect on precipitation pH is limited in both regions.

As described above, at the EANET sites where the concentration of acidic component tends to be higher than that of the basic component in annual basis, high acidity precipitation may be observed in monthly or daily basis. Table 3.3.1 summarizes the lowest pH value for each year from the observation data for 20 years. The lowest values were all observed at sites where the acid concentration sum was larger than the base concentration sum. And the lowest pH values are observed not only in urban sites but also in rural and remote sites from the latter half of the 2000s to the first half of the 2010s. This factor is considered to be due to the increase in the acid concentrations sum during the period, as shown later. In addition, it is believed that such data are acquired because EANET's wet deposition monitoring is performed with a high time resolution (daily) using a cooling storage device.

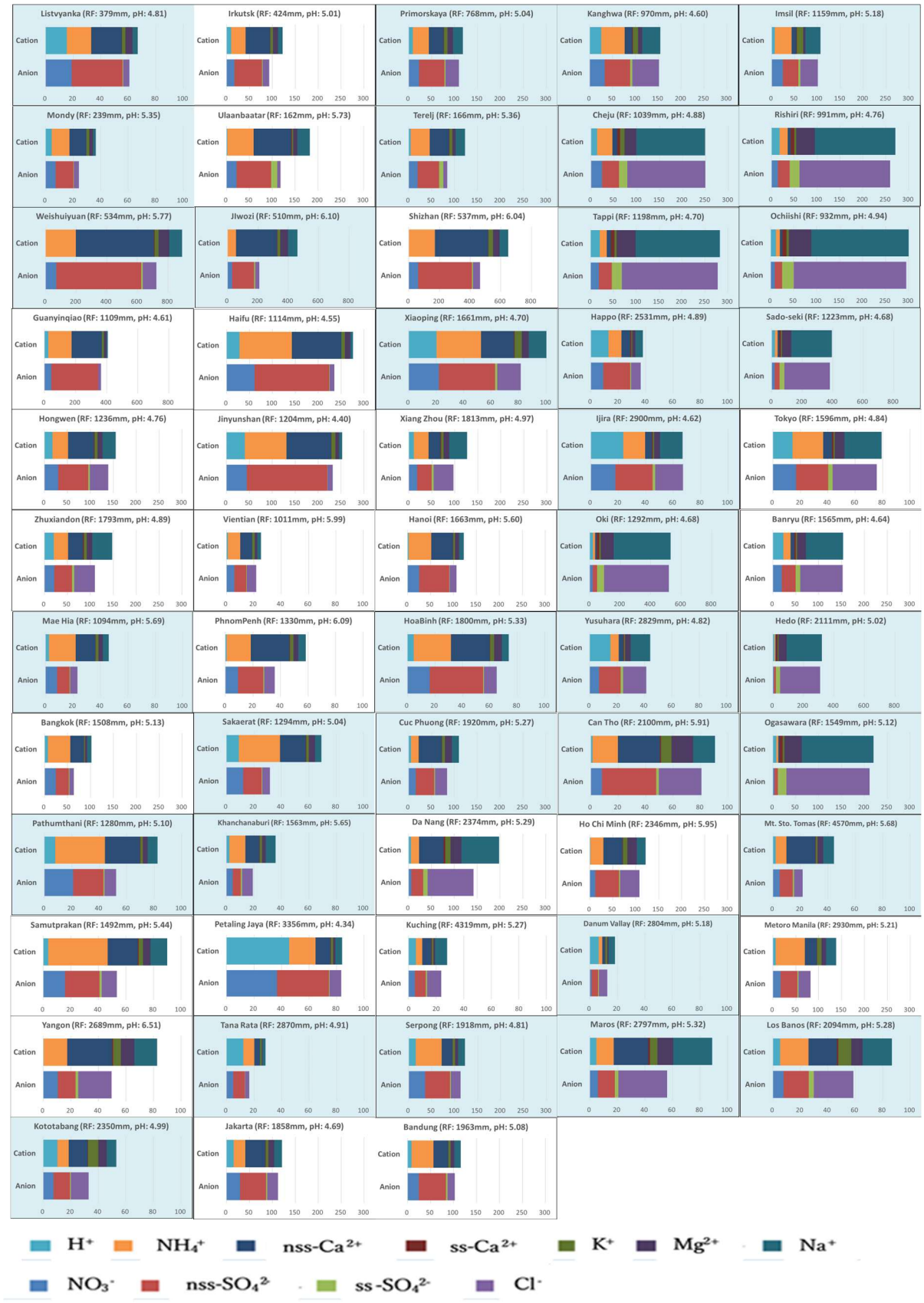

Figure 3.3.1. Ion balance of total precipitation collected in EANET sites between 2000 and 2019 1) Figures of remote and rural sites are hatched, 2) RF: Averaged annual precipitation, 3) Concentration unit: μeq L^{-1}, the scale changes according to the concentration, 0-100, 0-300, and 0-900 μeq L^{-1}.

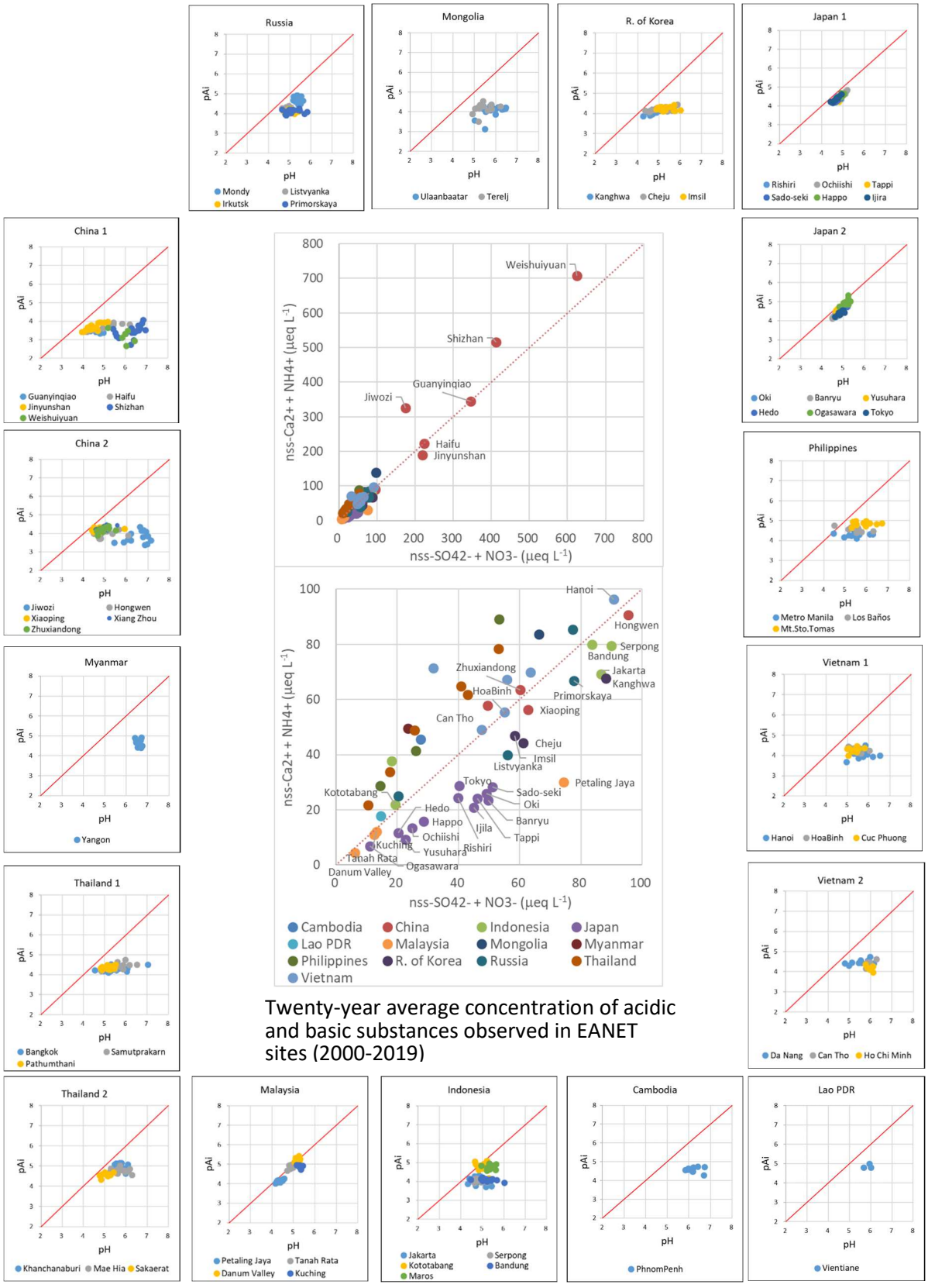

Twenty-year average concentration of acidic and basic substances observed in EANET sites (2000-2019)

Figure 3.3.2. Relationship between annual mean precipitation pH and pAi (input acidity) in EANET sites (2000-2019).

Table 3.3.1 Lowest precipitation pHs in twenty year's observation by EANET (2000-2019)

Year	Number of sites	Daily or event			Annual mean		
		pH	Site name	Precipitation (mm) and Date	pH	Site name	Precipitation (mm)
2000	40	3.54	Guanyinqiao (Ur)	1.6 (10/21)	4.22	Nanshan (Ru)	1259
2001	41	3.25	Jinyunshan (Ru)	2.1 (10/18)	4.18	Jinyunshan (Ru)	710
2002	41	3.16	Bandung (Ur)	14.5 (12/28)	4.23	Petaling Jaya (Ur)	2660
2003	44	3.41	Jinyunshan (Ru)	4.5 (12/2)	4.28	Petaling Jaya (Ur)	3041
2004	46	3.52	Xiaoping (Re)	14.8 (9/2)	4.33	Petaling Jaya (Ur)	2996
2005	47	3.40	Kanghwa (Ru)	1.0 (11/21)	4.25	Kanghwa (Ru)	811
2006	49	3.14	Listvyanka (Ru)	3.6 (8/17)	4.34	Cheju (Re)	1127
2007	49	3.35	Hedo (Re)	0.5 (11/3)	4.49	Banryu (Ur)	1273
2008	52	2.84	Haifu (Ur)	0.8 (9/13)	4.20	Haifu (Ur)	1010
2009	54	3.06	Haifu (Ur)	1.3 (11/27)	4.22	Haifu (Ur)	1066
2010	53	2.97	Jinyunshan (Ru)	1.1 (12/29)	3.94	Jinyunshan (Ru)	979
2011	53	3.08	Jinyunshan (Ru)	2.3 (4/3)	4.04	Jinyunshan (Ru)	848
2012	53	2.79	Haifu (Ur)	0.4 (5/27)	4.09	Jinyunshan (Ru)	1005
2013	52	3.17	Jinyunshan (Ru)	1.1 (1/16)	4.20	Jinyunshan (Ru)	1127
2014	53	3.11	Jinyunshan (Ru)	0.9 (1/26)	4.39	Jinyunshan (Ru)	1490
2015	57	3.37	Banryu (Ur)	2.0 (5/25-6/1)	4.39	Petaling Jaya (Ur)	3751
2016	57	3.55	Yusuhara (Re)	1.5 (8/16)	4.26	Petaling Jaya (Ur)	3432
2017	57	3.25	Kanghwa (Ru)	3.5 (2/19)	4.44	Kanghwa (Ru)	588
2018	57	3.57	Hedo (Re)	0.5 (7/27)	4.50	Petaling Jaya (Ur)	3848
2019	61	3.54	Jinyunshan (Ru)	0.5 (1/26)	4.68	Kanghwa (Ru)	502

➢ Ur: Urban, Ru: Rural, Re: Remote

Finally, Figure 3.3.3 shows the 20-year secular changes in acid concentration sums (nss-SO_4^{2-} + NO_3^-), base concentration sums (NH_4^+ + nss-Ca^{2+}) and H^+ concentrations for representative EANET sites. The higher acid concentration sums were observed in 2000s and 2010s at the rural and urban EANET sites in China, Republic of Korea, and Japan in Northeast Asia, in the comparison with base concentration sums. As the results, higher H^+ concentrations were observed at EANET sites mainly in 2000s in Korea, in 2010s in China, in 2000s and 2010s in Japan. After that, H^+ concentrations in these countries have been declining significantly. In Mongolia, the acid concentration sum in Ulaanbaatar has tended to be high in recent years. On the other hand, at rural and urban sites in Southeast Asian countries, the acid concentration sums and the H^+ concentrations have increased in recent years in Vietnam and Malaysia. Following the tendency of the base concentration sum, or completely independently, the acid concentration sums are maintained at a high level at some sites, and there are sites where the acid concentration sum tends to increase. The acid concentration sums at the remote site tend to decrease in Northeast Asia, as at the rural and urban sites. Besides, in Southeast Asia, there is no upward trend of acid concentration in remote sites. As mentioned here, precipitation acidity is the results on the balance between acids and bases dissolved in precipitation. Since the situation may change periodically due to air pollution in surrounding region in Northeast and Southeast Asian countries comparing with North America and European countries, it is important to continue wet deposition monitoring focusing on not only acids but also bases in precipitation in EANET countries.

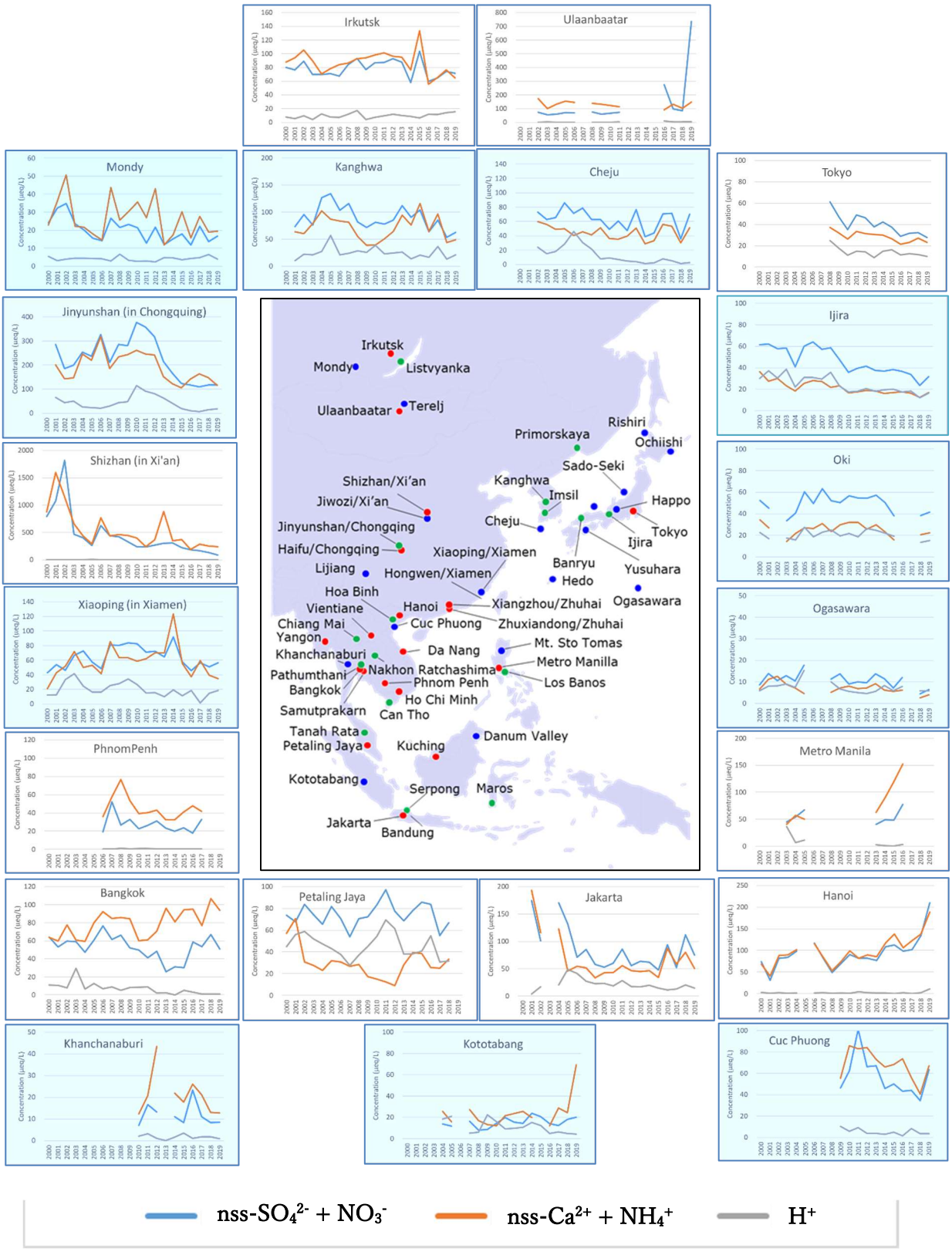

Figure 3.3.3. Long term trends of precipitation acidity (H^+) and concentrations of acids (nss-SO_4^{2-}+NO_3^-) and bases (nss-Ca^{2+}+NH_4^+) that acidified or neutralized precipitation in selected EANET sites (2000-2019). * Figures of remote and rural sites are hatched.

3.4. Spatial and temporal variation of wet deposition in East Asia

3.4.1 Comparison of wet deposition among EANET, NADP in US and EMEP in Europe

In this section, the trend of annual average of precipitation chemistry and annual wet deposition amount are compared among EANET, National Atmospheric Deposition Program (NADP) in US, and European Monitoring and Evaluation Program (EMEP) in Europe since 2000 to 2019 (the EMEP data is available until 2017). The data of precipitation chemistry and rainfall amount data of EMEP is collected from the annual data report of EMEP (https://projects.nilu.no/ccc/reports/).The data of annual precipitation-weighted mean concentrations and annual depositions from NADP were downloaded from the website (http://nadp.slh.wisc.edu/data/NTN/ntnAllsites.aspx).

In 1977, U.S. State Agricultural Experiment Stations (SAES) organized a project, later titled the NADP, to measure atmospheric deposition and study its effects on the environment. Sites in the NADP precipitation chemistry network began operations in 1978 with the goal of providing data on the amounts, trends, and geographic distributions of acids, nutrients, and base cations in precipitation. Reflecting the federal NAPAP (National Acidic Precipitation Assessment Program) role in the NADP, the network name was changed to NADP National Trends Network (NTN). The NTN network currently has 263 sites.

Measurements of air quality in Europe have been carried out under the "Co-operative programme for monitoring and evaluation of the long-range transmission of air pollutants in Europe" (EMEP) since 1 October 1977. From the start, priority was given to sulfur dioxide and sulfate in air, and pH and sulfate in precipitation, gradually increasing to include all main components in precipitation and ozone and nitrogen compounds in air. The EMEP data from 2018 for particulate matter, organic and elemental carbon, acidifying and eutrophying components in air and precipitation are presented in the report. In total, precipitation data from 89 stations and air data from 120 stations are presented in the report from 2018.

In order to compare the data among the three regions, the unit of concentration and deposition was transferred to that used in EANET in the following formulas and figures. The nss-SO_4^{2-} and nss-Ca^{2+} concentrations in NADP and nss-Ca^{2+} concentrations in EMEP were evaluated using the same method as EANET. Sea salt sulfate (calcium) was estimated from the concentration of sodium and the component ratio of sea water.

$[\text{nss-}SO_4^{2-}] = [SO_4^{2-}] - 0.06028\,[Na^+]$

$[\text{nss-}Ca^{2+}] = [Ca^{2+}] - 0.02161\,[Na^+]$

The wet deposition amount for the summary period of EMEP was calculated as:

Deposition amount ($mmol/m^2$) = C ($\mu mol/l$) × Rainfall (mm)/1000

In the comparison among three regions, it should keep in mind that in the following discussion the annual average concentration and annual deposition amount in EANET are obtained using the data from all of the urban, rural and remote sites, but urban site is excluded in EMEP and NADP network. Therefore, it is important to pay attention to the comparison of increasing and decreasing trends in each region.

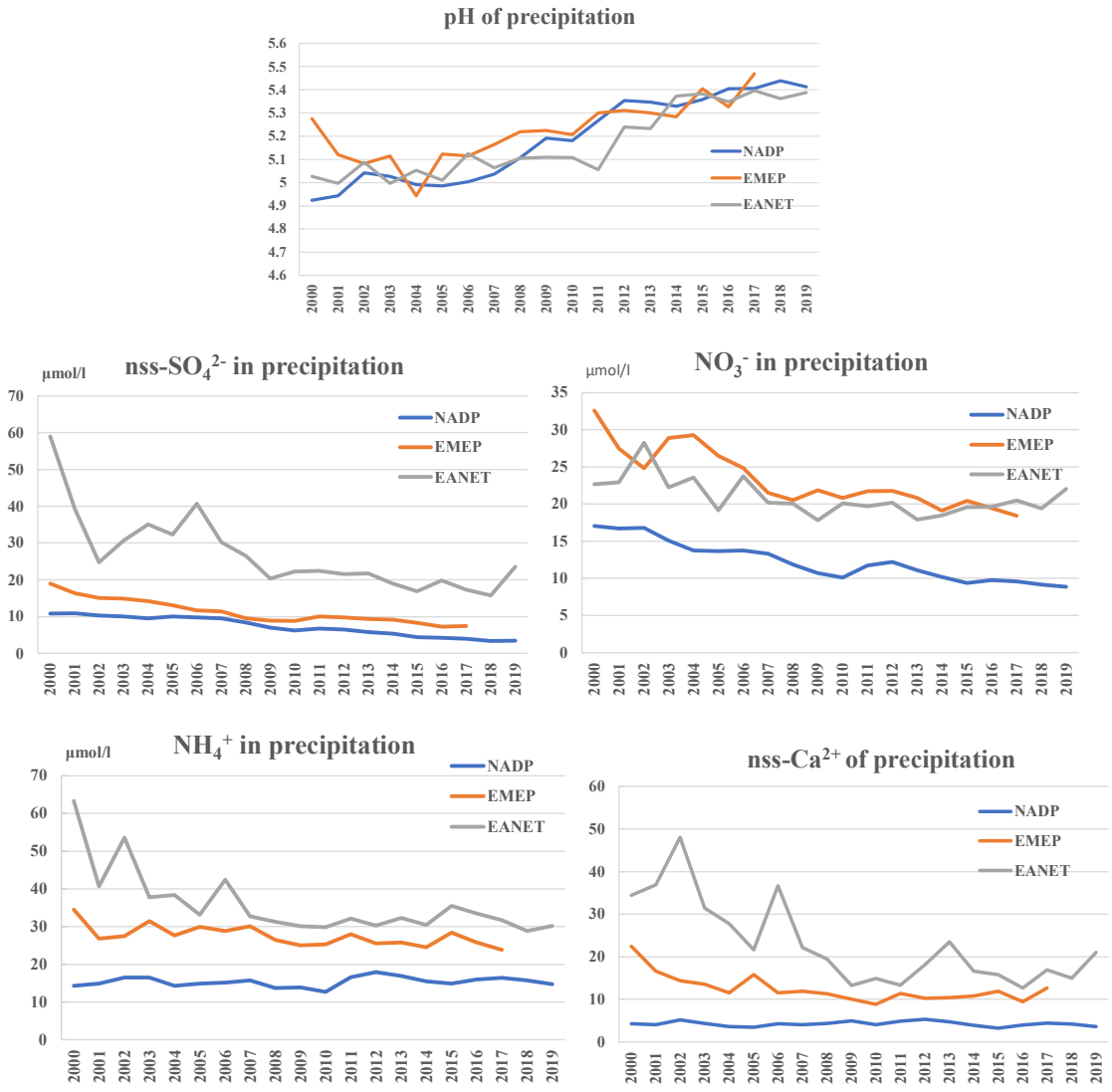

Note: Because of the abnormal value which is remarkable higher than the higher range limit (quartile 3 + 1.5xIQR), the following data has been excluded in the calcualtion of annual average
EANET: nss-SO_4^{2-} concentration from Weishuiyuan site in 2001 and 2002
nss-SO_4^{2-} concentration from Shizhan site in 2002
NH_4^+ concentration from Kototabang site in 2015
nss-Ca^{2+} concentration from Weishuiyuan site in 2001
EMEP: Data from Sztorhofdi site in 2006

Figure 3.4.1. The trend of annual average pH value, annual average concentration of nss-SO_4^{2-} NO_3^- NH_4^+ and nss-Ca^{2+} in precipitation from EANET, EMEP and NADP since 2000 to 2019.

The comparison of precipitation chemistry among EANET, NADP and EMEP is shown in the Figure 3.4.1. The pH value of precipitation shows significantly increasing trend (p<0.001) from all of the NADP (0.03 yr^{-1}), EMEP (0.02 yr^{-1}) and EANET (0.02 yr^{-1}) from 2000 to 2019. In 2000, the pH values of precipitation from EMEP, NADP and EANET were 5.3, 4.9 and 5.0 respectively. In 2017 the pH values of precipitation from EMEP, NADP and EANET were 5.5, 5.4 and 5.4 respectively. It suggests that the acid rain pollution in the all of the Europe, North America and East Asia has gradually reduced in the past 20 years.

The average of nss-SO_4^{2-} concentration from 2000 to 2017 in precipitation from EANET (25.9µmol/l) was significantly higher than that from EMEP (11.3 µmol/l) and NADP (7.6 µmol/l). The concentration of nss-SO_4^{2-} shows significantly declining trend (p<0.001) from all of the NADP (-0.43 µmol L^{-1} yr^{-1}), EMEP (-0.56 µmol L^{-1} yr^{-1}) and EANET (-1.25 µmol L^{-1} yr^{-1}). The concentration of NO_3^- in precipitation shows significantly decreasing trend (p<0.001) from NADP (-0.52 µmol L^-

^{1} yr^{-1}), EMEP (-0.97 μmol L^{-1} yr^{-1}) and slightly decreasing trend from EANET (-0.17 μmol L^{-1} yr^{-1}, p<0.05). The average concentration of NO_3^- was in similar level between EMEP (23.4 μmol/l) and EANET (20.8 μmol/l), and higher than the concentration in NADP (12.3 μmol/l). The concentration of NH_4^+ shows significantly decreasing trend from EANET (-0.68 μmol L^{-1} yr^{-1}, p<0.01), slightly decreasing trend from EMEP (-0.29 μmol L^{-1} yr^{-1}, p<0.05), and no clear change from NADP. The average concentration of NH_4^+ from EANET (35.1 μmol/l) was highest, followed by that from EMEP (27.5 μmol/l) and the concentration from NADP (15.5 μmol/l) was lowest. The average nss-Ca^{2+} concentration from 2000 to 2017 from EANET (22.9 μmol/l) was higher than that from EMEP (12.4 μmol/l) and NADP (4.2 μmol/l). The concentration of nss-Ca^{2+} shows overall declining trend from the EMEP (-0.32 μmol L^{-1} yr^{-1}, p<0.01) and EANET (-1.12 μmol L^{-1} yr^{-1}, p<0.01), but not clear change from NADP.

It can be concluded primarily that the increasing trend of pH value in precipitation from NADP, EMEP and EANET is probably due to more significant reduction of acid components (nss-SO_4^{2-} and NO_3^-) than alkali components (NH_4^+, and nss-Ca^{2+}) in the past 20 years.

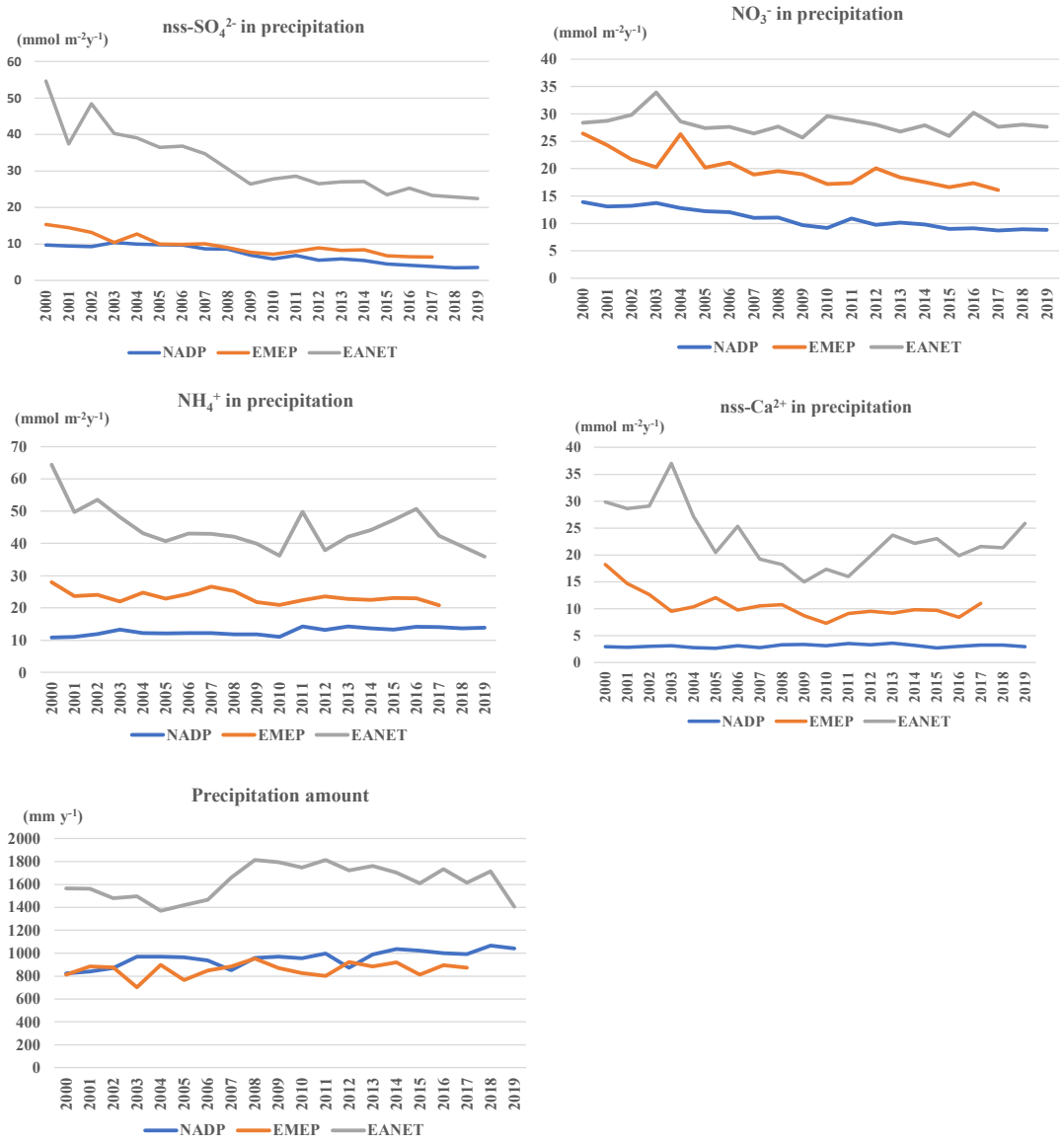

Note: Because of the abnormal value which is remarkable higher than the higher range limit (quartile 3 + 1.5xIQR), wet deposition of NH_4^+ from Kototabang site in EANET in 2015 has been excluded in the calcualtion of annual average

Figure 3.4.2. The trend of annual wet deposition amount of nss-SO_4^{2-} NO_3^- NH_4^+ and nss-Ca^{2+} and precipitation amount from EANET, EMEP and NADP since 2000 to 2019.

The comparison of wet deposition among EANET, NADP and EMEP is shown in the Figure 3.4.2. The average of wet deposition amounts of nss-SO_4^{2-}, NO_3^-, NH_4^+, and nss-Ca^{2+} from EANET (33.0, 28.3, 45.5, and 23.0 mmol m^{-2} y^{-1}, respectively) were the highest, and then was followed by those from EMEP (9.6, 19.9, 23.5, and 10.6 mmol m^{-2} y^{-1}, respectively), the lowest amounts were from NADP (7.5, 11.1, 12.6, and 3.1 mmol m^{-2} y^{-1}, respectively).

The wet deposition of nss-SO_4^{2-} shows significantly declining trend (p<0.001) from all of the NADP (-0.40 mmol m^{-2} y^{-1}), EMEP (-0.45 mmol m^{-2} y^{-1}) and EANET (-1.16 mmol m^{-2} y^{-1}) in recent 20 years. The wet deposition amount of NO_3^- doesn't show clear change from EANET, but which shows significantly declining trend (p<0.001) from EMEP (-0.44 mmol m^{-2} y^{-1}) and NADP (-0.28 mmol m^{-2} y^{-1}). The wet deposition amounts of NH_4^+ from NADP shows slightly increasing trend (0.14 mmol m^{-2} y^{-1}, p<0.05), and slightly decreasing trend from EANET (-0.58 mmol m^{-2} y^{-1}, p<0.05) but no significant trend was observed from EMEP. The wet deposition amounts of nss-Ca^{2+} from EMEP shows slightly declining trend (-0.23 mmol m^{-2} y^{-1}, p<0.05), but no significant trend was observed from NADP and EANET. The average precipitation amounts of EANET (1630mm) from 2000 to 2017 was much higher than the other two regions and the precipitation amounts of EMEP (856mm) and NADP (945mm) was in similar level. The precipitation amount from NADP shows significantly increasing trend (8.97 mm y^{-1}, p<0.001) in the past 20 years, but from the other networks doesn't show obvious trend.

3.4.2 Trends of wet deposition in Northeast Asia and Southeast Asia of EANET

The annual trend of the ion concentrations of precipitation and the wet deposition fluxes were estimated by the Mann-Kendall method. The trend analysis was focused on the wet deposition of H^+, nss-SO_4^{2-}, NO_3^-, NH_4^+, nss-Ca^{2+}, and the ion concentration of nss-SO_4^{2-}, NO_3^-, NH_4^+, nss-Ca^{2+}, pH, and the precipitation amount. The wet deposition fluxes and concentrations has been obtained from 2000 in EANET participating countries. The annual trends were estimated by the 11-year moving analysis within the 20-year period which satisfy the criteria of EANET (%PCL > 80% and %TP > 80%).

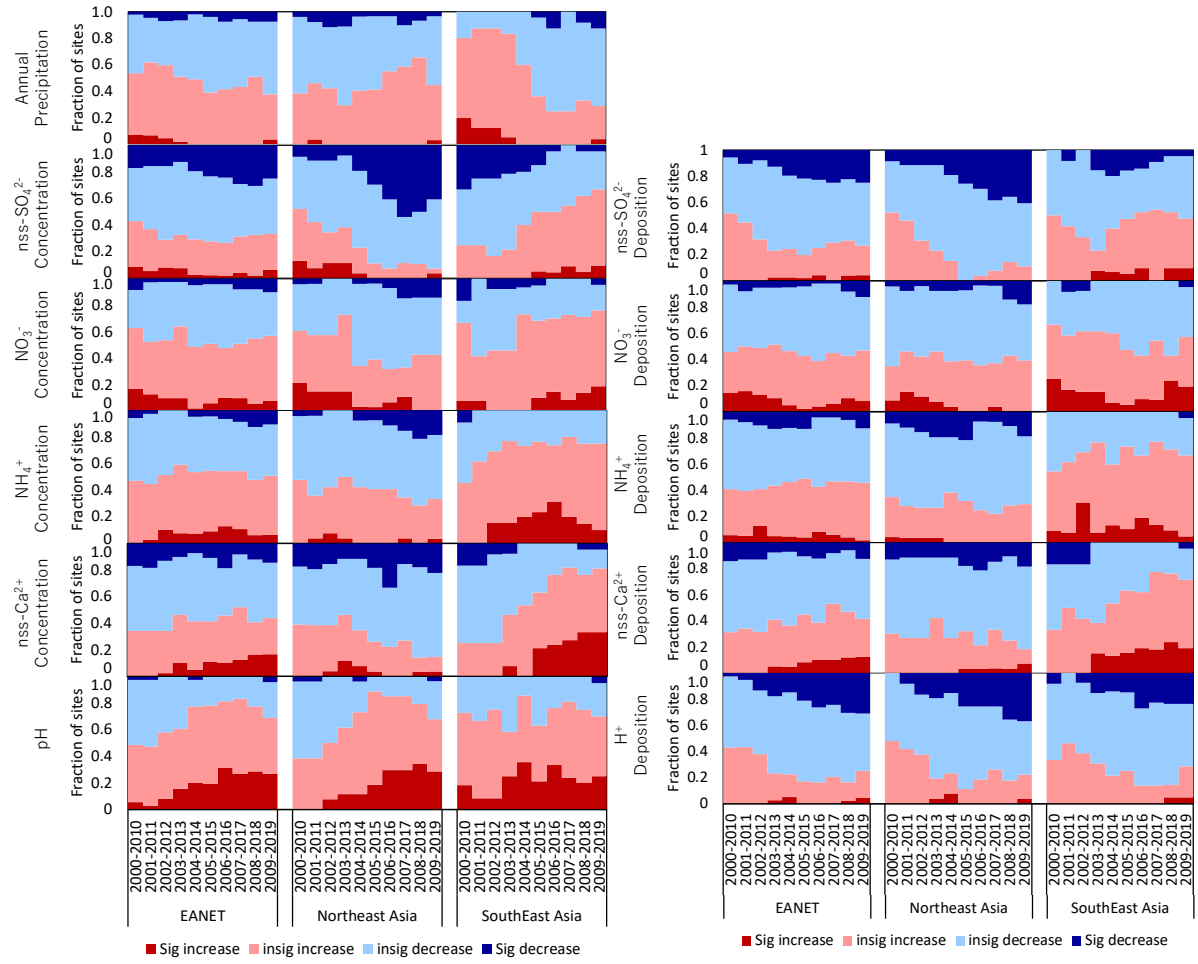

Figure 3.4.3. Percentage of significant positive trend (red), insignificant positive trend (light red), insignificant negative trend (light blue), and significant negative trend (blue) in EANET, northeast Asian sites, and southeast Asian sites, which are obtained by the Mann-Kendall test using the annual averaged concentrations of nss-SO_4^{2-}, NO_3^-, NH_4^+, nss-Ca^{2+}, pH, and precipitation amount, and the annual averaged wet deposition flux of nss-SO_4^{2-}, NO_3^-, NH_4^+, nss-Ca^{2+}, and H^+.

Figure 3.4.3 shows the percentage of EAENT monitoring sites where significant positive trend ($p < 0.05$), insignificant positive trend ($p > 0.05$), insignificant negative trend ($p > 0.05$), and significant negative trend ($p < 0.05$) in EANET participating countries, including Northeast Asian countries (Russia, Mongolia, China, Republic of Korea, Japan) and Southeast Asian countries (Cambodia, Indonesia, Lao P.D.R, Malaysia, Myanmar, Philippines, Thailand, and Vietnam).

The annual precipitation amount showed no significant trend in 20 years in both of Northeast Asian and Southeast Asian regions. The ratio of the significant negative trend of nss-SO_4^{2-} concentration has been increasing from the period of 2004-2014 to that of 2009-2019 in Northeast Asia. Especially, the significant negative trend of nss-SO_4^{2-} was obtained at EANET sites in China, Republic of Korea, and Japan recently (Figure 3.4.4). The significant deceasing rates of nss-SO_4^{2-} during 2009-2019 are obtained in Haifu (-10.86 μmol L^{-1} yr^{-1}, p <0.01), Jinyunshan (-11.58 μmol L^{-1} yr^{-1}, p<0.01), Shizhan (-9.92 μmol L^{-1} yr^{-1}, p<0.01), Xiaoping (-1.62 μmol L^{-1} yr^{-1}, p<0.01), Xiang Zhou (-0.78 μmol L^{-1} yr^{-1}, p<0.05), Zhuxiandong (-0.83 μmol L^{-1} yr^{-1}, p<0.05), Ijira (-0.50 μmol L^{-1} yr^{-1}, p<0.01), Oki (-0.60 μmol L^{-1} yr^{-1}, p<0.05), Banryu (-0.64 μmol L^{-1} yr^{-1}, p<0.05), Yusuhara (-0.54 μmol L^{-1} yr^{-1}, p<0.05), Tokyo (-0.70 μmol L^{-1} yr^{-1}, p<0.01), respectively.

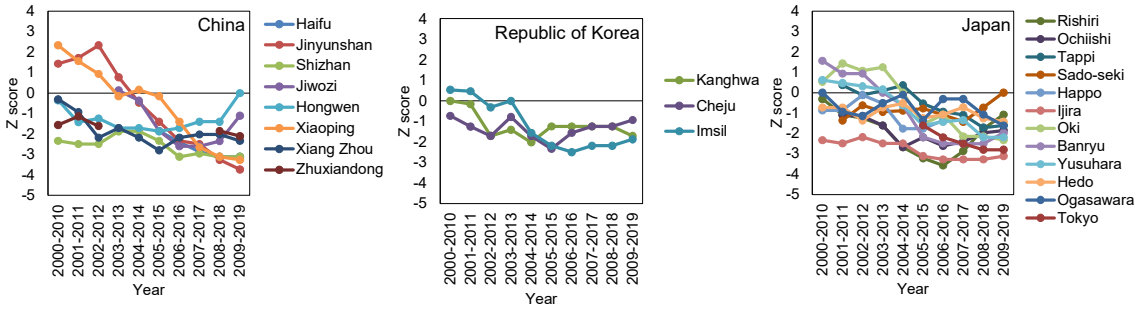

Figure 3.4.4. Moving trend analyses of nss-SO_4^{2-} concentration within 20 years at EANET sites in China, Republic of Korea, and Japan.

The concentration of NO_3^- did not have the significant trend in Northeast Asia and Southeast Asia. In the period from 2009 to 2019, the following monitoring sites shows the significant positive or negative trends of NO_3^-; Haifu (-3.05 μmol L^{-1} yr^{-1}, p<0.05), Jinyunshan (-3.10 μmol L^{-1} yr^{-1}, p<0.05), Yusuhara (-0.23 μmol L^{-1} yr^{-1}, p<0.05), Tokyo (-0.56 μmol L^{-1} yr^{-1}, p<0.05), Da Nang (-0.69 μmol L^{-1} yr^{-1}, p<0.05), Yangon (+1.67 μmol L^{-1} yr^{-1}, p<0.05), Mae Hia (+0.48 μmol L^{-1} yr^{-1}, p<0.05), Hoa Binh (+1.10 μmol L^{-1} yr^{-1}, p<0.05), Hanoi (+3.08 μmol L^{-1} yr^{-1}, p<0.01).

The number of the monitoring site which shows the significant positive trend of NH_4^+ and nss-Ca^{2+} was increasing in southeast Asian countries. Especially, the concentrations of NH_4^+ in Indonesia, Thailand, and Vietnam showed the positive trend recently (Figure 3.4.5).

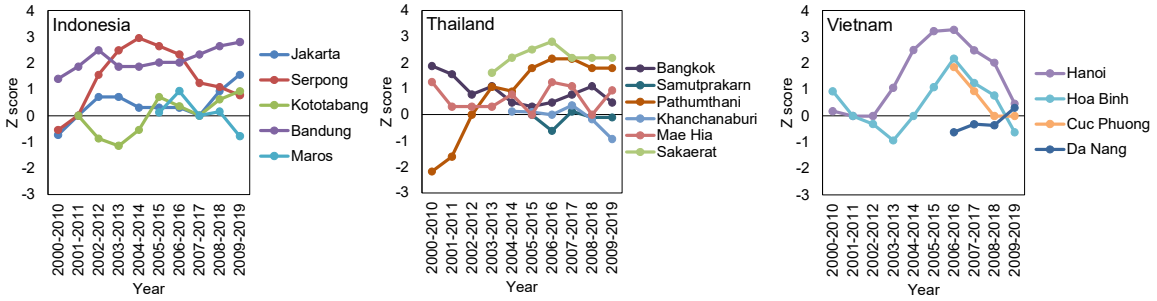

Figure 3.4.5. Moving trend analyses of NH_4^+ concentration within 20 years at EANET sites in Indonesia, Thailand, and Vietnam.

The significant positive trend of NH_4^+ during 2009-2019 were obtained in Sado-seki (+1.11 μmol L^{-1} yr^{-1}, p<0.05), Bandung (+1.82 μmol L^{-1} yr^{-1}, p<0.01), Sakaerat (+2.06 μmol L^{-1} yr^{-1}, p<0.05). The concentrations of nss-Ca^{2+} in Indonesia, Malaysia, and Vietnam showed the positive trend in 2009-2019 (Figure 3.4.6). The significant positive trends of nss-Ca^{2+} during 2009-2019 were obtained in Hongwen (+2.24 μmol L^{-1} yr^{-1}, p<0.05), Serpong (+1.19 μmol L^{-1} yr^{-1}, p<0.05), Maros (+0.75 μmol L^{-1} yr^{-1}, p<0.05), Kuching (+0.26 μmol L^{-1} yr^{-1}, p<0.05), Bangkok (+1.16 μmol L^{-1} yr^{-1}, p<0.01), Sakaerat (+1.27 μmol L^{-1} yr^{-1}, p<0.05), Hanoi (+3.45 μmol L^{-1} yr^{-1}, p<0.01), and Da Nang (+4.40 μmol L^{-1} yr^{-1}, p<0.01), respectively.

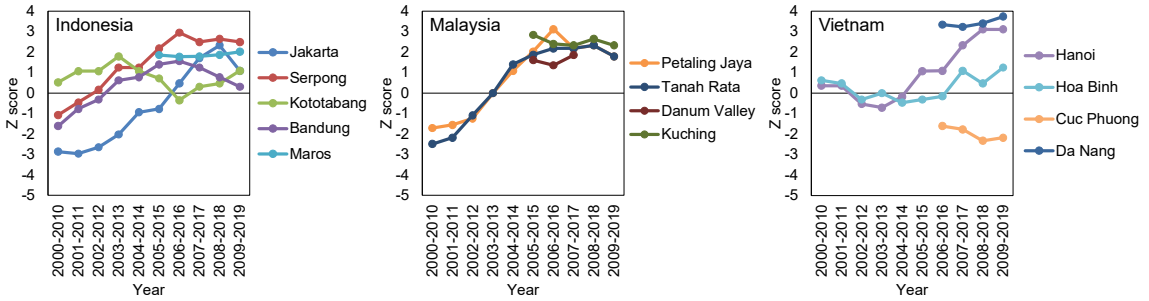

Figure 3.4.6. Moving trend analyses of nss-Ca^{2+} concentration within 20 years at EANET sites in Indonesia, Malaysia, and Vietnam.

The ratio of the significant positive trend of pH was been increasing from the period of 2002-2012 to that of 2009-2019 in both of Northeast Asia and Southeast Asia. The significant positive trends of pH during 2009-2019 were obtained in Haifu (+0.17 yr^{-1}, p<0.01), Jinyunshan (+0.11 yr^{-1}, p<0.01), Hongwen (+0.12 yr^{-1}, p<0.01), Serpong (+0.05 yr^{-1}, p<0.01), Kototabang (+0.06 yr^{-1}, p<0.01), Rishiri (+0.02 yr^{-1}, p<0.05), Ochiishi (+0.04 yr^{-1}, p<0.01), Yusuhara (+0.02 yr^{-1}, p<0.05), Imsil (+0.05 yr^{-1}, p<0.01), Primorskaya (+0.09 yr^{-1}, p<0.01), Bangkok (+0.10 yr^{-1}, p<0.05), Sakaerat (+0.05 yr^{-1}, p<0.05), and Da Nang (+0.13 yr^{-1}, p<0.01), respectively.

The trends of the wet deposition flux for nss-SO_4^{2-}, NO_3^-, NH_4^+ and nss-Ca^{2+} were similar with the trends of the ion concentrations. The trend of H^+ deposition flux shows the significant decrease from the period of 2002-2012 to that of 2009-2019 in both of Northeast Asia and Southeast Asia, which is the opposite trend of pH.

Based on the data analysis mentioned above, we prepared some maps to show geographical distribution of acids and bases wet deposition trends (in the periods of 2000-2010, 2005-2015, and 2009-2019) as shown below. The pH shows the increasing trend in Northeast Asian and Southeast Asian countries (Figure 3.4.7). The concentration of nss-SO_4^{2-} had the decreasing trend in Northeast Asian countries (Figure 3.4.8). There were no significant trends in the other components such as NO_3^- (Figure 3.4.9). The decline of the nss-SO_4^{2-} in North Asian countries contribute to increase pH. On the other hand, the concentration of nss-SO_4^{2-} in Southeast Asian countries had the insignificant trend. The concentration of nss-Ca^{2+} and NH_4^+ had the increasing trend in Southeast Asia (Figure 3.4.10, Figure 3.4.11). Therefore, the increasing trend of pH in Southeast Asian countries was possibly caused by increasing cation contribution (nss-Ca^{2+} and NH_4^+).

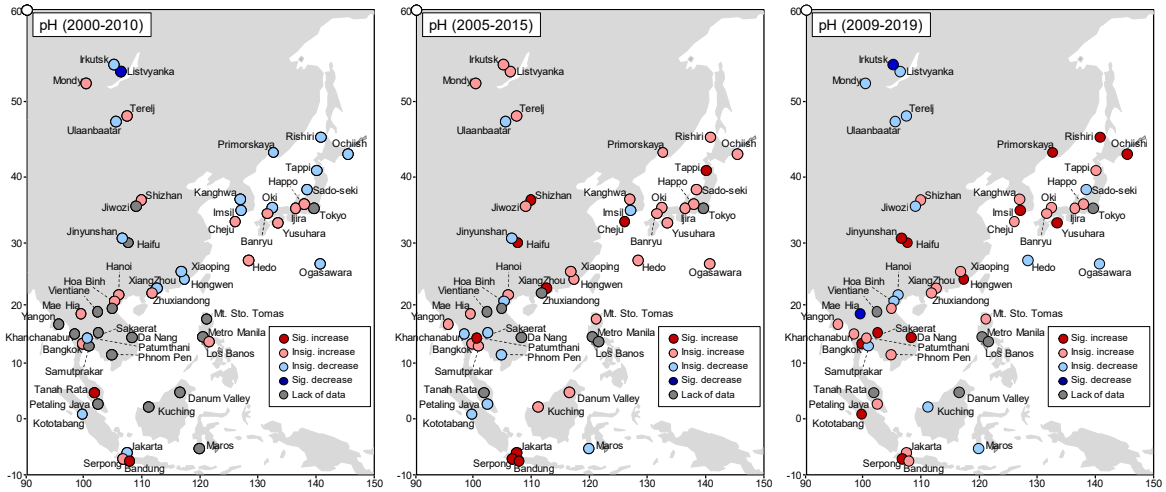

Figure 3.4.7. Spatial distribution of pH trend at EANET sites in the period of 2000-2010, 2005-2015, and 2009-2019.

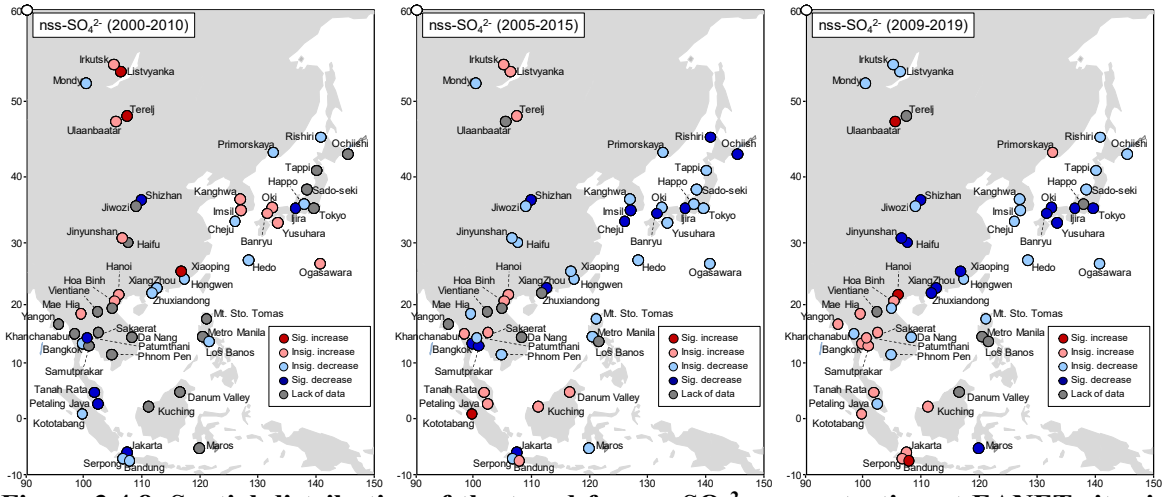

Figure 3.4.8. Spatial distribution of the trend for nss-SO_4^{2-} concentration at EANET sites in the period of 2000-2010, 2005-2015, and 2009-2019.

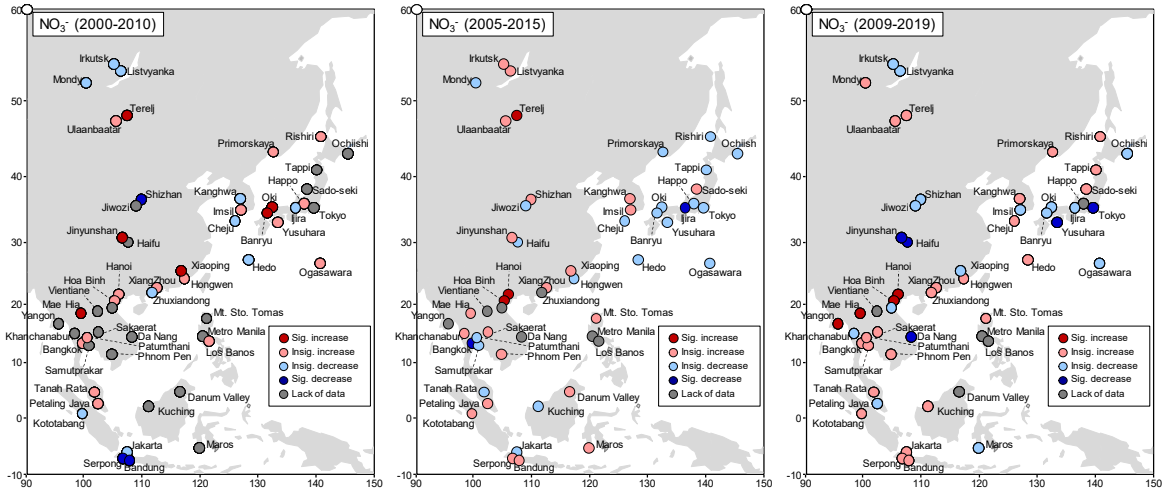

Figure 3.4.9. Spatial distribution of the trend for NO_3^- concentration at EANET sites in the period of 2000-2010, 2005-2015, and 2009-2019.

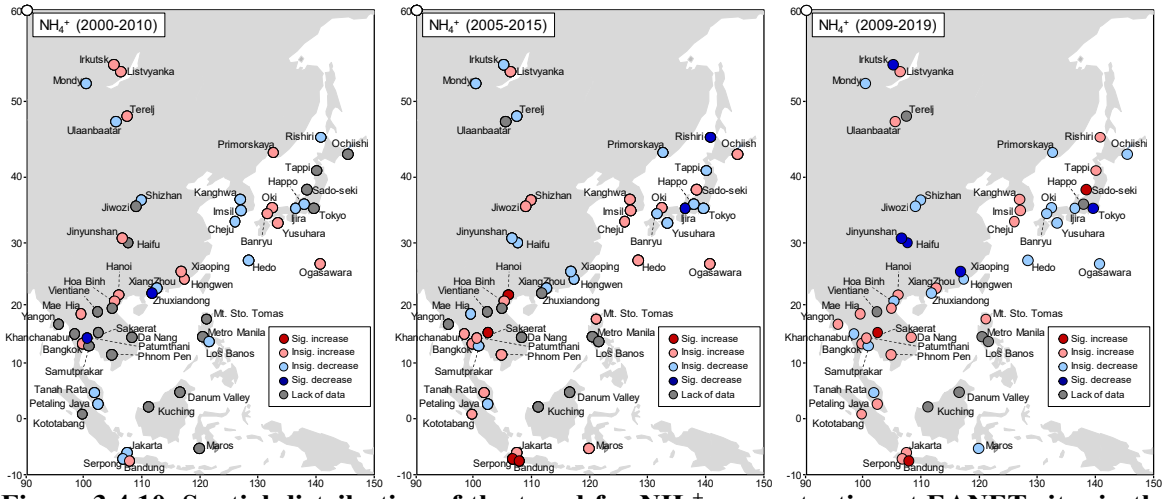

Figure 3.4.10. Spatial distribution of the trend for NH_4^+ concentration at EANET sites in the period of 2000-2010, 2005-2015, and 2009-2019.

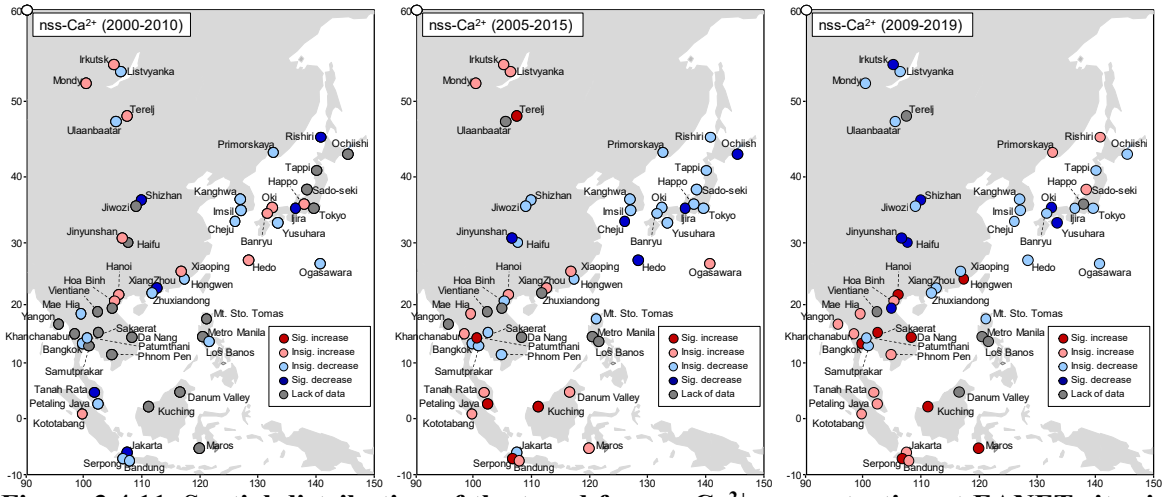

Figure 3.4.11. Spatial distribution of the trend for nss-Ca^{2+} concentration at EANET sites in the period of 2000-2010, 2005-2015, and 2009-2019.

3.5 Dry deposition assessment methodology

Dry deposition was estimated by the inferential method based on Technical Manual for Dry Deposition Flux Estimation in East Asia (EANET, 2010). The inferential method estimates the dry deposition based on the following equation:

$$F = C\ V_d \qquad (1)$$

where F is the dry deposition flux, C is the atmospheric concentration, and V_d is the deposition velocity. In this method, the atmospheric concentrations are measured. Contrarily, V_d values are inferred using a resistance model with some input data such as meteorological elements. The V_d is calculated from the following equations:

$$V_d = (R_a + R_b + R_c)^{-1} \quad \text{for gases} \qquad (2)$$
$$V_d = (R_a + V_{ds}^{-1})^{-1} + V_g \quad \text{for particles} \qquad (3)$$

where R_a is the aerodynamic resistance, R_b is the quasi-laminar layer resistance and R_c is the surface resistance, V_{ds} is the surface deposition velocity, and V_g is the gravitational settling velocity. For the R_a calculation, we set the reference height to 10 m over the zero-plane displacement height. The model adopts the R_c parameterization of Wesely (1989) with modifications of the outer surface resistance for SO_2 and NH_3. For the outer surface resistance, parameters of Erisman (1994) for SO_2 and Sumith at al. (2000) for NH_3 were used. The parameterization of V_{ds} for aerosol components followed Ruijgrok et al. (1997). This parameterization was in accordance with V_{ds} for aerosol components directly measured above forests in Japan (Matsuda et at., 2010; Matsuda et al., 2015). We used the parameters for forest surface in land use category to estimate deposition amounts to forests around each site.

For total sulfur dry deposition, dry depositions of SO_2 and particulate SO_4^{2-} were taken into account; for total nitrogen deposition, dry depositions of HNO_3, NH_3, particulate NO_3^- and particulate NH_4^+ were taken into account. We used concentrations of these components measured by the four-stage filter pack method to estimate the dry deposition amounts. So far, the total deposition amounts were assessed in Japanese EANET sites (Endo et al., 2011; Ban et al., 2016; Yamaga et al., 2021). In this report, total deposition amounts were adopted if data completeness of dry deposition was more than 75% and that of wet deposition amounts was more than 80% during the period.

Basically, the resistance model requires onsite and hourly meteorological data such as wind speed, temperature, relative humidity, solar radiation and precipitation amount to calculate V_d. The hourly data are currently available only at limited sites. Most sites report monthly data. Therefore, we calculated V_d using the monthly data. Regarding surface wetness (dry or wet), which is one of the key factors to determine V_d, we estimated percentage of wet surface period (wet-%) in a month from a regression line between monthly mean relative humidity and wet-%. And then monthly V_d was estimated from the following equation:

$$V_d = V_{d\text{-}dry} \text{ x dry-\%} + V_{d\text{-}wet} \text{ x wet-\%} \qquad (4)$$

where $V_{d\text{-}dry}$ and $V_{d\text{-}wet}$ are monthly V_d in the cases of dry and wet surface, respectively, dry-% is dry surface period in a month (dry-% = 100 − wet-%). The regression lines were made from the relationship between wet-% and wet surface period estimated by using available hourly meteorological data in Japan, Bangkok and Ulaanbaatar. Here, we determined as wet surfaces in the case over 85% in relative humidity. We used the regression line of Japan for the mid-latitude sites and that of Bangkok for the sites in Southeast Asia. We regarded $V_{d\text{-}dry}$ as V_d for the sites in Mongolia and Russia, because of low wet-% in Ulaanbaatar. Annual dry deposition amounts for each component calculated from monthly and hourly data were almost in agreement.

3.6 Spatial and temporal variation of total (dry and wet) deposition in East Asia

Figures 3.6.1, 3.6.2 and 3.6.3 show trends of annual amounts of total sulfur (S) deposition by dry and wet depositions at remote, rural and urban EANET sites, respectively. Low total S depositions were found at the remote sites located in northern inland (Mondy and Terelj) and Pacific Ocean (Ogasawara), and high total S depositions were found in the Japanese remote sites near Asian continent (Sado-seki and Oki). Dry deposition largely contributed to the high total S at Sado-seki and Oki. In Japanese remote sites except Rishiri and Ogasawara, more than 10 kg S/ha/year of total S deposition were found in many years. In these sites, the total S depositions had decreased around from 2013. Especially in Yusuhara and Happo, the decreases were started around from late 2000s. Clear decrease of wet S deposition was also found in Ijira (rural site) from early 2000s. More than 10 kg S/ha/year of total S deposition were found at all rural and urban sites. Especially high total S depositions more than 30 kg S/ha/year were found at urban sites in Southeast Asia (Hanoi, Bangkok and Petaling Jaya). At Hanoi and Bangkok, dry S depositions has decreased from 2000s.

Figures 3.6.4, 3.6.5 and 3.6.6 show trends of annual amounts of total nitrogen (N) deposition by dry and wet depositions at EANET sites in remote, rural and urban areas, respectively. Ban et al. (2016) estimated total N deposition at Japanese remote sites from 2003 to 2012 following the inferential method of EANET (2010), using hourly input data observed at each site. The amounts and trends of annual total N deposition estimated in this report using monthly data were almost the same as those of Ban et al. (2016). In remote sites, spatial and temporal trends of the total N depositions were similar to those of the total S depositions (low in northern inland (Mondy and Terelj) and Pacific Ocean (Ogasawara); high in Japanese sites near Asian continent (Sado-seki and Oki)). In Japanese remote sites except Rishiri and Ogasawara, more than 10 kg N/ha/year of total N deposition were found in many years. At the sites with high N deposition (Sado-seki and Oki), the total N depositions had decreased around from 2013. There was no clear decrease or increase trends in the total N depositions at other Japanese remote sites. Regarding rural sites, clear decrease of wet N deposition was found at Ijira, similar to that of wet S deposition. At Serpong, quite high total N depositions, more than 30 kg N/ha/year, were frequently found in 2010s. In urban sites, at Hanoi and Bangkok, dry N depositions has not clearly decreased from 2000s, unlike the decreases of dry S depositions.

Figures 3.6.7, 3.6.8 and 3.6.9 show trends of annual amounts of total nitrogen (N) deposition by oxidized N and reduced N at EANET sites in remote, rural and urban areas, respectively. Here oxidized N deposition is defined as sum of wet deposition of NO_3^- and dry depositions of HNO_3 and

particulate NO_3^-; reduced N deposition is defined as sum of wet deposition of NH_4^+ and dry depositions of NH_3 and particulate NH_4^+. In remote sites, reduced N deposition contributed more than half of total N deposition at lower N deposition sites (Mondy, Terelj, Rishiri and Ogasawara), and oxidized N deposition contributed more than half of total N deposition at higher N deposition sites (Sado-seki and Oki). At Sado-seki and Oki, the decreases of total N depositions were largely contributed by decreases of the oxidized N deposition. Regardless of the site categories, reduced N deposition contributed more than half of total N deposition in many years at the all sites in Russia, Mongolia and Southeast Asia, except Petaling Jaya.

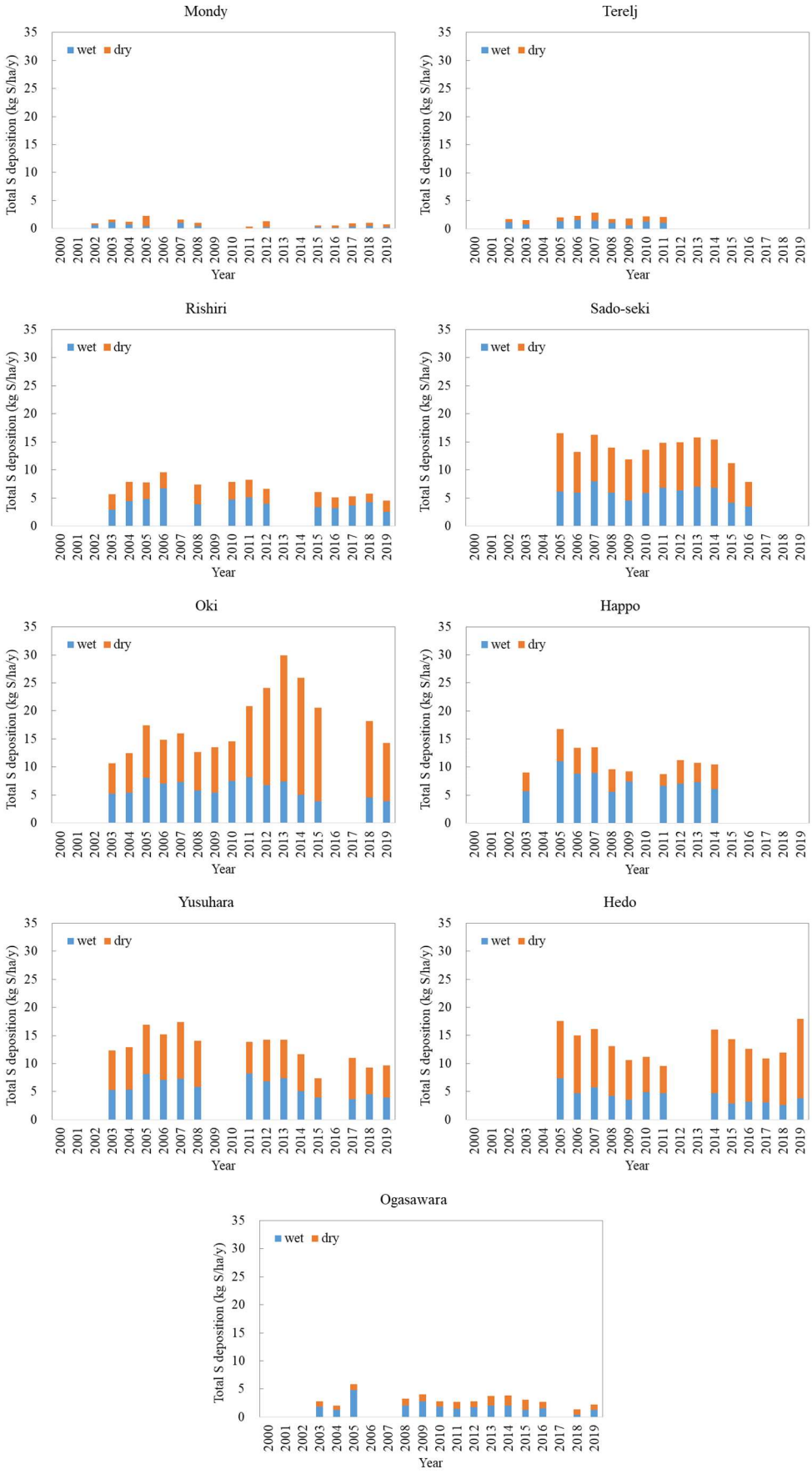

Figure 3.6.1. Trends of annual amounts of total sulfur deposition at EANET sites in remote areas. Blue and orange column indicates wet and dry deposition, respectively.

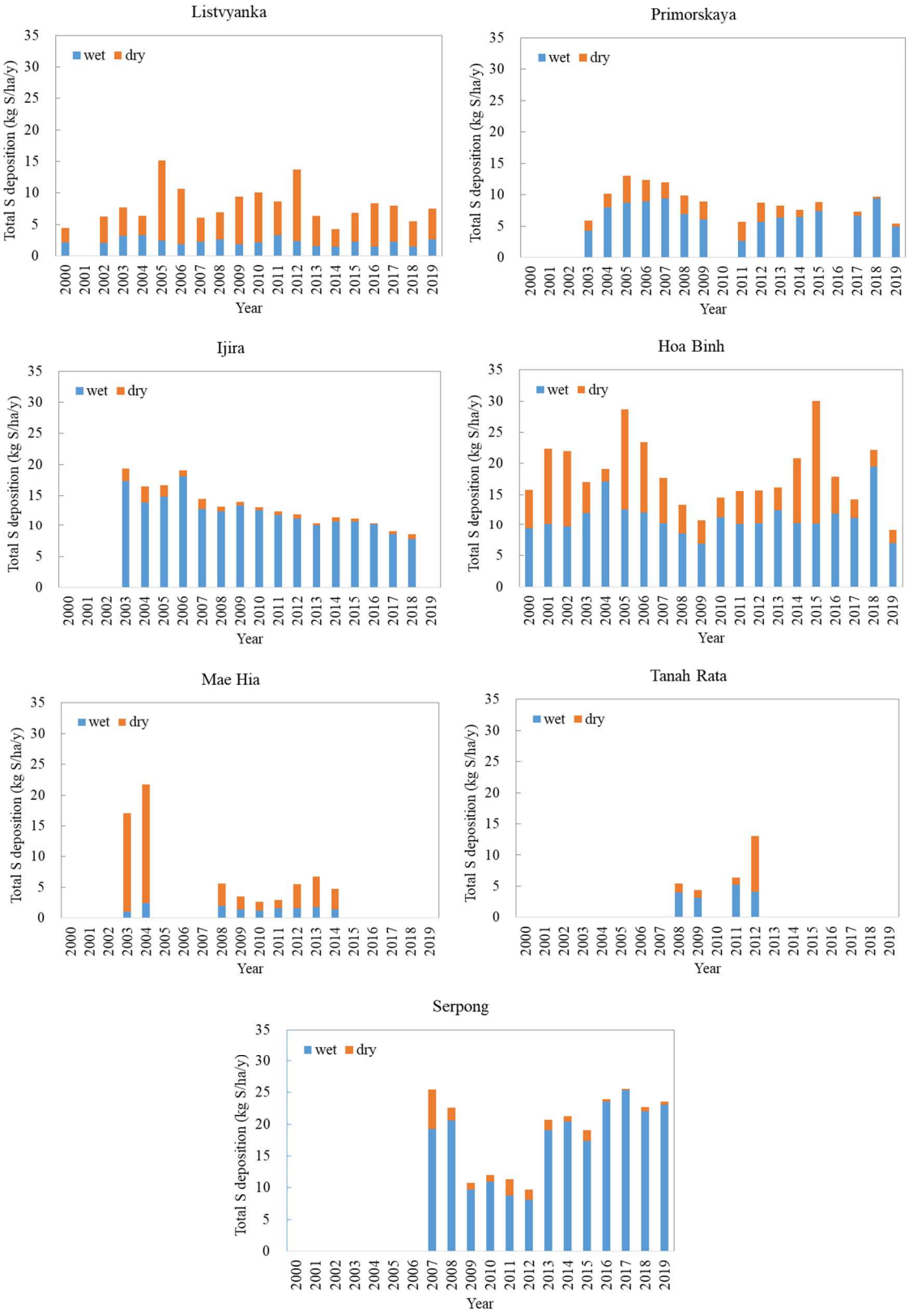

Figure 3.6.2. Trends of annual amounts of total sulfur deposition at EANET sites in rural areas. Blue and orange column indicates wet and dry deposition, respectively.

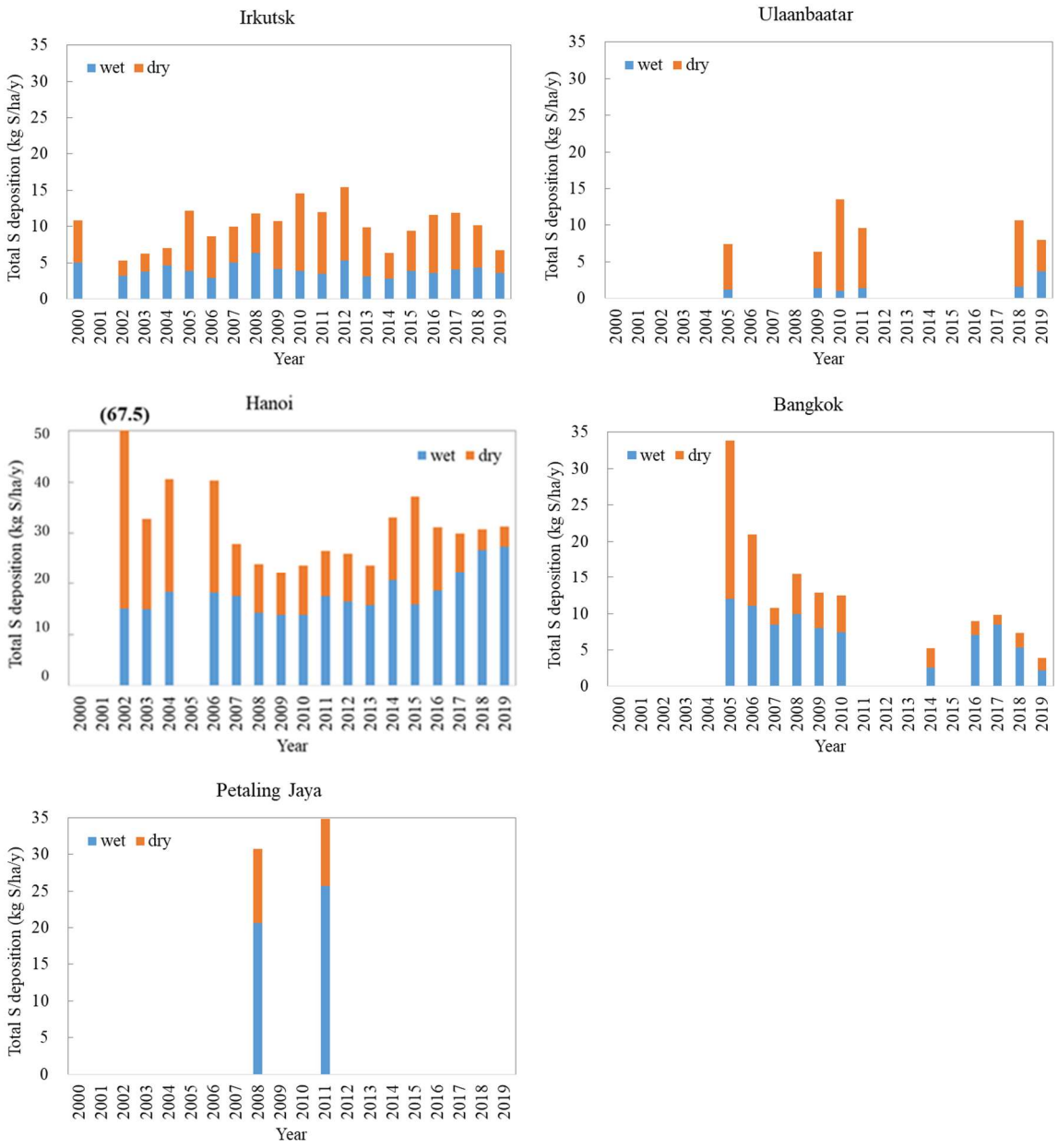

Figure 3.6.3. Trends of annual amounts of total sulfur deposition at EANET sites in urban areas. Blue and orange column indicates wet and dry deposition, respectively.

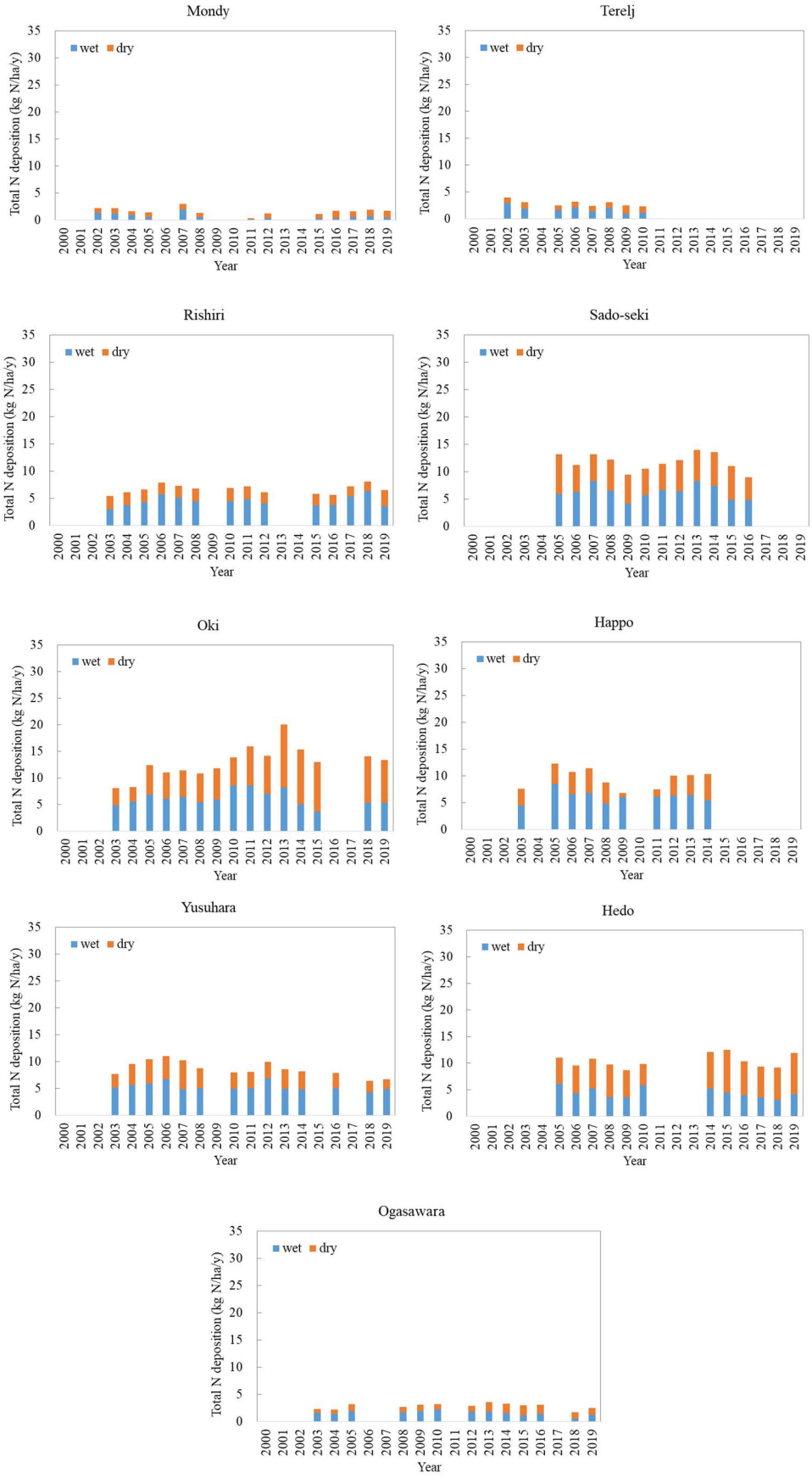

Figure 3.6.4. Trends of annual amounts of total nitrogen deposition at EANET sites in remote areas. Blue and orange column indicates wet and dry deposition, respectively.

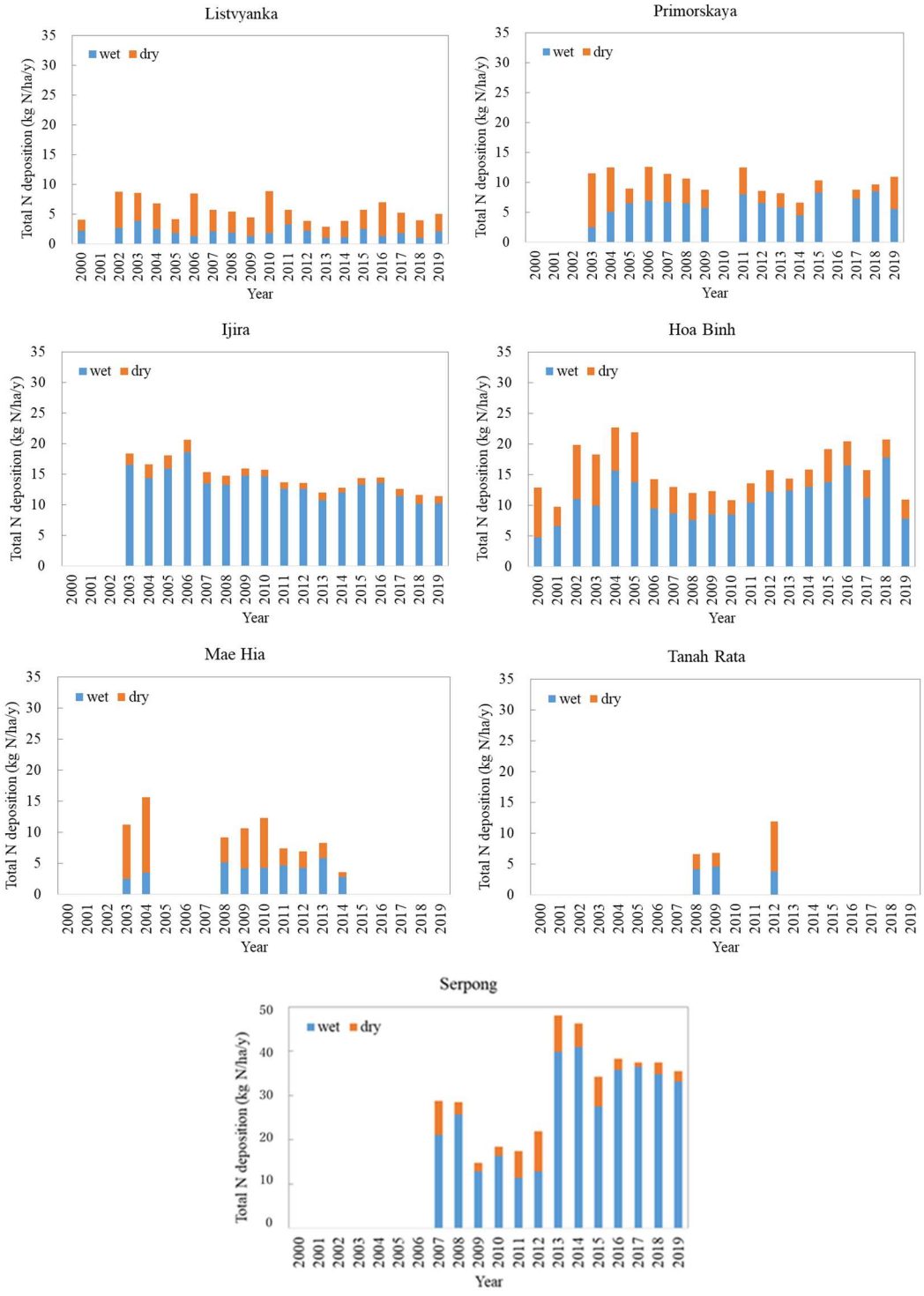

Figure 3.6.5. Trends of annual amounts of total nitrogen deposition at EANET sites in rural areas. Blue and orange column indicates wet and dry deposition, respectively.

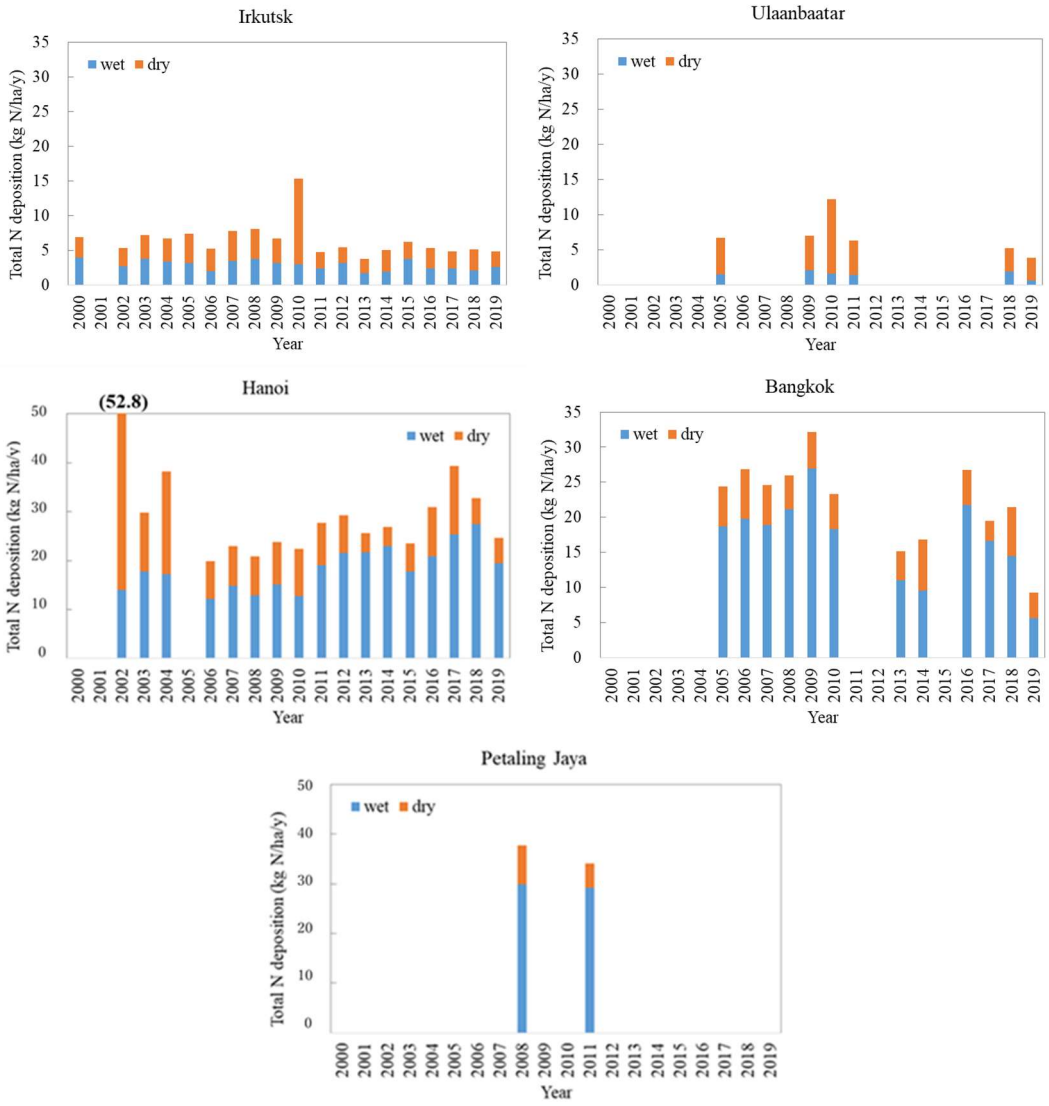

Figure 3.6.6. Trends of annual amounts of total nitrogen deposition at EANET sites in urban areas. Blue and orange column indicates wet and dry deposition, respectively.

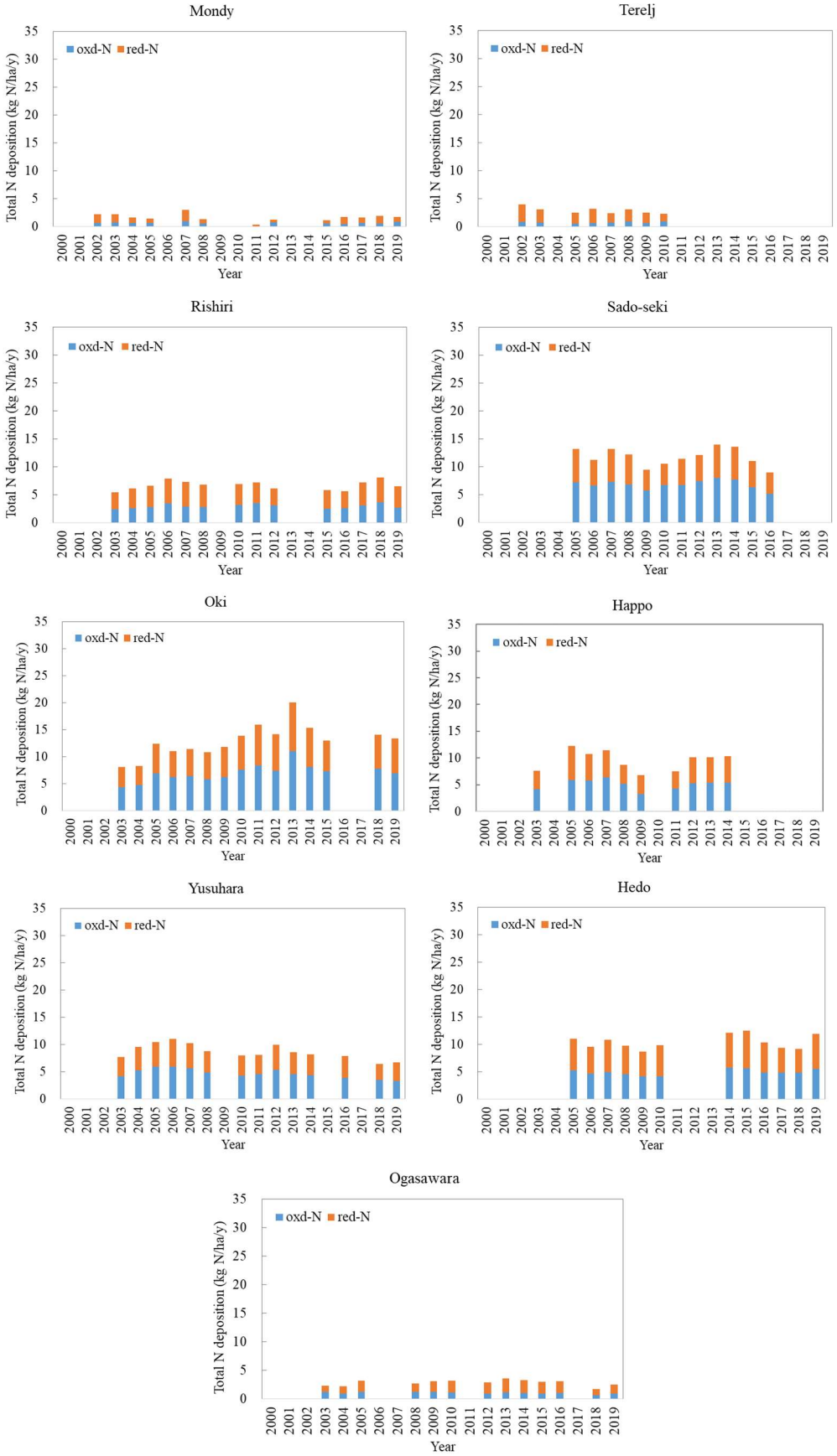

Figure 3.6.7. Trends of annual amounts of total nitrogen deposition at EANET sites in remote areas. Blue and orange column indicates oxidized and reduced nitrogen deposition, respectively.

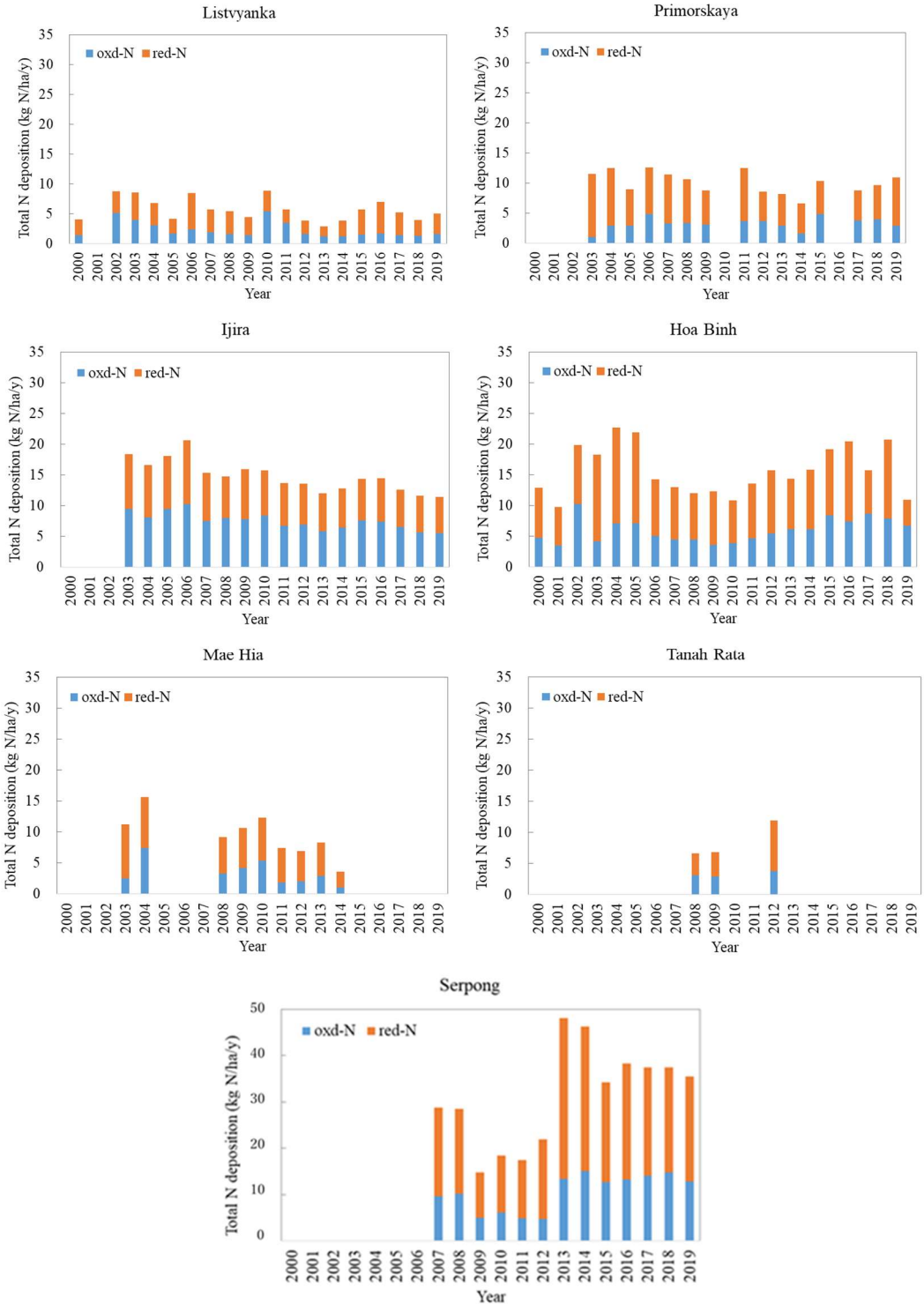

Figure 3.6.8. Trends of annual amounts of total nitrogen deposition at EANET sites in rural areas. Blue and orange column indicates oxidized and reduced nitrogen deposition, respectively.

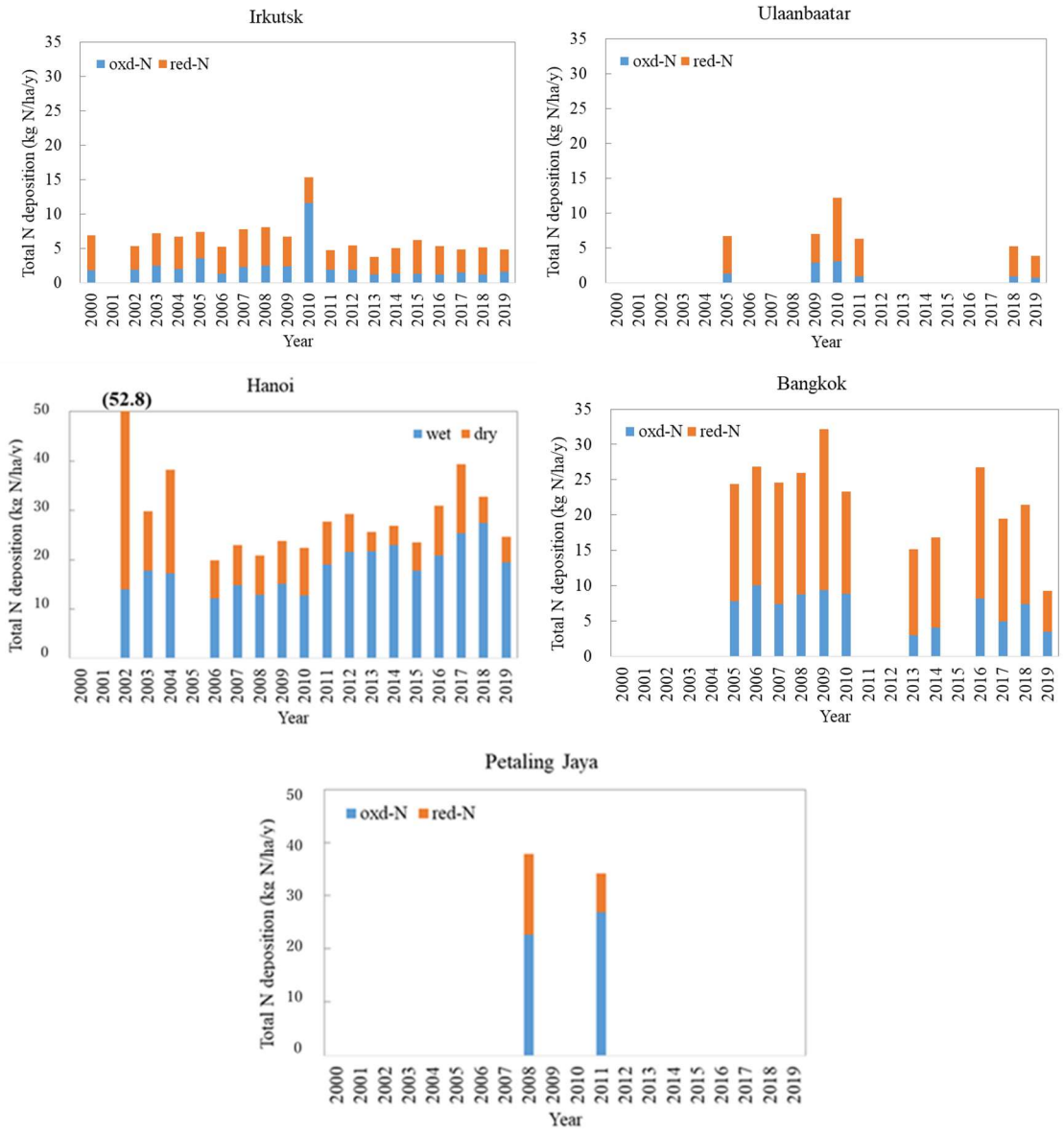

Figure 3.6.9. Trends of annual amounts of total nitrogen deposition at EANET sites in urban areas. Blue and orange column indicates oxidized and reduced nitrogen deposition, respectively.

The trend analyses (2000-2010, 2005-2015, and 2009-2019, respectively, by the Mann-Kendall method) were conducted for total deposition of sulfur, nitrogen, oxidized nitrogen and reduced nitrogen, respectively (Fig 3.6.10). Each Figure shows the trend analysis result of 10 years. If the number of data is less than 8, it will show lack of data. Generally, significant trends were observed from some stations in EANET during 2000-2019.

For the total deposition of sulfur, the significant decreasing trend was observed from the Hanoi site (2000-2010), Ijira site (2000-2010, 2005-2015 and 2009-2019), Primorskaya site (2005-2015), Yusuhara site (2005-2015) and Rishiri site (2009-2019); On the contrary, the significant increasing trend was observed from Irkutsk site during 2000 to 2010, Hanoi site (2009-2019) and Serpong site (2009-2019). For the total deposition of nitrogen, the significant decreasing trend was observed from the Ijira site (2005-2015 and 2009-2019), and significant increasing trend was observed from Oki site for the period from 2005 to 2015. For the total deposition of oxidized nitrogen, significant

decreasing trend was observed from Ijira site and Ogasawara site during 2005 to 2015 and 2009 to 2019, and Yusuhara site from 2005 to 2015; significant increasing trend was observed from Hanoi site (2005-2015 and 2009-2019) and Hoa Binh site (2009-2019). For the total deposition of reduced nitrogen, significant decreasing trend was observed from Terelj site (2000-2010) and Ijira site (2005 to 2015, and 2009-2019); significant increasing trend was found from Oki site (2000-2010 and 2005-2015).

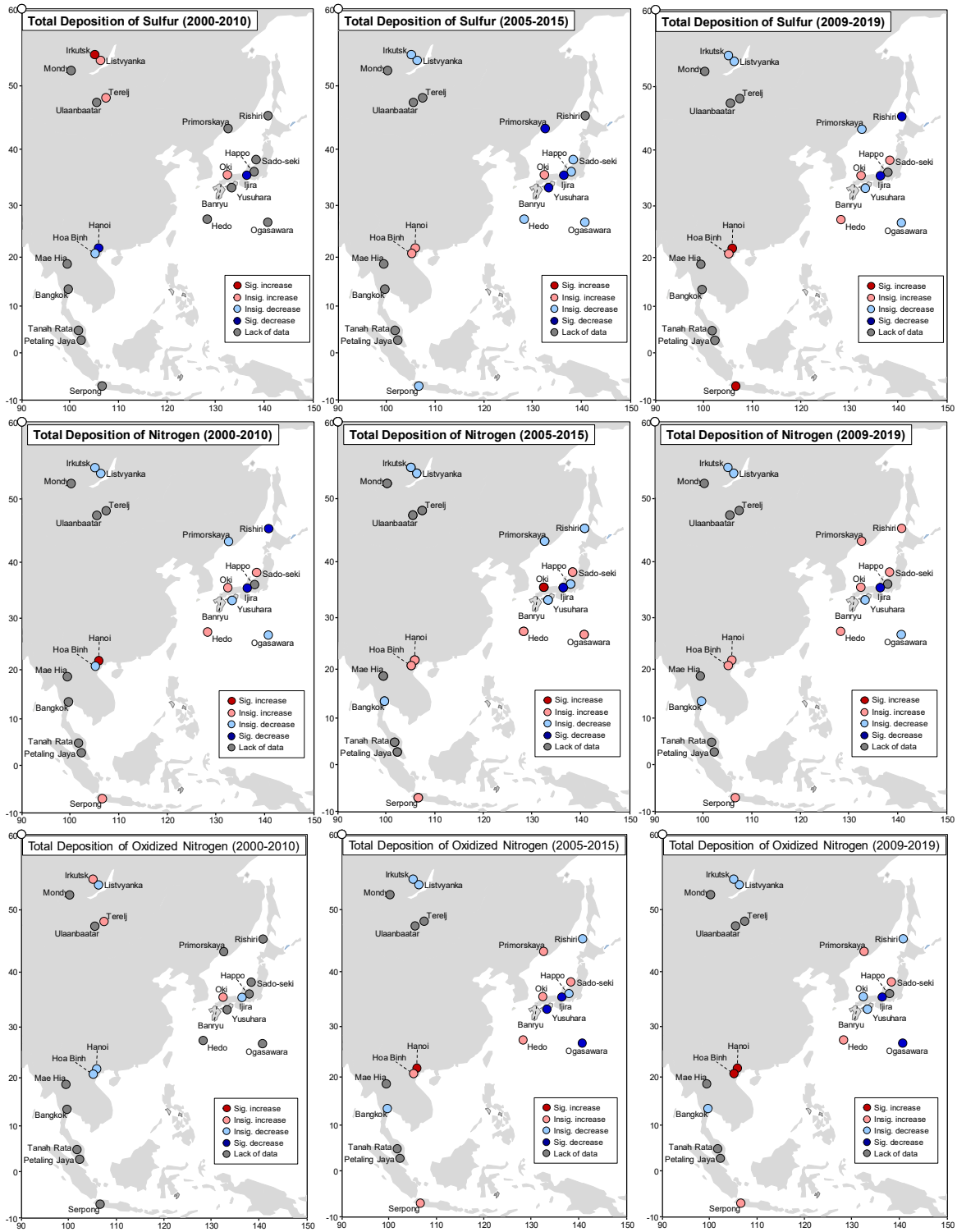

Figure 3.6.10 (1). Spatial distribution of the trend for total (wet and dry) deposition of sulfur, nitrogen and oxidized nitrogen at EANET sites in the period of 2000-2010, 2005-2015, and 2009-2019.

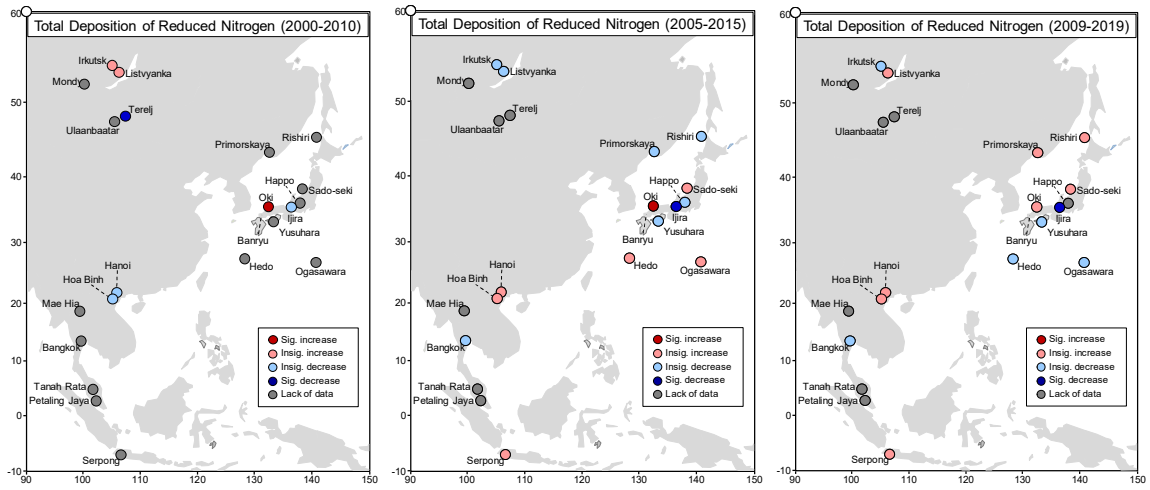

Figure 3.6.10 (2). Spatial distribution of the trend for total (wet and dry) deposition of reduced nitrogen at EANET sites in the period of 2000-2010, 2005-2015, and 2009-2019.

3.7 Summary and recommendations

In this chapter, we assessed spatial and temporal variations of wet and dry deposition using available EANET monitoring data during the period of 2000-2019.

Precipitation chemistry was evaluated mainly based on pH, pAi, the acid concentration sum (nss-SO_4^{2-} + NO_3^-) and the base concentration sum (NH_4^+ + nss-Ca^{2+}). The lowest pH values were all observed at sites where the acid concentration sum was larger than the base concentration sum. The acid concentration sums at the remote site tend to decrease in Northeast Asia, as at the rural and urban sites. In 2010s, H^+ concentrations in China, Korea and Japan have been declining significantly. The acid concentration sums have increased in recent years in Vietnam and Malaysia.

From the comparison of precipitation chemistry among EANET, NADP and EMEP, the pH values and nss-SO_4^{2-} concentrations showed significantly increasing and decreasing trend, respectively, in all networks from 2000 to 2019. The NO_3^- concentrations showed significantly decreasing trend from NADP, EMEP and slightly decreasing trend from EANET. The decreasing trend of nss-SO_4^{2-} concentration have been significant from the period of 2004-2014 to that of 2009-2019 in Northeast Asia, especially, in China, Republic of Korea, and Japan. The nss-SO_4^{2-} concentration in Southeast Asia had the insignificant trend. The NO_3^- concentration did not have the significant trend in Northeast Asia and Southeast Asia. Since the nss-Ca^{2+} and NH_4^+ concentration had the increasing trend, pH increasing trend in Southeast Asia was possibly caused by the increasing of the cations.

Total (dry and wet) deposition of S and N was evaluated at the sites carrying out the 4-stage filter pack monitoring in Russia, Mongolia, Japan, Vietnam, Thailand, Malaysia and Indonesia. Dry deposition was estimated by simplifying the inferential method using available monthly meteorological data. Low total S depositions were found at the remote sites located in northern inland and Pacific Ocean, and high total S depositions were found in the Japanese remote sites near Asian continent. In the high S deposition sites, the decreasing trend of S deposition was found in recent years. High total S depositions more than 30 kg S/ha/year were found at urban sites in Southeast Asia. The dry S depositions have decreased from 2000s at Hanoi and Bangkok. In remote sites, spatial and temporal trends of the total N depositions were similar to those of the total S depositions, and reduced N deposition contributed more than half of total N deposition at lower N deposition sites, and oxidized N deposition contributed more than half of total N deposition at higher N deposition sites. Regardless of the site categories, reduced N deposition contributed more than half

of total N deposition in many years at many sites, except at Sado-seki, Oki and Petaling Jaya. Trend analysis for total S and N, as well as oxidized and reduced N deposition, has shown a significant increase in some sites in Southeast Asia and a significant decrease in some sites in Northeast Asia, especially in the last decade.

Estimations of spatial and temporal variations of total deposition are important for assessing the impact on ecosystems including acidification and excess eutrophication. Current method to estimate dry deposition requires observations of gaseous and particulate S and N components and meteorological elements, therefore, there are only a limited number of sites that measure all items. To improve the situations, further expansion of monitoring by the 4-stage filter pack that measures the gaseous and particulate S and N components at the same time is expected at first. Moreover, chemical transport model is effective to estimate the deposition velocity, when the necessary items are limited. NADP developed a hybrid approach for estimating dry deposition using monitoring data and modeled data from chemical transport model (Schwede and Lear, 2014). Some use of the model for estimation of dry deposition should be considered for next step. Moreover, the latest information of the dry deposition process research should be taken into account to update the methodology.

3.8 References

Ban, S., Matsuda, K., Sato, K., Ohizumi, T. 2016. Long-term assessment of nitrogen deposition at remote EANET sites in Japan, Atmospheric Environment, 146, 70-78.

Endo, T., Yagoh, H., Sato, K., Matsuda, K., Hayashi, K., Noguchi, I., Sawada, K. 2011. Regional characteristics of dry deposition of sulfur and nitrogen compounds at EANET sites in Japan from 2003 to 2008, Atmospheric Environment, 45, 1259-1267.

Erisman, J. W. 1994. Evaluation of a surface resistance parameterization of sulphur dioxide, Atmospheric Environment, 28, 2583- 2594.

European Monitoring and Evaluation Program (EMEP) https://projects.nilu.no/ccc/reports/.

Hara, H. 1991. Acid Rain, - 3. How to read acid rain data -, Journal of Japan Society for Atmospheric Environment, 26, 3, A51-59.

Hara, H., Kitamura, M., Mori, A., Noguchi, I., Ohizumi, T., Seto, S., Takeuchi, T., Deguchi, T. 1995. Precipitation chemistry in Japan 1989-1993, Water Air & Soil Pollution 85 (4), 2307-2312.

Matsuda, K., Fujimura, Y., Hayashi, K., Takahashi, A., Nakaya, K. 2010. Deposition velocity of PM2.5 sulfate in the summer above a deciduous forest in central Japan, Atmospheric Environment, 44, 4582-4587.

Matsuda, K., Watanabe, I., Mizukami, K., Ban, S., Takahashi, A. 2015. Dry deposition of PM2.5 sulfate above a hilly forest using relaxed eddy accumulation, Atmospheric Environment, 107, 255-261.

National Atmospheric Deposition Program (NADP) http://nadp.slh.wisc.edu/data/NTN/ntnAllsites.aspx.

Network Center for EANET. 2000-2019. Acid Deposition Monitoring Network in East Asia (EANET) Data Report.

Network Center for EANET. 2010. Technical Manual for Wet Deposition Monitoring in East Asia -2010.

Network Center for EANET. 2010. Technical Manual for Dry Deposition Flux Estimation in East Asia.

Network Center for EANET. 2013. Technical Manual for Air Concentration Monitoring in East Asia.

Ohizumi, T. 2009. Atmospheric Deposition, - 2. Wet Deposition -, Journal of Japan Society for Atmospheric Environment, 44, 5, A17-24.

Ruijgrok, W., Tieben, H., Eisinga, P. 1997. The dry deposition of particles to a forest canopy: A comparison of model and experimental results, Atmospheric Environment, 31, 399-415.

Schwede, D.B., Lear, G.G. 2014. A novel hybrid approach for estimating total deposition in the United States, Atmospheric Environment, 92, 207-220.

Smith, R.I., Fowler D., Sutton, MA., Flechard, C., Coyle M. 2000. Regional estimation of pollutant gas dry deposition in the UK: model_ description, sensitivity analyses and outputs, Atmospheric Environment, 34: 3757-3777.

Wesely, M.L. 1989. Parameterization of surface resistances to gaseous dry deposition in regional-scale numerical models, Atmospheric Environment, 23, 1293-1304.

Yamaga, S., Ban, S., Xu, M., Sakurai, T., Itahashi, S., Matsuda, K., Trends of sulfur and nitrogen deposition from 2003 to 2017 in Japanese remote areas, Environmental Pollution (available online 27 July 2021) https://doi.org/10.1016/j.envpol.2021.117842.

4. Gas and Aerosol Pollution in East Asia

4.1 Introduction

4.1.1 Monitoring status by each country

Acid deposition is a phenomenon that acidic pollutants including sulfur dioxide (SO_2) and nitrogen oxides (NOx) are deposited to the Earth surface leading to acidification of freshwater, soils, and forests. This process is strongly affected by the variety of human activities such as power plants, industrial activities and car exhaust. In order to identify the linkage of acid deposition to those human activities, the research investigated the causal relationship has been conducted (Galloway, 1995, Schöpp et al., 2003, Yu et al., 2017).

The dry and wet deposition are influenced by the atmospheric chemical conversion of air pollutants including SO_2, O_3, NO, NO_2 (urban), HNO_3, HCl and NH_3 and the particulate components such as SO_4^{2-}, NO_3^-, Cl^-, NH_4^+ and PM_{10}. Especially, it is mostly focused on the sulfur dioxide (SO_2) and nitrogen oxides (NOx), which are because those components not only oxide shortly right after the deposition but show the conspicuous emission. The atmospheric chemistry of sulfur compounds in gas phase can be described as below equations (1) to (5).

$$SO_2 + OH\cdot + M \rightarrow HOSO_2\cdot + M \cdots (1)$$

$$HOSO_2\cdot + O_2 \rightarrow HO_2\cdot + SO_3 \cdots (2)$$

$$SO_3 + H_2O \rightarrow H_2SO_4 \cdots (3)$$

$$H_2SO_4 + 2NaCl \rightarrow 2HCl + Na_2SO_4 \cdots (4)$$

$$H_2SO_4 + 2NH_3 \rightarrow (NH_4)_2SO_4 \cdots (5)$$

$$NO_2 + OH + M \rightarrow HNO_3 + M \cdots (6)$$

$$NO_2 + O_3 \rightarrow NO_3 + O_2 \cdots (7)$$

$$NO_2 + NO_3 + M \rightarrow N_2O_5 + M \cdots (8)$$

$$N_2O_5 + H_2O \rightarrow 2HNO_3 \cdots (9)$$

$$N_2O_5 + NaCl \rightarrow ClNO_2 + NaNO_3 \cdots (10)$$

$$HNO_3 + NH_3 \leftrightarrow NH_4NO_3 \cdots (11)$$

Along with the conversion of sulfur compounds, the atmospheric reaction of nitrogen compounds is able to be expressed as above equations (6) to (11). M, which is mentioned in equations (1), (6) and (8), is possible to be any atmospheric molecules.

Once the pollutants are emitted in the air, they and their secondary pollutants can be deposited to local and distant location during transport/diffusion and chemical conversion process. The feature of long-range transportation shows that it is necessary to establish continuous monitoring network and to deal with this environmental phenomenon not only a domestic perspective but also as a regional or hemispherical problem. Therefore, EANET has conducted continuous monitoring in various countries for 20 years, and the number of gas and aerosol monitoring sites have been increased each year (Fig. 4.1.1).

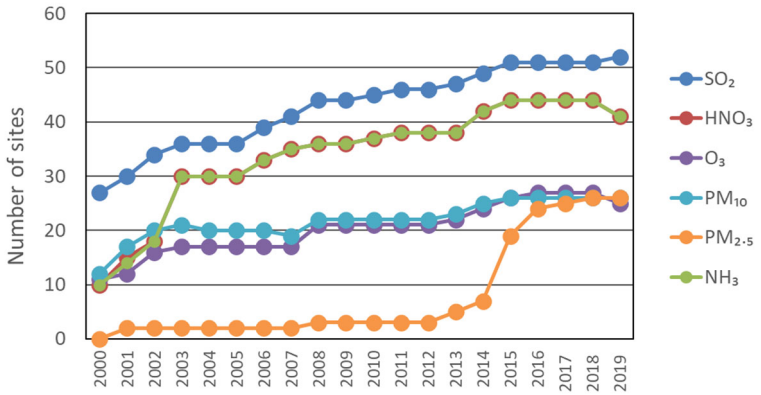

Figure 4.1.1 Annual variations of the number of gas and aerosol monitoring sites in EANET.

This will allow to establish the high-resolution monitoring network in East Asia and to provide the scientific evidence to policy makers to confront this environmental issue as well.

As described in Table 4.1.1, there were 54 air concentration monitoring sites operated in the EANET network as of 2019. The measuring components, which are SO_2, NO, NOx, $PM_{10/2.5}$, O_3, HNO_3, HCl, NH_3 and Particulate Matter Components (PMC), varies depending on the methodology at each site.

*In each country, simple historical and surrounding site description is required at each site (the meaning of each site, the reason why the site is chosen as the monitoring site for acid deposition.)
*Cambodia (Phnom Penh)
*China (Jinyunshan, Hongwen, Haibin-parkm, Wuzhishan, Lijiang)
*Indonesia (Jakarta, Serpong, Kototabang, Bandung)
*Japan (Rishiri, Ochiishi, Sado-seki, Happo, Ijira, Oki, Yusuhara, Hedo, Ogasawara, Tokyo, Niigata-maki, Tsushima)
*Lao PDR (Vientiane)
*Malaysia (Petaling Jaya, Tanah Rata, Danum Valley)
*Mongolia (Ulaanbaatar, Terelj)
*Myanmar (Yangon, Mandalay)
*Philippines (Metro Manila, Los Banõs, Mt. Sto. Tomas)

In case of EANET sites in Republic of Korea, there are three monitoring sites referred to Kangwha, Cheju (Kosan) and Imsil. The sites monitor those which SO_2, NO_2, O_3 and $PM_{10/2.5}$ with Automatic air monitor (AT), and HNO_3, HCl, NH_3 and PMC in $PM_{2.5}$ with Filter Pack (FP). Among those monitoring sites, Kangwha is located nearby the capital and expressed as the main site to describe the main concentration in Republic of Korea. In addition, Cheju (Kosan) site is located in remote region and represented as the background concentration of the country. Furthermore, Imsil monitoring site is placed on inland and remoted from the urban area. This feature shows that the site is described as the concentration of inland in Republic of Korea.

*Russia (Mondy, Listvyanka, Irkutsk, Primorskaya)
*Thailand (Bangkok, Samutprakarn, Pathumthani, Khanchanaburi, Chian Mai, Nakhon Ratchasima)
*Vietnam (Hanoi, Hoa Binh, Can Tho, Ho Chi Minh, Yen Bai)

Table 4.1.1. Sampling methods and parameters at respective EANET air concentration monitoring sites as of 2019.

Country	Site	Method	Parameter
Cambodia	Phnom Penh	AT*[2]	O_3, $PM_{2.5}$
		FP*[1]	SO_2, HNO_3, HCl, NH_3, PMC
China	Chongqing		
	- Jinyunshan	AT	SO_2, NO, NO_x*, PM_{10}
	Xiamen		
	- Hongwen	AT	SO_2, NO_2, PM_{10}
	Zhuhai		
	- Haibin-Park	AT	SO_2, NO_2, PM_{10}
	Wuzhishan	AT	SO_2, NO_2, PM_{10}
	Lijiang	AT	SO_2, NO_2, PM_{10}
Indonesia	Jakarta	AT	$PM_{2.5}$
		FP	SO_2, HNO_3, HCl, NH_3, PMC
		PS	SO_2, NO_2
	Serpong	FP	SO_2, HNO_3, HCl, NH_3, PMC
	Kototabang	PS	SO_2, NO_2
	Bandung	AT	O_3
		FP	SO_2, HNO_3, HCl, NH_3, PMC
		PS	SO_2, NO_2, NH_3, O_3
Japan	Rishiri	AT	SO_2, NO, NO_x*, O_3, $PM_{10/2.5}$
		FP	SO_2, HNO_3, HCl, NH_3, PMC
	Ochiichi	AT	SO_2, NO, NO_x*, O_3, $PM_{10/2.5}$
		FP	SO_2, HNO_3, HCl, NH_3, PMC
	Sado-seki	AT	SO_2, NO, NO_x*, O_3, $PM_{10/2.5}$
		FP	SO_2, HNO_3, HCl, NH_3, PMC
	Happo	AT	SO_2, NO, NO_x*, O_3, $PM_{10/2.5}$
		FP	SO_2, HNO_3, HCl, NH_3, PMC
	Ijira	AT	SO_2, NO, NO_x*, O_3, $PM_{10/2.5}$
		FP	SO_2, HNO_3, HCl, NH_3, PMC
	Oki	AT	SO_2, NO, NO_x*, O_3, $PM_{10/2.5}$
		FP	SO_2, HNO_3, HCl, NH_3, PMC
	Yusuhara	AT	SO_2, NO, NO_x*, O_3, $PM_{10/2.5}$
		FP	SO_2, HNO_3, HCl, NH_3, PMC
	Hedo	AT	SO_2, NO, NO_x*, O_3, $PM_{10/2.5}$
		FP	SO_2, HNO_3, HCl, NH_3, PMC
	Ogasawara	AT	SO_2, NO, NO_x*, O_3, $PM_{10/2.5}$
		FP	SO_2, HNO_3, HCl, NH_3, PMC
	Tokyo	FP	SO_2, HNO_3, HCl, NH_3, PMC
	Niigata-maki	AT	SO_2, NO, NO_x*, O_3
	Tsushima	AT	O_3, $PM_{10/2.5}$
Lao PDR	Vientiane	AT	NO, NO_2, NO_x, PM_{10}, $PM_{2.5}$
		FP*[1]	SO_2, HNO_3, HCl, NH_3, PMC
Malaysia	Petaling Jaya	FP*[1]	SO_2, HNO_3, HCl, NH_3, PMC
	Tanah Rata	FP*[1]	SO_2, HNO_3, HCl, NH_3, PMC
	Danum Valley	FP*[1]	SO_2, HNO_3, HCl, NH_3, PMC

Mongolia	Ulaanbaatar	AT	SO_2, NO, NO_2, NO_x, O_3, $PM_{10/2.5}$
		FP	SO_2, HNO_3, HCl, NH_3, PMC
	Terelj	FP	SO_2, HNO_3, HCl, NH_3, PMC
Myanmar	Yangon	AT	$PM_{2.5}$
		FP	SO_2, HNO_3, HCl, NH_3, PMC
	Mandalay	AT	$PM_{2.5}$
Philippines	Metro Manila	AT	NO, NO_2, NO_x, O_3, $PM_{10/2.5}$
		FP	SO_2, HNO_3, HCl, NH_3, PMC
	Los Baños	FP*[1]	SO_2, HNO_3, HCl, NH_3, PMC
	Mt. Sto. Tomas	FP*[1]	SO_2, HNO_3, HCl, NH_3, PMC
Republic of Korea	Kangwha	AT	SO_2, NO_2, O_3, $PM_{10/2.5}$
		FP	HNO_3, HCl, NH_3, PMC in $PM_{2.5}$
	Cheju	AT	SO_2, NO_2, O_3, $PM_{10/2.5}$
	(Kosan)	FP	HNO_3, HCl, NH_3, PMC in $PM_{2.5}$
	Imsil	AT*[2]	SO_2, NO_2, O_3, $PM_{10/2.5}$
		FP	HNO_3, HCl, NH_3, PMC in $PM_{2.5}$
Russia	Mondy	FP	SO_2, HNO_3, HCl, NH_3, PMC
		PS	O_3
	Listvyanka	FP	SO_2, HNO_3, HCl, NH_3, PMC
		PS	O_3
	Irkutsk	FP	SO_2, HNO_3, HCl, NH_3, PMC
		PS	O_3
	Primorskaya	FP	SO_2, HNO_3, HCl, NH_3, PMC
Thailand	Bangkok	AT	NO, NO_2, NO_x, O_3, $PM_{10/2.5}$
		FP	SO_2, HNO_3, HCl, NH_3, PMC
	Samutprakarn	AT	SO_2, NO, NO_2, NO_x, O_3, $PM_{10/2.5}$
	Pathumthani	FP*[1]	SO_2, HNO_3, HCl, NH_3, PMC
	Khanchanaburi*[1]	AT	SO_2, NO, NO_x*, O_3, $PM_{10/2.5}$
	(Vajiralongkorn Dam)	FP	SO_2, HNO_3, HCl, NH_3, PMC
	Chiang Mai		
	- Mae Hia	FP	SO_2, HNO_3, HCl, NH_3, PMC
	- Chang Phueak	AT	SO_2, NO, NO_2, NO_x, O_3, $PM_{10/2.5}$
	- Si Phum	AT	SO_2, NO, NO_2, NO_x, $PM_{10/2.5}$
	Nakhon Ratchasima		
	- Sakaerat	FP	SO_2, HNO_3, HCl, NH_3, PMC
	- Nai Mueang	AT*[2]	SO_2, NO, NO_2, NO_x, O_3, $PM_{10/2.5}$
Vietnam	Hanoi	FP	SO_2, HNO_3, HCl, NH_3, PMC
	Hoa Binh	AT	$PM_{2.5}$
		FP	SO_2, HNO_3, HCl, NH_3, PMC
	Can Tho	FP	SO_2, HNO_3, HCl, NH_3, PMC
	Ho Chi Minh	FP	SO_2, HNO_3, HCl, NH_3, PMC
	Yen Bai	FP	SO_2, HNO_3, HCl, NH_3, PMC

AT: Automatic Monitor, PS: Passive Sampler, FP: Filter pack, PMC: Particulate Matter Components.

NOx*: NOx measured by CLD in remote or rural sites.

Note: *1; 2-week intensive monitoring at Khanchanaburi site was implemented 3 times per year due to monitoring availability in the remote area.

There are different types of samplers to monitor the gas and aerosol pollutants. Filter pack method has been described as the most suitable method for monitoring gas and aerosol concentration in EANET. This is the reason why the Filter pack method is commonly used in most of the sites or used with other samplers. Passive samplers are used to monitor nitrogen oxides (NOx) and ozone (O_3) at several sites. Along with those samplers, the automatic air monitors have been introduced in some countries. Furthermore, the inferential method is applied for dry deposition measurement in EANET by the Task Force on Monitoring for Dry Deposition (TFMDD). The dry deposition flux is calculated by the product of atmospheric concentration and dry deposition velocity of each species under consideration. The deposition velocity is in turn estimated based on land surface properties and meteorological parameters. Direct flux observation has been conducted at selected sites on a research base for future improvement of the inferential method.

4.1.2 Review of previous PRSADs and highlight of this chapter

The concentrations of gaseous sulfur dioxide observed at EANET monitoring sites are presented in Fig. 4.1.2. Long-term averages of SO_2 concentration for the period 2000–2004 ranged widely from less than 0.5 ppb to more than 4.5 ppb. The sites with SO_2 concentrations greater than 3.5 ppb were located either in or near to urban areas. Besides these sites, the average SO_2 concentrations were at most 2.5 ppb, which is similar to SO_2 concentrations in the year 2000 at EMEP monitoring sites.

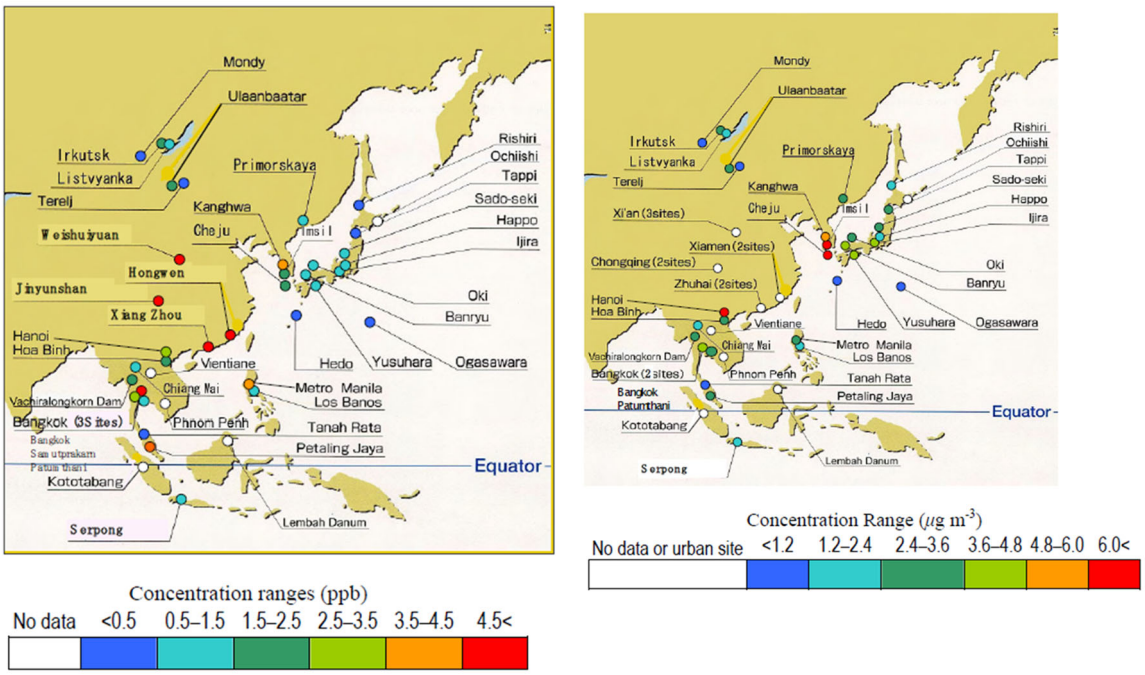

Figure 4.1.2 Spatial Distribution of annual SO_2 (Left) and particulate nss-SO_4^{2-} (Right) concentration (Average of 2000-04) [cited from PRSAD1].

Fig. 4.1.3 shows the average concentrations of sulfur- and nitrogen-containing species in both the aerosol and gaseous phases. These characteristics reflect both the importance of agricultural and natural sources of reduced atmospheric nitrogen in most areas and the significance of airborne sulfur transport to remote areas. It has been proposed that further studies investigate possible causes of these high concentrations measured at certain non-urban sites. PRSAD1 described the number of EANET monitoring sites with measurements of dry deposition (air concentrations) is not sufficient at present to be representative of the air quality in the respective cities or rural areas.

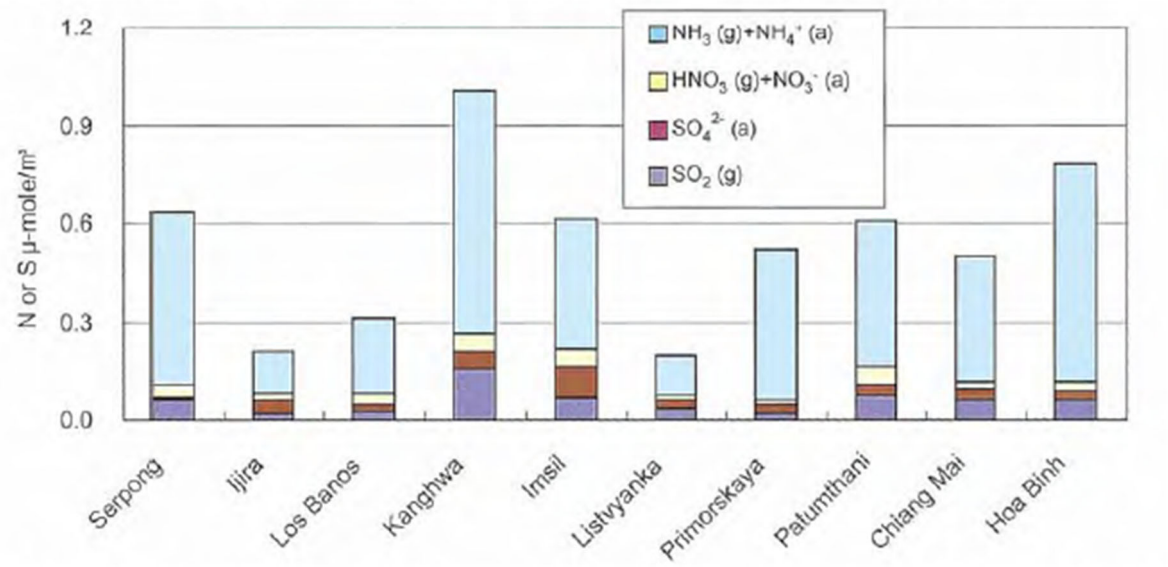

Figure 4.1.3 Average conc. of major acid and base compounds of sulfur and nitrogen at EANET rural monitoring sites in 2003 and 2004 [cited from PRSAD1].

Fig. 4.1.4 shows the spatial variation in the average annual SO_2 and PM_{10} concentrations at EANET sites from 2005 to 2009. In Northeast Asia, SO_2 at Jeju remote site were noticeably higher than those at the other remote sites within the East Asia region. Gas concentrations observed at the six EANET remote sites in Japan varied with increasing values from the monitoring sites from Rishiri site in the north down to Oki site in the south, except at the two-island southernmost remote sites, Hedo and Ogasawara, which showed very low concentrations. In Southeast Asia, the results of spatial variation analysis for air concentrations at most urban sites in South Asian regions for 2005 to 2009 showed NH_3 values that were generally three times higher than those for SO_2 suggesting that agriculture is a major activity in most Southeast Asian countries. PM_{10} concentrations are high at EANET sites in China, whereas it showed lower concentrations at Japanese EANET sites, most of which are classified as remote site. Moderate PM_{10} concentrations were observed at urban EANET sites in Thailand.

Fig. 4.1.5 shows the spatial variation of the five-year annual average of SO_2 from 2010 to 2014. High concentrations of SO_2 were observed at EANET sites in Russia, Mongolia, China, Thailand, and Indonesia. The highest five-year average SO_2 concentration from 2010–2014 was recorded at the Jinyunshan rural EANET site in China at 9.6 (7.6 – 12.9) ppb. However, the value was reduced 34% from the previous five-year average concentration, which is the highest reduction in SO_2 concentration at -0.46 ppb yr^{-1}. The sulfur components at all monitoring sites at EANET sites in China, Mongolia and Russia show distinctively seasonal cyclic pattern, which are low in the mid-summer and high during the winter period. Significant improvement of SO_2 concentration could have been linked to the pollution reduction policy applied in most of the cities in Southeast Asia. At EANET site in Jakarta, Indonesia, SO_2 concentration reduction ratio was -0.65 ppb yr^{-1}. However, concentration reduction of SO_4^{2-} is not enough in comparison with reduction of SO_2 concentration. In the Southeast Asia region, clear seasonal variation and the mutual relationship of SO_2 and sulfate was not recognized.

As shown in Fig. 4.1.6, SO_4^{2-} concentrations were found to be higher than NO_3^- and NH_4^+ at all urban sites. A high concentration of SO_4^{2-} can be seen in the middle latitudes (25-45° N) between 125-140° E, which corresponds to the Japanese remote sites and is due to the influence of sea salt.

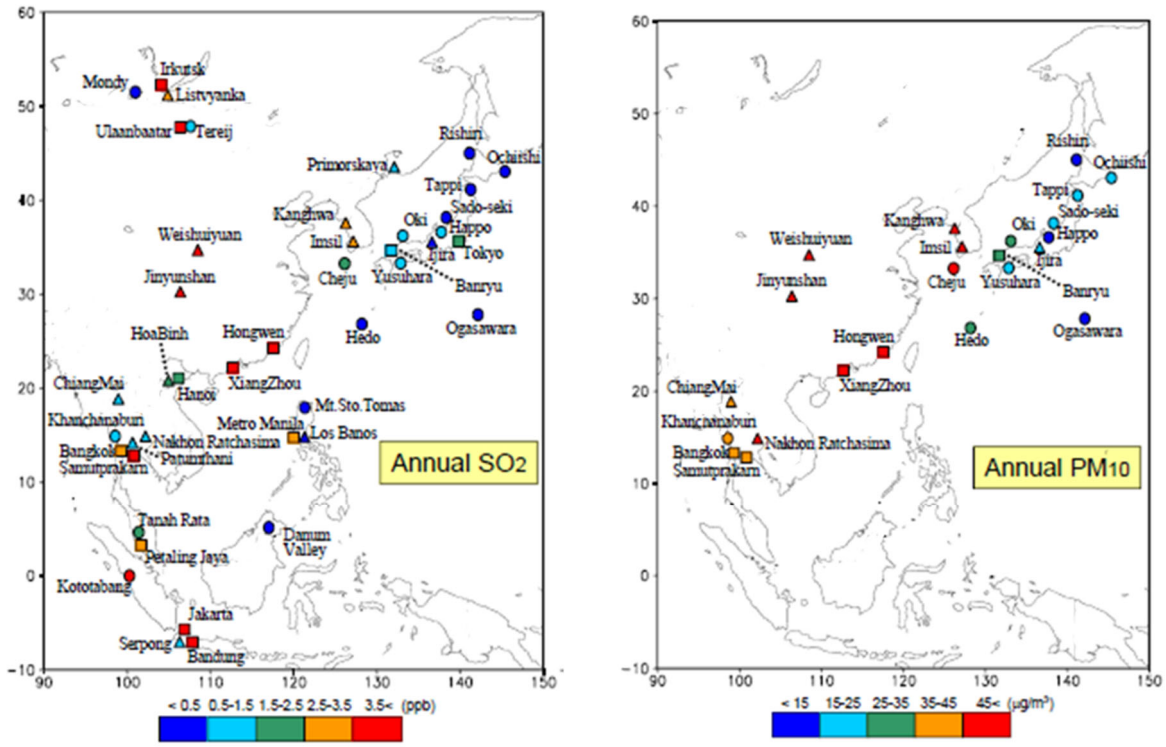

Figure 4.1.4 Spatial variation in the average annual SO_2 and PM_{10} conc. at EANET sites (2005-2009) [cited from PRSAD2].

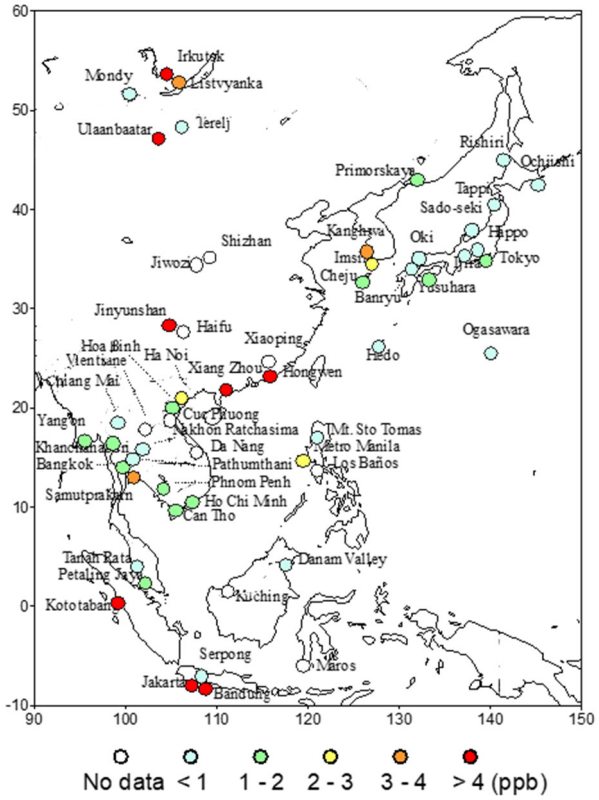

Figure 4.1.5 Spatial variation of the five-year annual average of SO_2 from 2010 to 2014 at EANET sites [cited from PRSAD3].

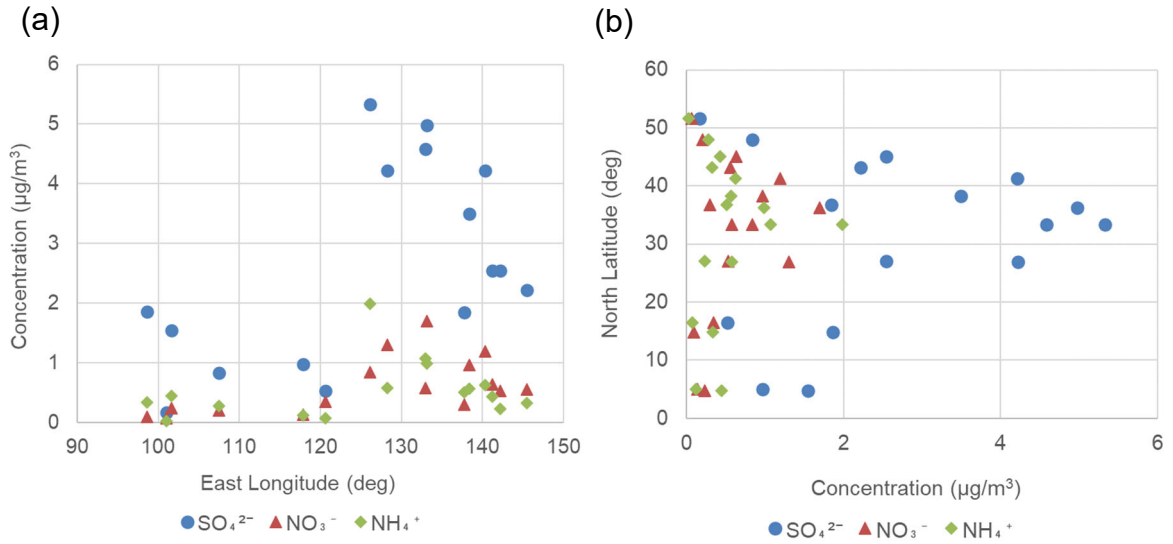

Figure 4.1.6 Spatial variation of the 5-year annual average of SO_4^{2-}, NO_3^- and NH_4^+ from 2010 to 2014 at remote site as a function of (a) longitude and (b) latitude [cited from PRSAD3].

The previous PRSADs showed clear regional characteristics of gas and aerosol concentrations in East Asia. Key discussions of this Chapter include the followings.

- How is the spatial variation of air concentrations in East Asia for recent 5 years (from 2015 to 2019)?
- How is the long term trends of gas and aerosol since beginning of EANET (from 2000 to 2019) and what factor may affect the trends?
- How is the current status of the gas and aerosol pollution in East Asia in relation with variations of atmospheric pollutant emissions? What is the important findings the state of air pollution in East Asia?

4.2 Spatial variation of air concentration

4.2.1 Geographical and climatic characteristics of EANET region

EANET countries are located on the eastern side of Eurasia continent, the Earth's largest and most diverse continent, and nearby islands. The enormous expanse of EANET region especially the huge latitudinal difference and its abundance of mountain and plateaus have resulted in great differences among regions in solar radiation, atmospheric circulation, precipitation, and climate as a whole, are subject overall to the world's widest climatic extremes.

The EANET region is dominated by a varied mix of climate regions. Subarctic, and temperate climates occur along the continent's northern and northeastern region; arid and highland climates occur in the region's interior and western parts; and tropical rainforest climates occur in southern region.

A continental climate, associated with large landmasses and characterized by an extreme annual range of temperature, prevails over a large part of Asia. In the mid-latitudes is the prevalent west wind as well as the isolating effect of the marginal mountain ranges. The influence of sea air from the Pacific Ocean extends only to the eastern margins of region. From the north, Arctic air has unimpeded access into the continent. In the south, tropical and equatorial air masses predominate, but their penetration to the center of Asia is restricted by the ridges of the mountainous belt stretching from the highlands of West Asia through the Himalayas to the mountains of southern China and

Southeast Asia; in the winter months (November through March), such penetration is further impeded by the density of the cold air masses over interior continent.

The diversity of climate and geography, in general, produce the most diverse forms of economic and energy consumption, as well as emissions of air pollutants. According to these significant spatial characteristic differences, analyses on dry deposition in the EANET regions are to be reported in two broadly classified as the Northeast and Southeast Asian sub-regions. In general, for the North-East Asian sub-region, the four seasons and the monsoon climate should be taken into account, as well as heating in winter. For South East Asia, the dry and rainy seasons are important climatic and meteorological factors.

Northeast Asia of EANET region comprises the eastern part of Russia, Mongolia, China, the Republic of Korea and Japan.

The Russian Far East under the influence of the Pacific Ocean has a monsoon climate that reverses the direction of wind in summer and winter, sharply differentiating temperatures. The climate of Russian Far East is characterized by frigid winters. The climate is Arctic or sub-Arctic for the northernmost part, a cold maritime for the east coast which has mild to warm summer. The average temperature in January is almost everywhere below -10 °C, and it goes down to -45 °C in the Eastern inland areas. The daily average in July is around freezing (0 °C) on the northern islands and along the Arctic coast, while it goes up to 20 °C in the southernmost areas. During winter, in most of the territory, the powerful Siberian Anticyclone dominates, except in the eastern seas, where the clashes between continental and maritime air masses give rise to intense low-pressure areas, which can bring heavy snowfalls.

During the long winter months, precipitation is scarce almost everywhere Owing to the greater availability of heat and energy, summer is almost everywhere the rainiest season, in fact, afternoon thunderstorms may occur in inland areas. On the other hand, the south-eastern areas receive even more rainfall in summer because they are affected by the Asian monsoon. In most of Siberia, yearly precipitation is between 150 and 500 mm. In the Far East, the Kamchatka peninsula is the wettest region of mainland Siberia: in some areas, precipitation exceeds 1,000 mm yr^{-1}, and a lot of snow can fall in winter.

The geography of Mongolia is varied, with the Gobi Desert to the south and cold, mountainous regions to the north and west. The whole of Mongolia is considered to be part of the Mongolian Plateau. The highest point in Mongolia is the Khüiten Peak in the far west at 4,374 m (14,350 ft). Most part of Mongolia consists of the Mongolian-Manchurian grassland steppe, with forested areas accounting for 11.2% of the total land area. Mongolia is high, cold and windy. It has an extreme continental climate with long, cold winters and short summers. Most of the country is hot in the summer and extremely cold in the winter, with January averages dropping as low as −30 °C. The annual average temperature in Ulaanbaatar is −1.3 °C, making it the world's coldest capital city. The country is usually at the center of a region of high atmospheric pressure and has averages 257 cloudless days a year. During summer the most of annual precipitation falls. Precipitation is highest in the north (average of 200 to 350 mm yr^{-1}) and lowest in the south, which receives 100 to 200 mm annually.

For China, the climate is extremely diverse; subtropical in the South to subarctic in the North. Tremendous differences in latitude, longitude, and altitude give a rise to sharp variations in precipitation and temperature within China, inducing complex climatic patterns.

The Korean Peninsula under the monsoon influence has a temperate climate with four distinct seasons. The movement of air masses from the Asian continent exerts greater influence on the Southern Korea's weather. About 74% of Japan is mountainous, with a mountain range running through each of the main islands and scattered plains and inter mountain basins.

Japan belongs to the temperate zone with four distinct seasons. Japan is generally a rainy country with high humidity. These are all climatic information of the Northeast Asian region.

Southeast Asia of EANET region lies on two geographic regions. Continental Southeast Asia comprises Cambodia, Laos, Myanmar, Thailand, Vietnam and Peninsular Malaysia, and Maritime Southeast Asia comprises Indonesia and the Philippines. The climate in Southeast Asia is mainly tropical and sub-tropical –hot and humid all year round with plentiful rainfall. Southeast Asia has a wet and dry season caused by seasonal shift in winds or monsoon. The tropical rain belt causes additional rainfall during the monsoon season and Typhoons sometimes hit the eastern part of the region and can cause heavy rain, flooding and damage. However, the mountain areas in the Northern region (Laos and Myanmar) and Southern region (Indonesia and Malaysia) have milder temperatures and drier climate.

4.2.2 Spatial distribution of SO_2, NO_2, NOx, O_3, PM_{10}, $PM_{2.5}$ (criteria air pollutants)

Fig. 4.2.1 shows the average concentrations of SO_2, NO_2, NOx, O_3, PM_{10}, $PM_{2.5}$ in each EANET country from 2015 to 2019. The spatial distribution of SO_2 at EANET sites in Russia and Mongolia, located in the northernmost part of Asia, is uneven. Listvyanka and Irkutsk in Russia have high concentrations, with 5-year averages of 2.84 ppb and 4.00 ppb, respectively, while Mondy and Primorskaya have only 0.18 ppb and 0.44 ppb. Ulaanbaatar in Mongolia has high SO_2 concentrations for many years, with a 5-year average of 9.10 ppb, the highest in the whole region of EANET, while Terelj has only 0.30 ppb. This significant difference in spatial distribution of concentration shows the influence of population distribution, as well as the effect of heating and fuel composition such as coal burning.

After continuous improvement, the SO_2 concentrations at EANET sites in China have significantly decreased, from a range of 3.9-7.5 ppb in 2014 to 0.1-2.9 ppb in 2019 for the 5 stations. The 5-year average range for the 5 stations is 0.1-3.54 ppb.

The SO_2 concentrations at all EANET sites in Japan are very low for a long time, with a 5-year average range of 0.03-1.3 ppb and the maximum value occurring in Tokyo. The SO_2 concentration range at the three EANET land sites in Republic of Korea was similar to that of China, with a 5-year average range of 0.66-2.44 ppb. The SO_2 concentration range at Cheju was similar to that of Japan, with a 5-year average of only 0.66 ppb.

Except for Indonesia, SO_2 concentrations at EANET sites in Southeast Asian countries are generally low. For 5-year average concentration, Phnom Penh of Cambodia is 0.80 ppb; Vientiane of Lao PDR is 0.4 ppb; 3 stations of Malaysia had a range of 0.05-1.20 ppb; Yangon of Myanmar was 0.58 ppb; the 3 stations in Philippines have a range of 0.15-0.40 ppb; the 9 stations in Thailand have a range of 0.46 ppb-1.90 ppb; the 5 stations in Vietnam have a range of 0.52-1.64 ppb. Higher SO_2 concentrations were found in Indonesia with 4 stations with 5-year average concentrations ranging from 0.88 ppb-5.58 ppb, while Jakarta reported the highest 5-year average of 5.58 ppb.

Among the ozone observations from 2015 to 2019 at EANET sites in eight countries of Cambodia, Indonesia, Japan, Mongolia, Philippines, Republic of Korea, Russia, and Thailand, Republic of Korea had the highest nationwide O_3 5-year average concentration of 40.5 ppb from 3 stations, with 44 ppb at Kangwha and Cheju stations and 33 ppb at Imsil. Japan reported the next highest nationwide averaged O_3 concentration from 13 stations with a 5-year average concentration range of 26-49 ppb. The 5-year average concentrations from 6 stations in Thailand range from 19 ppb to 27 ppb, while the 5-year average concentration of remaining countries are 18pp at Phnom Phenh in Cambodia,14 ppb at Bandung station in Indonesia, 11.4 ppb at Ulaanbaatar in Mongolia, and 8.5 ppb at Metro Manila in Philippines.

Among the NOx observations from 2015 to 2019 at EANET sites in six countries of China, Japan, Lao PDR, Malaysia, Mongolia, Philippines and Thailand, Ulaanbaatar site of Mongolia had the

highest NOx 5-year average concentration of 55.0 ppb. Metro Manila in Philippines reported the next highest 5-year averaged NOx concentration of 30.1 ppb. The 5-year averaged NOx concentrations are 22.4 ppb at Vientiane in Lao PDR and 14.7 ppb at Jinyunshan in China, respectively.

The 5-year average NOx concentrations of 6 EANET stations in Thailand has a range of 3.2-30.0 ppb. The nationwide average NOx concentrations of 12 stations in Japan has a range of 0.4-2.1 ppb, which is lower than other countries and has a small variation among sites.

Among the NO_2 observations from 2015 to 2019 at EANET sites in eight countries of China, Indonesia, Japan, Lao PDR, Mongolia, Philippines, Republic of Korea and Thailand, there are large spatial differences in the distribution of NO_2 concentrations. Indonesia has the highest NO_2 concentration level with a 5-year average concentration of 8.82 ppb, having an uneven spatial distribution with 5-year average concentrations of 46.2 ppb and 25.0 ppb at Bandung and Jakarta stations respectively, and only 1.1 ppb at Kototabang station. Similarly, the total 5-year average NO_2 concentration of four stations in China was 7.75 ppb, with higher concentrations of 14.1 ppb and 15.4 ppb at Hongwen site and Haibin-Park site and low concentration, only 0.9 ppb and 0.6 ppb at remote sites of Wuzhishan and Lijiang stations.

The NO_2 concentration at EANET sites in Republic of Korea were low and more uniformly distributed, with NO_2 concentrations ranging from 3.5 ppb to 6.0 ppb at the three stations. The concentrations of the six EANET stations in Thailand ranged from 8.6 ppb to 18.1 ppb, with small difference in concentration distribution.

Among the $PM_{2.5}$ observations from 2015 to 2019 at EANET sites in ten countries of Cambodia，Indonesia， Japan, Lao PDR, Mongolia, Myanmar, Philippines, Republic of Korea, Thailand, Vietnam, Mongolia had high $PM_{2.5}$ 5-year average concentration of 40.5 μg/m^3 at Ulaanbaatar of Mongolia. Jakarta of Indonesia reported high nationwide averaged $PM_{2.5}$ concentration of 41.0 μg/m^3. The $PM_{2.5}$ concentration in Hoa Binh of Vietnam is close to that of Jakarta of Indonesia, with a 5-year average concentration of 39.4 μg/m^3.

The 5-year average $PM_{2.5}$ concentrations at EANET sites in remaining countries are 20 μg/m^3 at Phnom Phenh in Cambodia, 32 μg/m^3 at Vientiane of Lao PDR, 29.4 μg/m^3 of Myanmar, 19 μg/m^3 at Metro Manila in Philippines, 16-30 μg/m^3 from 6 stations in Thailand. The nationwide average $PM_{2.5}$ concentrations of 12 stations is 9.06 μg/m^3 in Japan which is significantly lower than other countries.

Among the PM_{10} observations from 2015 to 2019 at EANET sites in seven countries of China, Japan, Lao PDR, Mongolia, Philippines, Republic of Korea and Thailand, there are large spatial differences in the distribution of PM_{10} concentrations. Ulaanbaatar of Mongolia has the highest PM_{10} concentration level with a 5-year average concentration of 110 μg/m^3. Vientiane of Lao PDR has the second highest PM_{10} concentration with 5-year average of 72 μg/m^3.

The PM_{10} concentration levels of EANET sites in China, Korea, the Philippines, and Thailand were similar. The 5-year average PM_{10} concentrations at four stations in China ranged from 8 to 48 μg/m^3 with the average concentration of 30.7 μg/m^3. The 5-year average PM_{10} concentrations at three stations in Korea, including Jeju Island, ranged from 8 to 48 μg/m^3 with the average concentration of 31.0 μg/m^3. The annual average PM_{10} concentration at Metro Manila of Philippines was 31 μg/m^3. The 5-years average PM_{10} concentrations at six stations in Thailand ranged from 28 to 51 μg/m^3 with the average concentration of 41.37 μg/m^3.

The 5-year nationwide average PM_{10} concentrations of 12 EANET stations in Japan has a range of 8-30 μg/m^3, with the average concentration of 19.9 μg/m^3, which is generally low and has a relatively large variation among sites.

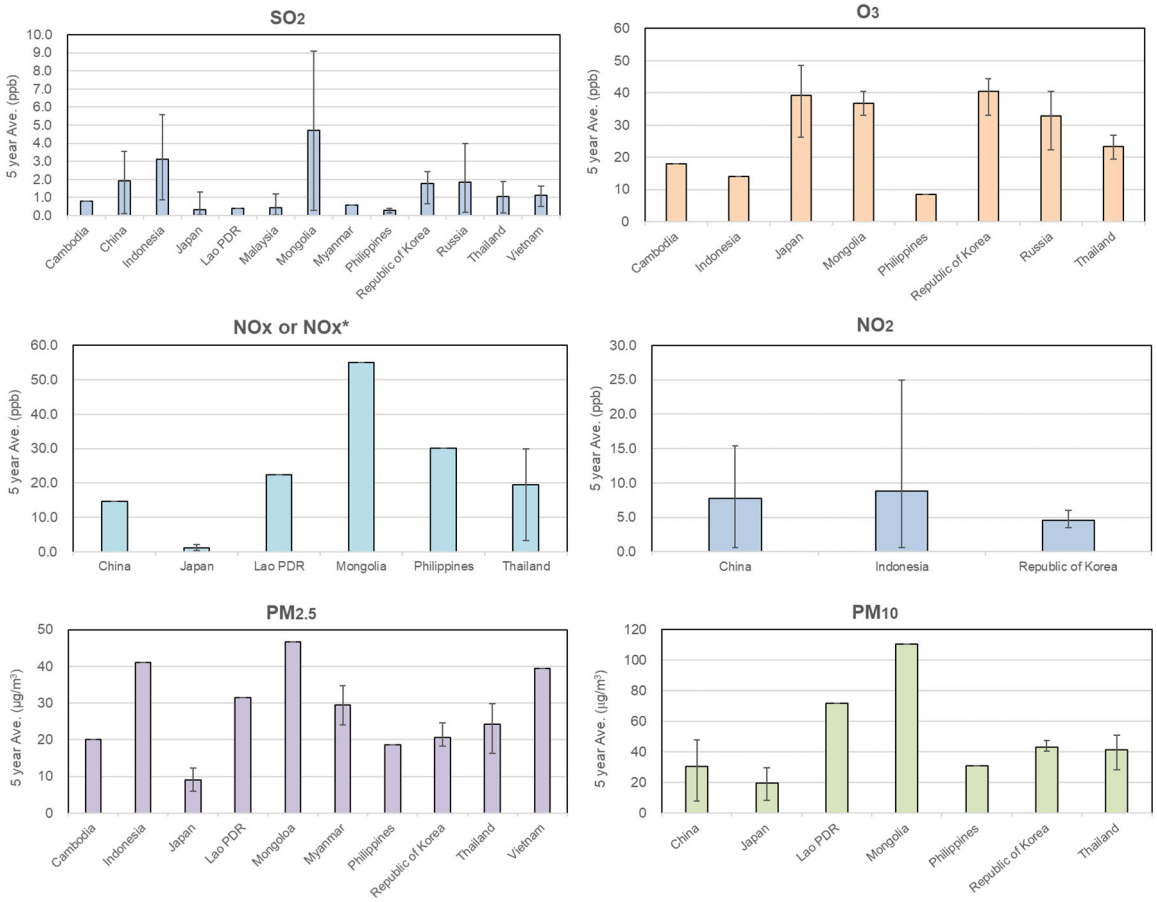

Figure 4.2.1 5-year average concentrations of SO_2, NO_2, NOx, O_3, PM_{10}, $PM_{2.5}$ at the monitoring sites of EANET in each country (Average from 2015 to 2019). Error bars denote standard deviations of all site data in each country.

4.2.3 Regional characteristics of SO_2, O_3, NOx/NO_2, $PM_{2.5}$, PM_{10}

The distribution of 5-year averages SO_2, NO_2, NOx, O_3, PM_{10}, $PM_{2.5}$ concentrations in the EANET region is shown in Fig. 4.2.2, and spatial variations of SO_2, NO_2, NOx, O_3, PM_{10}, $PM_{2.5}$ gas concentrations of at EANET remote sites as a function of longitude and latitude are shown in Fig. 4.2.3. It can be seen from the figures, the high SO_2 values in the EANET region are found in Mongolia and Russia in the north, where the 5-year average concentrations range from 1.86 ppb to 4.70 ppb, which is possibly related to the local coal combustion and winter heating. Other high SO_2 areas in the region occur at individual sites such as Indonesia Jakarta, Bundung and Jinyunshan in southwest China, which may be caused by the high sulfur content in local coal.

The SO_2 concentrations at other EANET stations in the region are generally low, especially for Republic of Korea and Japan in Northeast Asia with a 5-year average concentrations range of 0.03-1.3 ppb. The 5-year average SO_2 concentrations at stations in Southeast Asia countries of Myanmar, Thailand, Lao PDR and Vietnam range from 0.40 ppb to 1.14 ppb.

The distribution of O_3 concentrations at EANET sites is spatially different in Russia and Mongolia, which are located in the northern part of the EANET region, with concentrations ranging from 11 ppb to 40 ppb at four stations, and the maximum values are not found in the cities of Ulaanbaatar of Mongolia and Irkutsk of Russia, but in Mondy and Listvyanka of Russia. Unlike other pollutants, East Japan also has high overall ozone concentrations, with 5-year average concentrations of O_3 at 13 stations ranging from 26 ppb to 49 ppb, with a maximum value of 49 ppb at the Happo station.

O_3 concentrations in Indonesia are generally lower, with concentrations ranging from 8.5 ppb to 23.4 ppb.

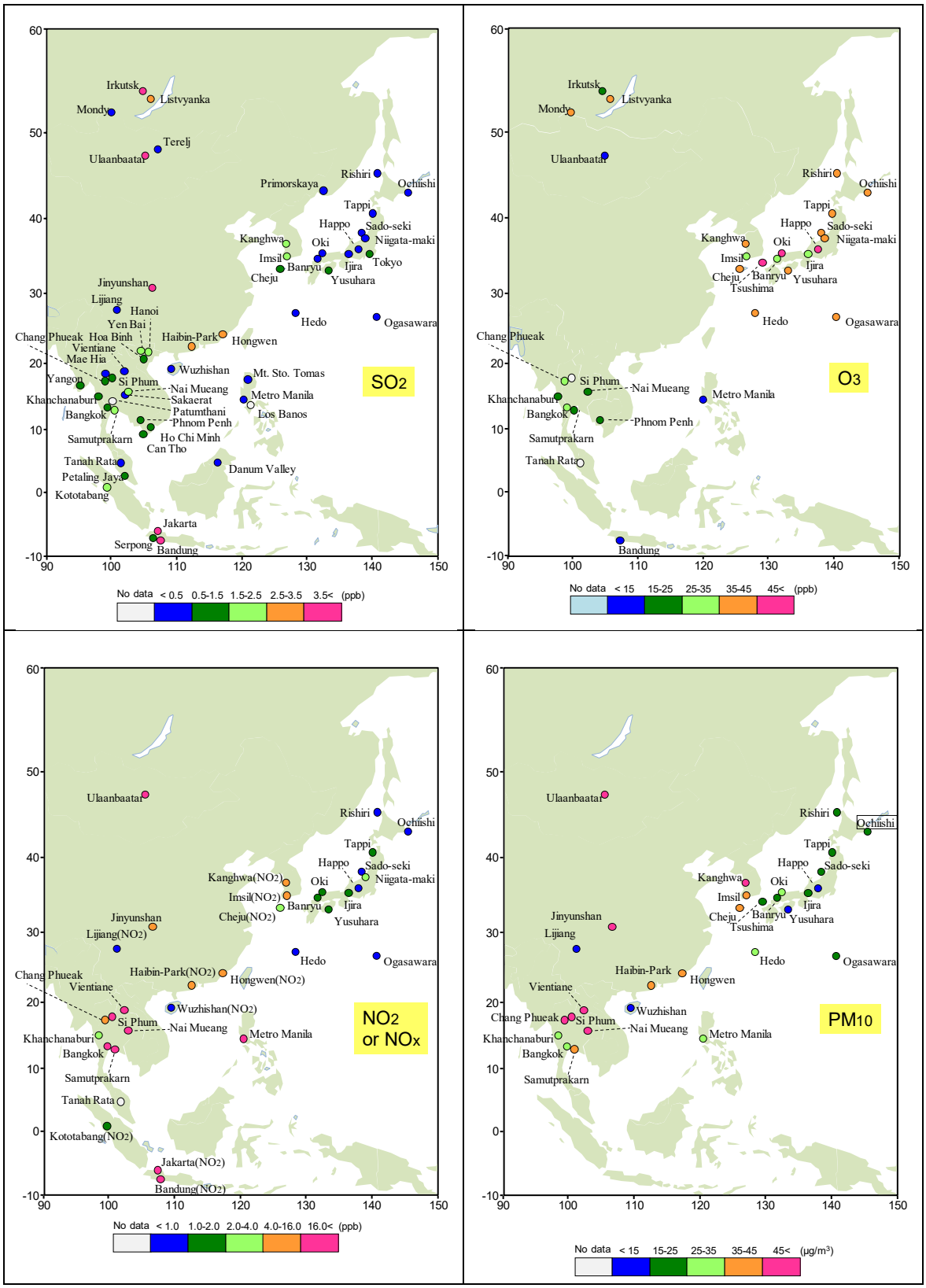

Figure 4.2.2 Spatial variations of gas and aerosol concentrations (SO_2, O_3, NO_2, NOx, PM_{10}, $PM_{2.5}$) at EANET sites. (5-year average from 2015 to 2019).

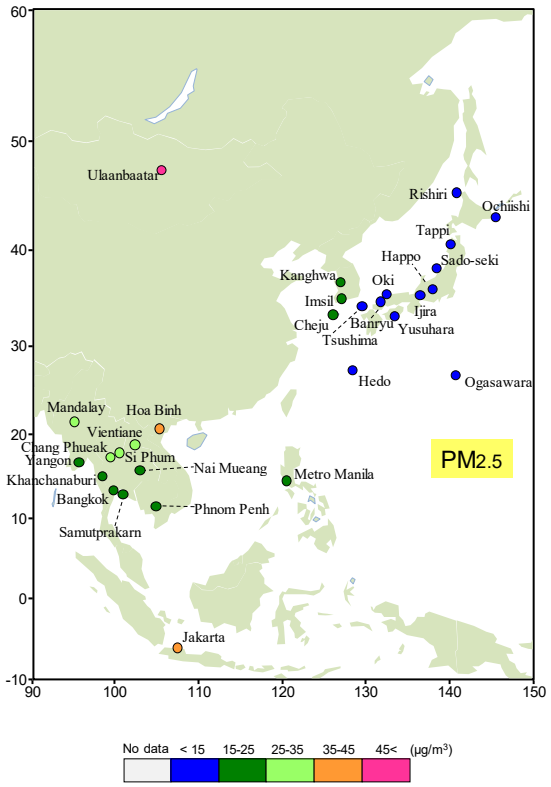

Figure 4.2.2 Spatial variations of gas and aerosol concentrations (SO_2, O_3, NO_2, NOx, PM_{10}, $PM_{2.5}$) at EANET sites. (5-year average from 2015 to 2019), Continued.

Despite the lack of data for adequate regional representation, it can be found generally that EANET sites in Japan and Russia have shown relatively high O_3 concentration level. The spatial differences in the northern part of the EANET region are large, with concentrations ranging from 11 ppb to 40 ppb at four sites of Russia and Mongolia and the maximum values occurring at Mondy and Listvyanka of Russia, not at the cities Ulaanbaatar of Mongolia and Irkutsk of Russia.

Unlike for other pollutants, EANET sites in Japan has relatively high ozone concentrations, with 5-year average concentrations of O_3 at 13 stations ranging from 26 ppb to 49 ppb and a maximum of 49 ppb at the Happo station. The concentrations of O_3 at EANET sites in Southeast Asia are generally lower in Philippines, Thailand, and Indonesia, with a range of 8.5-23.3 ppb.

The 5-year average NO_2 and NOx concentrations at the EANET sites are shown in Fig. 4.2.2. It can be seen that the highest NOx concentration of EANET region is found in Ulaanbaatar of Mongolia with a 5-year average concentration of 55.0 ppb. Southeast Asian sites, especially large cities such as Bangkok of Thailand, Metro Manila of Philippine, Jakarta of Indonesia, have relatively high NOx/NO_2 concentrations. The overall NO_2 and NOx concentrations in Japan are relatively low.

The overall $PM_{2.5}$ concentrations of EANET sites are low except for Ulaanbaatar of Mongolia, which shows a high concentration of 47μg/m^3. Hoa Binh of Vietnam and Jakarta of Indonesia showed higher $PM_{2.5}$ concentrations in Southeast Asia with a-year averaged concentration of 39 μg/m^3 and 41 μg/m^3. The remaining countries of Myanmar, Philippines, Thailand, and Lao PDR had a lower concentrations level ranging from 18.5 μg/m^3 to 31.5 μg/m^3. The overall concentrations in Japan and Korea are low, with their 5-year average concentrations of 9.06 μg/m^3 and 20.6 μg/m^3, respectively.

In addition to $PM_{2.5}$, PM_{10} also contains coarse particles, which are influenced by wind blow dust and sand storm. The highest 5-year average PM_{10} concentration in all EANET sites was 110 μg/m^3 at Ulaanbaatar, Mongolia, showing the influence of dust and sand storm. The higher PM_{10}

concentrations can be found Southeast Asia showing the influence of anthropogenic activities such as construction and traffic dust. 9 sites in Philippines, Thailand, and Lao PDR show generally higher concentrations than other regions, with concentrations ranging from 31.0 to 72.0 μg/m^3. The PM_{10} data in China stations show a wide range of concentrations between 8-48 μg/m^3. The highest PM_{10} concentration in Korea was similar to that of China, at 47.0 μg/m^3. PM_{10} concentration of Japan, on the other hand, is relatively low, with a 5-year average concentration range of 8.00-30.0 μg/m^3.

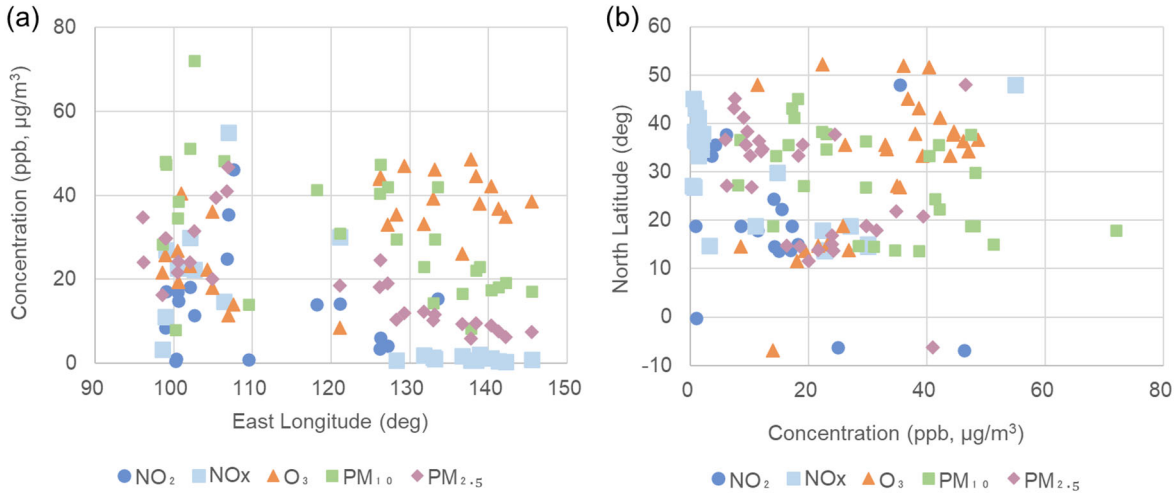

Figure 4.2.3 Spatial variations of gas and aerosol concentrations (NO_2, NOx, O_3, PM_{10}, $PM_{2.5}$) at EANET remote sites as a function of (a) longitude and (b) latitude. (5-year average from 2015 to 2019).

4.2.4 Spatial distribution of gas phase HNO_3, NH_3, HCl

Fig. 4.2.4 shows the average concentrations of HNO_3, NH_3 and HCl in each EANET country from 2015 to 2019. The concentration of HNO_3 at Hongwen station in China, is relatively high during the period from 2015 to 2019, ranging from 1.1 ppb to 1.2 ppb, with a 5-year average value of 1.15 ppb. The concentration at the EANET sites in Indonesia is the second highest in EANET region with a more consistent concentration distribution, the 5-year averaged HNO_3 concentration of 3 stations ranges from 0.62 ppb to 1.14 ppb during the period of 2015-2019.

The spatial distribution of HNO_3 concentrations at EANET sites in Japan and Malaysia showed a large fluctuation, with the 5-year average HNO_3 concentrations at 12 stations in Japan ranging from 0.03 ppb to 0.62 ppb. The 5-year average HNO_3 concentration at Petaling Jaya in Malaysia was 0.63 ppb, while those at Tanah Rata and Danum Valley were only 0.06 ppb. These variations would be caused by the spatial difference in population distribution and emission and atmospheric chemistry in Japan and Malaysia.

The HNO_3 concentrations at EANET sites in the rest of the countries are generally low, with the 5-year average concentration of 0.05 ppb in Mongolia, 0.09 ppb in Philippines, 0.09 ppb in Russia with a range of 0.04-0.17 ppb, 0.25 ppb in Myanmar with a range of 0.2-0.3 ppb, 0.25 ppb in Lao PDR, 0.47 ppb in Cambodia, and 0.40 ppb in Thailand. The HNO_3 5-year average concentration of 3 stations of Republic of Korea had a range of 0.19-0.14 ppb.

Ammonia affects particulate formation in the atmosphere as ammonium component and the acidity of deposition. Most EANET countries are agricultural countries where fertilizer use and livestock breeding are common practice. In Mongolia, as well as in China, there are also large pastoral areas. At the same time, population hygiene conditions in city and countryside, as well as ammonia escape

during denitrification of industrial and mobile sources can also affect ammonia concentrations. Generally, the atmosphere of most EANET countries can be classified as ammonia-rich condition.

There are various NH_3 concentration distributions in East Asia. Firstly, the spatial distribution of NH_3 in Philippines, Malaysia and Mongolia has a large variation. The 5-year average concentration at Metro Manila EANET station in Philippines is 13.20 ppb, while the average concentration at Mt. Sto. Tomas station is only 1.91 ppb.

Petaling Jaya EANET station had the highest 5-year average concentration of 9.61 ppb among the three stations in Malaysia, while Tanah Rata and Danum Valley stations had lower 5-year average concentrations of 1.23 ppb and 2.38 ppb. Ulaanbaatar station in Mongolia had a 5-year average concentration of 8.0 ppb and Terelj station with a 5-year average concentration of 1.70 ppb.

The NH_3 concentration at the Hongwen site in China is relatively high, with the average concentration of 9.99 ppb over 5-year. The 5-year average NH_3 concentration at the following three EANET stations in Indonesia ranged from 8.76 ppb to 9.18 ppb, with an overall average of 9.23 ppb. The 5-year average concentration at Cambodia EANET station was 7.20 ppb, the average NH_3 concentration at four EANET stations in Thailand ranged from 4.48 ppb to 8.85 ppb, and the average 5-year concentration at three stations in Republic of Korea ranged from 1.96 ppb to 7.70 ppb.

The other countries reported lower NH_3 concentrations for the 5 years. The 5-year average NH_3 concentration at the Yangon EANET station in Myanmar was 4.93 ppb, the 5 EANET stations in Vietnam had average NH_3 concentrations ranging from 1.42 ppb to 4.28 ppb with an overall average of 3.16 ppb, the Vientiane EANET station in Lao PDR had an average NH_3 concentration of 2.64 ppb, four EANET stations in Russia had average concentrations ranging from 1.18 ppb to 2.84 ppb. Ammonia concentrations in Japan were generally low, with a 5-year average of only 0.97 ppb at 12 EANET stations.

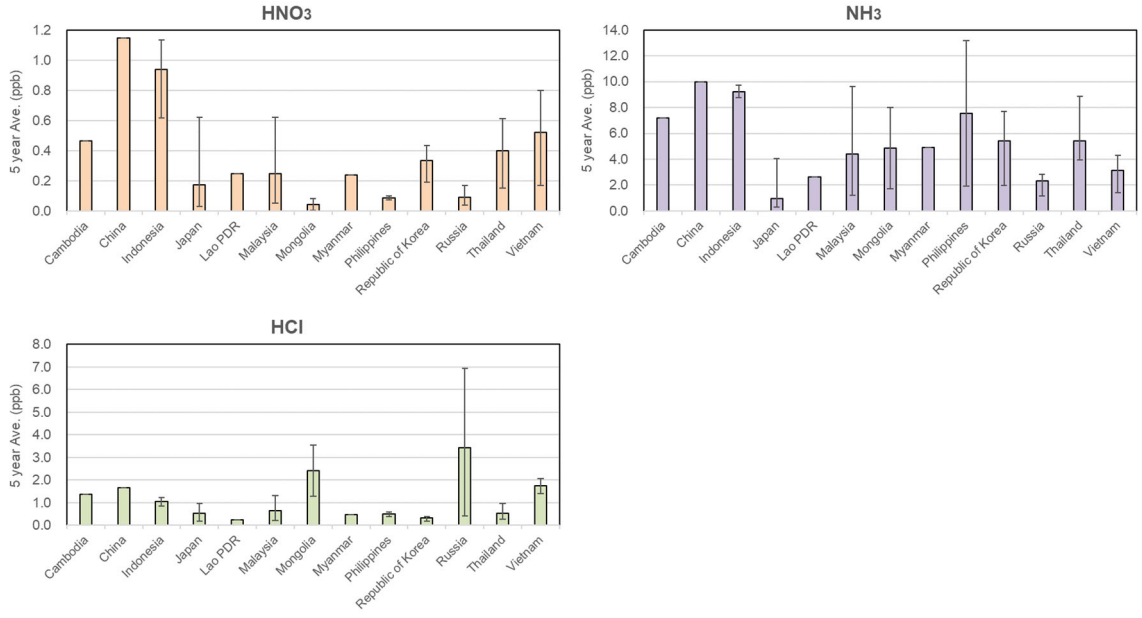

Figure 4.2.4 5-year average concentrations of HNO_3, NH_3 and HCl at the monitoring sites of EANET in each country (5-year average from 2015 to 2019).
Error bars denote standard deviations of all site data in each country.

Among the EANET countries, the highest HCl concentration is found in Russia with a 5-year average concentration of 3.43 ppb and with a large difference in the geospatial distribution. The average concentrations at Listvyanka and Irkutsk stations are 6.94 ppb and 4.40 ppb, while the 5-year average

concentrations at Mondy and Primorskaya stations are lower with 1.96 ppb and 0.42 ppb, respectively. The second highest concentration of HCl in the EANET region is found in Mongolia, where the 5-year average concentrations range from 1.30 ppb to 3.55 ppb.

The remaining countries have relatively similar lower HCl concentrations level. The 5-year average concentrations at EANET sites are 0.66 ppb in Malaysia, 0.53 ppb in Japan, 0.52 ppb in Thailand, 0.50 ppb in Philippines, 0.48 ppb in Myanmar and 0.25 ppb in Lao PDR. The differences among the three EANET stations in Republic of Korea were not significant, with 5-year average concentrations ranging from 0.20 to 0.48 ppb and average concentration of 0.33 ppb.

4.2.5 Regional characteristics of HNO_3, NH_3 and HCl

The distribution of 5-year average HNO_3, NH_3 and HCl concentrations in the EANET region is shown in Fig. 4.2.5, and spatial variations of HNO_3, NH_3 and HCl gas concentrations at EANET remote sites as a function of longitude and latitude are shown in Fig. 4.2.6. Atmospheric HNO_3 is mainly the secondary product of atmospheric chemical transformation and is easily removed by chemical transformation to nitrate and by dry and wet processes. Therefore, its concentration distribution is influenced by NOx emission, atmospheric chemical processes and removal processes.

Generally, there is an increasing trend of HNO_3 concentration in the EANET region from north to south. The HNO_3 concentrations are higher in Southeast Asian countries, such as Lao PDR, Myanmar, Cambodia and Vietnam, with 5-year average concentrations ranging from 0.24 ppb to 0.52 ppb. The HNO_3 concentrations in the northern EANET region such as Russia and Mongolia were significantly lower than those in other regions, with concentrations ranging from 0.05 ppb to 0.09 ppb. Republic of Korea and Japan have regional characteristics due to the population distribution, and the average concentration range is 0.18 ppb-0.34 ppb.

NH_3 is easy removed by dry and wet deposition due to its solubility in water. At the same time, NH_3 is easy to transform to ammonium salt aerosols such as sulfate and nitrate through gas-phase and liquid-phase non-homogeneous chemical reactions. Therefore, NH_3 could not transported over long distances and the NH_3 concentration is mainly affected by local emission such as agriculture, animal husbandry, population health conditions, and industrial and traffic emission including denitrification leaks.

There are no clear characteristics of spatial NH_3 concentrations distribution in Asia. High values of NH_3 in the EANET region occur mainly in large cities, indicating the influence of human activities and industrial distribution such as Ulaanbaatar of Mongolia, Hongwen of Xiamen city in China, Metro Manila of Philippine, Bangkok of Thailand, all 3 sites including Jakarta of Indonesia, Phnom Penh of Cambodia with a high concentration level of range of 7.20-13.20 ppb. Japan is lower overall for all sites, but Tokyo is also slightly higher than the other sites with 4.04 ppb.

There are no clear regional characteristics of HCl concentrations in EANET region. High values tend to occur at individual sites, such as Listvyanka and Irkutsk in Russia, Ulaanbaatar in Mongolia in the north, with 5-year average concentrations of 6.94 ppb, 4.40 ppb and 3.55 ppb, respectively. There are slight differences among the HCl concentrations in Southeast Asia, with Vietnam being relatively higher, with a concentration range of 1.40-2.06 ppb.

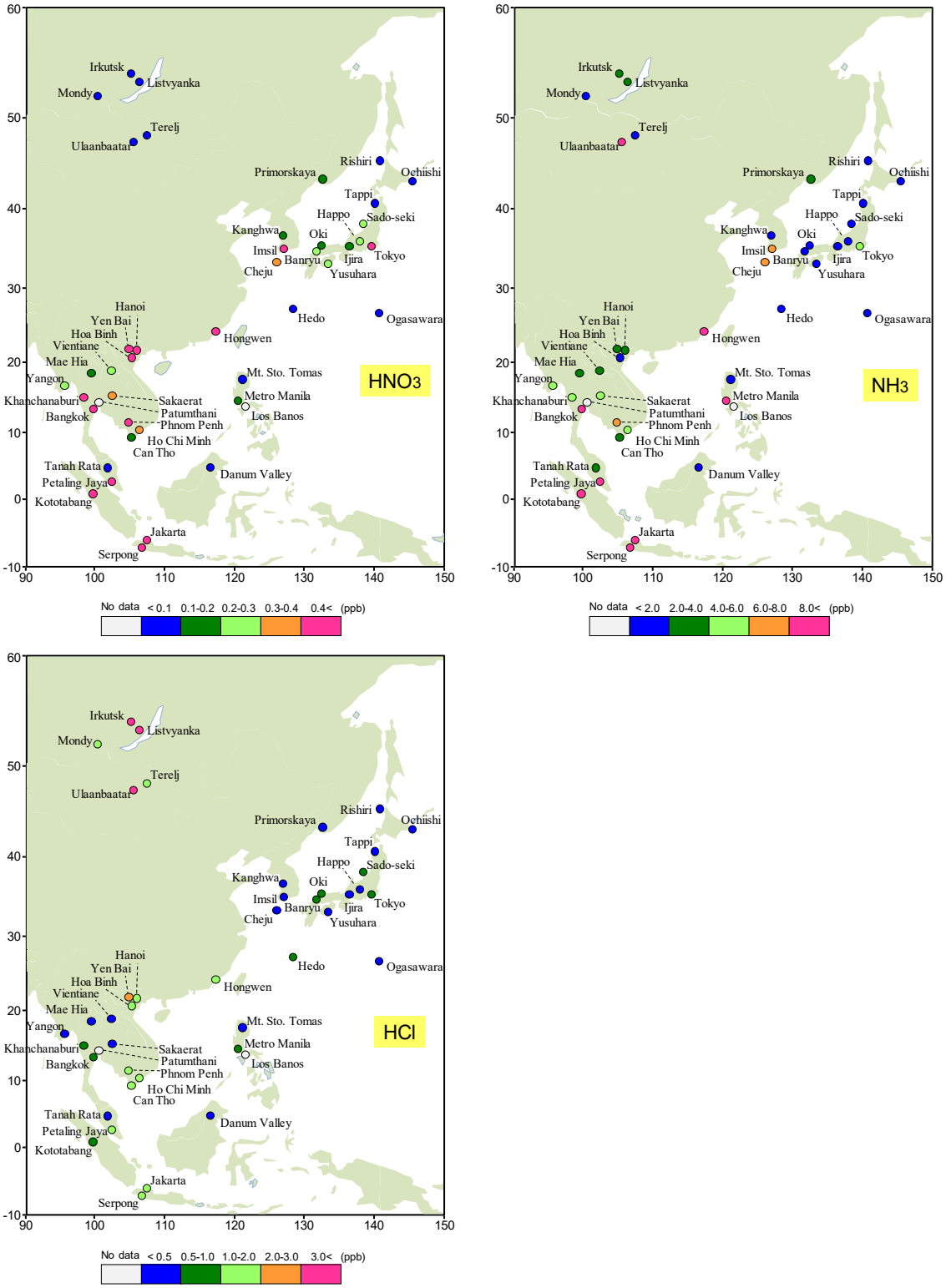

Figure 4.2.5 Spatial variations of gas concentrations (HNO_3, NH_3 and HCl) at EANET sites. (5-year average from 2015 to 2019).

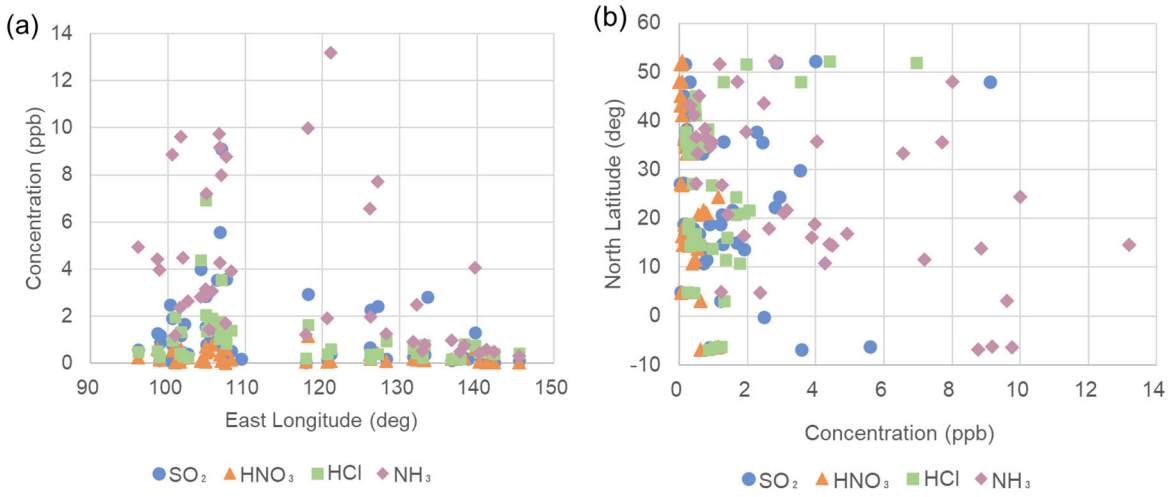

Figure 4.2.6 Spatial variation of gas concentrations (SO_2, HNO_3, NH_3 and HCl) at EANET remote sites as a function of (a) longitude and (b) latitude. (5-year average from 2015 to 2019).

4.2.6 Spatial distribution of SO_4^{2-}, NO_3^-, NH_4^+ and Ca^{2+} component in PM

Fig. 4.2.7 shows the average concentrations of SO_4^{2-}, NO_3^-, NH_4^+ and Ca^{2+} in each EANET country from 2015 to 2019. The highest SO_4^{2-} concentration was found at Hongwen of China, the only station reported data, with the 5-year average SO_4^{2-} concentration of 10.0 μg/m^3. The second highest 5-year averaged SO_4^{2-} concentration was found in Vietnam with the average of 5.59 μg/m^3 and a range of 3.89-7.46 μg/m^3 for the 5 stations, showing some differences in spatial distribution.

The 5-year average SO_4^{2-} concentrations of the remaining EANET countries were relatively low. The 5-year average SO_4^{2-} concentrations at Phnom Penh of Cambodia was 1.95 μg/m^3. The 5-year average SO_4^{2-} concentrations at 3 stations of Indonesia ranged from 4.66 μg/m^3 to 5.34 μg/m^3. 5-year average SO_4^{2-} concentrations at Vientiane of Lao PDR was 4.26 μg/m^3. 5-year average SO_4^{2-} concentrations at 3 stations in Malaysia ranged from 1.18 μg/m^3 to 3.66 μg/m^3. The 5-year average SO_4^{2-} concentrations at Yangon of Myanmar was 1.23 μg/m^3. The 5-year average SO_4^{2-} concentrations at 2 stations in Philippines ranged from 0.29 μg/m^3 to 2.35 μg/m^3. The 5-year average SO_4^{2-} concentrations at 3 stations in Republic of Korea ranged from 4.04 μg/m^3 to4.63 μg/m^3. The 5-year average SO_4^{2-} concentration at 5 stations in Thailand ranged from 0.76 μg/m^3 to 5.27 μg/m^3.

The SO_4^{2-} concentration levels at EANET sites in Japan, Mongolia and Russia were low and more consistent with a 5-year average range of 1.67-4.45 μg/m^3 for 12 stations in Japan, 0.51-1.68 μg/m^3 for 2 stations in Mongolia and 0.38-1.90 μg/m^3 for 3 stations in Russia respectively.

The highest NO_3^- concentration was found at EANET site of Hongwen in China, the only station reported data, with the 5-year average NO_3^- concentration of 7.94 μg/m^3. The second highest 5-year averaged NO_3^-concentration was found at EANET site in Vietnam with the average of 4.07 μg/m^3 and a range of 1.54-6.73 μg/m^3 for the 5 stations, showing some differences in spatial distribution.

The 5-year average NO_3^- concentrations of the remaining EANET countries were relatively low. The 5-year average NO_3^- concentrations at Phnom Penh of Cambodia was 1.66 μg/m^3. The 5-year average NO_3^- concentrations at 3 stations of Indonesia ranged from 1.15 μg/m^3 to 2.06 μg/m^3. The 5-year average NO_3^- concentration at 12 stations in Japan ranged from 0.34 μg/m^3 to 3.23 μg/m^3. The 5-year average NO_3^- concentrations at Vientiane of Lao PDR was 0.44 μg/m^3. The 5-year average NO_3^- concentrations at 3 stations in Malaysia ranged from 0.09 μg/m^3 to 1.56 μg/m^3. The 5-year average NO_3^- concentrations at Yangon of Myanmar was 0.80 μg/m^3. The 5-year average NO_3^- concentrations

at 2 stations in Philippines ranged from 0.21 μg/m^3 to 1.37 μg/m^3. The 5-year average NO_3^- concentrations at 3 stations in Republic of Korea ranged from 1.20 μg/m^3 to 3.06 μg/m^3. The 5-year average NO_3^- concentration at 4 stations in Thailand ranged from 0.21 μg/m^3 to 2.09 μg/m^3.

The NO_3^- concentration levels at EANET sites in Mongolia and Russia were low and more consistent with a 5-year average range of 0.01-0.16 μg/m^3 for 2 stations in Mongolia and 0.03-0.61 for 3 stations in Russia respectively.

The highest NH_4^+ concentration was found at EANET site of Hongwen in China, the only station reported data, with the 5-year average NH_4^+concentration of 3.26 μg/m^3. The second highest 5-year averaged NH_4^+ concentration was observed at EANET site in Republic of Korea with the average of 2.12 μg/m^3 and a range of 1.66-2.66 μg/m^3. The third highest 5-year averaged NH_4^+ concentration was found at EANET site in Vietnam with the average of 1.65 μg/m^3 and a range of 1.11-1.97 μg/m^3 for the 5 stations.

The 5-year average NH_4^+ concentrations of the remaining EANET countries were relatively low. The 5-year average NH_4^+ concentrations at Phnom Penh of Cambodia was 0.49 μg/m^3. The 5-year average NH_4^+ concentrations at 3 stations of Indonesia ranged from 0.71 μg/m^3 to 1.34 μg/m^3. The 5-year average NH_4^+ concentration at 12 stations in Japan ranged from 0.20 μg/m^3 to 1.17 μg/m^3 with the highest concentration occurring at Tokyo. The 5-year average NH_4^+ concentrations at Vientiane of Lao PDR was 1.17 μg/m^3. The 5-year average NH_4^+ concentrations at 3 stations in Malaysia ranged from 0.15 μg/m^3 to 1.03 μg/m^3. The 5-year average NH_4^+ concentrations at 2 stations in Mongolia ranged from 0.05 μg/m^3 to 1.48 μg/m^3. The 5-year average NH_4^+ concentrations at Yangon of Myanmar was 0.47 μg/m^3. The 5-year average NH_4^+ concentrations at 2 stations in Philippines ranged from 0.05 μg/m^3 to 0.57 μg/m^3. The 5-year average NH_4^+ concentrations at 4 stations in Russia ranged from 0.06 μg/m^3 to 0.66 μg/m^3. The 5-year average NH_4^+ concentration at 4 stations in Thailand ranged from 0.23 μg/m^3 to 1.09 μg/m^3.

The highest 5-year averaged Ca^{2+} concentration was found at EANET sites in Vietnam with the average of 2.28 μg/m^3 and a range of 1.61-3.73 μg/m^3 for the 5 stations. The second highest Ca^{2+} concentration was found at EANET sites of Hongwen in China and Phnom Penh in Cambodia, with the same 5-year average Ca^{2+} concentration of 1.68 μg/m^3.

The 5-year average Ca^{2+} concentrations of the remaining EANET countries were relatively low. The 5-year average Ca^{2+} concentrations at 3 stations of Indonesia ranged from 0.96 μg/m^3 to 1.40 μg/m^3. The 5-year average Ca^{2+} concentration at 12 stations in Japan ranged from 0.09 μg/m^3 to 44 μg/m^3 with the highest concentration occurring at Tokyo. The 5-year average Ca^{2+} concentrations at Vientiane of Lao PDR was 0.22 μg/m^3. The 5-year average Ca^{2+} concentrations at 3 stations in Malaysia ranged from 0.03 μg/m^3 to 0.54 μg/m^3. The 5-year average Ca^{2+} concentrations at 2 stations in Mongolia ranged from 0.15 μg/m^3 to 0.67 μg/m^3. The 5-year average Ca^{2+} concentrations at Yangon of Myanmar was 1.14 μg/m^3. The 5-year average Ca^{2+} concentrations at 2 stations in Philippines ranged from 0.33 μg/m^3 to 0.70 μg/m^3. The 5-year average Ca^{2+} concentrations at 3 stations in Republic of Korea ranged from 0.03 μg/m^3 to 0.09 μg/m^3. The 5-year average Ca^{2+} concentrations at 4 stations in Russia ranged from 0.05 μg/m^3 to 0.30 μg/m^3. The 5-year average Ca^{2+} concentration at 4 stations in Thailand ranged from 0.26 μg/m^3 to 0.97 μg/m^3.

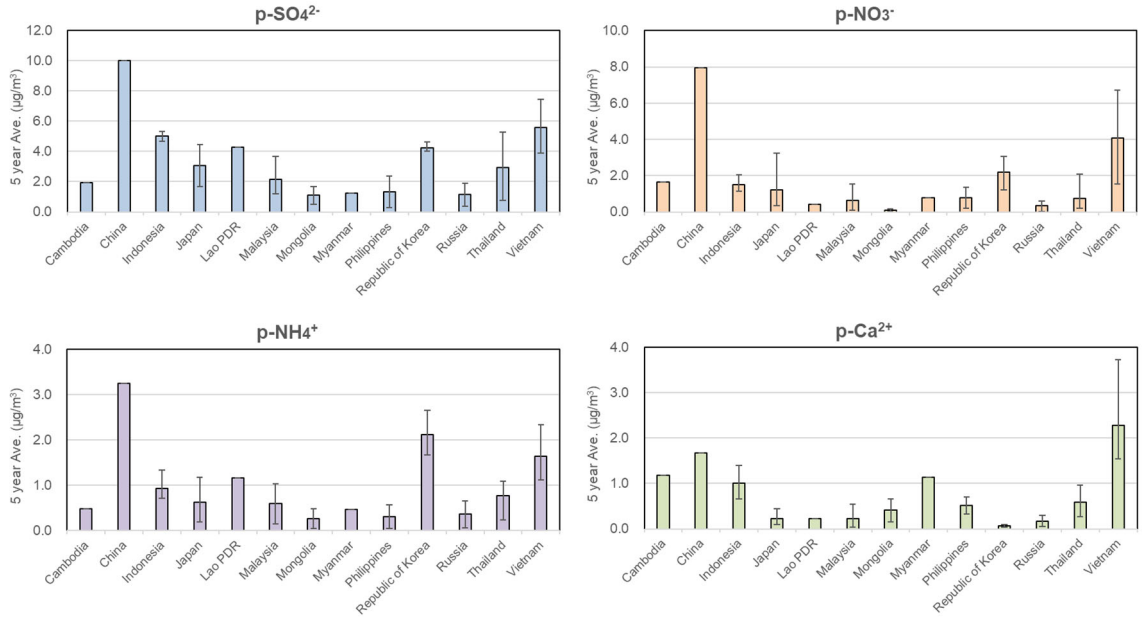

Figure 4.2.7 Average concentrations of particulate SO_4^{2-}, NO_3^-, NH_4^+ and Ca^{2+} at the monitoring sites of EANET in each country (5-year average from 2015 to 2019). Error bars denote standard deviations of all site data in each country.

4.2.7 Regional characteristics of SO_4^{2-}, NO_3^-, NH_4^+ and Ca^{2+} component in PM

The distribution of 5-year average SO_4^{2-}, NO_3^-, NH_4^+ and Ca^{2+} concentrations in the particulate matter in the EANET region is shown in Fig. 4.2.8, and spatial variations of SO_4^{2-}, NO_3^-, NH_4^+ and Ca^{2+} gas concentrations at EANET remote sites as a function of longitude and latitude are shown in Fig. 4.2.9. The distribution of SO_4^{2-} concentration in Southeast Asia is uneven. The highest SO_4^{2-} concentration in Southeast Asia was 7.47 μg/m^3 at Hanoi, Vietnam, and the lowest was 0.75 μg/m^3 at Mae Hia, Thailand. China has a high concentration of SO_4^{2-} with a 5-year average concentration of 10.0 μg/m^3 at Hongwen station. The SO_4^{2-} concentrations in Korea and Japan were lower and more evenly distributed, with concentrations ranging from 1.67 μg/m^3 to 4.63 μg/m^3. The concentrations in Mongolia and Russia in the north of EANET region were lower overall, with concentrations ranging from 0.51 to 1.90 μg/m^3.

NO_3^- is also an important component of the particulate matter. The Hongwen station of China has the highest concentration among the EANET sites in the region, with a 5-year average concentration of 7.94μg/m^3. EANET sites of Vietnam in Southeast Asia has an overall higher NO_3^- concentration level, with a concentration range of 1.54-6.73 μg/m^3 while other Southeast Asian EANET countries have relatively low NO_3^- concentrations. In Korea and Japan, lower NO_3^- concentrations with uneven spatial distribution can be found with a high concentration of 3.06 μg/m^3 at Kangwha of Korea and 3.23μg/m^3 at Tokyo of Japan. The overall lower concentrations were found in Mongolia and Russia in the northern region, with concentrations ranging from 0.51 μg/m^3 to 1.90 μg/m^3.

Higher NH_4^+ concentrations can be found at EANET sites in China, Vietnam and Korea. China has the highest NH_4^+ concentration, with a 5-year average concentration of 3.26 μg/m^3 at Hongwen, followed by the Republic of Korea, with concentrations ranging from 1.66 μg/m^3 to 2.66 μg/m^3. The overall NH_4^+ concentration distribution at EANET sites in Southeast Asia varies greatly, with the highest concentration of 2.34 μg/m^3 can be found at YenBai in northern part of Vietnam. The overall NH_4^+ concentrations at EANET sites in Japan, Russia and Mongolia are low.

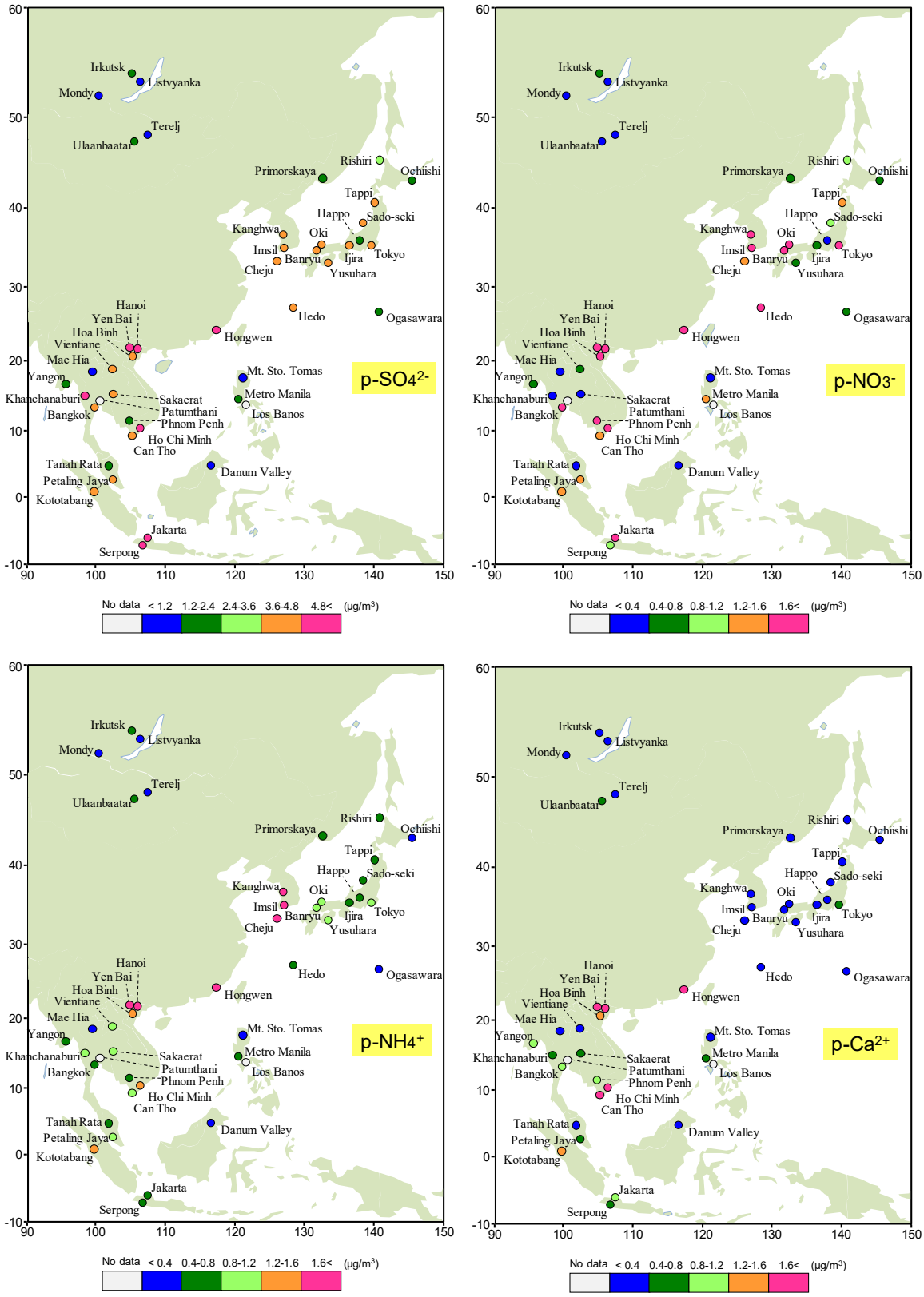

Figure 4.2.8 Spatial variations of aerosol component concentrations (particulate SO_4^{2-}, NO_3^-, NH_4^+ and Ca^{2+}) at EANET sites. (5-year average from 2015 to 2019).

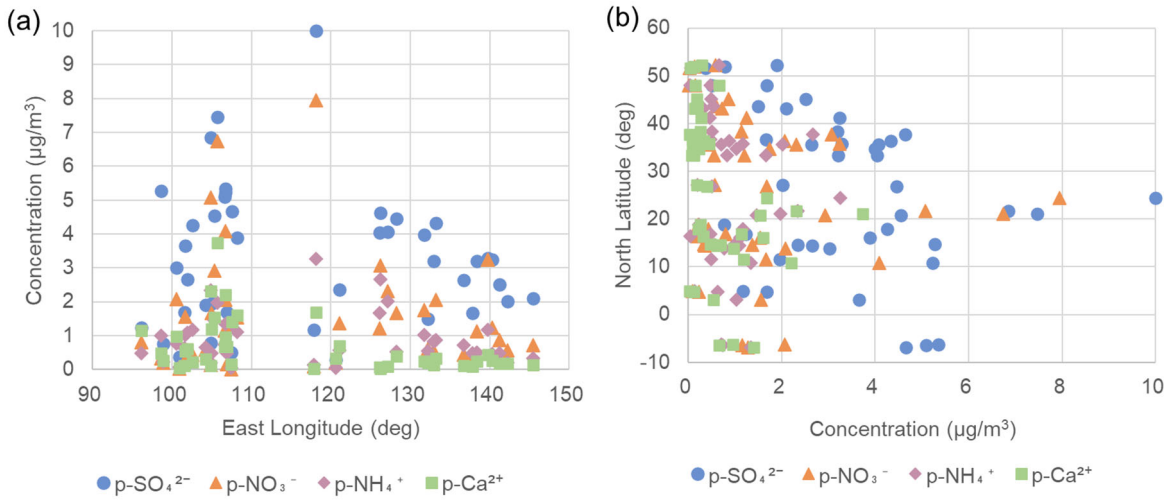

Figure 4.2.9 Spatial variations of aerosol component concentrations (particulate SO_4^{2-}, NO_3^-, NH_4^+ and Ca^{2+}) at EANET remote sites as a function of (a) longitude and (b) latitude. (5-year average from 2015 to 2019)

In EANET region, Vietnam has the highest average Ca^{2+} concentration with 5 stations ranging from 1.54 μg/m^3 to 3.71 μg/m^3, followed by Hongwen station in China with 1.68 μg/m^3, indicating possible influence from construction and traffic dust. Phnom Penh station in Cambodia and Bandung station in Indonesia showed 1.68 μg/m^3 and 1.19 μg/m^3, respectively while other Southeast Asian countries showed relatively low concentrations. The overall Ca^{2+} concentrations in Japan, Republic of Korea, Russia and Mongolia are low.

4.3 Temporal variation of air concentration

4.3.1 Annual variation of gas and aerosol concentrations at respective sites

It has been for 20 years since the regular activity of EANET started, so long term variations of gas and aerosol concentrations at the EANET sites will characterize the state of acidic deposition and related air pollutions in East Asia. In this section, annual variations of the major gaseous and aerosol concentrations at respective sites are discussed.

Fig. 4.3.1 shows annual variations of SO_2 concentration at respective EANET sites from 2000 to 2019. Except Weishuiyuan, the sites in China showed the remarkable decreasing trend over 20 years. The maximum SO_2 concentrations at Jinyunshan and Haibin-Park were 25.3 ppb in January 2010 and 5.28 ppb in December 2015 and then it showed decreasing trend. Except Tokyo, located in urban area and Yusuhara, located near volcanoes, the SO_2 concentrations at the sites in Japan were below 1 ppb. The SO_2 concentration at Happo was gradually decreased after showing the maximum value of 0.99 ppb in February 2011. The SO_2 concentration at Oki was 1.7 ppb in January 2010 and was annually decreased since 2010. The concentration of SO_2 at Tokyo was 3.08 ppb in August 2010 and was annually decreased. The maximum concentration of SO_2 at Yusuhara was 22.6 ppb in January 2010. The maximum SO_2 concentration at Ulaanbaatar, Mongolia was 35.1 ppb in December 2010 and kept the high level, but it drastically decreased after 2018. The tendency of SO_2 concentration change at Terelj, Mongolia was decreased, and it indicated the maximum value in winter of 2012. The maximum SO_2 concentrations at Imsil and Kangwha in Republic of Korea were 36.9 ppb in February 2010 and 4.1 ppb in January 2014 and then it showed decreasing trend over monitoring period. The SO_2 concentration at Cheju in Republic of Korea was 14.8 ppb of the highest concentration but was rapidly decreased since 4.60 ppb in December 2013. The annual SO_2

concentrations at the sites in Russia were fluctuated. The SO_2 concentration at Irkutsk in Russia showed the maximum value at 30.6 ppb in January 2018.

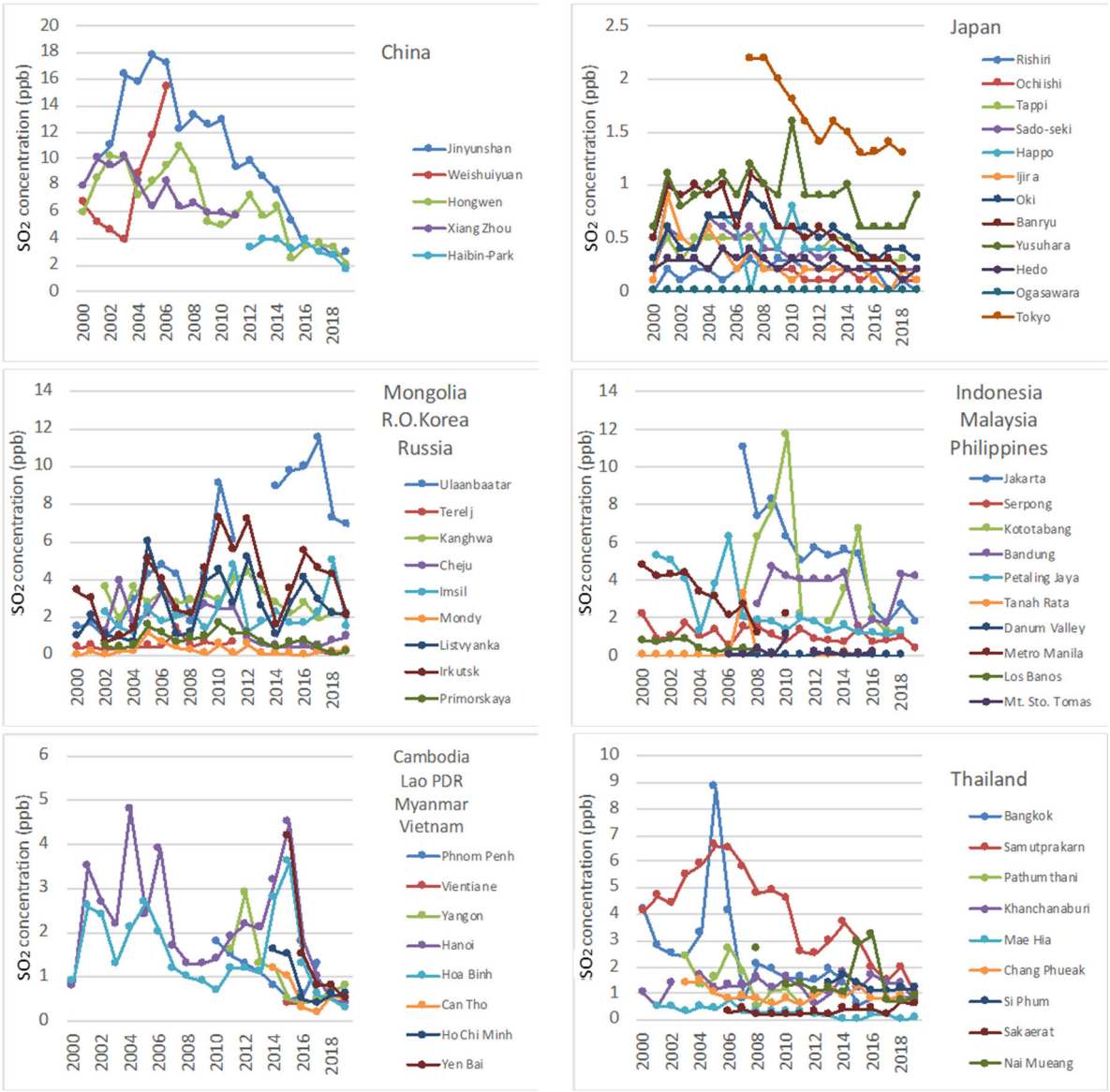

Figure 4.3.1 Annual variation of SO_2 concentration at respective EANET sites (Annual average from 2000 to 2019).

For SO_2 concentrations at EANET sites in Indonesia, Malaysia and Philippines, some sites showed remarkable decreasing trend. The maximum SO_2 concentration at Jakarta in Indonesia was 18.0 ppb in October 2008 and then it showed decreasing trend over monitoring period. The maximum SO_2 concentrations at Kototabang and Serpong in Indonesia were 6.32 ppb in April 2010 and 3.24 ppb in October 2011, respectively. The SO_2 concentration at Petaling Jaya in Malaysia was 2.98 ppb in June 2011 and was gradually decreased. At Tanah Rata in Malaysia, SO_2 was 0.7 ppb in June 2014 showing the highest concentration. At Los Banos in Philippines, the SO_2 concentration was recorded the highest values of 5.4 ppb in January 2010 and was gradually decreased. For SO_2 concentrations at EANET sites in Cambodia, Lao PDR, Myanmar and Vietnam, some sites showed remarkable decreasing trend after 2015. The SO_2 concentration at Phnom Penh in Cambodia was 2.2 ppb in November 2010 and was gradually decreased. The SO_2 concentration at EANET site of Vientiane in Lao PDR was 0.6 ppb both in February 2015 and June 2016. At EANET site of Yangon in Myanmar, the SO_2 concentration was 10.2 ppb in November 2012 and was annually decreased during the period.

The annual SO_2 concentrations in 2015 at EANET sites in Hanoi, Hoa Binh and Yen Bai in Vietnam were 4.5 ppb, 3.6 ppb and 4.2 ppb, respectively and then they were drastically decreased. The annual SO_2 concentration in 2005 at EANET site of Samutprakarn in Thailand was 6.6 ppb in maximum and then it was continuously decreased. For other sites in Thailand, the annual SO_2 concentrations were fluctuated.

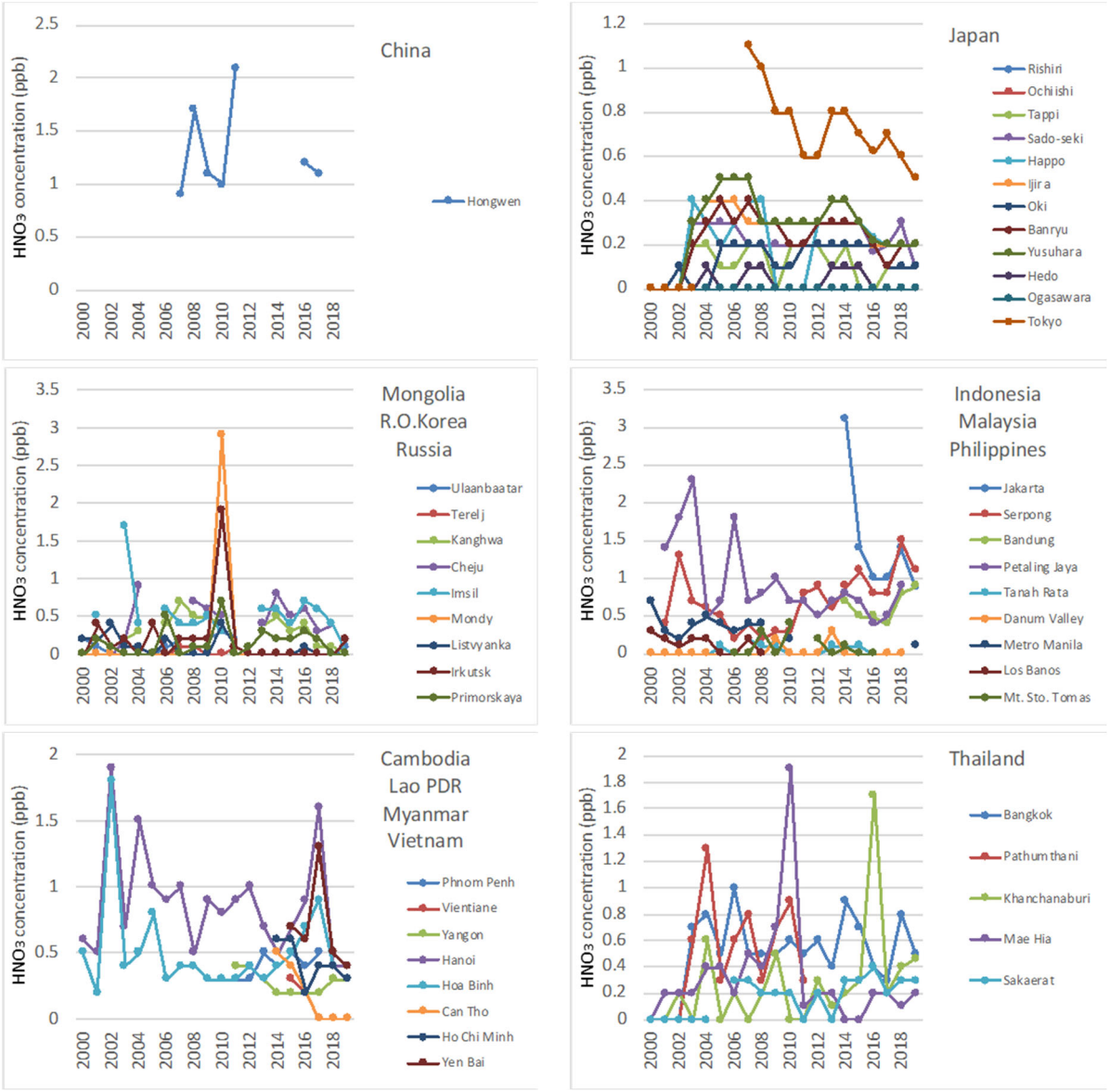

Figure 4.3.2 Annual variation of HNO_3 concentration at respective EANET sites (Annual average from 2000 to 2019).

Fig. 4.3.2 shows annual variations of HNO_3 concentration at respective EANET sites from 2000 to 2019. The annual HNO_3 concentration at Hongwen in China was between 1-2 ppb but there is no reported data after 2017. Except Tokyo, the HNO_3 concentrations at the EANET sites in Japan were below 0.6 ppb. The annual HNO_3 concentration at Tokyo in Japan was 1.1 ppb in 2007 and then it was continuously decreased. For the EANET sites in Mongolia, Republic of Korea and Russia, the annual HNO_3 concentrations were fluctuated and mostly lower than 1.0 ppb, whereas those at Mondy and Irkutsk in Russia were 2.9 ppb and 1.9 ppb in 2010, respectively.

For HNO_3 concentrations at EANET sites in Indonesia, Malaysia and Philippines, some sites showed remarkable decreasing or increasing trend. The annual HNO_3 concentration at Petaling Jaya in Malaysia was 1.8 ppb in June 2006 and it showed generally decreasing trend although there are fluctuations from year to year. The annual HNO_3 concentrations in 2014 at Jakarta in Indonesia were

3.1 ppb and then it was drastically decreased. The annual HNO_3 concentrations in 2008 at Serpong in Indonesia were 0.2 ppb and then it was continuously increased. At the EANET sites in Cambodia, Lao PDR, Myanmar and Vietnam, the annual HNO_3 concentrations were fluctuated and some sites showed high HNO_3 concentrations. The highest HNO_3 concentration at Phnom Penh, Cambodia was 0.8 ppb in August 2017. The HNO_3 concentration at Vientiane in Lao PDR showed the maximum value was 0.5 ppb in March 2015. The HNO_3 concentration at Yangon in Myanmar was rapidly increased from 2018 and showed the highest value of 19 ppb in September 2019. In 2002, the annual HNO_3 concentration at Hanoi and Hoa Binh in Vietnam were 1.9 ppb and 1.8 ppb, respectively. In 2017, the annual HNO_3 concentration at Hanoi, Hoa Binh and Yen Bai in Vietnam were 1.6 ppb, 0.9 ppb and 1.3 ppb, respectively. The annual HNO_3 concentrations at the EANET sites in Thailand were also fluctuated and some data showed high concentrations. The annual HNO_3 concentration at Pathumthani and Mae Hia in Thailand was 1.3 ppb in 2004 and 1.9 ppb in 2010, respectively.

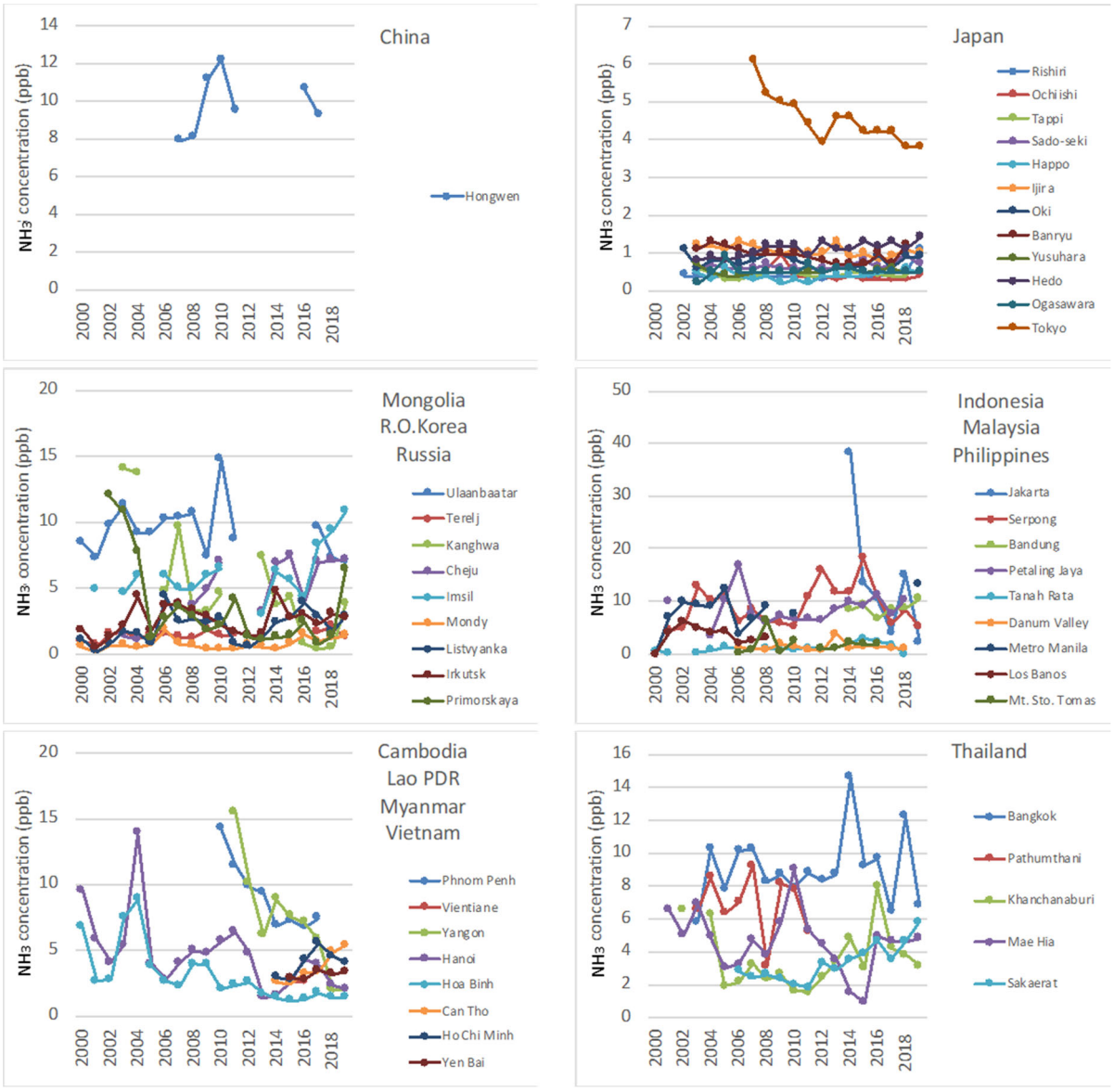

Figure 4.3.3 Annual variation of NH_3 concentration at respective EANET sites (Annual average from 2000 to 2019).

Fig. 4.3.3 shows annual variations of NH_3 concentration at respective EANET sites from 2000 to 2019. The annual NH_3 concentration at Hongwen in China was between 8-12 ppb, but there is no reported data after 2017. Except Tokyo, the NH_3 concentrations at the sites in Japan were below 1.5

ppb. The annual NH_3 concentration at Tokyo in Japan was 61 ppb in 2007 and then it was continuously decreased. For the sites in Mongolia, Republic of Korea and Russia, the annual NH_3 concentrations were fluctuated. The annual NH_3 concentrations in some years at Ulaanbaatar in Mongolia and at Cheju, Kangwha and Imsil in Republic of Korea exceeded 5.0 ppb, whereas those at Mondy in Russia were below 1.5 ppb. The annual NH_3 concentrations after 2017 at Ulaanbaatar in Mongolia was lower compared to those in former years of 2011. The annual NH_3 concentration at Kangwha in Republic of Korea was significantly decreased after 2016 (less than 1.0 ppb). The annual NH_3 concentrations at Irkutsk and Primorskaya in Russia were recorded as the highest of 23.5 ppb in February 2014 and 17.9 ppb in August 2019, respectively.

For the EANET sites in Indonesia, Malaysia and Philippines, the annual NH_3 concentrations were fluctuated but the concentrations were generally higher than those in Northeast Asia. The annual NH_3 concentration at Jakarta in Indonesia was 38.2 ppb in 2014, but it should be noted that the data completeness was less than the data quality objective (< 70%). The annual NH_3 concentration at Bandung in Indonesia show the highest value of 16.2 ppb, and then it showed a tendency to increase. The NH_3 concentration at Serpong in Indonesia was recorded as the highest of 34.7 ppb in November 2015. The NH_3 concentration at Danum Valley in Malaysia showed the maximum value at 10.1 ppb in July 2013 and then was decreased after that. The NH_3 concentration at Petaling Jaya in Indonesia was recorded as the highest of 18.2 ppb in June 2013.

For NH_3 concentrations at EANET sites in Cambodia, Lao PDR, Myanmar and Vietnam, some sites showed remarkably decreasing trend. The NH_3 concentration at Phnom Penh in Cambodia showed the highest value of 18.2 ppb in May 2010 and then it showed a trend to decrease the concentration every year. The NH_3 concentration at Vientiane in Lao PDR showed the maximum value was 0.4 ppb in February 2015. The NH_3 concentration at Yangon in Myanmar showed the highest value of 15.5 ppb in 2011 and then it also showed a decreasing trend. The NH_3 concentration at Hanoi in Vietnam was decreased after showing 9.92 ppb of max value in February 2011, and the annual variation at Hoa Binh in Vietnam was similar with that of Hanoi. The annual NH_3 concentrations at the EANET sites in Thailand were fluctuated. The annual NH_3 concentration at Pathumthani and Mae Hia in Thailand was 1.3 ppb in 2004 and 1.9 ppb in 2010, respectively. The highest NH_3 concentrations at Mae Hia, Nakhon Ratchasima and Sakaera in Thailand were 7.87 ppb in March 2016, 5.73 ppb in November 2012 and 10.6 ppb in January 2016, respectively.

Fig. 4.3.4 shows annual variations of HCl concentration at respective EANET sites from 2000 to 2019. The annual HCl concentration at Hongwen in China showed higher values of 14.5 ppb in 2010 and 13.3 ppb in 2011 but there is no reported data after 2017.The HCl concentrations at the sites in Japan were below 1.5 ppb. The HCl concentration at Ochiishi in Japan was 3.25 ppb in April 2012 showing the highest concentration. The highest HCl concentration at Ogasawara in Japan was 1.02 ppb in January 2011, and it was annually decreased. The HCl concentration at Oki in Japan was 1.5 ppb in August 2013 and was gradually decreased every year during monitoring period. The HCl concentration at Yusuhara, Japan was 0.71 ppb in January 2011, and it was decreased over whole monitoring period. For the sites in Mongolia, Republic of Korea and Russia, the annual HCl concentrations showed higher values (more than 5 ppb) after 2012. The HCl concentration at Cheju in Republic of Korea indicated the maximum value of 2.80 ppb in May 2019 increased rapidly from the lower level than 1 ppb. The HCl concentration at Kangwha in Republic of Korea: HCl was 1.5 ppb in May 2019 and was increased in the same year. The HCl concentration at Imsil in Republic of Korea was 2.3 ppb in June 2019 and its overall concentration was rapidly increased in 2019. The HCl concentrations at Irkutsk, Listvyanka and Mondy in Russia showed the maximum values of 21.7 ppb in January 2018, 21.3 ppb in October 2012 and 11.1 ppb in March 2018, respectively. The HCl concentrations at Primorskaya in Russia was 3.09 ppb in November 2010 and was generally decreased during monitoring period.

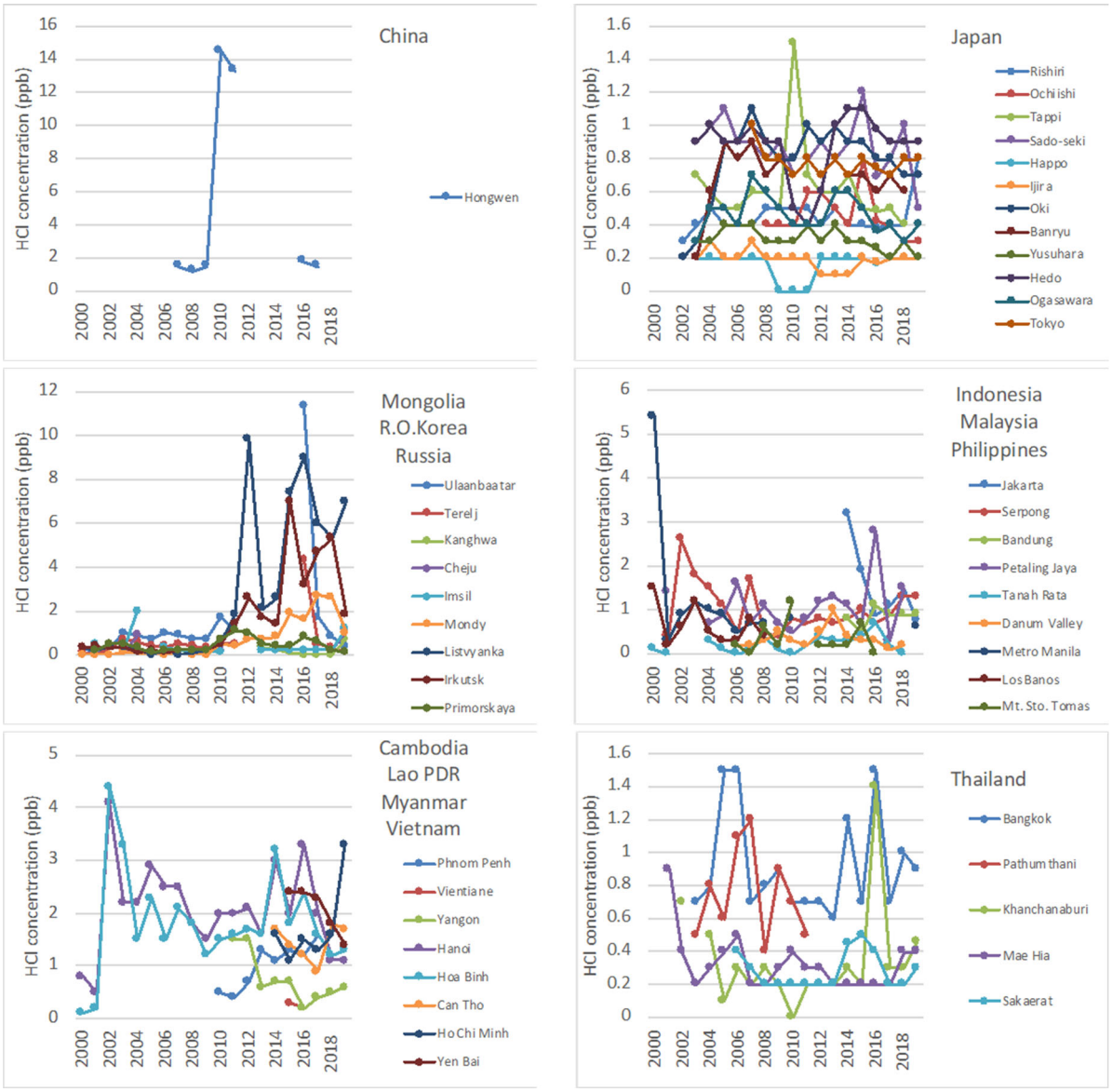

Figure 4.3.4 Annual variation of HCl concentration at respective EANET sites (Annual average from 2000 to 2019).

For the EANET sites in Indonesia, Malaysia and Philippines, the annual HCl concentrations were fluctuated but the high concentrations (more than 2 ppb) were occasionally observed. The highest HCl concentrations at Bandung and Serpong in Indonesia were 1.4 ppb in August 2016 and 5.52 ppb in December 2010, respectively. The HCl concentration at Danum Valley in Malaysia showed a maximum value at 3.00 ppb in February 2013, and it was decreased since 2013. The highest HCl concentration at Petaling Jaya in Malaysia: HCl was 6.7 ppb in December 2016, and it was annually decreased over whole monitoring period. The highest HCl concentrations at Metro Manila and Mt. Sto. Tomas in Philippines was 1.42 ppb in October 2010 and 2.56 ppb in December 2010, respectively. For HCl concentrations at EANET sites in Cambodia, Lao PDR, Myanmar and Vietnam, the sites in Vietnam showed remarkably decreasing trend. The HCl concentration at Phnom Penh in Cambodia was 2.3 ppb in March 2017, and it was annually increased. The HCl concentration at Vientiane in Lao PDR showed the maximum value of 0.4 ppb in January 2016. The HCl concentration at Yangon in Myanmar was 3.11 ppb in April 2012, and it was annually decreased over whole monitoring period. The HCl concentration at Hanoi in Vietnam was increased to 7.60 ppb in August 2016 but rapidly decreased since 7.10 ppb in October 2016. The HCl concentration at Yen Bai in Vietnam was 4 ppb in June 2016 and it was annually decreased. The annual variations of

HCl concentration at Hanoi and Hoa Binh in Vietnam are similar. Both sites show highest values of 4.1 ppb and 4.4 ppb in 2002, respectively and then those show decreasing trend. The annual HCl concentrations at the EANET sites in Thailand were fluctuated but lower than those in other Southeast Asian countries. The annual HCl concentrations at Bangkok, Mae Hia, Pathumthani and Sakaerat were 7.40 ppb in June 2016, 1.6 ppb in April 2019, 2.22 ppb in June 2010 and 1.4 ppb in January 2015, respectively.

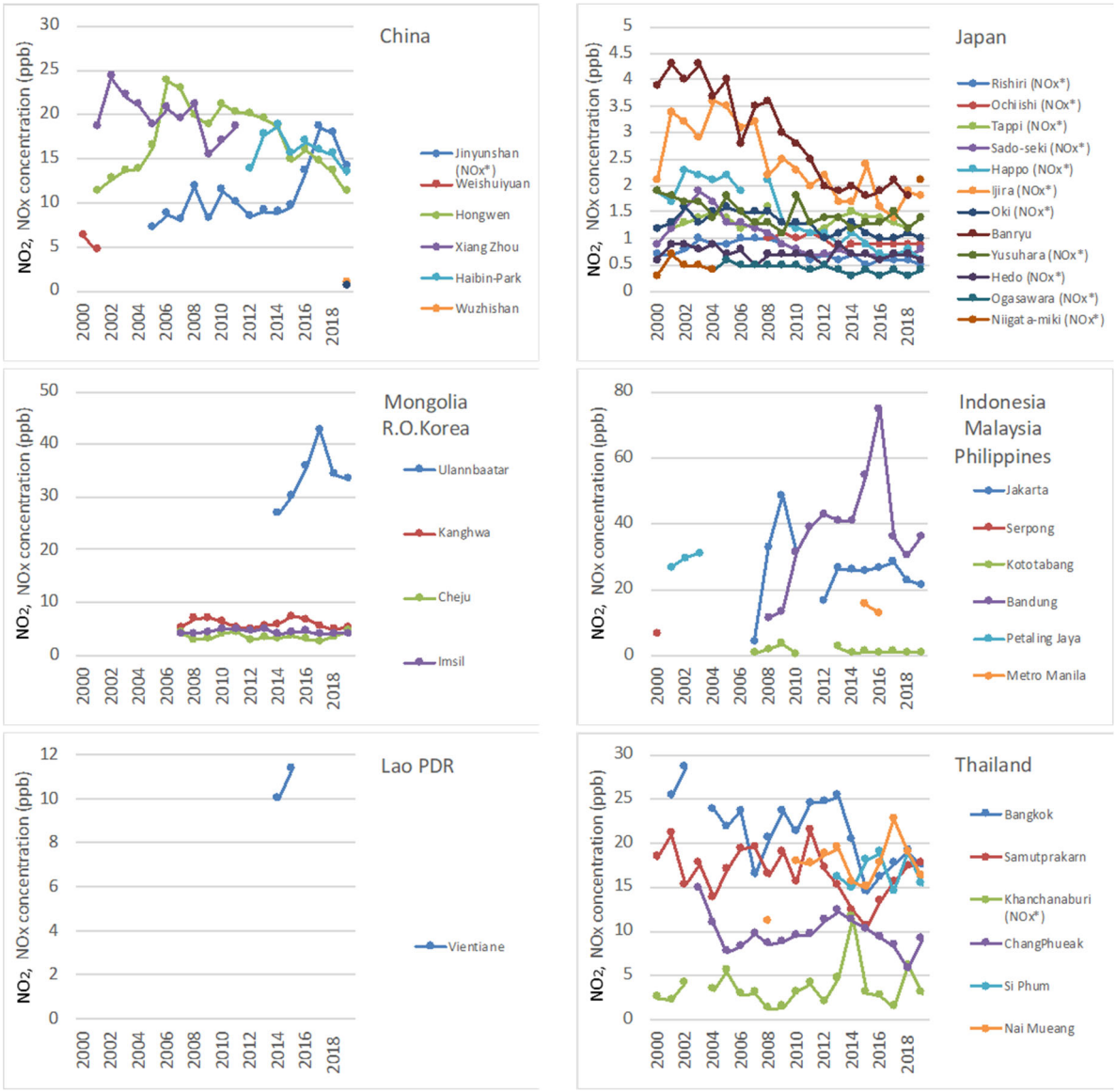

Figure 4.3.5 Annual variation of NO_2 or NOx concentration at respective EANET sites (Annual average from 2000 to 2019).

Fig. 4.3.5 shows annual variations of NO_2 or NOx concentration at respective EANET sites from 2000 to 2019. The annual NO_2 or NOx concentrations at the sites in China showed remarkably decreasing or increasing trend. The NO_2 concentration at Haibin-Park, China was 26.3 ppb in January 2019 showing the highest concentration, and it shows a slightly annually decreasing trend. The highest NOx concentration at Jinyunshan, China was 28.2 ppb in December 2017, and it showed remarkably increasing trend. The highest NO_2 concentrations at Lijiang and Wuzhishan in China were 0.9 ppb in May 2019 and 2.3 ppb in December 2019, respectively. The annual NO_2 or NOx concentrations at many sites in Japan showed remarkably decreasing trend. The highest annual NO_2 concentration at Banryu and annual NOx concentration at Ijira in Japan was 3.9 ppb in 2001 and 3.6

ppb in 2004, respectively. Then, those were continuously decreased. The highest concentrations of NOx at Hedo and Niigata-maki in Japan were 1.5 ppb in January 2015 and 2.8 ppb in February 2019, respectively. The highest concentration of NO_2 at Ulaanbaatar in Mongolia was 69.1 ppb in January 2017. It showed high level more than 25 ppb but decreased after 2016. The annual NO_2 concentrations at the sites in Republic of Korea were fluctuated. The highest concentration of NO_2 at Imsil and Kangwha in Republic of Korea were 11.5 ppb in December 2012 and 14.4 ppb in April 2015, respectively.

There are lots of missing data at the EANET sites in Malaysia, Philippines and Lao PDR. The sites in Indonesia showed high level of NO_2 more than 30 ppb. The highest concentration of NO_2 at Bandung in Indonesia was 140 ppb in September 2016 and it was significantly decreased after 2016. The highest concentration of NO_2 at Jakarta in Indonesia was 49.0 ppb in November 2010 and it was gradually decreased. The highest concentrations of NO_2 at Vientiane in Lao PDR and Metro Manila in Philippines was 20.6 ppb in January 2015 and 19.3 ppb in September 2015, respectively. The annual NO_2 concentrations at some sites in Thailand showed significantly decreasing trend. The highest concentration of NO_2 at Bangkok in Thailand was 41.8 ppb in January 2014 and it shows a trend to decrease gradually. The highest concentration of NO_2 at Chang Phueak in Thailand was 23.6 ppb in March 2007, and it was continuously decreased after 2013. The highest concentration of NOx at Khanchanaburi in Thailand was 35.5 ppb in June 2014, and the annual concentration in 2014 was much higher than that in the other years. The highest NO_2 concentrations at Nai Mueang and Samutprakarn and Si Phum in Thailand were 29 ppb in February 2018, 36.4 ppb in January 2019 and 45.7 ppb in July 2018, respectively.

Fig. 4.3.6 shows annual variations of O_3 concentration at respective EANET sites from 2000 to 2019. The annual O_3 concentrations at sites in Japan were fluctuated, but the O_3 concentration at Happo in Japan was continuously increased until 2008, and then the trend was drastically changed. The causes of this drastic change would be combined by change in meteorological conditions and concentrations of O_3 precursors. The highest O_3 concentrations at Happo, Hedo, Ijira, Niigata-maki, Ochiishi, Oki, Rishiri. Sado-seki and Tsushima in Japan were 83 ppb in April 2007, 58 ppb in April 2013, 48 ppb in May 2016, 54 ppb in May 2019, 54 ppb in April 2018, 66 ppb in May 2014, 53 ppb in April 2010, 65 ppb in May 2010 and 68 ppb in May 2019, respectively. The highest O_3 concentration at Ogasawara, Japan was 55 ppb in March 2019 and slightly increasing trend of annual concentration was observed. The highest O_3 concentration at Yusuhara in Japan was 59 ppb in May 2014 and its concentration had a trend to increase during whole monitoring period. The annual O_3 concentrations at the sites in Mongolia and Republic of Korea were also fluctuated. The highest O_3 concentration at Ulaanbaatar in Mongolia was 29 ppb in July 2016. The highest O_3 concentrations at Cheju, Imsil and Kangwha in Republic of Korea were 66 ppb in May 2014, 54 ppb in June 2015 and 69 ppb in June 2015, respectively. The O_3 concentrations at Cheju exceeded 55 ppb in high level especially in spring.

There is no long term O_3 concentration data at EANET sites in Indonesia, Malaysia, Philippines and Cambodia. The O_3 concentration at Bandung in Indonesia was 38 ppb as the highest value in May 2015 but represented a tendency to decrease. The highest O_3 concentration at Metro Manila in Philippines was 12 ppb in October 2015. The highest O_3 concentration at Phnom Penh in Cambodia was 31 ppb in December 2019. The O_3 concentration at some EANET sites in Thailand showed remarkably increasing trend and the annual concentrations were lower than those in Northeast Asia. The O_3 concentration at Bangkok in Thailand was similar levels except for the day having 120 ppb in March 2015. The O_3 concentration at Chang Phueak in Thailand was 47 ppb in March 2019 showing relatively high concentration. The highest O_3 concentration at Khanchanaburi in Thailand was 41.2 ppb in March 2010. At Nai Mueang in Thailand, the highest O_3 concentration was 40 ppb in March. The O_3 concentration at Samutprakarn in Thailand was 34 ppb in April 2015 as the maximum value. Its overall concentrations over monitoring period were gradually increased so high levels especially in spring and winter.

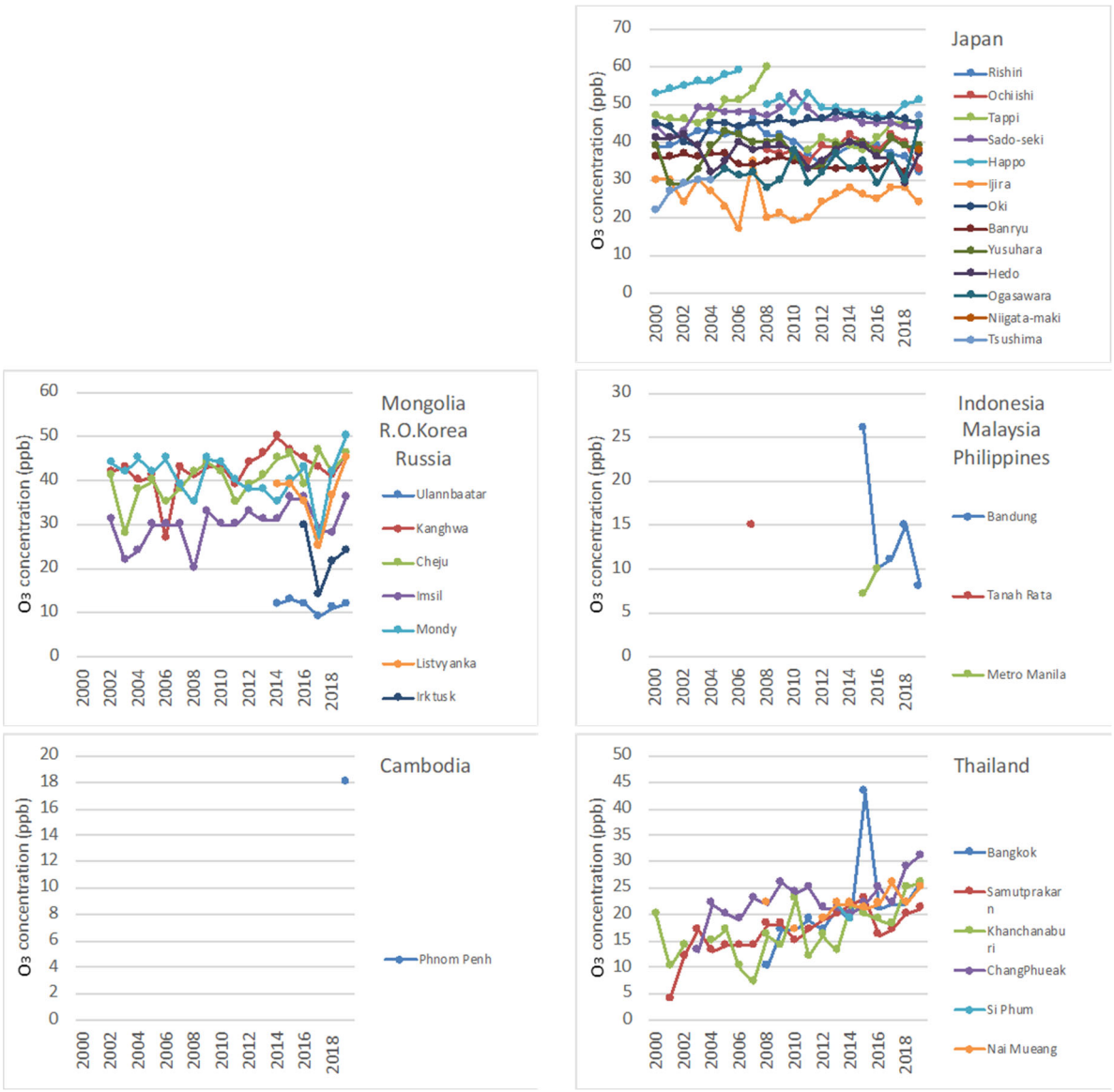

Figure 4.3.6 Annual variation of O_3 concentration at respective EANET sites (Annual average from 2000 to 2019).

Fig. 4.3.7 shows annual variations of PM_{10} concentration at respective EANET sites from 2000 to 2019. The annual PM_{10} concentrations at all sites in China showed decreasing trend. The highest PM_{10} concentrations at Haibin-Park, Jinyunshan, Lijiang and Wuzhishan in China were 76 μg/m^3 in December 2016, 119 μg/m^3 in January 2014, 15 μg/m^3 in May 2019 and 22 μg/m^3 in November 2019, respectively. The annual PM_{10} concentrations at some sites in Japan showed a slightly decreasing or increasing trend. The highest PM_{10} concentrations at Happo, Ijira, Ochiishi, Sado-seki, Tsushima and Yusuhara were 24 μg/m^3 in May 2011, 46 μg/m^3 in May 2011, 35 μg/m^3 in December 2010, 36 μg/m^3 in March 2013, 36 μg/m^3 in March 2019 and 36 μg/m^3 in May 2011, respectively. The PM_{10} concentration at Hedo in Japan was 78 μg/m^3 in October 2010 showing the highest value and its concentration was stable over whole monitoring period. The PM_{10} concentration at Ogasawara in Japan was 30 μg/m^3 in March 2010 with the highest concentration and its level was annually increased. The PM_{10} concentration at Oki in Japan was 47 μg/m^3 in November 2010 and it showed annually increasing trend. The PM_{10} concentration at Rishiri in Japan tended to increase and the highest concentration was 35 μg/m^3 in March 2014. The PM_{10} concentration at Ulaanbaatar in Mongolia showed very high concentration of 358 μg/m^3 in January 2014 but the annual concentration was kept above 100 μg/m^3 after 2015. The annual PM_{10} concentrations at sites in Republic of Korea

were fluctuated. The PM_{10} concentration at Cheju in Republic of Korea was 80 μg/m^3 in November 2010 and its concentration was gradually decreased. The highest PM_{10} concentrations at Imsil and Kangwha in Republic of Korea was 81 μg/m^3 in March 2019 and 80 μg/m^3 in February 2015, respectively.

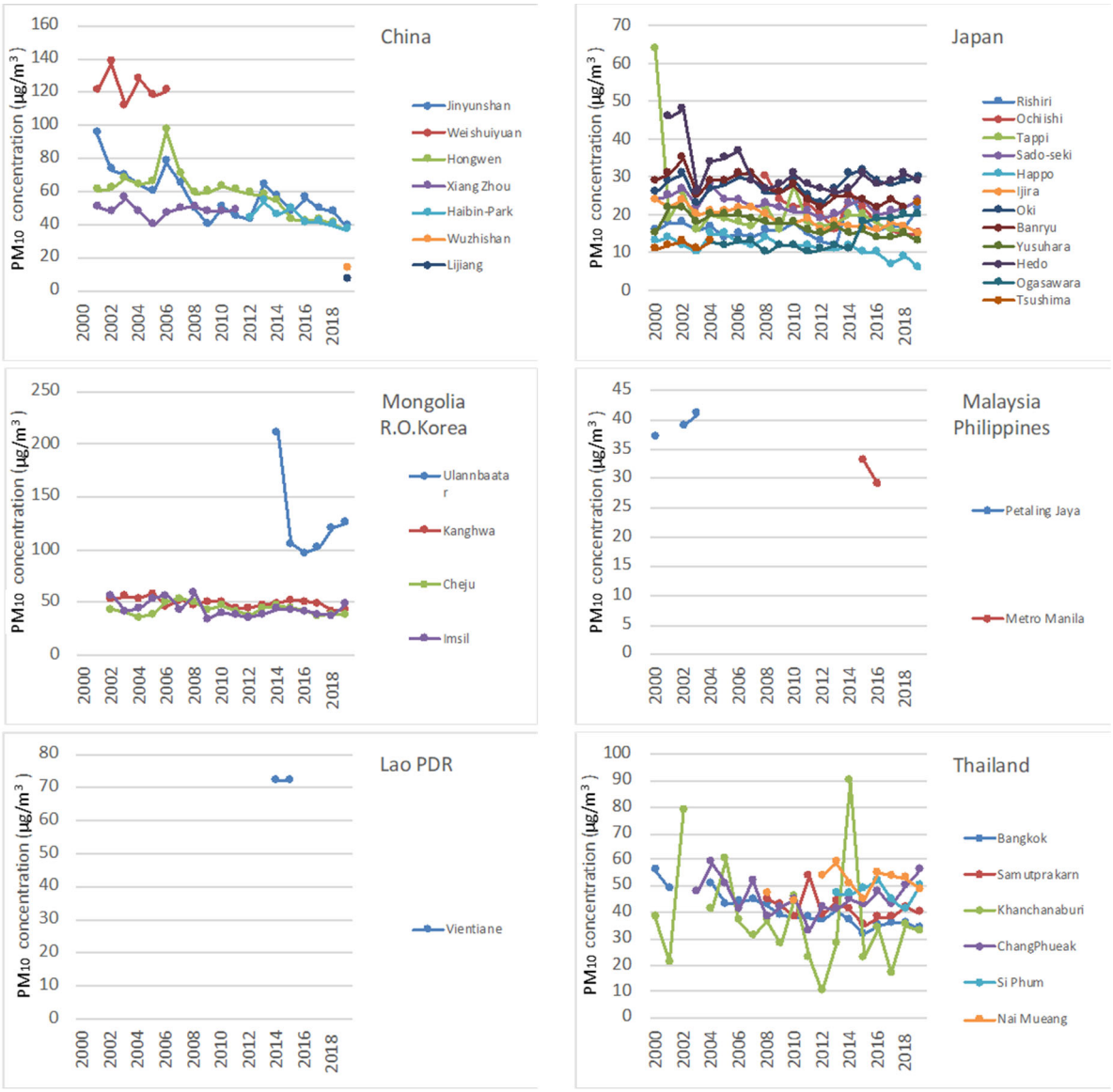

Figure 4.3.7 Annual variation of PM_{10} concentration at respective EANET sites (Annual average from 2000 to 2019).

There is no long term PM_{10} concentration data at EANET sites in Malaysia, Philippines and Lao PDR. The highest PM_{10} concentration at Metro Manila in Philippines was 38 μg/m^3 in October 2015. The annual PM_{10} concentrations at EANET sites in Thailand were fluctuated year by year. The highest PM_{10} concentration at Khanchanaburi and Si Phum in Thailand were 202 μg/m^3 and 118 μg/m^3, respectively. The highest PM_{10} concentration at Bangkok in Thailand was 78 μg/m^3 in December 2013, and the concentration of whole monitoring period had showed similar levels. The highest PM_{10} concentration at Chang Phueak, Thailand: PM_{10} was 132 μg/m^3 in March 2019, and it was gradually increased. The highest PM_{10} concentration at Nai Mueang in Thailand was 133 μg/m^3 in January 2015 and it was gradually decreased every year. The highest PM_{10} concentration at Samutprakarn in Thailand was 136 μg/m^3 in December 2013, and the level over whole monitoring period was gradually decreased.

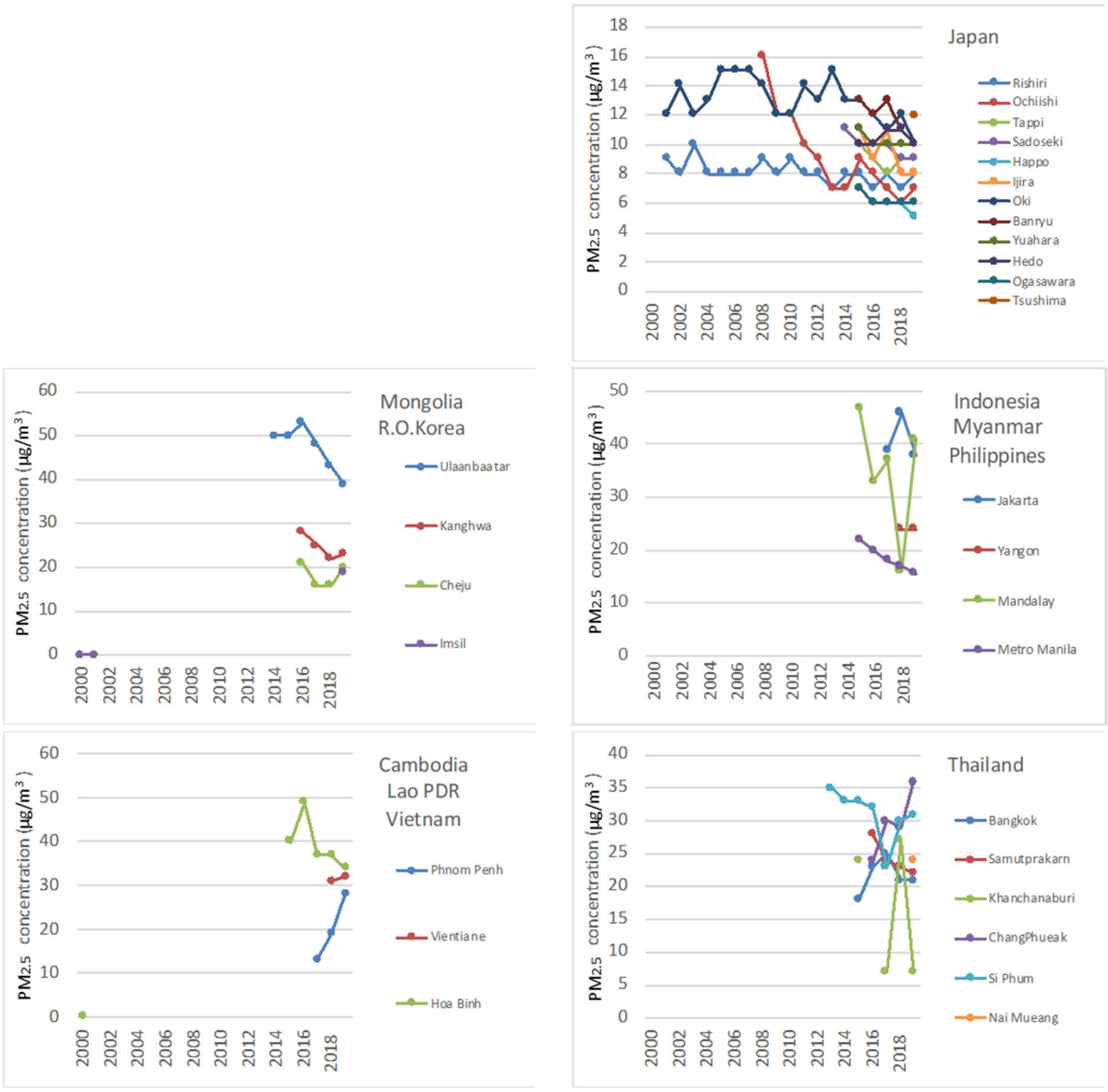

Figure 4.3.8 Annual variation of $PM_{2.5}$ concentration at respective EANET sites (Annual average from 2000 to 2019).

Fig. 4.3.8 shows annual variations of $PM_{2.5}$ concentration at respective EANET sites from 2000 to 2019. Except the sites in Japan, the annual data at most sites are available after 2014. The annual $PM_{2.5}$ concentrations at sites in Japan were lower (less than 15 μg/m^3), and there is clear decrease trend at Tsushima. The highest $PM_{2.5}$ concentrations at Happo, Hedo, Ijira, Ochiishi. Ogasawara and Tsushima in Japan were 12 μg/m^3 in April 2015, 15 μg/m^3 in February and March 2017, 15 μg/m^3 in May 2016 and in March and May 2017, 16 μg/m^3 in March 2014, 9 μg/m^3 in March 2018, 9 μg/m^3 in March 2019, respectively. The highest $PM_{2.5}$ concentrations at Oki, Rishiri, Sadoseki in Japan were 22.2 μg/m^3 in March 2011, 16 μg/m^3 in April 2018, and 16 μg/m^3 in May 2014, respectively. For these sites, the $PM_{2.5}$ concentration was generally decreased but the PM_{10} was increased. The highest $PM_{2.5}$ concentration at Yusuhara in Japan was 18 μg/m^3 in February 2016, and it exhibited the same pattern of PM_{10} with decreasing trend. The annual $PM_{2.5}$ concentrations at sites in Mongolia and Republic of Korea were continuously decreased after 2015. The highest $PM_{2.5}$ concentration at Ulaanbaatar in Mongolia was 148 μg/m^3 in January 2016 and exhibited high levels in winter like PM_{10}. At Cheju in Republic of Korea, $PM_{2.5}$ has a similar trend with PM_{10} and its concentration was high in March 2019 as level of 32 μg/m^3. The highest $PM_{2.5}$ concentration at Imsil in Republic of

Korea: $PM_{2.5}$ was 37 μg/m^3 in March 2019. At Kangwha in Republic of Korea, the $PM_{2.5}$ concentration over whole monitoring period was decreased. The highest $PM_{2.5}$ concentration was 37 μg/m^3 in March 2019 and had a same tread with PM_{10}.

For the EANET sites in Southeast Asian countries of Indonesia, Myanmar and Philippines, Cambodia, Lao PDR, Vietnam and Thailand, the annual $PM_{2.5}$ concentrations at Metro Manila in Philippines, Hoa Binh in Vietnam, Samutprakarn and Si Phum in Thailand showed decreasing trend. The highest $PM_{2.5}$ concentration at Jakarta in Indonesia was 61 μg/m^3 in July 2018. The highest $PM_{2.5}$ concentration at Yangon in Myanmar was 48 μg/m^3 in February 2019 showing the highest concentration with high levels in winter. The highest $PM_{2.5}$ concentration at Mandalay in Myanmar was 97 μg/m^3 in March 2016. The concentration was gradually decreased. The highest $PM_{2.5}$ concentration at Metro Manila in Philippines was 26 μg/m^3 in October 2015, and PM_{10} showed also the highest value at the same period. The highest $PM_{2.5}$ concentrations at Phnom Penh in Cambodia and Vientiane, Lao PDR were 37 μg/m^3 in February 2018 and 80 μg/m^3 in March 2019, respectively. The highest $PM_{2.5}$ concentrations at Bangkok in Thailand was 43 μg/m^3 in January 2019. At Chang Phueak in Thailand, the highest $PM_{2.5}$ concentration was 97 μg/m^3 in March 2019 showing the same case with PM_{10}. The highest $PM_{2.5}$ concentration at Khanchanaburi in Thailand was 63 μg/m^3 in March 2018 and it has the same seasonal feature with PM_{10}. The highest $PM_{2.5}$ concentration at Nai Mueang in Thailand was 43 μg/m^3 in December 2019. The highest $PM_{2.5}$ concentration at Samutprakarn in Thailand was 47 μg/m^3 in February 2017. Like PM_{10}, its level was slowly decreased by having high concentrations in dry season as well. The highest $PM_{2.5}$ concentration Si Phum in Thailand was 82 μg/m^3 in April 2016, and PM_{10} showed also the highest value at the same period. This indicated the same correlation each other and had a pattern of high levels in the same period.

Fig. 4.3.9 shows annual variations of particulate SO_4^{2-} concentration at respective EANET sites from 2000 to 2019. The annual particulate SO_4^{2-} concentration at Hongwen in China was increased from 2007 to 2011, and then it showed lower values in 2016 and 2017, there is no reported data after 2017. The particulate SO_4^{2-} concentrations at the sites in Japan showed decreasing trend. The highest particulate SO_4^{2-} concentration at Ijira, Ochiishi, Rishiri, Sado-seki in Japan were 6.82 μg/m^3 in May 2012, 12.06 μg/m^3 in December 2014, 6.24 μg/m^3 in May 2019 and 9.7 μg/m^3 in August 2013, respectively. The highest particulate SO_4^{2-} concentration at Hedo in Japan was 9.96 μg/m^3 in January 2015 and its overall concentration was gradually increased through whole monitoring period. At Ogasawara in Japan: the particulate SO_4^{2-} concentration was 5.41 μg/m^3 in March 2015, and it was generally sustained in high levels. The highest particulate SO_4^{2-} concentration at Oki in Japan was 8.1 μg/m^3 in May 2013, it was gradually decreased every year like SO_2. At Tokyo in Japan, the highest particulate SO_4^{2-} concentration was 10.2 μg/m^3 in August 2013. Like SO_2 concentration, while the annual concentration was decreased, it showed generally high levels in summer. The highest particulate SO_4^{2-} concentration at Yusuhara, Japan was 10.2 μg/m^3 in May 2012, and it was also decreased like SO_2. For some sites in Mongolia, Republic of Korea and Russia, the annual particulate SO_4^{2-} concentrations were decreased especially after 2008. The highest particulate SO_4^{2-} concentration at Terelj in Mongolia was 6.25 μg/m^3 in November 2016. The highest particulate SO_4^{2-} concentration at Ulaanbaatar in Mongolia was 3.37 μg/m^3 in February 2016 showing high levels in winter and it was significantly decreased since 2016. The highest particulate SO_4^{2-} concentrations at Cheju, Imail and Kanghwa in Republic of Korea were 35.1 μg/m^3 in January 2014, 21.2 μg/m^3 in May 2006 and 17.8 μg/m^3 in April 2008, respectively. The highest particulate SO_4^{2-} concentrations at Listvyanka and Mondy in Russia were 2.77 μg/m^3 in January 2014 and 1.27 μg/m^3 in March 2017, respectively. At Primorskaya in Russia, the particulate SO_4^{2-} concentration exhibited the maximum value at 9.77 μg/m^3 in February 2014, and its concentration was annually decreased over monitoring period.

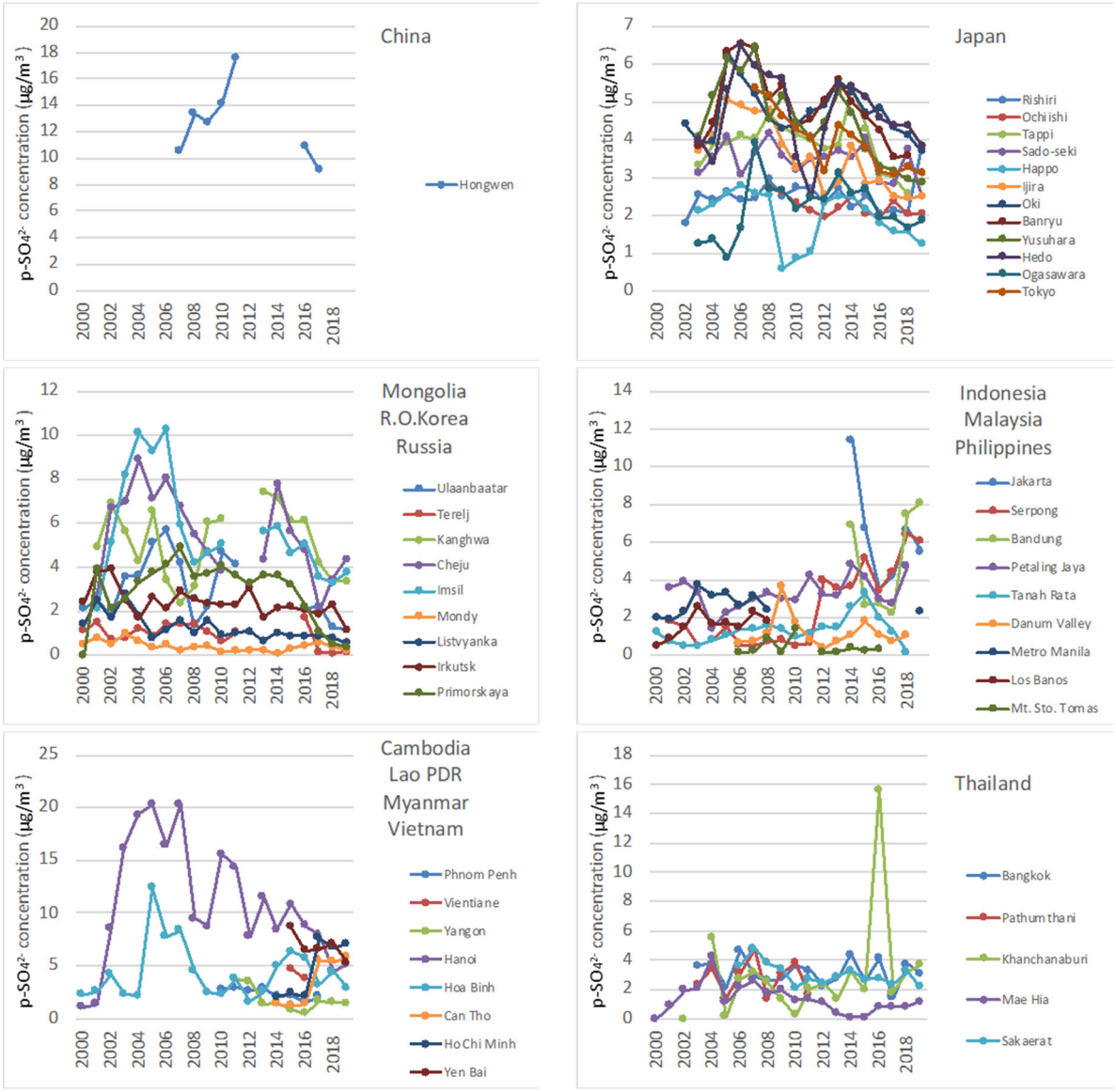

Figure 4.3.9 Annual variation of particulate SO_4^{2-} concentration at respective EANET sites (Annual average from 2000 to 2019).

For particulate SO_4^{2-} concentrations at EANET sites in Indonesia, Malaysia and Philippines, some sites showed increasing trend. The highest particulate SO_4^{2-} concentration at Bandung in Indonesia was 11.7 μg/m^3 in July 2019 having increase in general. The highest particulate SO_4^{2-} concentration at Jakarta in Indonesia was 19.7 μg/m^3, and it had a trend to decrease after that. The highest particulate SO_4^{2-} concentration at Serpong in Indonesia was 11.0 μg/m^3 in October 2018 and it showed annual increase. At Danum Valley in Malaysia, the maximum value of particulate SO_4^{2-} concentration was 5.55 μg/m^3 in March 2010, but it was rapidly decreased after. In October 2015, it showed high peak of 4.75 μg/m^3 in October 2015 and decreased again. The highest particulate SO_4^{2-} concentration at Petaling Jaya and Tanah Rata in Malaysia were 8.65 μg/m^3 in August 2018 and 10.2 μg/m^3 in October 2015, respectively. The highest particulate SO_4^{2-} concentration at Metro Manila and Mt. Sto. Tomas in Philippines were 6.07 μg/m^3 in October 2006 and 5.31 μg/m^3 in May 2008, respectively. For EANET sites in Cambodia, Lao PDR, Myanmar and Vietnam, the annual particulate SO_4^{2-} concentrations at Hanoi and Hoa Binh in Vietnam were remarkably decreased after 2005. The highest particulate SO_4^{2-} concentration at Phnom Penh in Cambodia was 5.85 μg/m^3 in April 2010, and it was annually decreased. At Vientiane in Lao PDR, the particulate SO_4^{2-} concentration was 10.2 μg/m^3 in November 2015 showing high levels in spring and winter like SO_2.

The highest particulate SO_4^{2-} concentration at Yangon in Myanmar was 7.51 μg/m^3 in April 2019 having generally high levels in spring and winter. The highest annual particulate SO_4^{2-} concentrations at Hanoi and Hoa Binh in Vietnam were 60.1 μg/m^3 in April 2007 and 39.5 μg/m^3 in February 2006, respectively. After these high peaks, the concentrations tended to continuously decrease. The highest annual particulate SO_4^{2-} concentration at Can Tho in Vietnam was 7.49 μg/m^3 in April 2017 and it tended to increase after 2017. The annual particulate SO_4^{2-} concentrations at the EANET sites in Thailand were also fluctuated but a specifically high peak was observed at Khanchanaburi in 2016. The highest particulate SO_4^{2-} concentration at Bangkok in Thailand was 19.3 μg/m^3 in April 2016 and its highest concentrations were occurred in dry season of 2014 and spring 2016, respectively. The highest particulate SO_4^{2-} concentration at Mae Hia in Thailand was 1.46 μg/m^3 in March 2011, and then it tended to decrease. At Khanchanaburi in Thailand, the particulate SO_4^{2-} concentration was 43.1 μg/m^3 in April 2016 and was high levels of concentration in spring.

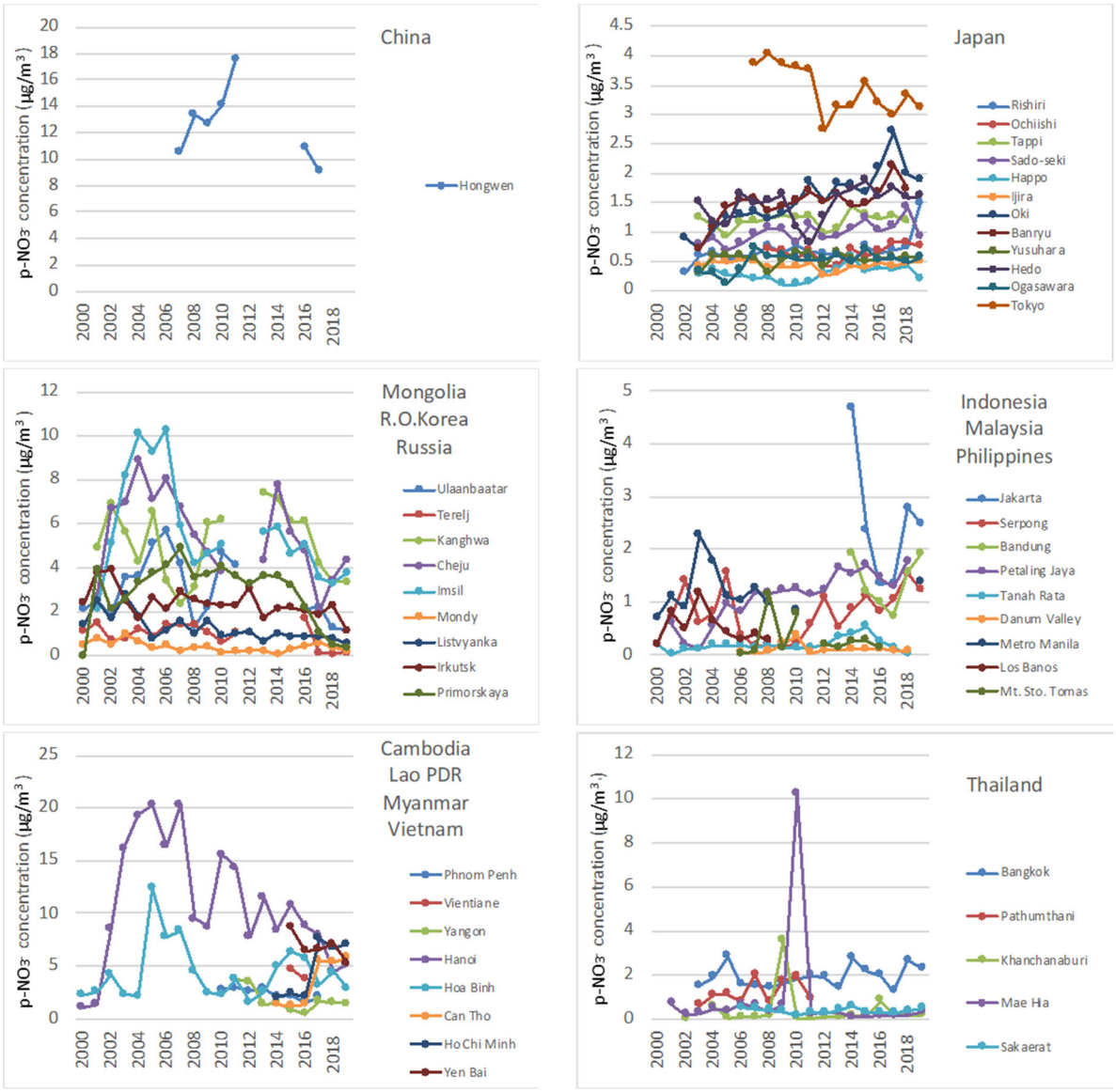

Figure 4.3.10 Annual variation of particulate NO_3^- concentration at respective EANET sites (Annual average from 2000 to 2019).

Fig. 4.3.10 shows annual variations of particulate NO_3^- concentration at respective EANET sites from 2000 to 2019. The annual particulate NO_3^- concentration at Hongwen in China was increased from 2007 to 2011, and then it showed lower values in 2016 and 2017. There is no reported data

after 2017. The particulate NO_3^- concentrations at some sites in Japan showed increasing trend. The highest particulate NO_3^- concentrations at Ijira and Ogasawara in Japan were 1.26 μg/m^3 in March 2013 and 2.3 μg/m^3 in March 2015, respectively. At Ochiishi in Japan, the particulate NO_3^- concentration was 1.98 μg/m^3 in May 2017 and the annual concentration was decreased every year. At Rishiri in Japan, both particulate NO_3^- and HNO_3 exhibited the highest values in 2019. The particulate NO_3^- concentration was 3.64 μg/m^3 in May showing the pattern of the highest value in spring. At Sado-seki in Japan, both particulate NO_3^- and HNO_3 were rapidly increased in 2018 showing the highest concentration of 8.32 μg/m^3 in March for particulate NO_3^- and 23 ppb in December for HNO_3. The highest particulate NO_3^- concentration at Tokyo in Japan was 6.57 μg/m^3 in February 2010, and it was annually decreased. For the sites in Mongolia, Republic of Korea and Russia, the annual particulate NO_3^- concentrations were fluctuated. The highest particulate NO_3^- concentration at Terelj and Ulaanbaatar in Mongolia were 0.65 μg/m^3 in December 2011 and 3.37 μg/m^3 in December 2011, respectively. Those were significantly decreased since 2016. At Cheju in Republic of Korea, a rapid increase in particulate NO_3^- concentration to 13.3 μg/m^3 was represented in May 2017, but the concentration over other period keeps lower than 4 μg/m^3. Even the highest concentration was occurred in spring 2017, a relatively high level is shown in winter during monitoring period. The highest particulate NO_3^- concentration at Imsil and Kangwha in Republic of Korea were 11.6 μg/m^3 in January 2018 and 13.4 μg/m^3 in December 2019, respectively. The highest particulate NO_3^- concentration at Irkutsk in Russia was 4.79 μg/m^3 in January 2018, and the overall concentration was decreased except for January 2018. At Listvyanka in Russia, the particulate NO_3^- concentration was 1.29 μg/m^3 in November 2016 having high levels in winter. The highest particulate NO_3^- concentration at Primorskaya in Russia was 6.68 μg/m^3 in March 2014.

For particulate NO_3^- concentrations at EANET sites in Indonesia, Malaysia and Philippines, some sites showed higher values after 2016. At Bandung in Indonesia, the particulate NO_3^- concentration was highly recorded as 4.5 μg/m^3 in June 2016, and its concentration had indicated an increasing tendency from 2017. The highest particulate NO_3^- concentration at Jakarta in Indonesia was 6.95 μg/m^3 in September 2015. The highest particulate NO_3^- concentration at Serpong in Indonesia was 2.88 μg/m^3 in August 2018. Its concentration was increased over monitoring period having a pattern of high levels in summer and winter. The highest particulate NO_3^- concentration at Danum Valley in Malaysia was 1.45 μg/m^3 in January 2010, and then it was rapidly decreased. The highest particulate NO_3^- concentration at Petaling Jaya in Malaysia was 4.35 μg/m^3 in March 2013, and higher values was recorded in summer of 2018. The highest particulate NO_3^- concentration at Tanah Rata in Malaysia was 1.51 μg/m^3 in October 2015. The highest particulate NO_3^- concentration at Metro Manila in Philippines was 2.16 μg/m^3 in November 2019. At Mt. Sto. Tomas in Philippines, the concentrations of particulate NO_3^- and HNO_3 were 3.14 μg/m^3 and 1.1 ppb in May 2010, and those were gradually decreased. For EANET sites in Cambodia, Lao PDR, Myanmar and Vietnam, the annual particulate NO_3^- concentrations at Hanoi and Hoa Binh in Vietnam had kept high level since 2008 and were rapidly increased in 2017. At Phnom Penh in Cambodia, the concentrations of particulate NO_3^- was 4.41 μg/m^3 in March 2015. Both particulate NO_3^- and HNO_3 had generally indicated a pattern of high levels in spring and winter. The particulate NO_3^- concentration at Vientiane in Lao PDR was 0.83 μg/m^3 in May 2016 and was high in spring and summer. At Yangon in Myanmar, the particulate NO_3^- concentration was rapidly increased in 2017 and recorded the maximum value of 23.6 μg/m^3 in December 2017. The highest annual particulate NO_3^- concentrations at Hanoi and Hoa Binh in Vietnam were 23.9 μg/m^3 in April 2007 and 12.4 μg/m^3 in February 2006, respectively. The highest annual particulate NO_3^- concentration at Can Tho in Vietnam was 4.00 μg/m^3 in April 2017 and it tended to increase after 2017. The annual particulate NO_3^- concentrations at the EANET sites in Thailand were also fluctuated but a specifically high peak was observed at Mae Hia in 2010. At Bangkok in Thailand, the particulate NO_3^- concentration was 16.8 μg/m^3 as the highest in February 2014 and showed similar concentration levels except for the winter in 2014 when had the highest concentration over whole monitoring period. The maximum values of particulate NO_3^- and HNO_3 at Mae Hia in Thailand were 68.2 μg/m^3 and 8.01 ppb in May 2010 but similar values in low concentration for both were kept after that. The highest particulate NO_3^- concentrations at Pathumthani, Khanchanaburi and Sakaerat in Thailand were 11.2 μg/m^3 in January 2017, 10.1 μg/m^3 in November 2009 and 1.62 μg/m^3 in January 2014, respectively.

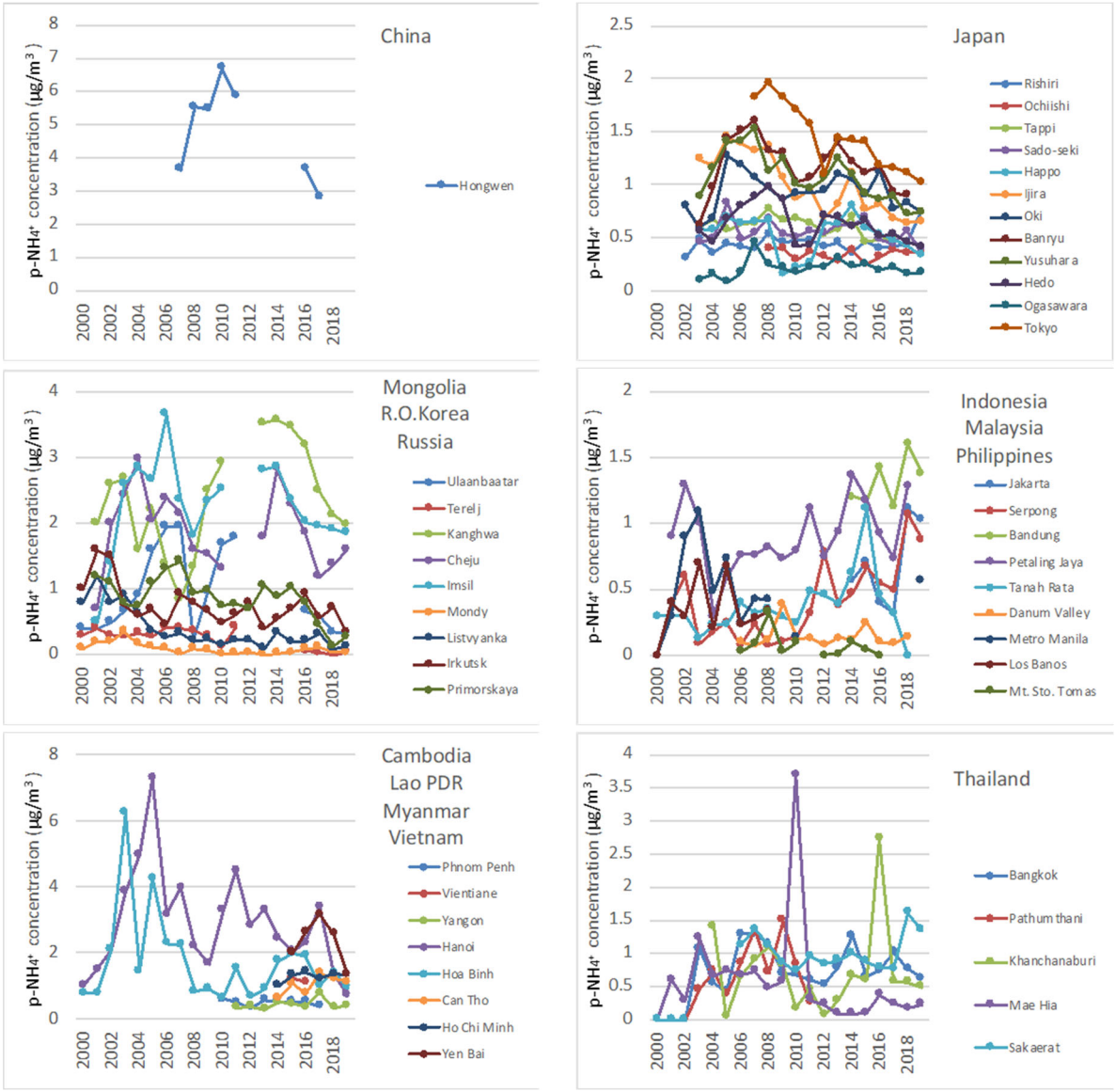

Figure 4.3.11 Annual variation of particulate NH_4^+ concentration at respective EANET sites (Annual average from 2000 to 2019).

Fig. 4.3.11 shows annual variations of particulate NH_4^+ concentration at respective EANET sites from 2000 to 2019. The annual particulate NH_4^+ concentration at Hongwen in China was increased from 2007 to 2011, and then it showed lower values in 2016 and 2017. There is no reported data after 2017. The particulate NH_4^+ concentrations at some sites in Japan showed decreasing trend. The highest particulate NH_4^+ concentration at Hedo, Oki and Tokyo were 1.62 µg/m^3 in January 2015, 1.96 µg/m^3 in February 2011 and 2.83 µg/m^3 in August 2013, respectively. The particulate NH_4^+ concentration at Happo in Japan exhibited the maximum value of 2.01 µg/m^3 in 2013 and slowly decreased after 1.82 µg/m^3 in April 2014. At Ijira in Japan, the particulate NH_4^+ concentration was 1.96 µg/m^3 in May 2012, and it was decreased over monitoring period. The particulate NH_4^+ concentration at Ochiishi in Japan was 0.9 µg/m^3 in February 2019, and it has been continuously decreased since 2008. At Ogasawara in Japan, the particulate NH_4^+ concentration was 0.55 µg/m^3 in December 2013, its level of concentrations was annually decreased. At Rishiri in Japan the highest particulate NH_4^+ concentration was 1.11 µg/m^3 in May 2019. Both NH_3 and the highest particulate NH_4^+ were significantly increased over monitoring period. At Sado-seki in Japan, both NH_3 and the highest particulate NH_4^+ showed the highest values of 2.3 ppb in May 2018 and 2.97 µg/m^3 in March

2018, respectively. NH_3 had a trend to increase the concentration, whereas particulate NH_4^+ was gradually decreased. The highest particulate NH_4^+ at Yusuhara in Japan was 2.44 μg/m^3 in May 2012, and it was generally high levels in spring having its decreasing trend over the period. For the sites in Mongolia, Republic of Korea and Russia, the annual particulate NH_4^+ concentrations were fluctuated. The particulate NH_4^+ concentration at Terelj in Mongolia was 0.63 μg/m^3 in March 2011. In this year, the particulate NH_4^+ were relatively high but were gradually decreased after that. While the particulate NH_4^+ concentration at Ulaanbaatar in Mongolia was annually decreased, and it showed high level of 5.02 μg/m^3 in 2011, especially in winter season. The particulate NH_4^+ concentration at Cheju in Republic of Korea was 10.5 μg/m^3 in January 2014 but had a trend to decrease gradually. The highest particulate NH_4^+ concentrations at Imsil and Kangwha in Republic of Korea were 5.41 μg/m^3 in January 2014 and 7.09 μg/m^3 in May 2014. Respectively. Then, it was gradually increased. The highest particulate NH_4^+ concentration at Irkutsk in Russia was 4.41 μg/m^3 in January 2018 having a pattern of high levels in winter. The highest particulate NH_4^+ concentrations at Listvyanka, Mondy and Primorskaya in Russia were 1.1 μg/m^3 in August 2017, 0.27 μg/m^3 in July 2017 and 2.18 μg/m^3 in November 2015, respectively.

For particulate NH_4^+ concentrations at EANET sites in Indonesia, Malaysia and Philippines, some sites showed clear increasing trend after 2010. In December 2019, the highest concentrations of NH_3 and particulate NH_4^+ were observed at Bandung in Indonesia were 16.2 ppb and 2.29 μg/m^3 in respective and both had showed a tendency to increase. The particulate NH_4^+ concentration at Jakarta in Indonesia was 1.84 μg/m^3 in May 2018, and it showed increasing trend. The particulate NH_4^+ concentration at Serpong in Indonesia was 1.91 μg/m^3 in December 2019, and it was increased during the period. The highest particulate NH_4^+ concentration at Danum Valley in Malaysia was 0.95 μg/m^3 in September 2015. At Petaling Jaya in Malaysia, the particulate NH_4^+ concentration was 2.62 μg/m^3 in April 2016, and it showed the maximum value in spring 2016. The highest concentrations of NH_3 and particulate NH_4^+ at Tanah Rata in Malaysia were 8.7 ppb and 3.96 μg/m^3 respectively in October 2015, and those time variation patterns are similar. The highest concentrations of NH_3 and particulate NH_4^+ at Metro Manila in Philippines were 25.1 ppb and 3.17 μg/m^3 in April 2019, respectively. The concentration of particulate NH_4^+ at Mt. Sto. Tomas in the Philippines was 0.95 μg/m^3 in May 2010, and then it was decreased. For EANET sites in Cambodia, Lao PDR, Myanmar and Vietnam, the annual particulate NH_4^+ concentrations at Hanoi and Hoa Binh in Vietnam had continuously decreased since 2005. The highest particulate NH_4^+ concentration at Phnom Penh in Cambodia was 1.34 μg/m^3 in April 2010. The highest particulate NH_4^+ concentration at Vientiane in Lao PDR was 3.09 μg/m^3 in November 2015 showing the highest annual concentration in 2015. At Yangon in Myanmar, the particulate NH_4^+ concentration was rapidly increased from November 2017, and its highest value was 8.72 μg/m^3 in December 2017. The particulate NH_4^+ concentration at Can Tho in Vietnam was 1.92 μg/m^3 in May 2017, and it had a trend to increase concentrations in spring. At Hanoi, Vietnam, the particulate NH_4^+ concentration was 9.93 μg/m^3 in December 2013 showing the maximum value, and it exhibits high concentration especially in winter. The highest particulate NH_4^+ concentration at Yen Bai in Vietnam was 7.61 μg/m^3 in March 2016, and the overall concentration was decreased since 2016. The annual particulate NH_4^+ concentrations at the EANET sites in Thailand were fluctuated, but specifically high peaks were observed at Mae Hia in 2010 and Khanchanaburi in 2016. The particulate NH_4^+ concentration at Bangkok in Thailand was 7.05 μg/m^3 in February 2017. This had a trend to generally increase in winter. The particulate NH_4^+ concentration at Mae Hia in Thailand was 1.31 μg/m^3 in May 2016, and it has the similar variation pattern with NH_3. The highest particulate NH_4^+ concentration at Nakhon Ratchasima in Thailand was 3.14 μg/m^3 in October 2013. Like NH_3, it has a pattern of high levels in spring and winter. The highest particulate NH_4^+ concentration at Pathumthani in Thailand was 2.49 μg/m^3 in November 2010. At Sakaerat in Thailand, the particulate NH_4^+ concentration was 2.87 μg/m^3 in February 2019, and it was increased over whole monitoring period.

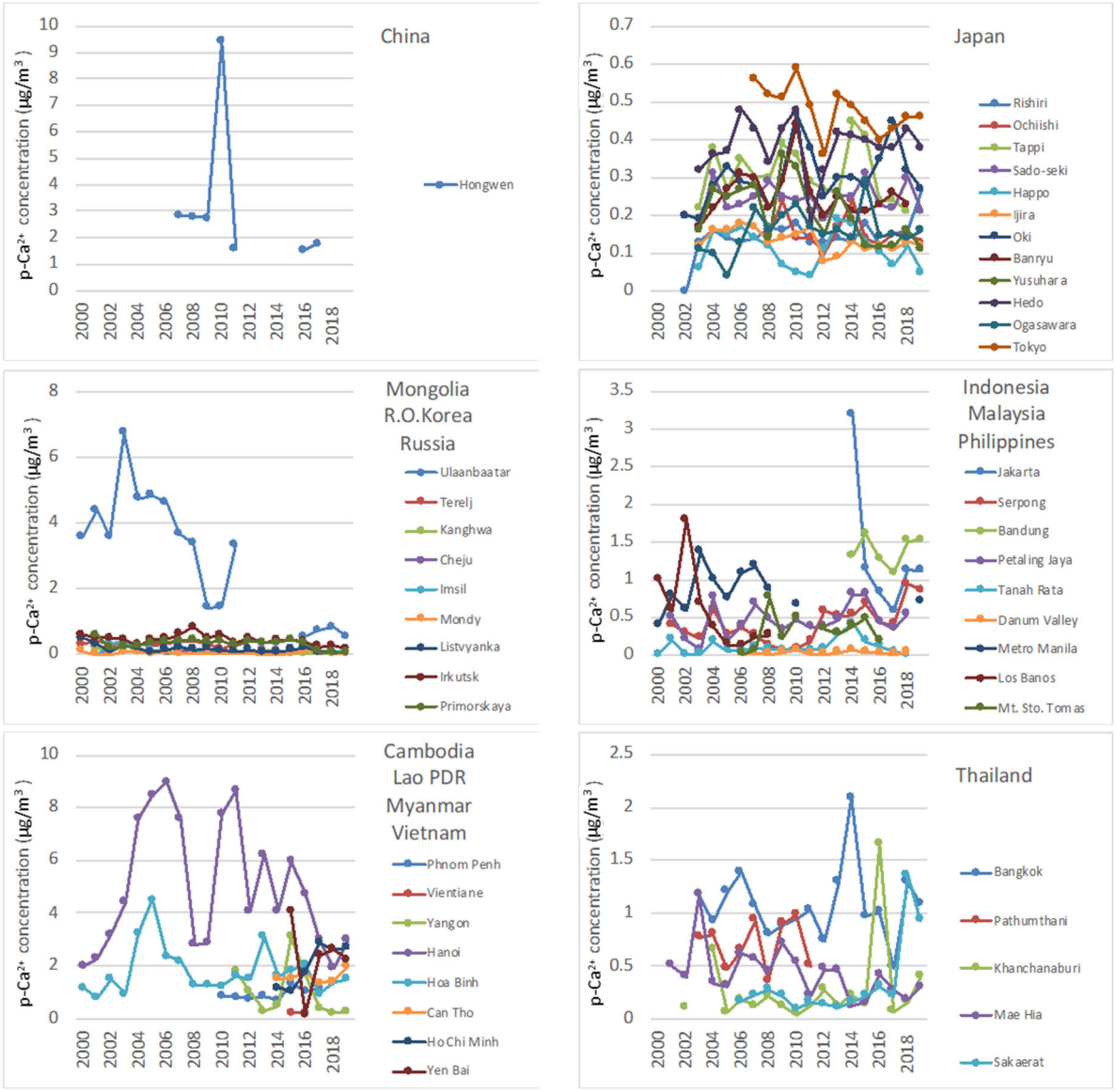

Figure 4.3.12 Annual variation of particulate Ca^{2+} concentration at respective EANET sites (Annual average from 2000 to 2019).

Fig. 4.3.12 shows annual variations of particulate Ca^{2+} concentration at respective EANET sites from 2000 to 2019. The annual particulate Ca^{2+} concentration at Hongwen in China was remarkably high in 2010, and it showed lower values in 2016 and 2017. There is no reported data after 2017. The particulate Ca^{2+} concentrations at the sites in Japan were fluctuated and low level (less than 0.5 μg/m^3). The highest values of particulate Ca^{2+} and Mg^{2+} at Happo in Japan were 0.97 μg/m^3 in March 2013 and 0.11 μg/m^3 in May 2014, respectively. Even both have a seasonal pattern of high level in spring, their concentrations are gradually decreased. The highest particulate Ca^{2+} concentration at Hedo, Ochiishi, Sado-seki in Japan were 2.44 μg/m^3 in March 2010, 3.08 μg/m^3 in December 2014 and 0.96 μg/m^3 in May 2014, respectively. The particulate Ca^{2+} concentration at Ijira in Japan was 0.6 μg/m^3 in May 2011 and had a seasonal pattern of high levels in spring. At Ogasawara in Japan, the overall particulate Ca^{2+} concentration during monitoring period showed high levels in fall and its concentration was 1.33 μg/m^3 in March 2015 and indicated high levels in spring. The highest particulate Ca^{2+} concentration at Oki in Japan was 1.3 μg/m^3 in November 2010 showing high levels in spring, and its concentration was annually decreased. At Rishiri in Japan, the particulate Ca^{2+} concentration was 0.51 μg/m^3 in April 2015, and it was high levels in spring. The highest particulate Ca^{2+} concentration at Tokyo in Japan was 1.68 μg/m^3 in July 2010, and it was annually decreased

over monitoring period. At Yusuhara, Japan, the particulate Ca^{2+} concentration showed high levels in spring with 1.15 μg/m^3 in March 2010, and it was generally decreased. For the sites in Mongolia, Republic of Korea and Russia, the annual particulate Ca^{2+} concentrations were fluctuated except decreasing trend in Ulaanbaatar in Mongolia. At Ulaanbaatar in Mongolia, the particulate Ca^{2+} concentration was 6.4 μg/m^3 in July 2011 showing the highest concentration, and it was decreased every year. The highest particulate Ca^{2+} concentration at Cheju, Imsil and Kangwha in Republic of Korea were 0.29 μg/m^3 in January 2014, 0.29 μg/m^3 in June 2018 and 0.31 μg/m^3 in May 2014. respectively. The particulate Ca^{2+} concentration at Kangwha showed decreasing trend. The highest particulate Ca^{2+} concentration at Irkutsk in Russia was 1.44 μg/m^3 in May 2010, and it had a trend to decrease during whole period. The highest particulate Ca^{2+} concentrations at Listvyanka, Mondy and Primorskaya in Russia were 0.46 μg/m^3 in July 2017, 0.21 μg/m^3 in July 2016 and 1.22 μg/m^3 in April 2012, respectively. The particulate Ca^{2+} concentration at Primorskaya showed decreasing trend.

For particulate Ca^{2+} concentrations at EANET sites in Indonesia, Malaysia and Philippines, some sites showed increasing or decreasing trend after 2012. The highest particulate Ca^{2+} concentration at Bandung in Indonesia was 11.7 μg/m^3 in October 2015, and it had overall increasing trend. At Jakarta in Indonesia, the particulate Ca^{2+} concentration was 5.56 μg/m^3 in November 2014 and Mg^{2+} was 0.47 μg/m^3 in August 2014. Both Ca^{2+} and Mg^{2+} had a trend to decrease in concentration levels. At Serpong in Indonesia, the highest concentrations of particulate Ca^{2+} and Mg^{2+} were 1.92 μg/m^3 and 0.22 μg/m^3 in August 2019, and these levels were increased over whole monitoring period. In addition, it generally had a pattern of high levels in summer. At Danum Valley in Malaysia, the particulate Ca^{2+} concentration was 0.27 μg/m^3 in March 2010 and Mg^{2+} was significantly decreased after showing the maximum value at 0.38 μg/m^3 in February 2010. The highest particulate Ca^{2+} concentration at Petaling Jaya and Tanah Rata in Malaysia was 1.86 μg/m^3 in July 2014 and 1.21 μg/m^3 in February 2014, respectively. At Metro Manila in Philippines, the particulate Ca^{2+} and Mg^{2+} concentrations were 1.49 μg/m^3 and 0.18 μg/m^3 in April 2010, respectively. The highest particulate Ca^{2+} concentration at Mt. Sto. Tomas in Philippines was 1.46 μg/m^3 in October 2015, and the overall concentration was gradually decreased.

For EANET sites in Cambodia, Lao PDR, Myanmar and Vietnam, the annual particulate Ca^{2+} concentrations at Hanoi and Hoa Binh in Vietnam largely fluctuated, and some site showed increasing trend since 2014. At Phnom Penh in Cambodia, the particulate Ca^{2+} and Mg^{2+} concentrations were 2.2 μg/m^3 and 0.31μg/m^3 in March 2015 respectively showing the pattern of high levels in spring. Both were gradually increased in concentration during whole monitoring period. At Vientiane in Lao PDR, the particulate Ca^{2+} concentration was 0.35 μg/m^3 in January 2015. The highest particulate Ca^{2+} concentration at Yangon in Myanmar was 12.9 μg/m^3 in November 2015, and it indicated high levels especially in spring. At Can Tho in Vietnam, the particulate Ca^{2+} concentration was recorded in 3.97 μg/m^3 in August 2016 and Mg^{2+} was 0.69 μg/m^3 in February 2017. Compare to Ca^{2+}, Mg^{2+} has a trend to increase the concentration over whole monitoring period. At Hanoi in Vietnam, the particulate Ca^{2+} and Mg^{2+} concentrations were 19.0 and 1.90 μg/m^3 in February 2010 showing the maximum values, and their concentrations were gradually decreased. The highest particulate Ca^{2+} concentration at Yen Bai in Vietnam was 5.29 μg/m^3 in December 2015. It was rapidly decreased in 2016 but increased in 2018 again. The annual particulate Ca^{2+} concentrations at the EANET sites in Thailand were fluctuated. At Mae Hia in Thailand, the maximum values of particulate Ca^{2+} and Mg^{2+} concentrations were 1.32 μg/m^3 in May 2010 and 0.11 μg/m^3 in April 2010, respectively. The highest particulate Ca^{2+} concentration at Pathumthani in Thailand was 2.07 μg/m^3 in November 2010. At Sakaerat in Thailand, the particulate Ca^{2+} concentration was 3.15 μg/m^3 in August 2018 showing the highest value. The overall concentration was increased and showed a pattern of high levels mainly in summer and winter.

4.3.2 Monthly variations of gas and aerosol concentrations at respective sites

Since there is a variety of characteristics of the EANET sites having different local emission sources of air pollutants and local climate, analysis of seasonal variation will also characterize regional features of acidic deposition and related air pollutions in East Asia. In this section, monthly variations of the major gaseous and aerosol concentrations at the selected EANET sites are discussed.

4.3.2.1 SO_2 and SO_4^{2-} in PM

Fig. 4.3.13 shows monthly variations of SO_2 and particulate SO_4^{2-} concentrations at the selected EANET sites. The monthly variations are demonstrated by the averages of 2000-2004, 2005-2009, 2010-2014 and 2015-2019, respectively (Same as for the other components shown in the following sections). Both SO_2 and particulate SO_4^{2-} concentrations were high in winter and low in summer at Ulaanbaatar in Mongolia due to high use of coal and the strong inversion layer below -20ºC. The particulate SO_4^{2-} concentration in summer during 2015-2019 was remarkably lower than those in previous years. As with Ulaanbaatar, both SO_2 and particulate SO_4^{2-} concentrations were high in winter and low in summer at Irkutsk in Russia due to coal combustion and low temperature in winter. The particulate SO_4^{2-} concentration in summer during 2015-2019 seem to be lower than those in previous years. Both SO_2 and particulate SO_4^{2-} concentrations were high in winter at Hongwen and Jinyunshan in China but the seasonal change was smaller than those at Ulaanbaatar and Irkutsk. At both sites, the SO_2 concentration in summer during 2015-2019 was remarkably lower than those in previous years, especially high concentrations in winter were disappeared during 2015-2019. At Kangwha in Republic of Korea, the SO_2 concentration in winter was clearly higher during 2010-2014, but high SO_2 concentration in winter was not observed during 2015-2019. For SO_2 and particulate SO_4^{2-} concentrations at Cheju in Republic of Korea, while the winter shows an obvious seasonal feature till 2014 shown high levels of concentration, there is no significant seasonal effect after concentration decrease. For the sites in Japan, the SO_2 concentration in winter and the particulate SO_4^{2-} concentration in summer were clearly higher at Rishiri, whereas both SO_2 and particulate SO_4^{2-} concentrations were higher in winter at Hedo. At Tokyo in Japan, both SO_2 and particulate SO_4^{2-} concentrations were higher in summer and the concentrations during 2015-2019 was remarkably lower than those in previous years,

At EANET site of Hanoi in Vietnam, the particulate SO_4^{2-} concentration higher in winter, but the concentration level and seasonal variation during 2015-2019 were clearly smaller than those in previous years. At EANET site of Mt. Sto. Tomas in Philippines, high peaks of SO_2 and particulate SO_4^{2-} concentrations were observed in May during 2005-2009 and 2010-2014, but such peak was not observed during 2015-2019. At EANET site of Phnom Penh in Cambodia, the SO_2 and particulate SO_4^{2-} concentrations tended to higher in dry season of January to March. At EANET site of Yangon in Myanmar, the SO_2 and particulate SO_4^{2-} concentrations tended to higher in dry season of January to March and October to December, and the SO_2 concentration during 2015-2019 was lower through the year. For the sites in Thailand, the SO_2 and particulate SO_4^{2-} concentrations were higher in dry season of January to April and October to December. At EANET site in Bangkok, the SO_2 concentration level and seasonal variation during 2015-2019 were clearly smaller than those in previous years. At Sakaerat, the SO_2 concentration from October to December during 2015-2019 was lower than those in previous years. At EANET site of Petaling Jaya in Malaysia, both SO_2 and particulate SO_4^{2-} concentrations were higher from June to August, and the SO_2 concentration during 2015-2019 was lower than those in previous years for whole year. At Danum Valley in Malaysia, high peaks of SO_2 and particulate SO_4^{2-} concentrations were observed from September to November, and the SO_2 concentration during 2015-2019 was lower than those in previous years. At EANET site of Serpong in Indonesia, the SO_2 and particulate SO_4^{2-} concentrations were higher from July to November. The overall concentration showed a pattern of high levels in dry season of May to October by exhibiting higher concentrations during 2015-2019.

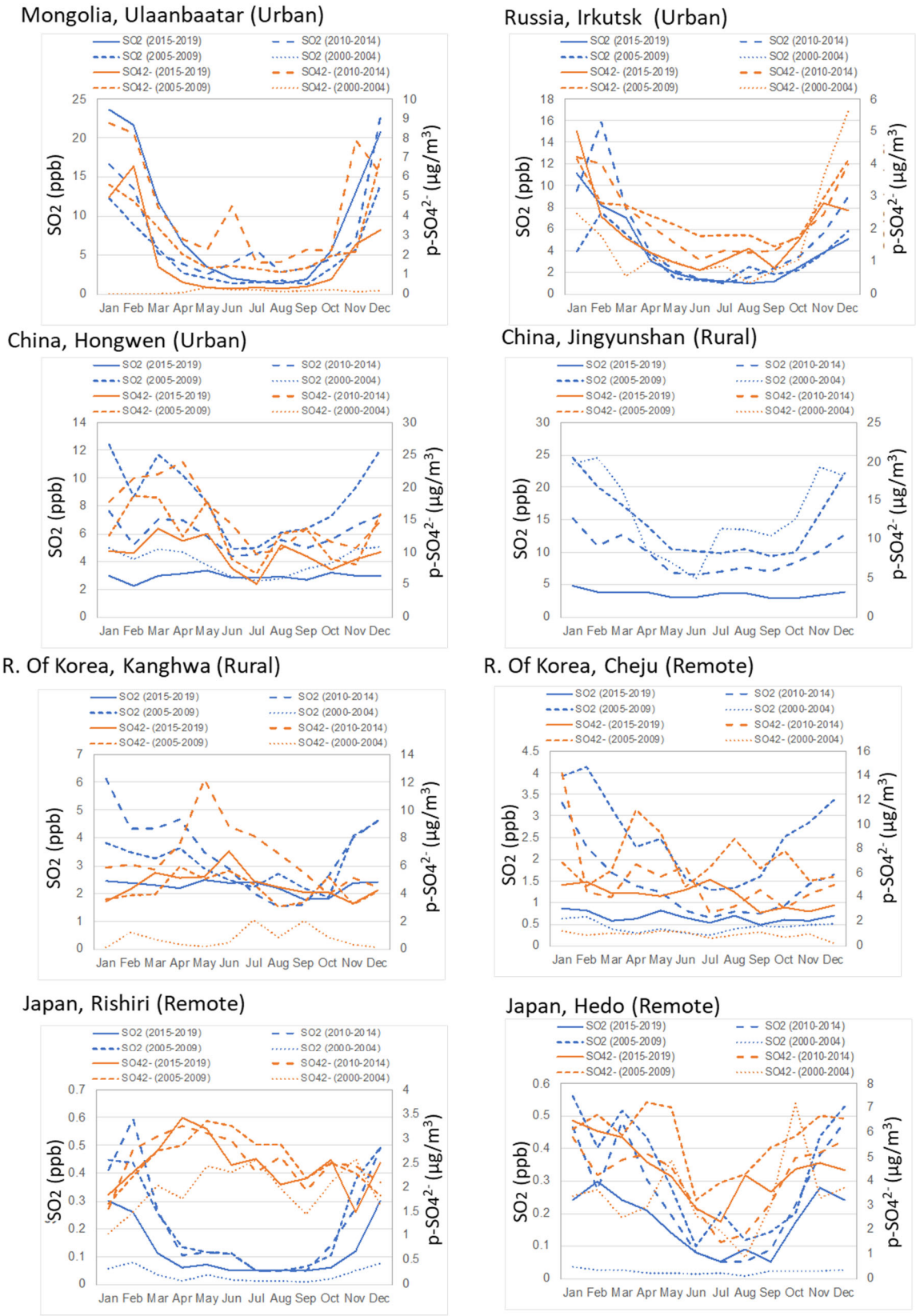

Figure 4.3.13 Monthly variations of SO_2 and particulate SO_4^{2-} concentrations at the selected EANET sites from north to south (Averages of 2000-2004, 2005-2009, 2010-2014 and 2015-2019).

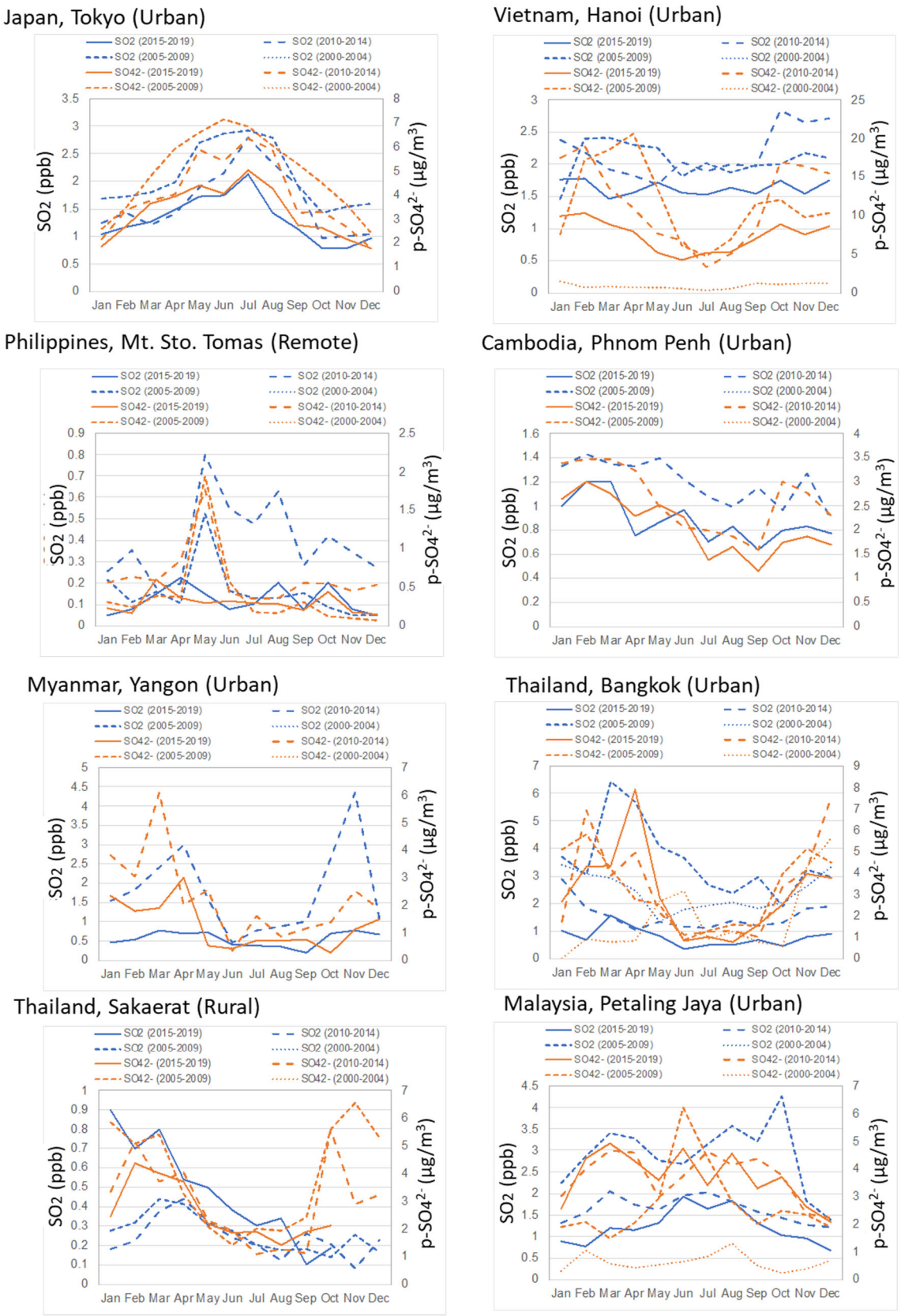

Figure 4.3.13 Monthly variations of SO_2 and particulate SO_4^{2-} concentrations at the selected EANET sites from north to south (Averages of 2000-2004, 2005-2009, 2010-2014 and 2015-2019), continued.

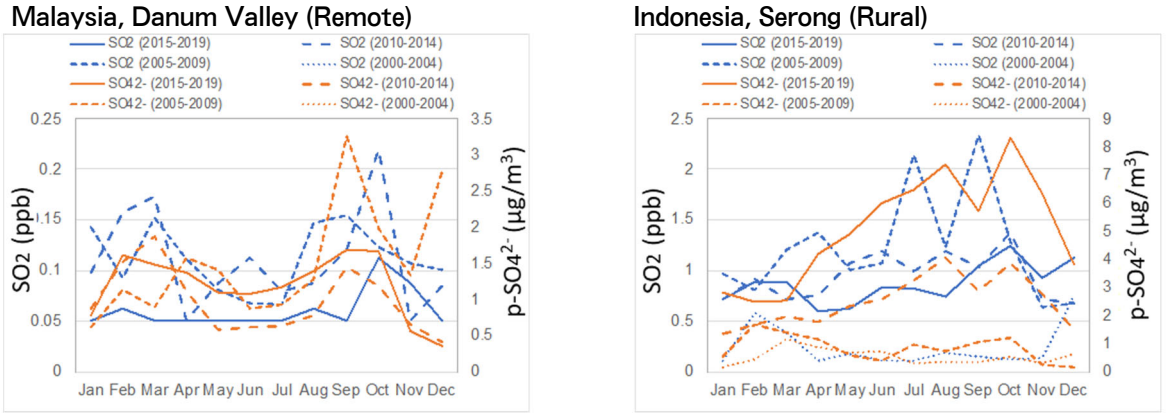

Figure 4.3.13 Monthly variations of SO_2 and particulate SO_4^{2-} concentrations at the selected EANET sites from north to south (Averages of 2000-2004, 2005-2009, 2010-2014 and 2015-2019), continued.

4.3.2.2 HNO_3 and NO_3^- in PM

Fig. 4.3.14 shows monthly variations of HNO_3 and particulate NO_3^- concentrations at the selected EANET sites. The particulate NO_3^- concentrations were high in winter and low in summer at Ulaanbaatar in Mongolia due to low volatility of nitrate aerosol and the strong inversion layer. For whole year, the HNO_3 and particulate NO_3^- concentrations during 2015-2019 were remarkably lower than those in previous years. As with Ulaanbaatar, both particulate NO_3^- concentrations were high in winter at Irkutsk in Russia. The particulate NO_3^- concentration in summer during 2015-2019 seem to be lower than those in previous years, and the HNO_3 concentration was remarkably lower during 2015-2019. At Hongwen in China, the HNO_3 concentration was higher in summer, whereas the particulate NO_3^- concentration was lower, which is possibly due to volatilization of nitrate aerosol in high temperature. At Kangwha in Republic of Korea, clear seasonal variations of high HNO_3 concentration in summer and high particulate NO_3^- concentration in winter were observed. However, there is no clear seasonal variation at Cheju in Republic of Korea. At both Kangwha and Cheju, the HNO_3 concentration during 2015-2019 was lower than those in previous years. For the sites in Japan, the HNO_3 concentration in summer and the particulate NO_3^- concentration in winter were clearly higher at Tokyo, but similar seasonal trend was not observed in the background sites of Rishiri and Hedo. This implies local photochemical formation of HNO_3 and particulate NO_3^- is considerable in urban area.

At EANET site of Hanoi in Vietnam, the HNO_3 concentration in summer and the particulate NO_3^- concentration in winter were clearly higher, but the similar seasonal trend was not observed in Hoa Binh. At both Hanoi and Hoa Binh, HNO_3 and particulate NO_3^- concentrations during 2015-2019 seem to be higher than those in previous years. At EANET site of Mt. Sto. Tomas in Philippines, high peaks of HNO_3 and particulate NO_3^- concentrations were observed in May and March during 2015-2019 and those concentrations were higher for whole year. At EANET site of Phnom Penh in Cambodia, the HNO_3 and particulate NO_3^- concentrations tended to higher in dry season of January to March and the concentrations during 2015-2019 were slightly lower than those in previous years. At Yangon in Myanmar, high peaks of HNO_3 and particulate NO_3^- concentrations were observed in May during 2015-2019 and January during 2010-2014, respectively. At EANET site of Bangkok in Thailand, both HNO_3 and particulate NO_3^- concentrations are lower in wet season from June to September. On the other hand, the particulate NO_3^- concentration was higher from June to September at Sakaerat in Thailand. For the EANET sites in Malaysia, the particulate NO_3^- concentration was higher from November to February at Danum Valley, whereas there is no clear seasonal variation in Petaling Jaya. At EANET site of Serpong in Indonesia, the HNO_3 and particulate NO_3^- concentrations were higher from July to November. The particulate NO_3^- concentrations were increased over monitoring period having a pattern of high levels in summer and winter during 2015-2019. The HNO_3 concentration was kept stable as the same level till summer of 2018 but was rapidly increased after fall.

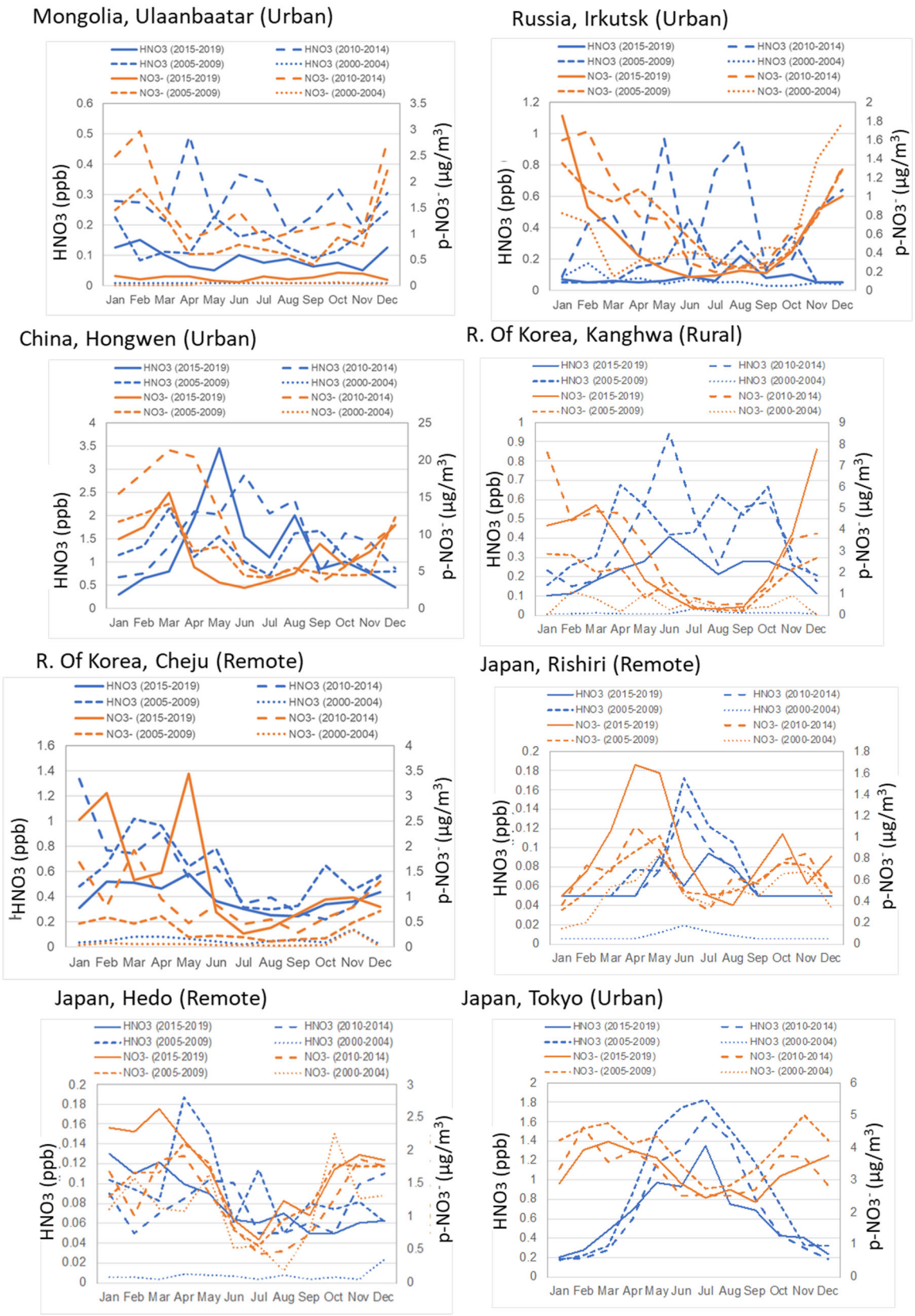

Figure 4.3.14 Monthly variations of HNO_3 and particulate NO_3^- concentrations at the selected EANET sites from north to south (Averages of 2000-2004, 2005-2009, 2010-2014 and 2015-2019).

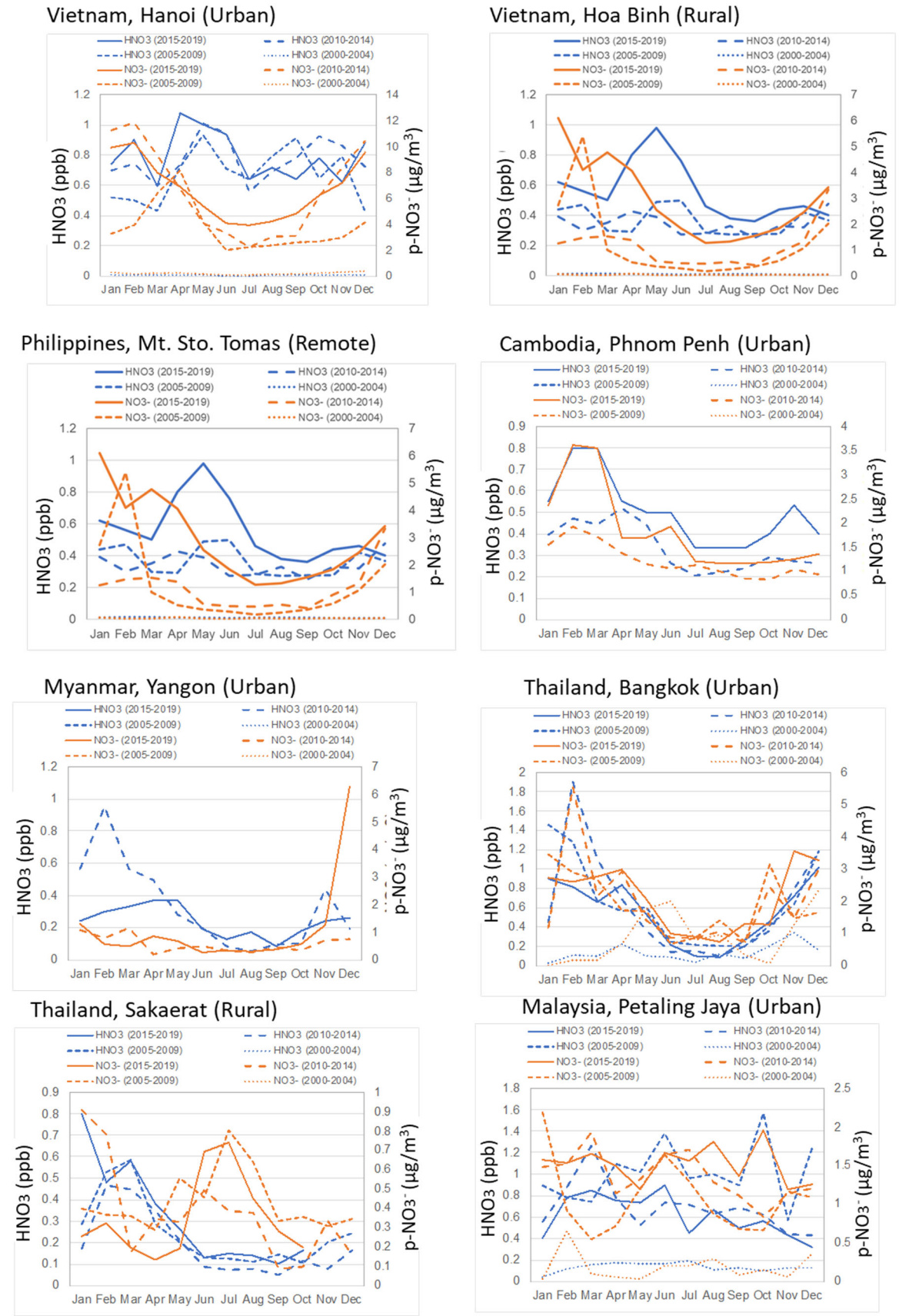

Figure 4.3.14 Monthly variations of HNO_3 and particulate NO_3^- concentrations at the selected EANET sites from north to south (Averages of 2000-2004, 2005-2009, 2010-2014 and 2015-2019), continued.

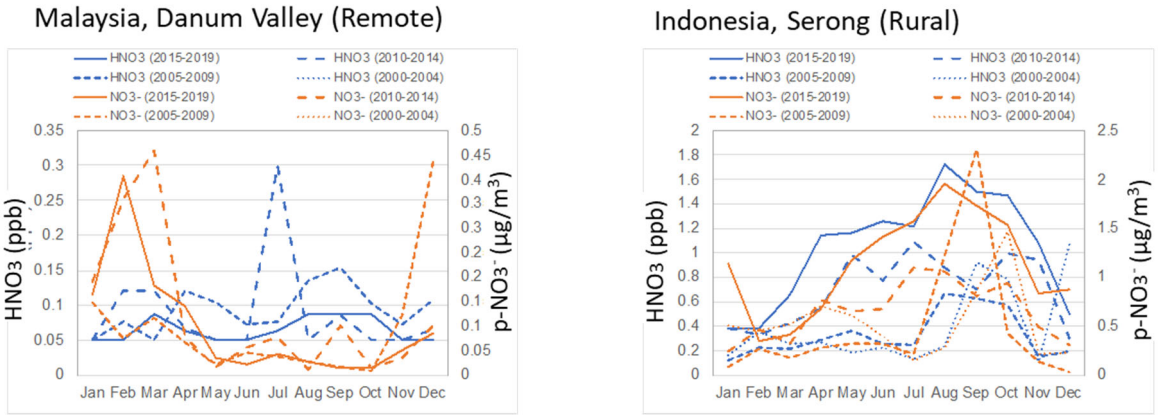

Figure 4.3.14 Monthly variations of HNO_3 and particulate NO_3^- concentrations at the selected EANET sites from north to south (Averages of 2000-2004, 2005-2009, 2010-2014 and 2015-2019), continued.

4.3.2.3 NH_3 and NH_4^+ in PM

Fig. 4.3.15 shows monthly variations of NH_3 and particulate NH_4^+ concentrations at the selected EANET sites. The particulate NH_4^+ concentrations were high in winter and low in summer at Ulaanbaatar in Mongolia due to low volatility of ammonium aerosol and the strong inversion layer. High concentration of NH_3 was observed in summer during 2010-2014, but the same trend was not observed during 2015-2019. Likely Ulaanbaatar, the particulate NH_4^+ concentrations were high in winter at Irkutsk in Russia and Hongwen in China, but there is no clear seasonal trend for NH_3. At Cheju and Kangwha in Republic of Korea, the NH_3 concentration was higher in summer and the particulate NH_4^+ concentration tends to be higher in spring (March to May). The similar seasonal trends of Cheju and Kangwha were observed at the background sites of Rishiri and Hedo in Japan. On the other hand, there is no clear seasonal trend of the particulate NH_4^+ at Tokyo in Japan, and both NH_3 and particulate NH_4^+ concentrations during 2015-2019 were slightly lower than those in previous years.

At EANET sites of Hanoi and Hoa Binh in Vietnam, the particulate NH_4^+ concentration was higher in winter, but there is no clear seasonal variation for NH_3. For whole year, the NH_3 concentration at Hoa Binh during 2015-2019 was lower than those in previous years. At EANET site of Mt. Sto. Tomas in Philippines, high peaks of NH_3 and particulate NH_4^+ concentrations were observed in March during 2005-2009 and 2010-2014 and May during 2005-2009 and 2010-2014, but the peak was shifted during 2015-2019. At EANET site of Phnom Penh in Cambodia, the NH_3 and particulate NH_4^+ concentrations tended to higher in dry season of January to March. At EANET site of Yangon in Myanmar, the NH_3 and particulate NH_4^+ concentrations tended to be higher in dry season of January to March and November to December. And the particulate NH_4^+ concentration during 2015-2019 was specifically high in December. For the EANET sites in Thailand, the NH_3 and particulate NH_4^+ concentrations were lower in wet season of June to September. At EANET site in Sakaerat, the NH_3 concentration during 2015-2019 was higher than those in previous years for whole year. At EANET site of Petaling Jaya in Malaysia, the NH_3 concentrations was higher from August to October, and the particulate NH_4^+ concentration was higher from March to June. On the other hand, at EANET site of Danum Valley in Malaysia, high particulate NH_4^+ concentration was observed in September and October. At EANET site of Serpong in Indonesia, the particulate NH_4^+ concentration showed low level, and the NH_3 concentrations were higher from April to November.

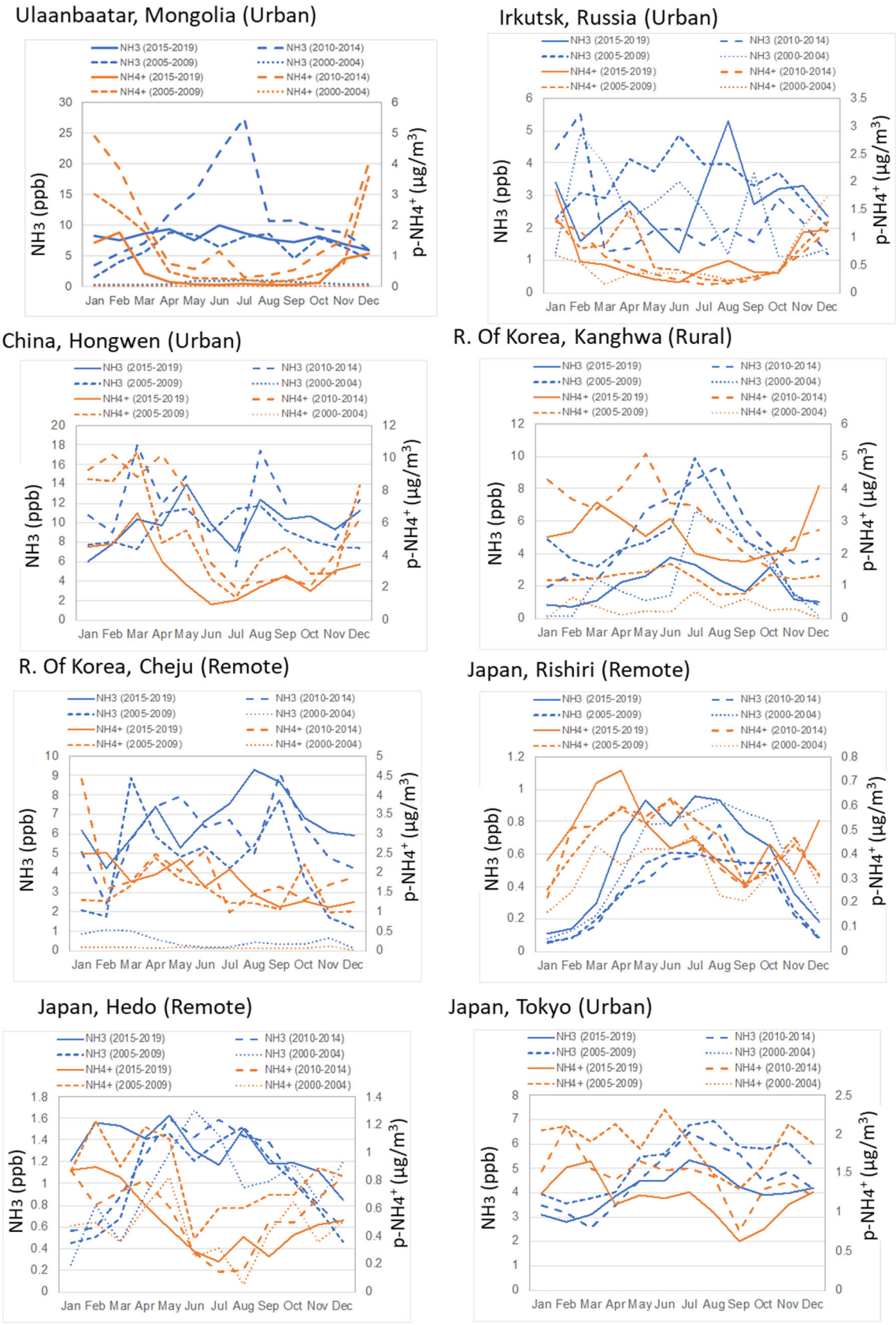

Figure 4.3.15 Monthly variations of NH_3 and particulate NH_4^+ concentrations at the selected EANET sites from north to south (Averages of 2000-2004, 2005-2009, 2010-2014 and 2015-2019).

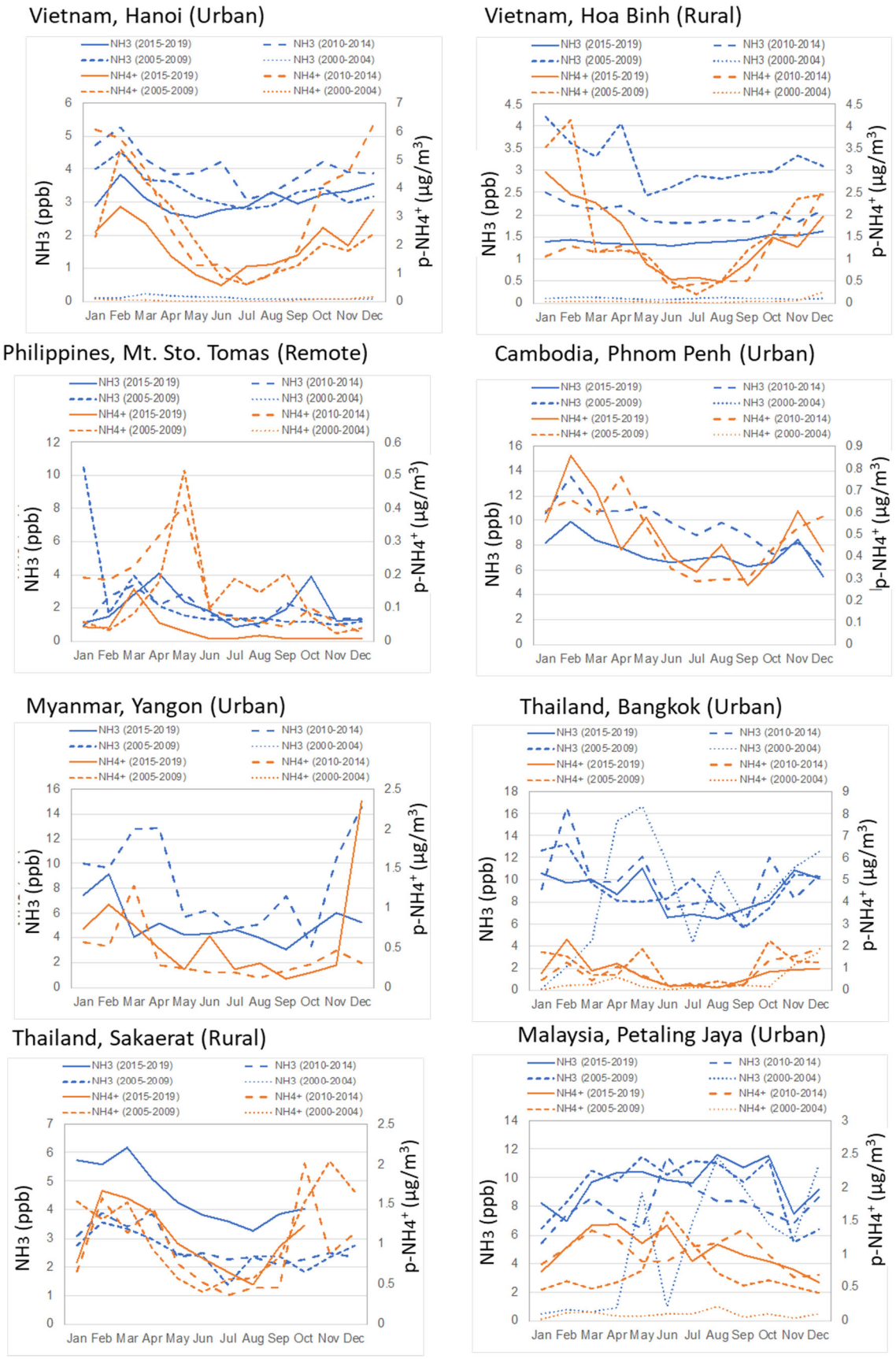

Figure 4.3.15 Monthly variations of NH_3 and particulate NH_4^+ concentrations at the selected EANET sites from north to south (Averages of 2000-2004, 2005-2009, 2010-2014 and 2015-2019), continued.

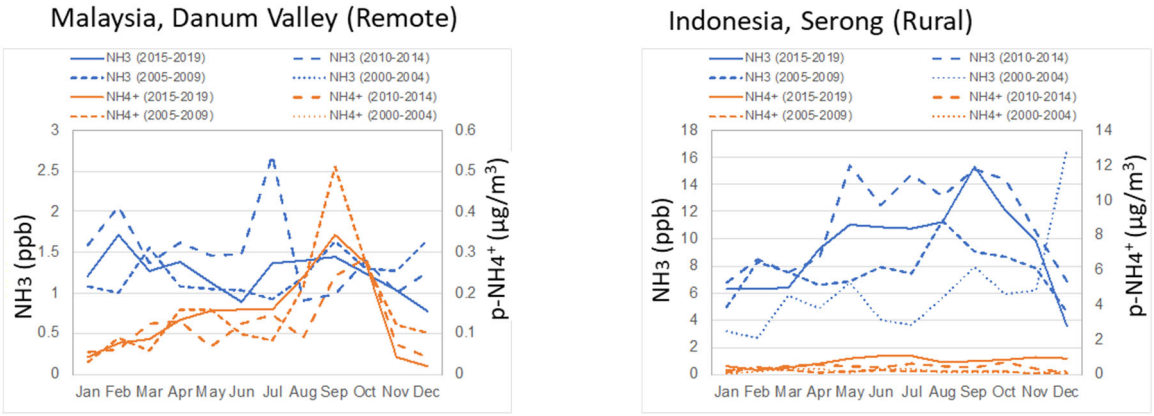

Figure 4.3.15 Monthly variations of NH_3 and particulate NH_4^+ concentrations at the selected EANET sites from north to south (Averages of 2000-2004, 2005-2009, 2010-2014 and 2015-2019), continued.

4.3.2.4 NO_2 and NOx

Fig. 4.3.16 shows monthly variations of NO_2 and NOx concentrations at the selected EANET sites. The NOx concentration was remarkably high in winter and low in summer at Ulaanbaatar in Mongolia due to the strong inversion layer in cold weather condition. Likely Ulaanbaatar, Jinyunshan in China showed higher NOx concentration in winter, which would be mainly caused by climate condition. For whole year, the NOx concentration during 2015-2019 was remarkably higher than those in previous years. At Hongwen in China, the NOx concentration was higher in winter, and the concentration during 2015-2019 was remarkably higher than those in during 2005-2009 and 2010-2014. At Kangwha and Imsil in Republic of Korea, the NOx concentration in winter was higher and the concentration level is not significantly changed from 2000 to 2019. At Rishiri in Japan, the NOx concentration was high in summer (April to July), whereas the NOx concentration at Hedo in Japan was higher in winter (November to February).

For the EANET sites in Thailand, the NOx concentration was lower in wet season of June to September. For a whole year, NOx concentration at Bangkok during 2015-2019 was remarkably higher than those in previous years, but the NOx concentration at Nai Mueang during 2010-2014 and 2015-2019 was higher than that during 2005-2009. At Jakarta in Indonesia, the NOx concentration was higher from April to October and the concentration at Bangkok during 2015-2019 tended to be lower than those in previous years.

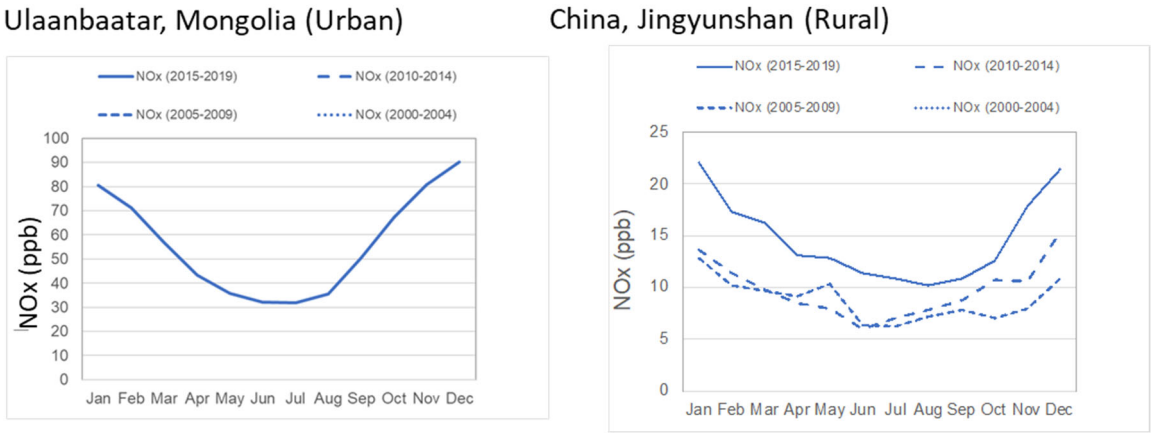

Figure 4.3.16 Monthly variations of NO_2 and NOx concentrations at the selected EANET sites from north to south (Averages of 2000-2004, 2005-2009, 2010-2014 and 2015-2019).

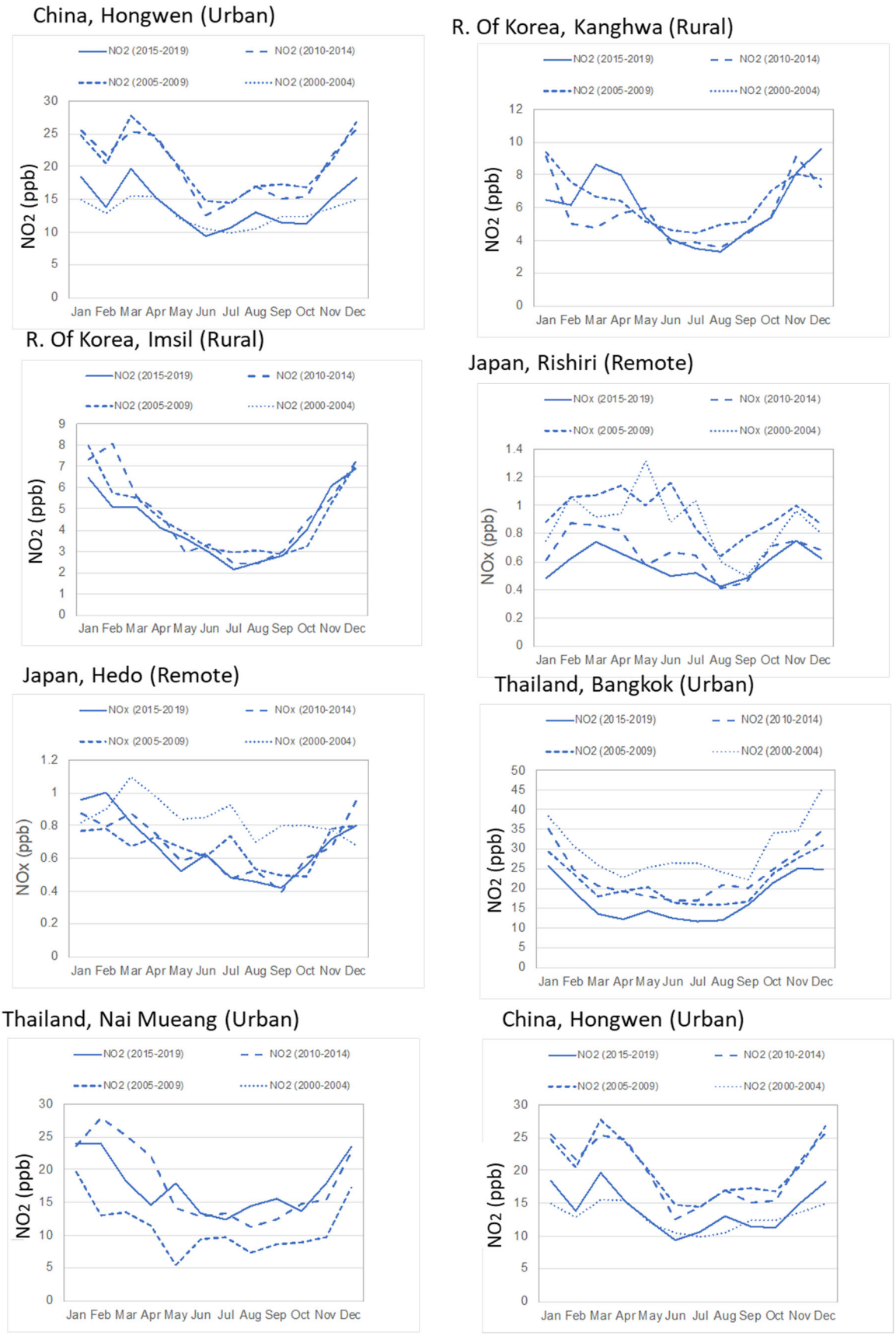

Figure 4.3.16 Monthly variations of NO_2 and NOx concentrations at the selected EANET sites from north to south (Averages of 2000-2004, 2005-2009, 2010-2014 and 2015-2019), continued.

4.3.2.5 O_3

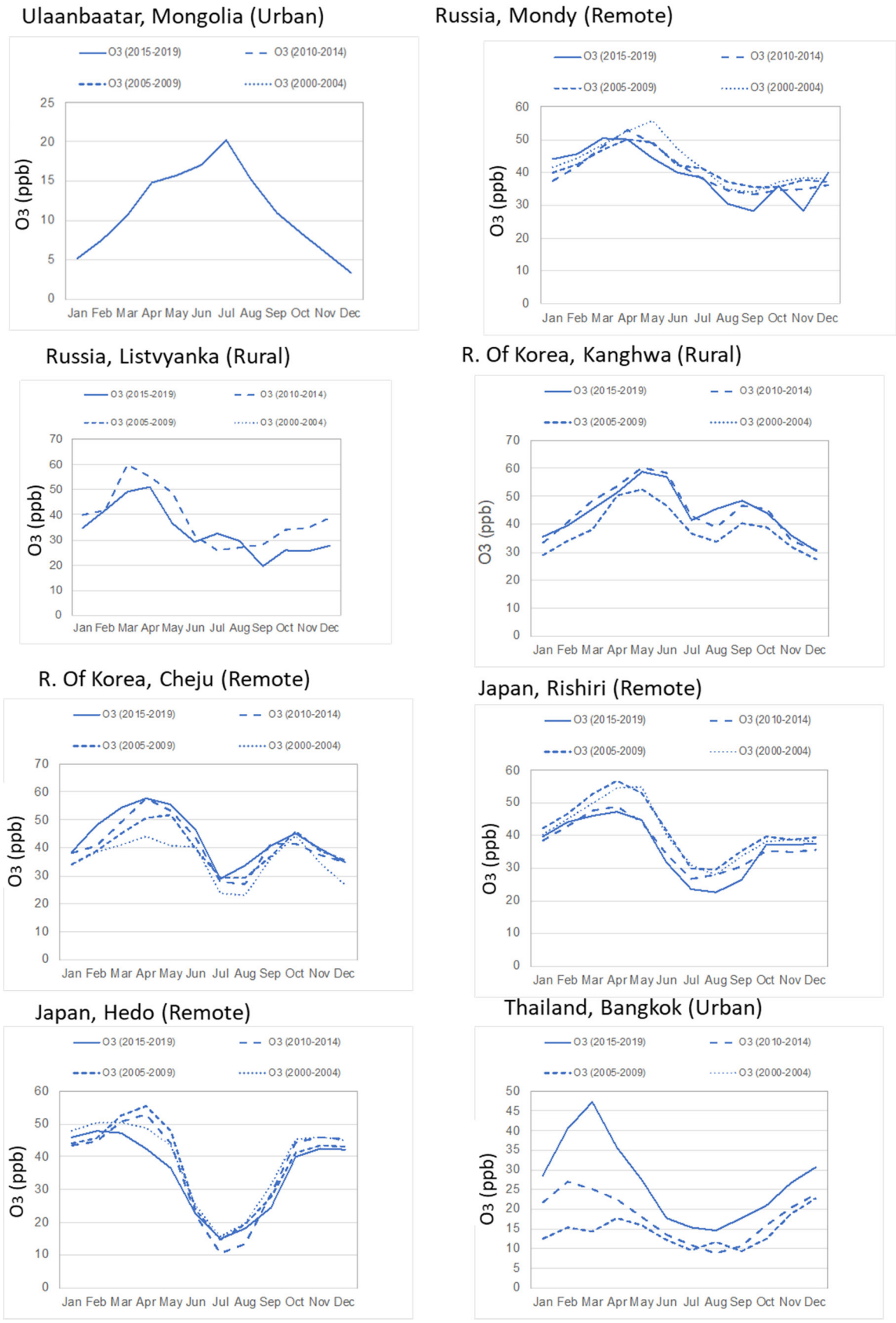

Figure 4.3.17 Monthly variations of O_3 concentrations at the selected EANET sites from north to south (Averages of 2000-2004, 2005-2009, 2010-2014 and 2015-2019).

Fig. 4.3.17 shows monthly variations of O_3 concentrations at the selected EANET sites. The O_3 concentration was remarkably high in summer at Ulaanbaatar in Mongolia due to the active photochemical reactions. At Mondy in Russia, the O_3 concentration was high in spring (March to May). Because there is no local emission sources of air pollutants, transportation across the Eurasia continent and lower stratosphere is major factor of variations. There is no significant change of O_3 concentration level from 2000 to 2019. The O_3 concentration at Listvyanka was also high in spring. For the sites in Republic of Korea, the O_3 concentrations was high in spring (April to May) and autumn (September to October). These trends will be determined by combination of local photo chemical production, long range transportation and regional climate condition. There is no significant change of O_3 concentration level at Kanghwa and Cheju from 2000 to 2019. The similar high O_3 concentration in spring was observed at the background sites of Rishiri and Hedo, but the O_3 concentration in summer was lower at these sites because the Pacific High including clean air covers the Japanese islands during the summer. For the O_3 concentration during 2015-2019, the concentration in spring and summer at Rishiri and the concentration in spring at Hedo were clearly lower than those in previous years.

At EANET site of Bangkok in Thailand, the O_3 concentrations was higher in dry season of February to May due to active photochemical reaction and lower O_3 wet deposition. For whole year, O_3 concentration at Bangkok during 2015-2019 was remarkably higher than those in previous years.

4.3.2.6 PM_{10} and $PM_{2.5}$

Fig. 4.3.18 shows monthly variations of PM_{10} and $PM_{2.5}$ concentrations at the selected EANET sites. Both PM_{10} and $PM_{2.5}$ concentrations were remarkably high in winter at Ulaanbaatar in Mongolia due to high use of coal and the strong inversion layer. Like Ulaanbaatar, the PM_{10} concentration at Jinyunshan and Hongwen in China was high in winter. For a whole year, the PM_{10} concentration at both sites during 2015-2019 was lower than those in previous years. At Kanghwa and Cheju in Republic of Korea, the PM_{10} concentration was high in spring (April to May) and autumn (October), and $PM_{2.5}$ was high in March. At Cheju, the PM_{10} concentration in summer during 2015-2019 was lower than those in previous years. At Rishiri in Japan, the PM_{10} and $PM_{2.5}$ concentrations were high in spring (March to May) and autumn (October to November). High PM_{10} concentration in spring was observed at Hedo in Japan. In spring, the PM_{10} concentration at Rishiri during 2015-2019 was higher than those during 2005-2009 and 2009-2014, whereas the PM_{10} concentration at Hedo during 2015-2019 was lower.

At EANET site of Hoa Binh in Vietnam, $PM_{2.5}$ was higher in dry season of November to March and biomass burning emission is one of the causes. The similar seasonal trend was observed at EANET sites, Vientiane in Lao PDR, Phnom Penh in Cambodia and Yangon in Myanmar. For the EANET sites in Thailand, the clear seasonal trend was observed at Bangkok, namely, both PM_{10} and $PM_{2.5}$ concentrations were remarkably high in dry season (October to April) and lower in wet season (May to September). For whole year, PM_{10} concentration at Bangkok during 2015-2019 was lower than those in previous years. The PM_{10} and $PM_{2.5}$ concentrations at EANET site of Chang Phueak in Thailand showed different seasonal variations from Bangkok. High peaks of PM_{10} and $PM_{2.5}$ concentrations was observed in March. The Chang Phueak site is located in northern Thailand and there is severe air pollution caused by biomass combustion in local area and neighboring countries. Only the PM_{10} data during 2000-2004 are available at EANET site of Petaling Jaya in Malaysia and there is no significant seasonal variations. At EANET site of Jakarta in Indonesia, the $PM_{2.5}$ concentration was higher from April to October. This seasonal trend was similar with those for other gas and particulate substances.

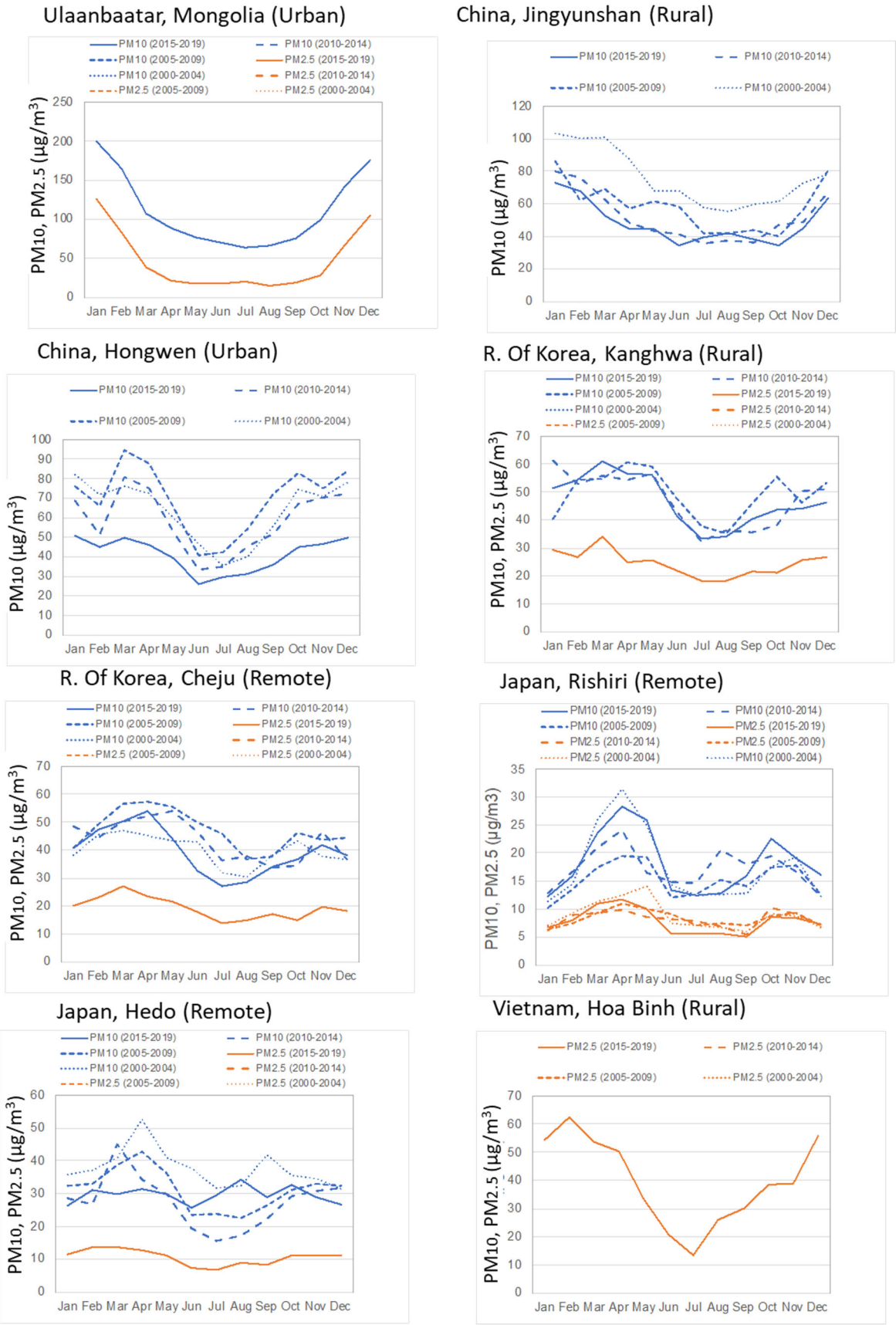

Figure 4.3.18 Monthly variations of PM_{10} and $PM_{2.5}$ concentrations at the selected EANET sites from north to south (Averages of 2000-2004, 2005-2009, 2010-2014 and 2015-2019).

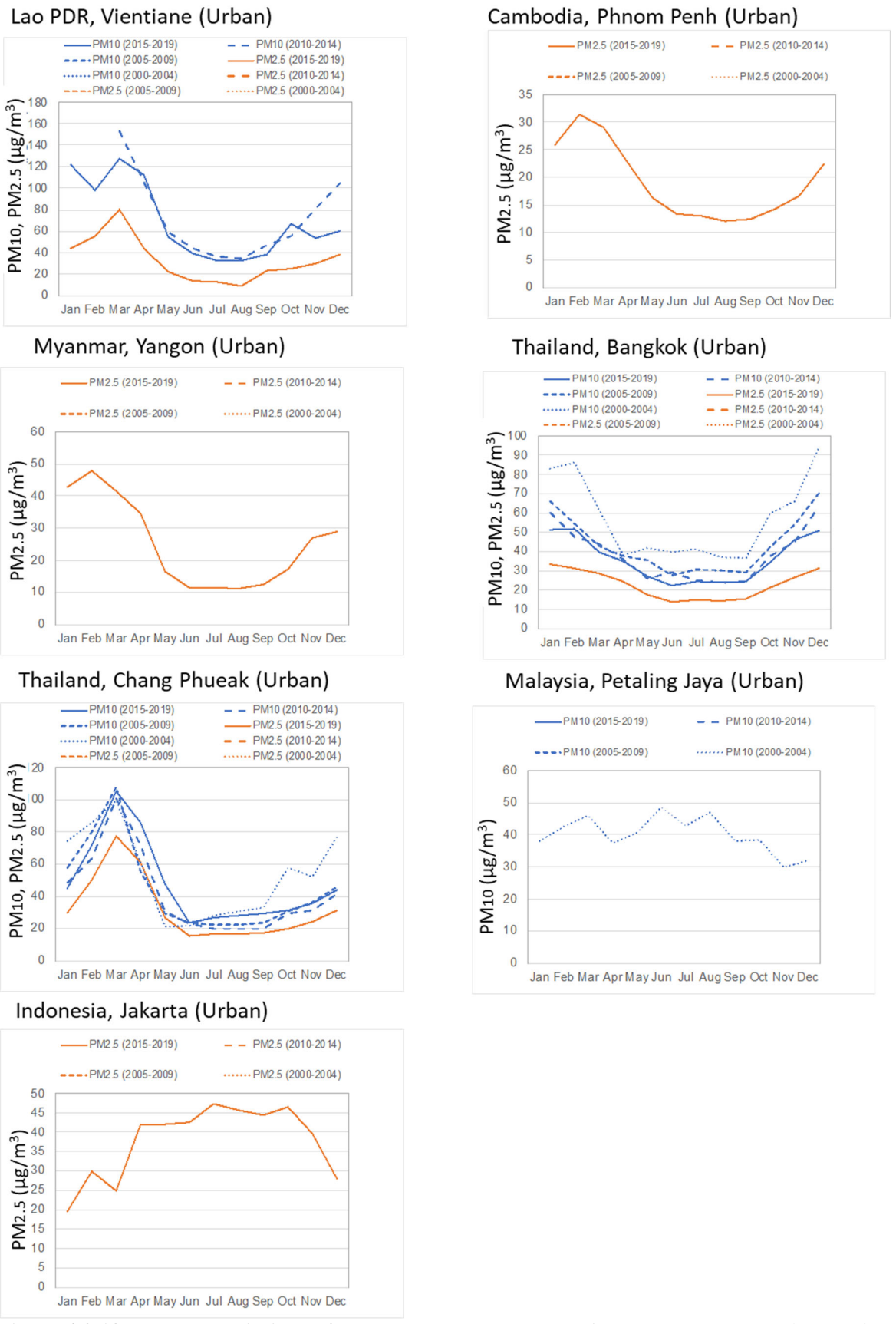

Figure 4.3.18 Monthly variations of PM_{10} and $PM_{2.5}$ concentrations at the selected EANET sites from north to south (Averages of 2000-2004, 2005-2009, 2010-2014 and 2015-2019), continued.

4.4 Assessment of gas and aerosol pollution in East Asia

The annual trends of the gas and aerosol concentration was estimated by the Mann-Kendall method. The trend analysis was focused on the annual average of atmospheric concentration of SO_2, NO_2, NOx, NH_3, O_3, PM_{10} and $PM_{2.5}$. The increasing and decreasing trend was evaluated by the slope and significance by the Mann-Kendall trend test.

Table 4.4.1. shows the annual trend of SO_2 concentration at each EANET site from 2000 to 2019. Among the 51 sites, 27 sites showed a significant decreasing trend (p<0.1) and 8 sites showed a strongly significant decreasing trend (p<0.001); Jinyunshan (-0.91 ppb yr^{-1}), Hongwen (-0.37 ppb yr^{-1}), Sado-seki (-0.37 ppb yr^{-1}), Banryu (-0.05 ppb yr^{-1}), Petaling Jaya (-0.10 ppb yr^{-1}), Samutprakarn (-0.25 ppb yr^{-1}) and Mae Hia (-0.02 ppb yr^{-1}). The decreasing trend of SO_2 at many sites in East Asia is associated with decrease of anthropogenic emission of SO_2. As described in Section 6.3., SO_2 emissions in EANET participating countries increased largely in early 2000s mainly due to contributions from coal-fired power plants, which increased rapidly along with large economic growth. Then, the SO_2 emissions showed decreasing trends after middle of 2000s reflecting effects of control measures. Not only atmospheric SO_2 concentration, nss-SO_4^{2-} concentration in precipitation showed significant decreasing trend in Northeast Asia, especially in China (Section 3.4.2).

Table 4.4.1. Annual trend of SO_2 concentration at each EANET site from 2000 to 2019.

unit: ppb yr^{-1}

Country	Site	Signific.	Slope
Cambodia	Phnom Penh	*	-0.20
China	Jinyunshan	***	-0.91
	Hongwen	***	-0.37
	Haibin-Park	*	-0.26
Indonesia	Jakarta	+	-0.23
	Serpong	*	-0.03
	Kototabang	*	-0.28
	Bandung		-0.08
Japan	Rishiri		0.00
	Ochiishi		0.00
	Tappi		0.00
	Sado-seki	***	-0.02
	Happo	**	-0.03
	Ijira	**	-0.02
	Oki	+	-0.02
	Banryu	***	-0.05
	Yusuhara		-0.01
	Hedo	*	-0.01
	Ogasawara		0.00
	Tokyo	***	-0.08
Lao PDR	Vientiane		0.00
Malaysia	Petaling Jaya	***	-0.10
	Tanah Rata	+	-0.04
	Danum Valley	*	-0.01
Mongolia	Ulaanbaatar		-0.40
	Terelj		0.00
Myanmar	Yangon	+	-0.13
Philippines	Metro Manila	**	-0.27
	Los Banos	+	-0.08
	Mt. Sto. Tomas		-0.04
Republic of Korea	Kanghwa	+	-0.06
	Cheju	*	-0.13
	Imsil		0.01
Russia	Mondy		-0.01
	Listvyanka		0.06
	Irkutsk		0.10
	Primorskaya		-0.03
Thailand	Bangkok		0.05
	Samutprakarn	***	-0.25
	Pathumthani		-0.19
	Khanchanaburi		0.01
	Mae Hia	***	-0.02
	Chang Phueak		-0.01
	Si Phum		-0.05
	Sakaerat	+	0.02
	Nai Mueang		-0.08
Vietnam	Hanoi	+	-0.09
	Hoa Binh	+	-0.07
	Can Tho		-0.13
	Ho Chi Minh		-0.20
	Yen Bai	+	-0.53

Siginificance
*** if trend at α = 0.001 level of significance
** if trend at α = 0.01 level of significance
* if trend at α = 0.05 level of significance
+ if trend at α = 0.1 level of significance

Table 4.4.2 and 4.4.3 show the annual trends of NO_2/NOx and NH_3 concentrations at each EANET site from 2000 to 2019, respectively. 11 sites among 17 EANET sites showed decreasing trend of

annual NO_2 concentration, but only 2 sites showed significant decreasing trend (p<0.1). These trends imply NO_2 concentration was fluctuated year-by-year.

Table 4.4.2. Annual trend of NO_2/NOx concentration at each EANET site from 2000 to 2019.

unit: ppb yr^{-1}

Country	Site	Signific.	Slope
China	Hongwen (NO2)		-0.14
	Haibin-Park (NO2)		-0.42
Indonesia	Jakarta (NO2)		-0.78
	Kototabang (NO2)		-0.07
	Bandung (NO2)		2.27
Japan	Banryu (NO2)	***	-0.14
Lao PDR	Vientiane (NO2)		1.40
Mongolia	Ulaanbaatar (NO2)		1.33
Philippines	Metro Manila (NO2)		-2.60
Republic	Kanghwa (NO2)		-0.06
of Korea	Cheju (NO2)		0.02
	Imsil (NO2)		-0.02
Thailand	Bangkok (NO2)	*	-0.42
	Samutprakarn (NO2)		-0.17
	ChangPhueak (NO2)		-0.05
	Si Phum (NO2)		0.08
	Nai Mueang (NO2)		0.30

unit: ppb yr^{-1}

Country	Site	Signific.	Slope
China	Jinyunshan (NOx*)	**	0.48
Japan	Rishiri (NOx*)	**	-0.02
	Ochiishi (NOx*)	*	-0.01
	Tappi (NOx*)		0.00
	Sado-seki (NOx*)	***	-0.05
	Happo (NOx*)	***	-0.10
	Ijira (NOx*)	***	-0.10
	Oki (NOx*)	**	-0.03
	Banryu (NOx)	***	-0.16
	Yusuhara (NOx*)	**	-0.03
	Hedo (NOx*)	+	-0.01
	Ogasawara (NOx*)	**	-0.01
	Niigata-miki (NOx*)		0.07
Lao PDR	Vientiane (NOx)		4.00
Mongolia	Ulaanbaatar (NOx)		0.00
Philippines	Metro Manila (NOx)		-6.30
Thailand	Bangkok (NOx)	***	-1.34
	Samutprakarn (NOx)	**	-0.81
	Khanchanaburi (NOx*)		0.03
	Chang Phueak (NOx)		-0.13
	Si Phum (NOx)		0.13
	Nai Mueang (NOx)		0.20

Siginificance
*** if trend at α = 0.001 level of significance
** if trend at α = 0.01 level of significance
* if trend at α = 0.05 level of significance
+ if trend at α = 0.1 level of significance

Table 4.4.3. Annual trend of NH_3 concentration at each EANET site from 2000 to 2019.

unit: ppb yr^{-1}

Country	Site	Signific.	Slope
Cambodia	Phnom Penh	*	-0.96
China	Hongwen		0.20
Indonesia	Jakarta		-4.80
	Serpong		0.08
	Bandung		0.28
Japan	Rishiri	*	0.00
	Ochiishi	*	-0.02
	Tappi		0.00
	Sado-seki	*	0.00
	Happo		0.01
	Ijira	**	-0.02
	Oki		0.00
	Banryu	**	-0.03
	Yusuhara		0.00
	Hedo	**	0.03
	Ogasawara		0.00
	Tokyo	***	-0.13
Lao PDR	Vientiane		0.07

unit: ppb yr^{-1}

Country	Site	Signific.	Slope
Malaysia	Petaling Jaya		0.14
	Tanah Rata	***	0.10
	Danum Valley		0.00
Mongolia	Ulaanbaatar		-0.04
	Terelj		0.03
Myanmar	Yangon	**	-1.35
Philippines	Metro Manila		0.04
	Los Banos		-0.45
	Mt. Sto. Tomas		0.13
Republic	Kanghwa	**	-0.60
of Korea	Cheju	**	0.35
	Imsil	*	0.20
Russia	Mondy	+	0.03
	Listvyanka	*	0.09
	Irkutsk		0.05
	Primorskaya	*	-0.23
Thailand	Bangkok		0.07
	Pathumthani		-0.11
	Khanchanaburi		0.08
	Mae Hia		-0.07
	Sakaerat	**	0.21
Vietnam	Hanoi	**	-0.20
	Hoa Binh	***	-0.17
	Can Tho	*	0.58
	Ho Chi Minh		0.33
	Yen Bai		0.16

Siginificance
*** if trend at α = 0.001 level of significance
** if trend at α = 0.01 level of significance
* if trend at α = 0.05 level of significance
+ if trend at α = 0.1 level of significance

12 sites among 22 EANET sites showed significant decreasing trend of annual NOx concentration (p<0.1) and 1 site showed significant increasing trend; Jinyunshan (0.48 ppb yr^{-1}, p<0.01). The anthropogenic NOx emission in East Asia increased largely from the early 2000s and continued to increase until 2011. Then, the emissions started to decrease by introduction of denitrification technologies (Section 6.3). The change in NOx emission would be associated with the decreasing trend of NOx, whereas the trend of NO_2 is more complex because most of NO_2 is produced by the atmospheric reaction of NO and O_3.

Among the 44 EANET sites, 10 sites showed a significant decreasing trend (p<0.05), and 8 sites showed a significant increasing trend (p<0.1) for annual NH_3 concentration. The following monitoring sites showed the strongly significant increasing or decreasing trend of NH_3 (p<0.001); Tokyo (-0.13 ppb yr^{-1}), Tanah Rata (0.10 ppb yr^{-1}), Hoa Binh (-0.17 ppb yr^{-1}). The NH_3 emissions from agricultural activities in EANET participating countries increased almost constantly from 1995 to 2015. Increase of NH_3 emission is caused by agricultural activities, synthetic fertilizer production, biofuel combustion, road vehicles and power plants (Section 6.3). Furthermore, recent researches pointed out that rapid SO_2 emission reductions cause significantly increase of ammonia concentrations in the Northeast Asia (Fu et al., 2017, Liu et al., 2018). It is important to consider the trend of NH_3 as well as counterpart species such as SO_2.

Table 4.4.4. Annual trend of O_3 concentration at each EANET site from 2000 to 2019.

unit: ppb yr^{-1}

Country	Site	Signific.	Slope
Indonesia	Bandung		-2.58
Japan	Rishiri	**	-0.35
	Ochiishi		0.23
	Tappi		0.33
	Sado-seki		-0.25
	Happo	**	-0.43
	Ijira		0.00
	Oki	**	0.17
	Banryu	***	-0.21
	Yusuhara		0.10
	Hedo	*	-0.23
	Ogasawara	**	0.48
	Niigata-maki	*	1.00
	Tsushima	*	1.13

unit: ppb yr^{-1}

Country	Site	Signific.	Slope
Mongolia	Ulaanbaatar		-0.25
Philippines	Metro Manila		3.00
Republic	Kanghwa	*	0.29
of Korea	Cheju	**	0.50
	Imsil	+	0.38
Russia	Mondy		-0.20
	Listvyanka		0.00
	Irktusk		0.29
Thailand	Bangkok	**	1.00
	Samutprakarn	***	0.53
	Khanchanaburi	+	1.00
	ChangPhueak	*	0.50
	Si Phum		-3.00
	Nai Mueang	+	0.60

Siginificance

*** if trend at α = 0.001 level of significance
** if trend at α = 0.01 level of significance
* if trend at α = 0.05 level of significance
+ if trend at α = 0.1 level of significance

Table 4.4.4., 4.4.5 and 4.4.6 show the annual trends of O_3, PM_{10} and $PM_{2.5}$ concentrations at each EANET site from 2000 to 2019, respectively.

Among the 28 EANET sites, 4 sites showed a significant decreasing trend (p<0.05), and 12 sites showed a significant increasing trend (p<0.1) for annual O_3 concentration. The following monitoring sites showed the strongly significant increasing or decreasing trend of O_3 (p<0.001); Banryu (-0.21 ppb yr^{-1}), Samutprakarn (0.53 ppb yr^{-1}). The Tropospheric Ozone Assessment Report (TOAR) Surface Ozone Database contains surface ozone data at thousands of monitoring sites around the world, densely located in mid-latitude North America, Western Europe and East Asia. According to the regional trend analysis of TOAR database, surface ozone concentration showed increasing trend over East Asia with the rate of 0.40 and 0.37 ppb yr^{-1} for summertime the average of daytime average and the daily maximum 8-hour average. Especially, the trends show a steep increase from 2011 to 2014. (Chang et al., 2017) Therefore, it is important to watch out the trend of surface ozone in East Asia combine EANET data with other monitoring database.

Table 4.4.5. Annual trend of PM_{10} concentration at each EANET site from 2000 to 2019.

unit: $\mu g/m^3\ yr^{-1}$

Country	Site	Signific.	Slope
China	Jinyunshan	**	-1.94
	Hongwen	***	-1.79
	Haibin-Park	*	-1.90
Japan	Rishiri		0.03
	Ochiishi	**	-1.00
	Tappi	+	-0.20
	Sado-seki	*	-0.21
	Happo	***	-0.33
	Ijira	***	-0.40
	Oki		0.10
	Banryu	***	-0.50
	Yusuhara	***	-0.43
	Hedo		-0.38
	Ogasawara	*	0.41
	Tsushima		0.61

unit: $\mu g/m^3\ yr^{-1}$

Country	Site	Signific.	Slope
Lao PDR	Vientiane		0.00
Mongolia	Ulaanbaatar		5.00
Philippines	Metro Manila		-4.00
Republic	Kanghwa	*	-0.50
of Korea	Cheju		-0.29
	Imsil		-0.47
Thailand	Bangkok	***	-1.00
	Samutprakarn		-0.40
	Khanchanaburi		-1.00
	ChangPhueak		0.13
	Si Phum		0.00
	Nai Mueang		0.20

Siginificance
*** if trend at α = 0.001 level of significance
** if trend at α = 0.01 level of significance
* if trend at α = 0.05 level of significance
+ if trend at α = 0.1 level of significance

Table 4.4.6. Annual trend of $PM_{2.5}$ concentration at each EANET site from 2000 to 2019.

unit: $\mu g/m^3\ yr^{-1}$

Country	Site	Signific.	Slope
Cambodia	Phnom Penh		7.50
Indonesia	Jakarta		-0.50
Japan	Rishiri	*	0.00
	Ochiishi	***	-0.67
	Tappi		-0.67
	Sadoseki	*	-0.33
	Happo		-0.42
	Ijira		-0.63
	Oki	+	-0.13
	Banryu		-0.58
	Yuahara		0.00
	Hedo		0.00
	Ogasawara		0.00

unit: $\mu g/m^3\ yr^{-1}$

Country	Site	Signific.	Slope
Lao PDR	Vientiane		1.00
Mongoloa	Ulaanbaatar		-2.33
Myanmar	Yangon		0.00
	Mandalay		-3.25
Philippines	Metro Manila	*	-1.55
Republic	Kanghwa		-2.33
of Korea	Cheju		-0.17
Thailand	Bangkok		0.38
	Samutprakarn	+	-1.50
	Khanchanaburi		-2.13
	ChangPhueak		3.50
	Si Phum	+	-1.00
Vietnam	Hoa Binh		-1.50

Siginificance
*** if trend at α = 0.001 level of significance
** if trend at α = 0.01 level of significance
* if trend at α = 0.05 level of significance
+ if trend at α = 0.1 level of significance

Among the 27 EANET sites, 12 sites showed a significant decreasing trend (p<0.1), and 1 site showed a significant increasing trend (p<0.05) for annual PM_{10} concentration. The following monitoring sites showed the strongly significant increasing or decreasing trend of PM_{10} (p<0.001); Hongwen (-1.79 $\mu g/m^3\ yr^{-1}$), Happo (-0.33 $\mu g/m^3\ yr^{-1}$), Ijira (-0.40 $\mu g/m^3\ yr^{-1}$), Banryu (-0.50 $\mu g/m^3\ yr^{-1}$), Yusuhara (-0.43 $\mu g/m^3\ yr^{-1}$), Bangkok (-1.00 $\mu g/m^3\ yr^{-1}$). The many sites in Northeast Asia showed significant decreasing trend, which implies it would be associated with change in emission of dust storm and primary emission and secondary formation of anthropogenic particulate matter.

Among the 26 EANET sites, 6 sites showed a significant decreasing trend (p<0.1) for annual $PM_{2.5}$ concentration. The Ochiishi (p<0.001, -0.67 $\mu g/m^3\ yr^{-1}$) and Oki (p<0. 1, -0.13 $\mu g/m^3\ yr^{-1}$) sites, which has been implemented $PM_{2.5}$ monitoring since 2008 and 2001, showed the significant increasing trend. Since many sites installed a $PM_{2.5}$ monitor after 2015, a clear trend has not been observed so far. The continuous monitoring is important to elucidate long term trend over East Asia.

4.5 Conclusion

EANET has conducted continuous monitoring in various countries in 20 years and the number of gas and aerosol monitoring sites have been increased each year. This will allow to establish the high-resolution monitoring network in East Asia and to provide the scientific evidence to policy makers to confront this environmental issue as well. There were 54 air concentration monitoring sites operated in the EANET network as of 2019. The measuring components, which are SO_2, NO, NO_2, NOx, $PM_{10/2.5}$, O_3, HNO_3, HCl, NH_3 and Particulate Matter Components (PMC), vary depending on the methodology at each site.

The spatial distribution of SO_2 in Russia and Mongolia varied by the influence of population distribution, as well as the effect of heating and fuel composition such as coal burning. After continuous improvement, SO_2 concentrations at Chinse EANET sites have been significantly reduced, and the 5-year average range for the 5 stations in China is 0.1 ppb-3.54 ppb. The SO_2 concentrations at all sites in Japan are very low for a long time, with a 5-year average range of 0.03 -1.3 ppb. The SO_2 concentration range at the three land sites in Republic of Korea is similar to that of China. Except for Indonesia, SO_2 concentrations in Southeast Asian countries are generally low for 5 year-average concentration.

Republic of Korea had the highest nationwide O_3 5-year average concentration (40.47 ppb from 3 stations), and Japan reported the next highest nationwide averaged O_3 concentration. On the other hand, O_3 concentration in Southeast Asian countries are lower. Mongolia had the highest NOx 5-year average concentration, and Philippines reported the next highest. There are large spatial differences in the distribution of NO_2 concentrations. Indonesia has the highest NO_2 concentration level.

Mongolia had the highest $PM_{2.5}$ 5-year average concentration of 40.5 $\mu g/m^3$ at Ulaanbaatar. Jakarta of Indonesia reported the next highest nationwide averaged $PM_{2.5}$ concentration of 41.0 $\mu g/m^3$. The $PM_{2.5}$ concentration in Hoa Binh of Vietnam is close to that of Jakarta of Indonesia, with a 5-year average concentration of 39.4 $\mu g/m^3$. The 5-year average $PM_{2.5}$ concentrations of remaining countries are less than 30 $\mu g/m^3$. Ulaanbaatar of Mongolia also has the highest PM_{10} concentration level with a 5-year average concentration of 110 $\mu g/m^3$. The PM_{10} concentration levels of EANET sites in China, Korea, the Philippines, and Thailand were similar. The 5-year nationwide average PM_{10} concentrations in Japan has a range of 8-30 $\mu g/m^3$.

The concentrations of HNO_3 at one Chinese site are high during the period from 2015 to 2019, with Hongwen concentrations ranging from 1.1 ppb to 1.2 ppb, with a 5-year average value of 1.15 ppb. The concentration at an EANET site in Indonesia has the second highest concentration in EANET region with a more consistent concentration distribution, the 5-year averaged HNO_3 concentration of 3 stations ranges from 0.62 ppb to 1.14 ppb. The HNO_3 concentrations in some countries are low, with the 5-year average concentration of less than 0.5 ppb.

There are various NH_3 concentration distributions in East Asia. The spatial distribution of NH_3 in Philippines, Malaysia and Mongolia has a large variation. One station of China has the highest NH_3 concentration among the EANET sites (9.99 ppb), followed by Indonesia (9.23 ppb). The 5-year average concentration at Cambodia station was 7.20 ppb, the average NH_3 concentration at four stations in Thailand ranged from 4.48 to 8.85 ppb, and the average 5-year concentration at three stations in Republic of Korea ranged from 1.96 to 7.70 ppb. The other countries reported lower average NH_3 concentrations for the 5 years.

The highest HCl concentration is found in Russia with a 5-year average concentration of 3.43 ppb and with a large difference in the geospatial distribution. The second highest concentration of HCl in the EANET region is found in Mongolia, where the 5-year average concentrations range from 1.30 ppb to 3.55 ppb. The remaining countries have relatively similar lower HCl concentrations level.

The highest SO_4^{2-} concentration was found at Hongwen of China, the only station reported data, with the 5-year average SO_4^{2-} concentration of 10.0 μg/m^3. The second highest 5-year averaged SO_4^{2-} concentration was found in Vietnam with the average of 5.59 μg/m^3 showing some differences in spatial distribution. The 5-year average SO_4^{2-} concentrations of the remaining countries were relatively low.

The highest NO_3^- concentration was found at Hongwen of China, the only station reported data, with the 5-year average NO_3^- concentration of 7.94 μg/m^3. The second highest 5-year averaged NO_3^- concentration was found in Vietnam with the average of 4.07 μg/m^3 and a range of 1.54-6.73 μg/m^3 for the 5 stations, showing some differences in spatial distribution. The 5-year average NO_3^- concentrations of the remaining countries were relatively low.

The highest NH_4^+ concentration was found at Hongwen of China, the only station reported data, with the 5-year average NH_4^+concentration of 3.26 μg/m^3. The second highest 5-year averaged NH_4^+ concentration was Republic of Korea with the average of 2.12 μg/m^3 and a range of 1.66 μg/m^3 to 2.66 μg/m^3. The third highest 5-year averaged NH_4^+ concentration was found in Vietnam with the average of 1.65 μg/m^3 and a range of 1.11-1.97 μg/m^3 for the 5 stations. The 5-year average NH_4^+ concentrations of the remaining countries were relatively low.

The highest 5-year averaged Ca^{2+} concentration was found in Vietnam with the average of 2.28 μg/m^3 and a range of 1.61-3.73 μg/m^3 for the 5 stations. The second highest Ca^{2+} concentration was found at Hongwen of China and Phnom Penh, with the same 5-year average Ca^{2+} concentration of 1.68 μg/m^3. The 5-year average Ca^{2+} concentrations of the remaining countries were relatively low.

Among the 51 sites, 27 sites showed a significant decreasing trend (p<0.1) and 8 sites showed a strongly significant decreasing trend (p<0.001). The decreasing trend of SO_2 at many sites in East Asia is associated with decrease of anthropogenic emission of SO_2. SO_2 emissions in EANET participating countries increased largely in early 2000s, and then it showed decreasing trends after middle of 2000s reflecting effects of control measures. On the other hand, among the 44 sites, 8 sites showed a significant increasing trend (p<0.1) for annual NH_3 concentration. The NH_3 emissions from agricultural activities in EANET participating countries increased almost constantly from 1995 to 2015, and rapid SO_2 emission reductions cause significantly increase of ammonia concentrations in the Northeast Asia.

Many sites observed significant increasing trend for annual O_3 concentration and the other surface ozone database in East Asia also showed increasing trend of summertime the average of daytime average and the daily maximum 8-hour average over East Asia. It is important to watch out the trend of surface ozone in East Asia combine EANET data with other monitoring database. Since many sites installed a $PM_{2.5}$ monitor after 2015, a clear trend of annual $PM_{2.5}$ concentration has not been observed so far. The continuous monitoring is important to elucidate long term trend over East Asia.

4.6 References

Chang, K-L, Petropavlovskikh, I, Cooper, OR, Schultz, MG and Wang, T, 2017. Regional trend analysis of surface ozone observations from monitoring networks in eastern North America, Europe and East Asia. Elem Sci Anth., 5: 50, https://doi.org/10.1525/elementa.243.

Fu, X., Wang, S., Xing, J., Zhang, X., Wang, T., Hao, J., 2017. Increasing Ammonia Concentrations, Reduce the Effectiveness of Particle Pollution Control Achieved via SO_2 and NO_X Emissions Reduction in East China, Environ. Sci. Technol. Lett. 4(6): 221–227, https://doi.org/10.1021/acs.estlett.7b00143.

Galloway JN., Schlesinger, WH., Levy II, H., Michaels, A., Schnoor, JL., 1995. Nitrogen fixation: Anthropogenic enhancement-environmental response, Global Biogeochemical Cycles, 9(2):235-252 https://doi.org/10.1029/95GB00158.

Liu, M., Huang, X., Song, Y. Xu, T., Wang, S., Wu, Z., Hu, M., Zhang, L., Zhang, Q., Pan, Y., Liu, X., Zhu, T., 2018, Rapid SO_2 emission reductions significantly increase tropospheric ammonia concentrations over the North China Plain, Atmos. Chem. Phys., 18, 17933–17943, https://doi.org/10.5194/acp-18-17933-2018.

Schöpp, W., Posch, M., Mylona, S., Johansson, M., 2003. Long-term development of acid deposition (1880–2030) in sensitive freshwater regions in Europe, Hydrol. Earth Syst. Sci., 7, 436–446, https://doi.org/10.5194/hess-7-436-2003.

Yu, L., Wang, Y., Zhang, X., Dörsch, P., and Mulder, J., 2017. Phosphorus addition mitigates N_2O and CH4 emissions in N-saturated subtropical forest, SW China, Biogeosciences, 14, 3097–3109, https://doi.org/10.5194/bg-14-3097-2017.

5. Impacts on Ecosystems in East Asia

5.1 Introduction

The EANET has been monitoring various ecosystem components, such as soil, forest vegetation, and inland water, to assess impacts of atmospheric deposition on ecosystems since 2000 when the regular-phase activity started. Important data sets over 10 years have been accumulated in many of monitoring sites, while the situations are different depending on monitoring items. Additionally, the EANET has been promoting a catchment-scale analysis considering biogeochemical cycles in forest ecosystems since 2010, in which interrelationships among atmospheric deposition, soil, vegetation, and inland water (mostly stream water) within a catchment area were also discussed qualitatively and/or quantitatively. In Sections 5.2 and 5.3, characteristics and long-term trends of soil, vegetation, and inland water are summarized based on the data sets until 2019 and their relationships with atmospheric deposition are discussed referring to the data at the nearest monitoring sites. The results from the regular-catchment monitoring sites and EANET-relevant study sites until 2019 are introduced in Section 5.4. Although the ecological monitoring above started in order to detect impacts of acid deposition, the results may also need to be discussed with other relevant factors, such as climate change.

5.2 Soil and vegetation monitoring

5.2.1 Soil monitoring

Soil monitoring has been conducted at 31 sites from 10 countries including the pre survey in 1999. Since 2000, the official survey records have been made following the "Technical Documents for Soil and Vegetation Monitoring in East Asia" (EANET, 2000). Metadata of each site and number of surveys are shown in Table 5.2.1, and 5.2.2, respectively. In these twenty years, 6 surveys were conducted at the most intensive sites, whereas some sites had no soil monitoring record since 2000 (Table 5.2.2). As previous chapters show, atmospheric environment has been improving in these 10 years, attention should be paid whether it reflects to soil chemical properties. This section focused mainly on soil pH(H_2O), because missing data were relatively small. Firstly, the distribution of entire-period-statistics of pH(H_2O) in each site and factors contributing the distribution are shown. Secondly, twenty-year-change in soil pH(H_2O) in relation to atmospheric environment is presented.

5.2.1.1 Distribution of soil pH(H_2O) among EANET sites

As shown in Table 5.2.1, geographical locations of soil monitoring sites of EANET cover very widespread area; it ranges from high-latitude region in northern hemisphere to low-latitude equatorial region. Latitude directly relates to climatic conditions and reflects diverse precipitation and air temperature. These climatic conditions also regulate vegetation and soil formation which comprises soil type.

Table 5.2.1 Metadata of soil monitoring sites.

Country	Site name	Site code	Corresponding atmospheric monitoring site	Geographical coordinates		MAP [*1]	Forest type [*2]	Soil type
				N Latitude	E Longitude	(mm y^{-1})		WRB [*3]
China	Jinyunshan	CNS004	Jinyunshan	29° 49'	106° 22'	1,207	Evergreen-coniferous	Not specified
	Dabagou	CNS007	Jiwozi	33° 50'	108° 48'	538	Evergreen-coniferous	Not specified
	Xiaoping	CNS009	Xiaoping	24° 51'	118° 2'	1,751	Evergreen-broad-leaved	Not specified
	Zhuxiandong	CNS011	Zhuxiandong	22° 12'	113° 31'	1,729	Evergreen-broad-leaved	Not specified
Indonesia	Bogor Research Forest	IDS002	Serpong	-6° 45'	106° 34'	1,902	Evergreen-broad-leaved	Not specified
Japan	Ijira	JPS006	Ijira	35° 34'	136° 42'	2,900	Evergreen-coniferous	Cambisols
	Yamato	JPS106	Ijira	35° 51'	136° 58'	2,900	Evergreen-coniferous	Andosols
	Banryu-2	JPS008	Banryu	34° 40'	131° 48'	1,565	Evergreen-broad-leaved	Cambisols
	Iwami Rinku FP	JPS108	Banryu	34° 37'	131° 47'	1,565	Evergreen-broad-leaved	Acrisols
Malaysia	Pasoh 1	MYS001	Petaling Jaya	2° 59'	102° 19'	3,380	Not specified	Not specified
	Pasoh 2	MYS101	Petaling Jaya	2° 59'	102° 19'	3,380	Not specified	Not specified
	UPMKB 1991	MYS005	—	3° 13'	113° 6'	—	Not specified	Not specified
	UPMKB 2008	MYS105	—	3° 13'	113° 6'	—	Not specified	Not specified
Mongolia	Bogdkhan Mountain	MNS001	Ulaanbaatar	47° 54'	106° 49'	162	Deciduous-coniferous	Not specified
	Terelj Mountain	MNS002	Terelj	47° 59'	107° 29'	164	Not specified	Not specified
Philippines	Mt. Makiling	PHS002	Los Baños	14° 10'	121° 11'	2,043	Evergreen-broad-leaved	Cambisols
	Up Quezon Land Grant	PHS102	Los Baños	14° 10'	121° 11'	2,043	Evergreen-broad-leaved	Nitisols
	La Mesa Watershed	PHS001	Metro Manila	14° 38'	121° 4'	2,881	Evergreen-broad-leaved	Not specified
	Boneco LTER Site	PHS003	Mt. Sto. Tomas	16° 25'	120° 36'	4,243	Evergreen-coniferous	Not specified
R. of Korea	Mt. Naejang	KRS003	Imsil	35° 36'	127° 11'	1,160	Evergreen-coniferous	Not specified
Russia	Irkutsk	RUS003	Irkutsk	52° 14'	104° 15'	424	Evergreen-coniferous	Luvisols
	Bolshie Koty	RUS002	Listvyanka	51° 51'	104° 54'	379	Evergreen-coniferous	Leptosols
	Pereemnaya river catchment	RUS102	Listvyanka	51° 56'	105° 17'	379	Evergreen-coniferous	Leptosols
	Ilchir Lake [*4]	RUS001	Mondy	51° 40'	101° 0'	239	Not specified	Gleysols
	Okinskoe Lake [*4]	RUS101	Mondy	51° 40'	101° 0'	239	Not specified	Podsols
	Solar Observatory	RUS201	Mondy	51° 40'	101° 0'	239	Deciduous-coniferous	Gleysols
	Primorskaya	RUS004	Primorskaya	—	—	768	Deciduous-broad leaved	Cambisols
Thailand	Vachiralongkorn Dam	THS004	Khanchanaburi	14° 46'	98° 35'	1,563	Evergreen-broad-leaved	Acrisols
	Vachiralongkorn Puye	THS104	Khanchanaburi	14° 46'	98° 35'	1,563	Evergreen-broad-leaved	Luvisols
Vietnam	Cave of Heaven [*4]	VNS002	Hoa Binh	20° 49'	105° 20'	1,800	Not specified	Not specified
	Thang Ranh [*4]	VNS102	Hoa Binh	20° 49'	105° 20'	1,800	Not specified	Not specified

*1, MAP is mean annual precipitation calculated from EANET wet deposition monitoring data.

*2, Forest type was decided from the dominant tree species reported in tree decline monitoring.

*3, Soil type is besed on soil classification of World Reference Base for Soil Resources (IUSS Working Group WRB, 2015).

*4, Grayed rows indicate sites having no official data since 2000.

Table 5.2.2 Times of monitoring and summary of chemical properties at each site from 2000 to 2019.

Country	Site code	Number of surveys	pH(H_2O)	pH(KCl)	Exchangeable cations ($cmol_c\ kg^{-1}$)					
					Ca^{2+}	Mg^{2+}	K^{+}	Na^{+}	Al^{3+}	H^{+}
China	CNS004	6	4.1 ± 0.2	3.5 ± 0.2	0.34 ± 0.26	0.08 ± 0.05	0.08 ± 0.03	0.02 ± 0.02	5.75 ± 1.64	0.92 ± 0.49
	CNS007	6	6.1 ± 0.2	5.1 ± 0.2	5.36 ± 1.87	0.67 ± 0.36	0.54 ± 0.24	0.15 ± 0.10	0.18 ± 0.17	0.55 ± 0.57
	CNS009	5	4.6 ± 0.2	4.0 ± 0.1	0.03 ± 0.03	0.06 ± 0.02	0.21 ± 0.08	0.09 ± 0.06	4.17 ± 1.48	0.50 ± 0.45
	CNS011	6	4.3 ± 0.3	3.7 ± 0.2	1.14 ± 1.36	0.39 ± 0.45	0.44 ± 0.57	0.22 ± 0.30	1.24 ± 1.15	2.35 ± 1.41
Indonesia	IDS002	5	4.2 ± 0.1	3.7 ± 0.1	1.05 ± 0.44	0.59 ± 0.67	0.09 ± 0.04	0.05 ± 0.06	4.09 ± 0.75	0.56 ± 0.31
Japan	JPS006	4	4.3 ± 0.3	3.5 ± 0.2	0.22 ± 0.14	0.40 ± 0.39	0.15 ± 0.08	0.10 ± 0.12	7.75 ± 2.20	1.03 ± 0.31
	JPS106	3	4.3 ± 0.3	3.9 ± 0.2	0.12 ± 0.09	0.17 ± 0.07	0.20 ± 0.06	0.03 ± 0.01	5.50 ± 4.74	0.69 ± 0.56
	JPS008	4	4.8 ± 0.2	3.9 ± 0.2	0.41 ± 0.47	0.35 ± 0.17	0.19 ± 0.06	0.22 ± 0.26	2.94 ± 0.59	0.54 ± 0.26
	JPS108	4	4.4 ± 0.2	3.6 ± 0.3	0.28 ± 0.28	0.36 ± 0.16	0.24 ± 0.07	0.08 ± 0.04	6.41 ± 2.08	0.98 ± 0.39
Malaysia	MYS001	3	4.3 ± 0.3	3.8 ± 0.2	0.24 ± 0.22	0.30 ± 0.27	0.20 ± 0.11	0.12 ± 0.03	3.02 ± 0.60	NA
	MYS101	2	4.3 ± 0.3	3.8 ± 0.3	0.07 ± 0.05	0.05 ± 0.06	0.05 ± 0.03	0.06 ± 0.04	3.35 ± 0.61	NA
	MYS005	2	5.3 ± 0.5	4.0 ± 0.7	1.36 ± 0.50	1.02 ± 0.19	0.06 ± 0.02	1.30 ± 0.17	1.84 ± 0.27	2.01 ± 0.30
	MYS105	2	4.8 ± 0.2	3.7 ± 0.1	0.78 ± 0.30	0.83 ± 0.22	0.04 ± 0.02	1.42 ± 0.13	1.52 ± 0.27	1.66 ± 0.28
Mongolia	MNS001	2	6.2 ± 0.6	5.3 ± 0.7	NA	NA	NA	NA	NA	NA
	MNS002	2	5.7 ± 0.3	4.7 ± 0.3	NA	NA	NA	NA	NA	NA
Philippines	PHS002	3	5.7 ± 0.6	4.9 ± 0.6	15.25 ± 4.44	12.76 ± 1.57	4.08 ± 1.27	2.15 ± 1.61	0.25 ± 0.53	0.35 ± 0.16
	PHS102	4	4.4 ± 0.3	3.8 ± 0.1	1.13 ± 1.43	0.37 ± 0.11	0.39 ± 0.17	0.33 ± 0.17	5.32 ± 1.34	0.66 ± 0.45
	PHS001	2	5.3 ± 0.3	4.2 ± 0.2	17.05 ± 7.78	5.07 ± 1.37	0.70 ± 0.47	2.24 ± 1.00	0.15 ± 0.14	0.19 ± 0.14
	PHS003	1	5.2 ± 0.2	5.0 ± 0.1	7.11 ± 1.18	0.86 ± 0.15	0.21 ± 0.03	0.39 ± 0.06	1.68 ± 0.35	0.35 ± 0.09
R. of Korea	KRS003	2	4.9 ± 0.2	4.0 ± 0.1	0.38 ± 0.36	0.17 ± 0.12	0.10 ± 0.04	0.08 ± 0.06	3.22 ± 0.49	0.31 ± 0.15
Russia	RUS003	2	6.3 ± 0.4	4.8 ± 0.7	17.29 ± 5.42	4.35 ± 1.51	0.23 ± 0.10	0.14 ± 0.04	0.13 ± 0.14	0.04 ± 0.03
	RUS002	2	5.7 ± 0.9	4.6 ± 0.9	15.66 ± 9.67	3.27 ± 1.87	0.43 ± 0.52	0.08 ± 0.04	1.05 ± 1.46	0.22 ± 0.24
	RUS102	1	4.8 ± 0.3	3.9 ± 0.6	4.24 ± 4.29	1.04 ± 1.09	0.36 ± 0.39	0.11 ± 0.05	8.30 ± 5.35	1.42 ± 0.56
	RUS001	0 (1)	ND	ND	ND	ND	ND	ND	ND	ND
	RUS101	0 (1)	ND	ND	ND	ND	ND	ND	ND	ND
	RUS201	1 (1)	7.4 ± 0.2	6.9 ± 0.1	100.36 ± 17.66	5.94 ± 1.90	1.98 ± 1.42	0.02 ± 0.02	NA	NA
	RUS004	2	5.2 ± 0.3	4.2 ± 0.7	10.28 ± 7.72	3.11 ± 1.22	0.38 ± 0.27	0.14 ± 0.05	0.71 ± 0.89	0.30 ± 0.07
Thailand	THS004	6	6.4 ± 0.5	5.5 ± 0.5	13.66 ± 10.14	7.79 ± 13.70	0.20 ± 0.36	0.19 ± 0.19	0.08 ± 0.08	7.43 ± 13.00
	THS104	4	5.1 ± 0.6	4.1 ± 0.3	2.38 ± 2.75	1.04 ± 0.75	0.03 ± 0.03	0.17 ± 0.13	1.26 ± 1.41	7.26 ± 14.19
Vietnam	VNS002	0 (1)	ND	ND	ND	ND	ND	ND	ND	ND
	VNS102	0 (1)	ND	ND	ND	ND	ND	ND	ND	ND

(), number of surveys including pre survey in 1999.

Mean ± SD.

NA represents "not analysed".

ND indicates no official data since 2000.

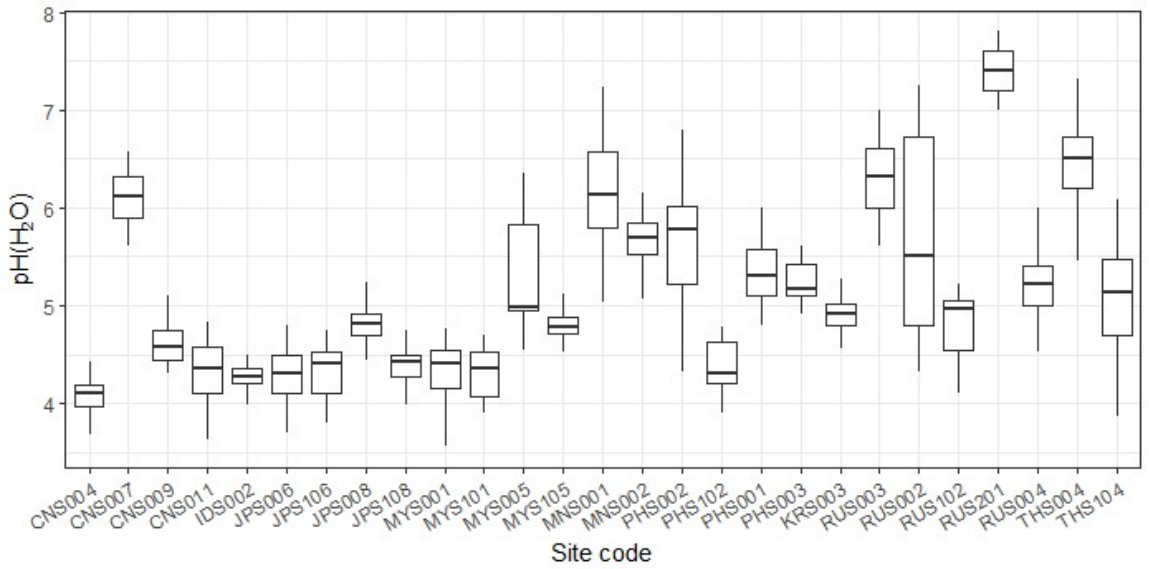

Figure 5.2.1. Entire-period-statistics of soil pH(H_2O) in each EANET site.
Middle cross bar, high and low ends of the box, and high and low ends of whiskers represent median, third and first quantile, maximum and minimum value.

Mean soil pH and concentrations of exchangeable cations are shown in Table 5.2.2, and as a representative of these measured items, distribution of pH(H_2O) among sites is shown in Figure 5.2.1. Mean pH(H_2O) ranged very widely from 4.0 to 7.4 among EANET sites. Soil pH(H_2O) of middle-latitude site (China, Japan, R. of Korea and Vietnam) tended lower compared to other sites. Variability within the same country (if there are multiple sits in a country) was also large. Similarly, pH(KCl) and soil exchangeable cations ranged widely; the average were 3.5 ~6.9 for pH(KCl), 0.03 ~ 100.36 $cmol_c\ kg^{-1}$ for Ca^{2+}, 0.05 ~ 12.76 $cmol_c\ kg^{-1}$ for Mg^{2+}, 0.03 ~ 4.08 $cmol_c\ kg^{-1}$ for K^+, 0.02 ~ 2.24 $cmol_c\ kg^{-1}$ for Na^+, 0.08 ~ 8.30 $cmol_c\ kg^{-1}$ for Al^{3+}, 0.04 ~ 7.43 $cmol_c\ kg^{-1}$ for H^+.

Figure 5.2.2 shows soil pH(H_2O) among soil types. Among 7 soil types, which appear in EANET soil monitoring sites, Gleysols had the highest pH(H_2O). Gleysols generally distributes in the locations where undrained and saturated with groundwater, which cause reduced soil condition (IUSS Working Group WRB, 2015). This soil type appeared in Solar Observatory site in Russia (RUS201). On the other hand, Andosols and Nitisols had the lowest value. Andosols is often generated from weathered volcanic ash and is rich in activated aluminum. This soil type appeared in Yamato site in Japan (JPS106). Nitisols contains clay-rich subsurface horizon and the CEC is relatively low. This soil type appeared in Up Quezon Land Grant in Philippines (PHS102). As shown, soil types are not reasonably corresponding to soil pH(H_2O); Acrisols, which contain activated aluminum, had relatively high pH(H_2O) in this survey. Soil type of almost half site has not been specified according to the international soil classification system (Table 5.2.1). If the soil classification completed throughout the EANET sites, relationships between soil type and soil chemical properties will be clearer.

Forest trees affect soil chemical properties through litter supply and decomposition of organic matters (Berg and McClaugherty, 2014). Figure 5.2.3 shows the difference in pH(H_2O) among forest types. This report distinguished forest type as [Evergreen or Deciduous] * [Coniferous or Broad leaved], therefore they fall into four categories. Among these forest types, Deciduous-coniferous forest had the highest soil pH(H_2O). This category consists mainly of *Larix sibirica*, which grows in Mongolia and Russia. On the other hand, Evergreen-coniferous forest had the lowest soil pH(H_2O). In this category, *Pinus* and *Chamaecyparis* species are mainly included. For five of 27 sites, forest type has not been specified because forest survey has never been conducted. If forest survey has conducted in more sites, it will enable to categorize forest types more precisely, and these information of forest (not only tree species but also ages, artificial or natural growth, and so on) will clarify the nutritional interaction between trees and soils.

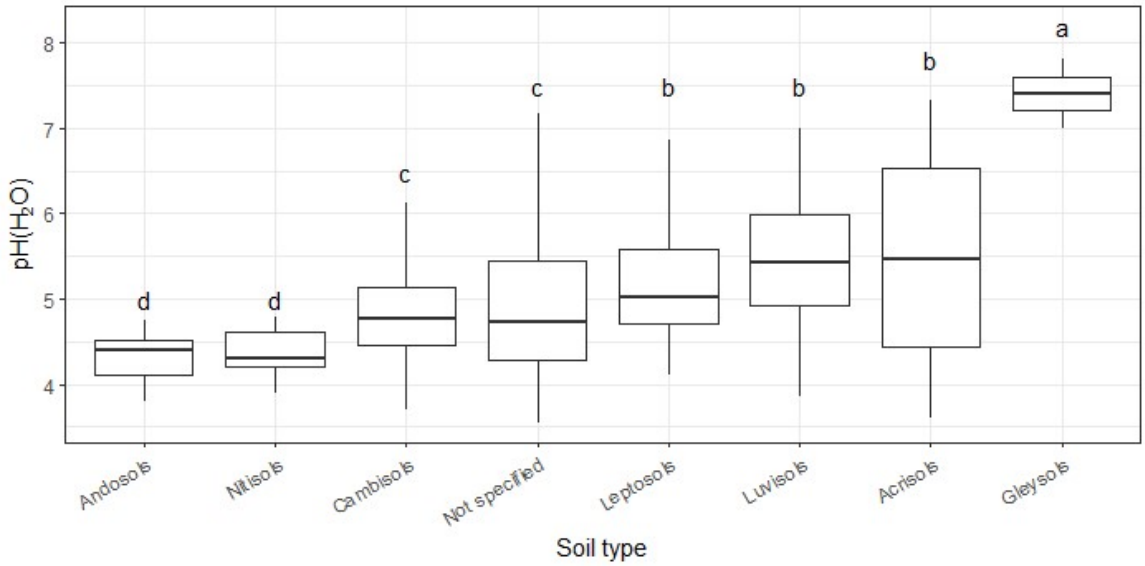

Figure 5.2.2. Soil pH(H_2O) among soil types.
Different alphabets represent significant difference ($p < 0.05$, Tukey HSD test). Explanations for box plot is the same as Fig. 5.2.1.

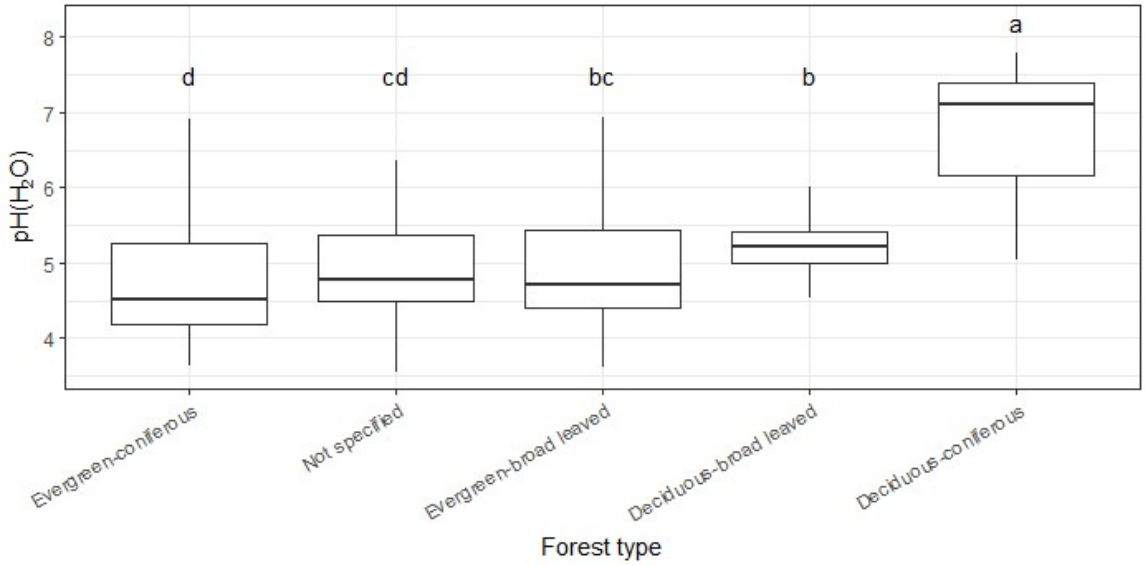

Figure 5.2.3. Soil pH(H_2O) among forest types.
Different alphabets represent significant difference ($p < 0.05$, Tukey HSD test). Explanations for box plot is the same as Fig. 5.2.1.

Relationships between mean annual precipitation and soil pH(H_2O), and latitude and soil pH(H_2O) are shown in Figure 5.2.4 and 5.2.5, respectively. The correlation between precipitation and soil pH(H_2O) was negative, whereas that between latitude and pH(H_2O) was positive, which means soil pH(H_2O) is low in the site where precipitation is high and latitude is low, that is near equatorial region. In fact, there was significant correlation between latitude and mean annual precipitation ($p < 0.001$, *t*-test), therefore the effect of climatic condition was significant on the soil chemical properties. Generally, high precipitation and air temperature induce chemical weathering of soil minerals and leaching of base cations, resulting in soil acidification and low soil pH(H_2O) (Breemen et al., 1984).

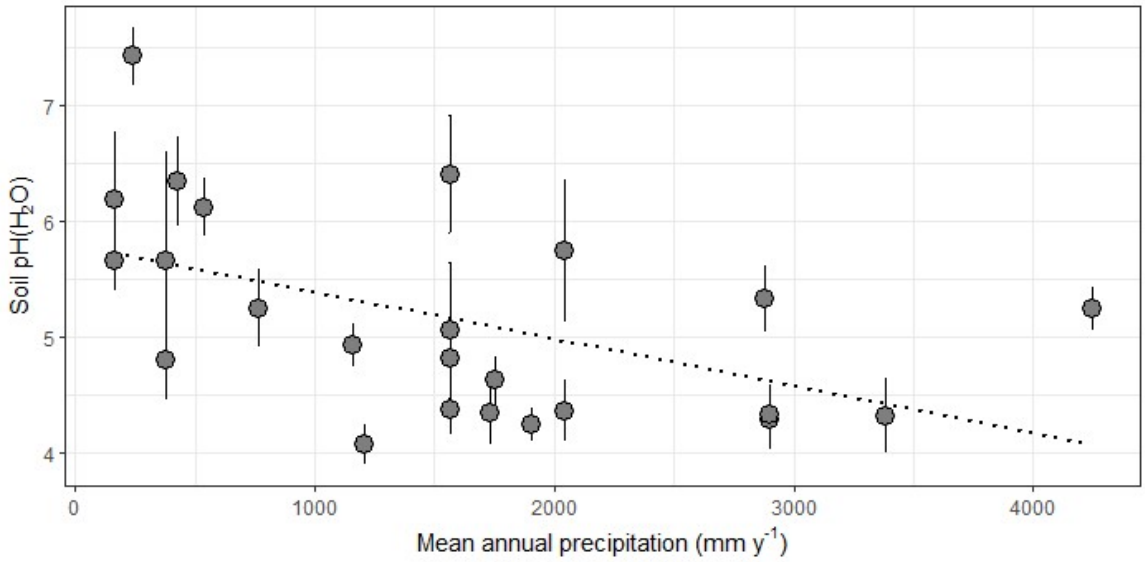

Figure 5.2.4. Relationship between mean annual precipitation and soil pH(H_2O) of each monitoring site.
Significant level of regression line is $p < 0.001$ (*t*-test).

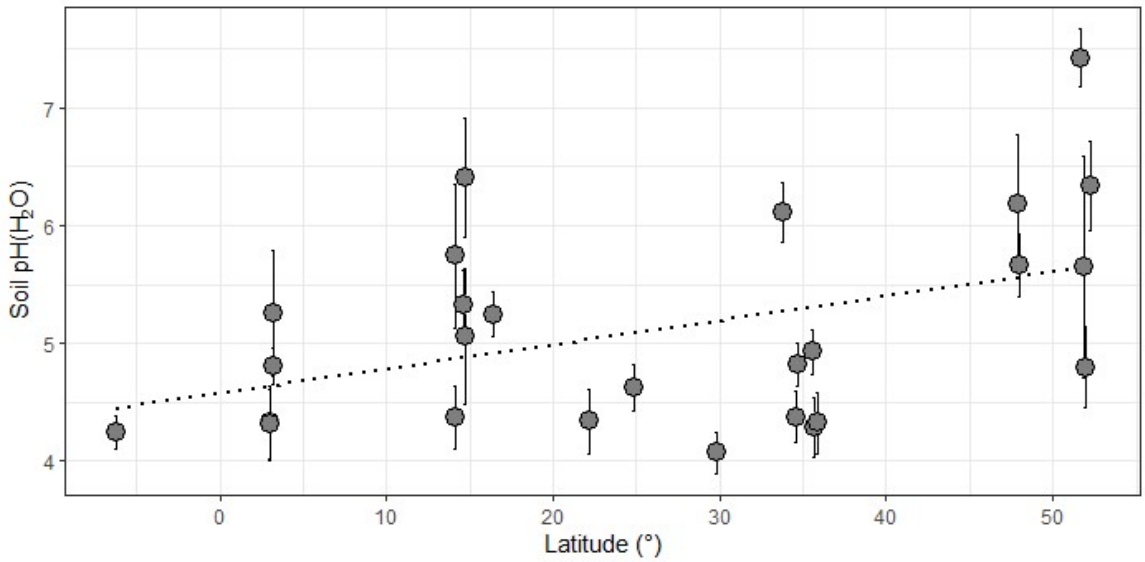

Figure 5.2.5. Relationship between latitude and soil pH(H_2O) of each monitoring site.
Significant level of regression line is $p < 0.001$ (*t*-test).

To elucidate which factor was the most important to control soil pH(H_2O) distribution among these four factors of soil type, forest type, mean annual precipitation and latitude, PLS-R (partial least squares regression) analysis was performed. This method is similar to multiple regression analysis but suitable to deal with explanation variables with multi-collinearity. The result showed that soil type and mean annual precipitation were the dominant factors for variation of pH(H_2O) (Table 5.2.3). As mentioned above, it was suggested that soil formation process and climatic conditions as represented by mean annual temperature affected soil chemical properties.

Table 5.2.3 Results of PLS-R

Explanatory variable for $pH(H_2O)$	VIP *
- Soil type	1.286
- Mean annual precipitation	1.254
- Forest type	0.834
- Latitude	0.277

*, VIP (variable importance for projection) means the strength of each explaining variable.

5.2.1.2 Temporal variation in soil $pH(H_2O)$ in relation to atmospheric environment

In the previous section showed that the inherent soil chemical properties at EANET sites varied widely and were influenced by soil formation process and precipitation. Therefore, it was suggested that sensitivity and response characteristics of soils to the outer environment would be vary among sites. As atmospheric quality has been improved in EANET countries in these 10 years, influences on soil chemical properties is also expected. This section shows the temporal change of soil $pH(H_2O)$ with some items from atmospheric monitoring. In addition, the relationships between atmospheric chemistries and soil $pH(H_2O)$ has been shown. The target sites were the sites which met the following three requirements.

- There were corresponding atmospheric monitoring stations.
- Soil monitoring data since 2000 were available.
- Soil monitoring surveys have been conducted more than 2 times.

Therefore, the monitoring data of 22 sites from 9 countries were used, and the following 9 sites (MYS005, MYS105, PHS003, RUS102, RUS001, RUS101, RUS201, VNS002, and VNS102) were omitted.

Figures 5.2.6 a and b illustrate temporal changes of $pH(H_2O)$ in each EANET site and the background band represents a trend of annual wet deposition of nss-SO_4^{2-} observed at corresponding atmospheric monitoring station to each soil monitoring site. At most of sites, the temporal change in soil $pH(H_2O)$ seemed to fluctuate following the trend of acid deposition. Annual wet deposition of nss-SO_4^{2-} tended decreasing in sites in China, Japan, Metro Manila in Philippines, and R. of Korea. Following this decrease, $pH(H_2O)$ in CNS009, CNS001 and JPS006 showed increasing trend (Figure 5.2.6 a). Although soil $pH(H_2O)$ should increase in response to this atmospheric trend theoretically, the temporal change of soil $pH(H_2O)$ did not necessarily obey this theory in some sites (e.g. CNS004, CNS007, JPS106, JPS008, JPS108 and KRS003). It was suggested that the effect of acid deposition from atmosphere on soil chemical properties was complicated because it reflected not only acid neutralization reaction of soil minerals but also other many processes including interactions between atmospheric deposition and forest trees and litter layer.

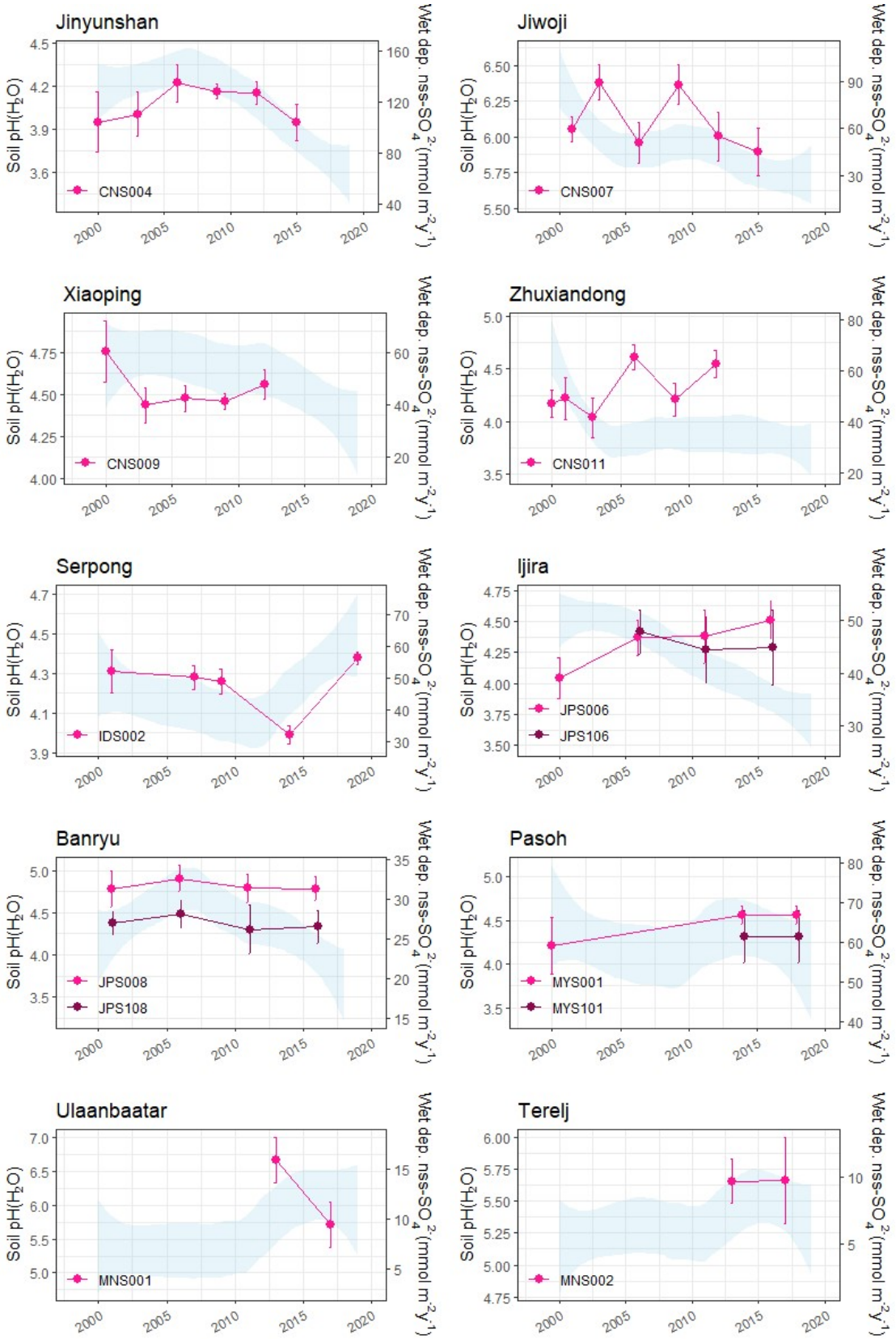

Figure 5.2.6 a. Temporal changes in soil pH(H_2O) with wet deposition nss-SO_4^{2-}.
Line chart represents soil pH(H_2O) at each survey year and band represents variation of wet deposition nss-SO_4^{2-} derived from loess (locally weighted scatter plot smooth) with 95% confidence interval.

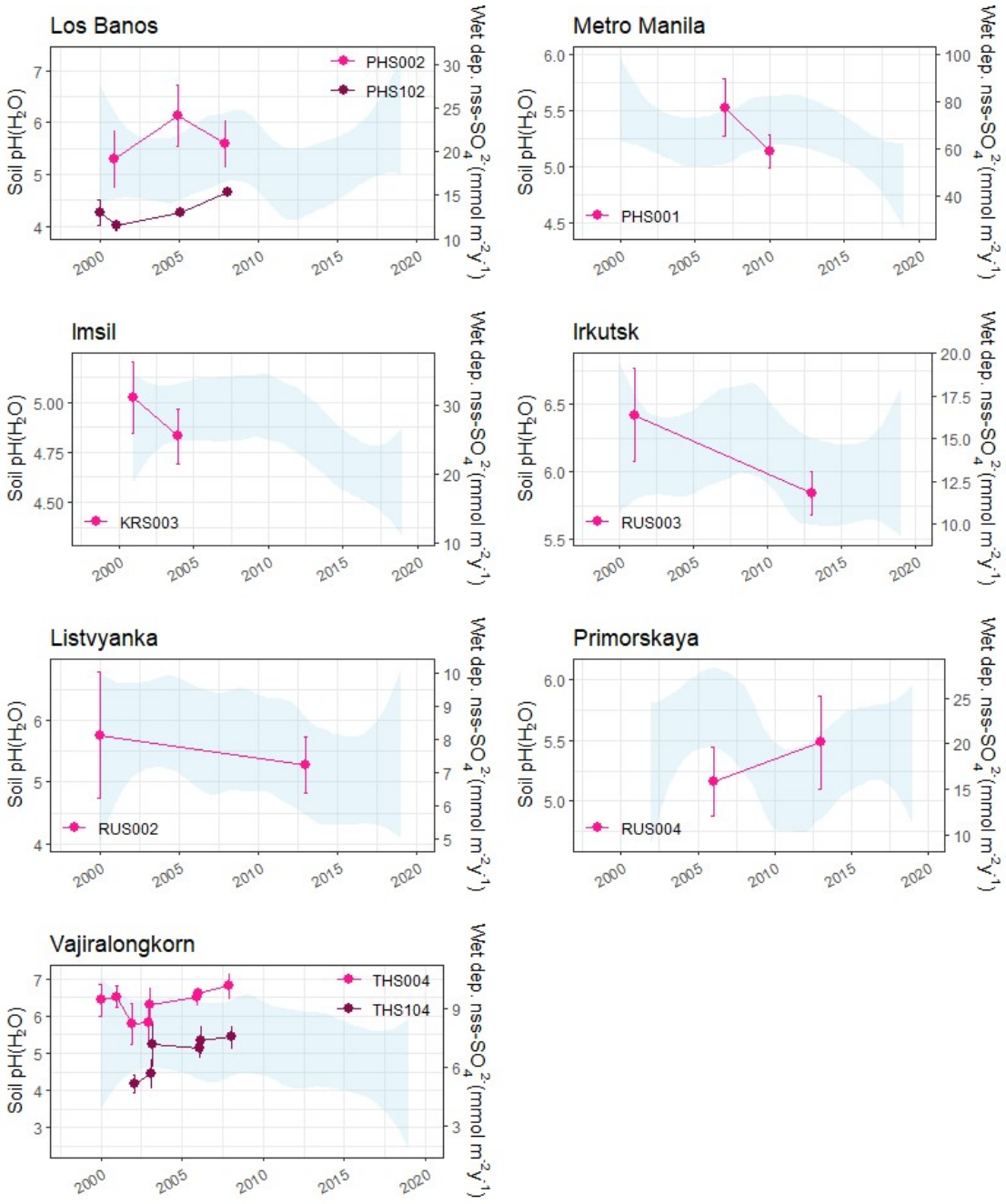

Figure 5.2.6 b. Temporal changes in soil pH(H_2O) with wet deposition nss-SO_4^{2-}.
Line chart represents soil pH(H_2O) at each survey year and band represents variation of wet deposition nss-SO_4^{2-} derived from loess (locally weighted scatter plot smooth) with 95% confidence interval.

To consider relationships between soil chemical properties and atmospheric depositions, regression analysis was conducted between soil pH(H_2O) and wet deposition pH, nss-SO_4^{2-}, nss-Ca^{2+}, NH_4^+ and NO_3^- (Table 5.2.4). The positive (+) correlation means that soil pH(H_2O) follows the fluctuation of wet deposition; when wet deposition increases, soil pH(H_2O) also increases. Ideally, increase in nss-SO_4^{2-}, NH_4^+ and NO_3^-, which behave acidifying substances in soil (Baba and Okazaki, 1998), will cause decrease in soil pH(H_2O). However, the sign of correlation varied between + and – among sites, implying the response to wet deposition of soil was not constant. In China, it was suggested that nss-Ca^{2+} was derived from calcareous substances in desert dust and

from anthropogenic emission sources, and nss-Ca^{2+} would contribute to neutralizing acid deposition and moderating soil acidification (Larssen and Carmichael, 2000; Duan et al., 2016). In addition to this interaction between atmospheric agents and soil, the diversity of soil chemical characteristics among sites and the complexity of soil reaction to acidifying substances from atmosphere were suggested to be related to these consequences.

Table 5.2.4 Slope of correlation between soil pH(H_2O) and items of wet deposition

Country	Site code	pH	nss-SO_4^{2-}	nss-Ca^{2+}	NH_4^+	NO_3^-
China	CNS004	ns	+	+	+	+
	CNS007	−	+	+	+	+
	CNS009	+	−	−	−	−
	CNS011	−	−	−	−	−
Indonesia	IDS002	−	ns	ns	−	−
Japan	JPS006	+	−	−	−	−
	JPS106	−	+	+	+	+
	JPS008	ns	+	+	+	+
	JPS108	ns	+	+	+	+
Malaysia	MYS001	+	−	ns	−	+
	MYS101	ns	ns	ns	ns	ns
Mongolia	MNS001	+	+	+	+	−
	MNS002	ns	ns	ns	ns	ns
Philippines	PHS002	ns	−	−	−	−
	PHS102	−	+	−	ns	−
	PHS001	−	+	+	−	−
R. of Korea	KRS003	+	+	−	+	−
Russia	RUS003	+	+	+	+	+
	RUS002	ns	ns	ns	ns	ns
	RUS004	+	−	−	−	−
Thailand	THS004	+	ns	−	ns	ns
	THS104	+	−	−	ns	ns

+, −, and ns represent significant-positive, significant-negative and not significant correlations, respectively.

5.2.1.3 Summary

The soil monitoring data since 2000 to 2019 were reviewed. The section 5.2.1.1 showed the diverse soil characteristics of EANET sites; the pH(H_2O) ranged from 3.5 to 7.5, and the factors controlling the widespread variation were suggested to be soil formation process and climatic conditions. In the section 5.2.1.2, temporal changes in soil pH(H_2O) was shown together with the items of wet deposition and it was suggested that the soil reaction was not necessarily parallel to the input of atmospheric deposition. Considering the diverse distribution of soil characteristics among EANET sites, it was also suggested the reaction process would be different for each site. However, there are considerable sites where soil monitoring has not been conducted enough times for these 20 years, implying insufficient framework to detect the ecological impacts resulted from changes in atmospheric environment. As this monitoring system will also provide valuable data for understanding the effects of climate change on ecosystems, soil monitoring should be continued more intensively.

5.2.2 Vegetation monitoring

5.2.2.1 Characteristics of monitoring stands

Vegetation monitoring has been conducted at 24 sites in 8 countries since 2000. The basic survey was principally carried out for the initial objectives (namely, establishment of baseline data and early detection of possible impact) in the participating countries in accordance with the *Technical Documents for Soil and Vegetation Monitoring in East Asia* (EANET 2000). These are performed in the same stand as soil monitoring and detailed metadata are shown in Table 5.2.1. However, there is a large variation in the content and frequency of surveys among sites. Regarding vegetation monitoring, it was assumed that comprehensive forest survey (General description of forest; GDF), tree decline survey (Observation of tree decline; OTD), and understory vegetation survey would be conducted. However, the only sites that have been surveyed more than once since 2015 are those in China and Japan (Figure 5.2.7). There are four monitoring sites that can track the diameter at breast height (DBH) growth of standing trees in China, two at Jinyunshan, and Dabagou and Xiaoping. Records from 2003 to 2015 are registered for the two sites of Jinyunshan. There also are four monitoring sites in Japan. Records have been registered for two sites (Banryu-2 and Iwami Rinku FP) since 2001, but monitoring of these sites has ended in 2018, and they have been replaced with two new sites (Sekido-san and Horyu-san). Records of Ijira and Yamato have been registered since 2006, and the data up to 2019 are available. Typically, trees subject to GDF are individually identified and recorded every 3 to 5 years. OTD is conducted every year for some GDF target trees, but the number of trees surveyed is small.

As shown in previous chapters, atmospheric environment has been improving over the last decade and it is necessary to verify whether it reflects on vegetation properties. In this section, temporal changes in DBH increase rate of individual trees and the total trunk cross-sectional area at breast height (BA) of the eight sites in Japan and China were analyzed. This is because these eight sites were the only sites where data was recorded in a continuously comparable manner. Firstly, the tree dynamics of each site will be described. Then, we consider what factors can explain their dynamics.

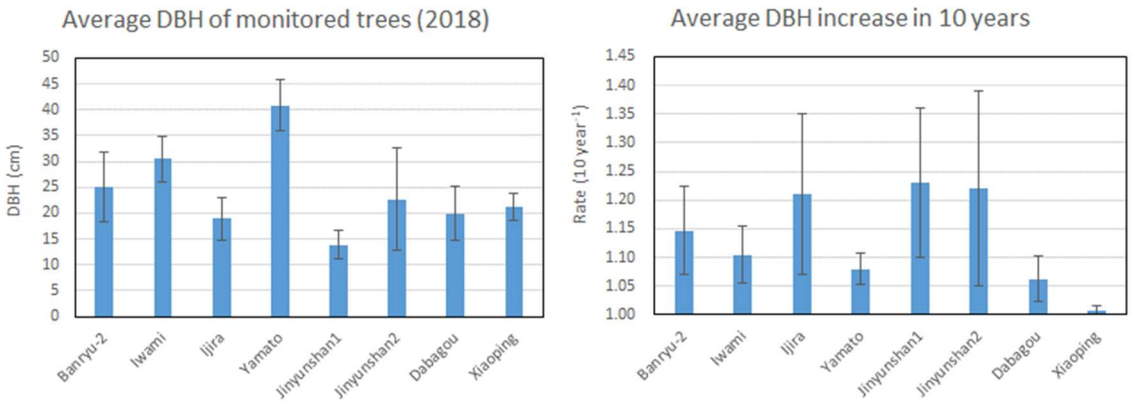

Figure 5.2.7. DBH of monitored trees for each stand and the rate of increase in DBH over the last 10 years in the tree decline survey (OTD). Vertical lines indicate standard deviation.

5.2.2.2 Stand dynamics

(1) Banryu-2 (JPS008)

This site faces the Sea of Japan and is expected to be easily affected by transboundary air pollution from the continent. It is an evergreen broad-leaved forest dominated by *Machilus thunbergii* and is composed of about 20 tree species. At this site, DBH data from 2001 to 2018 were analyzed for

GDF and OTD. The number of target trees of GDF were 80 in 2001. In 2006, 35 trees were thinned. By 2016, 13 trees had been recruited and 21 had died, bringing the number of trees surveyed to 34. The main cause of death was presumed to be competition with neighboring individuals, but there was also death due to bark beetles. Although the annual increase in DBH of individual trees showed a decreasing trend, some trees grew significantly from 2006 to 2010 after thinning (Figure 5.2.8a, b). The total BA of the trees surveyed by GDF decreased slightly in 2006 after thinning and has increased consistently since then, suggesting that the impact of thinning in 2006 was small (Figure 5.2.8c).

(2) Iwami Rinku FP (JPS108)

This site faces the Sea of Japan and is expected to be easily affected by transboundary air pollution from the continent. It is an evergreen broad-leaved forest dominated by *Castanopsis cuspidata* var. *sieboldii* and is composed of about 12 species of trees. At this site, DBH data from 2001 to 2018 were analyzed for GDF and OTD. The number of target trees of GDF were 141 in 2001. By 2016, 5 trees had been recruited and 44 had died, bringing the number of trees surveyed to 102. The main cause of death was presumed to be competition with neighboring individuals but eating marks of bark beetles were confirmed on more than 10 trees. The annual increase in DBH of individual trees was fairly constant throughout the period and showed no significant temporal changes (Figure 5.2.8d, e). In 2011, many bark beetle pits were found on *C. sieboldii*, and some *Quercus serrata* trees died or declined. However, the total BA of the trees surveyed by GDF continued to increase, suggesting that the impact of feeding damage on the stand was small (Figure 5.2.8f).

(3) Ijira (JPS006)

This site located inland in central Honshu Japan, and is expected to be susceptible to the urban atmosphere in Japan. It is a young cypress plantation, and the stand consists of almost one species, *Chamaecyparis obtusa*. At this site, DBH data from 2006 to 2019 were analyzed for GDF and OTD. The target trees of GDF were 121 in 2006. From 2006 to 2011, 37 trees were thinned. By 2016, 26 trees had been recruited and 3 had died, bringing the number of trees surveyed to 109. In the OTD survey, DBH was recorded for 8 trees in 2006, and 12 new trees were recorded from 2011. The annual increase in DBH of individual trees showed a decreasing trend (Figure 5.2.8g, h), but average DBH increase rate in recent 10 years was the largest among the monitoring sites in Japan (Figure 5.2.7). The total BA of the trees surveyed by GDF decreased slightly in 2011 after thinning and has increased in 2016, suggesting that the impact of thinning was small (Figure 5.2.8i).

(4) Yamato (JPS106)

This site located inland in central Honshu Japan, and is expected to be susceptible to the urban atmosphere in Japan. It is a matured cypress plantation, and the stand consists of one species, *Chamaecyparis obtusa*. At this site, DBH data from 2006 to 2019 were analyzed for GDF and OTD. The target trees of GDF were 48 in 2006. From 20011 to 2016, 19 trees were thinned. By 2016, no trees had been recruited and 4 had died, bringing the number of trees surveyed to 25. In the OTD survey, DBH was recorded for 20 trees in 2006, and 10 trees were replaced during the period. Therefore, the remaining 10 trees were continuously measured. The annual increase in DBH of individual trees showed a decreasing trend (Figure 5.2.8j, k). The total BA of trees surveyed by GDF decreased significantly in 2016 due to thinning, suggesting that the impact of thinning was very large (Figure 5.2.8l). On the other hand, no improvement in the growth of the remaining trees after thinning was observed (Figures 5.2.7, 5.2.8j, k).

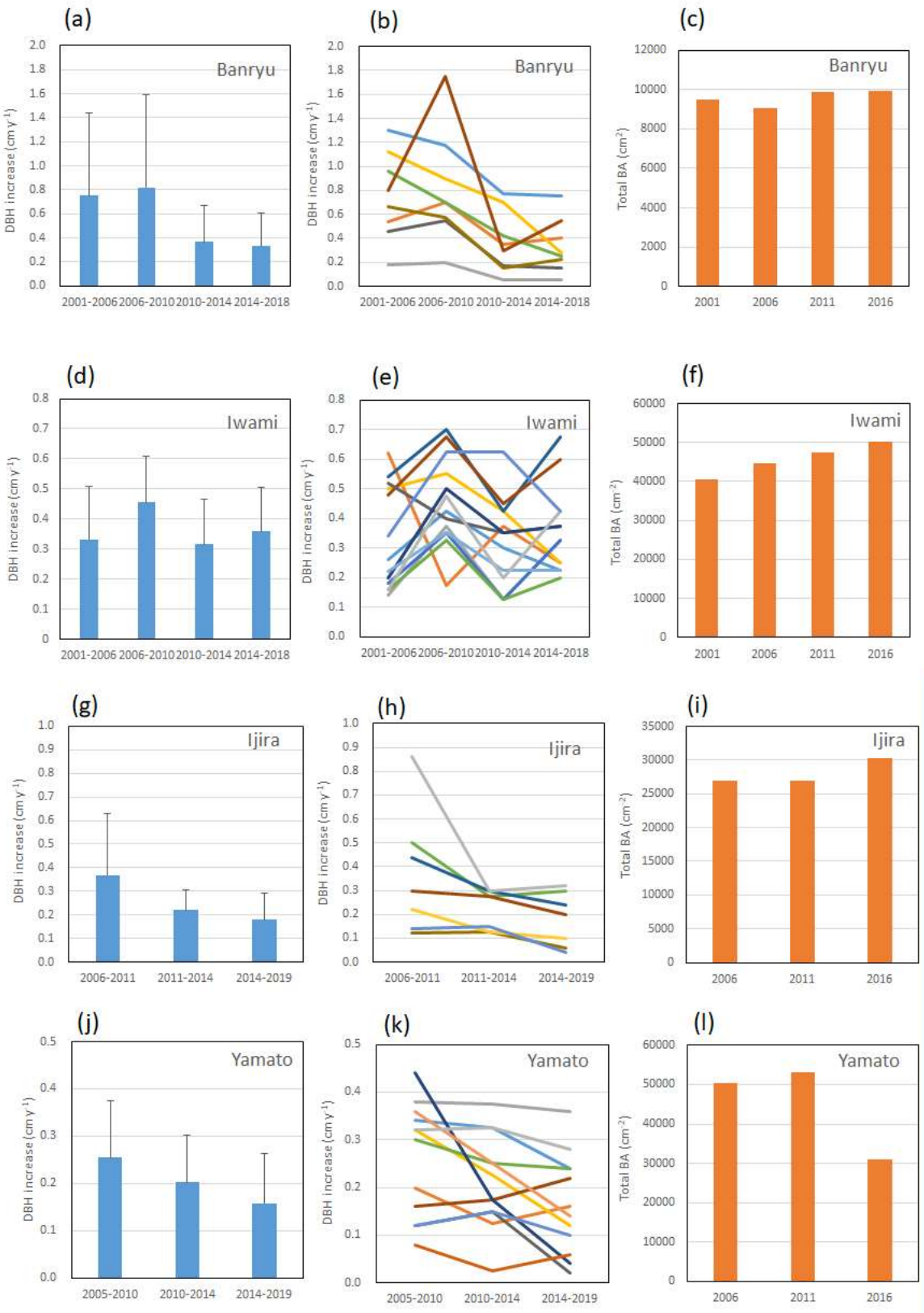
(a)
Banryu
DBH increase (cm y-1)
2001-2006 2006-2010 2010-2014 2014-2018
(b)
Banryu
DBH increase (cm y-1)
2001-2006 2006-2010 2010-2014 2014-2018
(c)
Banryu
Total BA (cm-2)
2001 2006 2011 2016
(d)
Iwami
DBH increase (cm y-1)
2001-2006 2006-2010 2010-2014 2014-2018
(e)
Iwami
DBH increase (cm y-1)
2001-2006 2006-2010 2010-2014 2014-2018
(f)
Iwami
Total BA (cm-2)
2001 2006 2011 2016
(g)
Ijira
DBH increase (cm y-1)
2006-2011 2011-2014 2014-2019
(h)
Ijira
DBH increase (cm y-1)
2006-2011 2011-2014 2014-2019
(i)
Ijira
Total BA (cm-2)
2006 2011 2016
(j)
Yamato
DBH increase (cm y-1)
2005-2010 2010-2014 2014-2019
(k)
Yamato
DBH increase (cm y-1)
2005-2010 2010-2014 2014-2019
(l)
Yamato
Total BA (cm-2)
2006 2011 2016

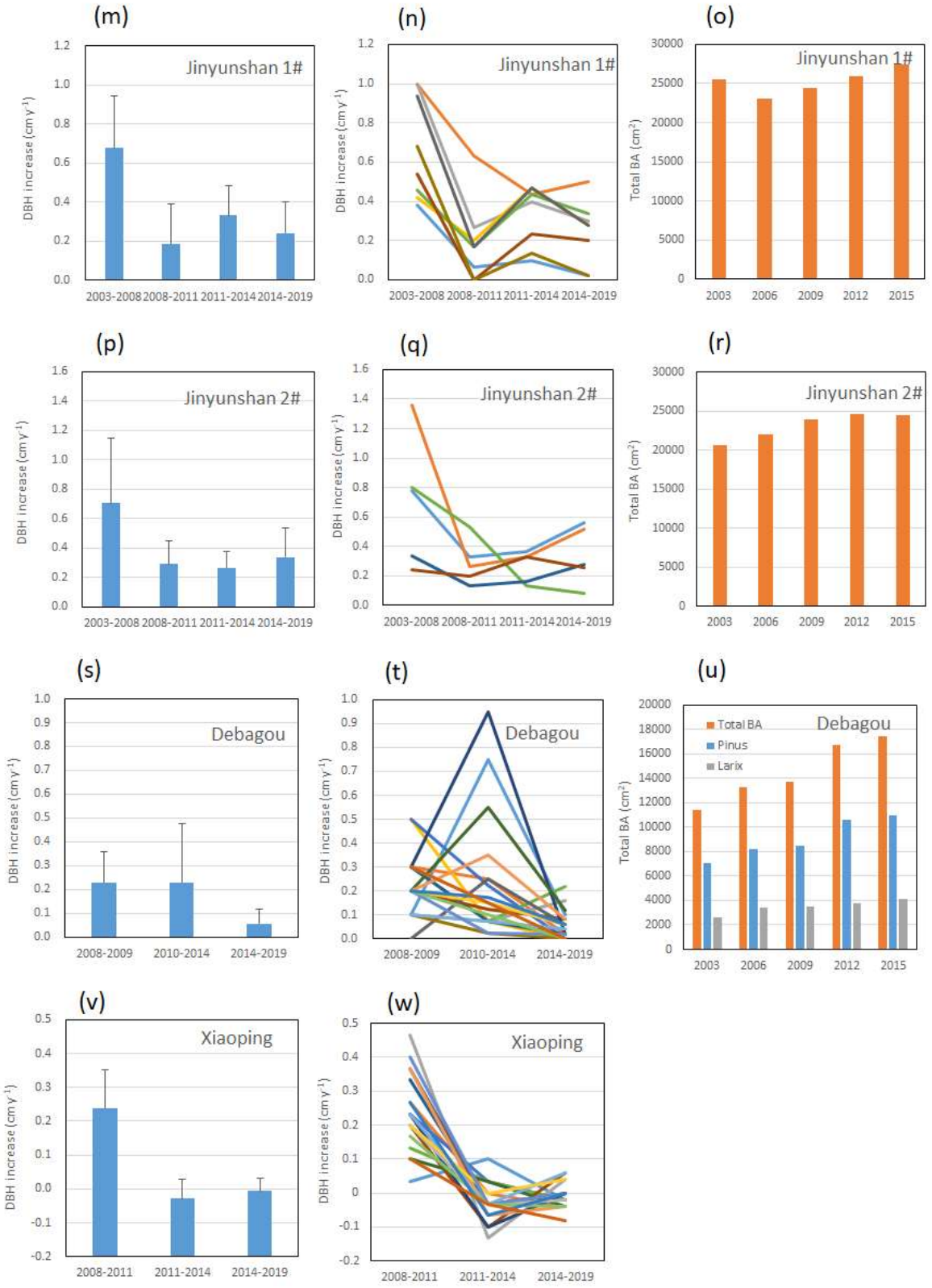

Figure 5.2.8. Average annual increase in DBH (left column) of OTD, DBH increase for each individual tree of OTD (middle column), and changes in total BA for each year at each GDF site (right column). Vertical lines indicate standard deviation. In the graphs showing the OTDs in the middle row (b, e, h, k, n, q, t, w), each colored line represents a different individual.

(5) Jinyunshan (CNS004)
Jinyunshan is located in the inland area of China and was selected as a rural site. The study area is set up with two stands (Jinyunshan-1, Jinyunshan-2), and Jinyunshan-1 is an evergreen mixed forest dominated by *Castanopsis carlesii var. spinulosa*, *Pinus massoniana* and *Symplocos setchuenensis* and is composed of about 14 tree species. Jinyunshan-2 is an evergreen broad-leaved forest composed of about 10 species including *Castanopsis fargesii*, *Elaeocarpus japonicus* and *Machilus pingii*. At both sites, DBH data from 2003 to 2019 were analyzed for GDF and OTD.

At Jinyunshan-1, the number of target trees of GDF were 104 in 2003. By 2006, 11 trees had been cut down and 11 trees had died. By 2015, one tree had been recruited and 5 trees had died, bringing the number of trees surveyed to 78. The main cause of death was presumed to be competition with neighboring individuals. In the OTD survey, DBH was recorded for 11 trees in 2008, and 2 trees died during the period. The annual increase in DBH of individual trees was fairly variable throughout the period (Figure 5.2.8m, n) but average DBH increase rate in recent 10 years was the largest among the monitoring sites (Figure 5.2.7). The total BA of the trees surveyed by GDF decreased slightly in 2006 after thinning, continued to increase until 2015, and has fully recovered (Figure 5.2.8o).

At Jinyunshan-2, the number of target trees of GDF were 75 in 2003. By 2006, 22 trees had been cut down and 5 additional trees had been cut by 2015. By 2015, 1 tree had been recruited and 1 tree had died, bringing the number of trees surveyed to 48. In the OTD survey, DBH was recorded for 9 trees in 2008, and 3 trees died during the period. The total BA of the trees surveyed by GDF increased in 2006 after thinning, suggesting that the impact of thinning was not negative (Figure 5.2.8r). On the other hand, the BA increase since 2009 has leveled off. The annual increase in DBH of individual trees appears to have declined in 2008, but has recently increased slightly (Figure 5.2.8p, q). In fact, the average DBH increase rate in recent 10 years was relatively large compared with other sites (Figure 5.2.7).

(6) Dabagou (CNS007)
Dabagou (Jiwozi) is located in the inland area of China and was selected as a remote site. It is a young coniferous plantation, and the stand mainly consists of two species, ever green *Pinus armandi* and deciduous *Larix gmelinii*, and is composed of about 14 tree species. At this site, DBH data from 2003 to 2019 were analyzed for GDF and OTD. The target trees of GDF were 66 in 2003. By 2016, no trees had been recruited and 1 had died, bringing the number of trees surveyed to 65. In the OTD survey, DBH was recorded for 20 *P. armandi* trees in 2008 and no dead trees were recorded during the period. However, the increase in DBH over the last 5 years was small (Figure 5.2.8s, t). In addition, average DBH increase rate in recent 10 years was small (Figure 5.2.7). The cause was presumed to be the interaction between individuals due to high tree density. On the other hand, the total BA of the trees surveyed by GDF continued to increase during the monitoring period (Figure 5.2.8u). This result is considered to be due to the difference in the surveyed stands of GDF and OTD, and is presumed to reflect the difference in stand characteristics.

(7) Xiaoping (CNS009)
Xiaoping is located near the sea in southern China and was selected as a remote site. The monitored stand is a plantation of evergreen broad-leaved tree, *Michelia macclurei* and consists of several other minor species. At this site, DBH data from 2003 to 2012 were recorded for GDF. However, at this site, individual IDs were not consistently assigned in GDF surveys, and GDF results could not be analyzed. Therefore, only OTD data from 2008 to 2019 were analyzed. In the OTD survey, DBH was recorded for 20 *M. macclurei* trees in 2008 and two trees had died by 2011, bringing the number of trees surveyed to 18. The characteristic of this site is that there was almost no increase in DBH in all the target trees during the observation period, and the average DBH increase rate in recent 10 years is almost zero (Figure 5.2.7, 5.2.8v, w). *M. macclurei* is not a fast-growing tree species by nature, but the cause of such extremely low growth rates is unknown.

5.2.2.3 Trend analysis for each stand

Tree growth is influenced by various environmental factors. Meteorological conditions (temperature, precipitation, strong winds, snowfall), CO_2 concentration, atmospheric depositions, intra- and inter- specific competition, diseases and pests, anthropogenic physical disturbance, etc (Forzieri et al. 2021; Hisao et al. 2019). The load of acid deposition (air pollution) is one of them. Assessing the effects of air pollution through field monitoring requires appropriate monitoring plans to distinguish the effects of air pollution from other factors. As a result of air pollution control measures in China, the amount of wet deposition of nss-SO_4^{2-}, which is an indicator of the intensity of regional air pollution, has been declining at each survey site since 2007 (Figure 5.2.6). In fact, the impact of transboundary air pollution from China on the Japanese archipelago has decreased significantly since 2008 (Okamoto et al. 2018). Since Banryu and Iwami are vulnerable to air pollution from the continent, it is possible that the reduction in transboundary air pollution had caused systematic changes in forest dynamics. However, in Banryu, the increase in DBH of the monitored trees has decreased since 2010, and the stand BA has hardly changed (Figure 5.2.8a, b, c).

At Iwami, there was no change in the annual increase in DBH during the monitoring period, and BA continued to increase as well (Figure 5.2.8d, e, f). Even considering the effects of logging and bark beetles, it is not clear whether the changes in the atmospheric environment had a positive effect on tree growth. Ijira and Yamato are located inland area and are monocultural coniferous plantation. It is considered that the influence of forest age and deforestation, that is, the influence of interaction between trees and human disturbance was large. In such situations, it is difficult to evaluate the effects of air pollution independently.

The impacts of the changes in atmospheric environment have been shown to vary with stand species diversity (Hisao et al. 2019). In the case of forest monitoring on Mt. Tateyama in the central mountainous region of Japan, the effects of transboundary air pollution on deciduous beech *Fagus crenata* and evergreen conifer *Cryptomeria japonica* were different and the beech trees became dominant as air pollution declined (Kume et al. 2020). At Dabagou's GDF site, evergreen pines and deciduous larch grow sympatrically (Figure 5.2.8u), and it is assumed that the environmental responses of these two tree species could be different. From 2003 to 2009, the rate of increase in DBH of larch was fast (Figure 5.2.9).

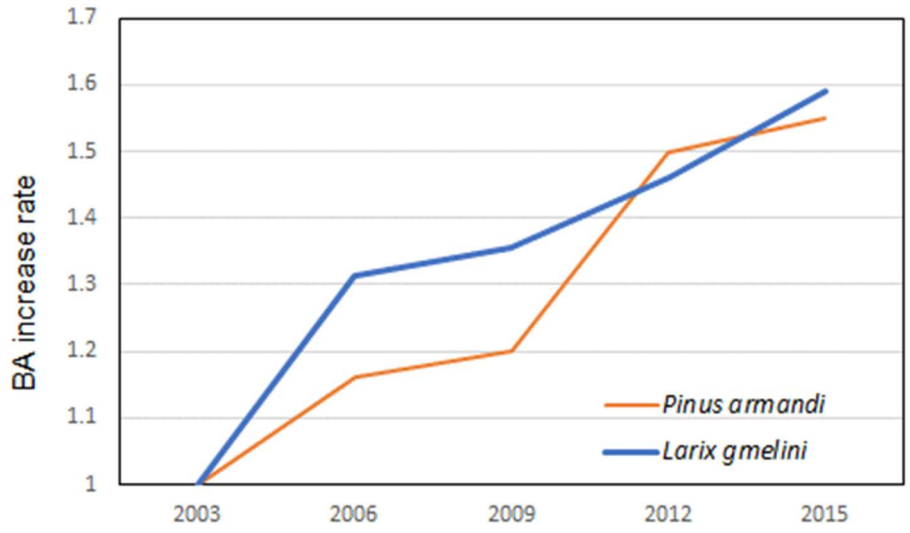

Figure 5.2.9. Changes in the BA increase rate of pine (*Pinus armandi*) and larch (*Larix gmelini*). Relative value with BA in 2003 as 1. The two species are mixedly planted.

However, as of 2015, the difference between the two species has disappeared. This result might indicate that there was a significant change in intraspecific relationships during the monitoring period, but analysis with additional data should be required to clarify the cause.

During the monitoring period, the factors that most affected the stand biomass of the monitoring sites were logging and thinning, and the effects of typhoons were also confirmed. The effects of bark beetles (*Platypus quercivorus*) have also been recorded in Japanese broad-leaved forests. Such results are similar to the trend of monitoring results in Europe (Forzieri et al. 2021). The other cause of mortality was due to competition with neighboring individuals, which is an aspect of biological interaction.

In conclusion, in order to quantitatively assess the impact of air pollution on a wide range of forests, it is necessary to identify individual trees and conduct long-term growth measurements at sites adjacent to air quality monitoring sites, with little or no anthropogenic disturbance. It is desirable that monitoring activities will be resumed and activated in countries other than Japan and China. Steady monitoring at many small sites may be more effective than investigating at a few large sites. In the case of planted forests, it may be possible to set up a more sensitive monitoring site by devising the species composition. By expanding and continuing such monitoring, it will be possible to conduct ecosystem impact assessment, including air pollution impact.

5.2.2.4 Summary

The EANET has been monitoring forest vegetation at 24 sites in 8 countries. The vegetation monitoring includes conduct comprehensive forest survey, tree decline survey, and understory vegetation survey, but the content and frequency of surveys vary widely. The only 8 sites that have been surveyed more than once since 2015 are in China and Japan. The amount of wet deposition of nss-SO_4^{2-}, which is an indicator of the intensity of regional air pollution, has been declining at each survey site since 2007. However, no corresponding increase in forest growth was observed. This may be due to anthropogenic disturbance, pest infestation (bark beetle), or intensified competition between individuals as the age of the forest increases. To quantitatively assess the impact of air pollution on a wide range of forests, it is necessary to identify individual trees and conduct long-term growth measurements with air quality monitoring with little or no anthropogenic disturbance.

5.3 Inland water chemistry and trend

5.3.1 Water chemistry

5.3.1.1 Site properties

In this section, the data on inland aquatic environment collected in 20 sites from 11 countries (Table 5.3.1) were analyzed. During the last five years, the monitoring in Banryu Lake ended in 2015, while that in Futago-ike Lake started in 2019. Futago-ike Lake consists of two neighboring lakes, Oike and Meike. Beside the sites listed in Table 5.3.1 four additional sites' data were also analyzed for Figure 5.3.1 and Figure 5.3.2: the Kamagatani River (as J1-1) and the Kobara River (as J1-2) which flow into the Ijira Lake in Japan and an additional sampling point in the Banryu Lake in Japan (as J2-1) and in Vachiralongkorn Dam in Thailand. Data from the starting year of each site to 2019 were used.

General properties of monitoring sites are important to interpret and evaluate the monitored chemical properties of inland water. Some properties such as area of a lake, water depth, water volume, altitude, precipitation etc. showed large variations among the sites in PRSAD 3, though there are many missing data. After five years, information is still insufficient as shown in the latest Data Report 2019 which shows the data on watershed area are available for 10 sites among the 20 sites. Information on surface geology and vegetation which are also essential for interpretation of water quality are available only for 9 sites in Indonesia, Japan, Mongolia, Russia and Thailand (Data report 2019).

5.3.1.2 Characteristic evaluation of water chemistry at each site

In order to show the characteristics of average water chemistry of each site, the relative ratios of respective elements were demonstrated by the tri-linear diagram in Figure 5.3.1 and the levels of average concentration of ionic elements were compared in Figure 5.3.2. In both figures, the total average concentration for the monitoring period of each site was used.

The tri-linear diagram shows balances among the major parameters, which is often used for characterization of inland waters. The center diamond plot, the left triangle plot and the right triangle plot show a balance between anions and cations, balance among cations, and balance among anions, respectively. Normally, nitrate ion is not added to the evaluation in the tri-linear diagram, but in this report, nitrate ion was added to the evaluation to understand the effects of nitrate ion. Figure 5.3.1 was very similar to the diagram made based on the average data until 2014 in PRSAD 3 and extracted characteristics of ionic composition of inland water at several sites in PRSAD 3 were true for the data until 2019 shown in Figure 5.3.1, too. The extracted characteristics were:

1) Ionic composition in Jinyunshan lake (C1) was peculiar, rich in SO_4^{2-} and $Ca^{2+} + Mg^{2+}$ and poor in alkalinity. Not only the relative ratio, but concentrations of SO_4^{2-} (0.62 meq L^{-1}) and NO_3^- (0.16 meq L^{-1}) were extremely high and the latter was the maximum among all the sites (Figure 5.3.2).

2) Composition in Jiwozi River (C3), Pereemnaya River (R1), Komarovka River (R2) and Ijira Lake (J1) were somewhat similar to that in Jinyunshan Lake and they (other than Ijira Lake) showed high SO_4^{2-} concentration next to Jinyunshan Lake (Figure 5.3.2). Ionic composition and concentration levels in the two rivers flowing into Ijira Lake were almost same as those in the lake.

3) Banyu Lake (J2) showed a very different characteristic from other sites: proportions of Cl^- and Na^+ to the total anions and the total cations, respectively, and their concentrations were extremely high suggesting the effect of sea salt.

4) Vachiralongkorn Dam (T1), Hoa Binh Reservoir (V1) and Tembaling River (M2) in Southeast Asian countries showed very high proportions of HCO_3^- and $Ca^{2+} + Mg^{2+}$ in anions and cations, respectively. Concentrations of these elements were extremely high in these sites and also in Pandin Lake (P1) as shown in Figure 5.3.2.

The tri-linear diagram based on the data from 2015 to 2019 was mostly similar to Figure 5.3.1. But the proportion of $NO_3^- + Cl^- + SO_4^{2-}$ increased slightly in Pereemnaya River (R1) and Komarovka River (R2), and decreased in Jinyunshan lake (C1) and Jiwozi River (C3). Although several years' averages of ionic compositions in these inland waters were relatively stable, the proportions of acidic anions in these sites have gradually been changing.

Table 5.3.1 List of inland aquatic environment monitoring sites

Country	Site name	Site ID
Cambodia	Sras Srang Lake	Ca1
China	Jinyunshan Lake	C1
	Xiaoping Dam	C2
	Jiwozi River	C3
	Zhuxiandong Stream	C4
Indonesia	Patengang Lake	I1
	Gunung Lake	I2
Japan	Ijira Lake	J1
	Banryu Lake	J2
	Futago-ike Lake	J3
Lao PDR	Nam Houm Lake	L1
Malaysia	Semenyih Dam	M1
	Tembaling River	M2
Mongolia	Terelj River	Mo1
Philippines	Pandin Lake	P1
	Ambulalakaw Lake	P2
Russia	Pereemnaya River	R1
	Komarovka River	R2
Thailand	Vachiralongkorn Dam	T1
Vietnam	Hoa Binh Reservoir	V1

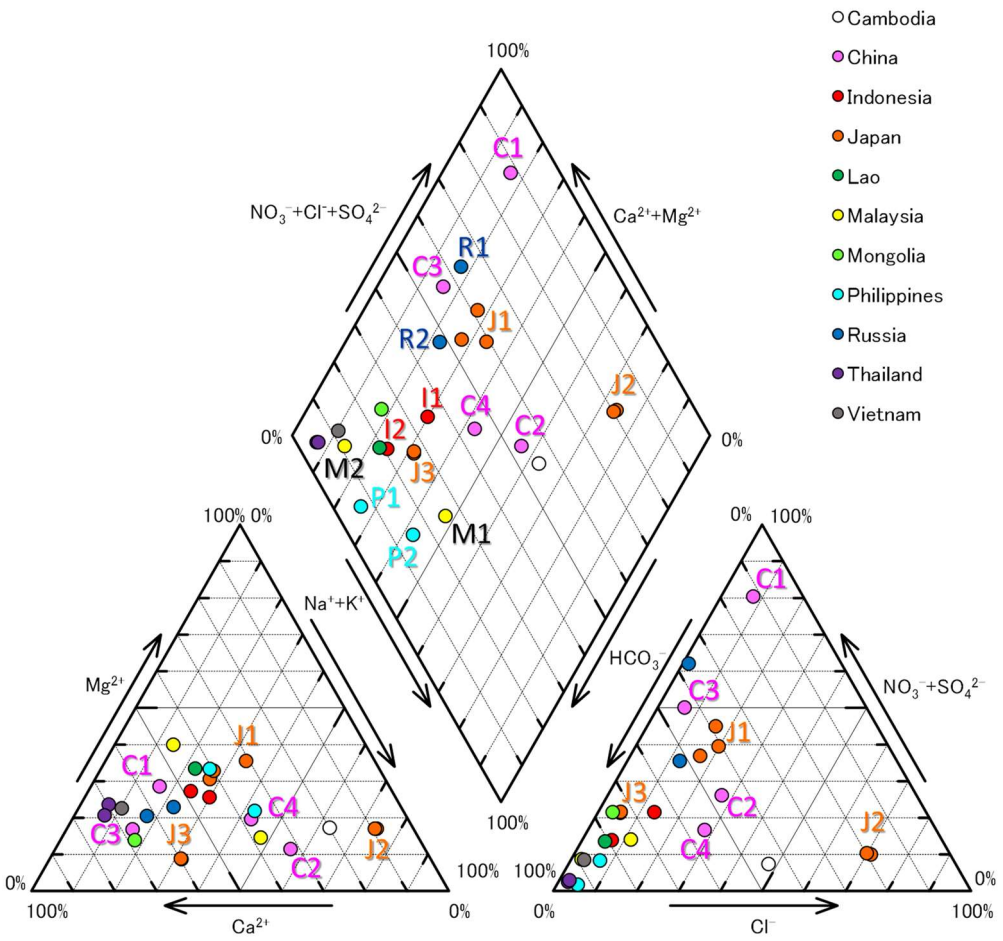

Figure 5.3.1. Piper trilinear diagram of the inland water chemistry from the EANET sites (drawn using the excel sheet by Hamada 2002). The total mean for the monitoring period was applied for the plot. HCO_3^- was based on alkalinity. Site IDs are indicated in Table 6.4.1.

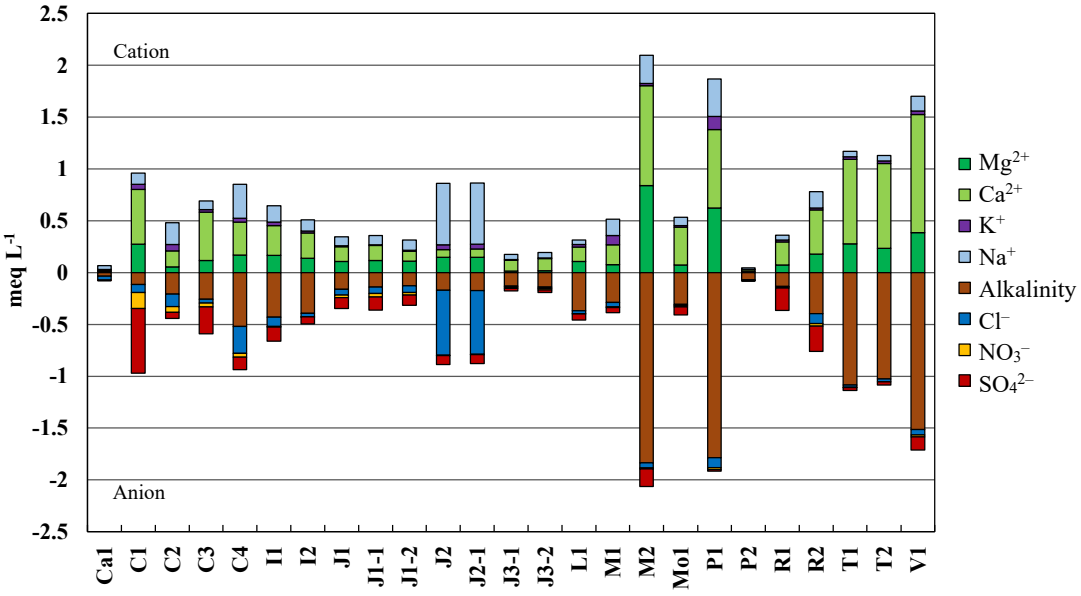

Figure 5.3.2. Mean concentration of ionic elements of inland water in each site for total monitoring period.

5.3.2 Spatial, seasonal and long-term patterns in inland water chemistry

5.3.2.1 Study sites

Water chemistry data of 20 inland sites covering the monitoring period from 2000 to 2019 were analysed in this section. The names and IDs of these sites are similar to those in Table 5.3.1 (section 5.3.1) with two exceptions. First, Futago-ike Lake (J3) was not included in this analysis, because monitoring at this site started in 2019 and only sites with at least five years monitoring data were used. Second, Vachiralongkorn Dam (T1) was divided into two separate sites; Vachiralongkorn Dam-1 (T1-1) in Ban Pong Chang and Vachiralongkorn Dam-2 (T1-2) in Ban Pang Pueng. Please refer to section 5.3.1 for the general properties of all monitoring sites.

5.3.2.2 Spatial patterns in inland water chemistry

The chemistry of inland waters in East Asia is rapidly changing resulting primarily from anthropogenic-induced major changes in atmospheric deposition (Obolkin et al., 2016; Mgelwa et al., 2020; Gao et al., 2020; Sase et al., 2021), thus necessitating continuous monitoring of these ecosystems. Here, the mean pH value, SO_4^{2-}, NO_3^-, Ca^{2+} and Mg^{2+} concentrations in inland waters over the last ten years (2010-2019) were calculated and their variability across EANET sites were showed (Figure 5.3.3). The low pH values were observed at Ambulalakao Lake (5.77), Sras Srang Lake (5.97) as well as Jinyunshan Lake (6.04), and the high at Tembaling River (7.99), Pandin Lake (7.82) and Vachiralongkorn Dam-2 (7.72), with 7.04 as the mean pH value across all inland sites.

On average, SO_4^{2-} concentrations varied greatly, from 0.08 to 30.71 mg L^{-1} and NO_3^- concentrations from 0.08 to 10.35 mg L^{-1}. The high SO_4^{2-} and NO_3^- concentrations were both found in Jinyunshan Lake, whereas the low concentrations of these water chemistry parameters were observed in Sras Srang Lake and Gunung Lake, respectively. Hoa Binh Reservoir had the highest mean concentrations of Ca^{2+} (22.00 mg L^{-1}), followed by Tembaling River (19.37 mg L^{-1}) and Vachiralongkorn Dam-2 (16.76 mg L^{-1}). Mg^{2+} concentrations in inland waters also varied greatly from 0.14 to 10.34 mg L^{-1}. Across all sites, the dominant anion was SO_4^{2-}, while the dominant cation was Ca^{2+}. The sites with the highest cation concentrations were generally characterized by higher pH values (Figure 5.3.3).

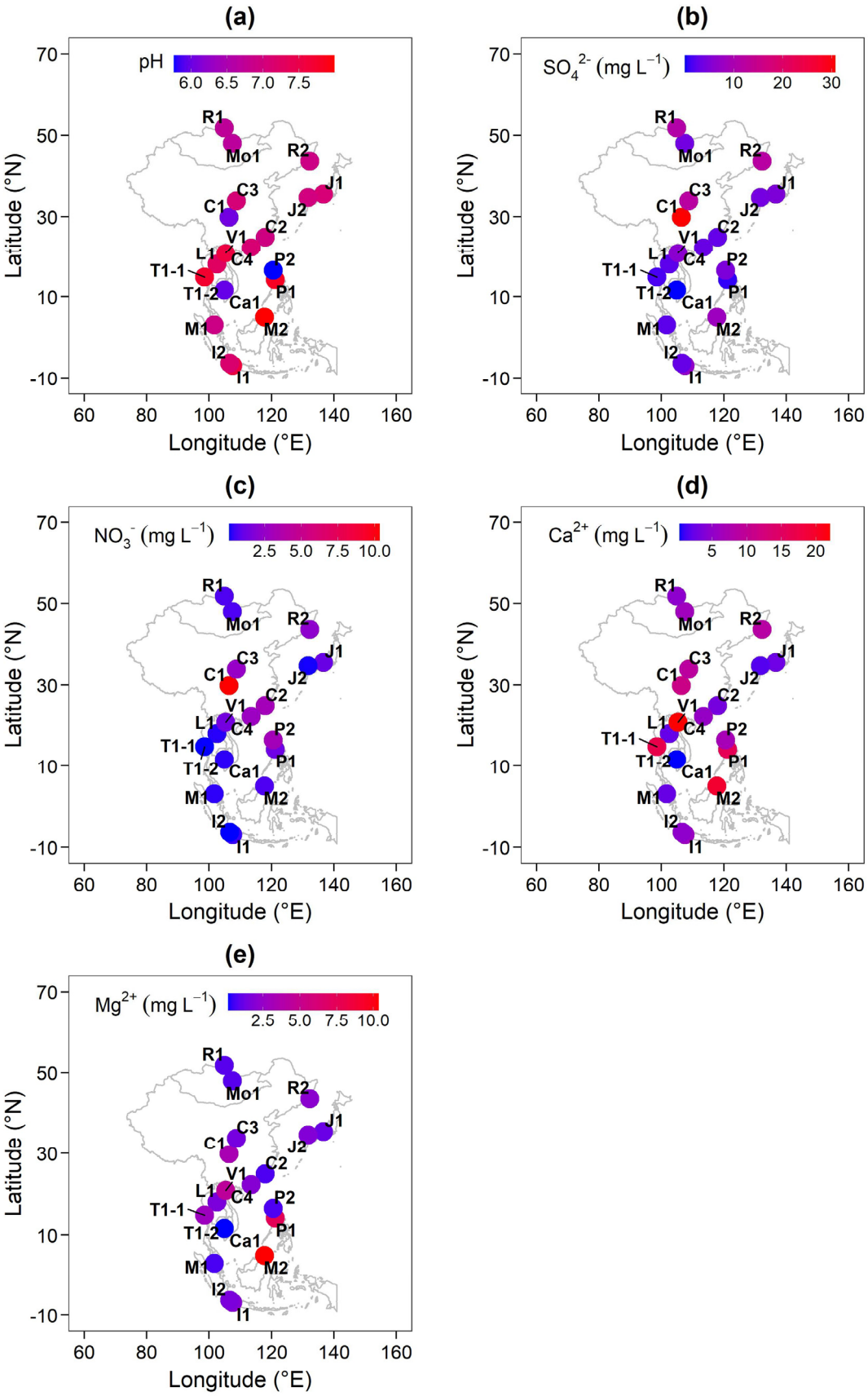

Figure 5.3.3. Spatial variability of pH values and concentrations of SO_4^{2-}, NO_3^-, Ca^{2+} and Mg^{2+} at 20 EANET inland sites. Note: values are the means from 2010 to 2019.

5.3.2.3 Seasonal patterns in inland water chemistry

Large seasonality of inland water chemistry was noted at some sites. For instance, distinct seasonal patterns in pH values and the concentrations of anions and cations are evident in the data collected from Jinyunshan and Ijira Lakes (Figure 5.3.4). For Jinyunshan Lake, pH values were relatively lower between spring and summer compared to autumn and winter. Concentrations of Ca^{2+}, SO_4^{2-} and NO_3^- revealed similar seasonal patterns, which were opposite to that of pH values. However, the seasonal variability was more prominent for NO_3^- than SO_4^{2-} and Ca^{2+} concentrations. For Ijira Lake, higher pH values were observed between May and September and lower values both at the end and the beginning of the year. This trend was the opposite of those of SO_4^{2-} and Ca^{2+} concentrations (Figure 5.3.4). Moreover, the concentrations of Mg^{2+} in the two aforementioned lakes and NO_3^- in Ijira Lake only showed negligible responses to seasonal changes. For Patenggang Lake, only Ca^{2+} responded clearly to seasonality, with its seasonal pattern similar to that of pH in Ijira Lake.

5.3.2.4 Long-term patterns in inland water chemistry and their relationships with atmospheric deposition

Jinyunshan Lake, Xiaoping Dam, Jiwozi River and Zhuxiandong Stream (China) showed overall decreasing trends in pH values and increasing trends in the concentrations of anions (especially SO_4^{2-}) from the beginning of the monitoring period to either the end of the first ten years or the beginning of the last ten years of the monitoring period, where overall increasing trends in pH values and decreasing trends in the concentrations of anions occurred (Figure 5.3.5). The discovered patterns of water chemistry across the four inland sites in China, especially those of pH values, suggest that these sites are currently recovering from their acidified states.

Using Jinyunshan Lake as an example, piecewise linear regression model in the segmented R package (Muggeo, 2008; R Development Core Team, 2020) indicated the occurrence of inflection points (breakpoints) at 2011, 2011, 2008, 2011 and 2010 for pH, SO_4^{2-}, NO_3^-, Ca^{2+} and Mg^{2+}, respectively. Before these points, the trends were decreasing for pH while increasing for anions and cations, and after these points, the trends were increasing for pH but generally decreasing for anions and cations (Figure 5.3.6).

Acid deposition, which has been associated with several detrimental environmental effects including ecosystem acidification and eutrophication (Bouwman et al., 2002), has become an issue of great concern in Asia, particularly the rapidly developing East Asia (Duan et al., 2016). Precipitation chemistry was therefore assessed at Jinyunshan, which is a deposition monitoring site nearest to Jinyunshan Lake, to understand the influence of atmospheric deposition on the observed patterns of water chemistry in this lake. Atmospheric H^+ deposition at Jinyunshan site was found to follow trends different from those of pH values in Jinyunshan Lake, with the year 2012 as the breakpoint between increasing and decreasing trends (Figure 5.3.6). The values of SO_4^{2-}, NO_3^-, Ca^{2+} and Mg^{2+} at the aforementioned lake and its nearest deposition site showed similar patterns, but with different locations of their breakpoints.

Ijira Lake in Japan has been generally experiencing increasing trend in pH values and decreasing trends in SO_4^{2-} and NO_3^- concentrations throughout the monitoring period (Figure 5.3.6). Assessment of precipitation chemistry at its nearest deposition site (namely Ijira) revealed decreasing trends in the deposition of H^+, SO_4^{2-} and NO_3^- constituents from the early 2000s to the

year 2019. The long-term patterns of water chemistry observed in Ijira Lake indicate continuous recovery of this lake from acidification and that decrease in deposition of acid constituents at Ijira site may have accelerated the recovery process.

Moreover, both a decreasing trend (2000-2008) and an increasing trend (2008-2019) in the values of pH were detected in Patenggang Lake (Indonesia). In addition to the decrease in H^+ deposition throughout the monitoring period at Bandung, which is the nearest deposition site of Patenggang Lake, the ongoing recovery of this lake from its acidified state might also be attributed to the significant increase in Ca^{2+} deposition (Figure 5.3.6).

Furthermore, while SO_4^{2-} and NO_3^- concentrations have been increasing, pH values have been decreasing over the entire monitoring period in Komarovka River (Russia). The increase in deposition of anions compared to cations at its nearest deposition site (such as Primorskaya), as evidenced by the lower ratio of base cation deposition ($Ca^{2+} + Mg^{2+} + K^+$) to strong acid deposition ($SO_4^{2-} + NO_3^- + Cl^-$) at this site, may be responsible for the observed decrease in pH values of the river.

Generally, most of the EANET inland sites are currently experiencing increasing values of pH in their surface waters. However, further reductions in atmospheric acid deposition are necessary to ensure their continued recovery from acidification.

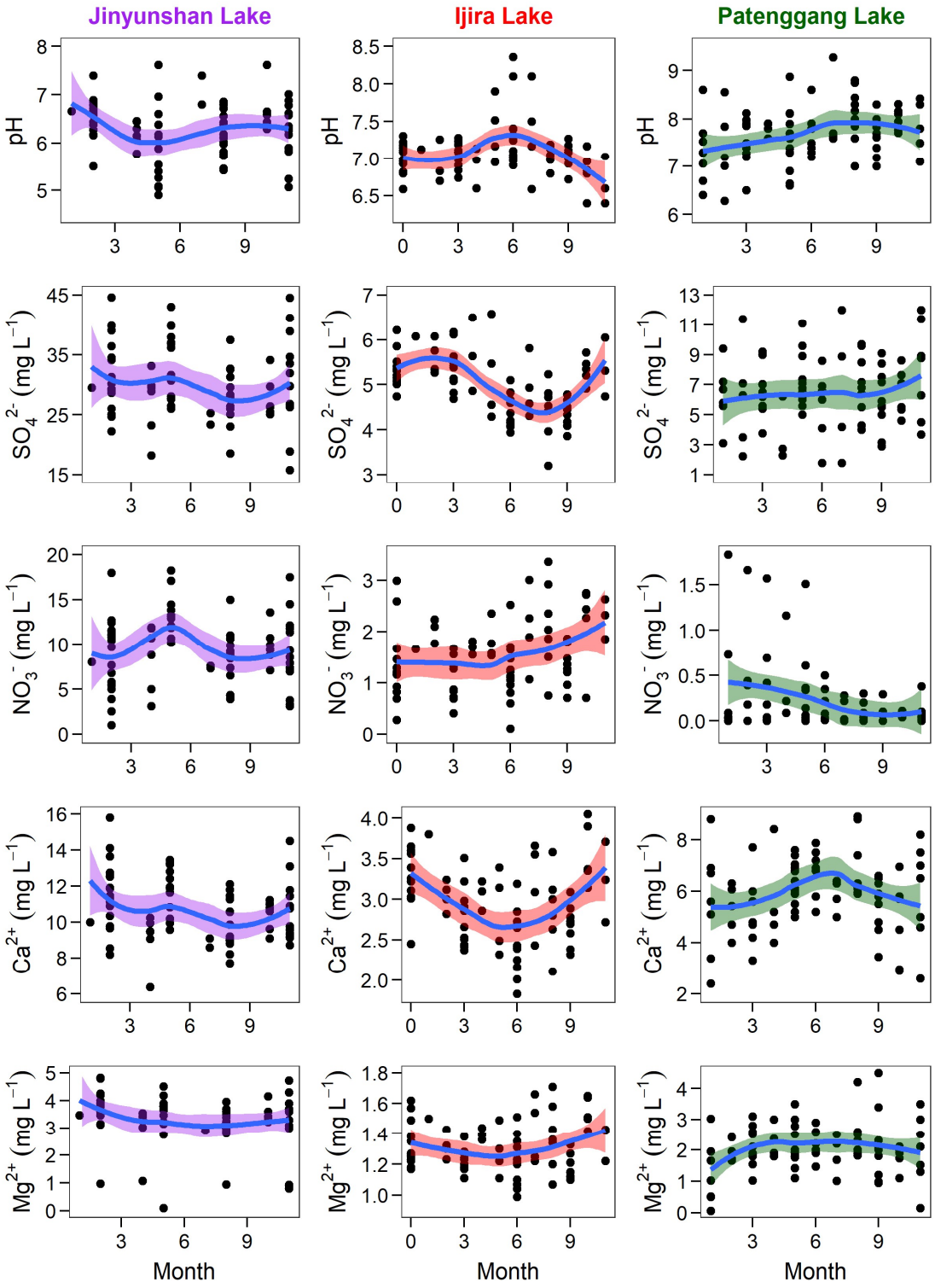

Figure 5.3.4. Seasonal variability of pH, SO_4^{2-}, NO_3^-, Ca^{2+} and Mg^{2+} values in three typical inland sites (Jinyunshan, Ijira and Patenggang Lakes, respectively)

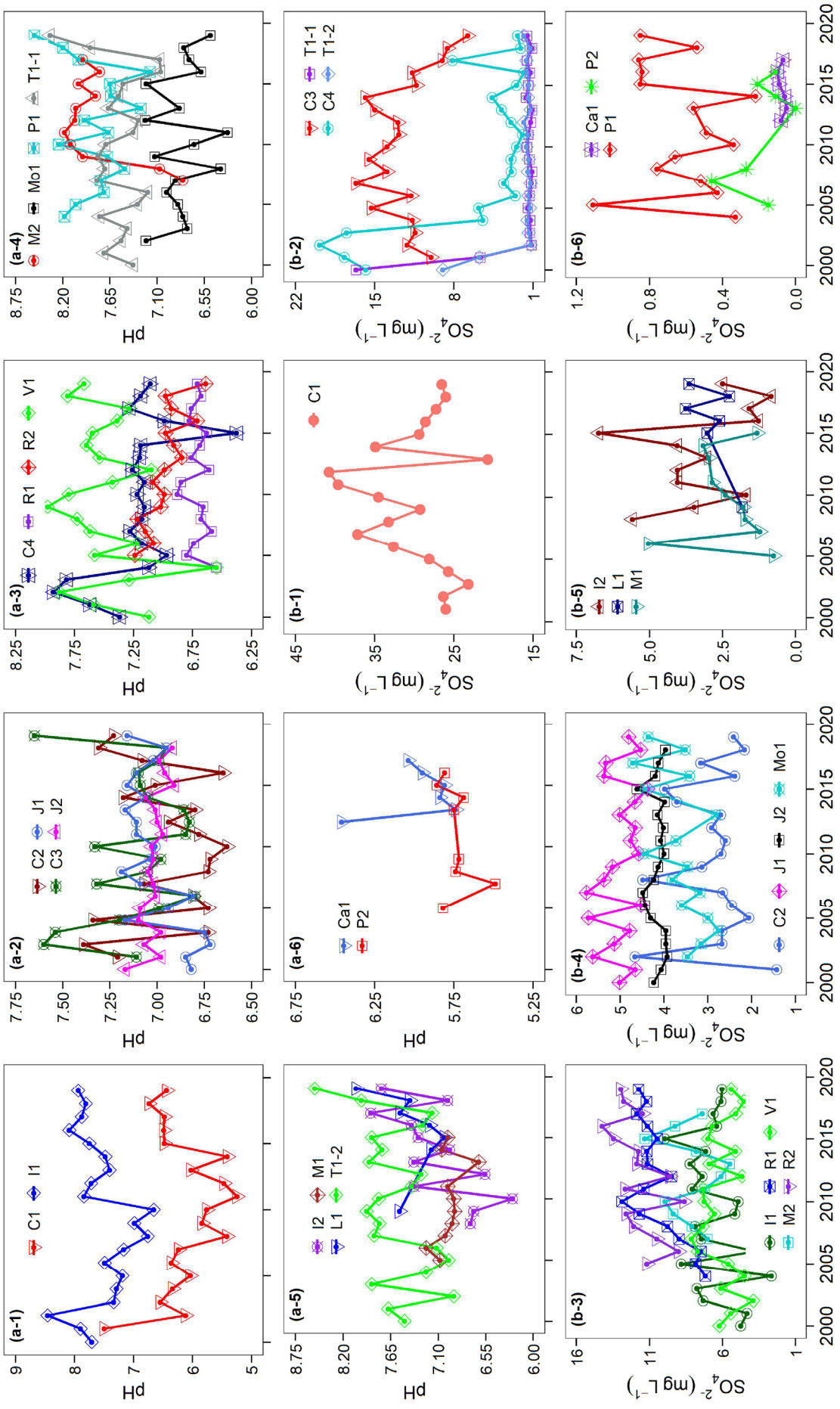
(a-1)
C1
I1
pH
(a-2)
C2
C3
J1
J2
pH
(a-3)
C4
R1
R2
V1
pH
(a-4)
M2
Mo1
P1
T1-1
pH
(a-5)
I2
L1
M1
T1-2
pH
(a-6)
Ca1
P2
pH
(b-1)
C1
SO4 2- (mg L-1)
(b-2)
C3
C4
T1-1
T1-2
SO4 2- (mg L-1)
(b-3)
I1
M2
R1
R2
V1
SO4 2- (mg L-1)
(b-4)
C2
J1
J2
Mo1
SO4 2- (mg L-1)
(b-5)
I2
L1
M1
SO4 2- (mg L-1)
(b-6)
Ca1
P1
P2
SO4 2- (mg L-1)
2000
2005
2010
2015
2020

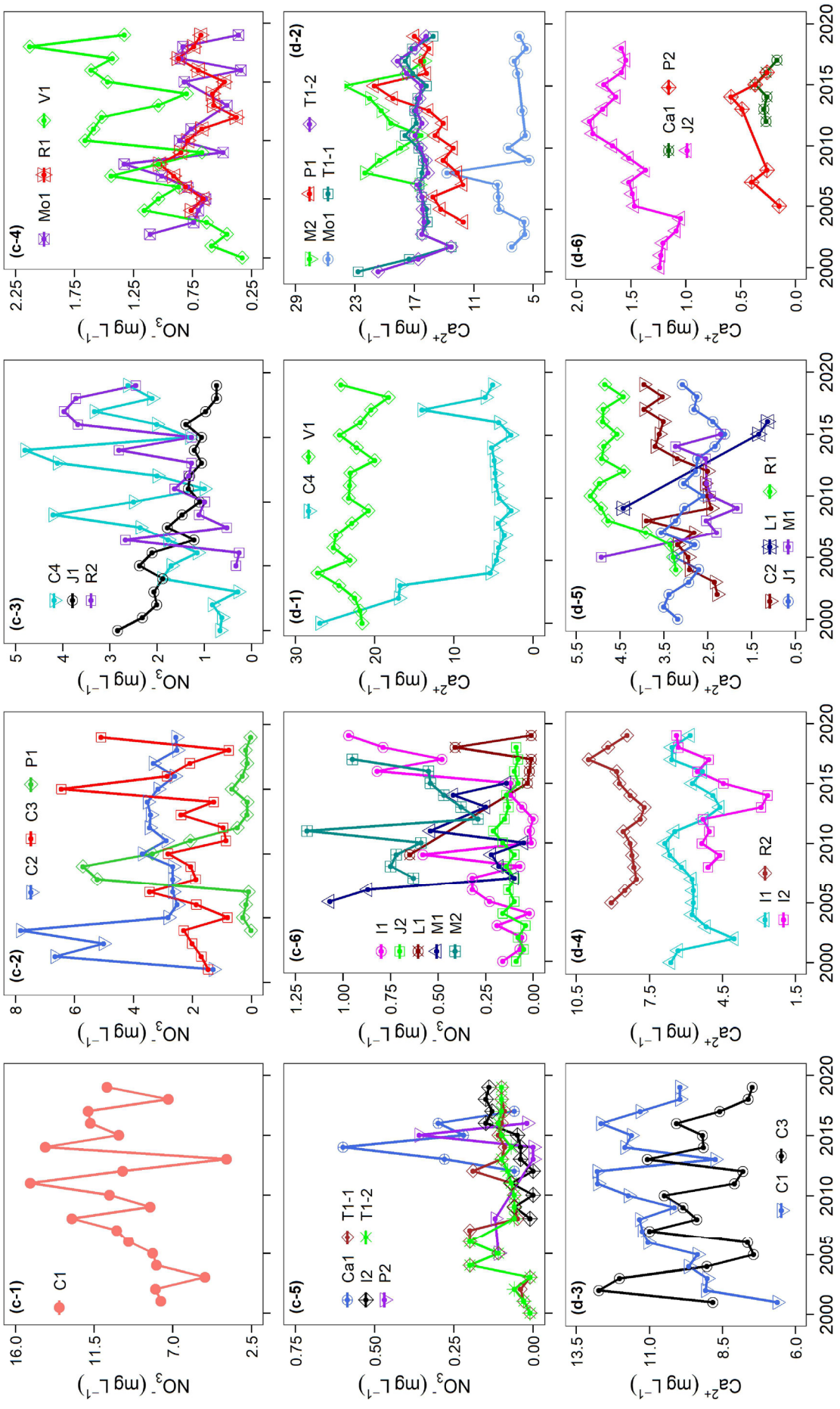
(c-1)
C1
(c-2)
C2 C3 P1
(c-3)
C4 J1 R2
(c-4)
Mo1 R1 V1
(c-5)
Ca1 I2 P2 T1-1 T1-2
(c-6)
I1 J2 L1 M1 M2
(d-1)
C4 V1
(d-2)
M2 Mo1 P1 T1-1 T1-2
(d-3)
C1 C3
(d-4)
I1 I2 R2
(d-5)
C2 J1 L1 M1 R1
(d-6)
Ca1 J2 P2
NO3- (mg L-1)
Ca2+ (mg L-1)
2000 2005 2010 2015 2020

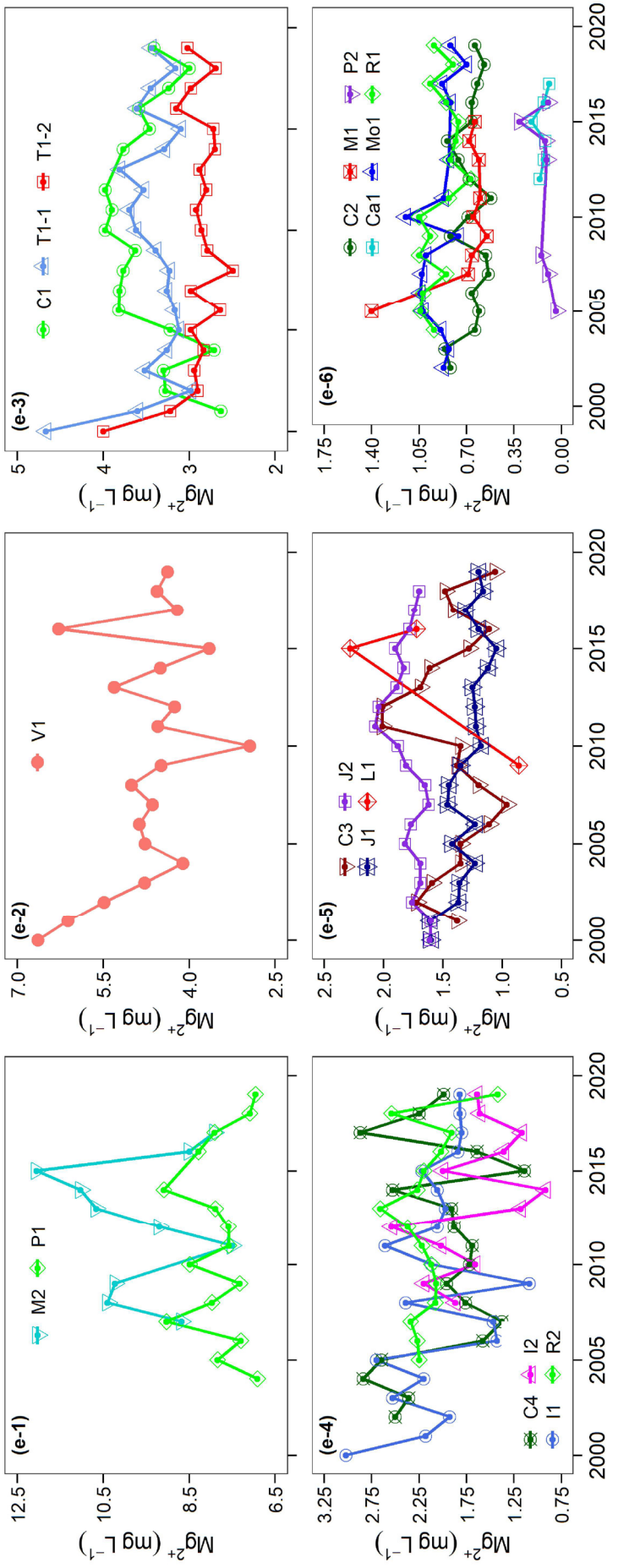

Figure 5.3.5. Long-term trends in pH values and concentrations of anions and cations in surface waters across the EANET inland sites from 2000 to 2019.

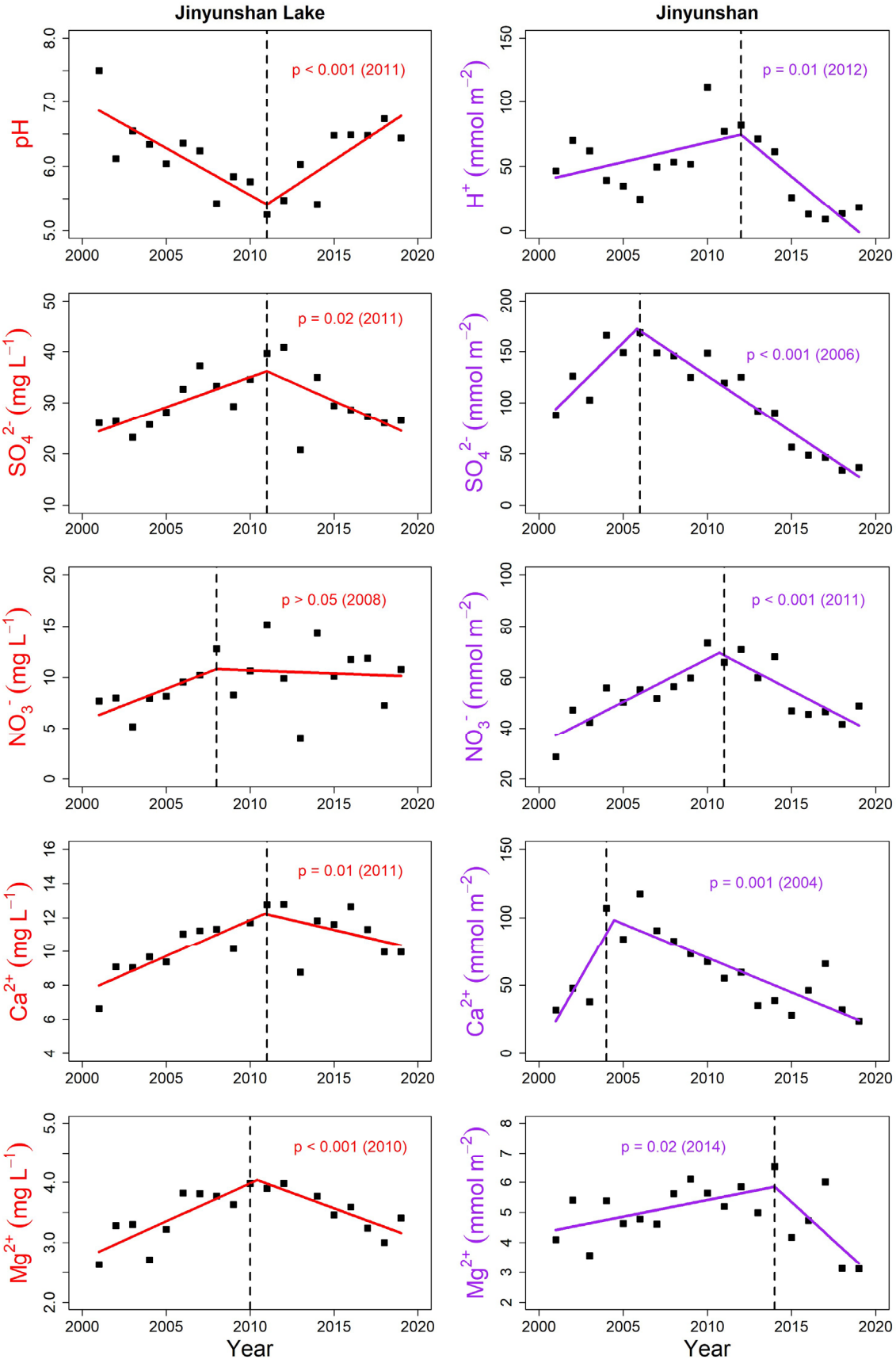
Jinyunshan Lake
Jinyunshan
pH
p < 0.001 (2011)
H+ (mmol m−2)
p = 0.01 (2012)
SO4 2- (mg L−1)
p = 0.02 (2011)
SO4 2- (mmol m−2)
p < 0.001 (2006)
NO3- (mg L−1)
p > 0.05 (2008)
NO3- (mmol m−2)
p < 0.001 (2011)
Ca2+ (mg L−1)
p = 0.01 (2011)
Ca2+ (mmol m−2)
p = 0.001 (2004)
Mg2+ (mg L−1)
p < 0.001 (2010)
Mg2+ (mmol m−2)
p = 0.02 (2014)
Year
Year

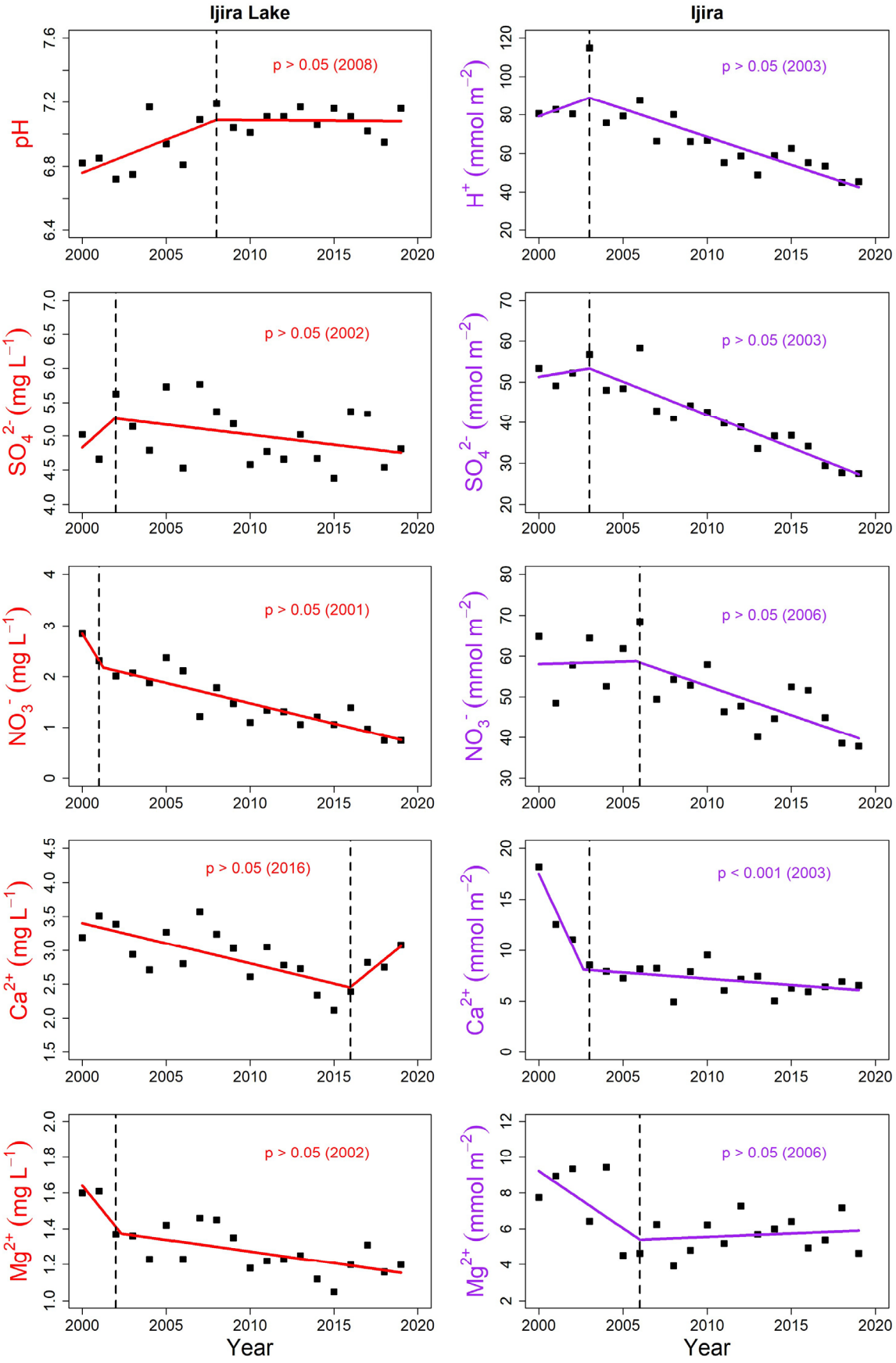
Ijira Lake
Ijira
pH
p > 0.05 (2008)
H^+ (mmol m^{-2})
p > 0.05 (2003)
SO_4^{2-} (mg L^{-1})
p > 0.05 (2002)
SO_4^{2-} (mmol m^{-2})
p > 0.05 (2003)
NO_3^- (mg L^{-1})
p > 0.05 (2001)
NO_3^- (mmol m^{-2})
p > 0.05 (2006)
Ca^{2+} (mg L^{-1})
p > 0.05 (2016)
Ca^{2+} (mmol m^{-2})
p < 0.001 (2003)
Mg^{2+} (mg L^{-1})
p > 0.05 (2002)
Mg^{2+} (mmol m^{-2})
p > 0.05 (2006)
Year
Year

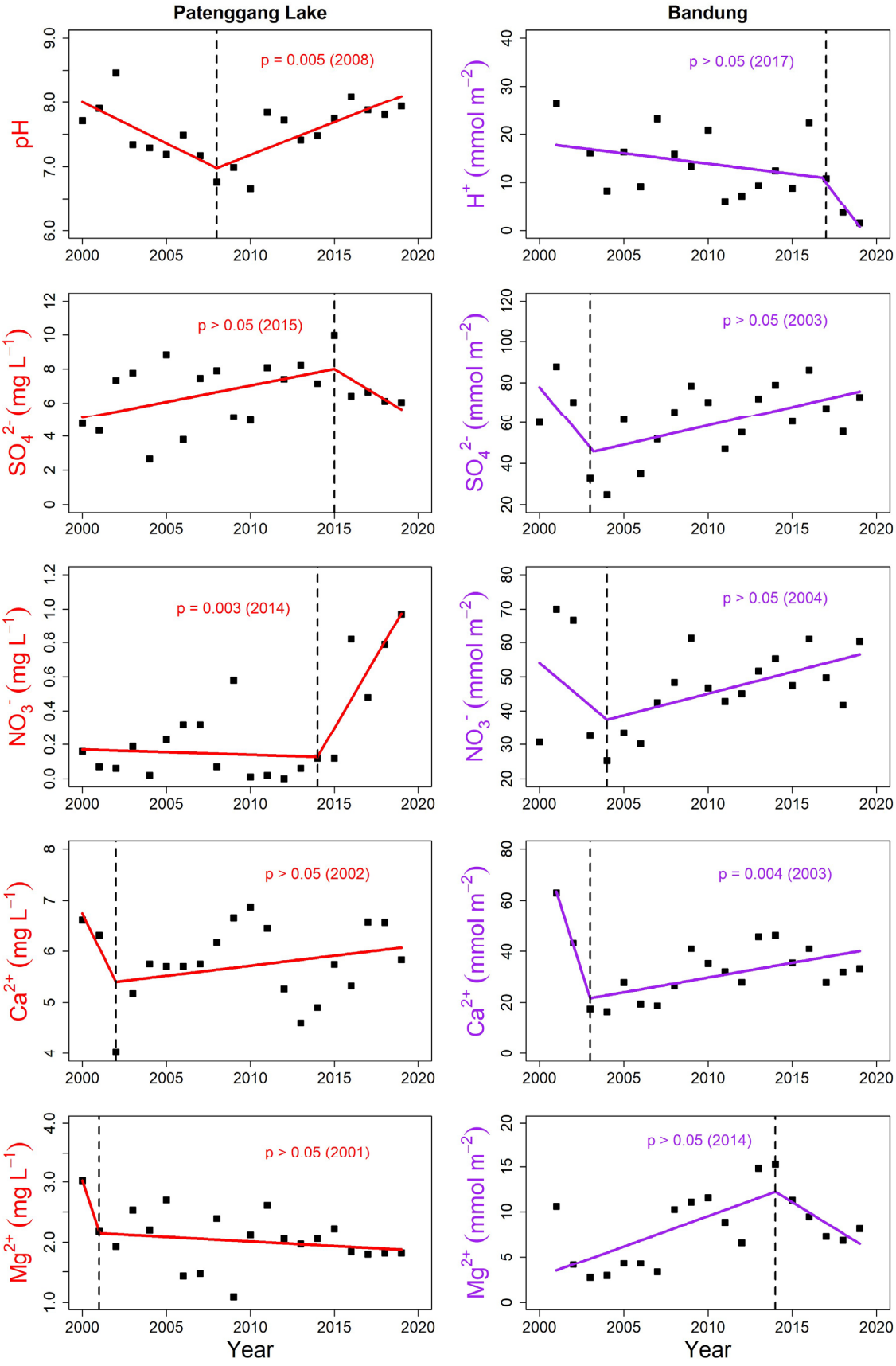

Figure 5.3.6. Long-term patterns of five selected chemical variables at three typical inland sites (Jinyunshan, Ijira and Patenggang Lakes) and their nearest deposition sites. The vertical dashed lines indicate the breakpoint locations as estimated by piecewise linear regression model.

5.3.3 Summary

The EANET has been monitoring inland water chemistry in 20 sites from 11 countries. Chemical properties, such as balance of ions, concentration levels, and seasonal changes, varied among the monitoring sites. Depending on the chemical properties, response of inland waters to atmospheric deposition was also different. However, several monitoring sites, such as Jinyunshan Lake, Xiaoping Dam, Jiwozi River and Zhuxiandong Stream in China, Patenggang Lake in Indonesia, and Ijira Lake in Japan, showed symptoms suggesting recovery from acidification. In some of sites, changing patterns of atmospheric deposition at the nearest monitoring sites were associated with those of ion concentrations in lakes/streams, respectively. It is suggested that further reduction in atmospheric acid deposition and its monitoring are necessary to ensure their continued recovery from acidification.

5.4 Catchment analysis

An integrated approach monitoring biogeochemical processes from atmospheric deposition through stream water chemistry is a valid one to evaluate effects of atmospheric deposition on terrestrial ecosystems, quantitatively and qualitatively. The catchment analysis is a prime example of the integrated approach. According to the recommendations described in the strategy papers for ecological monitoring (e.g., EANET 2020), the Network Center for the EANET (NC) has been conducting research activities on catchment analysis since 2002 at several reference forest sites, including the Kajikawa site (KJK) and the Lake Ijira catchment site (IJR) in Japan, in cooperation with scientists from the EANET countries (e.g., Yamashita et al. 2014; Sase et al. 2017, 2019, 2021), which contributed to development of the *Guideline for Catchment-scale Monitoring in East Asia* (EANET 2010). Currently, based on the guideline above, the regular catchment-scale monitoring is conducted at two sites, IJR since 2007 and the La Mesa Watershed (LMW) since 2019. Moreover, as the EANET Fellowship study (Zhigacheva et al. 2019), the data analysis on a catchment scale has been implemented for the Komarovka River catchment (KMR), where monitoring on atmospheric deposition, soil, vegetation, and inland water has been conducted as the EANET activities. In this section, results from the catchment analysis in these sites (Figure 5.4.1) were summarized.

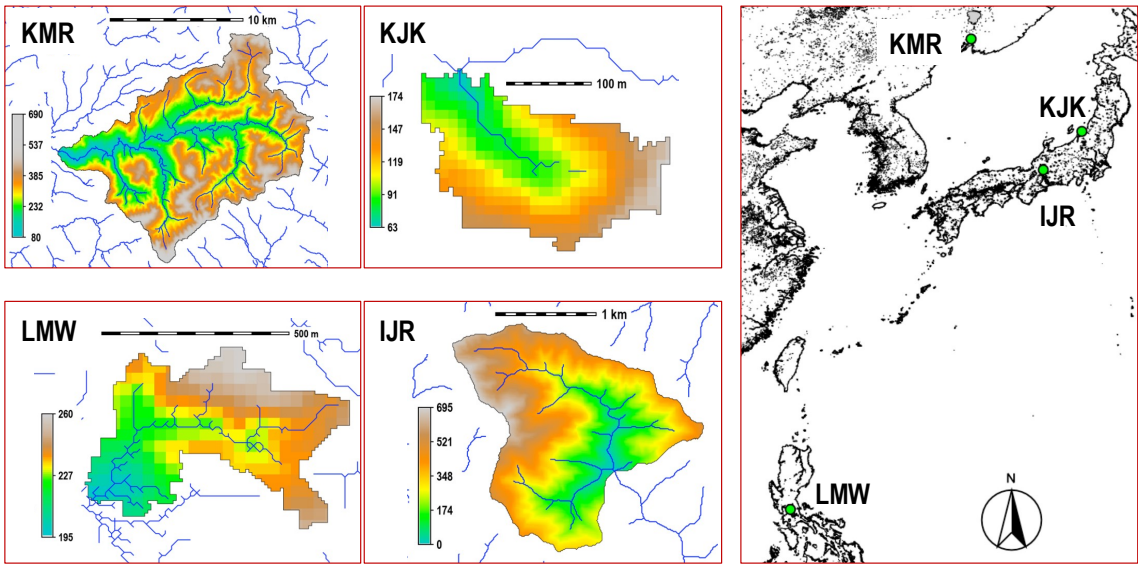

Figure 5.4.1. Site location and images of the respective catchment areas. IJR, Lake Ijira catchment; KJK, Kajikawa catchment, KMR, Komarovka River catchment; LMW, La Mesa Watershed Tower 1 catchment.

5.4.1 Ijira and Kajikawa

Field observations on a catchment scale at IJR and KJK have been implemented as the EANET activities since 2007 and 2002, respectively. In the case of IJR, the data on wet deposition and stream water chemistry since 2000 are also available, while the stream water data since 2000 are collected quarterly and its time resolution is too low to calculate discharges of water and materials from the stream precisely. For these two catchment sites, many of scientific papers have already been published based on the data from the national and EANET monitoring and/or relevant research activities. Based on the publications and the latest datasets, this section discusses the trends since 2007 and 2002 mainly for IJR and KJK, respectively.

1) Possible recovery from acidification and nitrogen saturation

Based on the long-term national monitoring data since 1988, it was reported that the stream water at IJR was acidified with increase of NO_3^- concentration in the mid-1990s, suggesting nitrogen (N)

saturation of the ecosystems. The highest levels of acid deposition among Japan contributed to the phenomena at IJR, although climatic anomalies, such as cool summer in 1993 and drought summer in 1994, triggered alteration of biogeochemical processes (Nakahara et al. 2010). However, recently Sase et al. (2019) pointed out that the stream water has been recovering from acidification and N saturation showing recovery of the pH to its original level (around 7.0) and a decline in NO_3^- concentration in the early 2000s. The recent trends of the stream water since 2007 are shown in Figure 5.4.2; pH and alkalinity did not show clear monotonic trends over the past decade; SO_4^{2-} concentration declined until 2011/2012 and then became stable, while NO_3^- concentrations have been declining continuously. Low values in pH and alkalinity observed in 2010/2011 and 2018 were accompanied with high concentrations of SO_4^{2-} and/or NO_3^-. In particular, pH and alkalinity showed clear increasing trends for several years after the low values in 2010/2011, while NO_3^- concentration was obviously declining. It is suggested that pH and alkalinity in the stream water at IJR were mainly regulated by NO_3^- leaching.

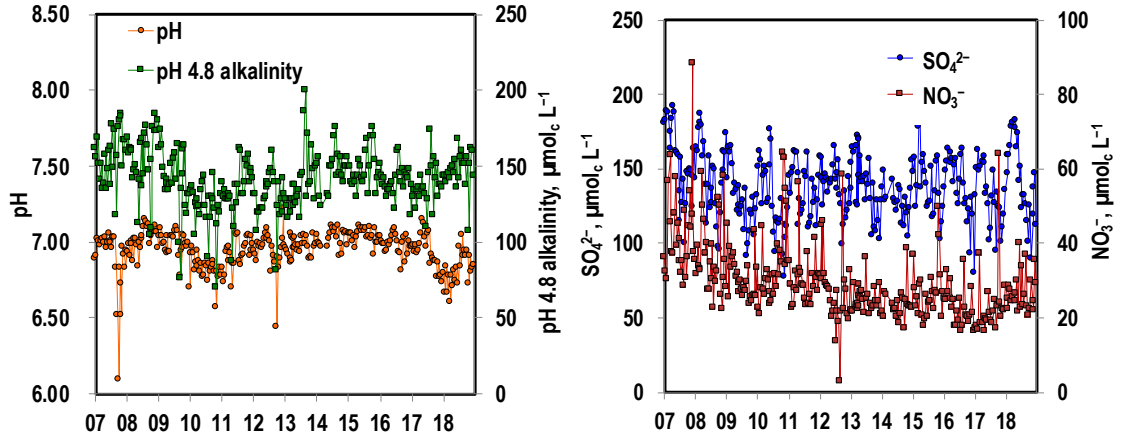

Figure 5.4.2. The pH and pH 4.8 alkalinity (left) and SO_4^{2-} and NO_3^- concentrations (right) in the stream water at IJR. The stream water was collected biweekly or twice monthly since November 2007.

Stream water chemistry at KJK did not show clear acidification phenomena during the observation period since 2002. Instead, the stream water showed phenomena thought to be recovery processes from acidification (Sase et al. 2021). The pH and alkalinity increased with decline of SO_4^{2-} concentration, especially after 2006/2007 (Figure 5.4.3). As shown in Figure 5.4.4, nss-S fluxes by RF and TF+SF declined in the same timing. It is suggested that the stream water chemistry at KJK was sensitively responded to changing atmospheric deposition (Sase et al. 2021). However, in the case of KJK, NO_3^- concentration has been increasing continuously after a slight decline until 2004 due to forest management. Reduction of N uptake with maturating of trees may contribute to N leaching in the stream water. In fact, according to the isotopic analysis of ^{17}O excess of NO_3^-, Nakagawa et al. (2018) estimated that the annual export flux of unprocessed atmospheric NO_3^- accounted for 9.4% ± 2.6% of the annual atmospheric NO_3^- deposition flux at KJK, while that at IJR accounted for 6.5% ± 1.8%. It is suggested that certain portions of NO_3^- were unused in the ecosystem and directly leached into the stream water.

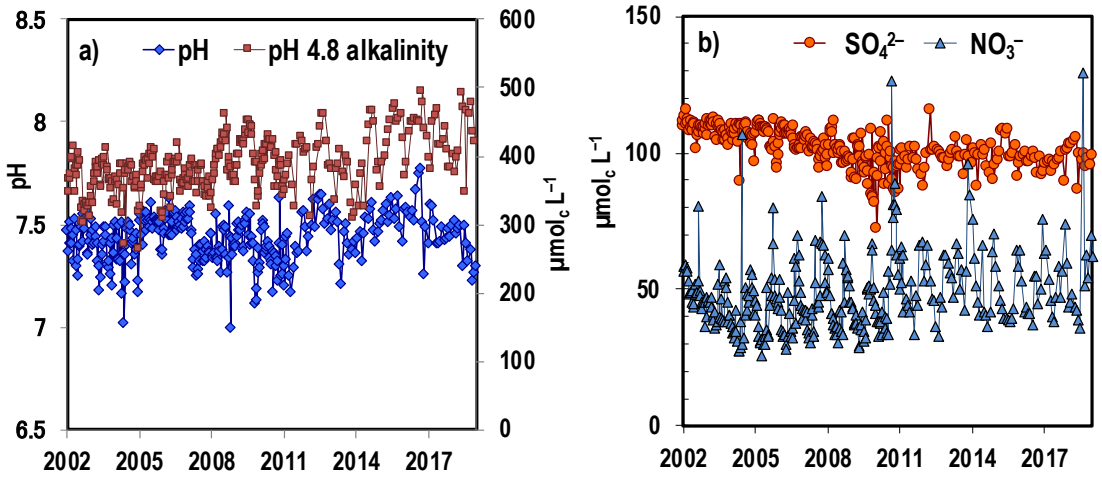

Figure 5.4.3. Long-term changes in (a) pH and alkalinity and (b) concentrations of SO_4^{2-} and NO_3^- in the stream water at KJK (modified after Sase et al. 2021).

2) Changing atmospheric deposition

Fluxes of S and dissolved inorganic N (DIN, as NO_3^- + NH_4^+) by wet deposition have been declining at IJR since 2000 and the declining trends became clearer after the peaks in 2006 (Sase et al. 2019). The trends were similar to those at KJK as shown in Figure 5.4.4 (updated with the latest data after Sase et al. 2021). The peak non-sea salt (nss) S flux by wet deposition was observed in 2006 at IJR, while those by rainfall outside canopy (RF) and throughfall and stemflow (TF+SF) were observed in 2005 and 2006, respectively (Sase et al. 2021). It is suggested that the deposition trends certainly reflected that of the SO_2 emissions in China (Lu et al. 2011).

Rapid decline of SO_4^{2-} concentration in the stream water for a few years from 2007 to 2009/2010 at IJR (see Figure 5.4.2) may also have reflected the S deposition trend. At KJK, the SO_4^{2-} concentration in stream water has been declining, in particular since 2006, with reduction of nss-S flux by TF+SF. It is suggested that SO_4^{2-} concentrations in stream water at both catchments were influenced by S fluxes by atmospheric deposition, even though that at IJR was strongly regulated by geological S as discussed later. In the case of KJK, reduction of SO_4^{2-} concentration seems to be strongly connected to recovery of the stream water from acidification (Sase et al. 2021)

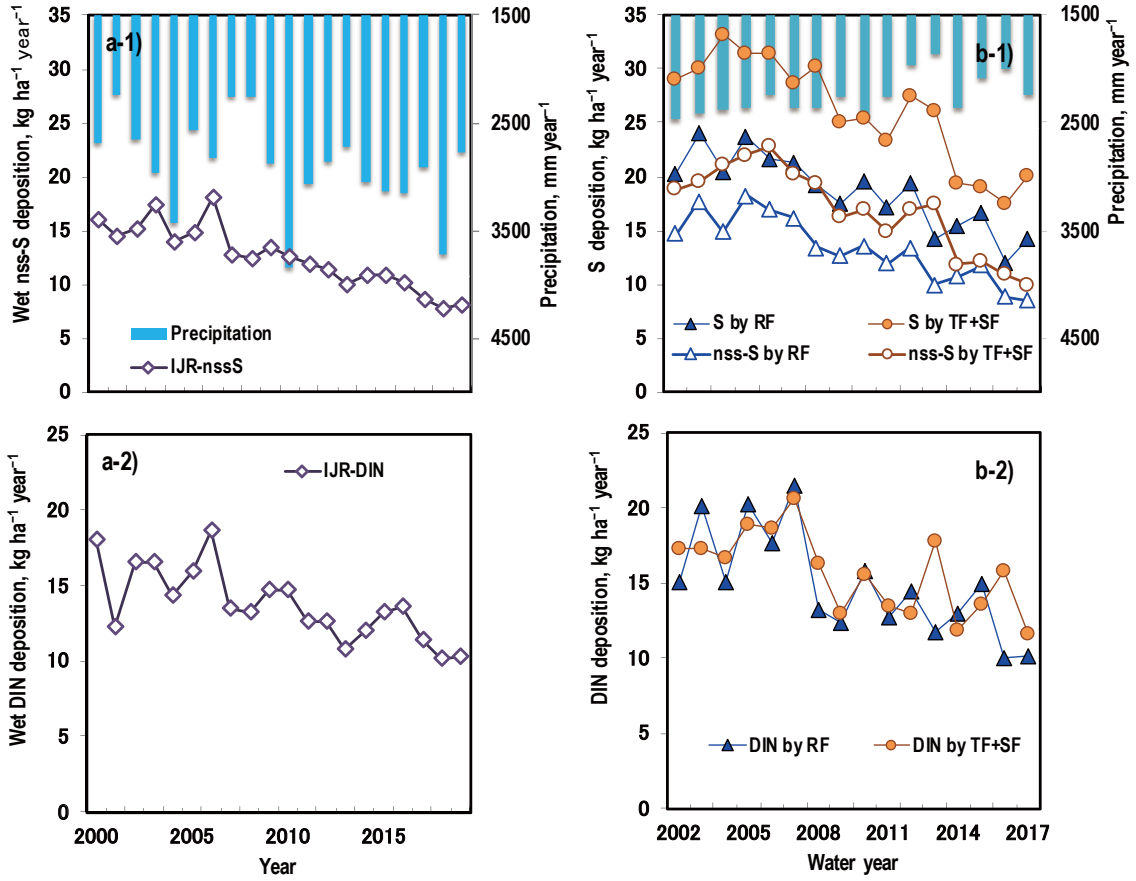

Figure 5.4.4. Annual fluxes of (1) S and/or non-sea salt (nss)-S and (2) DIN at (a) IJR and (b) KJK (updated with the latest data after Sase et al. 2021). Note: DIN, NO_3^- + NH_4^+, RF, rainfall outside canopy, TF+SF, throughfall and stemflow.

DIN flux by wet deposition at IJR showed a small peak in 2009/2010, which may have contributed to high NO_3^- concentrations and temporal acidification in 2010/2011 in the stream water. In fact, NO_X emissions in China had increased until 2012 (Zheng et al. 2018), which partly explained the observed trends. Sudden increase of NO_3^- concentration in 2011 in the stream water at KJK was similar to the phenomenon observed at IJR, although DIN flux by RF (bulk sampling) and TF+SF may have uncertainty. It is suggested that the stream water chemistry at IJR has been recovering from acidification and N saturation due to reduction of fluxes of S and N by atmospheric deposition, possibly reflecting the regional emission trends. However, high concentrations of SO_4^{2-} and NO_3^- with sudden decline of pH were observed in 2018 at IJR and KJK. Recovery processes should carefully be observed taking account of climate change. Moreover, NO_3^- concentration in the stream water has been continuously increasing at KJK, even though DIN flux was declining or not increasing at least. Various factors including forest maturation/management should be taken into account for mechanisms of N leaching. Integrated modeling from emissions to the stream water chemistry may help our understanding for these subjects.

3) Input-output budget

The input-output budgets of S on the catchment scale at IJR and KJK are shown in Figure 5.4.5. In the case of IJR, the S outputs were generally 2 - 3 times larger than the inputs, suggesting additional S sources other than atmospheric deposition, even though the input has been declining smoothly. Based on the S isotopic analysis, Sase et al. (2019) suggested that geological (rock) S largely contributed as a S source of the stream water. Simultaneously, it was suggested that S derived from atmospheric deposition has been accumulated in forest soil. It was also suggested that climatic changes, such as changes in precipitation amount/pattern and increase in temperature,

affect retention – release processes of S (Nakahara et al. 2010; Sase et al. 2021). In the United States, the impact of climatic conditions on S leaching was a major concern (Mitchell and Likens 2011). Recent increase in the net export at IJR should carefully be monitored with climatic conditions, although both input and output may have uncertainty. In the case of KJK, the input and output were relatively well balanced and both gradually declined. It was suggested that atmospheric S is a main source of the stream water S, which was supported also by the S isotopic analysis (Sase et al. 2021). However, because the response of the output to the input was delayed and slightly weaker than the input, the net export has been increased and the output exceeded the input sometimes. The similar phenomena were observed in Europe (Vuorenmaa et al. 2017). The S isotopic analysis suggested that S derived from atmospheric deposition was retained or cycled in the ecosystems and well homogenized before leaching to the stream water (Sase et al. 2021). In this process also, the impact of climatic conditions should carefully be monitored.

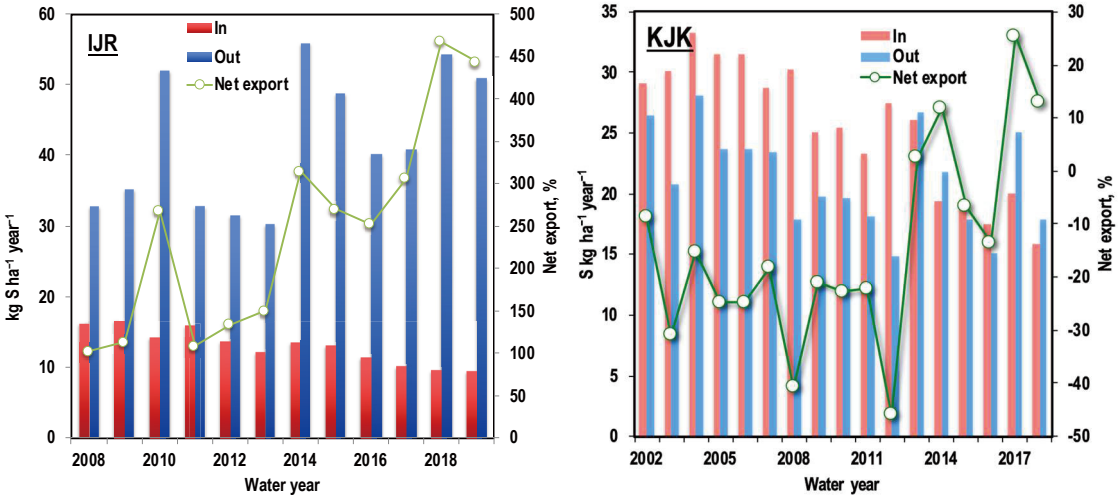

Figure 5.4.5. Input-output budgets of S at IJR (left) and KJK (right). Input of IJR, estimated as the flux by wet deposition and dry deposition, Input of KJK, estimated as the flux by TF+SF. Net export (%) = (output – input) / input × 100. The right figure was updated with the latest data after Sase et al. (2021). Water years were defined as November of one year to October of the following year and June of one year to May of the following year at IJR and KJK, respectively.

4) Differences in N leaching in two catchments

Recovery from N saturation (Sase et al. 2019) and progress of N saturation (Sase et al. 2021) were suggested at IJR and KJK, respectively, while DIN deposition seemed to be declining at both catchments, as previously mentioned. To understand changes in NO_3^- concentrations in stream water and stream water N outputs, their 3-year-moving averages are plotted with those of the atmospheric N input in Figure 5.4.6. The NO_3^- concentration at IJR clearly declined with the atmospheric N input, while those at KJK increased. On the other hand, the stream water N output at IJR did not declined recently and rather slightly increased and those at KJK slightly increased as well. The stream water N outputs were still lower than the 1:1 line of N balance but have been approaching the line (Figure 5.4.6 right). Although the atmospheric N inputs are partly utilized in the ecosystems, large portions of the inputs are leached to the stream waters at IJR and KJK; the latest N leaching ratios to the atmospheric N inputs were 67% and 75% at IJR and KJK, respectively (as the latest 3-year averages).

In the case of IJR, reduction of the atmospheric N deposition contributed to the recovery from N saturation, together with enhanced N uptake due to forest management and minimization of climatic anomalies (Sase et al. 2019). On the other hand, in the case of KJK, maturation of Japanese cedar trees may have reduced tree N uptake (Sase et al. 2021), which suppressed the contribution of N deposition reduction. Chiwa et al. (2019) suggested that Japanese cedar forest could be sensitive to the excess N deposition. The recent high precipitation amounts at IJR and the

continuous decline of precipitation at KJK appeared to have influenced on the stream water N outputs. In the case of IJR, the recent wetter conditions accelerated N leaching. A monsoon climate with warm and wet summer appeared to have contributed to N leaching from forest ecosystems (Fang et al. 2011). Thus, N leaching should carefully be monitored taking account of meteorological variability and forest conditions, even though the atmospheric N inputs have been declining. The current atmospheric N inputs are still enough large, over 10 kg ha^{-1} $year^{-1}$, which was suggested as the threshold value of N leaching (Wright et al. 1995).

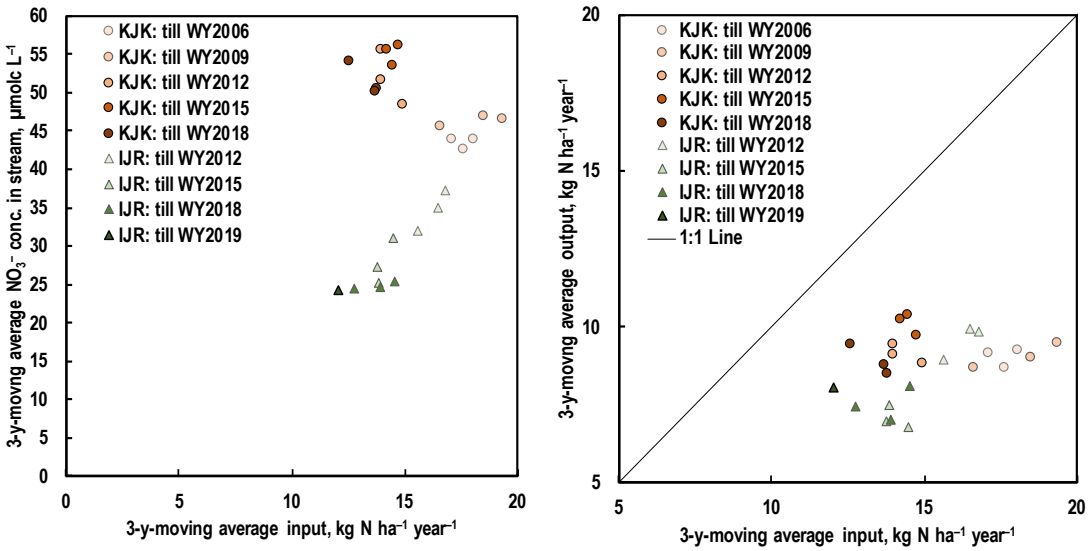

Figure 5.4.6. Changes in 3-year-moving averages of NO_3^- concentrations in stream water (left) and stream water N outputs with those of atmospheric N inputs at IJR and KJK. The data since 2007 to 2019 and the data since 2002 to 2019 were applied to calculate 3-year-moving averages at IJR and KJK, respectively. Water years (WYs) were defined as November of one year to October of the following year and June of one year to May of the following year at IJR and KJK, respectively. Water years were referred to by the following year and starting year for IJR and KJK, respectively; e.g., WY2019 at IJR, from November 2018 to October 2019; WY2018 at KJK, from June 2018 to May 2019. The N inputs were based on the total deposition by wet and dry deposition and deposition by TF+SF at IJR and KJK, respectively.

5) Seasonal variations and trends of dissolved elements on rainfall at KJK

Metal elements released into the atmosphere by human activities such as fossil fuel combustions flow into forest ecosystems by wet deposition (precipitation) and dry deposition (particulate matters) (Montoya-Mayor et al. 2013). Dissolved trace elements (TEs) are easy to move and easily incorporated into animals and plants. Some elements are necessary for lives, but excessive intake is harmful. Atmospheric wet deposition has been generally known as one of major pathway for air pollutants. Thus, understanding the concentration of elements contained in precipitation is very important in assessing the impact on forestry ecosystems (Zhu et al. 2016). Since KJK has been affected by transboundary air pollution originating from the Asian continent (Sase et al. 2008, Ohizumi et al. 2016), concentrations of TEs dissolved in precipitation were determined in order to evaluate the effects of transboundary air pollution in forest ecosystems more comprehensively (Morohashi et al. in preparation).

Rainfall samples (RF), which were collected monthly by a bulk sampler installed outside the forest canopy, were used for analysis of TEs for the period from January 2014 and December 2018. Trace elements ware directly determined by using the inductively coupled plasma mass spectrometer (ICP MS).

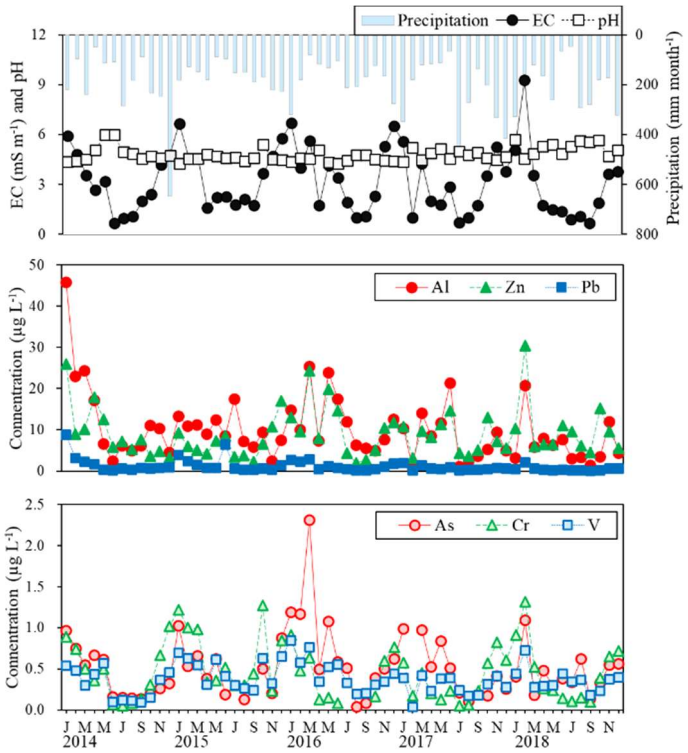

Figure 5.4.7. Monthly variations of EC, pH, Al, and TEs in RF at KJK.

Monthly precipitation, EC, pH, and concentrations of TEs in RF are shown in Figure 5.4.7. Precipitation amounts were higher in summer and winter than in other seasons. EC had a higher seasonal variation in winter than in summer, on the other hand, pH did not reveal a seasonal variation clearly. As previously reported, concentrations and fluxes of inorganic ions in RF showed clear seasonal fluctuations, high in winter and low in summer (Kamisako et al. 2008, Sase et al. 2008, 2021). Some TEs also showed similar seasonal variations to those of inorganic ions during this period. In particular, non-sea-salt sulfate ion (nss-SO_4^{2-}) was highly correlated with all TEs (Table 5.4.1).

Table 5.4.1 Relationship between the concentrations of nss-SO_4^{2-} and trace elements in RF at KJK

	nss-SO_4^{2-}	V	Cr	Zn	As	Sr	Pb
nss-SO_4^{2-}							
V	0.80**						
Cr	0.56**	0.69**					
Zn	0.71**	0.59**	0.35				
As	0.88**	0.78**	0.42*	0.70**			
Sr	0.76**	0.75**	0.84**	0.63**	0.71**		
Pb	0.61**	0.48*	0.47*	0.49**	0.46*	0.41	

* $P < 0.001$, ** $P < 0.0001$

To identify the potential sources of TEs in RF, the enrichment factors (EFs) were calculated by comparing the ratios of elements measured in rainfall versus the ratios of corresponding elements present in the earth crust. In this study, we chose Al as the reference element for the crustal source, and focused on V, Cr, Zn, As, Sr, and Pb. The EFs for these elements were found to be above 10, suggesting that they were derived from anthropogenic sources, such as fossil fuel combustion (Xing et al. 2017). The EFs of many elements showed an upward trend with seasonality, while that of Pb showed a downward trend (Figure 5.4.8). The S isotope analysis has revealed that S derived from coal combustion is being transported from the Asian continent to this area in winter (Ohizumi et al. 2016). The TEs, of which concentrations correlated with SO_4^{2-} concentrations, may also be transported across borders. On the other hand, decrease in EF of Pb may reflect changes in Pb

emissions at domestic and abroad. Year-to-year meteorological variability influences precipitation amounts and precipitation patterns, which may affect deposition processes of TEs and potential effects of TEs on living species.

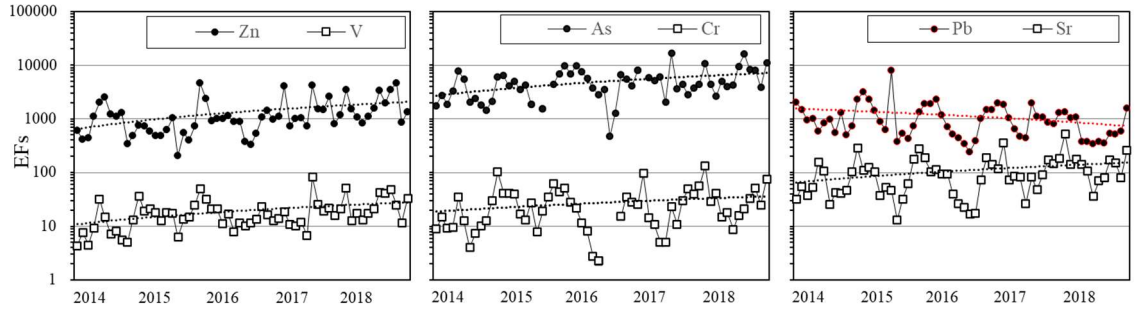

Figure 5.4.8. Trends of EFs in RF at KJK.

5.4.2 Komarovka River

At KMR (EANET site Primorskaya), the rainwater pH showed an increasing trend (Figure 5.4.9 left; $p < 0.01$). However, the stream water pH showed a declining trend (although the overall pH level was higher in stream water than in rainwater). Concentrations of SO_4^{2-} and NO_3^- in stream water have been increasing during the observation period ($p < 0.1$ and <0.001, respectively). The amplitude of NO_3^- concentrations in stream water has been increasing since around 2013. The SO_4^{2-} flux by wet deposition showed an inflection point in 2011, from a declining trend to an increasing trend. The NO_3^- flux by wet deposition showed no clear trend but relatively high deposition amounts were observed in the last several years. Relationship between the recent changing deposition and stream water chemistry should be assessed carefully.

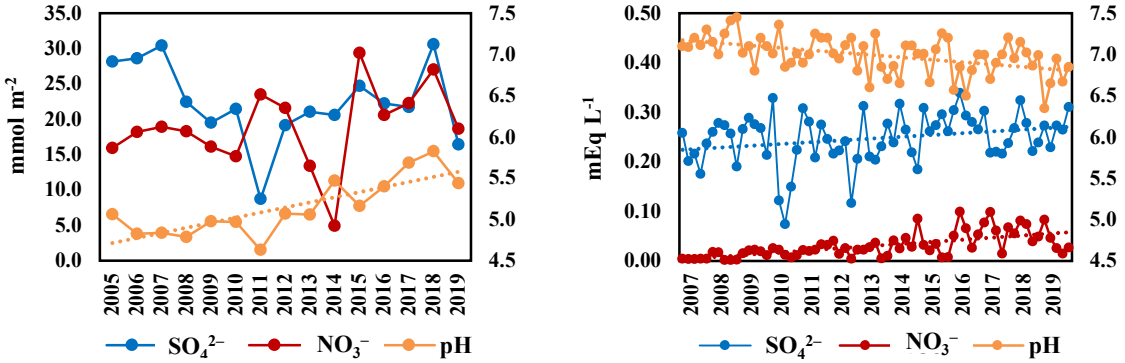

Figure 5.4.9. pH and annual fluxes of SO_4^{2-} and NO_3^- by wet deposition (left) and pH and concentrations of SO_4^{2-} and NO_3^- in stream water (right).

Balances between atmospheric inputs and outputs via stream water were estimated in Figure 5.4.10. The atmospheric inputs were estimated as sum of fluxes by wet deposition and dry deposition. As the outputs, material fluxes via stream water discharge were only considered here. The mean SO_4^{2-} output was more than two times higher than the input. It is suggested that S stored in soil within the catchment area has been mobilized. We may consider two possible sources; the first one is S accumulated in the past when the S deposition was higher than the present; the second one is geological S that had been distributed originally in the area. To identify sulfur sources for the stream water, S isotopic analysis may be utilized. For N compounds, the outputs for most years were lower than the inputs but relatively a high portion of N was discharged.

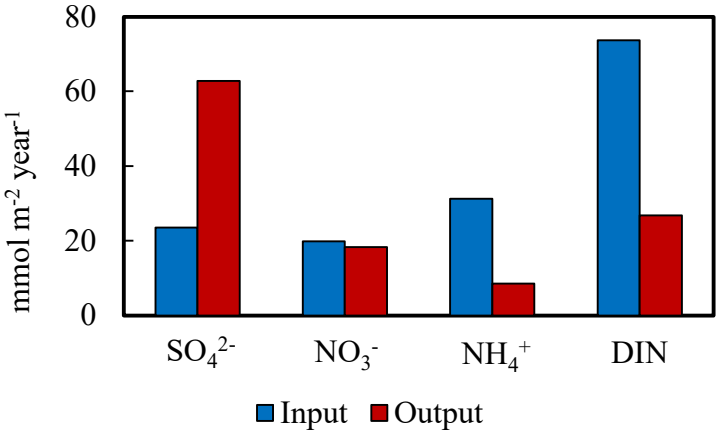

Figure 5.4.10. Input-Output balance (mean 2007-2017).

5.4.3 La Mesa Watershed

Characteristics of the Catchment

Another site has been newly added to the catchment monitoring sites being undertaken by EANET. This is the La Mesa Watershed Reservation (LMWR) located at 14˚75' N and 121˚10' E in Novaliches, Quezon City, Philippines (Andres *et al*., 2015). The watershed is considered to be the "lungs" of Metropolitan Manila being the only chunk of land with an intact forest in the area. To the northwestern side of the watershed lies Caloocan City, on the southeastern and southwestern side is the rest of Quezon City, while on the northeastern and northwestern sides are the Municipalities of San Mateo and Rodriguez, Province of Rizal. With a total area of 2,659.59 ha, the watershed has been proclaimed by virtue of Presidential Proclamation No. 1335 on 25 July 2007. LMWR is still considered as Unclassified Land on Public Domain, otherwise referred to as Public Forest per Land Classification Map No. 639 issued on 11 March 1927. It is a titled property under the Metropolitan Waterworks and Sewerage System (MWSS).

Following the Corona's Classification Scheme, the LMWR falls under Type 1 climate with two pronounced seasons, dry from November to April and wet from May to October. Rainfall for the most part is derived from the warm and moist southwest monsoon, as well as the convergent storm cells associated with the intertropical intensification and strong winds due to the frequent passage of tropical typhoons during the rainy season. The cooler and drier northeast monsoon occurs from October to January occasionally producing light rainfall. Mean annual rainfall is about 2,000 mm. Minimum temperature is 20 ˚C around January and February and the maximum of 35 ˚C occurs in April and May with a mean monthly temperature of 25 ˚C to 30 ˚C and mean annual temperature is at 27 ˚C. Relative humidity (RH) ranges from a maximum of 95% in August and September to a minimum of 55% in March and April with a mean annual RH of 76%. Surface elevation of the LMWR ranges from 40 to 260 m a.s.l. with a gently rolling to sloping topography with most of the areas having slopes of 18% and below. There are no flood prone areas within the watershed (Andres *et al*., 2015).

The monitoring small catchment is located in the upper northeastern portion of the LMWR near the Municipality of Rodriguez, Rizal (Figure 5.4.11).

Figure 5.4.11. The LMW catchment area being studied (left) and the stream where water is collected and analyzed (right).

Expected Outcomes in the Near Future

A weir has been designed to be constructed in the outlet of the stream where water is being collected for the laboratory analysis. This weir will be used to determine the stream discharge during the collection periods. However, due to travel restrictions brought about by the current COVID-19 pandemic the plan has been put on hold. In the meantime, stream discharge has been collected since 2019 and analyses done on the same. In addition to these, the atmospheric chemical inputs to the catchment analysis are being provided out of the data collected regularly at the Manila Observatory which is one of the monitoring stations of the EANET – Philippines.

5.4.4 Summary

Long-term data at two forest catchments, IJR and KJK, suggested that the catchment biogeochemical cycles have sensitively responded to the recent declining of atmospheric deposition (in particular, SO_4^{2-}) resulting in phenomena indicating recovery from acidification. However, NO_3^- concentration in stream water at KJK has been increasing, while DIN deposition has been declining. Moreover, decline rates of NO_3^- concentration in stream water at IJR has become slower in recent years. Forest types, maturation of trees and meteorological variability appeared to affect N leaching to stream water. It is suggested that interactions with climate change be taken into consideration in recovery processes from acidification and N saturation. New catchment analysis sites, KMR and LMW, may also contribute to further understanding of ecological response to atmospheric deposition and climate change.

5.5 Summary of the chapter

The EANET has been monitoring soil, (forest) vegetation, and inland water, to assess impacts of atmospheric deposition on ecosystems since 2000, and then promoting a catchment-scale analysis considering biogeochemical cycles in forest ecosystems since 2010. Important data sets over 10 years have been accumulated in many of monitoring sites. Although the ecological monitoring above started in order to detect impacts of acid deposition, the results suggested a necessity to be discussed with other relevant factors, such as climate change.

The soil monitoring clarified that the soil characteristics of EANET sites were quite diverse because of their soil formation processes and climatic conditions; e.g., the pH(H_2O) ranged from 3.5 to 7.5. Based on the comparison between temporal changes in soil pH(H_2O) and those of major variables in wet deposition, it was suggested that the soil reaction was not necessarily parallel to the input of atmospheric deposition. Considering the diverse distribution of soil characteristics among EANET sites, it was also suggested the reaction process would be different for each site. In addition to understanding the effects of atmospheric deposition, this monitoring system will also provide valuable data for understanding the effects of climate change on ecosystems. Therefore, more intensive soil monitoring is recommended.

The vegetation monitoring clarified that no increase in forest growth was observed corresponding to reduction of nss-SO_4^{2-} deposition. This may be due to anthropogenic disturbance, pest infestation (bark beetle), or intensified competition between individuals as the age of the forest increases. To assess the impact of air pollution on a wide range of forests quantitatively, it is necessary to conduct long-term growth measurements for identified individual trees in areas with little or no anthropogenic disturbance and monitor air quality simultaneously.

The inland water monitoring clarified that response of inland waters to atmospheric deposition was different depending on the chemical properties of the respective sites. However, in some of sites, changing patterns of atmospheric deposition at the nearest monitoring sites were associated with those of ion concentrations in lakes/streams, respectively. In fact, several monitoring sites showed symptoms suggesting recovery from acidification. It was suggested that further reduction in atmospheric acid deposition and its monitoring are necessary to ensure their continued recovery from acidification.

The catchment analysis clarified that biogeochemical cycles in two Japanese forest catchments have sensitively responded to the recent declining of atmospheric deposition (in particular, SO_4^{2-}) resulting in phenomena indicating recovery from acidification. However, it was also suggested that various factors, such as forest types, maturation of trees, and meteorological variability, affected N leaching to stream water. It was suggested that interactions with year-to-year meteorological variability be taken into consideration in recovery processes from acidification and N saturation. New catchment analysis sites may also contribute to further understanding of ecological response to atmospheric deposition and climate change.

In order to detect the effects of atmospheric deposition on forest ecosystems, data with low noise factors such as site disturbance (including anthropogenic disturbance) are required. It will be necessary to improve the system for better data acquisition regarding the control or understanding of anthropogenic disturbances (deforestation, non-execution of monitoring, site changes, etc.) in the monitoring program. In addition, the time response to the effects of atmospheric deposits on trees, soil, and water in ecosystems is different, and monitoring and model analysis that take into account the differences in time constants are required. In other words, as shown in the cases in Europe and the United States, it is important to continue monitoring ecosystems and model analyses using the monitoring results even after the atmospheric deposition has decreased sufficiently. Especially in the catchment area, it is expected that these combined effects will be observed as output. Therefore, in addition to the promotion of catchment area analysis in each region, it will be important to establish a system that includes site resetting of trees and soil in consideration of catchment areas in order to analyze the effects of atmospheric deposition and climate change.

5.6 References

Andres, E.P., M.S. Sabater, R. Espada Jr., E.C. Calzeta, and R.C Arjona. 2015. Vulnerability assessment of the La Mesa Watershed Reservation. Sylvatrop, The Technical Journal of Philippine Ecosystems and Natural Resources, January-December 2015, 25(1 and 2): 1-26.

Baba, M., Okazaki, M. 1998. Acidification in nitrogen-saturated forested catchment. Soil Science and Plant Nutrition, 44, 513–525.

Berg, B., McClaugherty, C. 2014. Plant Litter: Decomposition, Humus Formation, Carbon Sequestration, third ed. Springer.

Bouwman, A.F., Vuuren, D.P.V., Derwent, R.G., Posch, M., 2002. A global analysis of acidification and eutrophication of terrestrial ecosystems. Water, Air, and Soil Pollution 141, 349–382.

Breemen, N. Van, Driscoll, C. T., Mulder, J. 1984. Acidic deposition and internal proton sources in acidification of soils and waters. Nature, 307(5952), 599–604.

Chiwa, M., Tateno, R., Hishi, T., Shibata, H. 2019. Nitrate leaching from Japanese temperate forest ecosystems in response to elevated atmospheric N deposition, Journal of Forest Research, 24:1, 1–15, https://doi.org/10.1080/13416979.2018.1530082.

Duan, L., Yu, Q., Zhang, Q., Wang, Z., Pan, Y., Larssen, T., Tang, J., Mulder, J. 2016. Acid deposition in Asia: Emissions, deposition, and ecosystem effects. Atmospheric Environment, 146, 55–69.

EANET. 2020. Strategy Paper for Future Direction of EANET on Monitoring of Effects on Agricultural Crops, Forest and Inland Water by Acidifying Species and Related Chemical Substances. https://www.eanet.asia/resources/publications/

EANET. 2000. Technical documents for soil and vegetation monitoring in East Asia.

Fang, Y., Gundersen, P., Vogt, R.D., Koba K., Chen, F., Chen, X.Y., Yoh, M. 2011. Atmospheric deposition and leaching of nitrogen in Chinese forest ecosystems. Journal of Forest Research 16: 341-350. http://dx.doi.org/10.1007/s10310-011-0267-4.

Forzieri, G., Girardello, M., Ceccherini, G. et al. 2021. Emergent vulnerability to climate-driven disturbances in European forests. Nature Communications, 12, 1081. https://doi.org/10.1038/s41467-021-21399-7

Gao, Y., Zhou, F., Ciais, P., Miao, C.Y., Yang, T., Jia, Y.L., Zhou, X.D., Klaus, B.B., Yang, T.T., Yu, G.R., 2020. Human activities aggravate nitrogen-deposition pollution to inland water over China. National Science Review 7, 430–440.

Hisano, M., Chen, H.Y.H., Searle, E.B., Reich, P.B. 2020. Species-rich boreal forests grew more and suffered less mortality than species-poor forests under the environmental change of the past half-century. Ecology Letters, 22, 999-1008. https://doi.org/10.1111/ele.13259

IUSS Working Group WRB. 2015. World Reference Base for Soil Resources 2014, update 2015. International soil classification system for naming soils and creating legends for soil maps. World Soil Resources Reports No. 106. FAO, Rome.

Inomata, Y., Ohizumi, T., Saito, T., Morohashi, M., Yamashita, N., Takahashi, M., Sase, H., Takahashi, K., Kaneyasu, N., Fujihara, M., Iwasaki, A., Nakagomi, K., Shiroma, T., Yamaguchi, T. 2019. Estimate of transboundary transported anthropogenic sulfate deposition in Japan by using the sulfur isotopic ratio. Science of the Total Environment, 691, 779-788. https://doi.org/10.1016/j.scitotenv.2019.07.004.

Kamisako M, Sase H, Matsui,T, Suzuki H, Takahashi A, Oida T, Nakata M, Totsuka T, Ueda H.,2008. Seasonal and annual fluxes of inorganic constituents in a small catchment of a Japanese cedar forest near the Sea of Japan. *Water Air and Soil Pollution* 195: 51-61.

Kume, A., Fujimoto, M., Mizoue, N., Honoki, H., Nakajima, H., Ishida, M. 2020. Impact of reduced ozone concentration on the mountain forests of Mt. Tateyama, Japan. Environmental Pollution, 267, 115407. https://doi.org/10.1016/j.envpol.2020.115407.

Larssen, T., Carmichael, G. R. 2000. Acid rain and acidification in China: the importance of base cation deposition. Environmental Pollution, 110(1), 89–102.

Lu, Z., Zhang, Q., Streets, D.G. 2011. Sulfur dioxide and primary carbonaceous aerosol emission in China and India, 1996-2010. Atmospheric Chemistry and Physics 11: 9839-9864.

Mgelwa, A.S., Kabalika, Z., Hu, Y.L., 2020. Increasing importance of nitrate-nitrogen and organic nitrogen concentrations in bulk and throughfall precipitation across urban forests in southern China. Glob. Ecol. Conserv. 22, e00983 https://doi.org/10.1016/j.gecco.2020.e00983.

Mitchell, M.J., Likens, G.E., 2011. Watershed sulfur biogeochemistry: shift from atmospheric deposition dominance to climatic regulation. Environ. Sci. Technol. 45, 5267–5271. https://doi.org/10.1021/es200844n.

Montoya-Mayor, R., Fernández-Espinosa, A.J., Seijo-Delgado, I., Ternero-Rodríguez, M., 2013. Determination of soluble ultra-trace metals and metalloids in rainwater ana atmospheric deposition fluxes: A 2-year survey and assessment. Chemosphere 92: 882-891.

Muggeo, V.M., 2008. Segmented: an R package to fit regression models with broken-line relationships. R News 8, 20–25.

Nakagawa, F., Tsunogai, U., Obata, Y., Ando, K., Yamashita, N., Saito, T., Uchiyama, S., Morohashi, M,. Sase, H. 2018. Export flux of unprocessed atmospheric nitrate from temperate forested catchments: a possible new index for nitrogen saturation. Biogeosciences, 15: 7025-7042. https://doi.org/10.5194/bg-15-7025-2018.

Nakahara, O., Takahashi, M., Sase, H., Yamada, T., Matsuda, K., Ohizumi, T., Fukuhara, H., Inoue, T., Takahashi, A., Kobayashi, H., Hatano, R., Hakamata, T. 2010. Soil and stream water acidification in a forested catchment in central Japan. Biogeochemistry 97: 141-158. https://doi.org/10.1007/s10533-009-9362-4.

Obolkin, V., Khodzher, T., Sorokovikova, L., Tomberg, I., Netsvetaeva, O., Golobokova, L., 2016. Effect of long-range transport of sulphur and nitrogen oxides from large coal power plants on acidification of river waters in the Baikal region, East Siberia. International Journal of Environmental Studies 73, 452–461.

Ohizumi T, Take N, Inomata Y, Yagoh H, Endo T, Takahashi M, Yanahara K, Kusakabe M., 2016. Long-term variation of the source of sulfate deposition in a leeward area of Asian continent in view of sulfur isotopic composition. Atmospheric Environment 140: 42–51.

Okamoto, S., Tanimoto, H., Hirota, N., Ikeda, K., Akimoto, H., 2018. Decadal shifts in wind patterns reduced continental outflow and suppressed ozone trend in the 2010s in the lower troposphere over Japan. Journal of Geophysical Research: Atmospheres, 123. https://doi.org/10.1029/2018JD029266

R Development Core Team, 2020. R: A Language and Environment for Statistical Computing. R Foundation for Statistical Computing, Vienna, Austria.

Sase H, Takahashi A, Sato M, Kobayashi H, Nakata M, Totsuka T., 2008. Seasonal variation in the atmospheric deposition of inorganic constituents and canopy interactions in a Japanese cedar forest. Environmental Pollution. 152: 1-10.

Sase, H., Saito, T., Takahashi, M., Morohashi, M., Yamashita, N., Inomata, Y., Ohizumi, T., Nakata, M. 2021. Transboundary air pollution reduction rapidly reflected in stream water chemistry in forested catchment on the Sea of Japan coast in central Japan. Atmospheric Environment, 248: 118223. https://doi.org/10.1016/j.atmosenv.2021.118223.

Sase, H., Takahashi, M., Matsuda, K., Sato, K., Tanikawa, T., Yamashita, N., Ohizumi, T., Ishida, T., Kamisako, M., Kobayashi, R., Uchiyama, S., Saito, T., Morohashi, M., Fukuhara, H., Kaneko, S., Inoue, T., Yamada, T., Takenaka, C., Tayasu, I., Nakano, T., Hakamata, T., Ohta, S. 2019. Response of river water chemistry to changing atmospheric environment and sulfur dynamics in a forested catchment in central Japan. Biogeochemistry, 142: 357-374. https://doi.org/10.1007/s10533-019-00540-1.

Vuorenmaa, J., Augustaitis, A., Beudert, B., Clarke, N., de Wit, H.A., Dirnböck, T., Frey, J., Forsius, M., Indriksone, I., Kleemolaa, S., Kobler, J., Krám, P., Lindroos, A.- J., Lundin, L., Ruoho-Airola, T., Ukonmaanaho, L., Váňa, M., 2017. Long-term sulphate and inorganic nitrogen mass balance budgets in European ICP Integrated Monitoring catchments (1990–2012). Ecol. Indicat. 76, 15–29. https://doi.org/10.1016/j.ecolind.2016.12.040.

Wright, R.F., Roelofs, J.G.M, Bredemeier, M., Blanck, K., Boxman, A.W., Emmett, B.A., Gundersen, P., Hultberg, H., Kjønaas, O.J., Moldan, F., Tietema, A., van Breemen, N., van Dijk, H.F.G. 1995. NITREX: responses of coniferous forest ecosystems to experimentally changed deposition of nitrogen. Forest Ecology and Management 71: 163-169.

Xing J, Song,J, Yuan H, Wang Q, Li X, Li N, Duan L, Qu B., 2017. Atmospheric wet deposition of dissolved trace elements to Jiaozhou Bay, North China: Fluxes, sources and potential effects on aquatic environments. Chemosphere 174: 428-436.

Yamashita, N et al. 2014. Atmospheric deposition versus rock weathering in the control of streamwater chemistry in a tropical rain-forest catchment in Malaysian Borneo. Journal of Tropical Ecology, 30: 481-492. https://doi.org/10.1017/S0266467414000303.

Zheng, B., Tong, D., Li, M., Liu, F., Hong, C., Geng, G., Li, H., Li, X., Peng, L., Qi, J., Yan, L., Zhang, Y., Zhao, H., Zheng, Y., He, K., Zhang, Q. 2018. Trends in China's anthropogenic emissions since 2010 as the consequence of clean air actions. Atmospheric Chemistry and Physics 18, 14095–14111. https://doi.org/10.5194/acp-18-14095-2018

Zhigacheva, E et al. 2019. Investigation of atmospheric input and runoff discharge of sulfur and nitrogen compounds as the balance components of Komarovka river catchment by long-term observations at Russian EANET Primorskaya station (for 2005-2015). EANET Science Bulletin, Vol.5, 23-36.

Zhu J, Wang Q, Yu H, Li M, He N., 2016. Heavy metal deposition through rainfall in Chinese natural terrestrial ecosystems: Evidences from national-scale network monitoring. Chemosphere 164: 128-133.

6. Relevant Studies on Atmospheric Environment Assessment in the EANET Region

6.1 Introduction

Due to continuing rapid economic growth after the year of 2000, Asia keeps attracting much more concern than before from the view of global, hemispherical and regional air pollution. In addition to the effort of EANET, there have been many research activities and organizational initiatives focusing on regional air pollution in East Asia as well as in global and hemispherical perspectives. In this chapter, such research outputs and initiatives in the last few years are reviewed in order to provide useful information on the present status of acid deposition and regional air pollution. The covered topics are atmospheric observation, including satellite observation, emission inventory, chemical transport modeling (CTM), ecological and human health impact studies, which are not necessarily directly related to EANET, but would be useful for understanding air pollution and acid deposition in East Asia.

Figure 6.1.1 shows the overall structure of Chapter 6. In the first part, the observation studies (section 6.2), emission inventory studies (section 6.3) and CTM (section 6.4) are systematically reviewed. In the following part, the ecological impact assessment studies and the human health impact studies are reviewed in section 6.5 and section 6.6, respectively. In the final part, other international activities in EANET region are introduced in section 6.7 and the cross-chapter analysis of acid deposition based on measurements in EANET sites, emissions inventory, satellitte measurement, and CTM is carried out in section 6.8.

This chapter does not intend to provide a comprehensive review, but the atmospheric observational studies focusing on field campaign and satellite measurement as well as studies on acidification and nitrogen leaching in forest catchments (section 6.2), global and regional emision inventories (6.3), the Model Inter-Comparison Studies for Asia (MICS-Asia) utilizing EANET data for validation and analysis (section 6.4), ecological impact assessment studies on the national and/or regional scales (section 6.5) and impacts of $PM_{2.5}$ and ozone on human health (section 6.6) are introduced with higher priority. Additionally, some original analyses are conducted in the satellite observation (section 6.2), emission trend (section 6.3), health impacts (section 6.6) and acid deposition (section 6.8).

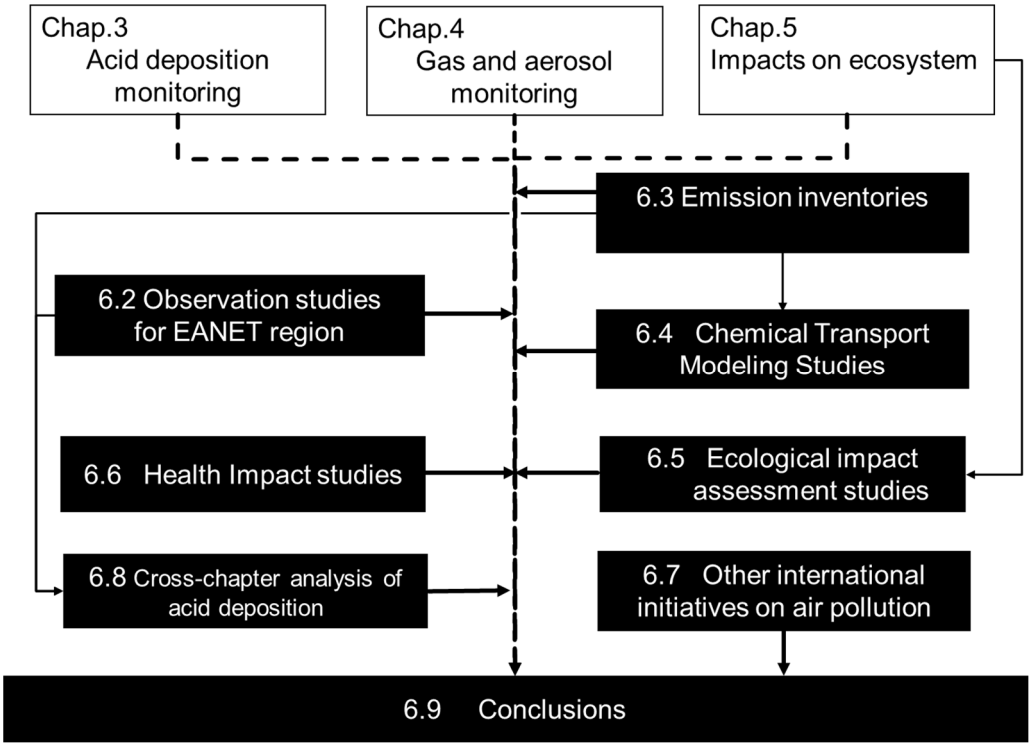

Figure 6.1.1. Overall strucrure of Chapter 6.

6.2 Observational studies for EANET region

6.2.1 Field campaigns for regional air quality

One of the objectives of acid deposition monitoring in EANET is to grasp the effect of acidification and the long-term trends of acidifying species and related chemical substances and the other relevant air pollutants. The long-term monitoring datasets are useful for evaluation of the impact on ecosystem and human health. However, in order to elucidate impacts of specific atmospheric events and chemical and physical processes relevant to assessing the effects of air pollutants, the intensive observational studies based on field campaigns will be helpful in addition to the long-term monitoring studies. In this section, field campaigns for acid deposition and regional air quality in East Asia are reviewed.

The 7-SEAS project has been established to characterize aerosol-meteorological interactions in Southeast Asia. The 7-SEAS program was organized through a collaborative effort with the United States and governments in Southeast Asia. There are a number of published research papers and project reports. This section introduce some important research results.

The international campaign of Dongsha Experiment was conducted in the northern Southeat Asian region from March to May 2010 (Lin et al., 2013). This is a pre-study of the 7SEAS which seeks to perform interdisciplinary research in the field of aerosol-meteorology and climate interaction in the Southeast Asian region, particularly for the impact of biomass burning on cloud, atmospheric radiation, hydrological cycle, and regional climate. The main goals of Dongsha Experiment are to develop an atmospheric observing platform in Dongsha Island and to characterize the chemical and physical properties of biomass burning aerosols in the northern Southeast Asian region. Two intensive observations of aerosol chemistry were conducted in March and April 2010, respectively. Overall, $PM_{2.5}$ mass concentrations were relatively high near burning source regions, while much

lower in Dongsha Island and background sites. The K^+ ion and levoglucosan, as the markers of biomass-burning smoke, were abundant near source regions, while decreasing from biomass-burning sources to downwind areas. For the Dongsha Experiment, OC and EC were also abundant in northern Southeast Asia and southern China, but much less elsewhere.

The Sonla campaign aimed to investigate aerosol chemical characteristics and to obtain the chemical profile of near-source biomass burning aerosols at a site in Sonla, Northern Vietnam (Lee et al., 2016). 24 hour sampling of $PM_{2.5}$ was conducted during the 7-SEAS campaign in the spring of 2012 and 2013. The collected particles were measured for mass concentrations, carbonaceous fractions and water-soluble components (Fig 6.2.1). The average $PM_{2.5}$ mass concentrations were 51±19 μg m^{-3} and 57±27 μg m^{-3} in 2012 and 2013, respectively. Carbonaceous contents of $PM_{2.5}$ were 59±9% and 58±9% in organic carbon (OC) and 9±3% and 10±3% in elemental carbon (EC) in 2012 and 2013, respectively. Of the 8 carbonaceous fractions for $PM_{2.5}$, OC3 (evolution temperature at 280°C–480°C) was most abundant in OC fractions, and EC1-OP (elemental carbon evolved at 580°C minus the pyrolized OC fractions) was predominant in EC fractions in most occasions. Among the measured water-soluble inorganic ions, NH_4^+ and SO_4^{2-} widely varied, indicating the influence of different trajectory origins. The trajectories were also distinguished with respect to char-EC to soot-EC ratio, and water-soluble OC, which shows that the concentrations were highest in the trajectory from the biomass burning source area.

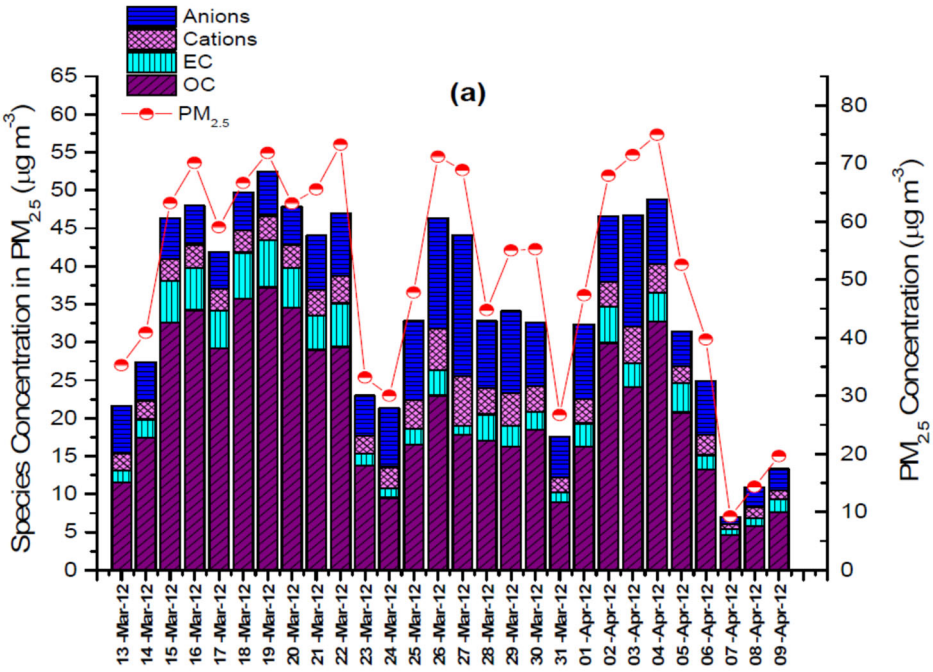

Figure 6.2.1. Temporal variations in $PM_{2.5}$ aerosol mass concentrations and inorganic ions and carbonaceous fractions in 2012 in Sonla, Northern Vietnam (Lee *et al.*, 2016).

The other international campaign, named as the 7-SEAS/BASELInE (Biomass-burning Aerosols & Stratocumulus Environment: Lifecycles and Interactions Experiment), has been conducted during February-May 2013 and March-April 2014. The 7-SEAS/BASELInE would provide a basis for a deeper improvement of the understanding of the lifecycles of regional biomass-burning aerosols, and their interactions with stratocumulus clouds during the Asian pre-monsoon season. In 2013, the direct aerosol radiative effects of biomass-burning aerosols over northern Indochina were estimated by the integration of observation and an optical and a radiative transfer model (Pani et al., 2016). The PM_{10} and black carbon mass at Doi Ang Khang, Thailand were 87±28 and 7±2 μg m^{-3}, respectively. Black carbon were the main contributor to the aerosol radiative forcing (ARF), while water insoluble, sea

salt and mineral dust components were negligible mainly due to their low extinction efficiency. The overall mean ARF was -8.0 and -31.4 W m^{-2} at top-of-atmosphere and at the surface, respectively. The observation of chemical components of biomass burning aerosols was conducted Doi Ang Khang (DAK; Biomass burning source) and Chiang Mai University (CMU; Urban location) in Thailand in 2014 (Khamkaew et al., 2016). The daily average $PM_{2.5}$ mass concentrations at DAK (80.8–83.3 μg m^{-3}) and CMU (90.7–93.1 μg m^{-3}) were well correlated. Concentrations of levoglucosan and K^+ were well correlated confirming that the $PM_{2.5}$ in these areas were mainly influenced by biomass burning activity. Principal component analysis revealed that biomass burning, road traffic, agricultural activity and soil re-suspension were plausible sources of $PM_{2.5}$ over the study locations.

Pan et al. (2012) conducted a three-year (2007-2010) observation campaign at ten selected sites in Northeast Asia to monitor wet and dry atmospheric deposition of different nitrogen species. Among the annual total deposition, 40% was comprised of the wet deposition and the rest 60% was dry deposition. Compared with gaseous nitrogen species, particulate nitrogen species were not the major contributor of dry deposition which contributed approximately 10% of the total dry deposition. The oxidized nitrogen species accounted for 21% of total nitrogen deposition, implying that other forms of gaseous nitrogen, such as NH_3, comprised a dominant portion of the total flux. The contribution of NO_3^- to nitrogen deposition was enhanced in certain urban and industrial areas, possibly due to the fossil fuel combustion. Liu et al. (2018) reported the long-term data sets including 3 years observations of $PM_{2.5}$ mass concentrations (2012–2014) and 1-year observations of $PM_{2.5}$ compositions (2012–2013). A distinct seasonal variability in $PM_{2.5}$ is observed, with highs in the winter and lows during the summer at urban sites. The chemical compositions of $PM_{2.5}$ were analyzed at six urban and background sites. The major $PM_{2.5}$ components at all the urban sites are organic matter (26.0 %), SO_4^{2-} (17.7 %), mineral dust (11.8 %), NO_3^- (9.8 %), NH_4^+ (6.6 %), elemental carbon (6.0 %). Similar chemical compositions of $PM_{2.5}$ were observed at background sites but were associated with higher fractions of organic matter (33.2 %) and lower fractions of NO_3^- (8.6 %) and elemental carbon (4.1 %).

The field campaign of free radical observation was conducted from January to March 2016 (Tan et al., 2018). It aimed to understand oxidative capacity during wintertime and to elucidate the secondary pollutants' formation mechanism in the Northeast Asia. Hydroxyl radical (OH), hydroperoxy radical (HO_2) and organic peroxy radical (RO_2) were observed in combination with observations of total reactivity of OH radical. The OH radical concentrations are nearly 2 times larger than those observed in previous winter campaigns in Birmingham (Heard et al., 2004), Tokyo (Kanaya et al., 2007), and NYC (Ren et al., 2006) during wintertime. During this campaign, the total primary production rate of total reactive radicals was dominated by the photolysis of HONO accounting for 46 % of the identified primary production pathways for reactive radicals. The McFAN project. An intensive field campaign was performed in winter of 2018 investigating the physicochemical mechanisms leading to haze formation with a focus on the contributions of multiphase processes in aerosols and fogs (Li et al., 2021). There are a strong relative humidity dependence of aerosol chemical compositions, suggesting an important role of multiphase chemistry. Compared with the low humidity period, both PM_1 and $PM_{2.5}$ showed higher mass fraction of secondary inorganic aerosols of nitrate, sulfate and ammonium and secondary organic aerosols during high humidity and fog episodes. The enhanced contributions were during high humidity and fog are most likely caused by aqueous-phase reactions favored by high relative humidity. The experiment provides new evidence of the key role of multiphase reactions in regulating aerosol chemical composition and physical properties in polluted regions.

The KORUS-AQ field study was conducted during May–June 2016 that is jointly sponsored by the National Institute of Environmental Research, Republic of Korea and the National Aeronautics and Space Administration of the United States (Crawford et al., 2021). KORUS-AQ consists of three aircraft observations, an extensive ground-based observation network, and three ship-based observations and air quality forecast models. Information gathered during this study is contributing to an improved understanding of the factors controlling air quality in Republic of Korea. KORUS-

AQ also provided a valuable scientific knowledge for future air quality–observing strategies involving geostationary satellite instruments being launched by both countries to examine air quality throughout the day over Asia and North America. Fig 6.2.2 shows the diurnal statistics of ozone with altitude by aircraft observation over the Seoul Metropolitan Area. A distinct diurnal pattern is observed in the lowest kilometer with median ozone values ranging from 68 ppb in the morning to 107 ppb in the afternoon. This wide range is related to both the overnight and early morning titration of ozone and the afternoon culmination of photochemical ozone production. Moving up to 1–2 km, median ozone values cover a smaller range (72–90 ppb) as the morning effects of titration by surface NOx emissions are reduced, and boundary layer depths in the afternoon do not always reach 2 km. The most distinctive features are layers between 2 and 4 km where median ozone values are in the vicinity of 75–80 ppb and almost all values exceed the 60 ppb 8-h average ozone standard for South Korea. This demonstrates that a substantial background ozone problem exists in addition to the local ozone production near the surface such that entrainment of air from the lower free troposphere alone is sufficient to violate the ozone standard. Whether the more modest ozone production rates (5–8 ppb) in the lower troposphere (2–4 km) is locally or regionally driven is immaterial to the idea that ozone can only be improved through a combination of measures taken both locally by Korea and regionally by neighboring countries.

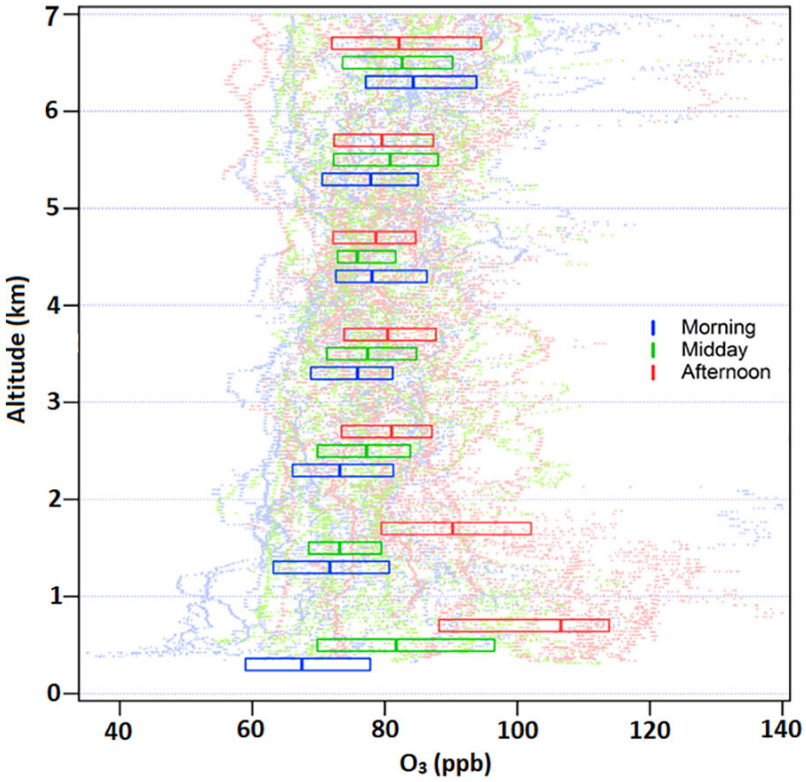

Figure 6.2.2. Vertical distribution of ozone observed by aircraft observation over the Seoul Metropolitan Area. Boxes showing median and inner quartile values for 1 km increments of altitude are plotted over the individual measurements separated into morning, midday, and afternoon observations (Crawford et al., 2021).

In early autumn 2012 and summer 2013, an intensive atmospheric observations campaign were carried out at the Field Museum TAMA of Tokyo University of Agriculture and Technology located in the suburbs of Tokyo. The observations focused on plant-derived VOCs and total OH reactivity in a typical area where anthropogenic and plant-derived substances are mixed (Ramasamy et al., 2018). The total OH reactivity, which gives the instantaneous loss rate of OH radicals due to reactive species, is an invaluable technique to understand regional air quality, as it gives the overall reactivity of the air mass, the fraction of each trace species reactive to OH, the fraction of missing sinks, O_3

formation potential, etc. The average measured OH reactivities during that autumn and summer were 7.4 s^{-1} and 11.4 s^{-1}, respectively. In summer, isoprene was the major contributor, accounting for 28.1% of the OH reactivity, as a result of enhanced light-dependent biogenic emission, whereas NO_2 was major contributor in autumn, accounting for 19.6%, due to the diminished contribution from isoprene as a result of lower solar strength (Fig 6.2.3). Most of the days in summertime, maximum O_3 mixing ratio observed above 50 ppb, whereas in autumn it was around 40 ppb mostly that indicates enhanced isoprene photochemistry might be a significant factor for the O_3 concentration level. Around the site, biogenic VOCs contributed twice higher than anthropogenic VOCs to OH reactivity. Higher missing OH reactivity (34%) was determined in summer, and linear regression analysis showed that oxygenated VOCs could be the potential candidates for missing OH reactivity. Lower missing OH reactivity (25%) was determined in autumn, and it was significantly reduced (11%) if the interference of peroxy radicals to the measured OH reactivity were considered.

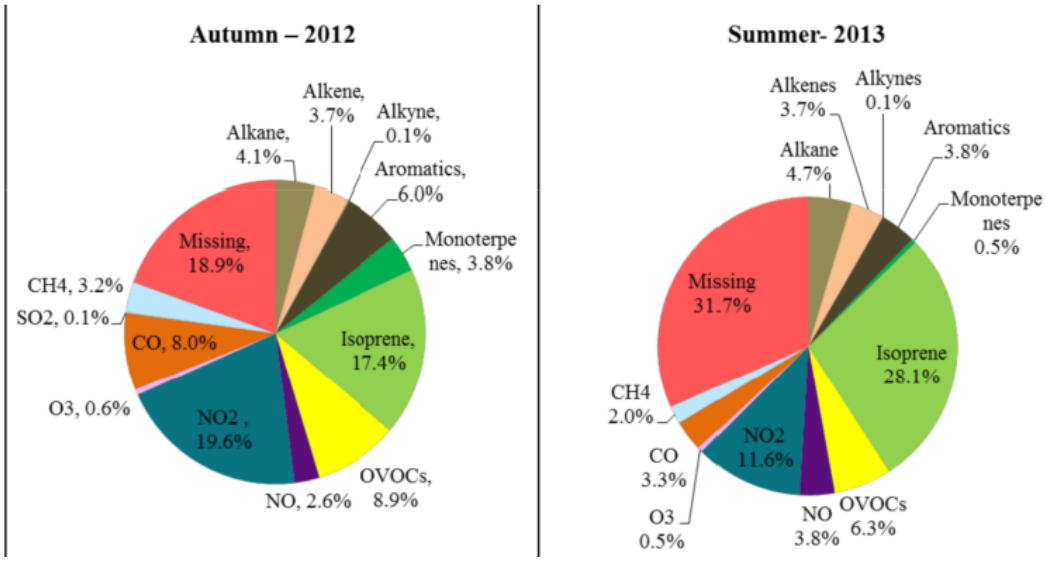

Figure 6.2.3. The average contribution of trace species to the total OH reactivity during autumn 2012 and summer 2013 campaign (Ramasamy et al., 2018).

6.2.2 Satellite observations

(1) NO_2 and SO_2

Satellite observations have been useful to monitor the air quality from space in near real time, and also widely used as a proxy for emissions. Representative satellite data is NO_2 column used to capture NO_x emissions. This space-based view of the NO_2 column was first reported by Richter et al. (2005) from 1996 to 2004. The NO_2 column above eastern China showed accelerated growth of 4%/yr in 1997 to 12%/yr in 2002. This rapid increase has continued up to 2011, the increase was 16%/yr from 1996 to 2011 over east central China (Hilboll et al., 2013). Increasing trends were common over most of China from 2005 to 2011 (Irie et al., 2016). Based on the linear relation between NO_2 column and anthropogenic NO_x emissions, it was estimated that anthropogenic NO_x emissions from China during 2000-2010 have almost doubled (Itahashi et al., 2014). As also indicated by the dataset of bottom-up emission inventory (see Section 6.3), the situation for NO_x emissions in China has been dramatically changed. The 11-year analysis of NO_2 column from 2005 to 2015 revealed the peak in 2011, and subsequent drop of around 40% from 2014 to 2015 over the north China plain (Krotkov et al., 2016). The analysis of the peak year over each province showed inhomogeneous spatial difference (van der A et al., 2017). In contrast to this declining trend over China, India showed a continuously increasing trend; therefore, it is anticipated that India could be the largest NO_x emission source under the current trends (Itahashi et al., 2019). SO_2 columns are also used to monitor SO_2

emissions (e.g., Lee et al., 2011; Li et al., 2010; 2013) both for anthropogenic and volcanic sources (e.g., Brenot et al., 2014). Although China was the largest source of anthropogenic SO_2 emission in Asia, its level was declined from 2007, and it was estimated that India surpassed China in its amount in 2016 by satellite-based estimation (Li et al., 2017).

In this section, the long-term trends of NO_2 and SO_2 column observed by satellite is presented. The analyzed areas are North East Asia (China, Republic of Korea, Japan, Mongolia, and Russia) and South East Asia (Vietnam, Cambodia, Lao PDR, Myanmar, Thailand, Malaysia, Indonesia, and Philippines). For Russia, to cover four EANET sites (see Fig. 1.5.1), the region of far east Russia from 90°E and up to 60°N are analyzed. The NO_2 and SO_2 column dataset, which was observed by Ozone Monitoring Instruments (OMI) onboard National Aeronautics and Space Administration (NASA) Earth Observing System (EOS) Aura satellite, is used in this section. Aura satellite was launched on 15 July 2004 in a sun-synchronous ascending polar orbit with a local equator crossing time of 13:45±0:15, and science-quality data operations began on 1 October 2004. The data from 2005 to 2019 are analyzed. Retrieval algorithms were based on the products provided by NASA. The level-3 daily product (OMNO2d) of the latest version 3.0 (Krotkov et al., 2019) for NO_2 column is used. This product contains the total and tropospheric column for all atmospheric conditions and for clear sky conditions (cloud fraction is less than 30%). The tropospheric column with screened for clear sky condition is analyzed. The level-3 daily product (OMSO2e) of the latest version 3.0 (Krotkov et al., 2015) for SO_2 column is used. This product contains the SO_2 in the planetary boundary layer. Both data of NO_2 and SO_2 column are gridded at a resolution of 0.25° × 0.25°. For SO_2 column, the smoothed method to average out the noise contained in SO_2 column is additionally adopted (Koukouli et al., 2016). This method smoothed the SO_2 column at each grid by weighted the surrounding eight cells, and if the negative values were found at grid, it was treated as zero value. The explosive volcanic eruptive events outside Asia had impacts on the Asian SO_2 column and these periods were discarded when averaging annual data in 2009 and 2011 based on the same approach in the previous report (Itahashi et al., 2018).

To clarify the long-term trends over North East and South East Asia, annual-averaged NO_2 columns are further analyzed. The result is shown in Fig. 6.2.4. The annual-averaged NO_2 column overall showed constant trends during these 15 years with 0.10 D.U. and 0.03 D.U. over North East Asia and South East Asia, respectively. In detail, North East Asia posed a slight declining trend in the late 2010s, whereas South East Asia showed a slight increase. This trend is generally matched to the estimation of bottom-up emission inventories (Section 6.3). In addition, to take into account the trend of anthropogenic emissions, biomass burning emissions could be an important source rather than anthropogenic sources especially over South East Asia and far east Russia.

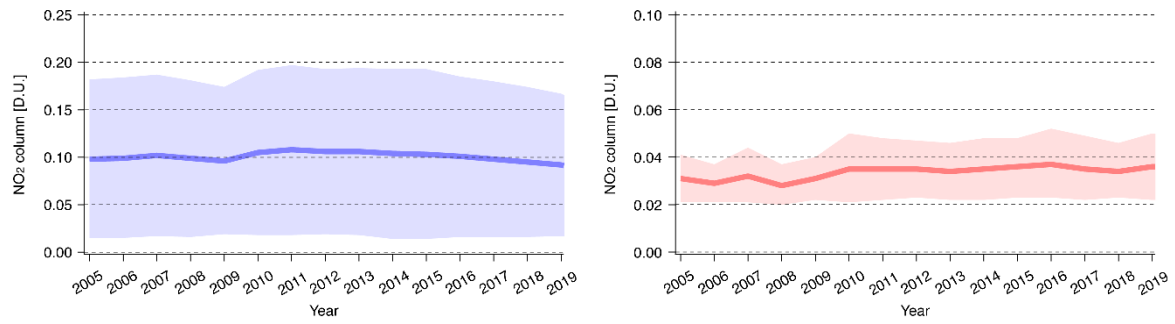

Figure 6.2.4. Temporal variation of annual-averaged NO_2 column from 2005 to 2019 over (left) North East Asia and (right) South East Asia.

The analysis of annual-averaged SO_2 column is presented in Fig. 6.2.5. North East Asia showed a peak in 2006-2007 and then declining. This trend is partly corresponded to the estimation of bottom-up emission inventories (Section 6.3), and partly due to the effect of volcanic SO_2 emissions around Japan. South East Asia showed peak in 2006 and 2008, and gradual increasing trends for SO_2 column.

These increasing trends found in SO_2 column are consistent to the growth of SO_2 emissions estimated by the bottom-up emission inventory (Section 6.3).

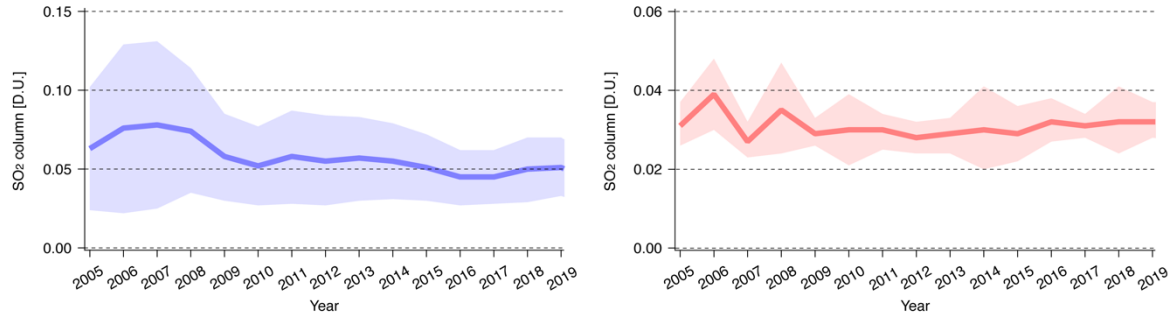

Figure 6.2.5. Temporal variation of annual-averaged SO_2 column from 2005 to 2019 over (left) North East Asia and (right) South East Asia.

(2) AOD

NO_x and SO_2 columns could be used as the proxy of NO_x and SO_2 emissions. These precursors produce secondary aerosols in the atmosphere with complex chemical reactions. The Aerosol Optical Depth (AOD) represents the attenuation of sunlight by aerosols and is an important measure of the aerosol column concentration (Kaufman et al., 2002). To obtain the long-term trends of AOD over Asian region, AOD measured by Moderate resolution Imaging Spectroradiometer (MODIS) onboard Terra satellite was analyzed. The MODIS product in the latest Collection 6.1 (Levy et al., 2013) was provided from 24 February 2000 to the present. Level 3 of MOD08_3D dataset gridded into 1.0°×1.0° (NASA, 2021) was used, and the product of AOD with Dark Targett (DT)/Dark Blue (DB) algorithms was analyzed.

The long-term trends of aerosol pollution status over North East Asia and South East Asia are analyzed, and shown in Fig. 6.2.6. Overall, the year-to-year variations were large; suggesting that the aerosol pollution did not straightforwardly relate to precursor emissions or satellite observations for NO_x and SO_2 column (Figs. 6.2.4 and 6.2.5). This would be because AOD contains both fine- and coarse-mode aerosols, and hence attributed to both anthropogenic and natural sources. Over North East Asia, it is noticed that the declining trend after 2013. Under the reduction of anthropogenic emissions from China, a decline in $PM_{2.5}$ concentration has been reported since 2013 (e.g., Zhang et al., 2019), and also influenced over downwind regions (e.g., Uno et al., 2020). Over South East Asia, for example, the highest peak was seen in 2015-2016 and then the drop was found in 2017. The broad impact caused by the biomass burning over this region will be large, and caused large year-to-year variation.

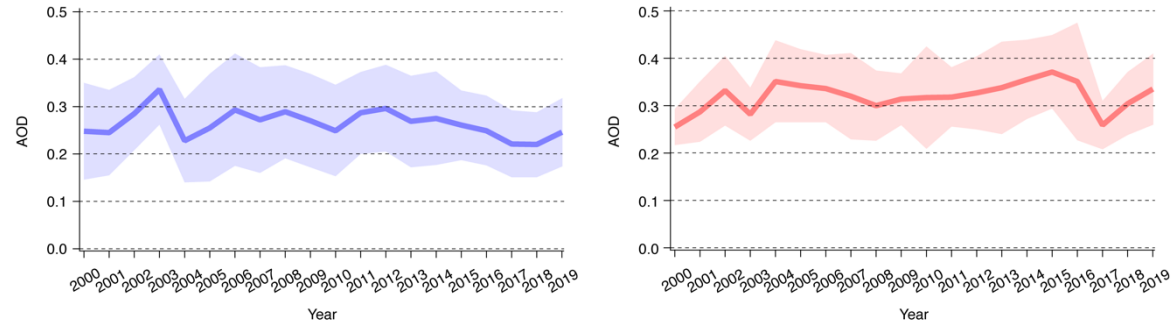

Figure 6.2.6. Temporal variation of annual-averaged AOD from 2000 to 2019 over (left) North East Asia and (right) South East Asia.

6.2.3 Acidification and nitrogen leaching in forest catchments

An integrated monitoring taking account of hydrological/biogeochemical processes in forest catchments is effective to assess effects of atmospheric deposition on terrestrial ecosystems. Therefore, as shown in Chapter 5.4, the EANET has been promoting the catchment-scale monitoring and relevant studies continuously. Of course, studies on acidification and nitrogen leaching in forest catchments have been conducted by many scientists outside the EANET community. There are also some more EANET-relevant studies which have been terminated. This section will review such other relevant studies in the East Asian region. The similar review on acidification and nitrogen leaching in forest catchments has already been done for the Review of the State of Air Pollution (RSAP) (EANET, 2015). At that time, the Executive Summary of RSAP pointed out the following situations:

- Inland water acidification, probably due to high acid loads, occurred over the last several decades in China, Japan and Russia, and both SO_4^{2-} and NO_3^- contributed to the acidification in the region. ANC of the bedrock geology is one of the most important factors for manifestation of inland water acidification.
- Based on input–output measurements conducted in Japan and China, the majority of ecosystems have high retention ability for nitrogen, whereas nitrogen saturation occurred in some particular forested ecosystems. Spatial distribution of nitrate concentrations in stream water in Japan showed that there were some areas with high concentration in the vicinity of large cities and intensive agricultural areas.

Although the scientific papers published until 2014 were reviewed in the RSAP, the atmospheric environment in the region has been dynamically changing for the last decade. The situations on forest catchments may have slightly be changed as responses to the changing atmosphere. Therefore, in this section, some updates will be highlighted, mainly based on relatively new literatures after 2010.

(1) Possible response to reduction of acid deposition

Acidification of inland water in China, Japan, and Russia was highlighted in RSAP published in 2015, as described above. However, at that time, emissions of sulfur dioxide (SO_2) and nitrogen oxide (NO_X), which mainly cause acid deposition and acidification of ecosystems, had already started declining in Northeast Asia (Kurokawa & Ohara, 2020). Thus, there was the question of when reduction of the emissions would be reflected in atmospheric deposition and ecosystem biogeochemistry. Duan et al. (2016) reviewed acid deposition in Asia comprehensively, from emissions to ecosystem impacts; high concentrations of SO_4^{2-} and NO_3^- in stream water could be observed with high S and N deposition, which was based on observations in forest catchments from China, Japan, and Korea. It was pointed out that relative low S leaching compared with S deposition indicated S adsorption in soil (Duan et al., 2016). As already shown in Chapter 5.4, atmospheric deposition of non-sea-salt (nss) SO_4^{2-} and dissolved organic nitrogen (DIN) by wet deposition and/or throughfall and stemflow (TF+SF) decreased for the period from the early 2000s to 2017/2018 in two EANET-relevant forest catchments in central Japan (Sase et al., 2021). Simultaneously, recovery of stream water from acidification has also been observed with decrease of SO_4^{2-} and/or NO_3^- concentrations in these forest catchments (Sase et al., 2019, 2021). It was also suggested that response of the ecosystems to reduction of S deposition was slightly delayed and weakened due to the internal S cycle (Sase et al., 2021). Thus, reduction of the emissions, especially reduction of SO_2 emissions, seems to have been reflected in atmospheric deposition and ecosystem response in China and Japan gradually for the last decade.

On the other hand, Komarovka River, located in a forest area of the Russian Far East, for which acidification of the river water was suggested in PRSAD3 (EANET, 2016), showed clearer acidification tendencies according to the data accumulated until 2019 (Zhigacheva in preparation), as shown in Chapter 5.4. In addition, Pereemnaya River, located in a forest area of the Baikal region, another EANET site in the East Siberia, showed a decline of pH with increase of SO_4^{2-} and NO_3^- concentrations for the period from 2001 to 2014, possibly due to an increase of SO_2 and NO_X emissions derived from coal thermal power plants in the region (Obolkin et al., 2016).

Emission trends of SO_2 and NO_X in Southeast Asia varies in the respective countries, although the regional emissions still continuously increased (Kurokawa & Ohara, 2020). Catchment studies in terms of acid deposition are very limited in the region except in some cases in the EANET-relevant forest catchments in Thailand and Malaysia. According to Kurokawa and Ohara (2020), SO_2 emissions in Thailand peaked in 1996, steeply decreased until 2001 and then decreased clearly after the small peak in 2005, while NO_X emissions in Thailand and both emissions in Malaysia still increased continuously. Sase et al. (2017) detected a specific response of forest catchment to reduction of SO_4^{2-} deposition at Sakaerat site in Nakhon Ratchasima Province, Thailand; stream water chemistry showed pH declining trend and increasing trends of SO_4^{2-} and other major-cation concentrations, due to changing precipitation pattern under the tropical savanna climate (Aw: the Köppen climate classification). The recovery process seems to be disturbed and rather retrogressed by changing climate. On the other hand, Baru Catchment in Danum Valley Conservation Area, which is located remote from cities in Sabah, Malaysia, did not show acidification/recovery trends during the surveys from 2008 to 2011 (Yamashita et al., 2014). They suggested that base cation leaching due to chemical weathering in deep strata neutralized stream water pH, resulting in increase of pH from 5.3 in the precipitation to 7.1 in the stream water. Importance of chemical weathering is highlighted in tropical rainforest climate (Af).

(2) Nitrogen leaching

Although RSAP (EANET, 2015) concluded the majority of ecosystems in China and Japan had high retention ability for nitrogen as described above, observational studies suggesting progress of nitrogen leaching could still be found for the last decade. Similar to the cases on acidification phenomena, studies on nitrogen leaching were reported mainly from Northeast Asia.

In the review by Duan et al. (2016) NO_3^- concentrations in stream waters were compared to N deposition amounts in forest catchments from China, Japan, and Korea and elevated NO_3^- concentrations in stream waters could be often observed with high N deposition. It was pointed out that elevated NO_3^- concentrations in stream water were observed even with N deposition below 10 kg ha^{-1} $year^{-1}$ (1.0 g m^{-2} $year^{-1}$) in Japan, while they are much lower than those in China.

In the Tatara River basin, Kyushu Island, southwestern Japan, Chiwa et al. (2012) found that the NO_3^- concentration in downstream water increased significantly for the period from 1977 to 2007 in spite of the reduction in agricultural activity and increases in sewage system wastewater treatment, suggesting effects of elevated atmospheric N deposition via upland forests in the basin. In Japan, emission peaks of NO_x and NH_3 were in the 1970s and 1980s, respectively and their emission rates were significantly smaller than those in China (Kurokawa & Ohara, 2020). It was suggested that the long-range transport of reactive N from the continent partly contributed to N saturation in the basin in addition to other forest conditions (Chiwa et al., 2012). The study above was conducted in the early 2010s and therefore reduction of NO_X emissions since 2011/2012 in China has not been reflected yet. In eastern Japan, Nishina et al. (2017) surveyed spatially NO_3^- concentrations in 608 independent small forested catchment water samples from northeastern suburbs of Tokyo where N deposition had increased over 30 years; The NO_3^- concentrations varied from 0.07 to 3.31 mg N L^{-1} and most of the variance of NO_3^- concentration could be explained by N deposition rates simulated by the atmospheric chemical transport model. It was also suggested that the catchment with dominant coniferous coverage, such as afforested area, had a strong sensitivity to N deposition of N leaching (Nishina et al., 2017). In the review, Chiwa et al. (2019) also pointed out that Japanese cedar and cypress, major afforested tree species in Japan, are arbuscular mycorrhizal (AM)-associated trees, which are susceptible to NO_3^- leaching in response to N deposition. It was suggested that several factors, including long-range transport of air pollutants, an Asian monsoon climate with warm and wet summer, and maturation/poor management of AM-associated plantations, would make Japanese temperate forests more sensitive to atmospheric N deposition (Chiwa et al., 2019). In the case of Lake Ijira catchment, one of the EANET sites, recovery processes from N saturation have been observed recently possibly due to reduction of N deposition, diminished effects of the past climatic anomalies, and forest management (Sase et al., 2019). On the other hand, continuous increase of

NO_3^- concentration in the stream water has been observed in Kajikawa catchment, in which planted Japanese cedar trees have been matured without forest managements (Sase et al., 2021).

(3) Summary

Aforementioned responses of forest catchments to changing emission/deposition of air pollutants are summarized in Table 6.2.1. Recovery from acidification is still not clear in many cases, probably because the datasets only until 2013/2014 could be used for these assessments. Even though S deposition decrease, response of ecosystems may slightly be delayed due to the internal S cycle (Sase et al., 2021). In some cases, acidification on deposition and/or stream water seems to be still ongoing. Changing climate may affect both deposition processes and ecosystem responses. Reduction of NO_X emissions after 2011/2012 has not been enough reflected in observational studies in forest areas. Moreover, not only N deposition but also other factors, such as climatic conditions and forest maturation and management, may influence N leaching processes. Monitoring and assessment for the next 5-year term will be more important to evaluate recovery from acidification and N leaching.

Table 6.2.1 Response of forest catchments to changing emission/deposition of pollutants in the EANET countries

Country	Monitored area (period)	Emission/ deposition	Stream water/ lake water	Source
Japan	Ijira FC (1988 – 2014)	SO_4^{2-} D decrease DIN D decrease (after 2006)	pH increase NO_3^- C decrease (after 2005/2006)	Sase et al. 2019
	Kajikawa FC (2002 – 2018)	SO_4^{2-} D decrease (after 2006) DIN D decrease (after 2007)	pH increase SO_4^{2-} C decrease (after 2006) NO_3^- C increase	Sase et al. 2021
	Tatara R basin	DIN D increase (1991 – 2007)	NO_3^- C increase (1977 – 2007)	Chiwa et al. 2012
	608 FC in the suburbs of Tokyo (spatial surveys)	Partly high DIN D (2007 – 2010)	Partly high NO_3^- C (2007 – 2010)	Nishina et al. 2017
Russia	Komarovka R (2005 – 2019)	No trend	pH decrease NO_3^- C increase	Zhigacheva in preparation
	Pereemnaya R (2001 – 2014)	SO_2 increase NO_X increase	pH decrease SO_4^{2-} C increase NO_3^- C increase	Obolkin et al. 2016
Malaysia	Baru FC (2008-2011)	No trend	No trend (well neutralized)	Yamashita et al. 2014
Thailand	Sakaerat FC	SO_4^{2-} D decrease	pH decrease SO_4^{2-} C increase	Sase et al. 2017

Note: R, river; FC, forest catchment; E, emission; D, deposition, C, concentration; L, leaching rate; DIN, dissolved inorganic nitrogen. Blue and yellow markers represent phenomena showing recovery from acidification and progress of acidification (or pollution), respectively.

6.3 Emission inventories

Air pollution, including acid deposition, is a crucial problem of atmospheric environment we have been facing. The fundamental reason why atmospheric environmental problems occur is clear: Concentrations of related species increased too much mainly due to emissions from anthropogenic activities. Therefore, for mitigating atmospheric environmental problems, it is important to find an effective way to reduce anthropogenic emissions and for this purpose, understanding details about the current status and trends of emissions are fundamentally important. It is a basic role of emission inventory which is defined as a dataset of air pollutants emissions estimated for specified source categories and related activities in certain administrative or geographical areas and in certain time periods.

In this section, global emission inventories, regional emission inventories in Asia, and national emission inventories in EANET member countries are reviewed. For methodologies to develop emission inventories, see emission inventory guidelines and manuals such as EMEP/EEA air pollutant emission inventory guidebook (https://www.eea.europa.eu/themes/air/air-pollution-sources-1/emep-eea-air-pollutant-emission-inventory-guidebook/emep) and ATMOSPHERIC BROWN CLOUDS EMISSION INVENTORY MANUAL (Shrestha et al., 2013).

6.3.1 Global emission inventories

(1) Overview of global emission inventories

Global emission inventories provide emissions data from all countries in the world, which are necessary for comparing and analyzing emissions among different countries and regions. For performing global model simulations, global gridded emission datasets are essential. Furthermore, for countries without national emissions data, we often have to rely on estimates from global emission inventories. Table 6.3.1 summarizes general information of major global anthropogenic emission inventories. Emission Database for Global Atmospheric Research (EDGAR) is a global database of anthropogenic emissions of greenhouse gases and air pollutants for sub-sector levels generally based on international statistics (Crippa et al., 2018). EDGAR has been providing both datasets for countries emissions and gridmaps. Evaluating the Climate and Air Quality Impacts of Short-Lived Pollutants (ECLIPSE) global emission fields provide gridded data not only for past years, but also for future projections estimated using the Greenhouse Gas and Air Pollution Interaction and Synergies (GAINS) integrated assessment model (Amman et al., 2011; Klimont et al., 2017). The EDGAR and ECLIPSE emissions inventories are developed based on consistent methodologies for each database. On the other hand, recently, "mosaic approaches" using independent emission inventories are also used for the development of global emission inventories. The Task Force Hemispheric Transfer of Air Pollution (TF HTAP) developed HTAPv2 emission database by compiling different national and regional inventories based on official and latest available regional information. In HTAPv2, EDGARv4.3 was used as default data and the MIX inventory, official emission inventories for the Model Intercomparison for Asia Phase III (MICS Asia III) (see Sect. 6.3.2) was used for the Asian region (Janssens-Maenhout et al., 2015). Recently, the Community Emission Data System (CEDS) inventory was developed for the Coupled Model Intercomparison Project Phase 6 (CMIP6). The CEDS calibrated default global emission estimates using independent national and regional emission inventories (Hoesly et al., 2018; McDuffe et al., 2020).

Table 6.3.1 General information of major global anthropogenic emission inventories

Names	Descriptions
EDGARv5.0	Species: SO_2, NO_x, CO, NMVOCS, NH_3, CO_2, CH_4, N_2O, PM_{10}, $PM_{2.5}$, BC, OC, and Mercury; Year: 1970-2015; Resolution; 0.1°×0.1°; https://edgar.jrc.ec.europa.eu
ECLIPSEv5 (v6: Baseline scenario)	Species: SO_2, NO_x, CO, NMVOCS, NH_3, CO_2, CH_4, PM_{10}, $PM_{2.5}$, BC, OC, and OM; Year: 1990-2050; Resolution; 0.1°×0.1°; https://iiasa.ac.at/web/home/research/researchPrograms/air/ECLIPSEv5.html https://iiasa.ac.at/web/home/research/researchPrograms/air/ECLIPSEv6.html
HTAPv2	Species: SO_2, NO_x, CO, NMVOCS, NH_3, PM_{10}, $PM_{2.5}$, BC, and OC; Year: 2008 and 2010; Resolution; 0.1°×0.1°;

	https://edgar.jrc.ec.europa.eu/dataset_htap_v2
CEDS	Species: SO_2, NO_x, CO, NMVOCS, NH_3, CO_2, CH_4, BC, and OC; Year: 1750-2014/1970-2017; Resolution; 0.5°×0.5°; https://gmd.copernicus.org/articles/11/369/2018 https://zenodo.org/record/3754964#.YHgs3ujN1hE

For atmospheric environmental problems, biomass burning is also an important source of related species especially in Southeast Asia. Global Fire Emissions Database (GFED) version 4 provides monthly, daily, and 3-hour emissions with burned area information (https://www.globalfiredata.org). The Fire Inventory from NCAR (FINN) version 1.0 provides daily, 1 km resolution, global estimates of air pollutants emissions from open biomass burning including wildfire, agricultural fires, and prescribed burning (https://www2.acom.ucar.edu/modeling/finn-fire-inventory-ncar).

For the development of accurate emission inventories and utilizing the data for improving atmospheric environment, international cooperation is essential among both scientific researchers and policy makers. The Global Emission InitiAtive (GEIA) created in 1990 is a community of emission experts for building emissions data access and analysis platforms and communicating with the emissions community through online resources and in-person meetings (http://www.geiacenter.org). GEIA is also collecting emission datasets which are provided from Emissions of atmospheric Compounds and Compilation of Ancillary Data (ECCAD), the GEIA data portal (https://eccad.aeris-data.fr).

(2) Trends of global emissions

Long historical trends of global emissions of SO_2, NO_2, and $PM_{2.5}$ are reviewed here. Figure 6.3.1 presents anthropogenic and open biomass and waste burning emissions from world regions during 1970-2015 and shares of emissions from EANET participating countries (PCs) except for Russia. Note that emissions from Russia are not included in those from EANET PCs in Sect. 6.3 because majority of emissions of Russia were not from the East Asia region. For Fig. 6.3.1, anthropogenic emissions from fuel combustion and industrial processes were obtained from REASv3.2 (see Table 6.3.2) and all others were from EDGARv5.0 (see Table 6.3.1). Details about emissions in EANET PCs are described in Sect. 6.3.2. Clear differences are found in the trends of anthropogenic emissions among regions as well as species. On the other hand, trends for biomass burning emissions of SO_2, NO_2, and $PM_{2.5}$ were growing continuously and their growth rates became slightly larger after late 2000s.

For SO_2, global anthropogenic emissions peaked prior to 1980 and decreased until around 2000. These features generally reflect changes of emissions in North America and Europe due to emission control policies in energy and industry sectors. After 2000, global SO_2 emissions increased again by about 7% until 2005 and then, turned to decrease by about 13% from 2005 in 2015. Shares of EANET PCs are about 15%, 44%, and 32% in 1970, 2005, and 2015, respectively. On the other hand, shares of emissions in South Asia increased largely recently from about 9% in 2005 to 16% in 2015. Asia is the largest emitter region of SO_2 and about half of SO_2 emissions are from Asia in 2015.

For NO_x, global anthropogenic emissions continuously increased until early 2010s and then, decreased slightly. Similar to SO_2, majority of NO_x emissions were from North America and Europe in 1970 and the emission amounts and their shares in global total showed decreasing trends. The trends after the early 2000s reflect temporal variation of NO_x emissions from Asia. The emissions increased largely by the early 2010s and then decreased slightly. Correspondingly, shares of emissions from EANET PCs to global total increased from 12% in 1970 to about 38% in 2011 and then, slightly decreased to 35% in 2015. NO_x emissions are mainly from the combustion of coal, oil, and gas with high temperatures in such as power and large industrial plants and the transport sector especially road transport. The reduction of NO_x emissions in North America, Europe, and East Asia

was basically due to control measures for these sources. However, the decreasing rates were much smaller than those of SO_2 indicating difficulty of controlling NO_x emissions.

Anthropogenic $PM_{2.5}$ emissions are mainly from small combustion such as in residential sector and small industrial plants. In addition, contributions from open biomass and waste burning are larger for $PM_{2.5}$ compared to SO_2 and NO_x. Even in 1970, the share of EANET PCs was about 34% and Asia was the largest emitter region where the share was nearly half global total. Emissions generally increased until the early 2000s reflecting trends of Asia and Africa. Then, emissions in EANET PCs showed slightly decreasing trends while those in Africa continued to increase. On the other hand, emissions from Europe, North America, and Russia decreased largely especially after 1990s. As a result, global emissions were almost stable after 2000. Shares of EANET PCs peaked in early 2000s (about 54%) and in 2015, contribution rates of total emissions in EANET PCs and whole Asia were about 44%, and 65%, respectively.

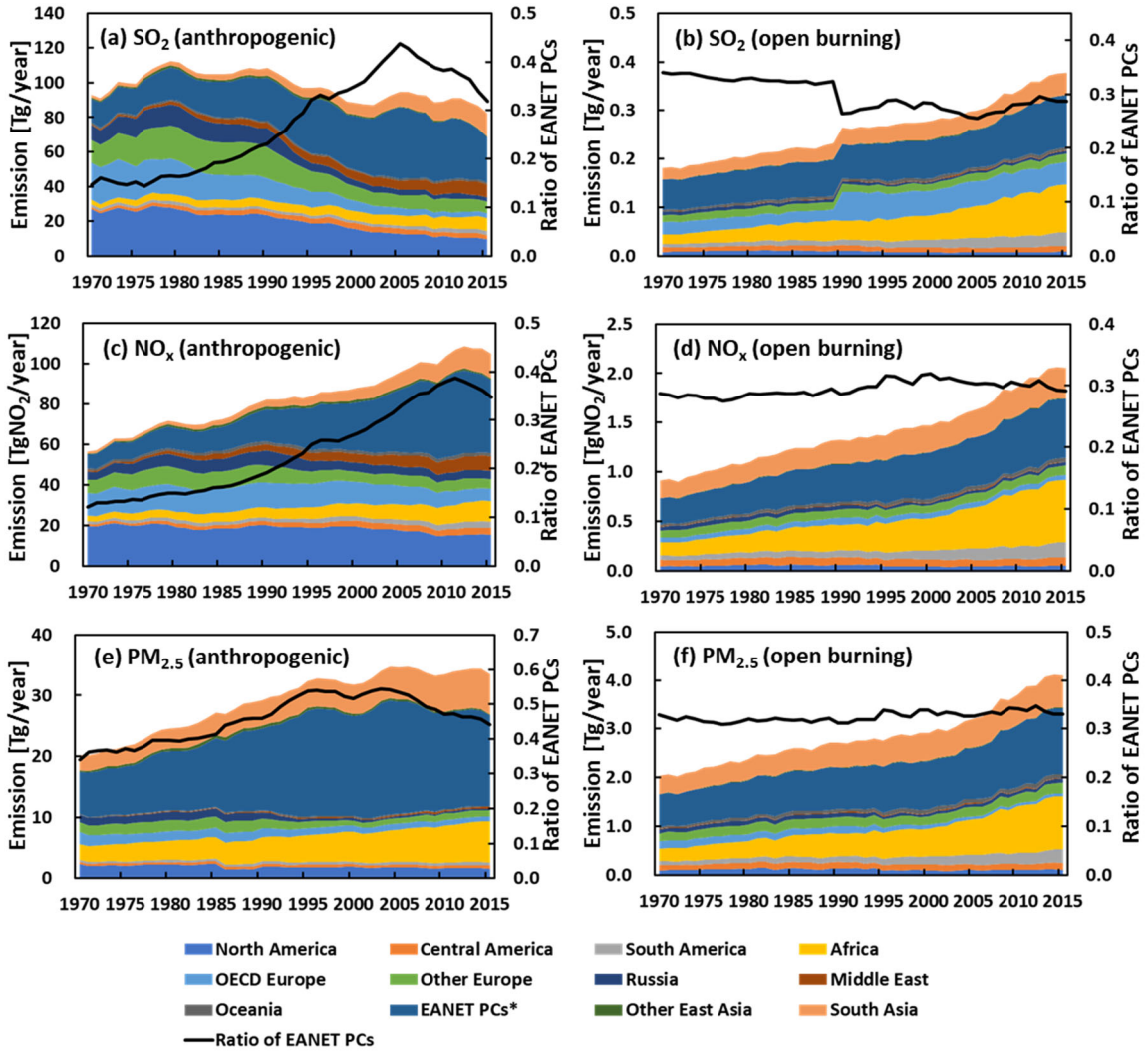

Figure 6.3.1. Time series of global anthropogenic (left panels) and open biomass and waste burning (right panels) emissions of (a,b) SO_2, (c,d) NO_x, and (e,f) $PM_{2.5}$ from world regions. Lines provide ratios of total emissions of EANET participating countries (PCs) except for Russia to global total emissions. Emissions from fuel combustion and industrial processes in Asian regions were from REASv3.2 and all others were from EDGARv5.0. (*In Sect. 6.3, emissions from Russia are not included in those from EANET PCs because majority of emissions of Russia were not from the East Asia region.)

6.3.2 Regional emission inventories in East Asia

(1) Overview of emission inventories in East Asia

With an increase in demand for energy, motorization, and industrial and agricultural products, all the anthropogenic air pollutant emissions in East Asia increased drastically during these 6 decades. On the other hand, situations of the trends were different among countries, sources, and species and thus, spatial and temporal variation of emissions in East Asia are becoming complicated (Kurokawa & Ohara, 2020). Therefore, development of emission inventories focusing on the Asian region has been conducted and continuous efforts for their updates and new development are required.

The earliest Asian emission inventory developed by Kato and Akimoto (1992), estimated SO_2 and NO_x emissions in East, Southeast, and South Asia in 1975, 1980, and 1985-1987. Akimoto and Narita (1994) provided gridded data with a resolution of 1°×1°. There are two major project-based emission inventories in Asia. Streets et al. (2003a, b, 2006) developed Asian emission inventories for the Transport and Chemical Evolution over the Pacific (TRACE-P) field campaign and Zhang et al. (2009) created its successor data for the Intercontinental Chemical Transport Experiment-Phase B (INTEX-B) project. Woo et al. (2020) developed Comprehensive Regional Emissions inventory for Atmospheric Transport Experiment (CREATE) based on GAINS-Asia model. The Regional Emission inventory in ASia (REAS) series provided historical emission datasets in Asia: REASv1.1 for actual emissions during 1980-2003 and projected ones in 2010 and 2020 (Ohara et al., 2007), REASv2.1 focusing on the period between 2000 and 2008 (Kurokawa et al., 2013), and REASv3.2 for a long historical period from 1950 to 2015 (Kurokawa & Ohara, 2020). For East Asian countries, a lot of research-based national emission inventories have been developed. MEIC (Multi-resolution Emission Inventory for China) developed by Tsinghua University is a widely used emission inventory data base for China (Zheng et al., 2018). Zhao et al. (2013, 2014) developed recent and projected emission inventories of air pollutants in China. For Japan, several project-based emission data sets were developed such as the Japan Auto-Oil Program (JATOP) Emission Inventory-Data Base (JEI-DB) (JPEC, 2014) and emission data for Japan's Study for Reference Air Quality Modeling (J-STREAM) (Chatani et al., 2018). Pham et al. (2008) and Permadi et al. (2017) developed emission inventories in Thailand and Indonesia, respectively. Furthermore, similar to global data, a mosaic-based emission inventory was developed in Asia. The MIX inventory, a component of the HTAPv2 inventory as described in Sect. 6.3.1, is a mosaic of up-do-date regional emission inventories (Li et al., 2017): MEIC for China, JEI-DB for Japan, Clean Air Policy Support System (CAPSS) inventory for the Republic of Korea (Lee et al., 2011), and REASv3.2 for default. Table 6.3.2 summarizes general information of major regional emission inventories in Asia.

Table 6.3.2 General information of major regional emission inventories in Asia

Names	Descriptions
REASv3.2	Species: SO_2, NO_x, CO, NMVOCS, NH_3, CO_2, PM_{10}, $PM_{2.5}$, BC, and OC; Year: 1950-2015; Resolution; 0.25°×0.25°; https://doi.org/10.5194/acp-20-12761-2020
INTEX-B	Species: SO_2, NO_x, CO, NMVOCS, PM_{10}, $PM_{2.5}$, BC, and OC; Year: 2006; Resolution; 0.5°×0.5°; https://doi.org/10.5194/acp-9-5131-2009
TRACE-P	Species: SO_2, NO_x, CO, NMVOCS, NH_3, CO_2, CH_4, BC, and OC; Year: 2000; Resolution; 0.5°×0.5°; https://doi.org/10.1029/2002JD003093
CREATE	Species: SO_2, NO_x, CO, NMVOCS, NH_3, CO_2, CH_4, N_2O, PM_{10}, and $PM_{2.5}$;

	Year: 2010; Resolution; 0.1°×0.1°; https://doi.org/10.3390/su12197930
MIX	Species: SO_2, NO_x, CO, NMVOCS, NH_3, CO_2, PM_{10}, $PM_{2.5}$, BC, and OC; Year: 2008 and 2010; Resolution; 0.25°×0.25°; https://doi.org/10.5194/acp-17-935-2017

(2) Trends of SO_2 and NO_x emissions in East Asia

Emissions of SO_2 and NO_x provide fundamental information for assessing acid deposition. In addition, NO_x is an important precursor of tropospheric ozone and both SO_2 and NO_x play roles as precursors of secondary $PM_{2.5}$. Therefore, these species are treated as essential species in anthropogenic emission inventories and were targets of the first comprehensive emission inventory in Asia (Kato and Akimoto, 1992). Anthropogenic emissions of SO_2 and NO_x in EANET PCs from major sector categories during 1995-2015 are shown in Fig. 6.3.2 and those from major fuel types are provided in Fig. 6.3.3. The emissions of PCs in Northeast Asia (NEA: total of China, Japan, Mongolia, and Republic of Korea) and Southeast Asia (SAE: total of Cambodia, Indonesia, Lao PDR, Malaysia, Myanmar, Philippines, Thailand, and Vietnam) are also provided in Figs. 6.3.2 and 6.3.3. In general, structures and trends of SO_2 and NO_x emissions in EANET PCs and NEA are similar, but those in SEA are different.

In EANET PCs and NEA, most SO_2 emissions were from coal combustion in power plants and industry sector controlling trends of total emissions. Drastic changes were found in the 2000s. Emissions increased largely in early 2000s mainly due to contributions from coal-fired power plants, which increased rapidly along with large economic growth. Then, emissions showed decreasing trends after middle of 2000s reflecting effects of control measures, especially flue gas desulfurization (FGD) introduced to large coal-fired power plants and industrial plants in NEA. According to Figs. 6.3.2 and 6.3.3 based on REASv3.2, total emissions of EANET PCs and NEA in 2015 became smaller than those in 1990. SO_2 emissions in SEA were almost stable before 2010, but after 2010, emissions from coal fired power plants increased rapidly. Actually, for SEA, majority of SO_2 emissions were from heavy fuel oil combustions in 1995, but more than half of total emissions were from coal combustions in 2015 as shown in Fig. 6.3.3.

For NO_x, most emissions in EANET PCs and NEA were from coal combustion in power and industry plants and road transport sector especially for diesel vehicles. NO_x emissions increased largely from the early 2000s and continued to increase until 2011. But then the emissions started to decrease by introduction of denitrification technologies such as selective catalytic reduction (SCR) to large power plants and regulations for road vehicles in NEA. Compared to SO_2, timing of the decrease was later and reduction ratios were smaller for NO_x emissions. These features are similar to the case of other countries including North America and Europe. On the other hand, NO_x emissions in SEA especially from diesel road vehicles and coal power plants increased largely and doubled from 1995 to 2015. According to Fig. 6.3.2, for SEA, about half of the increased amounts from 1995 to 2015 were by emissions from road transport sector. For SO_2 and NO_x emissions, contributions from open biomass and waste burning are relatively small in EANET PCs (both NEA and SEA).

In Sect. 6.3, emissions are reviewed based on bottom-up emission inventories where emissions are calculated using activity data such as energy consumption and corresponding emission factors. But there are inevitable uncertainties in the activity data and emission factors. Furthermore, it is impossible to estimate real-time emissions by the bottom-up approach. There is another approach to estimate emissions using observation data, chemical transport models, and numerical algorisms (Ex. Ding et al., 2017 and Itahashi et al., 2019 for top-down NO_x emissions). Recently, satellite observation data of air pollutants have become available in a finer scale. For understanding emissions in East Asia, analyzing both bottom-up and top-down emissions are becoming an important issue.

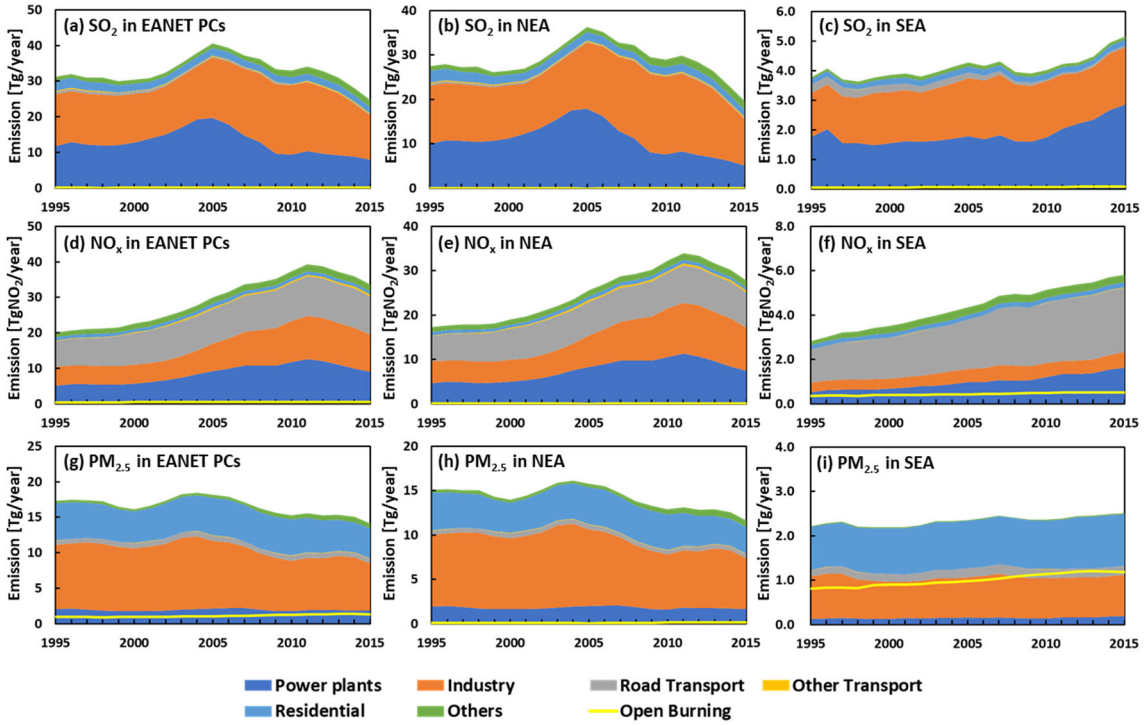

Figure 6.3.2. Time series of anthropogenic emissions from major sector categories (areas) and open biomass and waste burning (yellow lines) of (a, b, c) SO_2, (d, e, f) NO_x, and (g, h, i) $PM_{2.5}$ in (a, d, g) East Asia (total of EANET PCs), (b, e, h) NEA, and (c, f, i) SEA during 1995-2015. Emissions were obtained from REASv3.2 except for those from open biomass and waste burning taken from EDGARv5.0.

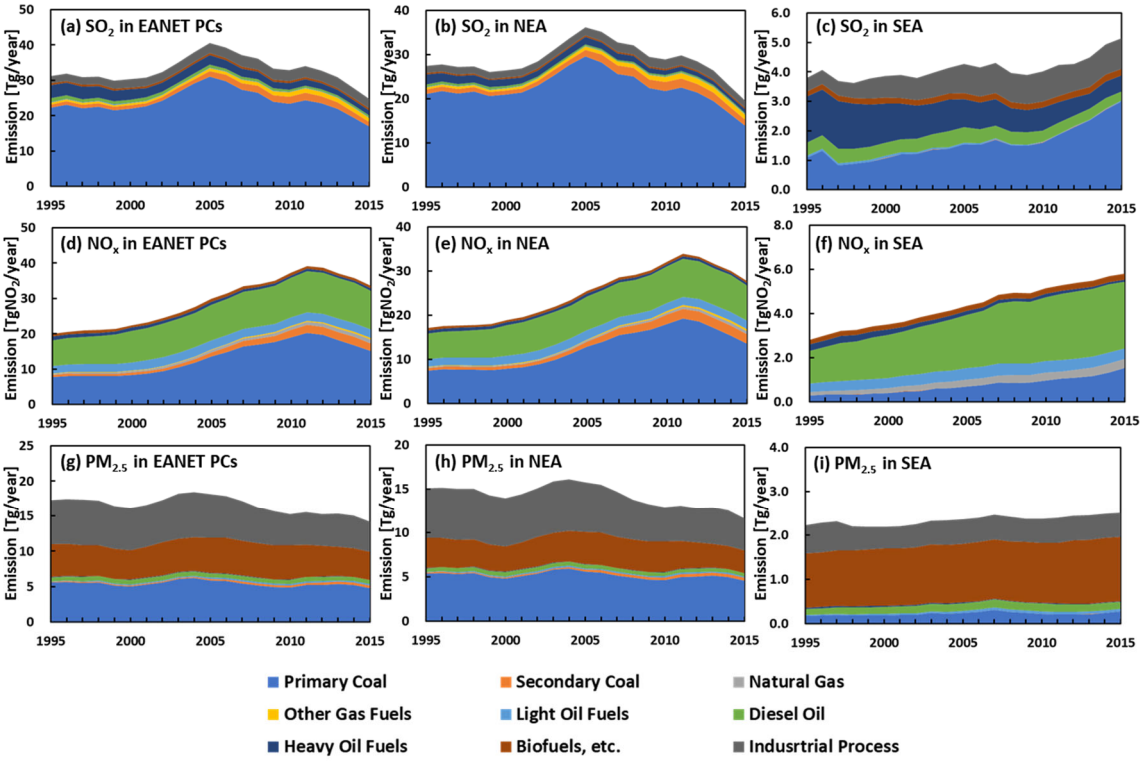

Figure 6.3.3. Time series of anthropogenic emissions from major fuel types of (a, b, c) SO_2, (d, e, f) NO_x, and (g, h, i) $PM_{2.5}$ in (a, d, g) East Asia (total of EANET PCs), (b, e, h) NEA, and (c, f, i) SEA during 1995-2015. Emissions were obtained from REASv3.2 except for those from open biomass and waste burning taken from EDGARv5.0.

(3) Trends of emissions of $PM_{2.5}$ in East Asia

Time series of $PM_{2.5}$ emissions during 1995-2015 in EANET PCs, NEA, and SEA from each major sector category including open biomass and waste burning are presented in Fig. 6.3.2 and those from major fuel types are provided in Fig. 6.3.3. Note that $PM_{2.5}$ and its component species in this section include only primary species directly emitted from such as combustion and industrial processes. The same as the cases for SO_2 and NO_x, structures and trends of $PM_{2.5}$ emissions in EANET PCs and NEA are similar, but those in SEA are different.

Emissions in EANET PCs and NEA slightly decreased before 2000 and then increased until the middle of 2000s mainly controlled by coal consumption in the industry and residential sectors and industiral process emissions in NEA. Then, emissions showed decreasing trends due to the effects of control measures on the industry sector and decreased biofuel consumption in the residential sector in NEA. For SEA, most anthropogenic emissions were from the industry and residential sector similar to NEA, but relative ratios of residential emissions mainly from biofuel combustion were larger than NEA (about 46% to total in 2015). On the other hand, in addition to anthropogenic emissions, contributions from open biomass and waste burning emissions in SEA were relatively large (about 32% to total in 2015) compared to NEA.

According to REASv3.2 used for Figs. 6.3.2 and 6.3.3, shares of $PM_{2.5}$ emissions in 2015 from power plants, industry, and residential sectors in EANET PCs/NEA/SEA were 12%/14%/5%, 43%/48%/25%, and 27%/26%/31%, respectively and those from coal comsuption, biofuel usage, and indusrrial process (non-combustion) were 34%/39%/11%, 28%/22%/58%, and 30%/32%/22%, respectively.

(4) Trends of NH_3 emissions in East Asia

NH_3 is an important species for assessing the status of air pollution, especially to evaluate acid deposition and secondary $PM_{2.5}$. In addition, NH_3 is a key species in the nitrogen cycle and thus, affects status of the ecosystem as well as air quality. Figure 6.3.4 provides NH_3 emissions from major sector categories including open and waste biomass burning in EANET PCs, NEA, and SEA during 1995-2015. Obviously, most NH_3 emissions in EANET PCs (both NEA and SEA) are from agricultural sources: fertilizer application and manure management. (Note that "Fertilizer Application" in Fig. 6.3.4 includes contributions from both synthetic fertilizer and animal manure used as fertilizer.) According to global emission inventories, most countries have the same features (McDuffie et al., 2020), but it is much important in Asia because agriculture is an important industry in most countries in Asia, especially SEA. In addition, to sustain increasing number of population, improving the efficiency of agricultural production is also an important issue causing increasing amounts of fertilizer consumption and numbers of livestock. According to REASv3.2 used for Fig. 6.3.4, NH_3 emissions in EANET PCs/NEA/SEA from agricultural activities increased almost constantly in these two decades (about 20%/18%/57% from 1995 to 2015). Major NH_3 emission sources other than agricultural activities are latrines, industrial process in synthetic fertilizer production and biofuel combustion. Furthermore, three-way catalyst to road vehicles and denitrification equipment introduced to power plants emit NH_3 which might be becoming important sources in EANET PCs. For NH_3 emissions, contributions from open biomass burning were larger than those for SO_2 and NO_x. Note that uncertainties of NH_3 emissions are generally higher than other species due to lack of emission factors based on local information. Researches for country specific emission factors in Asia especially for agricultural sources are necessary.

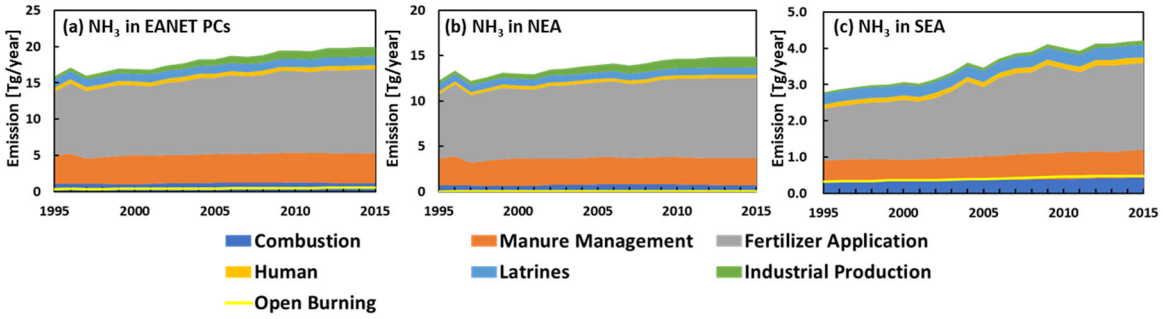

Figure 6.3.4. NH_3 emissions from major sector categories (areas) and open biomass and waste burning (the yellow line) in (a) East Asia (total of EANET PCs), (b) NEA, and (c) SEA during 1995-2015. Emissions were obtained from REASv3.2 except for those from open biomass and waste burning taken from EDGARv5.0.

(5) Trends of $NMVOC_S$ emissions in East Asia

NMVOCSs are organic chemical compounds including hazardous species such as benzene and toluene. But, in air pollution problems, NMVOCs are treated as an important precursor of tropospheric ozone which is not only a harmful air pollutant but also controls chemical substances related to acid deposition. Therefore, understanding and controlling anthropogenic NMVOCs emissions are expected to be a more important issue in Asia. Figure 6.3.5 shows time series of NMVOCs emissions from major sector categories in EANET PCs, NEA, and SEA during 1995-2015. Similar to SO_2, NO_x, and $PM_{2.5}$, structures and trends of NMVOCs emissions in EANET PCs and NEA are close. For SEA, trends of emissions are similar to those of EANET PCs and NEA, but sector contributions are different. NMVOCs emissions in EANET PCs (both NEA and SEA) increased almost monotonically until 2015 mainly due to contributions from stationary non-combustion sources as well as road transport including evaporative emissions. According to REASv3.2 used for Fig. 6.3.5, a share of emissions in EANET PCs/NEA from stationary combustion and road transport was about 56%/55% in 1995, but in 2015, that of stationary non-combustion sources were about 53%/64% and in particular, emissions from solvent and paint uses were nearly 37%/47% of total emissions. On the other hand, half of the increase of NMVOC emissions in SEA during 1995 and 2015 was by road vehicles and majority of the rest was stationary non-combustion sources. In SEA, emissions from stationary combustion and those from open biomass and waste burning were relatively large compared to NEA. For stationary combustion, most emissions were from biofuel combustion in the residential sector. For precursors of ozone and $PM_{2.5}$, NMVOC emissions not only from anthropogenic sources but also biogenic sources, where high reactive species such as Isoprene and Terpene are emitted, should be taken into consideration.

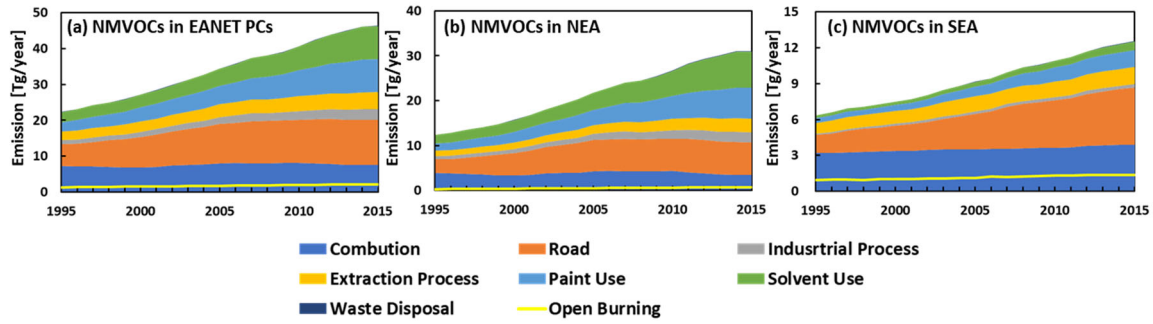

Figure 6.3.5. NMVOCs emissions from each sector category (areas) and open biomass and waste burning (the yellow line) in (a) East Asia (total of EANET PCs), (b) NEA, and (c) SEA during 1995-2015. Note that "Road" includes contributions from both exhaust and evaporative emissions and "Extraction Process" includes emissions from extraction and handling of fossil fuels, oil refinery, transport and depots, and service stations. Emissions were obtained from REASv3.2 except for those from open biomass and waste burning taken from EDGARv5.0.

6.3.3 National emission inventories in EANET member countries

In air quality management, emission inventories have essential roles providing such as trends and status of emissions and input data for air quality models necessary to assess contributions and impacts from each emission source on air quality, echo system, human health, etc. In this section, emissions in East Asia were reviewed and discussed based on research-based emission inventories such as REASv3.2. However, in the development of the research-based emission inventories, there are a lot of limitations such as accessibility of local data including detailed national statistics for activity data and information of technologies related to estimating emission factors. In addition, it is difficult to secure enough budgets to develop emission inventories regularly or in the necessary time interval especially focusing on a specific country. Therefore, a national emission inventory officially supported and maintained by each country is preferable for air quality management. However, the situation and policies for the national emission inventory are different from country to country. The current status of national emission inventories in EANET member counties is summarized in Table 6.3.3 based on information provided by SAC members of each participating country. EANET is expected to play an important role in supporting capacity building and information sharing for national emission inventories.

Table 6.3.3 Current status of national emission inventories in EANET member countries

No	Country	Status	Species	References
1	Cambodia	1. UNFCC National GHG EI	1. CO_2, CH_4, N_2O, and HFCs	1. National GHG Emissions Inventory Report (https://unfccc.int/sites/default/files/resource/National_GHG_Inventory_Cambodia.pdf)
2	China	1. National Emission Amounts 2. Second Pollution Source Census	1. and 2. SO_2, NO_x, and PM	1. Ministry of Ecology and Environment of China has an environmental statistical reporting system, which collect emission data from local government of provinces and cities. 2. In 2020, China central government has conducted Second Pollution Source Census, which is largest ever emission inventory work by central government and the base year is 2017.
3	Indonesia	1. UNFCCC National GHG EI	1. CO_2, CH_4, N_2O, CF_4, and C_2F_6 (CO and NO_x for agriculture, forestry and other land use)	1. INDONESIA SECOND BIENNIAL UPDATE REPORT (https://unfccc.int/sites/default/files/resource/Indonesia-2nd_BUR.pdf)
4	Japan	1. $PM_{2.5}$EI of MEOJ	1. Primary $PM_{2.5}$, SO_2, CO,	1. Information for PM2.5EI of Ministry of Environment Japan (MOEJ) (in Japanese)

		2. NMVOCs EI of MEOJ 3. UNFCCC National GHG EI	SPM, NO_x, VOCs, and NH_3 2. NMVOCs 3. CO_2, CH_4, N_2O, HFCs, PFCs, SF_6, NF_3, SO_2, NO_x, CO, and NMVOCs	(http://www.env.go.jp/air/osen/pm/info.html #INVENTORY) 2. Information for NMVOC EI (MEOJ) (in Japanese) (https://www.env.go.jp/air/osen/voc/inventory.html) 3. National Greenhouse Gas Inventory Report of JAPAN (https://unfccc.int/sites/default/files/resource/jpn-2021-nir-13apr21.zip)
5	Lao PDR	1. UNFCCC National GHG EI[3]	1. CO_2, CH_4, and N_2O	1. THE FIRST BIENNIAL UPDATE REPORT OF THE LAO PDR (https://unfccc.int/sites/default/files/resource/The%20First%20Biennial%20Update%20Report-BUR_Lao%20PDR.pdf)
6	Malaysia	1. UNFCCC National GHG EI	1. CO_2, CH_4, N_2O, HFCs, PFCs, SF_6 and NF_3	1. THIRD BIENNIAL UPDATE REPORT TO THE UNFCCC (https://unfccc.int/sites/default/files/resource/MALAYSIA_BUR3-UNFCCC_Submission.pdf)
7	Mongolia	1. Case study of National EI	1. SO_2, NO_x, TSP, PM_{10}, $PM_{2.5}$, CO, NMVOC, and NH_3	1. National Emission Inventory using The National Emission Inventory Guideline for Air Pollutants, Batbayar. J, Amarzaya. E, National Agency for Meteorology and Environmental Monitoring (NAMEM), MNE (https://www.envpol.mne.gov.mn)
8	Myanmar	1. UNFCCC National GHG EI	1. CO_2, CH_4, N_2O, CO, NO_x, NMVOCs, SO_2, SF_6, and ODSs	1. MYANMAR'S INITIAL NATIONAL COMMUNICATION UNDER THE UNITED NATIONS FRAMEWORK CONVENTION ON CLIMATE CHANGE (UNFCCC)(https://unfccc.int/resource/docs/natc/mmrnc1.pdf)
9	Philippines	1. EI of EMB	1. PM, SO_2, NO_x, CO, and VOC	1. Philippines National Air Quality Status Report 2016-2018 (https://air.emb.gov.ph/wp-content/uploads/2021/07/NAQSR-2016-2018- FV.pdf) Philippine Emission Inventory 2018 (https://air.emb.gov.ph/emission-inventory-

				2018) DENR-Environmental Management Bureau (EMB) Website (https://emb.gov.ph)
10	Republic of Korea	1. National Air Pollutants Emission Service 2. UNFCCC National GHG EI	1. SO_2, NO_x, CO, VOC, NH_3, TSP, PM_{10}, and $PM_{2.5}$ 2. CO_2, CH_4, N_2O, HFCs, PFCs, and SF_6	1. Information for National Air Pollutants Emission Service (in Korean) (http://airemiss.nier.go.kr/mbshome/mbs/airemiss/index.do) 2. Third Biennial Update Report of the Republic of Korea (https://unfccc.int/sites/default/files/resource/Third%20Biennial%20Update%20Report%20of%20the%20ROK%20under%20the%20UNFCCC.pdf)
11	Russia	1. UNFCCC National GHG EI	1. CO_2, CH_4, N_2O, HFCs, PFCs, SF_6, NF_3, SO_2, NO_x, CO, and NMVOC	1. Russian Federation. 2021 Common Reporting Format (CRF) Table (https://unfccc.int/sites/default/files/resource/rus-2021-crf-15apr21.zip)
12	Thailand	1. EI System Web Application has been developed in 2020 and still ongoing improved and revised. The EI is planned to use as AQM tool for local Administration (not yet implemented) 2. UNFCCC National GHG EI	1. $PM_{2.5}$, PM_{10}, NO_x, N_2O, SO_2, CO, NMVOC, NH_3, BC, and OC 2. CO_2, CH_4, N_2O, SO_2, NO_x, CO, and NMVOCs	1. Pollution Control Department. Air Quality and Noise Management Division, 2021. 2. THAILAND THIRD BIENNIAL UPDATE REPORT (https://unfccc.int/sites/default/files/resource/BUR3_Thailand_251220%20.pdf)
13	Vietnam	1. UNFCCC National GHG EI	1. CO_2, CH_4, N_2O, and HFCs	1.VIET NAM THIRD BIENNIAL UPDATED REPORT (https://unfccc.int/sites/default/files/resource/Viet%20Nam_BUR3.pdf)

6.4 Chemical transport modeling studies

In this section 6.4, studies related to the chemical transport model (CTM) are reviewed. Subsection 6.4.1 presented the brief introduction for CTM, and Subsection 6.4.2 and 6.4.3 respectively reviewed the related CTM studies for atmospheric composition (mainly focused on $PM_{2.5}$ and O_3) and acid deposition.

6.4.1 Introduction of CTM studies

Air pollutants and depositions are affected by not only local sources but also the long-range transport. Observation network such as 202 is vitally important to measure phenomena in the atmosphere. However, interpreting such phenomena from observation itself is sometimes difficult due to the complex impacts of both nearby and distant sources. Chemical transport models (CTMs), which numerically representing the processes of emissions, transport, chemical reactions, and depositions, have been recognized as an important approach. The emission data is one of the important input dataset for CTMs prepared using emission inventories (see, Section 6.3). Another important input data is the meteorological field generated by the meteorological model. For example, the meteorological data of wind fields are used for the transport (advection and diffusion) process. The chemical reactions and depositions are internally calculated by CTMs, but required temperature and relative humidity in the chemical reaction processes are also taken from meteorological fields. The application of CTMs varies the target phenomena. With regard to the horizontal grid resolution, CTMs can be divided into two types of framework; the regional CTMs and the global CTMs. Generally, the regional CTMs targeted local-to-regional scales with a few to tens kilometers and the global CTMs targeted whole over the world with coarse-resolution greater than a hundred kilometers. Because the targeted domain by the regional CTMs also affected by the global-scale ambient pollution, the lateral boundary condition for the regional CTMs are taken from global CTMs. CTMs have been developed by each researcher or group; however, the open-source models are also available currently. For example, the Community Multiscale Air Quality (CMAQ) modeling system (Byun and Schere, 2006) released by the U.S. Environmental Protection Agency (EPA) is one of the typical regional CTM. Not only to understand the spatiotemporal behavior of air pollutants by CTMs, CTMs can be also applied to investigate the important processes. For example, by reducing the specific emission sources and then conduct the additional simulation, the impact caused by the specific emission sources can be estimated. These applications are so-called the source-receptor (S/R) analysis, and the simplest way is changing the input emission data and subsequently conducting the additional simulation using different emissions (i.e., brute-force method). Other ways are the tagged tracer method and the direct method (Clappier et al., 2017). The former is using tags for S/R analysis. In this case, the tags can be applied for the emission source itself or the source region where air pollutants formed. The latter is the method to directly calculate sensitivities for S/R analysis on along with simulation (i.e., decoupled direct method; DDM). Today, CTMs researches are one of an important approach to foster our understanding on the air quality. The example of a feedback loop between observation and CTMs is illustrated in Figure 6.4.1.

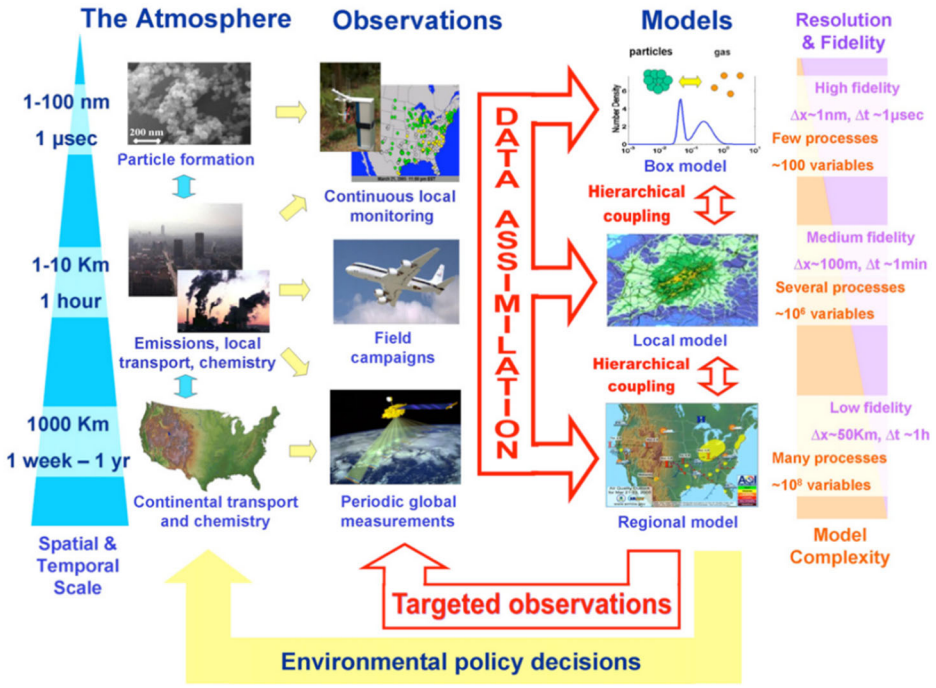

Figure 6.4.1. Information feedback loops between models and observations as they relate to predicting air quality. Complex CTMs incorporate chemical, aerosol, radiation modules, and use information from meteorological simulations (e.g., wind and temperature fields, turbulent diffusion parameterizations) and from emission inventories to produce chemical weather forecasts. Yellow arrows represent the data flow for predictions using the first principles. Another source of information for concentrations of pollutants in the atmosphere is the observations. Data assimilation combines these two sources of information to produce an optimal analysis state of the atmosphere, consistent with both the physical/chemical laws of evolution through the model (first principles) and with reality through measurement information. Pink arrows illustrate the data flow for dynamic feedback and control loop from measurements/data assimilation to simulation. Targeted observations locate the observations in space and time such that the uncertainty in predictions is minimized (source: Fig. 1 of Carmichael et al., 2008a).

Although CTMs are based on state-of-the-art science, it should be taken into accounts that uncertainties are existing in CTMs (Carmichael et al., 2008a). An interpretation based on one CTM can cause misunderstanding of phenomena due to its uncertainty. To further our understanding of CTMs over Asia, the Model Inter-Comparison Study for Asia (MICS-Asia) has been established. Phase I was conducted in 1998–2000 (Carmichael et al., 2002), Phase II was in 2003–2008 (Carmichael et al., 2008b), and Phase III was in 2010–2020. MICS-Asia Phase I focused on sulfur (SO_2 and SO_4^{2-}) concentrations and deposition in January and May 1993. Observation datasets of sulfur were prepared by a cooperative monitoring network in East Asia (Fujita et al., 2000). A total of 18 sites located in China, Republic of Korea, and Japan were compared with models. MICS-Asia Phase II extended its focus on O_3 and PM (Carmichael et al., 2008b). To compare the seasonality, the four representative months of March, July, and December 2001 and March 2002 were analyzed. Historically, consistent and reliable observation dataset over the Asian region has been a bottleneck for the analysis of ambient concentration and deposition, and hence the evaluation of CTM. To address this issue, EANET has been established in 2001 and providing observation data up to now. In MICS-Asia Phase II, the EANET observation data at 43 sites were compared with models. As the lesson learned in Phase II, emission data were made to be uniform; however, participant models used different modeling domains with different horizontal and vertical structures and also used different meteorological models. In MCS-Asia Phase III, the targeted year was 2010 to fully cover the entire year. The modeling domain was coordinated, and the modeling inputs data such as meteorological

field and emission data are also unified. For emission data, the topic 2 of MICS-Asia Phase III established the MIX emission inventory (Li et al., 2017). In the following subsections of 6.4.2 and 6.4.3, scientific results from MICS-Asia activities are presented. In addition, relevant results from CTMs studies conducted over East Asia are also reviewed.

6.4.2 Atmospheric composition

The analysis for O_3 and relevant species in MIICS-Asia Phase II was summarized (Han et al., 2008). Features on the spatial distribution were consistently reproduced by models over the western Pacific Rim, and well captured day-to-day variation especially in July 2001. However, larger differences were found over southern China and northern Southeast Asia, and in addition, all models failed to represent O_3 behavior over the upper troposphere. The overview of model evaluation and intercomparison for O_3 in MICS-Asia Phase III was reported (Li et al., 2019). Models captured the key patterns of monthly and diurnal variations; however, large positive biases in models during the summer season were found over the North China Plain and western Pacific Rim. It was suggested that most models in MICS-Asia Phase III missed the key processes for O_3 formation. To seek the current modeling performance in detail, because the model overestimation during summer was not detected in MICS-Asia Phase II but found in Phase III, some selected models were further analyzed (Akimoto et al., 2019; 2020). The model included the heterogeneous reaction of HNO_3 (on soot surface) $\rightarrow$ NO + NO_2 led to a better agreement with observation for NO and nighttime O_3. In addition to this chemical reaction, the vertical transport was considered as the important factor to make the difference in the model performance of O_3 at Beijing and Tokyo (Akimoto et al., 2019). At the western Pacific Rim, long-range transport from the Asian continent, in-situ photochemical production, and dry deposition process over oceans were identified as the key points to lead model overestimation (Akimoto et al., 2020).

The following studies are related to O_3 analysis over Asia. Yamaji et al. (2006) performed CMAQ simulations for East Asia in 2002. The results showed that in summer, O_3 production by emissions in the area was the largest, especially in most of China, and the area around the Yangtze River accounted for most of the O_3 concentration. On the other hand, in winter and early spring, the O_3 influx from outside the East Asian region contributes significantly to the surface O_3 concentration over this area. It was also concluded that O_3 in Japan was characterized by spring and autumn peaks and low concentrations in summer. The spring peak could be separated from the results of two impact simulations, i.e., inflow from outside the region in early spring and photochemical production by emissions within the region in late spring. Nagashima et al. (2010) introduced the tagged tracer method into the global CTM of CHASER (Sudo et al., 2002). By tagging the emission sources, the contribution of each source region to the surface O_3 concentration in East Asia in the early 2000s was estimated. The results showed that in the cold season, O_3 transported from remote areas outside of East Asia contributed about half of the East Asian surface O_3, while in the warm season, O_3 produced within the region mostly contributed. This result is shown in Figure 6.4.2. Li et al. (2016) conducted O_3 simulation for the East Asian region in 2010 with the tagged tracer method in a regional CTM of NAQPMS (Wang et al., 2001). They reported that the contribution of long-range transport from outside East Asia accounted for most of the annual surface ozone in the Korean Peninsula, Japan, and remote areas. On the other hand, the contribution of homegrown O_3 in the Korean peninsula and Japan was same level or higher than the contribution of O_3 produced in China. Under the situation of a high amount of anthropogenic emission in East Asia, appropriate emission regulation strategies are desired to reduce O_3 pollution. In contrast to this situation over East Asia, Southeast Asia are also affected by biomass burning emissions. Ammuyalojaroen et al. (2014) conducted the model simulation with different emission inventories. The result pointed out the variability of simulated O_3 concentration were small against anthropogenic emission inventories but large for biomass burning emissions. Marvin et al. (2021) also revealed the importance of biomass burning emissions to form local O_3 during biomass burning seasons.

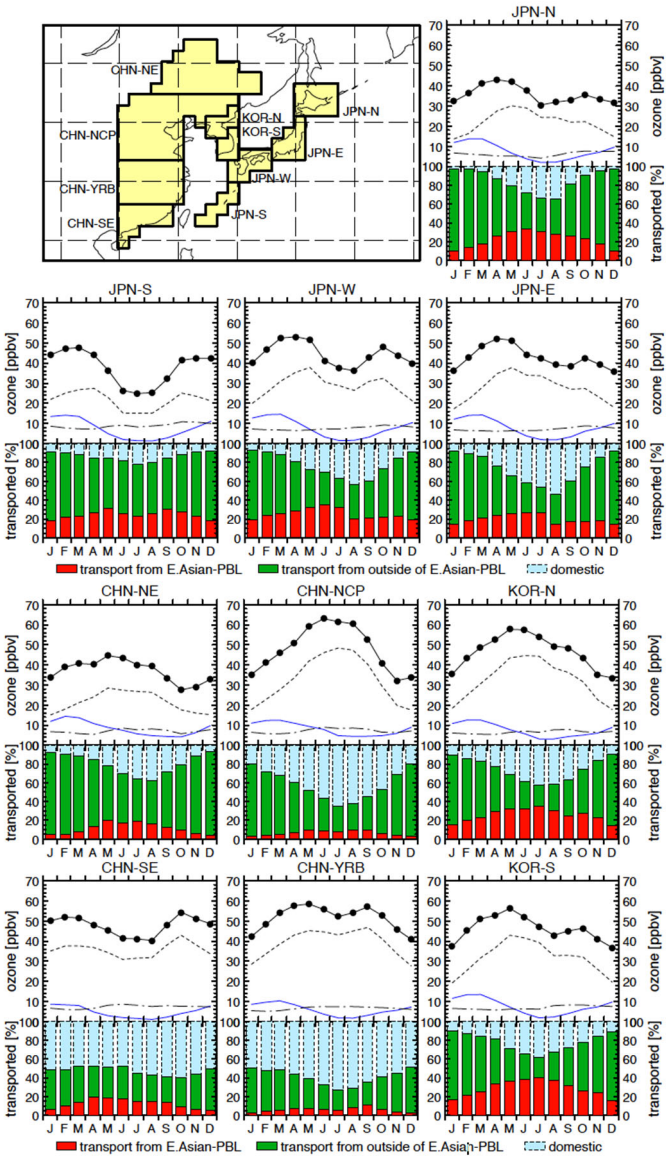

Figure 6.4.2. (Top plots of each figure) Seasonal variations of the area averaged monthly mean surface O3 with contributions from the stratosphere (blue solid lines), PBL (black dashed lines), and FT (black dash-dotted lines), calculated by the model. The map shows the areas of averaging. (Bottom plots of each figure) Red bars indicate the contribution (%) of O3 originating from the PBL in the East Asian source region, green bars from outside of the East Asian PBL, and pale blue bars from domestic pollution (see details in the manuscript). All values are averaged for 6 years (source: Fig. 4 of Nagashima et al., 2010).

The model intercomparison on MICS-Asia Phase II for inorganic aerosol components was reported (Hayami et al., 2008). The participated models performed well for SO_4^{2-} and total ammonium (NH_3 and NH_4^+); however, models constantly and considerably underestimated total nitrate (HNO_3 and NO_3^-). On the other hand, NO_3^- was slightly overestimated in MICS-Asia Phase III (Chen et al., 2019). The comparison between Phase II and Phase III was also conducted, and it was reported that the spread of root mean square error was smaller and the correlation coefficient was improved in Phase III. In phase III, negative bias in SO_4^{2-} was found, and this reason was considered as the insufficient oxidation process from SO_2 to SO_4^{2-} (Tan et al., 2020). Alongside evaluating the secondary aerosols, investigations of precursor-gases are also important (Kong et al., 2020). Another important approach is the online simulation in CTMs. Theoretically, meteorological parameters, e.g., radiation, temperature, boundary height are related to aerosol behavior. The meteorology and

chemistry should be inherently coupled together, and this approach is called online-coupled CTMs (Zhang, 2008). Under MICS-Asia Phase III, online-coupled model intercomparison have been also conducted. Simulated aerosol optical depth during clean periods were similar whereas peak values during severe haze periods were different because of the different inorganic aerosol components and hygroscopic growth efficiency (Gao et al., 2018). The aerosol direct radiative forcing during January 2010 was estimated, and the average reduction in near-surface temperature was estimated as 0.3-1.6 °C during severe haze events. For the estimated aerosol direct radiative forcing, it was indicated that the aerosol mixing status was important, in addition, black carbon played a key role although the composition on $PM_{2.5}$ was small (Gao et al., 2020).

Related to aerosol, the following studies revealed its behavior over Asia. Li et al. (2014) estimated the S/R relation of PM_{10}, and results showed that the largest attributions were self-contributions in China (49%), Korea (42%), and Japan (39%. Over China, by dividing into seven regions, local and inter-regional contributions of SO_4^{2-} and NO_3^- were estimated (Ying et al., 2014). Wintertime sulfate concentrations demonstrated a more significant inter-regional southward transport pattern and wider spatial distributions than nitrate, and this feature was significant during winter than summer. Although the cities were mostly affected by local region emissions, the influence of the long-range transport were obvious for SO_4^{2-}. Over downwind region of China, many studies have been conducted to clarify the long-range transport. Over Republic of Korea, the effect of emission controls on both China and Republic of Korea have been examined (Kim et al., 2021). The importance of international collaboration for efficient pollution mitigation in terms of NH_3 control has been suggested. Itahashi et al. (2012) applied the DDM, which directly calculated sensitivities to emissions, with CMAQ to two high concentration events observed at EANET's Oki site in July 2005, and the result showed that the seasonal impact showed that local impacts were significant for Korea, and Japan in summer. Based on various numerical method, Chatani et al. (2020) investigated the S/R analysis of $PM_{2.5}$ in Japan. They clarified that transport from outside Japan plays a key role for secondary $PM_{2.5}$ components, and the non-linearity influence is essential to derive effective strategies to reduce secondary $PM_{2.5}$ pollution. Over Southeast Asia, various studies based on CTMs have been published. Lee et al. (2017) conducted an analysis of severe haze events in Southeast Asia, 2003-2014, using WRF-Chem. According to this analysis, most of them were affected by biomass burning, and averaged over the last decade, the contribution of aerosols generated by biomass burning during low-visibility days were 39% in Bangkok, Thailand, 36% and 33% respectively in Kuala Lumpur and Kuching, Malaysia, and 34% in Singapore. The impact of biomass burning is large over Southeast Asia both for O_3 and $PM_{2.5}$. Nguyen et al. (2019) conducted the both offline and online modeling over continental Southeast Asia, and reported the importance of aerosol direct effect which decreased meteorological parameters of the shortwave radiation, temperature, the planetary boundary height (PBL), and wind speed; subsequently enhanced $PM_{2.5}$ concentration whereas reduced O_3 concentration.

6.4.3 Acid deposition

In MICS-Asia Phase I, estimates of deposition were consistent among different models, but varied by a factor of 5 at some locations (Carmichael et al., 2002). The reason for this variability was determined to be the input data of emissions and meteorological field. It was also found that the model structure of vertical resolution was more important than the parameterization used in the chemical conversion and removal processes. In Phase I, the target species for deposition analysis was limited only sulfur wet deposition. In Phase II, focuses were extended into the dry deposition of aerosols of SO_4^{2-}, NO_3^-, NH_4^+ and the relevant gas species of SO_2, HNO_3, NH_3, and the wet deposition of SO_4^{2-}, NO_3^-, NH_4^+. Total of 37 EANET sites for wet deposition over four representative months were compared with models (Wang et al., 2008). The models generally reproduced acid depositions in China, Korea, Japan, and Southeast Asia, but could not accurately describe depositions in inland areas such as Mongolia and Russia. These differences were attributed to differences in meteorology, chemical mechanisms, and deposition parameterizations. In Phase III, the targeted species further included the dry deposition of H_2SO_4, NO and NO_2 in addition to the species on Phase II. Moreover, total of 54 EANET sites including southeast Asian countries were analyzed, and the analyzed period

covered 2010 entire year. The overview paper for wet deposition presented the annual accumulated deposition status over Asia (Itahashi et al., 2020). The models generally captured the wet deposition observed at EANET sites, but underestimated SO_4^{2-} and NH_4^+ and the differences among models were large for NO_3^-. The result for total N deposition (defined as the sum of dry and wet deposition of NO, NO_2, HNO_3, and NO_3^-) are shown in Figure 6.4.3. It showed large variation among models over each country; suggesting the large uncertainties related deposition processes in the current model. The comparison between deposition amount and anthropogenic emission over each country indicated the role of other emission sources or the long-range transport from outside of its country. Although the model estimated deposition had large variabilities, the possibilities of the importance of long-range transport of nitrogen, and lateral boundaries, especially north Asia, and biomass burning, especially over southeast Asia have been suggested from this model intercomparison study. Over Asia, wet deposition was dominant factor compared to the dry deposition, and the importance of dry deposition over land were commonly found in all models. The meteorological modeling performance for precipitation itself is one of the keys to improve the wet deposition performance. In previous studies, publicly available observation data over China, where is one of the dominant emission sources in Asia, were limited. However, a nationwide observation has been established and the advantage in MICS-Asia Phase III is to use such observation data over China. The reactive nitrogen over China was analyzed and the result showed that wet deposition amount of NH_4^+ was underestimated by all models (Ge et al., 2020).

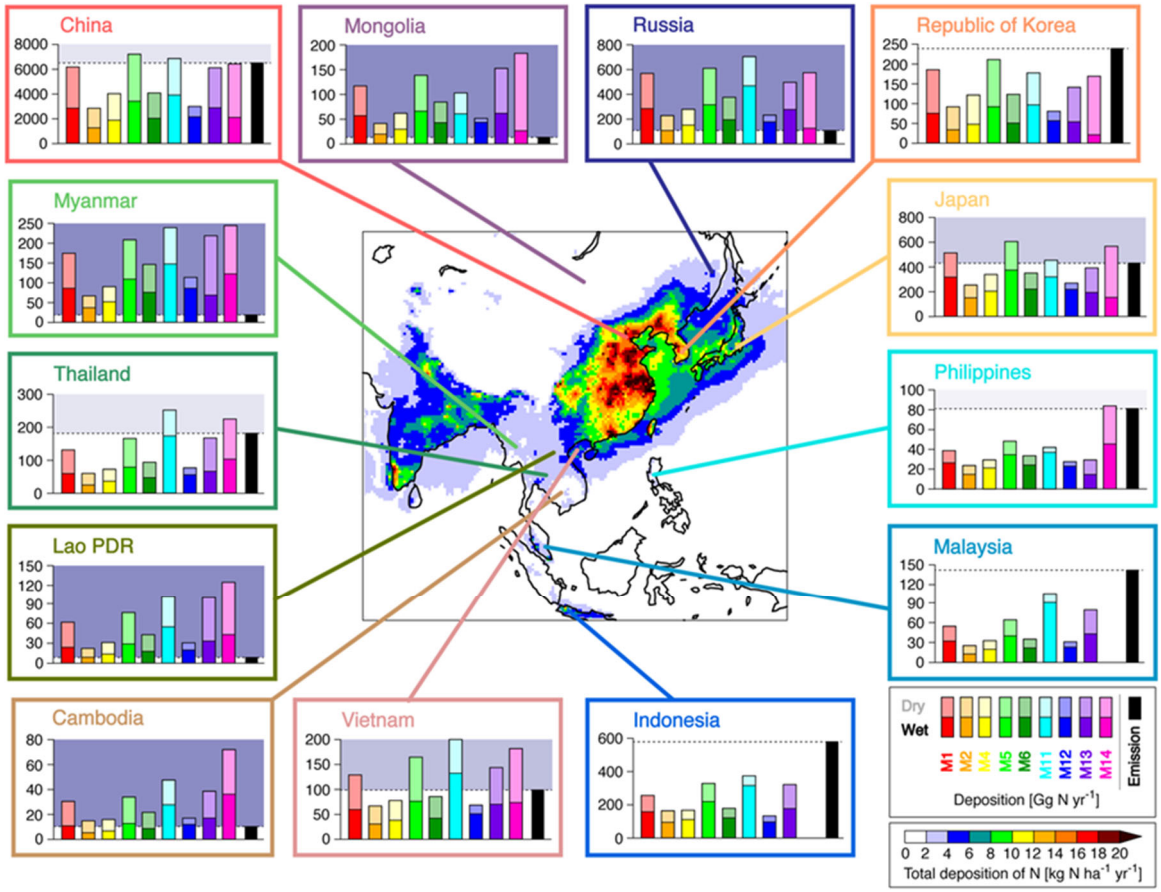

Figure 6.4.3. Map of the annual accumulated total N deposition over Asia. The cumulative bar graphs show dry deposition (light colors) and wet deposition (dark colors), with different colors representing different models and black representing the amount of anthropogenic NO_X emissions. The background blue areas of the graphs indicate an excess of total deposition compared to emissions, and their transparency is based on the number of models making this prediction (i.e., bolder colors indicate that more of the nine models simulated the excess) (quoted with modification: Fig. 10 of Itahashi et al., 2020).

Other studies for deposition analyses over Asia are as follows. Lin et al. (2008) conducted a sensitivity analysis of emissions to acid deposition using CMAQ by the brute force method for 2001. The results showed that emissions from eastern China made a considerable contribution greater than 20% to acid deposition over East Asia's wide area during the analysis period. On the other hand, the transport from outside of Asia also has an enormous impact, with northwest China, Mongolia, and Russia having a huge impact compared to the others. Furthermore, the impact of volcanoes on sulfur deposition in Japan was more significant than the results before this study, pointing to the importance of pollutant emissions from volcanoes on a sulfur deposition. Kajino et al. (2011) used the regional CTM of Regional Air Quality Model (RAQM) (An et al., 2002; Han, 2007) to investigate the S/R relationship of sulfur deposition in East Asia in 2002. The investigated regions are divided into three Chinese areas, Republic of Korea, and Japan. The results showed that the largest contribution on each region was self-contribution, accounting for 53-84%. The contribution of emissions from Japanese volcanoes was significant for the northwestern Pacific. Kajino et al. (2013) used RAQM2 (Kajino et al., 2012) to perform a S/R analysis of total nitrate deposition in Japan, China, and Korea for 2006 using the brute force method. The effect of sea salt on total nitrate was also examined. As a result, each country's largest contribution was from its own emissions in the summer season. In the presence of sea-salt particles, total nitrate deposition to Korea and Japan increased about 10-25%, and that in the ocean increased about 40%. However, sea salt contribution to source-receptor analysis was almost smaller than 10%, especially in summer, and smaller than 4% in all regions. Zhao et al. (2015) analyzed nitrogen deposition over the Pacific Northwest and estimated the contribution of various sources. The annual averaged total deposition in the Pacific Northwest ranged from 0.8 to 20 kg N/ha. Ship and marine emissions made a small contribution to the deposition near the continent but were important far from the continent. As one example, the value of 10 kg N/ha has been proposed to diagnose the threat for biodiversity on land (Bleeker et al., 2011). As suggested from these studies and also Figure 6.4.3, East Asia could be facing this threat due to the expansion of anthropogenic emissions. To diagnose the nitrogen deposition with finer-resolution in both time and space, CTM can be a useful approach. However, as seen in Figure 6.4.3, the model estimated nitrogen burden still contains uncertainties; therefore, further improvements in modeling processes are indeed required tasks for future study in Asia.

6.5 Ecological impact assessment studies

The EANET has been monitoring atmospheric deposition and its effects on ecosystems since 2001. Many of sites have already accumulated the data for more than 10 years. However, the number of monitoring sites is still limited for ecological monitoring on soil, vegetation, inland water, and forest catchments. Therefore, only by the EANET data, it is difficult to assess impacts of air pollution/total atmospheric (wet + dry) deposition on ecosystems on the East Asian scale. Fortunately, impacts of atmospheric deposition on ecosystems have also been assessed by scientists in the region on the national and/or regional scales, although the number of studies were not many recently. In this section, the recent studies on ecological impact assessment in the region are briefly summarized and a future view on forest environmental risk assessment is presented.

6.5.1 Risk of acidification and eutrophication

Excess inputs of acidic substances and reactive nitrogen (Nr) species from anthropogenic sources may cause acidification and eutrophication of ecosystems. To abate the risks of acidification and eutrophication, ecological impact assessment should be conducted on the regional scale. In the Convention on Long-range Transboundary Air Pollution, United Nations Economic Commission for Europe (UNECE), the Protocol to Abate Acidification, Eutrophication and Ground-level Ozone (Gothenburg Protocol) was adopted in 1999. In the Gothenburg Protocol, “critical loads (CLs)” of acidification and nutrient nitrogen as well as “critical levels” of ozone were clearly mentioned as concerns for setting emission ceilings. The "CL" is defined as “a quantitative estimate of an exposure to one or more pollutants below which significant harmful effects on specified sensitive elements of

the environment do not occur, according to present knowledge" (UNECE, 2005). Thus, the CLs of acidification and nutrient nitrogen are the maximum amounts of acidifying deposition and eutrophying nitrogen deposition an ecosystem can tolerate in the long term without being damaged, respectively. An integrated assessment model, "Regional Air Pollution Information and Simulation (or Information Systems, RAINS)" developed by International Institute for Applied Systems Analysis (IIASA), which used the CL concept, was utilized for international negotiations for the protocols above. Recently, it was confirmed that decreasing emissions have reflected in concentrations and fluxes of S and N compounds in deposition and runoff in forest catchments in Europe (Forsius et al., 2021); It was also pointed out that emission abatement actions had their intended effects on CL exceedances and ecosystem impacts. Thus, regional ecological impact assessments have certainly contributed to risk abatement of acidification and eutrophication in the case of Europe.

In Asia, a similar integrated assessment utilizing the CL concept, RAINS-ASIA, was promoted by IIASA in cooperation with the World Bank and the Asian Development Bank in the 1990s (Shah et al., 2000; IIASA, 2008). According to the IIASA website, this was the "first" integrated assessment of air pollution in Asia, which was conducted with a large international network of scientific collaborators from 20 countries in Asia. Unfortunately, the second assessment has not been conducted on the regional scale, at least by international initiatives like the EANET. Several studies were conducted by scientists on the national or regional scale, although they did not cover the whole EANET region.

Zhao et al. (2011) calculated CL exceedances and assessed soil acidification risks on the national scale in China taking account of the future scenario of PM emission control. Since base cation (BC) deposition derived from anthropogenic emissions may have an important role in neutralizing soil acidification (Larssen and Carmichael, 2000), it was suggested that acidification risks increased in some parts of the country due to a decrease in BC deposition with PM emission control. Duan et al. (2016) also emphasized the importance of BC (in particular Ca) deposition even for the risk of regional soil acidification.

Xie et al. (2020) produced empirical-N CL map for the Northeast Asian region, including China, Korea and Japan (Figure 6.5.1). The empirical CLs for each vegetation type were estimated based on the literatures conducting field N fertilization experiments. According to their assessment, the area of CL exceedance in East Asia decreased by at least 4.6% during 2010 – 2015, and they concluded that NO_x emission reduction (by 15% for the same period) in China had great benefits to natural ecosystems (Xie et al., 2020). They also suggested the importance of NH_3 emission reduction.

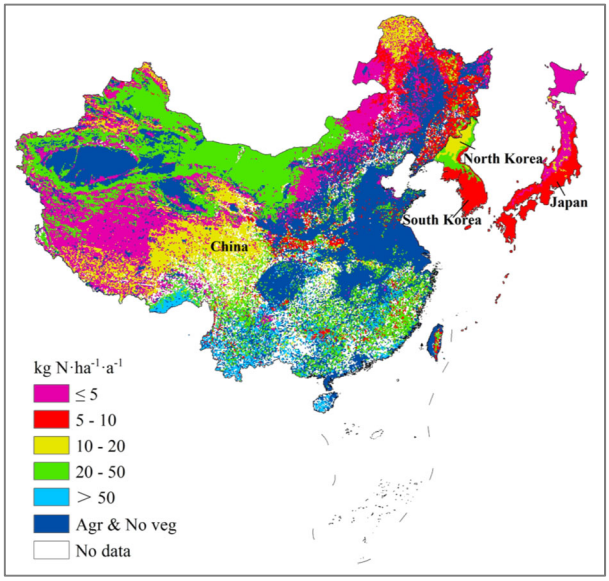

Figure 6.5.1. Empirical N critical load map based on the minimums of the critical load ranges for major forest and grassland ecosystems in East Asia. Wide-distributed agricultural fields and no vegetation regions (Agr & No veg), with theoretically very low sensitivity to N deposition and thus high critical loads, are also showed in the map (Xie et al., 2020).

In the EANET, to promote regional impact assessment, "Workshop on regional impact assessment of atmospheric deposition and air pollution on forest ecosystems" was held on 21-22 November 1999, Niigata, Japan in cooperation with the International Co-operative Programme on Assessment and Monitoring of Air Pollution Effects on Forests (ICP Forests) under CLRTAP, UNECE. In the summary of the workshop, it was pointed out that the regional impact assessment has contributed to policy making on air pollution abatement in Europe, while efforts should also be made to further promote regional impact assessments to provide scientific inputs useful for policy making in East Asia (EANET, 2019). It was also suggested that modeling and satellite observation be more integrated to support and extend assessment to cover the region and high quality of the monitoring data is essential to validate the output of these different approaches. In the workshop, a study on regional impact assessments using CLs of acidification and eutrophication was presented by the EANET scientific community (Yamashita et al., 2019), which has been promoted as one of the activities in line with the "Strategy Paper on Future Direction of EANET on Monitoring of Effects on Agricultural Crops, Forest and Inland Water by Acidifying Species and Related Chemical Substances (EANET, 2020)". In the near future, the study output is expected to be published as a scientific paper.

6.5.2 Environmental risk assessment of ozone

Risk assessments of ozone and PM have also been conducted on the national and regional scales, although no study covered the whole EANET region. Scientists from China and Europe have recently assessed ozone risk on Asian forests using different indices (Figure 6.5.2; De Marco et al., 2020). So far, concentration-based indices, such as AOT40 or W126, were widely used for the assessment of ozone impacts in Europe and the United States, respectively, a flux-based index, PODY, which is considered a stomatal ozone uptake, has been recommended to be used. As shown in Figure 6.5.2, the spatial distributions of risks using the respective indices are slightly different. It is suggested that further elaboration on the indices is necessary. Also, a regional assessment for the whole EANET region is expected to be conducted in the near future.

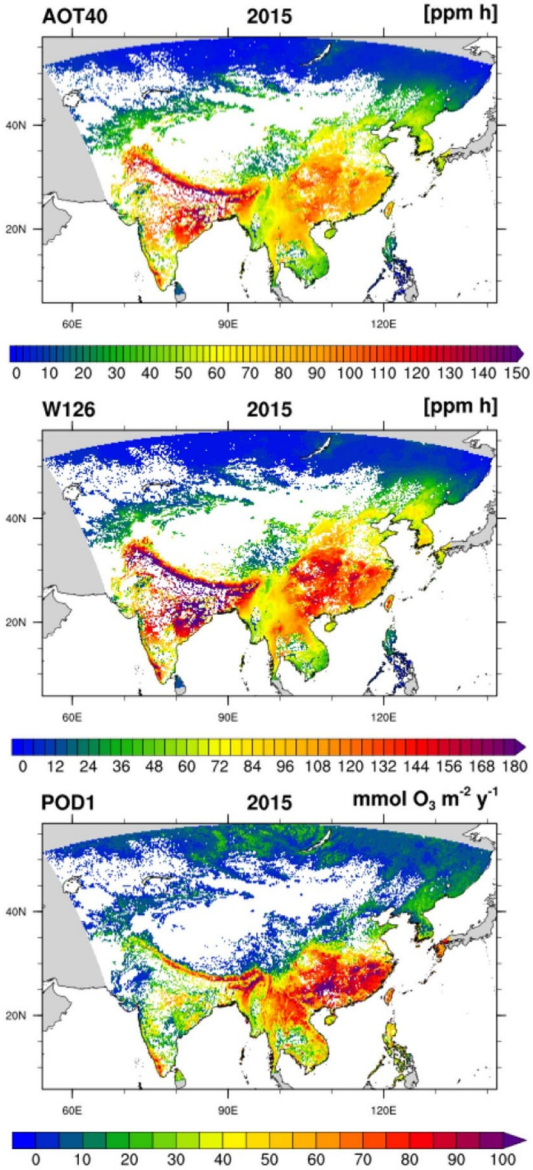

Figure 6.5.2. Ozone risk assessment for Asian forests estimated by three metrics (AOT40, W126 and POD1) in 2015. White color represents grid points without forest cover and grey color is used outside the domain (De Marco et al., 2020).

Exposure to ozone may reduce CO_2 uptake of forest trees. However, it is difficult to detect the effect in an actual forest areas. Reduction of CO_2 fixation rate expected to forest trees is also a risk of ozone in the context of climate change. Kinose et al. (2020) studied the impacts of ozone on CO_2 uptake for representative Japanese broadleaf tree species (Figure 6.5.3) and estimated that the mean O_3-induced reduction in annual CO_2 uptake was 14.0%, 10.6%, 8.6%, and 15.4% in *Fagus crenata*, *Quercus serrata*, *Quercus mongolica* var. *crispula*, and *Betula platyphylla* var. *japonica*, respectively. It was suggested that the atmospheric O_3 concentration be reduced by approximately 28%, 20%, 17%, and 49% to abate the O_3-induced reductions in photosynthetic CO_2 uptake to 5% in *F. crenata*, *Q. serrata*, *Q. mongolica* var. *crispula*, and B. *platyphylla* var. *japonica*, respectively (Kinose et al., 2020). Impact assessment of ozone should be promoted to keep both tree health and carbon absorption.

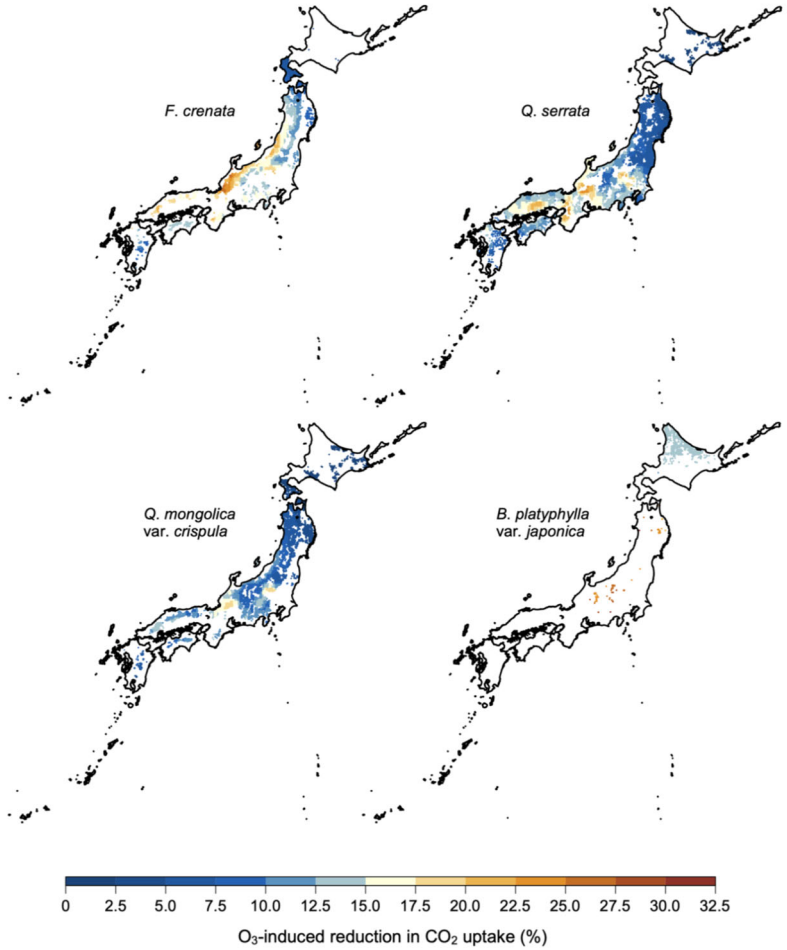

Figure 6.5.3. Spatial distribution of 5-year mean O_3-induced reduction in annual CO_2 uptake per unit leaf (Kinose et al., 2020).

6.5.3 The future of forest environmental risk assessment

Changes in the atmospheric environment affect forest tree dynamics through changes in the rates of CO_2 absorption and material cycles. The EANET has been monitoring atmospheric deposition and its effects on ecosystems and to assess impacts of air pollution/total atmospheric (wet + dry) deposition on ecosystems on the East Asian scale. Part of the premise is that forest monitoring can assess the impact of increased loads of anthropogenic atmospheric deposition on ecosystems. In reality, ecosystems are affected by various environmental factors, so it is necessary to separate the effects of atmospheric deposition from these variable factors (Figure 6.5.4).

Increased mean air temperature promotes the respiration rate of plants and microorganisms and affects the chemical properties of soil and the growth period of vegetation. The El Niño/Southern Oscillation (ENSO) often affects weather and climate extremes (Ropelewski & Halpert, 1992; IRI, 2021), and these phenomena cause physical disturbance to vegetation through typhoons and floods, in addition to the biological aspects of ecosystems.

Material cycling in ecosystems is driven by the uptake of CO_2 from the atmosphere through photosynthesis, and an increase in atmospheric CO_2 concentration increases the efficiency of CO_2 fixation in chloroplasts, leading to an increase in leaf photosynthesis and a decrease in transpiration (Ainsworth & Rogers, 2007; Kirschbaum & McMillan, 2018). An increase in atmospheric CO_2 concentration will also affect the soil environment through changes in the quality and quantity of leaf litter, decomposition rates, and even root growth (Madhu & Hatfield, 2013). While the reduction

of acid deposition mitigates the reduction of photosynthetic activity due to air pollution stress, it may also inhibit the amount of vegetation growth through a reduced supply of nitrogen and sulfur into the ecosystem (de Vries et al., 2014).

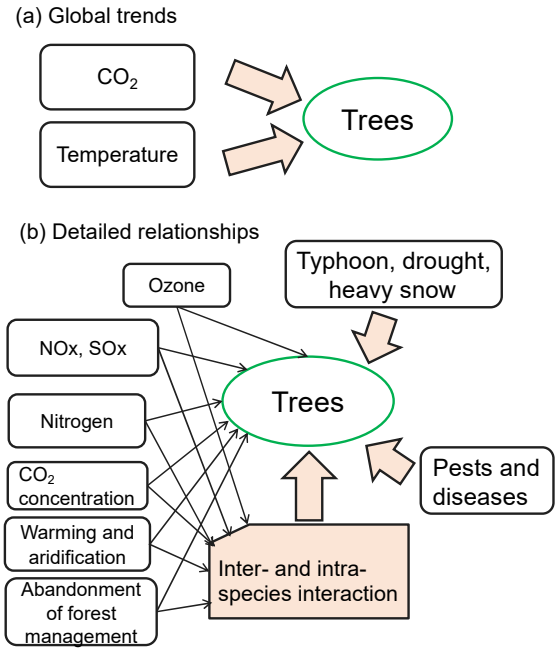

Figure. 6.5.4. Global trends of environmental issues and actual detailed relationships between forest trees and various environmental factors.

The results of long-term forest monitoring have revealed that the species diversity of ecosystems is important for the environmental response of vegetation (Hisano, 2019). In other words, it has been clarified that forests with high species diversity can respond more positively to increases in CO_2 concentrations, air temperatures, or drought. In addition, as shown by Kume et al. (2020), mixed vegetation with different species that respond differently to atmospheric ozone concentrations may exhibit stable growth as a community in response to air pollution effects, as each species grows in a complementary manner in response to changes in air pollution stress.

As mentioned above, forest ecosystems are exposed to various risks associated with global environmental change, and air pollution is one of the risk factors with relatively high regional characteristics (Figure 6.5.5). In order to assess the risk of air pollution effects through field monitoring, it is necessary to have an assessment method to discriminate between the different responses of the forest itself (de Vries et al., 2014), such as the effects of different tree species and species diversity, and other factors.

In the East Asia region, there are few forest sites that have been stably monitored for a long period of time with high accuracy, and there is limited data available in the public domain (Liang & Gamarra, 2020). In order to conduct an effective environmental risk assessment of ozone and PM, enhanced vegetation information is needed, and such information would be useful for risk assessment of global environmental change.

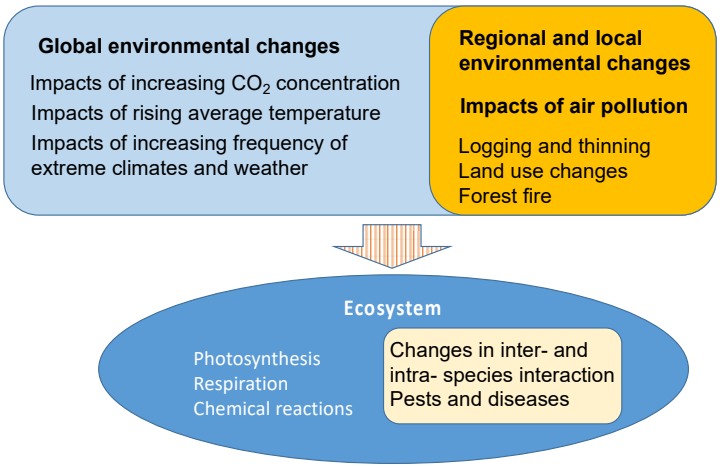

Figure 6.5.5. Global and regional/local environmental changes and their effects on ecosystems.

6.6 Health impact studies

The health impact study on air pollution is mainly conducted by biological and epidemiological studies. Epidemiological studies are effective against public health problems such as air pollution. The epidemiology was defined as "the study of the distribution and determinants of health-related states or events in specified populations, and the application of this study to the prevention and control of health problems" (Last, 2001). In ancient times, the effects of air pollution in the London Smog episode and epidemiological surveys on the effects of air pollution in Yokkaichi, Japan are well known.

The indoor air pollution affects people indoors with gases and particulate matter that are emitted from burning fuels in stoves and kitchen cooking stoves, while the outdoor air pollution is the air pollution contained in the air, which affects the person breathing it, indoors or outdoors. This chapter deals with the outdoor air pollution for broader consideration. The number of premature mortality is often used as an index as an endpoint (event for which occurrence is predicted) for the health impact assessment. The exposure-response function estimated by epidemiological studies calculates the probability of premature mortality (death shorter than life expectancy at that age) in people who have been exposed to a certain concentration of air pollutants for a certain period of time.

$PM_{2.5}$ and ozone have been focused for not only significant health effects but also characteristics as transboundary air pollutants in recent years. This chapter focuses on recent epidemiological findings of $PM_{2.5}$ and ozone in East Asia.

6.6.1 Impacts of $PM_{2.5}$ on human health

Previous epidemiological and toxicological studies have accumulated evidence on the health effects of particulate air pollution. Especially, fine particles with an aerodynamic diameter of less than 2.5 μm ($PM_{2.5}$) can easily penetrate deeply into the lung and cause various biological responses, such as oxidative stress and inflammation. The evidence established the causal link of exposure to $PM_{2.5}$ with respiratory and cardiovascular diseases, and lung cancer. Recently, there has also been increasing interest in the health effects of $PM_{2.5}$ on diabetes, the cenetral nervous system, and maternal outcomes.

Based on the health risk function underpinned by epidemiological evidence, the health burden

attributable to $PM_{2.5}$ has been assessed. Here, we will summarize the research progress about the health impacts of $PM_{2.5}$ in the East Asian region.

(1) Epidemiological studies and health risk function of $PM_{2.5}$

Burden of disease (which interchangeably indicates health burden hereafter), the sum of mortality and morbidity (Murray & Lopez, 1997), has been utilized to quantify the health impacts of air pollutants at the population level (Shiraiwa et al., 2017; Ezzati et al., 2002). Mortality and Disability Adjusted Life Years (DALY) are the metrics used to quantify the health burden. DALYs are the sum of the years of life lost to due to premature mortality (YLLs) and the years lived with a disability (YLDs) due to specific diseases or risk factors.
The mortality attributable to $PM_{2.5}$ ($D_{PM2.5}$) is calculated using population attributable fraction (PAF):

$$D_{PM2.5} = D_{total} \times PAF$$

where D_{total} (total number of deaths) is the product of the mortality rate and population. Here, PAF is calculated from relative risk (RR) of the corresponding levels of $PM_{2.5}$, as the following equation:

$$\mathrm{PAF} = \frac{RR - 1}{RR}$$

RR is derived from the exposure-response function based on epidemiological studies.

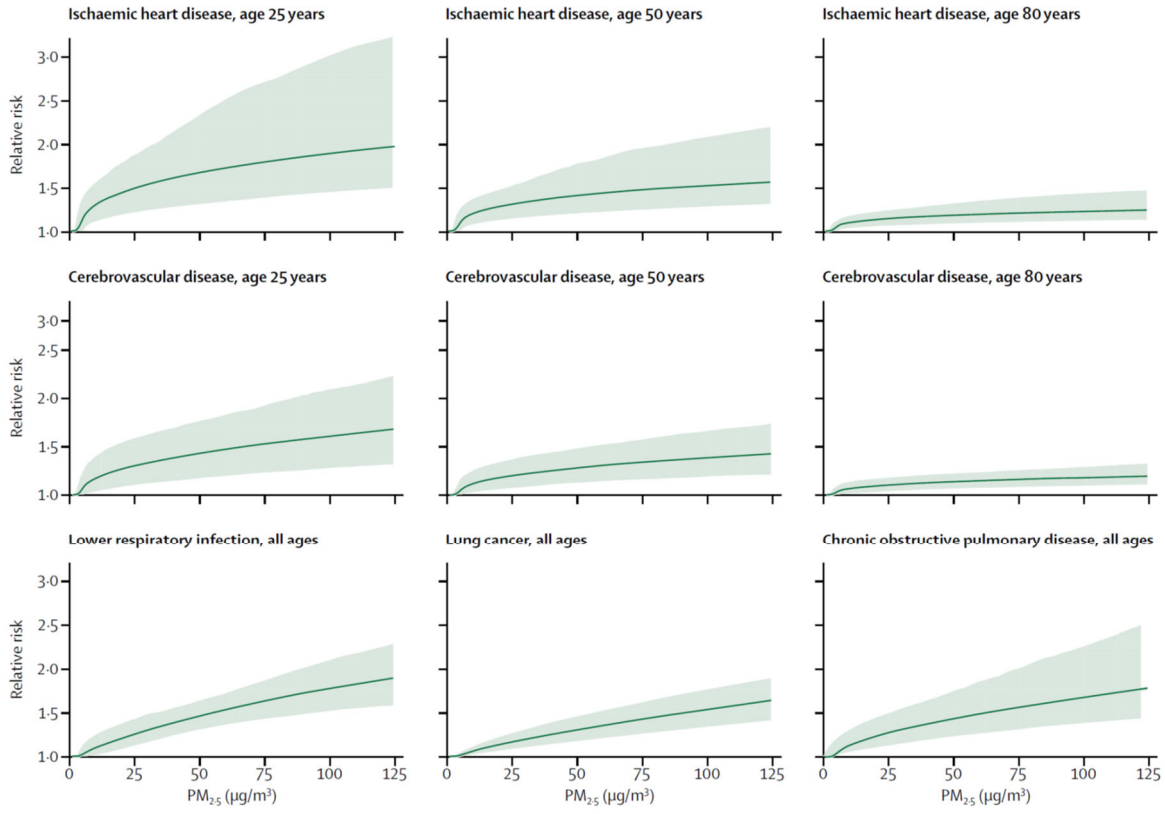

Figure 6.6.1. Visualization of the concentration-response health risk function of $PM_{2.5}$ and diseases (Cohen et al., 2017).

Air pollution epidemiological studies can be classified into studies using short- or long-term exposure. Short-term refers to the time scale of days to weeks while long-term refers to that over months and years. The health effects of short-term exposure to $PM_{2.5}$ is assessed by time-series

analyses and case-crossover design while that of long-term exposure is evaluated by longitudinal cohort studies. Because the study design is different between these two types, the different health risk functions can be defined. The function of short-term exposure may underestimate the number of attributable deaths compared to the function of long-term exposure because studies using short-term exposure cannot account for the underlying chronic conditions (Künzli et al., 2001).

Most of the cohort studies were from areas where the concentration was relatively low and the shape of $PM_{2.5}$-mortality relationship is unknown. This has led to the development of an integrated exposure-response (IER) function for $PM_{2.5}$ and mortality by combining the results of epidemiological studies from ambient air pollution, active smoking, secondhand tobacco smoke, and household cooking smoke (Burnett et al., 2014). However, the IER function requires a strong assumption about equivalent exposure and toxicity, and has thus been further developed into the Global Exposure Mortality Model (GEMM), accounting for these limitations, using several cohort studies across the globe (Burnett et al., 2018) and Asia (Yin et al, 2018). The parameters of the risk function for GEMM vary by age and causes (ischemic heart disease, cerebrovascular disease, lower respiratory infection, chronic obstractive pulmonary disease, and lunc cancer) (Figure 6.6.1).

(2) Burden of diseases attributable to $PM_{2.5}$ and its projection in East Asia

The Global Burden of Disease study (GBD 2019 Risk Factors Collaborators, 2020) used the population-weighted annual average concentration of $PM_{2.5}$ which was estimated using the measurements of satellite-derived aerosol optical depth, ground-based monitoring stations, chemical transport models and land-use modeling. The annual mortality attributable to ambient $PM_{2.5}$ in East Asia (13 participating countries of EANET) is 1.805 million in 2019, which is slightly larger than that in 2010 (1.564 million). The annual DALYs attributable $PM_{2.5}$ also increased from 38.6 to 43.4 million years. The change in age distribution partialy contributed to in the increases in attributable mortality and DALYs from 2010 to 2019. Indeed, the percentage change in age-standardized rate for mortality and DALYs show a decreasing trend except for Japan and Mongolia (GBD 2019 Risk Factors Collaborators, 2020).

There has been increasing number of literatures estimating the country- or region- specific mortality attributable to $PM_{2.5}$. For an example, in a study in Ulaanbaatar, Mongolia estimated the annual average concentration of $PM_{2.5}$ measured at the city center exceeded 75μg/m^3 during 2009-2010, which shows a clear seasonal variation. It is considered that coal and wood combustion in the low-income traditional housing area are the main sources. The estimated attributable mortality to air pollution was not low (Allen et al., 2013). These countries- and region- specific studies are useful to evaluate the impacts of specific air pollution measures although the estimates have uncertainty and further studies are warranted to estimate more accurate health impacts. According to a study (Dasadhikari et al., 2019) which estimated the mortality attributable due to $PM_{2.5}$ by sector from 2010 to 2015. In the Asian-Pacific region, agricultural, industrial, and residential sectors are the largest emission sources in 2015.

It is of interest about how the burden of disease due to $PM_{2.5}$ will change in the future in which when climate change has impacts on air quality including $PM_{2.5}$ and ozone. Silva et al. (2016) estimated the attributable mortality due to $PM_{2.5}$ under various scenarios by atmospheric modeling. Because of reduced emissions, $PM_{2.5}$ concentration of 2100 is expected to decrease in all scenarios. The mortality attributable to $PM_{2.5}$ in 2100 is expected decrease in East Asia as well as other regions. However, some scenarios show increase in mortality during 2030 and 2050.

(3) Summary

The health impact assessments of $PM_{2.5}$ provide important input for environmental policy making. There still remains uncertainty in effect estimates due to the uncertainty in health risk function which should be improved.

6.6.2 Impacts of ozone on human health

In the last decade, progress in both exposure science and health monitoring has paved the way for several developments in air pollution health risk assessment. Among these developments are studies which focused on the role of ozone on human health. Ozone studies have been gaining traction through the years, though at a rate comparably slower than other well-documented criteria pollutants, such as particulate matter and nitrogen dioxide. Ozone is a secondary pollutant which is formed via a complex photochemical interaction together with its chemical precursors, namely volatile organic compounds (VOC) and the oxides of nitrogen ($NO_x = NO_2+NO$) (Finlayson-Pitts and Pitts, 1993). Governmental policies targeting the reduction of ozone concentrations have been largely coursed through the regulation of its chemical precursors (Wang et al., 2017). In 2008, approximately 30% of world total NO_x emissions were from East Asia (including Northeast and Southeast Asia) (Akimoto et al., 2015). The high levels of precursors together with the presence of photochemical reactions led to substantial and steady increase of ozone in the region (Takahashi et al., 2020). The succeeding sections will summarize the developments in the past decade regarding ozone pollution and its effect on human health in the East Asian region.

(1) Epidemiological evidence

Health risks associated to ozone exposure can be simplified into two types: short-term and long-term. Short-term exposures usually last within days and weeks, whereas long-term take several months to years. Short-term exposures are usually paired with similar short-term health outcomes in the same temporal scale such as daily respiratory-related mortality or outpatient asthma visits. Whereas, health outcome measures from cohort studies such as lung cancer and chronic obstructive pulmonary disorder (COPD) among others, have been usually used alongside long-term exposure.

(2) Short-term association

In Japan, NO_2-adjusted, same-day ozone exposure was associated with increase in cardiorespiratory co-morbidity outpatient visits (Seposo et al., 2020). Whereas, in Moscow, Russia, a 10-$\mu g/m^3$ increase in the average of same-day and previous day's ozone concentration was associated with increase in all-cause non-accidental mortality (Revich & Shaposhnikov, 2010).

(3) Long-term association

Cohort studies in Asia, though have been increasing in recent years, are still few in contrast to the long-standing cohort studies in the Americas and Europe. Nevertheless, evidence in the long-term effect of ozone on health in the region has been gradually accumulating due to the viability of research attributed to the developments in exposure science measurements, health outcome monitoring and exposure-health matching. In South Korea, children who had the previous history of bronchiolitis and who were exposed to high levels of ozone were prone to developing asthma (Kim et al., 2013). Extensive evidence linking ozone to other long-term health outcomes such as COPD, myocardial infarction (MI), congestive heart failure (CHF) and diabetes (Kazemiparkouhi et al., 2020; Zanobetti & Schwartz, 2011) have been well-documented in the Americas and Europe, however, evidence has been scarce in the East Asian region.

(4) Ozone-related health burden and its future projection

In contrast to the wide spectrum of candidate health outcomes which were examined in $PM_{2.5}$-related cohort studies, ozone-related cohort studies have mostly observed a consistent finding whereby COPD mortality is associated to ozone pollution. In the recent GBD 2019 study, the authors utilized an inverse-variance weighted meta-analysis of the five cohorts, which estimated the relative risk of dying from COPD due to ozone exposure is at 1.06 (95% CI: 1.03, 1.10) (GBD 2019 Risk Factors Collaborators, 2020); visualized in Figure 6.6.2. Health risks below a theoretical minimum risk exposure level (TMREL) are assumed to be approaching the null association. Previous studies used

a uniform distribution sourced out from the cohort studies (GBD 2019 Risk Factors Collaborators, 2020), with studies utilizing TMREL values of 32.4 ppb or 33.3 ppb (Anenberg et al., 2010; Anenberg et al., 2019).

Utilizing a global chemical transport model, Silva et al. (2016) estimated that 35% of the 493 (95% CI: 122 – 989) thousand global burden of ozone-related respiratory mortality occurred in East Asia. Energy, residential and commercial, industry, land transportation, and shipping and aviation sectors were observed to contribute to the anthropogenic ozone emission in the region. In a similar global health burden estimation, Anenberg et al. (2018) noted that a substantial proportion of the ozone-related asthma emergency room visits occurred in Asia.

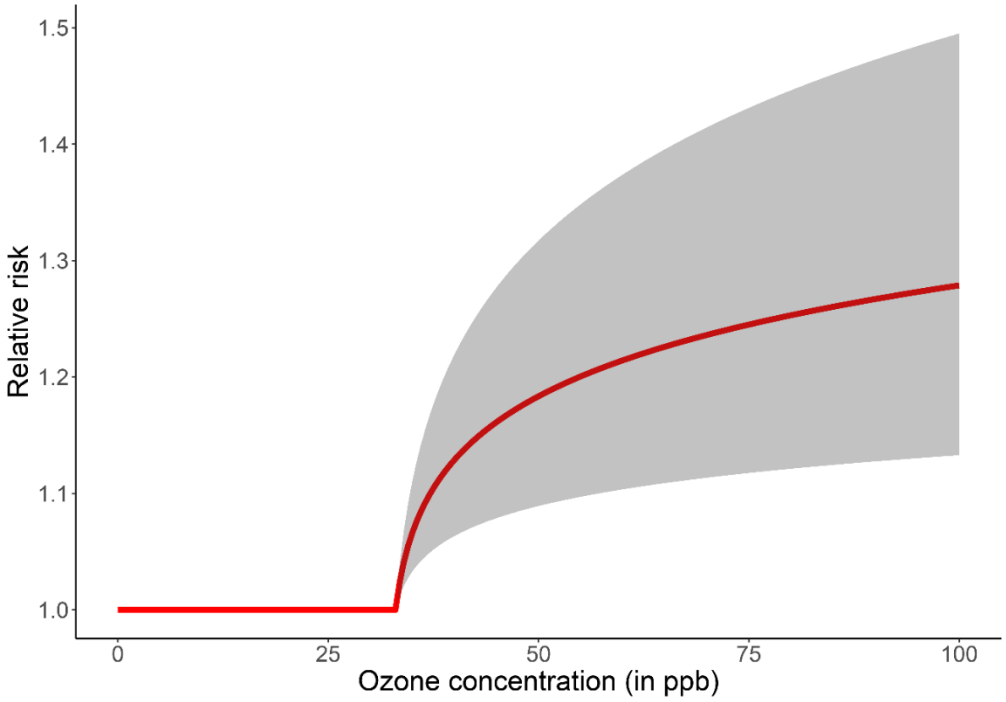

Figure 6.6.2. Visualization* of the concentration-response health risk function of ozone and COPD.

* Utilizing the ozone-COPD risk estimate from GBD 2019. Central estimate (in red) with 95% Confidence Interval in grey-shaded area.

A systematic analysis of the 2017 Global Burden of Disease (GBD) study revealed that ozone exposure resulted to an overall chronic respiratory disease-related, age-standardized DALY of 120.21 (45.70 – 193.34) per 100,000 population in Southeast Asia, East Asia, and Oceania (Soriano et al., 2020). In GBD 2019, East Asia (13 participating countries of EANET) has a total of 108,205 ambient ozone pollution-attributable deaths, which was 31% lower than the 2010 GBD estimate of 156,844.

Near- and far-term projections in ozone concentration have been projected to result to excesses in premature respiratory-related death. Silva et al. (2016) noted that future excess ozone-related mortality is discernable particularly in East Asia with 127,000 deaths per year under the representative concentration pathway (RCP) 8.5, which approximately constitutes 47.5% of global excess mortality in 2030 relative to 2000 concentrations. In brief, RCPs are scenarios which contain information regarding emission, concentration, and land-use trajectories (Moss et al., 2010). Further down in 2050, East Asia is projected to have the highest ozone-related mortality at 518,000 deaths per year under the RCP 6.0 pathway.

(5) Summary

There has been significant progress in the past decade in elucidating not only the ozone-related health risks, but also the current and prospective health burden. The current developments in the field of ozone-health association provide an opportunity for policymakers alike to anchor future policies regarding ozone-related reduction measures with the currently available evidence from the region.

6.7 Other international initiatives on air pollution

Impacts on public and individual health and climate change are the well known scourges of air pollution. According to State of Global Air 2020, which is issued by the Health Effects Institute and the Institute for health Metrics and Evalution's global Burden of Disease project, air pollution is 4th leading risk factor for death globally, continuing to exceed the impacts of other widely recognized risk factors for chronic disease like obesity (high body-mass index), high cholesterol, and malnutrition (Figure 6.7.1). Furthermore, air pollution contributed to 6.7 million deaths in 2019. It was also pointed out that the findings in 2019 show that little or no progress has been made in many parts of the world. Major disparities continue to exist; air quality has improved in many high-income countries over the past several decades, while dangerous levels of air pollution persist in low- and middle-income countries.

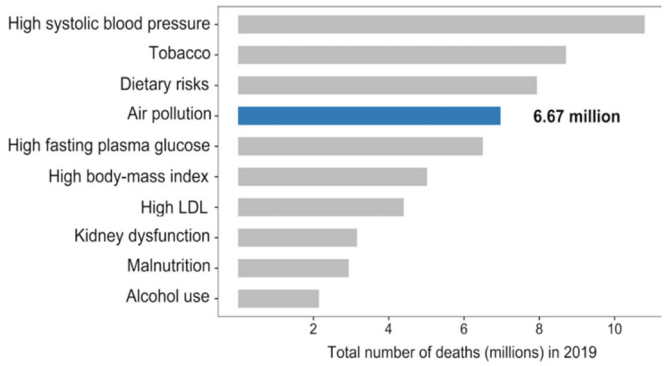

Figure 6.7.1. Global Ranking of Risk Factors by Total Deaths from all Causes in 2019.
Data: State of Global Air 2020

Looking at the East Asia region, air pollution is a severe health crisis as well, and perhaps even more serious situation than the world. There are over 4 million lives jeopardizing due to exposure from outdoor and household air pollution in the Asia Pacific. The more significant numbers of the victims are the vulnerable ones: women, the elderly, and the poor.

In order to deal with air pollution and get better air quality, not only the EANET but also lots of international organizations in the world have been conducting serial activities including monitoring air pollutants, evaluating and analyzing the monitoring data, providing efficient solutions how to improve, and so on.

In this chapter, the efforts of several international initiatives, Concretely, the Global Atmosphere Watch (GAW) Programme of World Meteorological Organization (WMO), the Task Force on Hemispheric Transport of Air Pollution (TF HTAP), Joint Research Project for Long-range Transboundary Air Pollutants in Northeast Asia (LTP) and Asia Pacific Clean Air Partnership (APCAP) will be introduced. By reviewing these initiatives' activities, the EANET can learn their advantages on how to address air pollution. Overmore, the EANET is also able to find out the possibility to build or strengthen the cooperative relationship with other international initiatives.

6.7.1 WMO/GAW

The Global Atmosphere Watch (GAW) programme of World Meteorological Organization (WMO) is a partnership involving the Members of WMO, contributing networks and collaborating organizations and bodies which provides reliable scientific data and information on the chemical composition of the atmosphere, its natural and anthropogenic change, and helps to improve the

understanding of interactions between the atmosphere, the oceans and the biosphere. EANET has been closely collaborating with WMO for a long time. A WMO officer participated in EANET meetings as an observer and in workshops organized by the EANET Network Center and the EANET Secretariat. Some experts involved in EANET activities have contributed to WMO/GAW as members of scientific advisory groups. In August 2018, the Letter of Arrangement for the recognition of EANET as a contributing network for WMO/GAW was signed by the chairperson of the Nineteenth Session of the Intergovernmental Meeting of EANET and the Deputy Secretary-General of WMO. In this section, scientific outcomes made by collaboration between the EANET community and WMO/GAW are introduced.

A global assessment of precipitation chemistry and deposition was implemented by the Scientific Advisory Group for Precipitation Chemistry (SAG-PC) of WMO/GAW (Vet *et al*., 2014). Some experts involved in EANET activities are co-authors of this scientific paper. This assessment was accomplished by presenting quality assured measurement-based data from monitoring networks including EANET and long-term research studies around the world, complemented by model results generated by 21 Eulerian global models that participated in the Coordinated Model Studies of the Task Force on Hemispheric Transport of Air Pollution (TF HTAP). The monitoring data set was used to create global wet deposition maps for two time periods, 2000–2002 and 2005–2007, and was complemented by the TF HTAP ensemble-mean modeling results for the base year 2001.

This assessment indicated global characteristics of sulfur and nitrogen depositions. Highest sulfur wet deposition occurred in the major established and emerging industrial areas in the northeastern United States, western Europe, and East Asia. Wet deposition of nitrogen was highest in eastern North America, southern Europe, northeast India, southeast Asia, and northern Oceania. In industrialized regions, oxidized nitrogen (NO_3^-) was often a larger contributor to nitrogen wet deposition than reduced nitrogen (NH_4^+). In regions of intensive agriculture and many low deposition areas over the oceans, reduced nitrogen was often larger. The deposition of reduced nitrogen continued to exceed oxidized nitrogen deposition. Model-based dry and total deposition of nitrogen were highest in the eastern United States, western Europe, South Asia and eastern China.

Vet *et al.*(2014) reported the measurement-based 3-year average patterns of nitrogen wet deposition for 2000–2002 and 2005–2007, respectively. The wet deposition patterns were consistent with nitrogen emissions patterns with the additional influences of long range transport and precipitation amount. In 2000–2002 and 2005–2007, the highest 3-year average measured wet deposition occurred in Europe and Asia, ranging from 12.00-24.55 kg N ha^{-1} a^{-1} and 12.00–27.07 kg N ha^{-1} a^{-1}, respectively. The lowest levels of wet deposition (<1.0 kg N ha^{-1} a^{-1}) occurred in western North America, northern Europe, and Russian Federation and the highest values (>7 kg N ha^{-1} a^{-1}) occurred in eastern North America, southern Europe, northeast India, Southeast Asia and northern Oceania.

Temporal changes were discussed by the comparison of the data for 2000–2002 and 2005–2007. In Europe, sulfur wet deposition levels in 2005–2007 were remarkably lower than in 2000–2002, which is attributable to large SO_2 emission reductions which began after 1990. In Asia, the average percent change of sulfur wet deposition was an increase of 8.5%, but both major increases and decreases occurred in some areas. Major changes in the anthropogenic emissions of NO_x and NH_3 have occurred from 2000 to 2007 and have been documented in various parts of the world. These include major NO_x emission reductions in Europe, eastern Canada, and the eastern U.S., and major NO_x and NH_3 emission increases in India and China. Consistent with the continental changes in emissions, median wet deposition of nitrogen decreased in North America and Europe and increased in Africa and Asia.

Another assessment of global and regional trends of atmospheric sulfur was implemented by the international cooperation among 10 regional measurement networks including EANET, WMO/GAW and others in Europe and North America (Aas *et al*., 2019). Trends in observations of sulfur components in air and precipitation from major regional networks and estimates from six

different global aerosol models were compared for the years from 1990 to 2015. Fig. 6.7.2 (a), (b) and (c) show trends of SO_2, sulfate in aerosol and sulfate wet deposition calculated by the Meteorological Synthesizing Center-West of the Co-operative Programme for Monitoring and Evaluation of the Long-range Transmission of Air Pollutants in Europe (EMEP MSC-W) model over the 1990–2015 period, respectively.

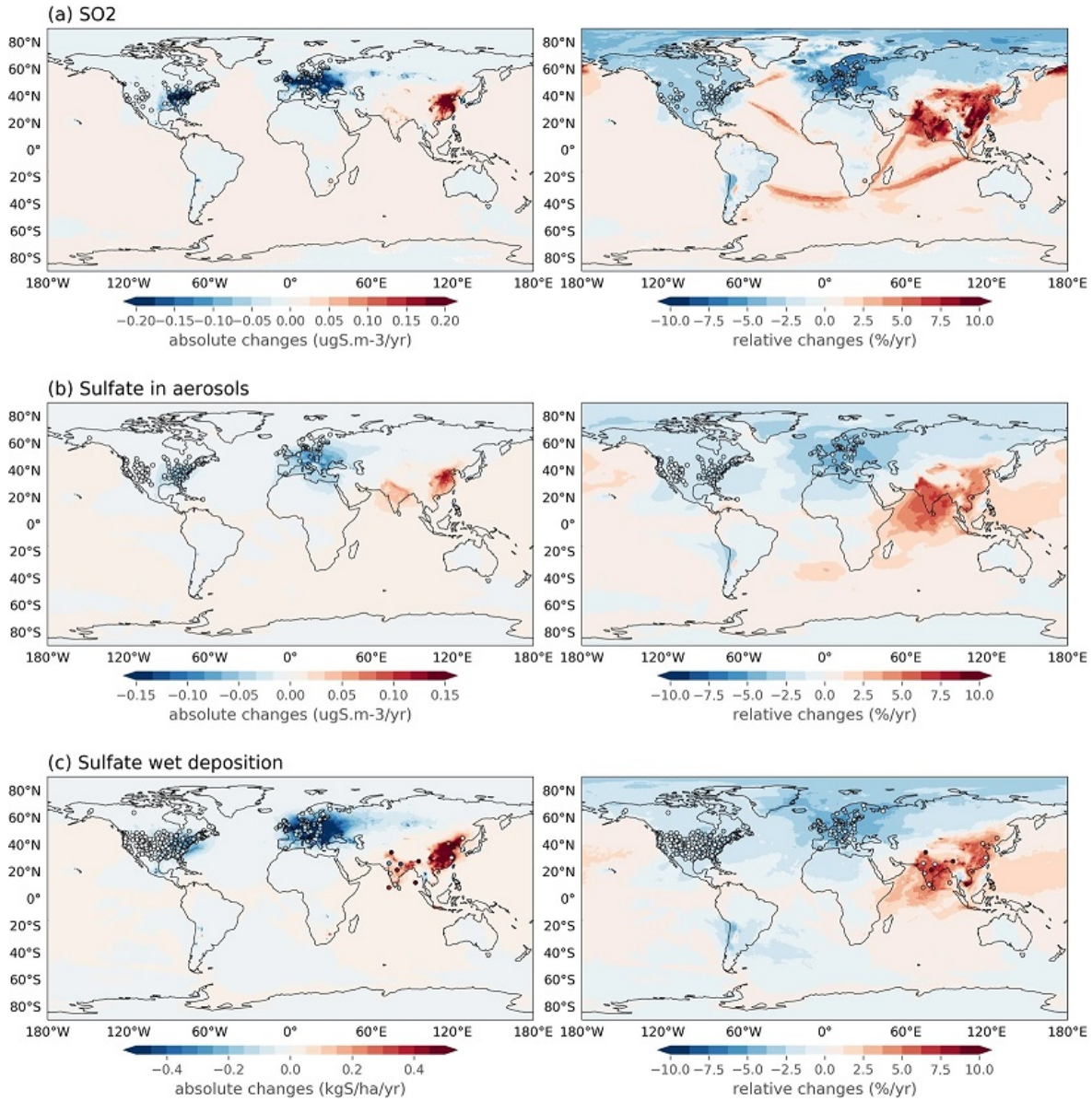

Fig 6.7.2. Absolute (left) and relative (right) trends of air concentrations and wet deposition calculated by the EMEP MSC-W model with observed trends superimposed (open circles), of (a) SO_2, (b) sulfate in aerosol and (c) sulfate wet deposition over the 1990–2015 period. (Aas *et al.*, 2014).

In North America and in Europe, concentrations of the primary emitted compound of SO_2 showed greater decreases than the secondary sulfate in aerosols and in precipitation. This non-linear relationship is seen in both model results and observations. This may partly be explained by the increasing oxidation capacity of the atmosphere during these twenty years. In the early 1990's, SO_2 emissions were still high, and the oxidation of SO_2 to sulfate was limited to some extent by the availability of the oxidants such as H_2O_2, OH and O_3. As the emissions decreased, more oxidants became available, and SO_2 was more efficiently oxidized to sulfate. In addition, less acidity in the environment probably leads to more efficient dry deposition of SO_2, which would also contribute to

a larger reduction in SO_2 concentrations with respect to sulfate. The decrease trend of sulfur wet deposition was lesser than that of SO_2, but larger than those of sulfate in aerosols, because both SO_2 and sulfate are efficiently scavenged by rain water, and thus the wet deposition trend represents a mix of SO_2 and sulfate in aerosols. It should be noted that increase of SO_2 concentrations in East Asia is larger than those of sulfate in aerosol and wet deposition.

Europe had the largest reductions in sulfur emissions in the first part of the period while the highest reduction came later in North America and East Asia. The sulfur emissions in East Asia clearly increased from 2000 to 2005 followed by a decrease, while in India a steady increase trend over the whole period has been found by both observations and models. The remarkable changes in global SO_2 emissions over the last decades have affected atmospheric composition on a regional and global scale with a large impact on air quality, atmospheric deposition and the radiative forcing of sulfate aerosols. Reproduction of historical atmospheric pollution levels based on global aerosol models and emission changes is crucial to prove that such models are able to predict future scenarios.

6.7.2 TF HTAP

There are also close relations with TF HTAP. The TF HTAP was organized in 2005 under the UNECE Convention on Long-range Transboundary Air Pollution (CLRTAP) (http://www.unece.org/env/lrtap/welcome.html). CLRTAP mandated the TF HTAP to work in partnership with scientists across the world to improve knowledge on the intercontinental or hemispheric transport and formation of air pollution; its impacts on climate, ecosystems, and human health; and the potential mitigation opportunities. For HTAP Phase 1 (HTAP1) more than 20 global models participated, and conducted joint modelling experiments. The focus was the meteorological year 2001. TF HTAP produced the first assessment of the intercontinental transport of air pollution in the Northern Hemisphere is summarized in 2010 (TF HTAP, 2010a, b). In 2012, the TF HTAP launched a new phase of HTAP Phase 2 to provide up-to-date information. The objectives of the HTAP2 activity are summarized in the report (Galmarini et al., 2017). This HTAP2 had a close relation to the regional modeling experiments of the Air Quality Model Evaluation International Initiative (AQMEII) over Europe and North America, and the MICS-Asia over Asia. Under the framework of HTAP2 and for the input dataset of global modeling experiment, the emission inventory of HTAP_v2.2 has been created (Janssens-Maehnout et al., 2015). The emission dataset of MIX emission inventory for MICS-Asia Phase III (Li et al., 2017) also aimed to support the HTAP2 experiments.

6.7.3 Joint research project for Long-range Transboundary Air Pollutants in Northeast Asia (LTP)

In order to promote environmental management, to take a leading role in regional environmental management, also to contribute to global environmental improvement, the Tripartite Environment Ministers Meeting (TEMM) mechanism is established among three countries, Korea, China and Japan. Three ministers have been holding the meeting on an annual basis since 1999 and achieved great results. Except for Ministerial Meetings, there are other two meeting levels within this mechanism. One is Director-Generals' Meetings, and the other is Working-Level Meetings. Under the Working-Level Meeting of TEMM, there are 25 specific projects, and the Joint Research Project for LTP is the one of working level project.

For the sake of establishing a common understanding of the mechanism of transboundary movement of pollutants, the three countries of Korea, China, and Japan have held LTP Expert Meetings since1995 which was even earlier than the first TEMM meeting. The objectives of the Joint Research Project for LTP are to study the state of air quality, the influence of neighboring countries, and the policy making of each country to improve the air quality. The Joint Research Project for LTP has been executed in the five stages as below.

Table 6.7.1 History of the Joint Research Project for LTP

Stages and duration	Achievements of each stage
1st stage (2000–2004)	Built the foundation for collaborative research of measurements and modeling
2nd stage (2005–2007)	Drew the S–R (Source–Receptor) relationship for sulfur compounds by using the emission data agreed upon by the three counties
3rd stage (2008–2012)	Updated the emission inventory and extend the research area to nitrogen compounds
4th stage (2013–2017)	Focused on the S–R relationship of $PM_{2.5}$ concentrations over Korea, China, and Japan
5th stage (2018-2022)	

To get a better understanding of the current situation of long-range transport of air pollutants in Northeast Asia, the Joint Research Project for LTP is implementing two main research activities. Concretely, monitoring and modeling analysis activities. The Joint Research Project for LTP has 12 monitoring sites which are located 9 cities in three countries (Figure 6.7.3) in line with an agreement of the Joint Operating Committee.

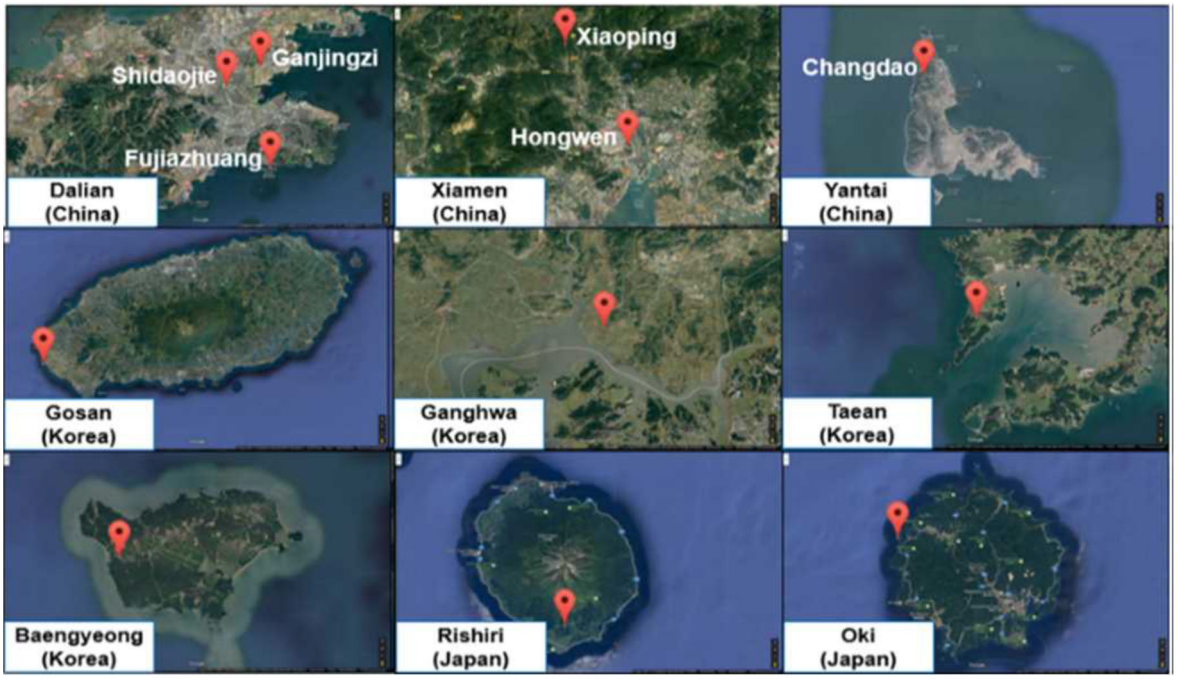

Figure 6.7.3. Locations of monitoring sites in three countries for LTP project.
Data: Summary Report of the 4th Stage (2013-2017) LTP Project https://www.me.go.kr/home/file/readDownloadFile.do?fileId=184686&fileSeq=1 accessed on 1 October 2021.

Through analyzing the monitoring data and model simulation, the expert group of Joint Research Project for LTP has got the following results regarding transboundary movement of air pollutants and these results were reported to TEMM 21, while the expert shared the view that methodologies need to be further improved.

1. The first Summary Report for TEMM jointly produced by the three countries on long– range transboundary air pollutants in Northeast Asia. In order to investigate the characteristics of air

pollution, three countries have carried model simulations based on the same recent emission inventory generated through the LTP Meeting.
2. The annual average concentrations of SO_2, NO_2, $PM_{2.5}$ and PM_{10} have shown a decreasing trend in recent years in the LTP monitoring sites in China, Japan, and Korea.
3. It was agreed that, even though there are some uncertainties in modeling and limitations in monitoring, the three countries have successfully diagnosed the decreasing trend of air pollution in Northeast Asia.
4. The modeling results of the three countries are quite similar with some exceptions and are in line with the monitoring data and basic natural settings of Northeast Asia.
5. The dominant contribution to the concentrations in each country is domestic emission in general and highlights the importance of emission reductions for improving domestic and regional air quality.
6. Further research on species‐targeted monitoring and emission reduction will effectively contribute to improve air quality through continuous cooperation among the three countries.

6.7.4 APCAP[1]

The United Nations Environment Assembly is the world's highest-level decision-making body on the environment, with a universal membership of all 193 Member States. The Assembly sets priorities for global environmental policies and develops international environmental law. At the first session of the UN Environment Assembly, air pollution was identified as a top priority that requires immediate action. In the Asia Pacific region, there were several international initiatives that has been struggled with air pollution, however, there was a need to set-up a coordination mechanism to bring together different frameworks and initiatives to maximize synergies and to consolidate available evidence to identify the most effective solution to reduce emissions and improve health and wellbeing.

Asia Pacific Clean Air Partnership (APCAP) was established in 2015 in response to the above situation and social needs as a mechanism and platform to promote coordination and collaboration among various clean air initiatives in Asia Pacific.

The Asia Pacific Clean Air Partnership aims to
- Serve as a mechanism for better coordination and collaboration of clean air programs in the region.
- Provide a platform to generate and share knowledge on air pollution initiatives, policies and technologies in the Asia Pacific region.
- Strengthen institutional capacity, provide technical assistance on air quality management; and support air quality assessments to identify solutions for clean air.

The APCAP Joint Forum and Science Panel are important vehicles to achieving the above aims.

APCAP has sixteen member countries since 2015. Namely, Afghanistan, Cambodia, India, Iran, Japan, Republic of Korea, Malaysia, Maldives, Mongolia, Nepal, New Zealand, Pakistan, Philippines, Singapore, Sri Lanka, Thailand. In 2019, Gyeonggi Provincial Government from Republic of Korea joined the partnership.

The activities APACP has been conducted can be summarized into two phases. The first phase was from 2014 to 2018. The second phase has started in 2019, and will be continued until 2023. The first phase has 3 main components. Concretely, 1) regional cooperation and information sharing on air pollution control; 2) strengthening the science and policy interface on air pollution issue; 3) strengthening member countries' capacity building.

[1] https://www.unep.org/asia-and-pacific/asia-pacific-clean-air-partnership/what-we-do, accessed to the web site on 27 April 26, 2021.

(1) APCAP Joint Forum

The APCAP Joint Forum is the key venue in the Asia Pacific for sharing the latest policy-relevant scientific knowledge, and information on the state of national and international efforts. The Joint Forum also aims to identify priority air quality issues, promote regional approaches to combat the priority issues where appropriate and identify appropriate forums and existing mechanisms to help address air pollution challenges of the region. The inaugural Asia Pacific Clean Air Partnership Joint Forum was organized in November 2015, in response to the 2014 UN Environment Assembly (UNEA) resolution on air quality (1/7) where countries called for immediate and coordinated action to address air pollution and its impacts. The meeting provided an opportunity to enhance synergies among various air pollution initiatives in the region, and promoted science policy dialogue.

The second APCAP Joint Forum was held in March 2018 under the theme of "Solutions Landscape for Clean Air". The major discussion point for both sessions is shown in Table 6.7.2.

Tale 6.7.2 Discussion point of APCAP Joint Forum

Major Discussion point for the first session in 2015	Major discussion point for the second session in 2018
➢ Review and discussions of the latest policy relevant scientific developments related to air pollution and control measures; ➢ Review and comments on the Assessment report on air pollution including Short Lived Climate Pollutants (SLCPs) in Asia Pacific; ➢ Review and comments on country and regional progress on implementation of the United Nations Environment Assembly (UNEA) resolution on air quality and synergetic implementation of the air quality related resolution by the UNEA and other air quality related activities in Asia Pacific; ➢ Review and presentation of the governance and working modalities of the APCAP.	➢ discuss and share the latest science, evidence and impacts of air pollution; ➢ share and exchange practical and innovative solutions at national and local levels, featuring policy, finance, and technology; ➢ report on progress on air quality actions region arising from the 2014 UN Environment Assembly resolution and discussions at the 2015 Asia Pacific Clean Air Partnership Joint Forum; and ➢ develop a plan for the Asia Pacific Clean Air Partnership Joint Forum to implement the UN Environment Assembly resolutions on air quality in the region.

(2) APCAP Science Panel

APCAP Science Panel was established to bring together scientific expertise from the multiple regional initiatives to provide clear policy options based on the best science to support action on air pollution in Asia Pacific.

The current members of APCAP Science panel consist of 12 experts as shown below:

- Chair: Jiming Hao, Chair, China
- Vice Chair: Hajime Akimoto, Japan
- Markus Amann, Austria
- Jiang Kejun, China
- Zhang Shiqiu, China
- Veerabhadran Ramanathan, India
- Jayaraman Srinivasan, India
- Kalpana Balakrishnan, India
- Teruyuki Nakajima, Japan
- Young Sunwoo, Republic of Korea
- Rajasekhar Balasubramanian, Singapore
- Nguyen Thi Kim Oanh, Thailand

"Air Pollution in Asia Pacific: Science-Based Solutions Report" and three clean air policy briefs: (1) $PM_{2.5}$ and ozone co-benefits of co-control; (2) Reducing exposure to particulate matter in indoor environments; and (3) Policy showcase: Clean energy transition in China were developed by APCAP Science Panel during the first phase. These four deliverables are widely known all over the world.

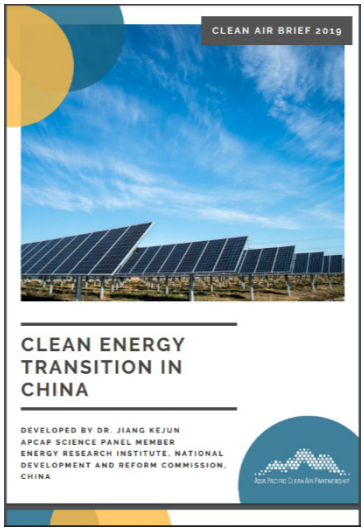

In the "Air Pollution in Asia Pacific: Science-Based Solutions Report", 25 practical measures are introduced to deal with air pollution. The report used the highest quality data available and state-of-the-art modelling to identify the most effective 25 measures to reduce air pollution. The analysis, which takes the region's considerable diversity into account, groups the selected measures into three categories that are fully described within the report:

- Conventional emission controls focusing on emissions that lead to the formation of fine particulate matter;
- Further (next-stage) air-quality measures for reducing emissions that lead to the formation of $PM_{2.5}$ and are not yet major components of clean air policies in many parts of the region; and
- Measures contributing to development priority goals with benefits for air quality.

The report pointed out that if the 25 identified measures are effectively implemented, 1 billion people in Asia could enjoy air quality that conforms to the WHO Guideline by 2030, compared to only

about 360 million in 2015. The reductions in outdoor air pollution could reduce premature mortality by a third, and about 2 million premature deaths from indoor air pollution could be avoided each year. These 25 measures also provided benefits for food and water security, environmental protection and the mitigation of climate change.

The specific measures to be taken are as Table 6.7.3.

Table 6.7.3 The proposed 25 measures by APCAP Science Panel

Regional application of conventional measures	
Post-combustion controls	Introduce state-of-the-art end-of-pipe measures to reduce sulphur dioxide, nitrogen oxides and particulate emissions at power stations and in large-scale industry
Industrial process emissions standards	Introduce advanced emissions standards in industries, e.g., iron and steel plants, cement factories, glass production, chemical industry, etc.
Emissions standards for road vehicles	Strengthen all emissions standards; special focus on regulation of light- and heavy-duty diesel vehicles
Vehicle inspection and maintenance	Enforce mandatory checks and repairs for vehicles
Dust control	Suppress construction and road dust; increase green areas
Next-stage air quality measures that are not yet major components of clean air policies in many parts of Asia and the Pacific	
Agricultural crop residues	Manage agricultural residues, including strict enforcement of bans on open burning
Residential waste burning	Strictly enforce bans on open burning of household waste
Prevention of forest and peatland fires	Prevent forest and peatland fires through improved forest, land and water management and fire prevention strategies
Livestock manure management	Introduce covered storage and efficient application of manures; encourage anaerobic digestion
Nitrogen fertilizer application	Establish efficient application; for urea also use urease inhibitors and/or substitute with, for example, ammonium nitrate
Brick kilns	Improve efficiency and introduce emissions standards
International shipping	Require low-Sulphur fuels and control of particulate emissions
Solvent use and refineries	Introduce low-solvent paints for industrial and do-it-yourself applications; leak detection; incineration and recovery
Measures contributing to development priority goals with benefits for air quality	

Clean cooking and heating	Use clean fuels – electricity, natural gas, liquefied petroleum gas (LPG) in cities, and LPG and advanced biomass cooking and heating stoves in rural areas; substitution of coal by briquettes
Renewables for power generation	Use incentives to foster extended use of wind, solar and hydro power for electricity generation and phase out the least efficient plants
Energy efficiency for households	Use incentives to improve the energy efficiency of household appliances, buildings, lighting, heating and cooling; encourage rooftop solar installations
Energy efficiency standards for industry	Introduce ambitious energy efficiency standards for industry
Electric vehicles	Promote the use of electric vehicles
Improved public transport	Encourage a shift from private passenger vehicles to public transport
Solid waste management	Encourage centralized waste collection with source separation and treatment, including gas utilization
Rice paddies	Encourage intermittent aeration of continuously flooded paddies
Wastewater treatment	Introduce well-managed two-stage treatment with biogas recovery
Coal mining	Encourage pre-mining recovery of coal mine gas
Oil and gas production	Encourage recovery of associated petroleum gas; stop routine flaring; improve leakage control
Hydrofluorocarbon, (HFC) refrigerant replacement	Ensure full compliance with the Kigali Amendment

6.8 Cross-chapter analysis of acid deposition

This section demonstrates three examples of cross-chapter analysis based on observed wet depositions in Chapter 3, observed column density from satellite measurements in section 6.2.2, emission inventory in section 6.3 and the results from CTM study in section 6.4. Section 6.8.1 compares the long-term trends of observed wet depositions analyzed in Chapter 3 with emission inventories in EANET, NADP and EMEP for 20 years (2000-2019). In section 6.8.2, the trends of total (wet and dry) depositions estimated in Chapter 3 are compared with those of column density and emission inventory in Japan as an example of national scale analysis. Furthermore, in section 6.8.3, the observation-based total (wet and dry) depositions are compared with the simulated depositions by CTM. So far, CTM has been verified mainly by observed wet depositions and/or gas/aerosol concentrations, and this study provides the first results of the verification for total deposition in East Asia. The analyses in this section will provide useful information on trend factors of acid depositions in East Asia.

6.8.1 Trends of wet depositions and emissions among EANET, NADP and EMEP

Long-term trends of wet depositions (observations in section 3.4.1) and emissions (emission

inventory in section 6.3) are compared among EANET, NADP and EMEP regions for 20 years (2000-2019). EANET region is separated to Northeast Asia (China, Korea, Japan and Mongolia; NE Asia) and Southeast Asia (other countries; SE Asia). Figure 6.8.1 shows the multiple trends of concentrations in precipitation, wet depositions and emissions for sulfur and oxidized nitrogen in each region. Additionally, the relative ratios of emission and column density (satellite measurements in section 6. 2) to the average during 2005-2015 is added for covering the emission trends in EANET region in the whole period during 2000-2019. The trends of NOx emissions are well consistent with those of column densities of NO_2 for the period during 2005-2015. For SO_2, the emission trends were almost similar to the column densities, though the latter shows a large fluctuation.

The SO_2 and NO_x emissions in SE Asia increased since 2000, while the emissions in NE Asia decreased from 2005 and 2011 for SO_2 and NO_x, respectively. Total amount of emissions for SO_2 as well as NO_x in EANET was around two times of those in NADP and UNEP, which decreased gradually since 2000. After 2015, the column density of NO_2 was almost stable in SE Asia, but slightly decreased in NE Asia. On the other hand, the column density of SO_2 after 2015 increased in SE Asia, but was not clear trend in the same period in NE Asia.

Wet depositions of SO_4^{2-} and NO_3^- in EANET region were higher than those in NADP and EMEP. Wet depositions of SO_4^{2-} in NE Asia decreased to one quarter for the period during 20 years in spite of the increase of SO_2 emissions before 2006. Inversely, the wet depositions of SO_4^{2-} in SE Asia increased after the last half of the 2000's in response to the increasing SO_2 emissions and became higher than that in NE Asia after 2013. The crossing point of increasing trend in SE Asia and decreasing trend in NE Asia is found around 2012. For NO_3^-, the wet depositions in NE Asia slightly decreased after 2011 according to the decrease of NO_x emissions. Wet depositions for NO_3^- in SE Asia were higher than other regions since 2001 and increased after the last half of the 2000's in response to the increase of NO_x emissions. The trends of the concentration in precipitation of SO_4^{2-} and NO_3^- are similar to those of their wet depositions in NE Asia as well as SE Asia after the middle of the 2000's.

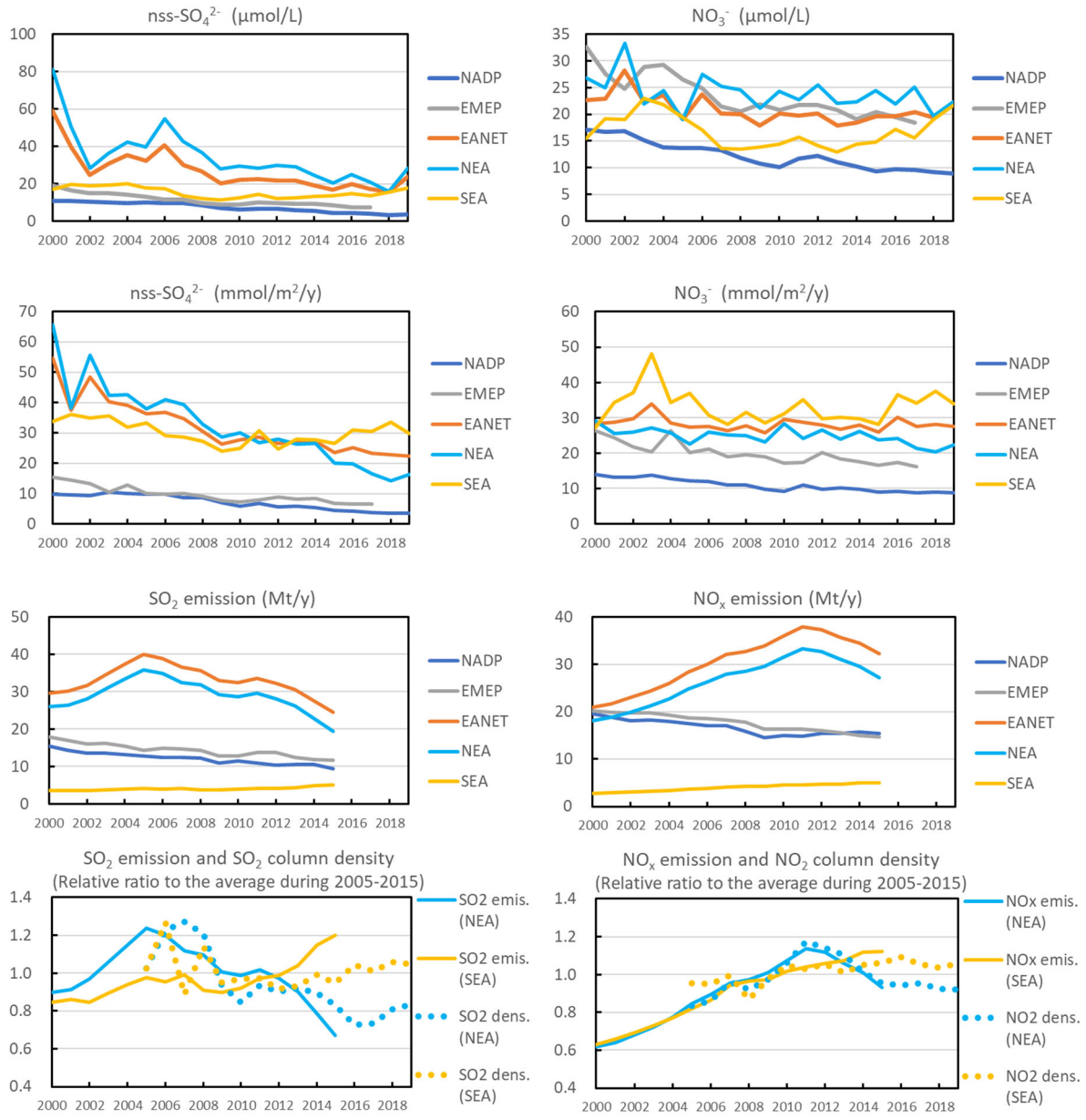

Figure 6.8.1. 20-years trends of observed concentrations in precipitation, observed wet depositions emissions and emissions of sulfur (left) and oxidized nitrogen (right) in EANET, NADP and EMEP regions during 2000-2019. The bottom shows the relative ratios of emission and column density (satellite measurements) to the average during 2005-2015 in EANET region. The emissions are approximately calculated as NADP = North America and EMEP = OECD Europe + Other Europe + Russia. The regional averaged column densities of SO_2 and NO_2 in EANET region are obtained by the area-weighted average of the column densities of each country.

6.8.2 National scale analysis of trends of depositions and emission - Japan case –

As an example of national scale analysis, the trends of total (wet and dry) depositions (sulfate and oxidized nitrate), column density (SO_2 and NO_2), and emissions (SO_2 and NO_x) are compared in Japan (respectively). In the analysis, the total depositions in Oki and Hedo are excluded as their trends have large fluctuations. Additionally, the total deposition in Ogasawara is also excluded as

there are little influence by Japanese emissions.

The 20-years trends of total deposition of sulfate and oxidized nitrate observed in each site, column density around Japan from OMI, and emission from emission inventory in Japan are shown in Fig. 6.8.2. These values are normalized by the averaged values during 2005-2015. The sulfur deposition had the negative trend with -3.0 % year^{-1} of annual rate. The trend was correlated with that of SO_2 emissions as well as SO_2 column density in Japan while the annual rate was higher than those of the emissions (-1.6 % year^{-1}) and the column density (-0.9 % year^{-1}).-It's likely that these differences were caused by the decrease of SO_2 emissions in Northeast Asia since 2005 (see Fig.6.3.2). The trend of oxidized nitrogen deposition also was negative with -1.1 % year^{-1} of annual rate. However, the trend wasn't monotonous and became upward during 2009-2013. It was considered that the complicated changes were influenced by the regional variability of annual changes of NO_x emissions in Northeast Asia. For interpretation precisely, more careful analysis using CTM is needed.

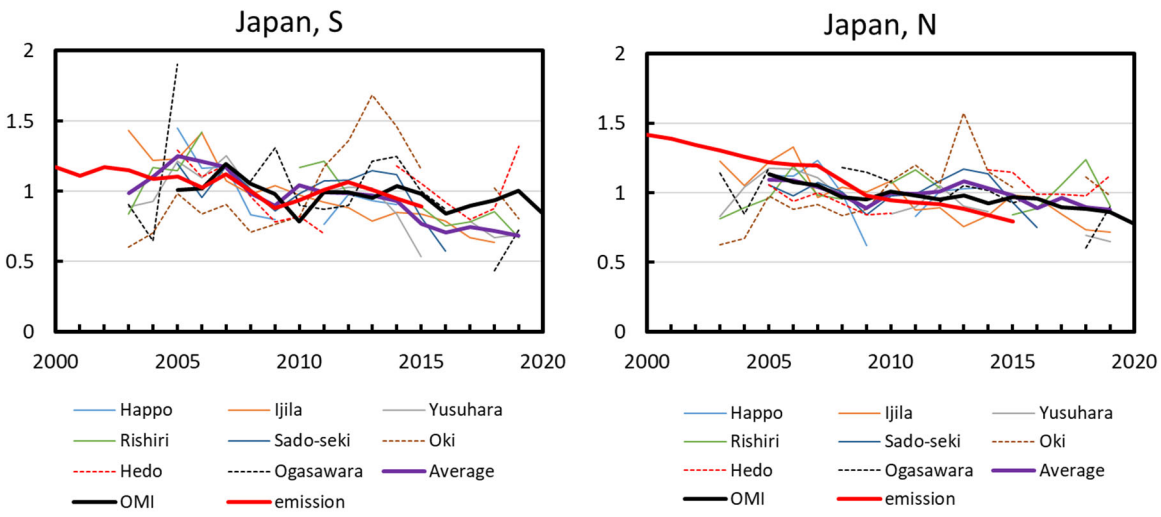

Figure 6.8.2. Long-term trends of observed total depositions of sulfate (left) and oxidized nitrate (right) in each site in Japan (purple: averaged value), column density of SO_2 and NO_2 from satellite OMI measurements over Japan, and SO_2 and NO_x emissions in Japan during 2000-2019. All values are normalized by the averaged values during 2005-2015.

6.8.3 Comparison of EANET observation and CTM results from MICS-Asia Phase III

Total sulfur and nitrogen deposition analyzed in Chapter 3 is compared to CTM results taken from MICS-Asia Phase III (Itahashi et al., 2020). In this analysis, 6 sites in Japan were averaged, 2 sites in Russia and 2 sites in Mongolia were averaged as North Asia, and 2 sites in Vietnam and 2 sites in Thailand and 1 site in Indonesia were averaged as Southeast Asia. Generally, total sulfur and nitrogen deposition both for wet and dry components over Japan were well captured by CTM (Figure 6.8.3). In its nitrogen components, both oxidized and reduced nitrogen deposition were reproduced by CTM. Over North Asia, total sulfur and nitrogen deposition were underestimated by CTM. As the component of nitrogen, both oxidized and reduced nitrogen were underestimated by CTM. As found in MICS-Asia, deposition over North Asia excessed its emission amount in these countries (Itahashi et al., 2020). Therefore, the long-range transport within Asian region and import from northern boundary of modeling domain (i.e., global-scale impacts) should be further investigated to consider this modeling underestimation issue. The modeling performance over Southeast Asia were complexed. Total sulfur wet and dry deposition were generally captured by CTM within its multi-model variations, whereas total nitrogen wet deposition was underestimated and total nitrogen dry deposition was overestimated. In its components, oxidized nitrogen tended to be underestimated and

reduced nitrogen tended to be overestimated over Southeast Asia. For wet deposition process, the improvements in precipitation amounts by meteorological model could contribute to refine the wet deposition over Southeast Asia (Itahashi et al., 2021). The uncertainties in emission as input source into CTM were relatively larger over this region; therefore, further examinations based on the cross-cutting studies based on observation (both ground-based and space-borne), emission inventories, and CTM are furthermore required to foster our understanding on air quality over Asia.

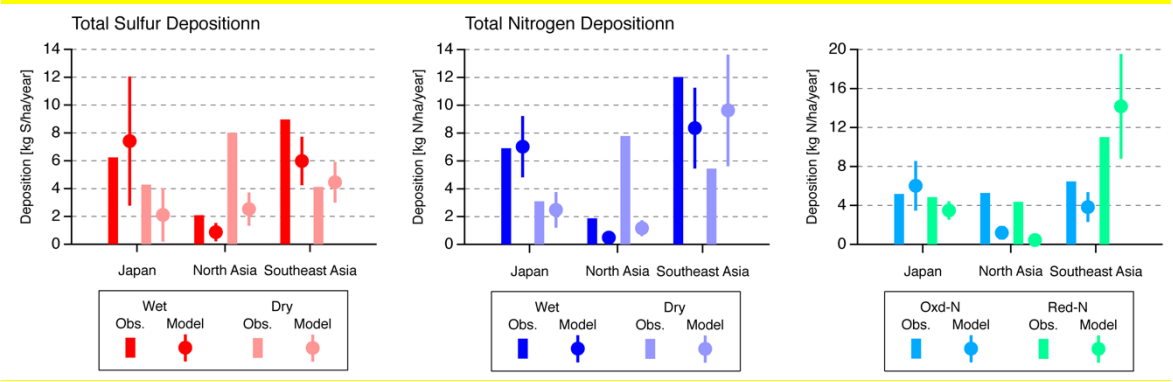

Figure 6.8.3. Comparison for total sulfur and nitrogen deposition between observation and CTM model simulation. See details for observation in Chapter 3. The result of CTM model simulations were taken from MICS-Asia phase III (Itahashi et al., 2020). The circle is ensemble mean and the vertical bar is deviation among models.

6.9 Conclusions

As has been seen in this Chapter, substantial numbers of studies have been carried out in the last few years to elucidate the cause and response of regional acid deposition and air pollution and their human health and ecological impacts in East Asia based on observational and modeling studies. Additionally, some original and/or summarized analysis are conducted in the satellite observation, acidification in forest catchments, impacts studies on human health and ecological system, and trends of air quality, acid deposition, and their environmental impacts. Most of those studies reviewed and conducted in this Chapter are deeply related to EANET from the viewpoints that EANET monitoring data have been fully used or the results were obtained in the EANET "additional activities" by collaboration of scientists of participating countries. These kinds of scientific investigations are crucial for EANET for passing messages of implication of the activities to policy makers and the public. More active integration of emission inventory, model simulation, monitoring including satellite observation, and human health and ecological impact studies would be a key for the future successful operation of EANET.

6.10 References

(6.2)

Brenot, H., Theys, N., Clarisse, L., van Geffen, J., van Gent, J., Van Roozendael, M., van der A, R., Hurtmans, D., Coheur, P.-F., Clerbaux, C., Valks, P., Hedelt, P., Prata, F., Rasson, O., Sievers, K., and Zehner, C. 2014. Support to Aviation Control Service (SACS): an online service for near-real-time satellite monitoring of volcanic plumes. Nat. Hazards Earth Syst. Sci. 14: 1099–1123.

Chiwa, M., Onikura, N., Ide, J., Kume, A. 2012. Impact of N-saturated upland forests on downstream N pollution in the Tatara River Basin, Japan. Ecosystems 15: 230-241. https://doi.org/10.1007/s10021-011-9505-z.

Chiwa, M., Tateno, R., Hishi, T., Shibata, H. 2019. Nitrate leaching from Japanese temperate forest ecosystems in response to elevated atmospheric N deposition, Journal of Forest Research, 24:1, 1-15, https://doi.org/10.1080/13416979.2018.1530082.

Crawford, J. H., Ahn, J-Y., Al-Saadi, J., Chang, L., Emmons, L. K., Kim, J., Lee, G., Park, J-H., Park, R. J., Woo, J. H., Song, C-K., Hong, J-H., Hong, Y-D., Lefer, B. L., Lee, M., Lee, T., Kim, S., Min, K-E., Yum, S. S., Shin, H. J. & 11 others, Kim, Y-W., Choi, J-S., Park, J-S., Szykman, J. J., Long, R. W., Jordan, C. E., Simpson, I. J., Fried, A., Dibb, J. E., Cho, S. & Kim, Y. P., 2021. The Korea–United States Air Quality (KORUS-AQ) field study, Elementa: Science of the Anthropocene, 9(1), 00163.

Duan, L., Yu, Q., Zhang, Q., Wang, Z., Pan, Y., Larssen, T., Mulder, J., 2016. Acid deposition in Asia: emissions, deposition, and ecosystem effects. Atmos. Environ. 146, 55–69. https://doi.org/10.1016/j.atmosenv.2016.07.018

EANET 2015. Review on the State of Air Pollution in East Asia (edited by Task Force on Research Coordination, Scientific Advisory Committee, Acid Deposition Monitoring Network in East Asia), Network Center for the EANET, Niigata, Japan. 411p.

EANET 2016. Third Periodic Report on the State of Acid Deposition in East Asia, Part I - III.

Heard, D. E., Carpenter, L. J., Creasey, D. J., Hopkins, J. R., Lee, J. D., Lewis, A. C., Pilling, M. J., Seakins, P. W., Carslaw, N., and Emmerson, K. M. 2004. High levels of the hydroxyl radical in the winter urban troposphere, Geophysical Research Letter, 31, L18112.

Hilboll, A., Richter, A., Burrows, J. P. 2013. Long-term changes of tropospheric NO_2 over megacities derived from multiple satellite instruments. Atmos. Chem. Phys. 13: 4145–4169.

Irie, H., Muto, T., Itahashi, S., Kurokawa, J., and Uno, I. 2016. Turnaround of tropospheric nitrogen dioxide pollution trends in China, Japan, and South Korea. SOLA. 12: 170-174.

Itahashi, S., Uno, I., Irie, H., Kurokawa, J., and Ohara, T. 2014. Regional modeling of tropospheric NO_2 vertical column density over East Asia during the period 2000-2010: comparison with multisatellite observations. Atmos. Chem. Phys. 14: 3623-3635.

Itahashi S., Uno I., Irie H., Kurokawa J., and Ohara T. 2018. Impacts of biomass burning emissions on tropospheric NO_2 vertical column density over continental Southeast Asia, in: Land-Atmospheric Research Applications in South and Southeast Asia, Springer Remote Sensing/Photogrammetry, edited by: Vadrevu K., Ohara T., Justice C., Springer, Cham, 67–81, https://doi.org/10.1007/978-3-319-67474-2_4.

Itahashi,S., Yumimoto, K., Uno, I., Hayami, H., Fujita, S., Pan, Y-P., Wang, Y. 2018. A 15-year record (2001-2015) of the ratio of nitrate to non-seasalt sulfate in precipitation over East Asia. Atmos. Chem. Phys. 18: 2835-2852.

Itahashi, S., Yumimoto, K., Kurokawa, J., Morino, Y., Nagashima, T., Miyazaki, K., Maki, T., and Ohara, T. 2019. Inverse estimation of NOx emissions over China and India 2005-2016: contrasting recent trends and future perspectives. Environ. Res. Lett. 14: 124020.

Kanaya, Y., Cao, R., Akimoto, H., Fukuda, M., Komazaki, Y., Yokouchi, Y., Koike, M., Tanimoto, H., Takegawa, N., and Kondo, Y. 2007. Urban photochemistry in central Tokyo: 1. Observed and modeled OH and HO2 radical concentrations during the winter and summer of 2004, Journal of Geophysical Research, 112, D21312.

Kaufman, Y.J., Tanre, D., and Boucher, O. 2002. A satellite view of aerosols in the climate system. Nature. 419: 215–23

Khamkaew, C., Chantara, S., Janta, R., Pani, S. K., Prapamontol, T., Kawichai, S., Wiriya, W. and Lin, N. H. 2016. Investigation of Biomass Burning Chemical Components over Northern Southeast Asia during 7-SEAS/BASELInE 2014 Campaign. Aerosol and Air Quality Research, 16, 2655-2670.

Koukouli, M.E., Balis, D.S., van der A, R.J., Theys, N., Hedelt, P., Richter, A., Krotkov, N., Li, C., and Taylor, M. 2016. Anthropogenic Sulphur dioxide load over China as observed from different satellite sensors. Atmos. Environ. 145: 45–59.

Krotkov, N. A., Li, C., and Leonard, P.: OMI/Aura Sulfur Dioxide (SO2) Total Column L3 1 day Best Pixel in 0.25 degree × 0.25 degree V3, Greenbelt, MD, USA, Goddard Earth Sciences Data and Information Services Center (GES DISC), https://doi.org/10.5067/Aura/OMI/DATA3008, 2015.

Krotkov, N.A., McLinden, C.A., Li, C., Lamsal, L.N., Celarier, E.A., Marchenko, S.V., Swartz,

W.H., Bucsela, E.J., Joiner, J., Duncan, B.N., Boersma, K.F., Veefkind, J.P., Levelt, P.F., Fioletov, V.E., Dickerson, R.R., He, H., Lum Z. and Streets, D.G. 2016. Aura OMI observations of regional SO_2 and NO_2 pollution changes from 2005 to 2015. Atmos. Chem. Phys. 16: 4605–4629.

Krotkov, N. A, Lamsal, L. N., Marchenko, S. V., Celarier, E. A., Bucsela, E. J., Swartz, W. H., Joiner , J. and the OMI core team. 2019. OMI/Aura NO_2 Cloud-Screened Total and Tropospheric Column L3 Global Gridded 0.25 degree x 0.25 degree V3, NASA Goddard Space Flight Center, Goddard Earth Sciences Data and Information Services Center (GES DISC), Accessed: 14 January, 2021, 10.5067/Aura/OMI/DATA3007.

Kurokawa J., Ohara, T. 2020. Long-term historical trends in air pollutant emissions in Asia: Regional Emission inventory in ASia (REAS) version 3. Atmospheric Chemistry and Physics 20: 12761–12793. https://doi.org/10.5194/acp-20-12761-2020.

Lee, C., Martin, R.V., Donkelaar, A., Lee, H., Dickerson, R.R., Hains, J.C., Krotkov, N., Richter, A., Vinnikov, K., and Schwab, J.J. 2011. SO_2 emissions and lifetimes: Estimates from inverse modeling using in situ and global space-based (SCIAMACHY and OMI) observations, J. of Geophys. Res. –Atmospheres, 116: D06304.

Lee, C. T., Ram, S. S., Nguyen, D. L., Chou, C. C., Chang, S. Y., Lin, N. H., Chang, S. C., Hsiao, T. C., Sheu, G. R., Ou-Yang, C. F., Chi, K. H., Wang, S. H., Wu, X.C. 2016. Aerosol Chemical Profile of Near-Source Biomass Burning Smoke in Sonla, Vietnam during 7-SEAS Campaigns in 2012 and 2013. Aerosol and Air Quality Research 16, 2603-2617.

Levy, R.C., Mattoo, S., Munchak, L.A., Remer, L.A., Sayer, A.M., Patadia, F., and Hsu, N.C. 2013. The collection 6 MODIS aeorosol products over land and ocean. Atmos. Meas. Tech. 6: 2989–3034.

Li, G., Su, H., Ma, N., Tao, J., Kuang, Y., Wang, Q., Hong, J., Zhang, Y., Kuhn, U., Zhang, S., Pan, X., Lu, N., Tang, M., Zheng, G., Wang, Z., Gao, Y., Cheng, P., Xu, W., Zhou, G., Zhao, C., Yuan, B., Shao, M., Ding, A., Zhang, Q., Fu, P., Sun, Y., Pöschl, U., Cheng, Y. 2021. Multiphase chemistry experiment in Fogs and Aerosols in the North China Plain (McFAN): integrated analysis and intensive winter campaign 2018. Faraday Discussions 226, 207-222.

Li, M., Zhang, Q., Kurokawa, J.-I., Woo, J.-H., He, K., Lu, Z., Ohara, T., Song, Y., Streets, D. G., Carmichael, G. R., Cheng, Y., Hong, C., Huo, H., Jiang, X., Kang, S., Liu, F., Su, H., and Zheng, B. 2017. MIX: a mosaic Asian anthropogenic emission inventory under the international collaboration framework of the MICS-Asia and HTAP, Atmos. Chem. Phys., 17: 935–963.

Lin, N. H., Tsay, S. C., Maring, H. B., Yen, M. C., Sheu, G., R., Wang, S. H., Chi, K. H., Chuang, M. T., Ou-Yang, C. F., Fu, J. S., Reid, J. S., Lee, C. T., Wang, L. C., Wang, J. L., Hsu, C. N., Sayer, A. M., Holben, B. N., Chu, Y. C., Nguyen, X. A. Sopajaree, K., Chen, S. J., Cheng, M. T., Tsuang, B. J., Tsai, C. J., Peng, C. M., Schnell, R. C., Conway, T., Chang, C. T., Lin, K. S., Tsai, Y. I., Lee, W. J., Chang, S. C., Liu, J. J., Chiang, W. L., Huang, S. J., Lin, T. H., Liu, G. R. 2013. An overview of regional experiments on biomass burning aerosols and related pollutants in Southeast Asia: From BASE-ASIA and the Dongsha Experiment to 7-SEAS, Atmospheric Environment, Volume 78, 1-19.

Liu, Z., Gao, W., Yu, Y., Hu, B., Xin, J., Sun, Y., Wang, L., Wang, G., Bi, X., Zhang, G., Xu, H., Cong, Z., He, J., Xu, J., Wang, Y. 2018. Characteristics of PM2.5 mass concentrations and chemical species in urban and background areas of China: emerging results from the CARE-China network, Atmospheric Chemistry and Physics 18, 8849–8871.

NASA. 2021. LAADS DAAC, Accessed: 30 June 2021, https://ladsweb.modaps.eosdis.nasa.gov

Nishina, K., Watanabe, M., Koshikawa, M.K., Takamatsu, T., Morino, Y., Nagashima, T., Soma, K., Hayashi, S. 2017. Varying sensitivity of mountainous streamwater base-flow NO3– concentrations to N deposition in the northern suburbs of Tokyo. Scientific Reports 7: 7701. https://doi.org/10.1038/s41598-017-08111-w.

Obolkin, V., Khodzher, T., Sorokovikova, L., Tomberg, I., Netsvetaeva O., Golobokova, L. 2016. Effect of long-range transport of sulphur and nitrogen oxides from large coal power plants on acidification of river waters in the Baikal region, East Siberia, International Journal of Environmental Studies, 73 (3): 452-461. http://dx.doi.org/10.1080/00207233.2016.1165481.

Sase, H., Saito, T., Takahashi, M., Morohashi, M., Yamashita, N., Inomata, Y., Ohizumi, T., Nakata,

M. 2021. Transboundary air pollution reduction rapidly reflected in stream water chemistry in forested catchment on the Sea of Japan coast in central Japan. Atmospheric Environment, 248: 118223. https://doi.org/10.1016/j.atmosenv.2021.118223.

Sase, H., Takahashi, M., Matsuda, K., Sato, K., Tanikawa, T., Yamashita, N., Ohizumi, T., Ishida, T., Kamisako, M., Kobayashi, R., Uchiyama, S., Saito, T., Morohashi, M., Fukuhara, H., Kaneko, S., Inoue, T., Yamada, T., Takenaka, C., Tayasu, I., Nakano, T., Hakamata, T., Ohta, S. 2019. Response of river water chemistry to changing atmospheric environment and sulfur dynamics in a forested catchment in central Japan. Biogeochemistry, 142: 357-374. https://doi.org/10.1007/s10533-019-00540-1.

Sase, H., Yamashita, N., Luangjame, J., Garivait, H., Kietvuttinon, B., Visaratana, T., Kamisako, M., Kobayashi, R., Ohta, S., Shindo, J., Hayashi, K., Toda, H., Matsuda, K. 2017. Alkalinization and acidification of stream water with changes in atmospheric deposition in a tropical dry evergreen forest of northeastern Thailand. Hydrological Processes, 31: 836-846. http://dx.doi.org/10.1002/hyp.11062.

Pan, Y. P., Wang, Y. S., Tang, G. Q., Wu, D. 2012. Wet and dry deposition of atmospheric nitrogen at ten sites in Northern China, Atmospheric Chemistry and Physics 12(14), 6515-6535

Pani, S. K., Wang, S. H., Lin, N. H., Lee, C. T., Tsay, S. C., Holben, B. N., Janjai, S., Hsiao, T. C., Chuang, M. T., Chantara, S. 2016. Radiative Effect of Springtime Biomass-Burning Aerosols over Northern Indochina during 7-SEAS/BASELInE 2013 Campaign. Aerosol and Air Quality Research 16, 2802-2817.

Ramasamy, S., Nagai, Y., Takeuchi, N., Yamasaki, S., Shoji, K., Ida, A., Jones, C., Tsurumaru, H., Suzuki, Y., Yoshino, A., Shimada, K., Nakashima, Y., Kato, S., Hatakeyama, S., Matsuda, K., Kajii, Y. 2018. Comprehensive measurements of atmospheric OH reactivity and trace species within a suburban forest near Tokyo during AQUAS-TAMA campaign, Atmospheric Environment, 184, 166–176.

Ren, X., Brune, W. H., Mao, J., Mitchell, M. J., Lesher, R. L., Simpas, J. B., Metcalf, A. R., Schwab, J. J., Cai, C., Li, Y., Demerjian, K. L., Felton, H. D., Boynton, G., Adams, A., Perry, J., He, Y., Zhou, X., and Hou, J. 2006. Behavior of OH and HO2 in the winter atmosphere in New York city, Atmospheric Environment, 40, 252–263.

Richter, A., Burrows, J. P., Nues, H., Granier, C., and Niemeier, U. 2005. Increase in tropospheric nitrogen dioxide over China observed from space. Nature. 437: 129–132.

Tan, Z., Rohrer, F., Lu, K., Ma, X., Bohn, B., Broch, S., Dong, H., Fuchs, H., Gkatzelis, G. I., Hofzumahaus, A., Holland, F., Li, X., Liu, Y., Liu, Y., Novelli, A., Shao, M., Wang, H., Wu, Y., Zeng, L., Hu, M., Kiendler-Scharr, A., Wahner, A., Zhang, Y. 2018. Wintertime photochemistry in Beijing: observations of ROx radical concentrations in the North China Plain during the BEST-ONE campaign, Atmospheric Chemistry and Physics 18, 12391–12411.

Uno, I., Wang, Z., Itahashi, S., Yumimoto, K., Yamamura, Y., Yoshino, A., Takami, A., Hayasaki, M., and Kim, B-G. 2020. Paradigm shift in aerosol chemical composition over regions downwind of China. Sci. Rep. 10: 6450.

van der A, R. J., Mijling, B., Ding, J., Koukouli, M. E., Liu, F., Li, Q., Mao, H., and Theys, N. 2017. Cleaning up the air: effectiveness of air quality policy for SO_2 and NOx emissions in China, Atmos. Chem. Phys. 17: 1775-1789.

Yamashita, N., Sase, H., Kobayashi, R., Leong, K-P., Hanapi, J.M., Uchiyama, S., Urban, S., Toh, Y-Y., Muhamad, M., Gidiman, J., Chappell, N.A. 2014. Atmospheric deposition versus rock weathering in the control of streamwater chemistry in a tropical rain-forest catchment in Malaysian Borneo. Journal of Tropical Ecology, 30: 481-492. http://dx.doi.org/10.1017/S0266467414000303.

Zhang, Q., Zheng, Y., Tong, D., Shao, M., Wang, S., Zhang, Y., Xu, X., Wang, J., He, H., Liu, W., Ding, Y., Lei, Y., Li, J., Wang, Z., Zhang, X., Wang, Y., Cheng, J., Liu, Y., Shi, Q., Yan, L., Geng, G., Hong, C., Li, H., Liu, F., Zheng, B., Cao, J., Ding, A., Gao, J., Fu, Q., Huo, J., Liu, B., Liu, Z., Yang, F., He, K. and Hao, J. 2019. Drivers of improved $PM_{2.5}$ air quality in China from 2013 to 2017. Proc. Natl. Acad. Sci. U. S. A. 116: 24463–9.

(6.3)

Akimoto, H. and Narita, H. 1994. Distribution of SO_2, NO_x, and CO_2 emissions from fuel combustion

and industrial activities in Asia with 1° × 1° resolution, Atmos. Environ., 28: 213–225.

Amann, M., Bertok, I., Borken-Kleefeld, J., Cofala, J., Heyes, C., Höglund-Isaksson, L., Klimont, Z., Nguyen, B., Posch, M., Rafaj, P., Sandler, R., Schöpp, W., Wagner, F., and Winiwarter, W. 2011. Cost-effective control of air quality and greenhouse gases in Europe: Modeling and policy applications, Environ. Modell. Softw., 26: 1489–1501.

Chatani, S., Yamaji, K., Sakurai, T., Itahashi, S., Shimadera, H., Kitayama, K., and Hayami, H. 2018. Overview of model inter-comparison in Japan's Study for Reference Air Quality Modeling (J-STREAM), Atmosphere, 9: 19.

Crippa, M., Guizzardi, D., Muntean, M., Schaaf, E., Dentener, F., van Aardenne, J. A., Monni, S., Doering, U., Olivier, J. G. J., Pagliari, V., and Janssens-Maenhout, G. 2018. Gridded emissions of air pollutants for the period 1970–2012 within EDGAR v4.3.2, Earth Syst. Sci. Data, 10: 1987–2013.

Ding, J., Miyazaki, K., van der A, R. J., Mijling, B., Kurokawa, J.-I., Cho, S., Janssens-Maenhout, G., Zhang, Q., Liu, F., and Levelt, P. F. 2017. Intercomparison of NO_x emission inventories over East Asia, Atmos. Chem. Phys., 17: 10125–10141.

Hoesly, R. M., Smith, S. J., Feng, L., Klimont, Z., Janssens-Maenhout, G., Pitkanen, T., Seibert, J. J., Vu, L., Andres, R. J., Bolt, R. M., Bond, T. C., Dawidowski, L., Kholod, N., Kurokawa, J.-I., Li, M., Liu, L., Lu, Z., Moura, M. C. P., O'Rourke, P. R., and Zhang, Q. 2018. Historical (1750–2014) anthropogenic emissions of reactive gases and aerosols from the Community Emissions Data System (CEDS), Geosci. Model Dev., 11: 369–408.

Itahashi, S., Yumimoto, K., Kurokawa, J., Morino, Y., Nagashima, T., Miyazaki, K., Maki, T., and Ohara, T. 2019. Inverse estimation of NO_x emissions over China and India 2005–2016: contrasting recent trends and future perspectives, Environ. Res. Lett., 14: 124020.

Janssens-Maenhout, G., Crippa, M., Guizzardi, D., Dentener, F., Muntean, M., Pouliot, G., Keating, T., Zhang, Q., Kurokawa, J., Wankmüller, R., Denier van der Gon, H., Kuenen, J. J. P., Klimont, Z., Frost, G., Darras, S., Koffi, B., and Li, M. 2015. HTAP_v2.2: a mosaic of regional and global emission grid maps for 2008 and 2010 to study hemispheric transport of air pollution, Atmos. Chem. Phys., 15: 11411–11432.

JPEC. 2014. Emission inventory of $PM_{2.5}$ and profiles of emission sources, Report of Ministry of Environment of Japan, 1094 p.

Kato, N. and Akimoto, H. 1992. Anthropogenic emissions of SO_2 and NO_x in Asia: emissions inventories, Atmos. Environ., 26: 2997–3017.

Klimont, Z., Kupiainen, K., Heyes, C., Purohit, P., Cofala, J., Rafaj, P., Borken-Kleefeld, J., and Schöpp, W. 2017. Global anthropogenic emissions of particulate matter including black carbon, Atmos. Chem. Phys., 17: 8681–8723.

Kurokawa, J., Ohara, T., Morikawa, T., Hanayama, S., Janssens-Maenhout, G., Fukui, T., Kawashima, K., and Akimoto, H. 2013. Emissions of air pollutants and greenhouse gases over Asian regions during 2000–2008: Regional Emission inventory in Asia (REAS) version 2, Atmos. Chem. Phys., 13: 11019–11058.

Kurokawa, J. and Ohara, T. 2020. Long-term historical trends in air pollutant emissions in Asia: Regional Emission inventory in ASia (REAS) version 3, Atmos. Chem. Phys., 20: 12761-12793.

Lee, D.-G., Lee, Y.-M., Jang, K.-W., Yoo, C., Kang, K.-H., Lee, J.-H., Jung, S.-W., Park, J.-M., Lee, S.-B., Han, J.-S., Hong, J.-H., and Lee, S.-J. 2011. Korean national emissions inventory system and 2007 air pollutant emissions, Asian J. Atmos. Environ., 5: 278–291.

Li, M., Zhang, Q., Kurokawa, J.-I., Woo, J.-H., He, K., Lu, Z., Ohara, T., Song, Y., Streets, D. G., Carmichael, G. R., Cheng, Y., Hong, C., Huo, H., Jiang, X., Kang, S., Liu, F., Su, H., and Zheng, B. 2017. MIX: a mosaic Asian anthropogenic emission inventory under the international collaboration framework of the MICS-Asia and HTAP, Atmos. Chem. Phys., 17: 935–963.

McDuffie, E. E., Smith, S. J., O'Rourke, P., Tibrewal, K., Venkataraman, C., Marais, E. A., Zheng, B., Crippa, M., Brauer, M., and Martin, R. V. 2020. A global anthropogenic emission inventory of atmospheric pollutants from sector- and fuel-specific sources (1970–2017): an application of the Community Emissions Data System (CEDS), Earth Syst. Sci. Data, 12: 3413–3442.

Ohara, T., Akimoto, H., Kurokawa, J., Horii, N., Yamaji, K., Yan, X., and Hayasaka, T. 2007. An Asian emission inventory of anthropogenic emission sources for the period 1980–2020, Atmos. Chem. Phys., 7: 4419–4444.

Permadi D. A., Sofyan, A., and Oanh, N. T. K. 2017. Assessment of emissions of greenhouse gases and air pollutants in Indonesia and impacts of national policy for elimination of kerosene use in cooking, Atmos. Environ., 154: 82–94.

Pham, T. B. T., Manomaiphiboon, K., and Vongmahadlek, C. 2008. Development of an inventory and temporal allocation profiles of emissions from power plants and industrial facilities in Thailand, Sci. Total Environ., 397: 103–118.

Shrestha, R. M., Kim Oanh, N. T., Shrestha, R. P., Rupakheti, M., Rajbhandari, S., Permadi, D. A., Kanabkaew, T., and Iyngararasan, M. 2013. Atmospheric Brown Clouds (ABC) Emission Inventory Manual, United Nations Environment Programme, Nairobi, Kenya, 174 p.

Streets, D. G., Bond, T. C., Carmichael, G. R., Fernandes, S. D., Fu, Q., He, D., Klimont, Z., Nelson, S. M., Tsai, N. Y., Wang, M. Q., Woo, J.-H., and Yarber, K. F. 2003a. An inventory of gaseous and primary aerosol emissions in Asia in the year 2000, J. Geophys. Res., 108: 8809.

Streets, D. G., Yarber, K. F., Woo, J.-H., and Carmichael, G. R. 2003b. Biomass burning in Asia: Annual and seasonal estimates and atmospheric emissions, Global Biogeochem. Cy., 17: 1099.

Streets, D. G., Zhang, Q., Wang, L., He, K., Hao, J., Wu, Y., Tang, Y., and Carmichael, G. R 2006. Revisiting China's CO emissions after the Transport and Chemical Evolution over the Pacific (TRACE‐P) mission: Synthesis of inventories, atmospheric modeling, and observations, J. Geophys., Res., 111: D14306.

Woo, J.-H., Kim, Y., Kim, H.-K., Choi, K.-C., Eum, J.-H., Lee, J.-B., Lim, J.-H., Kim, J., and Seong, M. 2020. Development of the CREATE Inventory in Support of Integrated Climate and Air Quality Modeling for Asia, sustainability, 12: 7930.

Zhang, Q., Streets, D. G., Carmichael, G. R., He, K. B., Huo, H., Kannari, A., Klimont, Z., Park, I. S., Reddy, S., Fu, J. S., Chen, D., Duan, L., Lei, Y., Wang, L. T., and Yao, Z. L. 2009. Asian emissions in 2006 for the NASA INTEX-B mission, Atmos. Chem. Phys., 9: 5131–5153.

Zhao, Y., Zhang, J., and Nielsen, C. P. 2014. The effects of energy paths and emission controls and standards on future trends in China's emissions of primary air pollutants, Atmos. Chem. Phys., 14: 8849–8868.

Zheng, B., Tong, D., Li, M., Liu, F., Hong, C., Geng, G., Li, H., Li, X., Peng, L., Qi, J., Yan, L., Zhang, Y., Zhao, H., Zheng, Y., He, K., and Zhang, Q. 2018. Trends in China's anthropogenic emissions since 2010 as the consequence of clean air actions, Atmos. Chem. Phys., 18: 14095–14111.

(6.4)

Ammuyalojaroen, T., Barth, M. C., Emmons, L. K., Carmichael, G. R., Kreasuwum, J., Prasitwattanaseree, S., and Chantara, S. 2014. Effects of different emission inventories on modeled ozone and carbon monoxide in Southeast Asia. Atmos. Chem. Phys. 14: 12983–13012.

An, J., Ueda, H., Wang, Z., Matsuda, K., Kajino, M., and Cheng, X. 2002. Simulations of monthly mean nitrate concentrations in precipitation. Atmos. Environ. 36: 4159–4171.

Akimoto, H., Nagashima, T., Li, J., Fu, J.S., Ji, D., Tan, J., and Wang, Z. 2019. Comparison of surface ozone simulation among selected regional models in MICS-Asia III – effects of chemistry and vertical transport for the causes of difference. Atmos. Chem. Phys. 19: 603–615.

Akimoto, H., Nagashima, T., Kawano, N., Li, J., Fu, J.S., and Wang, Z. 2020. Discrepancies between MICS-Asia III simulation and observation for surface ozone in the marine atmosphere over the Northwestern Pacific Asian rim region. Atmos. Chem. Phys. 20: 15003–15014.

Bleeker, A., Hicks, W.K, Dentener, F., Galloway, J and Erisman, J.W. 2011. N deposition as a threat to the world's protected areas under the convection on biological diversity. Environ. Pollut., 159: 2280–2288.

Byun, D. and Schere, K. L. 2006. Review of the governing equations, computational algorithms, and other components of the models-3 Community Multiscale Air Quality (CMAQ) modeling system. Appl. Mech. Rev., 59: 51–77.

Carmichael, G.R., Calori, G., Hayami, H., Uno, I., Cho, S. Y., Engardt, M., Kim, S.-B., Ichikawa, Y., Ikeda, Y., Woo, J.-H., Ueda, H., and Amann, M. 2002. The MICS-Asia study: model intercomparison of long-range transport and sulfur deposition in East Asia. Atmos. Environ. 36: 175–199.

Carmichael, G. R., Sandu, A., Chai, T., Daescu, D. N., Constantinescu, E. M., and Tang, Y. 2008a. Predicting air quality: Improvements through advanced methods to integrate models and measurements. J. Comp. Phys., 227(7): 3540–3571.

Carmichael, G.R., Sakurai, T., Streets, D., Hozumi, Y., Ueda, H., Park, S.U., Fung, C., Han, Z., Kajino, M., Engardt, M., Bennet, C., Hayami, H., Sartelet, K., Holloway, T., Wang, Z., Kannari, A., Fu, J., Matsuda, K., Thongboonchoo, N., and Amann, M. 2008b. MICS-Asia II: The model intercomparison study for Asia Phase II methodology and overview of findings. Atmos. Environ. 42: 3468–3490.

Chatani, S., Shimadera, H., Itahashi, S., and Yamaji, K. 2020. Comperehensive analysis of source sensitivities and apportionments of PM2.5 and ozone over Japan via multiple numerical techniques. Atmos. Chem. Phys. 20: 10311–10329.

Chen, L., Gao, Y., Zhang, M., Fu, J. S., Zhu, J., Liao, H., Li, J., Huang, K., Ge, B., Lee, H-J., Wang, X., Lam, Y-F., Lin, C-Y., Itahashi, S., Nagashima, T., Kajino, M., Yamaji, K., Wang, Z., and Kurokawa, J. 2019. MICS-Asia III: Multi-model comparison and evaluation of aerosol over East Asia. Atmos. Chem. Phys. 19: 11911–11937.

Clappier, A., Belis, C. A., Pernigotti, D., and Thunis, P. 2017. Source apportionment and sensitivity analysis: two methodologies with two difference purposes. Geosci. Model Dev. 10: 4245–4256.

Fujita, S., Takahashi, A., Weng, J-H., Huang, L-F., Kim, H-K., Li, C-K., Huang, F.T.C., Jeng, F-T., 2000. Precipitation Chemistry in East Asia, Atmos. Environ. 34: 525-537.

Gao, M., Han, Z., Liu, Z., Li, M., Xin, J., Tao, Z., Li, J., Kang, J.-E., Huang, K., Dong, X., Zhuang, B., Li, S., Ge, B., Wu, Q., Cheng, Y., Wang, Y., Lee, H.-J., Kim, C.-H., Fu, J.S., Wang, T., Chin, M., Woo, J.-H., Zhang, Q., Wang, Z., and Carmichael, G.R. 2018. Air quality and climate change, Topic 3 of the Model Inter-Comparison Study for Asia Phase III (MICS-Asia III)–Part 1: Overview and model evaluation. Atmos. Chem. Phys. 18: 4859–4884.

Gao, M., Han, Z., Tao, Z., Li, J., Kang, J.-E., Huang, K., Dong, X., Zhuang, B., Li, S., Ge, B., Wu, Q., Lee, H.-J., Kim, C. -H., Fu, J. S., Wang, T., Chin, M., Li, M., Woo, J.-H., Cheng, Y., Wang, Z., and Carmichael, G.R. 2020. Air quality and climate change, Topic 3 of the Model Inter-Comparison Study for Asia Phase III (MICS-Asia III)–Part 2: aerosol radiative effects and aerosol feedbacks. Atmos. Chem. Phys. 20: 1147–1161.

Ge, B., Itahashi, S., Sato, K, Xu, D., Wang, J., Fan, F., Tan, Q., Fu, J. S., Wang, X., Yamaji, K., Nagashima, T., Li, J., Kajino, M., Liao, H., Zhang, M. G., Wang, Z., Li, M., Woo, J-H., Kurokawa, J., Pan, Y., Wu, Q., Liu, X., and Wang, Z. F. 2020. Model inter-comparison study for Asia (MICS-Asia) phase III: multimodel comparison of reactive nitrogen deposition over China. Atmos. Chem. Phys. 20: 10587–10610.

Han, Z. 2007. A regional air quality model: Evaluation and simulation of O_3 and relevant gaseous species in East Asia during spring 2001. Environ. Modell. Software, 22: 1328–1336.

Han, Z., Sakurai, T., Ueda, H., Carmichael, G. R., Streets, D., Hayami, H., Wang, Z., Holloway, T., Engardt, M., Hozumi, Y., Park, S. U., Kajino, M., Sartelet, K., Fung, C., Bennet, C., Thongboonchoo, N., Tang, Y., Chang, A., Matsuda, K., and Amann, M. 2008. MICS-Asia II: Model intercomparison and evaluation of ozone and relevant species. Atmos. Environ. 42: 3491–3509.

Hayami, H., Sakurai, T., Han, Z., Ueda, H., Carmichael, G.R., Streets, D., Holloway, T., Wang, Z., Thongboonchoo, N., Engardt, M., Bennet, C., Fung, C., Chang, A., Park, S.U., Sartelet, K., Matsuda, K., and Amann, M. 2008. MICS-Asia II: Model intercomparison and evaluation of particulate sulfate, nitrate and ammonium. Atmos. Environ. 42: 3510–3527.

Itahashi, S., Uno, I. and Kim, S. 2012. Source Contributions of Sulfate Aerosol over East Asia Estimated by CMAQ-DDM. Environ. Sci. Technol. 46(12): 6733–6741.

Itahashi, S., Hayami, H., Yumimoto, K. and Uno, I. 2017. Chinese province-scale source apportionments for sulfate aerosol in 2005 evaluated by the tagged tracer method. Environ. Pollut., 220: 1366–1375.

Itahashi, S., Ge, B.Z., Sato, K., Fu, J.S., Wang, X.M., Yamaji, K., Nagashima, T., Li, J., Kajino, M., Liao, H., Zhang, M.G., Wang, Z., Li, M., Kurokawa, J., Carmichae, G.R., and Wang, Z.F. 2020. MICS-Asia III: overview of model intercomparison and evaluation of acid deposition over Asia, Atmos. Chem. Phys. 20: 2667–2693.

Kajino, M., Ueda, H., Sato, K. and Sakurai, T. 2011. Spatial distribution of the source-receptor relationship of sulfur in Northeast Asia. Atmos. Chem. Phys. 11: 6475–6491.

Kajino, M., Inomata, Y., Sato, K., Ueda, H., Han, Z., An, J., Katata, G., Deushi, M., Maki, T., Oshima, N., Kurokawa, J., Ohara, T., Takami, A. and Hatakeyama, S. 2012. Development of the RAQM2 aerosol chemical transport model and predictions of the Northeast Asian aerosol mass, size, chemistry, and mixing type. Atmos. Chem. Phys. 12: 11833–11856.

Kajino, M., Sato, K., Inomata, Y. and Ueda, H. 2013. Source–receptor relationships of nitrate in Northeast Asia and influence of sea salt on the long-range transport of nitrate. Atmos. Environ. 79: 67–78.

Kim, E., Kim, B-U., Kim, H. C.. and Kim, S. T. 2021. Sensitivity of fine particulate matter concentrations in South Korea to regional ammonia emissions in Northeast Asia. Environ. Pollut., 273: 116428.

Kong, L., Tang, X., Zhu, J., Wang, Z., Fu, J.S., Wang, X., Itahashi, S., Yamaji, K., Nagashima, T., Lee, H.-J., Kim, C.-H., Lin, C.-Y., Chen, L., Zhang, M., Tao, Z., Li, J., Kajino, M., Liao, H., Sudo, K., Wang, Y., Pan, Y.-P., Tang, G., Li, M., Wu, Q., Ge, B., and Carmichael, G.R. 2020. Evaluation and uncertainty investigation of the NO_2, CO and NH_3 modeling over China under the framework of MICS-Asia III. Atmos. Chem. Phys. 20: 181–202.

Kuribayashi, M., Ohara, T., Morino, Y., Uno, I., Kurokawa, J., and Hara, H. 2012. Long-term trends of sulfur deposition in East Asia. Atmospheric Environment 59, 461-475.

Lee, H.-H., Bar-Or, R. Z., and Wang, C. 2017. Biomass burning aerosols and the low-visibility events in Southeast Asia. Atmos. Chem. Phys. 17: 965–980.

Li, J., Yang, W., Wang, Z., Chen, H., Hu, B., Li, J., Sun, Y., Huang, Y., 2014. A modeling study of source-receptor relationships in atmospheric particulate matter over Northeast Asia. Atmos. Environ. 91, 40–51.

Li, J., Yang, W., Wang, Z., Chen, H., Hu, B., Li, J., Sun, Y., Fu, P. and Zhang, Y. 2016. Modeling study of surface ozone source-receptor relationships in East Asia. Atmospheric Research. 167: 77–88.

Li, J., Nagashima, T., Kong, L., Ge, B., Yamaji, K., Fu, J.S., Wang, X., Fan, Q., Itahashi, S., Lee, H.-J., Kim, C.-H., Lin, C.-Y., Zhang, M., Tao, Z., Kajino, M., Liao, H., Li, M., Woo, J.-H., Kurokawa, J., Wu, Q., Akimoto, H., Carmichael, G.R., and Wang, Z. 2019. Model evaluation and inter-comparison of surface-level ozone and relevant species in East Asia in the context of MICS-Asia phase III Part I: Overview. Atmos. Chem. Phys. 19: 12993–13015.

Li, M., Zhang, Q., Kurokawa, J., Woo, J.-H., He, K.B., Lu, Z., Ohara, T., Song, Y., Streets, D.G., Carmichael, G.R., Cheng, Y.F., Hong, C.P., Huo, H., Jiang, X.J., Kang, S.C., Liu, F., Su, H., and Zheng, B. 2017. MIX: a mosaic Asian anthropogenic emission inventory for the MICS-Asia and the HTAP projects. Atmos. Chem. Phys. 17: 935–963.

Lin, M., Oki, T., Bengtsson, M., Kanae, S., Holloway, T. and Streets, D.G. 2008. Long-range transport of acidifying substances in East Asia—Part II: Source–receptor relationships. Atmos. Environ. 42: 5956–5967.

Marvin, M. R., Palmer, P. I., Latter, B. G., Siddans, R., Kerridge, B. J., Latif, M. T., and Khan, M. F. 2021. Photochemical environment. Atmos. Chem. Phys. 17: 935–963.

Morino, Y., Ohara, T., Kurokawa, J., Kuribayashi, M., Uno, I., and Hara, H. 2011. Temporal variations of nitrogen wet deposition across Japan from 1989 to 2008. J. of Geophys. Res. Atmos. 116: D06307.

Nagashima, T., Ohara, T., Sudo, K. and Akimoto, H. 2010. The relative importance of various source regions on East Asian surface ozone. Atmos. Chem. Phys. 10: 11305–11322.

Nguyen, G. T. H., Shimadera, H., Uranishi, K. Matsuo, T., Kondo, A., and Thepanondh, S. 2019. Numerical assessment of $PM_{2.5}$ and O_3 air quality in continental Southeast Asia: Baseline simulation and aerosol direct effects investigation. Atmos. Environ. 219: 117054.

Sudo, K., Takahashi, M., Kurokawa, J. and Akimoto, H. 2002. CHASER: A global chemical model of the troposphere 1. Model description. Journal of Geophys. Res.: Atmos. 107(D17): 4339.

Tan, J. N., Fu, J.S., Carmichael, G.R., Itahashi, S., Tao, Z.N., Huang, K., Dong, X.Y., Yamaji, K., Nagashima, T., Wang, X.M., Liu, Y.M., Lee, H.J., Lin, C.Y., Ge, B.Z., Kajino, M., Zhu, J., Zhang, M.G., Liao, H., and Wang, Z.F. 2020. Why do models perform differently on particulate matter over East Asia? A multi-model intercomparison study for MICS-Asia III. Atmos. Chem. Phys. 20: 7393–7410.

Wang, Z., Maeda, T., Hayashi, M., Hsiao, L.F., and Liu, K. Y. 2001. A nested air quality prediction modeling system for urban and regional scales: application for high ozone episode in Taiwan. Water Air Soil Pollut. 130: 391–396.

Wang, Z., Xie, F., Sakurai, T., Ueda, H., Han, Z., Carmichael, G.R., Streets, D., Engards, M., Hollowway, T., Hayami, H., Kajino, M., Thongboonchoo, N., Bennet, C., Park, S.U., Fung, C., Chang, A., Sartelet, K., and Amann, M. 2008. MICS-Asia II: Model inter-comparison and evaluation of acid deposition. Atmos. Environ. 42: 3528–3542.

Yamaji, K., Ohara, T., Uno, I., Tanimoto, H., Kurokawa, J. and Akimoto, H. 2006. Analysis of the seasonal variation of ozone in the boundary layer in East Asia using the Community Multi-scale Air Quality model: What controls surface ozone levels over Japan? Atmos. Environ. 40: 1856–1868.

Ying, Q., Wu, L., and Zhang, H. 2014. Local and inter-regional contributions to $PM_{2.5}$ nitrate and sulfate in China. Atmos. Environ. 94: 582–592.

Zhao, Y., Zhang, L., Pan, Y., Wang, Y., Paulot, F. and Henze, D. K. 2015. Atmospheric nitrogen deposition to the northwestern Pacific: seasonal variation and source attribution, Atmos. Chem. Phys. 15: 10905–10924.

Zhang, Y. 2008. Online-coupled meteorology and chemistry models: history, current status, and outlook. Atmos. Chem. Phys. 8: 2895–2932.

(6.5)

Ainsworth, E.A., Rogers, A. 2007. The response of photosynthesis and stomatal conductance to rising [CO2]: mechanisms and environmental interactions. Plant, Cell & Environment, 30, 258-270. https://doi.org/10.1111/j.1365-3040.2007.01641.x

De Marco, A., Anav, A., Sicard, P., Feng, Z., Paoletti, E. 2020. High spatial resolution ozone risk-assessment for Asian forests. Environ. Res. Lett. 15, 104095. https://doi.org/10.1088/1748-9326/abb501.

de Vries, W., Dobbertin, M.H., Solberg, S. et al. 2014. Impacts of acid deposition, ozone exposure and weather conditions on forest ecosystems in Europe: an overview. Plant and Soil, 380, 1–45. https://doi.org/10.1007/s11104-014-2056-2

Duan, L., Yu, Q., Zhang, Q., Wang, Z., Pan, Y., Larssen, T., Mulder, J., 2016. Acid deposition in Asia: emissions, deposition, and ecosystem effects. Atmos. Environ. 146, 55–69. https://doi.org/10.1016/j.atmosenv.2016.07.018

EANET 2020, Strategy Paper on Future Direction of EANET on Monitoring of Effects on Agricultural Crops, Forest and Inland Water by Acidifying Species and Related Chemical Substances, Updated at the 6th Meeting of the Task Force on Soil and Vegetation Monitoring and adopted by the Scientific Advisory Committee of the EANET at its 20th Session.

EANET 2019. Summary of the workshop. Workshop on regional impact assessment of atmospheric deposition and air pollution on forest ecosystems 21-22 November 2019, Niigata, Japan. EANET/ WRIA/ 3

Forsius, M., Posch, M., Holmberg, M., Vuorenmaa, J., Kleemola, S., Augustaitis, A., Beudert, B., Bochenek, W., Clarke, N., de Wit, H.A., Dirnböck, T., Frey, J., Grandin, U., Hakola, H., Kobler, J., Krám, P., Lindroos, A-J., Löfgren, S., Pecka, T., Rönnback, P., Skotak, K., Szpikowski, J., Ukonmaanaho, L., Valinia, S., Váňa, M. 2021. Assessing critical load exceedances and ecosystem impacts of anthropogenic nitrogen and sulphur deposition at unmanaged forested catchments in Europe. Science of the Total Environment 753, 141791. https://doi.org/10.1016/j.scitotenv.2020.141791

Hisano, M., Chen, H. Y. H., Searle, E. B., Reich, P. B. 2019. Species‐rich boreal forests grew more and suffered less mortality than species‐poor forests under the environmental change of the past half‐century. Ecology Letters, 22, 999– 1008. https://doi.org/10.1111/ele.13259

IIASA 2008, RAINS-Asia: The First Integrated Assessment of Air Pollution in Asia (visited on 26 April 2021). https://iiasa.ac.at/web/home/research/researchPrograms/air/rains-asia1.html

IRI (International Research Institute on Climate and Society) 2021. *ENSO Resources.* https://iri.columbia.edu/our-expertise/climate/enso/

Kinose, Y., Yamaguchi, M., Matsumura, H., Izuta T. 2020. Impact assessment of ozone absorbed through stomata on photosynthetic carbon dioxide uptake by Japanese deciduous forest trees: Implications for ozone mitigation policies. Forests 11, 137. https://doi.org/10.3390/f11020137.

Kirschbaum, M.U.F., McMillan, A.M.S. 2018. Warming and elevated CO_2 have opposing influences on transpiration. Which is more important?. Curr Forestry Rep 4, 51–71. https://doi.org/10.1007/s40725-018-0073-8

Kume, A., Fujimoto, M., Mizoue, N., Honoki, H., Nakajima, H., Ishida, M. 2020. Impact of reduced ozone concentration on the mountain forests of Mt. Tateyama, Japan. Environmental Pollution, 267, 115407. https://doi.org/10.1016/j.envpol.2020.115407.

Larssen, T., Carmichael, G.R., 2000. Acid rain and acidification in China: the importance of base cation deposition. Environ. Pollut. 110, 89-102. https://doi.org/10.1016/S0269-7491(99)00279-1

Liang, J., Gamarra, J.G.P. 2020. The importance of sharing global forest data in a world of crises. Sci Data 7, 424. https://doi.org/10.1038/s41597-020-00766-x

Madhu, M., Hatfield, J.L. 2013 Dynamics of plant root growth under increased atmospheric carbon dioxide. Agronomy Journal, 105, 657-669. https://doi.org/10.2134/agronj2013.0018

Ropelewski, C.F., Halpert, M.S. 1992. Global and regional scale precipitation patterns associated with the El Niño/Southern oscillation. Monthly Weather Review 115, 1606–1626. https://doi.org/10.1175/1520-0493(1987)115<1606:GARSPP>2.0.CO;2

Shah, J., Nagpal, T., Johnson, T., Amann, M. , Carmichael, G.R., Foell, W., Green, C., Hettelingh, J-P., Hordijk, L., Li, J., Peng, C., Pu, Y., Ramankutty, R., Streets, D. 2000. Integrated analysis for acid rain in Asia: Policy implications and results of RAINS-Asia model. Annual Review of Energy and the Environment 25, 339-375. https://doi.org/10.1146/annurev.energy.25.1.339.

UNECE 2005. 1999 Protocol to Abate Acidification, Eutrophication and Ground-level Ozone to the Convention on Long-range Transboundary Air Pollution. UNECE Homepage, https://unece-modl.dotsoft.gr/protocols

Xie, D., Zhao, B., Wang, S., Duan, L. 2020. Benefit of China's reduction in nitrogen oxides emission to natural ecosystems in East Asia with respect to critical load exceedance. Environment International 136 (2020) 105468. https://doi.org/10.1016/j.envint.2020.105468

Yamashita, N., Sase, H., Kurokawa, J., Morino, Y., Kuribayashi, M., Ohara, T. 2019. Regional impact assessment on acidification/N saturation in the East Asia: a critical loads approach. Workshop on regional impact assessment of atmospheric deposition and air pollution on forest ecosystems Abstract Book, EANET/ WRIA/ 2/ 22/ O7.

Zhao, Y., Duan, L., Lei, Y., Xing, J., Nielsen, C.P., Hao, J.M., 2011. Will PM control undermine China's efforts to reduce soil acidification? Environmental Pollution 159, 2726-2732. https://doi.org/10.1016/j.envpol.2011.05.018.

(6.6)

Akimoto, H., Kurokawa, J., Sudo, K., Nagashima, T., Takemura, T., Klimont, Z., et al. 2015. SLCP co control approach in east asia: Tropospheric ozone reduction strategy by simultaneous reduction of nox/nmvoc and methane. Atmospheric Environment 122:588-595.

Allen, R.W., Gombojav, E., Barkhasragchaa, B., Byambaa, T., Lkhasuren, O., Amram, O., Takaro, T.K., Janes, C.R. 2013. An assessment of air pollution and its attributable mortality in Ulaanbaatar, Mongolia. Air Qual Atmos Health. 6(1):137-150

Anenberg SC, Horowitz LW, Tong DQ, West JJ. 2010. An estimate of the global burden of anthropogenic ozone and fine particulate matter on premature human mortality using atmospheric modeling. Environmental health perspectives 118:1189-1195.

Anenberg, S.C., Henze, D.K., Tinney, V., Kinney, P.L., Raich, W., Fann, N., et al. 2018. Estimates of the global burden of ambient [formula: See text], ozone, and [formula: See text] on asthma incidence and emergency room visits. Environ Health Perspect 126:107004.

Anenberg SC, Miller J, Henze DK, Minjares R, Achakulwisut P. 2019. The global burden of

transportation tailpipe emissions on air pollution-related mortality in 2010 and 2015. Environmental Research Letters 14:094012.

Burnett, R.T., Pope, III,C.A., Ezzati, M., Olives, C., Lim, S.S., Mehta, S., Shin S., Singh, H.H., Hubbell, B., Brauer, M., Cohen, A. 2014. An integrated risk function for estimating the global burden of disease attributable to ambient fine particulate matter exposure. Environ. Health Perspect. 122, 397-403.

Burnett, R., Chen, H., Szyszkowicz, M., Fann, N., Hubbell, B., Pope, C.A., et al. Global estimates of mortality associated with long-term exposure to outdoor fine particulate matter. 2018. Proc Natl Acad Sci U S A. 115(38):9592-9597.

Cohen, J.A., Brauer, M., Burnett, R., Anderson, H.R., Frostad, J., Estep, K., Balakrishnan, K., Brunekreef, B., Dandona, L., Dandona, R., Feigin, V., Freedman, G., Hubbell, B., Jobling, A., Kan, H., Knibbs, L., Liu, Y., Martin, R., Morawska, L., Pope III, C.A., Shin, H., Straif, K., Shaddick, G., Thomas, M., Dingenen, V.R., Donkelaar, V.A., Vos, T., Murray, J.L.C., Forouzanfar, H.M. 2017. Estimates and 25-year trends of the global burden of disease attributable to ambient air pollution: an analysis of data from the Global Burden of Diseases Study 2015. Lancet 2017; 389: 1907–18.

Dasadhikari, K., Eastham, S.D., Allroggen, F., Speth, R.L., Barrettet, S.R.H. 2019. Evolution of sectoral emissions and contributions to mortality from particulate matter exposure in the Asia-Pacific region between 2010 and 2015. Atmospheric Environment, 116916.

Finlayson-Pitts. B.J., Pitts, J.N. 1993. Atmospheric chemistry of tropospheric ozone formation: Scientific and regulatory implications. Air & Waste 43:1091-1100.

GBD 2019 Diseases and Injuries Collaborators. 2020. Global burden of 87 risk factors in 204 countries and territories, 1990–2019: a systematic analysis for the Global Burden of Disease Study 2019. Lancet. 396(10258): 1223–1249.

Kazemiparkouhi, F., Eum, K-D., Wang, B., Manjourides, J., Suh, H.H. 2020. Long-term ozone exposures and cause-specific mortality in a us medicare cohort. Journal of Exposure Science & Environmental Epidemiology 30:650-658.

Kim, B.J., Seo, J.H., Jung, Y.H., Kim, H.Y., Kwon, J.W., Kim, H.B., et al. 2013. Air pollution interacts with past episodes of bronchiolitis in the development of asthma. Allergy 68:517-523.

Künzli, N., Medina, S., Kaiser, R., Quénel, P., Horak, F. Jr., Studnicka, M. 2001. Assessment of deaths attributable to air pollution: should we use risk estimates based on time series or on cohort studies? Am J Epidemiol. 153:1050-1055.

Last, J.M., A dictionary of epidemiology 2001. 4th ed. Oxford, Oxford University Press.

Moss, R.H., Edmonds, J.A., Hibbard, K.A., Manning, M.R., Rose, S.K., van Vuuren, D.P., et al. 2010. The next generation of scenarios for climate change research and assessment. Nature 463:747-756.

Murray, C.J., Lopez, A.D. 1997. Global mortality, disability, and the contribution of risk factors: Global Burden of Disease Study. Lancet. 349:1436-42.

Revich, B., Shaposhnikov, D., 2010. The effects of particulate and ozone pollution on mortality in moscow, russia. Air Quality, Atmosphere & Health 3:117-123.

Seposo, X., Ueda. K., Sugata, S., Yoshino, A., Takami, A., 2020. Short-term effects of air pollution on daily single- and co-morbidity cardiorespiratory outpatient visits. Sci Total Environ 729:138934.

Shiraiwa, M., Ueda, K., Pozzer, A., Lammel, G., Kampf, C.J., Fushimi, A., Enami, S., Arangio, A.M., Fröhlich-Nowoisky, J., Fujitani, Y., Furuyama, A., Lakey, P.S.J., Lelieveld, J., Lucas, K., Morino, Y., Pöschl, U., Takahama, S., Takami, A., Tong, H., Weber, B., Yoshino, A., Sato, K. 2017. Aerosol Health Effects from Molecular to Global Scales. Environ Sci Technol. 51: 13545-13567

Silva, R.A., Adelman, Z., Fry, M.M., West, J.J., 2016. The impact of individual anthropogenic emissions sectors on the global burden of human mortality due to ambient air pollution. Environmental Health Perspectives 124:1776-1784.

Silva, R.A., West, J.J., Lamarque, J.F., Shindell, D.T., Collins, W.J., Dalsoren, S., Faluvegi, G., Folberth, G., Horowitz, L.W., Nagashima, T., Naik, V., Rumbold, S.T., Sudo, K., Takemura, T., Bergmann, D., Cameron-Smith, P., Cionni, I., Doherty, R.M., Eyring, V., Josse, B.,

MacKenzie, I.A., Plummer, D., Righi, M., Stevenson, D.S., Strode, S., Szopa, S., Zengast, G. 2016. The effect of future ambient air pollution on human premature mortality to 2100 using output from the ACCMIP model ensemble. Atmos. Chem. Phys. 16, 9847–9862

Soriano, J.B., Kendrick, P.J., Paulson, K.R., Gupta, V., Abrams, E.M., Adedoyin, R.A., et al. 2020. Prevalence and attributable health burden of chronic respiratory diseases, 1990–2017: A systematic analysis for the global burden of disease study 2017. The Lancet Respiratory Medicine 8:585-596.

Takahashi, M., Feng, Z., Mikhailova, T.A., Kalugina, O.V., Shergina, O.V., Afanasieva, L.V., et al. 2020. Air pollution monitoring and tree and forest decline in east asia: A review. Science of The Total Environment 742:140288.

Wang, T., Xue, L., Brimblecombe, P., Lam, Y.F., Li, L., Zhang, L. 2017. Ozone pollution in china: A review of concentrations, meteorological influences, chemical precursors, and effects. Science of The Total Environment 575:1582-1596.

Yin, P., Brauer, M., Cohen, A., Burnett, R.T., Liu, J., Liu, Y., Liang, R., Wang, W., Qi, J., Wang, L., et al. Long-term exposure to fine particulate matter and cardiovascular disease mortality in China: a cohort study. 2018. Environ. Health Perspect. 2017, 125, 117002.

Zanobetti, A., Schwartz, J. 2011. Ozone and survival in four cohorts with potentially predisposing diseases. American journal of respiratory and critical care medicine 184:836-841.

(6.7)

Aas W., Mortier A., Bowersox V., Cherian R., Faluvegi G., Fagerli H., Hand J., Klimont Z., Galy-Lacaux C., Lehmann C.M.B., Lund Myhre C., Myhre G., Olivie D., Sato K., Quaas J., Rao P.S.P., Schulz M., Shindell D., Skeie R.B., Stein A., Takemura T., Tsyro S., Vet R. and Xu X. 2019. Global and regional trends of atmospheric sulfur. Scientific Reports 9: 95.

Galmarrini, S., Koffi, B., Solazzo, E., Keating, T., Hogrefe, C., Schulz, M., Benedictow, A., Griesfeller, J. J., Janssens-Maenhout, G., Carmichael, G., Fu, J. and Dentener, F. 2017. Technical note: Coordination and harmonization of the multi-scale, multi-model activities HTAP2, AQMEII3, and MICS-Asia3: simulations, emission inventories, boundary conditions, and model output formats. Atmos. Chem. Phys., 17: 1543–1555.

Janssens-Maenhout, G., Crippa, M., Guizzardi, F., Dentener, F., Muntean, M., Pouliot, G., Keating, T., Zhang, Q., Kurokawa, J., Wankmuller, R., Danier van der Gon, H., Kuenen, J.J.P., Kilmont, Z., Frost, G., Darras, S., Koffi, B. and Li, M. 2015. HTAP_v2.2: a mosaic of regional and global emission grid maps for 2008 and 2010 to study hemispheric transport of air pollution. Atmos. Chem. Phys. 15: 11411–11432.

Li, M., Zhang, Q., Kurokawa, J., Woo, J. -H., He, K. B., Lu, Z., Ohara, T., Song, Y., Streets, D. G., Carmichael, G. R., Cheng, Y. F., Hong, C. P., Huo, H., Jiang, X. J., Kang, S. C., Liu, F., Su, H., and Zheng, B. 2017. MIX: a mosaic Asian anthropogenic emission inventory for the MICS-Asia and the HTAP projects. Atmos. Chem. Phys., 17: 935–963.

TF HTAP (Task Force Hemispheric Transport of Airpollution). 2010a. Part A, Ozone and Particulate Matter, in: Economic Commission for Europe, edited by: Dentener, F., Keating, T., and Akimoto, H., Air Pollution Studies, 17, UNECE, Geneva, 1–728.

TF HTAP (Task Force Hemispheric Transport of Airpollution). 2010b Part D, Answers to Policy Relevant Science Questions, edited by: Keating, T., Zuber, A., Dentener, F., Seddon, J., Travnikov, O., Gusev, A., Carmichael, G., Parrish, D., and Grano, D., UNECE, Geneva.

Vet, R., Artz, R. S., Carou, S., Shaw, M., Ro, C. -U., Aas, W., Baker, A., Bowersox, V. C., Dentener, F., Galy-Lacaux, C., Hou, A., Piennar, J. J., Gillett, R., Forti, M. C., Gromov, S., Hara, H., Khodzher, T., Mahowald, N. M., Nickovic, S., Rao, P. S. P., and Reid, N. W. 2014. A global assessment of precipitation chemistry and deposition of sulfur, nitrogen, sea salt, base cations, organic acids, acidity and pH, and phosphorous. Atmos. Environ., 93: 3–100.

World Meteorological Organization Global Atmosphere Watch (WMO GAW). 2017. Global Atmosphere Watch Workshop on Measurement-Model Fusion for Global Total Atmospheric Deposition (MMF-GTAD). World Meteorological Organization. Geneva, Switzerland, GAW Report No. 234.

World Meteorological Organization Global Atmosphere Watch (WMO GAW). 2019. Global

Atmosphere Watch Expert Meeting on Measurement-Model Fusion for Global Total Atmospheric Deposition. World Meteorological Organization. Geneva, Switzerland, GAW Report No. 250.

(6.8)

Itahashi, S., Ge, B.Z., Sato, K., Fu, J.S., Wang, X.M., Yamaji, K., Nagashima, T., Li, J., Kajino, M., Liao, H., Zhang, M.G., Wang, Z., Li, M., Kurokawa, J., Carmichae, G.R., and Wang, Z.F. 2020. MICS-Asia III: overview of model intercomparison and evaluation of acid deposition over Asia, Atmos. Chem. Phys. 20: 2667–2693.

Itahashi, S., Ge, B.Z., Sato, K., Wang, Z., Kurokawa, J., Tan, J., Huang, K., Fu, J.S., Wang, X.M., Yamaji, K., Nagashima, T., Li, J., Kajino, M., Carmichael, G.R., and Wang, Z.F. 2021. Insights into seasonal variation of wet deposition over southeast Asia via precipitation adjustment from the findings of MICS-Asia III, Atmos. Chem. Phys. 21: 8709–8734.

7. Summary and Recommendations for Future Activities

7.1 Introduction

The atmosphere surrounding us is essential for the survival of mankind. However, acid deposition and related air pollution became very serious in some area. Acidic substances deposited on the surface of forest, soil, inland water as well as buildings as wet or dry deposition, are exacerbating their properties and moreover, are also a significant threat to human health.

EANET has been regularly monitoring acid deposition in East Asia since 2000. Thanks to the sincere efforts of the participating countries of Acid Deposition Monitoring Network in East Asia, the amount of sulfur dioxide and nitrogen oxides released in East Asia has been decreasing since around 2010 and it seems that the environmental impact of acid rain itself is being mitigated. However, there remain serious problems of air pollution including substances related to acid deposition such as ozone and $PM_{2.5}$ in this area. Impacts of acid deposition and related air pollution on human health and ecosystems are now of significant concern not only in the East Asian region but also in all over the world.

EANET published scientific review reports three times on the status of the acid deposition in East Asia in every five years based on the EANET monitoring data obtained in 2000-2004, 2005-2009, and 2010-2014 (PRSAD1 2006, PRSAD2 2011, PRSAD3 2016). The year 2020 marks the 20th anniversary of the establishment of EANET, and we have decided to compile a report on our activities over the last 20 years. Therefore, this report is the Fourth Periodic Report (PRSAD4) on the conditions of acid deposition and related atmospheric pollutants in East Asia based on 20-year monitoring data from 2000 to 2019.

Drafting Committee (DC) of experts from 13 participating countries was established in 2019 to prepare this report. The DC prepared the implementation plan for PRSAD4 and prepared the format and contents of this report. PRSAD4 consists of three parts: Part 1: Regional Assessment, Part 2: National Assessment, and Part 3: Executive Summary.

In drafting this report, the DC appointed Lead Authors and Contributors. The DC and the Lead Author examined the importance of chemical components in precipitation and temporal and spatial fluctuations in atmospheric concentrations in order to investigate the effects of acid deposition in detail and determine the current state of acid rain. In order to investigate the long-term fluctuations of acid deposition, this report also conducted a trend analysis based on the 2000-2019 data.

In addition to the monitoring of acid deposition continued by each Participating Country since the founding of EANET it is necessary to enhance the capability of research to investigate the mechanism of the acid deposition and related air pollution caused by ozone and/or PM2.5 in the whole region of East Asia. For that purpose, the enhancement of capabilities on modeling studies investigating air pollution status and changes in each participating country and emission inventory studies as the base data for such modeling study are important. Of course, it is still very important to study on the effects of air pollution on agricultural crops, forest ecosystem and inland water in order to improve the atmospheric environment in the East Asian region. Those studies are desirable to be done under cooperation among Participating Countries.

In order to increase the influence of EANET, it is necessary to strengthen collaboration with relevant international organizations, research institutes, and countries, including diversification of funding mechanism. From this perspective, the activities consist of the continuation of long-term activities, including new projects that can address the challenges in East Asia, considering the changing situation. Activities also include provisions for ongoing assessment and reporting of acidification

and air pollution to policy makers and the implementation of appropriate research to assess the effects of acid deposition and related air pollutants.
Moreover, there is evidence which suggests that the climate change and atmospheric issues are likely to be solved simultaneously if coordinated measures and actions from the governments, enterprises and the public are undertaken, with consideration on co-benefits during the design and implementation of related strategies. Thus, efforts to reduce the emission of acid deposition and related air pollution could simultaneously solve climate change issues.

Under such circumstances EANET decided to expand its scope from current activities focusing on monitoring of acid deposition to broader activities, including air pollution measures. In the Twenty-second Session of the Intergovernmental Meeting on the EANET (IG22) held in 2020 it was agreed that some activities related to air pollution can be an interest to Participating Countries of the EANET, and the scope expansion should include types of activities and/or substances or target areas related to air pollution beyond acid deposition.

7.2 Summary

7.2.1 Data Quality (Chapter 2)

Quality Assurance and Quality Control (QA/QC) plays an important role in acid deposition monitoring to ensure that the measurement to be accurate, comparable and quantifiable quality. EANET produced four QA/QC programs (Wet Deposition, Air Concentration, Soil and Vegetation, Inland Aquatic Environment) in 2000. Those are composed of several procedure types: i) siting, ii) sampling procedures and sample handling, iii) chemical analysis, and iv) QA/QC for the measurement data at each site. Several documents regarding QA/QC have been developed by EANET to guide receiving reliable data that can be comparable among the participating countries as well as with other monitoring networks outside of the East Asian region.

The Inter-Laboratory Comparison project is also used for all analytical laboratories for the EANET monitoring involved. The purposes of this project are to evaluate the analytical systems through the evaluation of analytical results, analytical instruments and their operating condition and other relevant and appropriate practices. The Inter-Laboratory Comparison surveys were carried out 22 times, 15 times, 21 times, 20 times for wet deposition, dry deposition, soil and inland aquatic environment, respectively.

The annual measurements in a participating country are subjected to the data qualification by the National QA/QC manager and the national committee of data evaluation of each country. Some suspected datasets will be as a feedback to the analytical laboratories or appropriate organizations.
All datasets are eventually collected at the Network Center (NC) where the datasets are further examined and qualified through communications with national centers. The datasets qualified so far are submitted to the international data verification group for the final checking. The international experts of the monitoring activities qualify each of the datasets in a careful and detailed manner. After discussion between NC and national centers, the verified datasets are submitted to the Scientific Advisory Committee to be scientifically and technically approved. The annual data report are actually completed after SAC consideration, which will be officially and finally approved by the Intergovernmental Meeting.

Data Completeness is one of the data quality indicators when measurement data are summarized statistically in monthly, seasonal or annual periods. If large amounts of data are missing or regarded as invalid during the summary period, the summarized statistics (e.g., the mean, median, maximum and minimum values) can be highly misleading. Therefore, periodic reporting of summarized data for long-term regional monitoring network activities should be based on operational measurements with as few missing data as possible.

7.2.2 Wet and Dry Deposition of Acidic Substances in East Asia (Chapter 3)

Spatial and temporal variations of wet and dry deposition using available EANET monitoring data during the period of 2000-2019 are assessed in Chapter 3 of the main text.

Under the EANET framework, there are currently 61 wet deposition monitoring sites and 54 dry deposition monitoring sites located in 13 EANET member countries. In accordance with EANET criteria, the wet and dry deposition monitoring sites are categorized into three types: urban, rural, and remote. Sampling techniques, sample storage and analysis, data processing, QA/QC procedures of all monitoring sites and laboratories participating in EANET are conducted according to EANET's Guidelines and Manuals.

The 20-year secular changes in acid concentration sums (nss-SO_4^{2-} + NO_3^-), base concentration sums (NH_4^+ + nss-Ca^{2+}) and H^+ concentrations for representative sites are monitored in the EANET region. At the rural and urban sites, higher acid concentration sums were observed in 2000s and 2010s in China, Republic of Korea, and Japan in Northeast Asia, in comparison with base concentration sums. As the results, higher H^+ concentrations were observed mainly in 2000s in Korea, in 2010s in China, in 2000s and 2010s in Japan. After that, H^+ concentrations in these countries have been declining significantly. In Mongolia, the acid concentration sum in Ulaanbaatar has tended to be high in recent years. On the other hand, at rural and urban sites in Southeast Asian countries, the acid concentration sums and the H^+ concentrations have increased in recent years in Vietnam and Malaysia. Following the tendency of the base concentration sum, or completely independently, the acid concentration sums are maintained at a high level at some sites, and there are sites where the acid concentration sum tends to increase. The acid concentration sums at the remote site tend to decrease in Northeast Asia as at the rural and urban sites. Besides, in Southeast Asia, there is no upward trend of acid concentration in remote sites. As mentioned here, precipitation acidity is the results of the balance between acids and bases dissolved in precipitation. Since the situation may change periodically due to air pollution in surrounding region in Northeast and Southeast Asian countries, it is important to continue wet deposition monitoring focusing on not only acids but also bases in precipitation in EANET countries.

Based on the EANET data, geographical distribution of acids and bases and wet deposition trends (in the periods of 2000-2010, 2005-2015, and 2009-2019) were analyzed. The pH shows the increasing trend in Northeast Asian and Southeast Asian countries. The concentration of nss-SO_4^{2-} had the decreasing trend in Northeast Asian countries. There were no significant trends in the other components such as NO_3^-. The decline of the nss-SO_4^{2-} in North Asian countries contributes to increase pH. On the other hand, the concentration of nss-SO_4^{2-} in Southeast Asian countries had the insignificant trend. The concentration of nss-Ca^{2+} and NH_4^+ had the increasing trend in Southeast Asia. Therefore, the increasing trend of pH in Southeast Asian countries was possibly caused by increasing cation contribution (nss-Ca^{2+} and NH_4^+).

From the comparison of precipitation chemistry among EANET, NADP (National Atmospheric Deposition Program) and EMEP (European Monitoring and Evaluation Programme), the pH values and nss-SO_4^{2-} concentrations showed significantly increasing and decreasing trend, respectively, in all these networks from 2000 to 2019. The NO_3^- concentrations showed significantly decreasing trend in NADP, EMEP and slightly decreasing trend in EANET. The decreasing trend of nss-SO_4^{2-} concentration has been significant from the period of 2004-2014 to that of 2009-2019 in Northeast Asia, especially, in China, Republic of Korea, and Japan. The nss-SO_4^{2-} concentration in Southeast Asia had the insignificant trend. The NO_3^- concentration did not have the significant trend in Northeast Asia and Southeast Asia. Since the nss-Ca^{2+} and NH_4^+ concentration had the increasing trend, pH increasing trend in Southeast Asia was possibly caused by the increasing of the cations.

Total (dry and wet) deposition of S and N was evaluated at the sites carrying out the wet-only and the 4-stage filter pack monitoring in Russia, Mongolia, Japan, Vietnam, Thailand, Malaysia and Indonesia. Wet deposition was estimated by the product of precipitation amount and concentration.

Dry deposition was estimated by simplifying the inferential method using available monthly meteorological data. Low total S depositions were found at the remote sites located in northern inland and Pacific Ocean, and high total S depositions were found in the Japanese remote sites near Asian continent. In the high S deposition sites, the decreasing trend of S deposition was found in recent years. High total S depositions more than 30 kg S/ha/year were found at urban sites in Southeast Asia. The dry S depositions have decreased from 2000s at Hanoi and Bangkok. In remote sites, spatial and temporal trends of the total N depositions were similar to those of the total S depositions, and reduced N deposition contributed more than half of total N deposition at lower N deposition sites. Oxidized N deposition contributed more than half of total N deposition at higher N deposition sites. Regardless of the site categories, reduced N deposition contributed more than half of total N deposition in many years at many sites, except at Sado-seki, Oki and Petaling Jaya. Trend analysis for total S and N, as well as oxidized and reduced N deposition, has shown a significant increase in some sites in Southeast Asia and a significant decrease in some sites in Northeast Asia, especially in the last decade.

Estimations of spatial and temporal variations of total deposition are important for assessing the impact on ecosystems including acidification and excess eutrophication. Current method to estimate dry deposition requires observations of gaseous and particulate S and N components and meteorological elements, while there are only a limited number of sites that measure all items. To improve the situations, further expansion of monitoring by the 4-stage filter pack that measures the gaseous and particulate S and N components at the same time is expected at first. Moreover, chemical transport model is effective to estimate the deposition velocity, when the necessary items are limited. NADP developed a hybrid approach for estimating dry deposition using monitoring data and modeled data from chemical transport model. Some use of the model for estimation of dry deposition should be considered for next step. Moreover, the latest information of the dry deposition process research should be taken into account to update the methodology.

7.2.3 Gas and Aerosol Pollution in East Asia (Chapter 4)

Monitoring Status by each country

EANET has conducted continuous monitoring in various countries for 20 years and the number of gas and aerosol monitoring sites increased each year. This will allow to establish the high resolution monitoring network in East Asia and to provide the scientific evidence to policy makers to confront this environmental issue as well. There were 54 air concentration monitoring sites operated in the EANET network as of 2019. The measuring components, which are SO_2, NO, NO_2, NOx, $PM_{10}/_{2.5}$, O_3, HNO_3, HCl, NH_3 and Particulate Matter Components (PMC), vary depending on the methodology utilized at each site.

SO_2, NO_2, NOx, O_3, PM_{10} and $PM_{2.5}$ concentrations

The spatial distribution of SO_2 in Russia and Mongolia varied by the influence of population distribution as well as the effect of heating and fuel composition. After continuous improvement, SO_2 concentrations in China have been significantly reduced, and the 5-year average range for the 5 stations in China is 0.1 ppb-3.54 ppb. The SO_2 concentrations at all sites in Japan are very low for a long time, with a 5-year average range of 0.03 ppb-1.3 ppb. The SO_2 concentration range at the three land sites in Republic of Korea is similar to that of China. Except for Indonesia, SO_2 concentrations in Southeast Asian countries are generally low for 5 year-average concentration.

Republic of Korea had the highest nationwide O_3 5-year average concentration (40.47 ppb from 3 stations), and Japan reported the next highest nationwide averaged O_3 concentration. On the other hand, O_3 concentration in Southeast Asian countries are lower. Mongolia had the highest NOx 5-year average concentration, and Philippines reported the next highest. There are large spatial differences in the distribution of NO_2 concentrations. Indonesia has the highest NO_2 concentration level.

Mongolia had the highest $PM_{2.5}$ 5-year average concentration of 40.47 μg/m^3 at Ulaanbaatar. Jakarta of Indonesia reported the next highest nationwide averaged $PM_{2.5}$ concentration of 41.00 μg/m^3. The $PM_{2.5}$ concentration in Hoa Binh of Vietnam is close to that of Jakarta of Indonesia, with a 5-year average concentration of 39.4 μg/m^3. The 5-year average $PM_{2.5}$ concentrations of remaining countries are less than 30 μg/m^3. Ulaanbaatar of Mongolia also has the highest PM_{10} concentration level with a 5-year mean concentration of 110.40 μg/m^3. The PM_{10} concentration levels in China, Korea, the Philippines, and Thailand were similar. The 5-year nationwide average PM_{10} concentrations in Japan has a range of 8 to 30 μg/m^3.

Among the 51 sites, 27 sites showed a significant decreasing trend and 8 sites showed a strongly significant decreasing trend. The decreasing trend of SO_2 at many sites in East Asia is associated with decrease of anthropogenic emission of SO_2. SO_2 emissions in EANET participating countries increased largely in early 2000s mainly due to contributions from coal-fired power plants, which increased rapidly along with large economic growth. Then, the SO_2 emissions showed decreasing trends after middle of 2000s reflecting effects of control measures.

Many sites observed significant increasing trend of annual O_3 concentration and the other surface ozone database in East Asia also showed increasing trend of summertime mean of daytime average and the daily maximum 8-hour average over East Asia. It is important to watch out the trend of surface ozone in East Asia by combining EANET data with other monitoring database. Since many sites installed a $PM_{2.5}$ monitor after 2015, a clear trend of annual $PM_{2.5}$ concentration has not been observed so far. The continuous monitoring is important to elucidate long term trend over East Asia.

HNO_3, NH_3 and HCl concentrations

The concentration of HNO_3 at one monitoring site of China is high during the period from 2015 to 2019, with Hongwen concentrations ranging from 1.1 ppb to 1.2 ppb, with a 5-year average value of 1.15 ppb. The concentration in Indonesia is the second highest in EANET region with a more consistent concentration distribution, the 5-year averaged HNO_3 concentration of 3 stations ranges from 0.62 ppb to 1.14 ppb. The HNO_3 concentrations in some countries are low, with the 5-year mean concentration of less than 0.5 ppb.

There are various NH_3 concentration distributions in East Asia. The spatial distribution of NH_3 in Philippines, Malaysia and Mongolia has a large variation. China has the relatively high NH_3 concentration among the countries with a 5-year average concentration of 9.99 ppb at Hongwen site, followed by Indonesia with an overall average of 9.23 ppb. The 5-year mean concentration at Cambodia station was 7.20 ppb, the average NH_3 concentration at four stations in Thailand ranged from 4.48 to 8.85 ppb, and the mean 5-year concentration at three stations in Republic of Korea ranged from 1.96 to 7.70 ppb. The other countries reported lower average NH_3 concentrations for the 5 years.

The highest HCl concentration is found in Russia with a 5-year mean concentration of 3.43 ppb and with a large differences in the geospatial distribution. The second highest concentration of HCl in the EANET region is found in Mongolia, where the 5-year mean concentrations range from 1.30 ppb to 3.55 ppb. The remaining countries have similar relatively lower HCl concentration levels.

Among the 44 sites, 8 sites showed a significant increasing trend of annual NH_3 concentration. The NH_3 emissions from agricultural activities in EANET participating countries increased almost constantly from 1995 to 2015, and rapid SO_2 emission reductions cause significantly increase of ammonia concentrations in the Northeast Asia.

SO_4^{2-}, NO_3^-, NH_4^+ and Ca^{2+} component concentrations in particulate matter

The highest SO_4^{2-} concentration was found at Hongwen of China, the only station reported data, with the 5-year average SO_4^{2-} concentration of 10.00 μg/m^3. The second highest 5-year averaged SO_4^{2-} concentration was found in Vietnam with mean of 5.59 μg/m^3 showing some differences in spatial distribution. The 5-year mean SO_4^{2-} concentrations of the remaining countries were relatively low.

The highest NO_3^- concentration was found at Hongwen of China, the only station reported data, with the 5-year average NO_3^- concentration of 7.94 μg/m^3. The second highest 5-year averaged NO_3^- concentration was found in Vietnam with mean of 4.07 μg/m^3 and a range of 1.54 μg/m^3-6.73 μg/m^3 for the 5 stations, showing some differences in spatial distribution. The 5-year mean NO_3^- concentrations of the remaining countries were relatively low.

The highest NH_4^+ concentration was found at Hongwen of China, the only station reported data, with the 5-year average NH_4^+concentration of 3.26 μg/m^3. The second highest 5-year averaged NH_4^+ concentration was Republic of Korea with mean of 2.12 μg/m^3 and a range of 1.66 μg/m^3 to 2.66 μg/m^3. The third highest 5-year averaged NH_4^+ concentration was found in Vietnam with mean of 1.65 μg/m^3 and a range of 1.11to 1.97 μg/m^3 for the 5 stations. The 5-year mean NH_4^+ concentrations of the remaining countries were relatively low.

The highest 5-year averaged Ca^{2+} concentration was found in Vietnam with mean of 2.28 μg/m^3 and a range of 1.61 to 3.73 μg/m^3 for the 5 stations. The second highest Ca^{2+} concentration was found at Hongwen of China and Phnom Penh, with the same 5-year average Ca^{2+} concentration of 1.68 μg/m^3. The 5-year mean Ca^{2+} concentrations of the remaining countries were relatively low.

7.2.4 Impacts on Ecosystems in East Asia (Chapter 5)

The EANET has been monitoring various ecosystem components, such as soil, forest vegetation, and inland water, to assess impacts of atmospheric deposition on ecosystems since 2000 when the regular-phase activity started. Important data sets over 10 years have been accumulated in many of monitoring sites, while the situations are different depending on monitoring items. Additionally, the EANET has been promoting a catchment-scale analysis considering biogeochemical cycles in forest ecosystems since 2010, in which interrelationships among atmospheric deposition, soil, vegetation, and inland water (mostly stream water) within a catchment area were also discussed qualitatively and/or quantitatively. Although the ecological monitoring above started in order to detect impacts of acid deposition, the results may also need to be discussed with other relevant factors, such as climate change.

Soil monitoring has been conducted at 31 sites from 10 countries including the surveys in 1999 during the preliminary phase. The soil monitoring data since 2000 to 2019 showed the diverse soil characteristics of EANET sites, which were controlled by various factors, such as soil formation process and climatic conditions. Comparison of temporal changes in soil pH(H_2O) with the major items of wet deposition suggested that the soil reaction was not necessarily parallel to the input of atmospheric deposition. It was also suggested that the reaction process would be different for each site. However, there are considerable sites where soil monitoring has not been conducted enough times for these 20 years, implying insufficient framework to detect the ecological impacts resulted from changes in atmospheric environment. As this monitoring system will also provide valuable data for understanding the effects of climate change on ecosystems, soil monitoring should be continued more intensively.

Monitoring on forest vegetation has been conducted at 24 sites in 8 countries. The vegetation monitoring includes implementations of the comprehensive forest survey, tree decline survey, and understory vegetation survey, but the content and frequency of surveys vary widely. The only 8 sites that have been surveyed more than once since 2015 are in China and Japan. The wet deposition amount of nss-SO_4^{2-}, which is an indicator of the intensity of regional air pollution, has been declining at each survey site since 2007. However, no corresponding increase in forest growth was observed. This may be due to anthropogenic disturbance, pest infestation (bark beetle), or intensified

competition between individuals as the age of the forest increases. To quantitatively assess the impact of air pollution on a wide range of forests, it is necessary to identify individual trees and conduct long-term growth measurements with air quality monitoring with little or no anthropogenic disturbance.

Monitoring on inland water chemistry has been conducted in 20 sites from 11 countries. Chemical properties, such as balance of ions, concentration levels, and seasonal changes, varied among the monitoring sites. Depending on the chemical properties, response of inland waters to atmospheric deposition was also different. However, several monitoring sites, such as Jinyunshan Lake, Xiaoping Dam, Jiwozi River and Zhuxiandong Stream in China, Patenggang Lake in Indonesia, and Ijira Lake in Japan, showed symptoms suggesting recovery from acidification. In some of sites, changing patterns of atmospheric deposition at the nearest monitoring sites were associated with those of ion concentrations in lakes/streams, respectively. It is suggested that further reduction in atmospheric acid deposition and its monitoring are necessary to ensure their continued recovery from acidification.

Long-term data at two forest catchments, Lake Ijira catchment (IJR) and Kajikawa catchment (KJK), suggested that the catchment biogeochemical cycles have sensitively responded to the recent declining of atmospheric deposition (in particular, SO_4^{2-}) resulting in phenomena indicating recovery from acidification. However, NO_3^- concentration in stream water at KJK has been increasing, while DIN deposition has been declining. Moreover, decline rates of NO_3^- concentration in stream water at IJR have become slower in recent years. Forest types, maturation of trees and meteorological variability appeared to affect N leaching to stream water. It is suggested that interactions with climate change (or year-to-year meteorological variability) should be taken into consideration in recovery processes from acidification and N saturation. New catchment analysis sites, Komarovka River (KMR) and La Mesa Watershed (LMW), may also contribute to further understanding of ecological response to atmospheric deposition and climate change.

7.2.5 Relevant Studies on Atmospheric Environment Assessment in the EANET Region (Chapter 6)

In addition to the effort of EANET, there have been many research activities and organizational initiatives focusing regional air pollution in East Asia as well as in global and hemispherical perspectives. In this chapter, such research outputs and initiatives in the last few years are reviewed in order to provide useful information on present status of acid deposition and regional air pollution. The covered topics are atmospheric observation including satellitte observation, emission inventory, chemical transport modeling (CTM), ecosystem and human health impact studies, which are not necessarily directly related to EANET, but would be useful for understanding air pollution and acid deposition in East Asia.

Figure 7.2.1 shows the overall structure reprinted from Chapter 6 in the main text. In the first part, the observation studies (section 6.2), emission inventory studies (section 6.3) and CTM (section 6.4) are systematically reviewed. In the following part, the ecosystem impact assessment studies and the human health impact studies are reviewed in section 6.5 and section 6.6, respectively. In the final part, other international activities in EANET region are introduced in section 6.7 and the combined analysis of long-term trends of acid deposition and gas/particles based on ground and satellite measurements and emissions is carried out in section 6.8.

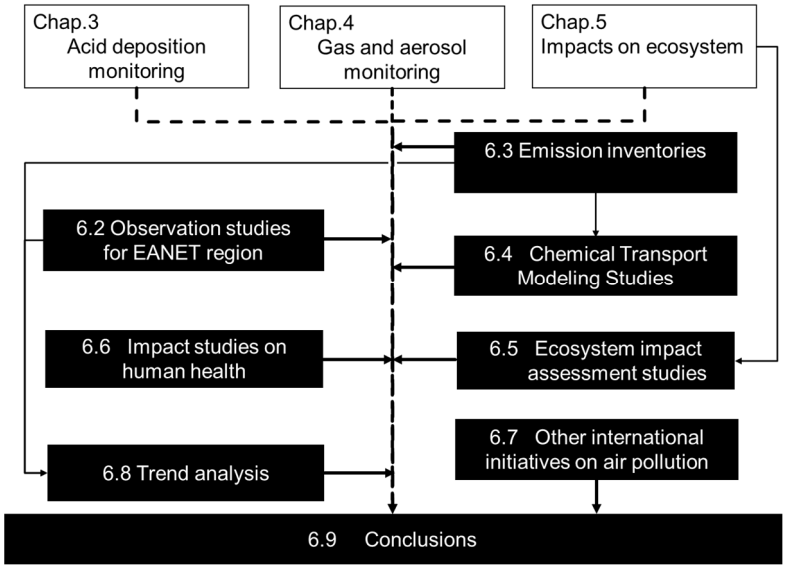

Figure 7.2.1. Overall strucrure of Chapter 6.

This chapter does not intend to provide comprehensive review, but the atmospheric observational studies focusing on field campaign and satellite measurement as well as studies on acidification and nitrogen leaching in forest catchments (section 6.2), the Model Inter-Comparison Studies for Asia (MICS-Asia) utilizing EANET data for validation and analysis (section 6.4), ecosystem impact assessment studies on the national and/or regional scales (section 6.5) and impacts of $PM_{2.5}$ and ozone on human health (section 6.6) are introduced with higher priority. Additionally, some original analysis are conducted in the satellite observation (section 6.2), emission trend (section 6.3) and long-term trends of acid deposition and air quality (section 6.8).

7.3. Recommendations for future activities

7.3.1. Data quality

The objectives of QA/QC programs are to obtain reliable and comparable monitoring data among the participating countries in East Asian region, as well as with other networks by ensuring data accuracy, precision, representativeness, and completeness in the acid deposition monitoring. For that purpose, the Network Center (NC) has been evaluating the monitoring data and trying to improve their quality. However, the data evaluation can be done only by checking the submitted report and data from each participating country. It is obvious that each participating country should continue to improve their data quality according to some reliable guidelines for QA/QC activities considering their respective capabilities. Therefore, EANET published QA/QC Guidebook for Acid Deposition Monitoring Network in East Asia -2016 (https://www.eanet.asia/wp-content/uploads/2019/04/QAQC_Guidebook2016.pdf). In addition, closer communication between each national QA/QC manager and the NC and the regular submission of the information regarding data quality are desirable. Therefore, the National Monitoring Plan of each Participating Country should be reviewed every year and also should be revised, if necessary, according to this QA/QC Guidebook.

It is noteworthy that there was a remarkable improvement of the quality of analysis after collaborative research between a participating country and the NC. That shows the efficiency of technical mission to improve the capacity of each Participating Country. Since 2020, however, it became quite difficult to keep the technical mission by dispatching member(s) of the NC to Participating countries requesting dispatch because of the spread of COVID-19. It is not clear when the spread of COVID-

19 will subside, but it is necessary to keep going the technical mission even if the face-to-face collaboration to deal with technical issues on monitoring of acid deposition and air pollution is difficult. We may proceed by use of discussion and instructions on the web.

The Inter-Laboratory Comparison (ILC) project has been implemented for all analytical laboratories involved for the EANET monitoring. Analytical systems, *i.e.*, analytical instruments and their operating conditions utilized by the laboratories could be evaluated through ILC by use of standard samples prepared by the NC and by comparison of submitted data from each laboratory. It must be important to continue ILC to confirm and improve the ability of the laboratories implementing EANET monitoring. The validity of this evaluation needs to be checked in an objective way, and the results should be feedbacked to each laboratory.

It is already more than 20 years since the start of monitoring in EANET Participating Countries, but it is still difficult to say that the monitoring systems in all the countries are very stable. In order to eliminate the missing of data for a long period or to attain the data quality objectives (DQOs) for maintaining the completeness of the data it is necessary to avoid power failure at the site due to lightning damage or unstable power supply, failure of the sampling inlet, malfunction of monitoring equipments due to deterioration over time or severe meteorological conditions, lack of financial and technical resources to repair the instruments, and so on. Timely inspection and renewal of monitoring instruments are very important. In order to improve data completeness, the alternative instruments for replacing the failed instruments should be kept in a laboratory, and lightning conductor, surge protector and/or uninterruptible power system (UPS) should be equipped in the station.

7.3.2 Wet and dry deposition of acidic substances in East Asia

East Asia is quite different from western countries considering its geographical, climatological, as well as ecological environment. In order to reflect such diverse environment, it is necessary to set up a sufficient number of monitoring sites which can represent their surrounding environment. There are currently (as of July 2021) 61 wet deposition monitoring sites and 54 dry deposition monitoring sites installed in 13 EANET Participating Countries. Those monitoring sites are categorized into three types in accordance with EANET criteria, *i.e.*, urban, rural, and remote sites. Sampling techniques, sample storage and analysis, data processing and QA/QC procedures of all monitoring sites and laboratories are conducted according to EANET's guidelines. In PRSAD3 it was recommended that Participating Countries and NC should pay attention to the expansion of new monitoring sites and restoration of dormant sites by quickly providing economical and technical supports. Although the number of monitoring sites are increasing, it is still insufficient to describe the wet and dry deposition status of the whole area of each country. It is desirable to arrange denser sites according to the capabilities of each country. Not only the number of monitoring sites but also the situation of monitoring sites is not yet satisfactory. It still requires the effort of each Participating Country and NC. Unfortunately, however, the spread of COVID-19 made it more difficult for NC to support local staff on site. Therefore, online consultation concerning technical support by NC should be utilized more effectively.

Wet deposition monitoring is carried out based on the wet deposition manual established in 2010. Basically, there is no big problem concerning the measurements of wet deposition. However, there are still some data not acceptable from a point of view of QA/QC. In order to improve data quality in wet deposition monitoring, more attention should be paid to eliminate unknown ionic species and to elaborate the commonly used monitoring procedures at each monitoring site by utilizing the manual. After that, it becomes important to evaluate the obtained data by utilization of modeling analysis as well as comparison with the data reported by other networks such as NADP, EMEP, etc. There are wet deposition monitoring data in East Asia for more than 20 years. Thus, such long-term variation of regional deposition should be analyzed in comparison with the change of emission amount of air pollutants in the region for getting insight into the effect of domestic air pollution control measures.

Estimations of spatial and temporal variations of total deposition are important for assessing the impact on ecosystems including acidification and excess eutrophication. Dry deposition was estimated by the inferential method based on Technical Manual for Dry Deposition Flux Estimation in East Asia (EANET, 2010) (for details refer to Chapter 3 of this report). Namely, current method for estimating dry deposition is based on observations of gaseous and particulate S and N components and meteorological elements. At present, there are only a limited number of sites that measure all those items in East Asia. Thus, it is very important to ensure monitoring sites which measure gaseous and particulate S and N components by use of simple but reliable method such as 4-stage filter pack and getting reliable meteorological data. As a way to compliment limited number of data, chemical transport model is effective to estimate the deposition velocity. NADP has developed a hybrid approach for estimating dry deposition using monitoring data and modeled data from chemical transport model (Schwede and Lear, 2014). These days model analyses are indispensable to evaluate the field data and to analyze the effects of air pollution and acidic deposition. Utilization of model analyses is strongly recommended for estimation of dry deposition.

7.3.3 Gas and aerosol pollution in East Asia

It goes without saying that acidic deposition is the main target of EANET. However, substances related to acid deposition, such as precursor gases of acidic substances, ozone as one of the products of atmospheric chemical reactions to form acidic substances in air, and particulate matters as the products of neutralization reactions of acidic substances in the atmosphere, are also the targets of EANET from the early stage. These days more attention is paid to in wider area of air pollutants. Climate change is obviously not the target of EANET, but because of the possible co-benefit, the control of air pollution could simultaneously mitigate climate change. The reduction of emission of air pollutants could reduce the climate change related substances, which will be possible targets of EANET in the future. If common benefits for acid rain and climate change can be obtained, it will be a great driving force for solving environmental problems. Scope expansion of EANET adopted by IG 23 encouraged us to extend our targets and interests to wider area.

At present, however, acid deposition is still a big environmental problem in East Asia. We need to face to the improvement of monitoring activities for acid deposition and related substances.

SO_2 and SO_4^{2-}
Concentration of SO_2 has improved and reducing trend has been seen especially in the north eastern part of EANET region. Concentration of SO_4^{2-} is also coming down in many participating countries. Therefore, it can be said that mitigation measures for sulfur compounds can be recognized as successful in the region. The shift to electric vehicles and the regulations on the use of low-sulfur fuel in ships (started in January 2020) are expected to continue to reduce SO_2 and SO_4^{2-}, but it is important to continue monitoring and aim for further environmental improvement.

NO_2, NOx, HNO_3^- and NO_3^-
During the past 20 years, East Asian countries met rapid increase of NOx both from industrial sector and transportation sector because rapid activating industrial activities and rapid increase of traffic, whereas there was remarkable decrease of NOx emission in northeastern part of EANET region observed from ~2010 and reduction of NOx emissions in East Asia due to the decline in economic activity caused by COVID-19 from 2020. It is expected that the use of fossil fuels will decrease rapidly toward a decarbonized society, and the amount of NOx emissions will be further reduced. Changes in NOx concentrations in air can affect the surface ozone concentrations, too. Thus, changes in NOx emissions need to be monitored based on an accurate grasp of NOx and NO_3^- depositions.

NH_3-NH_4^+
Because of the advance of agriculture in Asia, emission of ammonia and ammonium is increasing. Ammonia is an important atmospheric basic-compounds which can neutralize acids. In order to accurately evaluate the concentration of PM, accurate integration of ammonium salt emissions is

essential, and more accurate monitoring of NH_3 and NH_4^+ considering each country's capability is needed.

O_3
Ozone is assumed as an important gaseous species related to acid deposition. It is because ozone is a secondary product produced in the air by chemical reactions involving HOx radicals which are also important agents to form acids in the air. Ozone is a toxic gas harmful for not only human health but also plants and animals. Moreover, it is a strong greenhouse gas. Ozone is pointed out as one of SLCPs (short-lived climate pollutants). Mitigation measures for ozone is, thus, co-beneficial from either point of view of air pollution and global warming. Ozone was intensively monitored in the urban area so far from a point of view of the effects on human health. More extensive monitoring of ozone is needed from the viewpoints described above. As already described, ozone is a secondary pollutant produced in the air by the photochemical reactions of NOx and VOCs; not a pollutant emitted directly by human activity. Thus, it is important to enhance the capabilities of each participating country on simulation-model analyses in addition to field monitoring to know the mechanisms of pollution and to estimate its spatial and temporal distribution. And for the purpose of verification, remote sensing technology including satellite measurements should be taken into view in the near future.

Particulate Matter (PM)
The main target of monitoring in the EANET is mass concentrations (PM_{10} and $PM_{2.5}$). And the enhancement of capabilities of each participating country on decreasing the concentration of PM is of great importance. In addition, dust and sand storm in Northeast Asia and haze in Southeast Asia should be included in PM monitoring.

7.3.4 Impacts on ecosystems in East Asia

Serious forest decline is not observed in East Asian countries. That is very fortunate for us living in East Asia. We hope such situation lasts long, but it is not guaranteed. That is because the effects of acid deposition and its related atmospheric substances on the growths of forest trees have not enough been clarified in EANET monitoring sites and their surroundings so far. These days the effects of atmospheric pollutants, such as ozone and PM, are assumed more serious to forest trees than acid precipitation. Therefore, under the expanded scope of the EANET, ozone and PM should be monitored more extensively to evaluate their risks to the forest ecosystems.

As for inland water environment, the EANET has been monitoring inland water chemistry for twenty years. Among those monitoring sites, several sites showed symptoms suggesting recovery from acidification. However, response of inland waters to atmospheric deposition is quite different depending on the chemical properties of the water in the monitored lakes/rivers. Although changing patterns of ion concentrations in lakes/rivers in some monitoring sites were well synchronized with those of atmospheric deposition at the nearest monitoring sites, there remains several technical issues that need to be improved.

According to the recommendations described in PRSAD3, the following points have been progressed during the last five years,

- The catchment monitoring/analysis have been promoted to discuss effects of atmospheric deposition on inland waters more precisely. The long-term data at Lake Ijira catchment (IJR) and Kajikawa catchment (KJK) illustrated changes in atmospheric deposition and consequent ecosystem responses, which have already been published in international scientific journals. Moreover, the new regular catchment monitoring has started in La Mesa Watershed in 2019 and the catchment-scale analysis has been applied to the data on Komarovka River as the fellowship research.

- In addition to analysis of ion/element concentrations, the isotopic analysis has been applied to samples collected the catchment sites above to discuss possible origins of elements and/or their dynamics in ecosystems, as a new trial for the NC research activities as well as the national monitoring of Japan. The isotopic data have certainly contributed to interpretation of the data on IJR and KJK.

However, the subjects above progressed only in a few countries, and therefore, similar trials should be promoted in other EANET countries to discuss relationship between atmospheric deposition and ecosystems. Moreover, the following subject remains as the regional network:

- The number of the EANET sites for ecological monitoring is too small to cover the entire region. A huge variety of forest ecosystems are distributed throughout the region with diversity of climate, geology, vegetation, soil, and human activity. Therefore, a scale-up approach is crucial for a regional risk assessment. Efforts should be made to assess the regional risks of acidification on the East Asian scale to continue the EANET monitoring in the high-risk areas more effectively.

Those points have not been cleared yet. Thus, they are still valid as future recommendations of the EANET. These points should be addressed as quickly as possible.

Additionally, in order to detect the effects of atmospheric deposition on forest ecosystems, the following points improving the monitoring program and assessment can be recommended:

- To obtain data with low noise factors, such as site disturbance (including local anthropogenic disturbance)
- To improve the system for better data acquisition regarding the control or understanding of anthropogenic disturbances (deforestation, non-execution of monitoring, site changes, etc.)
- To implement monitoring and model analysis considering the differences in time constants, since the time response of ecosystems to atmospheric deposition is different.
- To continue monitoring ecosystems and model analyses using the monitoring results even after the atmospheric deposition has decreased sufficiently.

Especially in the catchment area, it is expected that these combined effects of atmospheric deposition and climate change will be observed as output. Therefore, in order to analyze the effects on forest ecosystems, beside the promotion of catchment area analysis in each region, the following point can be recommended:

- To establish a system that may reset of monitoring sites on soil and forest vegetation in consideration of catchment areas.

7.3.5 Emission inventories

Problems of atmospheric environment are mainly caused by increasing emissions from anthropogenic activities related to demands for energy, motorization, and industrial and agricultural products. For consideration of effective mitigation measures for the problems, it is fundamentally important to understand current status and trends of emissions from air and climate pollutants. Furthermore, it is indispensable to develop gridded emission data to atmospheric models to analyze the status of the atmospheric environment over wider areas of global or continental scale and examine effectiveness of control measures. Major roles of emission inventory are to obtain detailed information of emission sources and provide input emission data to atmospheric models for making appropriate atmospheric environmental policies based on scientific results.

East Asia is now the regions of the world with the large air pollutant emissions. Therefore, estimation of emissions in East Asia is important not only for understanding local air pollution, but also for large scale air pollution and global climate change.

Recently, the quality of emission inventories in Asian region is improving. Members of NC have been collaborating with researchers from various research institutes to develop and improve mosaic emission inventories composed of reliable national and regional inventories under the framework of the Model Inter-Comparison Study for Asia (MICS-Asia) project. EANET has provided some assistance with this. In the EANET Emission Inventory Workshop, which was held in October, 2021, many technical officers and researchers of EANET participating countries, particularly those of Southeast Asia, participated and learned roles of emission inventory in air quality management and basic knowledge of development and application of emission inventory. However, continuous efforts for elaboration of emission inventory are necessary. Therefore, it is recommended that research activities (e.g., survey of detailed activity data and emission factors) and capacity building for their activities are required in EANET participating countries. In addition, the national emission inventory officially supported and maintained by each participating country is preferable for the air quality management of this area.

In East Asia, in addition, there are many natural emissions in addition to emissions from anthropogenic activities. Major related air pollutants are biogenic volatile organic compounds (BVOC) emitted by plants especially in tropical and sub-tropical areas, soil dust transported as Yellow Sand Dust over Northeastern area, and haze resulted from biomass burning in Southeastern area. In general, uncertainty in the emission inventory of those items is very large. More and continuous studies to understand and evaluate the fundamental model and key parameters of the emission estimations for natural sources may be effective in the research and capacity building activities for targeting these region.

Verification, improvement, and updates of emission inventories based on ground and satellite observations, chemical transport modeling, and inverse modeling are essential to reduce uncertainties. This work requires strong collaborative and integrated research among emission inventory developing, monitoring, chemical transport modeling, and inverse modeling groups. These activities have possibility to help future QA/QC of national emission inventory in EANET participating countries.

7.3.6 Modeling activities

Monitoring of air pollutants including acid deposition carried out in the EANET is an essential activity to know the phenomena taking place in the atmosphere over the East Asia. However, interpreting such phenomena based only on the observational data is sometimes difficult due to the complex impacts of many types of origins of pollutants. Furthermore, available observation data are spatially scare over the East Asia and target species and chemical components are not enough. Chemical transport model (CTM) is an important and powerful tool to grasp the surface concentrations, spatial distribution of deposition, and temporal variation of air pollutants. Therefore, modeling studies based on CTMs validated through EANET monitoring data are effective to achieve detailed and easy-to-read analysis of spatial and temporal variability in PM, ozone, acid deposition and other monitoring species. However, attention should be paid to the uncertainty existing in CTMs. In order to avoid misinterpretation based on a single CTM, MICS-Asia has been established and it is still in operation. In MICS-Asia, further efforts are planned such as analyzing more specific air pollution events typically occur in East Asia and utilizing model simulated results for impact assessment of ecosystem and human health. EANET should provide capacity building activities for atmospheric modeling similar to the EANET Emission Inventory Workshop held on October 2021 and encourage scientists in the participating countries to join projects such as MICS-Asia in order to support more transparent discussions on the present status of the atmospheric environment.

A significant advance has been made in acid deposition modeling in the past 20 years in East Asia. Reliable model analysis results were reported from Southeast Asia, too, in recent years. However, there is still differences among the models. In the recent MICS-Asia studies the participated models performed well for SO_4^{2-} and total ammonium (NH_3 and NH_4^+), but estimation of total nitrate (HNO_3 and NO_3^-) still has uncertainties. Regional scale evaluations of acidification and nitrogen leaching

should be still kept going. Collaboration of atmospheric modeling and impact studies should be maintained to make clear the relationship between atmospheric deposition and its impacts to ecosystems. It is recommended to encourage collaborative works between researchers of different scientific fields such as atmospheric chemistry and ecosystems.

7.3.7 Health impact studies

Impacts of acid deposition has been mainly investigated from a point of view of impacts on plants. The main substances affecting public health are nitrogen oxides (NOx), sulfur dioxide (SO_2), tropospheric ozone (O_3), and PMs. Epidemiological studies have indicated that symptoms of bronchitis for children was associated with long-term exposure to Nitrogen Dioxide (NO_2). SO_2 can affect the respiratory system and functions of the lungs, and causes eye irritation. Excessive O_3 exposure can cause breathing problems, aggravate asthma and reduce lung functions. In recent years, fine particles ($PM_{2.5}$) are of significant concern, as these tiny particles penetrate into the lungs, affecting both the respiratory and vascular systems.

Even if there is still uncertainty at the moment, air pollution measures are required considering the adverse health effects at present and expected in the near future in East Asia. During the past 20 years, participating countries of the EANET have made great efforts to reduce emissions of acid deposition and related pollutants through methods such as effective policies, advanced technologies and best practices. Therefore, assessment on effectiveness of various measures contributing to emission reduction of acid deposition and related air pollution considering the adverse effects caused by multiple air pollutants is necessary, which could figure out applicable measures to further improve the air quality.

7.4 References

EANET. 2006. Periodic Report on the State of Acid Deposition in East Asia, Part I-III: Acid Deposition Monitoring Network in East Asia, Niigata, Japan.

EANET. 2011. Second Periodic Report on the State of Acid Deposition in East Asia, Part I-III: Network Center for the EANET, Niigata, Japan.

EANET. 2016. Third Periodic Report on the State of Acid Deposition in East Asia, Part I-III: Acid Deposition Monitoring Network in East Asia, Bangkok, Thailand.

Schwede, D.B., Lear, G.G. 2014. A novel hybrid approach for estimating total deposition in the United States, Atmospheric Environment, 92, 207-220.

Network Center for EANET. 2010. Technical Manual for Dry Deposition Flux Estimation in East Asia.

Kurokawa, J., Wang, Z., Woo, J., Carmichael, G., Fu, J. S., Zhang, Q., Han, Z., Thongboonchoo, N., Chuang, M-T., Lam, Y. F., Li, J., Nagashima, T., Zhang, M., Itahashi, S., Ge, B., Li, M., Gao, M., Sato, K., Minoura, H. and Akimoto, H. 2020. The Model Inter-Comparison Study for Asia (MICS-Asia): Phase III and next steps, EANET Science Bulletin, 5, 99-112.

List of the Secretariat of the Drafting Committee for the Preparation of the Fourth Periodic Report

Asia Center for Air Pollution Research (ACAP)
1182 Sowa, Nishi-ku, Niigata-shi, 950-2144, Japan
Tel; +81-25-263-0550
Fax; +81-25-263-0566
E-mail; eanet@acap.asia

Name	Position	Department
Dr. Shiro Hatakeyama	Director General	
Dr. Erdenebat Eldev-Ochir	Deputy Director General	
Mr. Kenichiro Fukunaga	Deputy Director General	
Dr. Ken Yamashita	Head	Planning and Training Department
Dr. Meihua Zhu	Senior Researcher	Planning and Training Department
Ms. Ayako Aoyagi	Administrative Staff	Planning and Training Department
Dr. Keiichi Sato	Head	Atmospheric Research Department
Dr. Mingqun Huo	Senior Researcher	Atmospheric Research Department
Mr. Ryo Matsuya	Senior Researcher	Atmospheric Research Department
Mr. Takuya Momoi	Senior Researcher	Atmospheric Research Department
Dr. Akie Yuba	Senior Researcher	Atmospheric Research Department
Ms. Mari Futami	Researcher	Atmospheric Research Department
Dr. Hiroyuki Sase	Head	Ecological Impacts Research Department
Dr. Rieko Urakawa	Senior Researcher	Ecological Impacts Research Department
Mr. Hiroki Yotsuyanagi	Senior Researcher	Ecological Impacts Research Department
Mr. Masayuki Morohashi	Senior Researcher	Ecological Impacts Research Department
Dr. Tsuyoshi Ohizumi	Head	Data Management Department
Dr. Junichi Kurokawa	Chief Senior Researcher	Data Management Department
Mr. Hiroshi Machida	Senior Researcher	Data Management Department
Dr. Yuusuke Kiriyama	Researcher	Data Management Department
Ms. Kumiko Nakamura	Researcher	Data Management Department

Acid Deposition Monitoring Network in East Asia (EANET)

URL: http://www.eanet.asia

Secretariat for the EANET

United Nations Environment Programme
Asia and the Pacific Office

2nd Floor, United Nations Building, Rajdamnern Nok Avenue, Bangkok 10200, Thailand
TEL: +662-288-1627
FAX: +662-280-3829
e-mail: eanetsecretariat@un.org
URL: http://www.eanet.asia
URL: http://www.unep.org/asia-and-pacific/restoring-clean-air/eanet

Network Center for the EANET

Asia Center for Air Pollution Research (ACAP)

1182 Sowa, Nishi-ku, Niigata-shi 950-2144, Japan
TEL: +81-25-263-0550
FAX: +81-25-263-0566
e-mail: eanet@acap.asia
URL: http://www.acap.asia